Cardiovascular Specific Gene Expression

Edited by
Pieter A. Doevendans, Robert S. Reneman and Marc van Bilsen

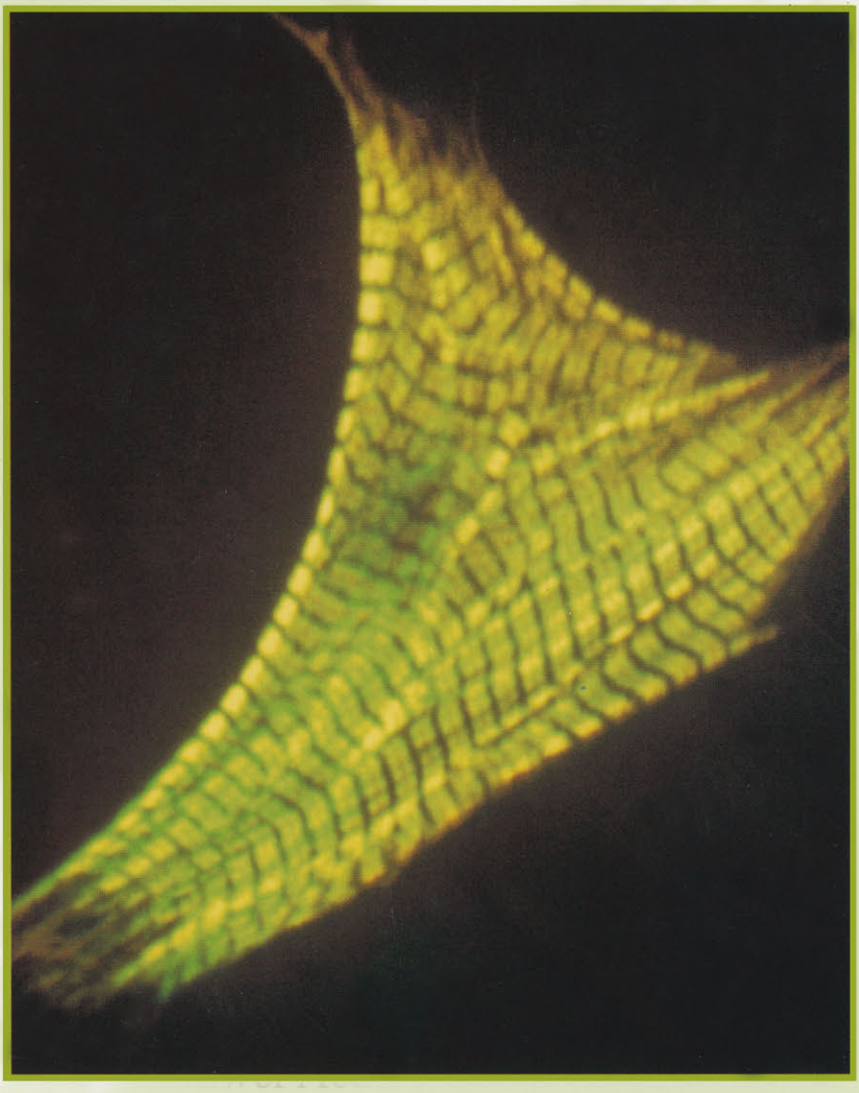

Springer-Science+Business Media, B.V.


EUROPEAN SCIENCE FOUNDATION
E·S
F


CARIM


Federation of European Physiological Societies
FEPS
1991


molecular
M C M
cardiology maastricht

Developments in Cardiovascular Medicine

VOLUME 214

The titles published in this series are listed at the end of this volume.

Cardiovascular Specific Gene Expression

edited by

PIETER A. DOEVENDANS
Department of Cardiology
Academic Hospital Maastricht,
Maastricht, The Netherlands

ROBERT S. RENEMAN
CARIM,
Academic Hospital Maastricht,
Maastricht, The Netherlands

and

MARC VAN BILSEN
Department of Physiology
Academic Hospital Maastricht,
Maastricht, The Netherlands

Cardiovascular Research Institute Maastricht (CARIM)
Maastricht University
PO Box 616
6200 MD MAASTRICHT
The Netherlands

This publication has been made possible by educational grants from the Royal Netherlands Academy of Arts and Sciences and the Netherlands Heart Foundation.

SPRINGER-SCIENCE+BUSINESS MEDIA, B.V.

A C.I.P. Catalogue record for this book is available from the Library of Congress.

ISBN 978-90-481-5189-9 ISBN 978-94-015-9321-2 (eBook)
DOI 10.1007/978-94-015-9321-2

Cover picture by and with the courtesy of David Becker
Legend to the cover picture:
Transiently transfected neonatal rat cardiomyocytes assemble normal sarcomeres. Primary cultures of neonatal rat cardiomyocytes were transfected with expression plasmids harboring human beta myosin heavy chain cDNA. Two days after transfection the cells were fixed and immunostained using an epitope specific antibody recognizing the human protein. The fluorochrome conjugated to the secondary antibody was visualized via epifluorescene and confocal microscopy.

Printed on acid-free paper

Table of Contents

List of Contributors ix

Preface xiii

1. Cardiology approaching the year 2000. A clinician's look at molecular cardiology
Hein J.J. Wellens 1

Part One : **Cardiovascular specific gene expression**

2. The transcriptional building blocks of the heart
Diego Franco, Robert Kelly, Peter Zammit, Margaret E. Buckingham and Antoon F.M. Moorman 7

3. A cardiac-specific troponin I promoter. Distinctive patterns of regulation in cultured fetal cardiomyocytes, adult heart and transgenic mice
Stefano Schiaffino, Simonetta Ausoni, Caterina Millino, Elisa Calabria, Claudia Sandri and Raffaella Di Lisi 17

4. Mice deficient in muscle LIM protein (MLP) reveal a pathway to dilated cardiomyopathy and heart failure
Pico Caroni 27

5. Regulation of endothelial cell specific receptor tyrosine kinase gene expression during development and disease
Thorsten M. Schlaeger 35

6. Smoothelins: one gene, two proteins, three muscle cell types .... so far
Guillaume J.J.M. van Eys, Carlie J.M. de Vries, Sander S.M. Rensen, Victor L.J.L. Thijssen, Edward L.C. Verkaar, Gisela P.G.M. Coolen, Wiel M.H. Debie, Marco C. de Ruiter and Sevilla D. Wadleigh-Detera 49

Part Two : **Transcription regulation**

7. Regionalization of transcriptional potential in the myocardium: 'cardiosensor' transgenic mice

Robert G. Kelly, Peter S. Zammit, Diego Franco, Antoon F.M. Moorman and Margaret E. Buckingham 67

8. Human troponin genes: transcriptional regulation and chromosomal organization
Paul J.R. Barton, Pankaj K. Bhavsar, Kimberley A. Dellow, Philip J. Townsend, Magdi H. Yacoub and Nigel J. Brand 75

9. Retinoid signaling: insight from genetically engineered mice
Pilar Ruiz-Lozano and Kenneth R. Chien 87

10. Ventricular expression of the atrial regulatory myosin light chain gene
Pieter A. Doevendans, Ronald Bronsaer, Pilar Ruiz-Lozano, Jan Melle van Dantzig and Marc van Bilsen 99

11. Expression of rat gap junction protein connexin 40 in the heart
W. Antoinette Groenewegen 117

Part three : **Ion channels and gap junction**

12. Sympathetic regulation of cardiac delayed rectification: relationship to cardiac arrhythmias
Robert S. Kass 125

13. The sarco(endo)plasmic reticulum Ca^{2+} pumps in the cardiovascular system
Anne-Marie Lompré, Olivier Vallot, Marielle Anger and Anne Ozog 139

14. Potassium channels; genes, proteins, and patients
Connie Alshinawi and Arthur A.M. Wilde 151

15. Expression of Cx43 in cardiac and aortic muscle cells of hypertensive rats
Jacques-Antoine Haefliger and Paolo Meda 161

16. Genetic engineering and cardiac ion channels
Andrew A. Grace, Richard C. Saumarez and Jamie I. Vandenberg 171

Part four : **Intracellular signaling**

17. Receptor tyrosine kinase signaling in vasculogenesis and angiogenesis
Thomas I. Koblizek, Werner Risau and Urban Deutsch 179

18. Molecular analysis of vascular development and disorders
Peter Carmeliet and Désiré Collen 193

19. Crosstalk between the estrogen receptor and the insulin-like growth factor (IGF-1) receptor. Implications for cardiac disease
Christian Grohé, Rainer Meyer and Hans Vetter 227

20. Expression of basic helix-loop-helix proteins and smooth muscle phenotype in the adult rat aorta
Paul R. Kemp and James C. Metcalfe 237

21. Expression of the IGF system in acute and chronic ischemia
Elisabeth Deindl, René Zimmermann and Wolfgang Schaper 245

22. Long-chain fatty acids and signal transduction in the cardiac muscle cell
Marc van Bilsen, Karin A.J.M. van der Lee and Ger J. van der Vusse 257

Part five : **DNA transfer**

23. Reduction of kidney renin expression by ribozymes
Matthew G.F. Sharp, Jörg Peters and John J. Mullins 269

24. Receptor-dependent cell specific delivery of antisense oligonucleotides
Erik A.L. Biessen and Theo J.C.van Berkel 285

25. Tissue-specific gene delivery by recombinant adenoviruses containing cardiac-specific promoters
Wolfgang-Michael Franz, Thomas Rothmann, Matthias Müller, Norbert Frey and Hugo Albert Katus 301

26. Catheter-mediated delivery of recombinant adenovirus to the vessel wall to inhibit restenosis
Olivier Varenne, Peter Sinnaeve, Désiré Collen, Stefan P. Janssens and Robert D. Gerard 319

Index 325

List of Contributors

Connie Alshinawi
Academic Medical Center, University of Amsterdam, Department of Clinical and Experimental Cardiology, PO Box 22700, 1100 DE AMSTERDAM, The Netherlands.
Co-author: Arthur A.M. Wilde

Paul J.R. Barton
Molecular Biology Group, Department of Cardiothoracic Surgery, National Heart and Lung Institute, Imperial College School of Medicine, Dovehouse Street, LONDON SW3 6LY, United Kingdom
Co-authors: Pankaj K. Bhavsar, Kimberley A. Dellow, Philip J. Townsend, Magdi H. Yacoub and Nigel J. Brand

Theo J.C. van Berkel
Division of Biopharmaceutics, LACDR, University of Leiden, PO Box 9503, 2300 RA LEIDEN, The Netherlands
Co-author: Erik A.L. Biessen

Marc van Bilsen
Department of Physiology, Cardiovascular Research Institute Maastricht (CARIM), Maastricht University, PO Box 616, 6200 MD MAASTRICHT, The Netherlands
Co-authors: Karin A.J.M. van der Lee and Ger J. van der Vusse

Peter Carmeliet
Center for Transgene Technology and Gene Therapy, Campus Gasthuisberg, Herestraat 49, Universiteit Leuven, B-3000 LEUVEN, Belgium.
Co-author : Désiré Collen

Pico Caroni
Friedrich Miescher Institute, Maulbeerstrasse 66, CH-4058 BASEL, Switzerland

Elisabeth Deindl
Max-Planck-Institute for Physiological and Clinical Research, W. G. Kerckhoff-Institute, Department of Experimental Cardiology, Benekestraße 2, D-61231 BAD NAUHEIM, Germany
Co-authors: René Zimmermann and Wolfgang Schaper

Pieter A. Doevendans
Department of Cardiology, Cardiovascular Research Institute Maastricht, PO Box 5800, 6202 AZ MAASTRICHT, The Netherlands
Co-authors: Ronald Bronsaer, Pilar Ruiz-Lozano, Jan Melle van Dantzig and Marc van Bilsen

Guillaume J.J.M. van Eys
Department of Molecular Biology and Genetics, University of Maastricht, P.O. Box 616, 6200 MD MAASTRICHT, The Netherlands
Co-authors: Carlie J.M. de Vries, Sander S.M. Rensen, Victor L.J.L. Thijssen, Edward L.C. Verkaar, Gisela P.G.M. Coolen, Wiel M.H. Debie, Marco C. de Ruiter and Sevilla D. Wadleigh-Detera

Diego Franco
Department of Anatomy and Embryology, University of Amsterdam, Spui 21, 1012 WX AMSTERDAM, The Netherlands
Co-authors: Antoon F. M. Moorman, Robert Kelly, Peter Zammit and Margaret Buckingham

Wolfgang-Michael Franz
Medizinische Klinik II, Universität Lübeck, Ratzeburger Allee 160, D-23538 LÜBECK, Germany
Co-authors : Thomas Rothmann, Matthias Müller, Norbert Frey and Hugo Albert Katus

Robert D. Gerard
Center for Transgene Technology and Gene Therapy, Flanders Interuniversity Institute for Biotechnology, KU Leuven, 49 Herestraat B-3000 LEUVEN, Belgium
Present address: Vector Core Laboratory and Supervisor, NGVL, Center for Gene Therapy, University of Michigan, 1150 West Medical Center Drive, ANN ARBOR, MI 48109-0688, USA
Co-authors: Olivier Varenne, Peter Sinnaeve, Désiré Collen and Stefan P. Janssens

Andrew A. Grace
Department of Biochemistry, University of Cambridge, Tennis Court Road, CAMBRIDGE CB2 1QW, United Kingdom
Co-authors: Richard C. Saumarez and Jamie I. Vandenberg

Christian Grohé
Medizinische Univ.-Poliklinik, University of Bonn, Wilhelmstr. 35–37, D-53111 BONN, Germany
Co-authors: Rainer Meyer and Hans Vetter

W. Antoinette Groenewegen
Department of Medical Physiology & Sports Medicine, Utrecht University, PO Box 80043, 3508 TA UTRECHT, The Netherlands

Jacques-Antoine Haefliger
Department of Internal Medicine B, University Hospital, Laboratoire de Biologie Moléculaire 19-1359, Centre Hospitalier Universitaire Vaudois, CH-1011 LAUSANNE, Switzerland

Co-author: Paolo Meda

Robert S. Kass
Department of Pharmacology, Columbia University, College of Physicians and Surgeons, 630 W. 168th St, PH 7W, Room 318, NEW YORK, NY 10032, USA

Robert G. Kelly
Department of Molecular Biology, Pasteur Institute, 28 Rue du Dr Roux, F-75724 PARIS Cedex 15, France
Co-authors: Peter S. Zammit, Diego Franco, Antoon F.M. Moorman and Margaret E. Buckingham

Paul R. Kemp
Section of Cardiovascular Biology, Department of Biochemistry, University of Cambridge, Tennis Court Road, CAMBRIDGE, CB2 1QW, United Kingdom
Co-author: James C. Metcalfe

Thomas I. Koblizek
Department of Molecular Cell Biology, Max-Planck-Institute for Physiological and Clinical Research, Kerckhoff Institute, Parkstr. 1, D-61231 BAD NAUHEIM, Germany
Present address: New York University Medical Center, Department of Pharmacology, 550 First Avenue, NEW YORK, NY 10016, USA
Co-authors: Werner Risau and Urban Deutsch

Anne-Marie Lompré
CNRS ERS 570, Groupe "Gènes et Protéines Musculaires", Université Paris-Sud, Bat. 433 – F-91405, ORSAY, France
Co-authors: Olivier Vallot, Marielle Anger and Anne Ozog

Robert S. Reneman
Department of Physiology, Cardiovascular Research Institute Maastricht (CARIM), Maastricht University, PO Box 616, 6200 MD MAASTRICHT, The Netherlands

Pilar Ruiz-Lozano
Department of Medicine, School of Medicine, University of California, 0613 Basic Science Building, LA JOLLA, CA 92093-0613, USA
Co-author: Kenneth R. Chien

Matthew G. F. Sharp
Centre for Genome Research, King's Buildings, University of Edinburgh, West Mains Road, EDINBURGH EH9 3JQ, United Kingdom
Co-authors: Jörg Peters and John J. Mullins

Stefano Schiaffino
Department of Biomedical Sciences, CNR Center of Muscle Biology and Physiopathology, University of Padova, Viale G. Colombo 3, I-35121 PADOVA, Italy
Co-authors: Simonetta Ausoni, Caterina Millino, Elisa Calabria, Claudia Sandri and Raffaella Di Lisi

Thorsten M. Schlaeger
Max Planck-Institüt für Physiologische und Klinische Forschung, Kerckhoff-Institut, Parkstraße 1, D-61231 BAD NAUHEIM, Germany

Hein J.J. Wellens
Department of Cardiology, Cardiovascular Research Institute Maastricht, PO Box 5800, 6202 AZ MAASTRICHT, The Netherlands

Preface

Improving our insights into the genetic predisposition to cardiovascular disease is one of the most important challenges in our field in the next millennium, not only to unravel the cause of disease but also to improve the selection of patients for particular treatments. Nowadays, for example, subjects with a cholesterol above a particular plasma level are exposed to a cholesterol lowering regime based upon the beneficial outcome of epidemiological studies which include subjects not prone to the disease, despite a plasma cholesterol above the accepted level. Identification of the patients who are genetically predisposed to the consequences of this disorder will reduce the number of subjects unnecessarily treated and, hence, the costs of health care. Because in most cardiovascular diseases the genetic component is a consequence of more than one gene defect, only limited progress has as yet been made in identifying subjects genetically at risk. For example, in hypertension only in less than 10% of the patients the genetic defect has been identified.

It has been known for quite some time that in heart and blood vessels fetal genes are upregulated or induced when they are exposed to such disorders as high blood pressure and ischemia. Little is known about the function of these genes in the cardiac and vascular adaptation to these disorders; only guesses can be made. Therefore, it is of utmost importance to obtain more information about the specific role of these genes in fetal development and the molecular mechanisms involved in this consistently observed switch to a "fetal program" in most of the adaptation processes.

To get better insight into the genetic defects playing a role in the origin of cardiovascular diseases and into the function of the fetal genes upregulated or induced when heart and blood vessels are exposed to a changing environment, close collaboration between basic and clinical scientists is a prerequisite. Therefore, in December 1997 we brought together these scientists to discuss the expression of specific genes in the cardiovascular system. The organizers were delighted that internationally renown scientists and young investigators accepted our invitation to participate in this discussion. The book presented here is a reflection of the papers presented at the workshop. The discussions were vivid and very interesting but these are not included in the book, because to the opinion of the editors most of the chapters include the essence of the discussions held. On behalf of the editors I would like to thank the authors for their contributions, making this book a good reflection of our present knowledge of cardiovascular specific gene expression.

Without ignoring the contribution of others, it is my pleasure to thank Pieter Doevendans and Marc van Bilsen for their hard work. Without them we would not have been in a situation to look back at a fantastic scientific happening.

Robert S. Reneman

1. CARDIOLOGY APPROACHING THE YEAR 2000. A CLINICIAN'S LOOK AT MOLECULAR CARDIOLOGY

Hein J.J. Wellens

Introduction

Unfortunately, the incidence of cardiovascular disease is still growing. As recently commented upon by Braunwald [1], world wide in 1990 29% of all deaths were caused by cardiovascular disease and this is expected to rise to 36% in 2020. Incidence and ability to lower the number of cardiovascular deaths varies considerably from country to country. As shown by Sans et al. [2] standardized mortality from ischemic heart disease may vary in Europe from 70 (France) to 700/100.000 (Russia) for men and from 36 (France) to 370/100.000 (Russia) for women in the age group 0-64 years.
Graying of the population and reduction in mortality from acute ischemic syndromes have resulted in a larger patient population with coronary heart disease which, as shown for the Netherlands in figure 1, will result in a growing number of cardiovascular deaths in the coming years.
Against this background it is clear that for many years to come we will be treating cardiac patients and the obvious question is: What has molecular and cell biology to offer in this battle?

Better understanding of the disease

Understanding of the processes responsible for cardiac and vascular disease have made important strides in the past decade thanks to the use of molecular biologic research. Also, the role of genetic influences is being unraveled. Still, we are looking at the tip of the iceberg. We know that only a few cardiovascular diseases have a monogenetic background but even there the situation is more complex than we expected. Typical examples are the long QT syndrome and hypertrophic cardiomyopathy. What presents clinically as a similar abnormality may have marked differences in the chromosomal location of the abnormal gene. Also we have become aware of the complexity of reactions or repair processes after a noxious substance or trigger. Prevention or suppression of expression of one genetic pathway frequently is followed by the

P.A. Doevendans et al. (eds.), Cardiovascular specific gene expression, 1-5.

development of a new pathway preventing palliation or cure. Unfortunately, much too often the non-transparency of these processes make the clinician believe that nature is too complex to become unraveled, understood, and controlled.

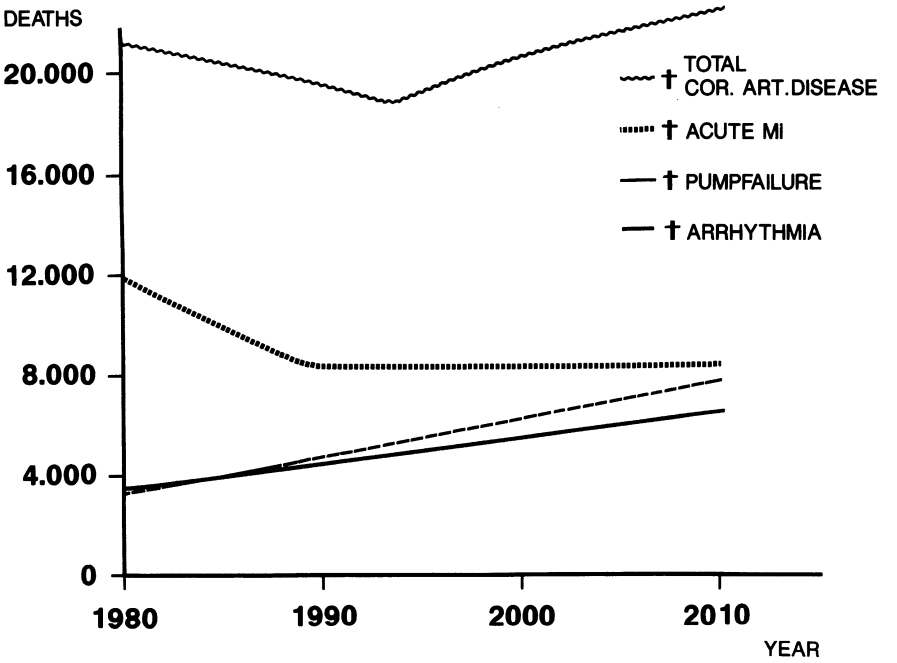

Figure 1. *The incidence of death from acute myocardial infarction, pump failure and cardiac arrhythmias in recent years in the Netherlands. Although mortality from acute myocardial infarction fall, mortality from pump failure and cardiac arrhythmias increased, resulting in an increase in total mortality from cardiac diseases.*

Development of new diagnostic and therapeutic strategies

In recent years we have seen the development of new strategies to diagnose and treat ischemic syndromes, lipid disorders, congestive heart failure, etc. Unfortunately, many of these established strategies are frequently not applied. Less than half of the patients who should be treated with thrombolytics because of a myocardial infarction actually receive that medication. The same holds for beta-blocking agents after a myocardial infarction [3] or the use of lipid lowering agents in case of atherosclerotic disease, independent of the lipid values. This suggests that new strategies coming from the molecular-biologic and genetic laboratory may even be more difficult to apply. The wide gap between the basic scientist and the clinician threatens to delay or even prevent the introduction of that knowledge into clinical medicine. This can be illustrated by table 1. In this table, possible cardiovascular therapies based on information from

molecular biology are listed. Most clinicians will be familiar with the pathological expression of cardiovascular disease, but their understanding of the basic processes resulting in the interventions suggested in the right column in table 1 will be disappointing. This stresses the necessity to bridge the rapidly widening gap between basic science and clinical medicine. Failure to understand basic mechanisms seduces the clinician to use a therapeutic shot gun approach. Restenosis after balloon dilatation of an artery is a complex process, including thrombosis and repair by proliferation and migration of cells to the inner wall of the vessel. Attempts to interfere with components of this process, like the use of antithrombotic drugs have not been successful. These disappointing results led to the use of irradiation of the vessel wall, so called brachytherapy, with the intent to halt the repair process after balloon-induced damage to the vessel wall. Such an approach is not based on the understanding of the processes leading to restenosis but simply prevents the vessel lumen directed movement of the repair process. Many of our current therapies are not interfering with basic processes during disease. For example, congestive heart failure may have different causes like hypertension, valvular, ischemic or myocardial disease. Often however, our therapy is aimed at reducing circulatory volume, or decreasing afterload rather than correcting the myocardial changes that resulted in pump failure.

Table 1. Molecular therapies for vascular diseases (from Gibbons and Dzau [4])

Pathologic event	**Therapeutic target**
Plaque rupture	Metallo proteinase inhibitors Leucocyte adhesion blockers
Thrombosis	Glyco protein IIb/IIIa-receptor blockers, tissue factor inhibitors, antithrombosis
Endothelial dysfunction	NO donors, anti-oxidants
Endothelial injury	VEGF, IGF
Dysregulated cell growth	Cell-cycle inhibitors
Dysregulated apoptosis	Integrin antagonists
Matrix modification	Metallo proteinase inhibitors Plasmin antagonists

Bridging the gap

Molecular and cellular biology and molecular genetics are of major importance for our understanding of normal and abnormal cardiovascular function. But how long will it take before this information becomes therapeutically useful? Essential in this process is to bridge the gap between basic science and clinical medicine. For the clinician there are several problems, such as the understanding of the language of the basic scientist,

the necessity to closely follow new information and to appreciate the value of mechanism specific fine tuning above the shotgun approach. In this regard the approach recently suggested by Judith Swain [5] is worth considering. In view of the changes in academic medicine currently taking place in the United States, she pointed out that if academics is to survive in academic medicine, closely knit groups performing four different types of activities have to be formed. Table 2 shows how these four groups all working in the cardiovascular area differ as to their involvement in research and patient care. However, close contact between these four groups, for example, in a daily meeting, where information and ideas are exchanged will lead to growing mutual understanding and cooperation. It is obvious that funding of such a situation requires a major change in thinking of hospital administrators and guru's of medical faculties.

Table 2. The "ideal" approach to bring basic information into academic medicine (adapted from Swain [5])

	Research	**Patient care**
Physician scientist	only	--
Clinical investigator	mostly	--
Clinical educator	--	mostly
Master clinician	--	only

Conclusion

More than ever there is a need for understanding and cooperation between basic science and clinical medicine. However, important conceptual and structural changes are required to make this possible.

References

1. Braunwald E. Shattnek Lecture - Cardiovascular Medicine at the turn of the millennium: Triumphs, concerns, and opportunities. New Engl J Med 1997;337:1360-69.
2. Sans S, Kesteloot H, Kromhout D, on behalf of the Task Force. The burden of cardiovascular diseases mortality in Europe. Eur Heart J 1997;18:1231-48.
3. Avanzini F, Zuanetti G, Latini R, Colombo F, Santoro E, Maggione AP, Franzosi MG, Tognoni G, on behalf of the Gruppo Italiano di Stadio sulla Sopravvivenza nell' Infarto Miocardico (GISSI) Investigators. Use of beta-blocking agents in secondary prevention after myocardial infarction: a case for evidence-based medicine? GISSI experience 1984-1993. Eur Heart J 1997;18:1447-56.
4. Gibbons GH, Dzau VJ. Molecular therapies for vascular diseases. Science 1996;272:689-93.
5. Swain JL. Is there room left for academics in academic medicine? J Clin Invest 1996;98:1071-73.

2. THE TRANSCRIPTIONAL BUILDING BLOCKS OF THE HEART

Diego Franco, Robert Kelly, Peter Zammit, Margaret Buckingham, and Antoon F.M. Moorman

Introduction

Within the adult heart, it is convention to distinguish working myocardium (atrial and ventricular) from conduction system myocardium, each characterized by distinct functional properties and patterns of gene expression [1]. In the tubular heart, expression of most contractile genes such as myosin and actin isoforms show either homogeneous expression or a gradient along the antero-posterior myocardial tube. At this stage, the heart exerts a peristaltoid contraction wave with a posterior-anterior pacemaker polarity. With further development, five different functional cardiac segments can be distinguished [2]. Two fast contracting segments, the atria and ventricles grow out from the outer curvature of the primary heart tube. They are flanked by slow conducting segments reminiscent to the primary cardiac tube, i.e. inflow tract, atrioventricular canal and outflow tract [3]. The ventricles are characterised at this stage by a trabeculated morphology. Eventually, an outer ventricular compact myocardial layer is formed which shows a distinct pattern of gene expression [4]. At this stage, no morphological ventricular conduction system is identifiable albeit that the heart exerts a synchronous contraction wave from apex to the arterial pole. As the heart undergoes septation, each cardiac segment is divided into right and left components. Transgenic mice carrying regulatory sequences of myosin light chain genes have shown a distinct transcriptional potential in right and left atrial and ventricular components [5,6]. The first morphological evidence of a ventricular conduction system can be traced to the fetal stage.

In the present study we have compared the pattern of expression of cardiac specific genes during embryogenesis and we have integrated these data into a model of cardiac transcriptional regulation. Furthermore, the arrangement of the distinct cardiac building blocks explains the coordinated contraction and the ECG. Hence, the formation of the cardiac ventricular conduction system does not need an extra-cardiac non-myocardial origin.

P.A. Doevendans et al. (eds.), Cardiovascular specific gene expression, 7-16.

Materials and methods

Previously characterised expression patterns of myosin heavy chain (MHC) and myosin light chain (MLC) isoforms [see for a review 7,8], muscle-specific creatine kinase and Gln2 [9,10], and transgenic mice carrying regulatory sequences of MLC3F gene, i.e. 3F-*nlacZ*-2E [5], and 3F-*nlacZ*-9 [11] have been used to illustrate the developmental profile of transcriptional potential during cardiac development.
To gain insight into the development of the conduction system, mouse embryos ranging from embryonic day (E) 8.5 to E18.5 were collected and processed for *in situ* hybridisation as previously described [11]. Serial sections were hybridised with complementary cRNA probes against MLC2a [12], and MLC2v [13] isoforms, atrial natriuretic factor [ANF, 14], slow skeletal troponin C [15], cardiac troponin C [15], and SERCA2 [16] mRNAs. To gain insight into three-dimensional patterns of gene expression, computer-aided three-dimensional reconstructions were generated.

Results

The tubular heart
In the early tubular heart, two types of expression patterns are observed, a homogeneous expression or a gradient along the antero-posterior cardiac tube (figure 1), with the possible exception of MLC2v which has been described to be restricted to the ventricular myocardium as early as the cardiac tube stage [13].

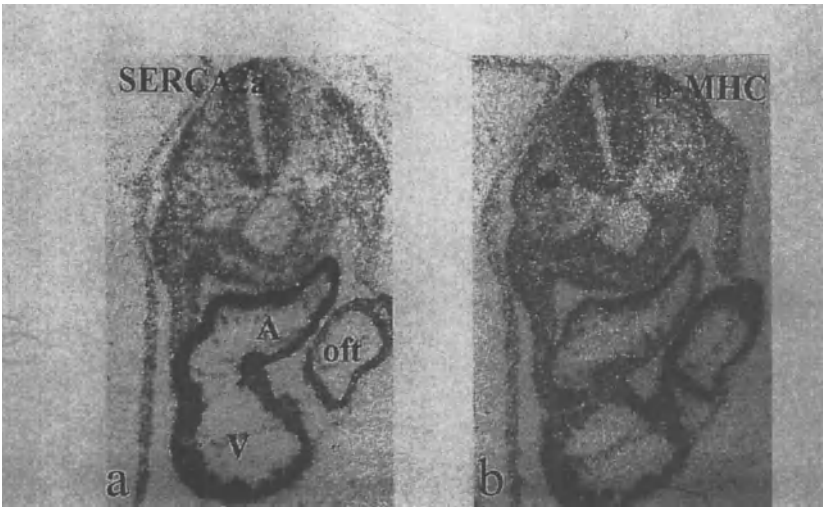

Figure 1. In situ *hybridisation of E10 rat heart hybridized with a cRNA probe against sarcoplasmatic reticulum calcium-ATPase (SERCA2a) mRNA (a) and beta myosin heavy chain (β-MHC) mRNA (b). Note the gradual decrease of expression from the posterior (atrial; A) to the anterior (outflow tract, oft) pole of the heart for the SERCA2 mRNA (a). In essence, the opposite pattern is observed for β-MHC mRNA (b). V, ventricle.*

The five segment heart

With further development, five functional segments can be distinguished in the embryonic heart, i.e. inflow tract, atria, atrioventricular canal, ventricles, inflow tract. α-MHC and the regulatory MLC2a mRNAs become confined to inflow tract, atrial and atrioventricular canal myocardium and, interestingly, remain transiently expressed in outflow tract myocardium (figure 2a). Conversely, β-MHC and MLC2v is expressed mostly in outflow tract, ventricular and atrioventricular canal myocardium. Remarkably both genes (MLC2a and MLC2v) are also expressed in inflow tract myocardium (figure 2b). Thus, co-expression of MHC and regulatory MLC isoforms is observed in the remaining myocardium of the primary heart tube, whereas a down-regulation of "atrial-specific" genes is observed in the ventricle and a down-regulation of "ventricular-specific" genes is observed in the atria.

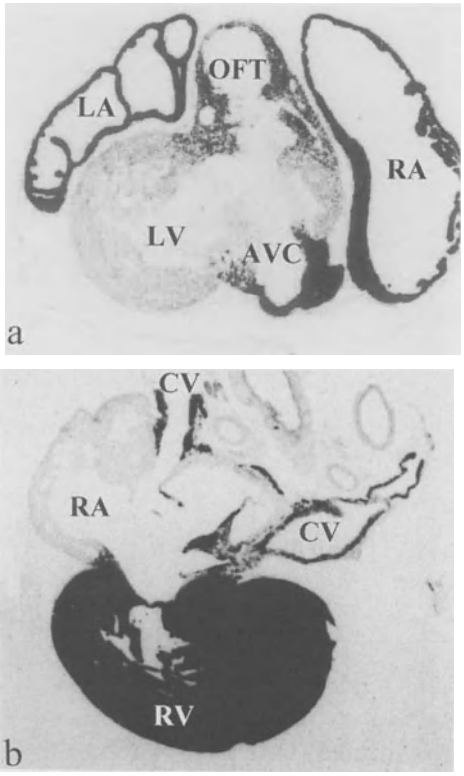

Figure 2. *(a)* In situ *hybridisation of E14 mouse heart hybridised with a cRNA probe against myosin light chain 2a (MLC2a) mRNA. (b)* In situ *hybridisation of a rat newborn (one-day old) hybridised with a cRNA probe against myosin light chain 2v (MLC2v) mRNA. Expression of MLC2a is confined to the atrial myocardium, atrioventricular canal myocardium and outflow tract myocardium. Only low level of expression is observed in the ventricular myocardium. MLC2v mRNA expression is confined to the ventricular myocardium and to the myocardial cells surrounding the caval veins (derivatives from the embryonic inflow tract). Observe that no expression of the MLC2v is observed in the atrial myocardium. LA, left atrium; LV, left ventricle; RA, right atrium; RV, right ventricle; AVC, atrioventricular canal; OFT, outflow tract; CV, caval veins.*

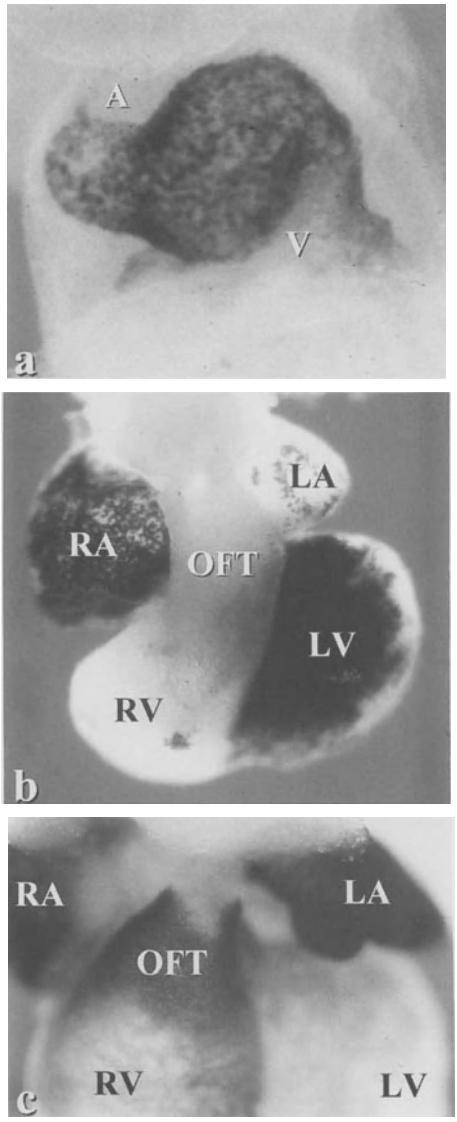

Figure 3. *Whole-mount X-gal coloration of 3F-nlacZ-2E transgenic mouse embryos at E8.5 (a) and E10.5 (b) days of gestation. Observe that expression of the transgene is even along the myocardium at E8.5 and becomes confined to the embryonic left ventricle and right atrium at E10.5. Whole-mount in situ hybridisation of a E14.5 mouse heart hybridised with a dig-labeled cRNA probe against MCL2a mRNA-expression of MLC2a endogenous transcript is mainly confined to the atrial myocardium and to the outflow tract myocardium, whereas low levels of expression remain detectable in the ventricular myocardium. It is important to highlight that endogenous expression of MLC2a mRNA, at this stage, is higher in the right ventricular myocardium than in the left ventricular myocardium. A, anterior pole; V, venous pole; LA, left atrium; LV, left ventricle; RA, right atrium; RV, right ventricle; AVC, atrio-ventricular canal; OFT, outflow tract.*

The seven segment heart

Soon after cardiac looping, right and left atrial and ventricular primordia can be observed. Transgenic mice carrying β-galatosidase reporter gene under transcriptional control of regulatory sequences of the MLC3F gene locus demonstrate a differential transcriptional potential between right and left atrial and ventricular domains [5]. Detailed analysis of the developmental profile of transgene expression demonstrates that right/left differential transgene expression develops after cardiac looping (figure 3a and 3b) [11]. Differential expression of endogenous genes also has been observed for different MHC and MLC isoforms during development (figure 3c; table 1).

Table 1. Summary of the differential expression in the right compact myocardial (RCM) layer versus the left compact myocardial (LCM) layer of MHC and MLCs isoforms during development. >, higher than; =, equal to.

αMHC	RCM>LCM	from E12.5 to E18.5
βMHC	LCM>RCM	at birth
MLC1a	RCM>LCM	from E12.5 to E16.5
MLC1v	RCM=LCM	
MLC2a	RCM>LCM	from E14.5 to E18.5
MLC2v	RCM=LCM	
MLC3f	RCM>LCM	from E9.5 to E10.5

The eighth cardiac segment?

Further differences in gene expression are observed in the ventricular component of the developing heart. With the formation of the compact myocardium, differences in gene expression between the trabeculations and the compact myocardium are observed. In essence, "atrial-specific" isoforms are more highly expressed in the trabeculations than in the compact myocardium, whereas "ventricular-specific" isoforms are expressed at low levels in the trabeculations as compared to the compact myocardium [4]. Two examples that illustrate this paradigm are the expression of ANF and SERCA2; ANF mRNA is highly expressed in the ventricular trabeculations and in the atrial myocardium, but not in the compact myocardium or in the atrioventricular canal (figure 4). SERCA2 mRNA is more highly expressed in the atria than in the ventricles and interestingly shows a steep decrease in expression in atrioventricular canal as well as in the trabeculations.

Discussion

The pattern of expression of distinct cardiac muscle genes in the developing heart suggests that at least seven different transcriptional domains can be distinguished, i.e. outflow tract, right ventricle, left ventricle, atrioventricular canal, right atrium, left atrium and inflow tract. Eventually an eighth domain will be developed, namely the

ventricular conduction system. We propose herein a model of transcription that accounts for the progressive formation of these distinct domains during cardiogenesis. In the early tubular heart, most genes show homogeneous expression or gradients along the antero-posterior (AP) cardiac tube. Consequently, we suggest thus that cardiac transcription activators (AA, anterior activator; PA, posterior activator) are also expressed as gradients along the AP axis (figure 5a). This hypothesis is underscored by the expression pattern of dHAND described by Biben & Harvey [17].

We suggest that at least two cardiac transcriptional repressors are expressed in the embryonic heart; a "ventricular-specific" atrial repressor (VS-AR) inducing down-regulation of atrial genes in the ventricles, and a "atrial-specific" ventricular repressor (AS-VR) inducing down-regulation of ventricular genes in the atria (figure 5b). This hypothesis is underscored by the pattern of expression of MHC and regulatory MLCs in the embryonic heart. Co-expression of "atrial-specific" and "ventricular-specific" isoforms is observed in the slow-conducting cardiac flanking segments, whereas expression in the fast-conducting atrial and ventricular myocardial populations is restricted to "atrial-specific" or "ventricular-specific" isoforms, respectively (figure 5c). It is tempting to speculate that transient differences in gene expression between right/left components can be ascribed to a temporal difference in the maturation process between the right and left compact myocardial layers.

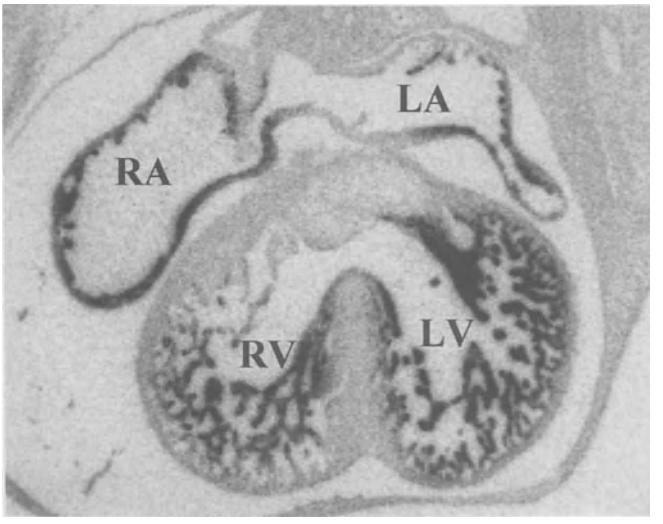

Figure 4. In situ *hybridisation of an E14 mouse heart hybridised with a cRNA probe against ANF mRNA. Note that ANF mRNA expression is confined to the atrial myocardium and the ventricular trabeculated myocardium. LA, left atrium; LV, left ventricle; RA, right atrium; RV, right ventricle.*

In this line, the maturation of the left ventricular compact myocardium would precede that of the right ventricular compact layer. This differential transcriptional potential between right and left cardiac chambers is, nonetheless, maintained in the adult heart [5,18]. The differential gene expression phenotype observed between the trabeculated and the compact myocardium of the ventricles might also be explained in terms of maturation. Based on the expression pattern of contractile genes, the compact myocardium displays a more mature phenotype than the trabeculations [4,8], whereas based on the expression pattern of genes involved in impulse conduction [19,20] as well as on direct measurements of their conductive properties [21], the trabeculations display a more advanced phenotype. This "ambiguous" phenotype of the trabeculations is characteristic of the adult ventricular conduction system as well.

Morphological identification of the ventricular conduction system is first observed at the late fetal stage. However, some characteristics of the adult conduction system are observed in the embryonic heart; the trabeculations share with the ventricular conduction system, i.e. the bundle branches, a weak SERCA2 mRNA expression and a high level of expression of ANF, desmin and α-smooth-muscle actin. Taken together, these data suggest that the ventricular conduction system originates from the embryonic ventricular trabeculated layer.

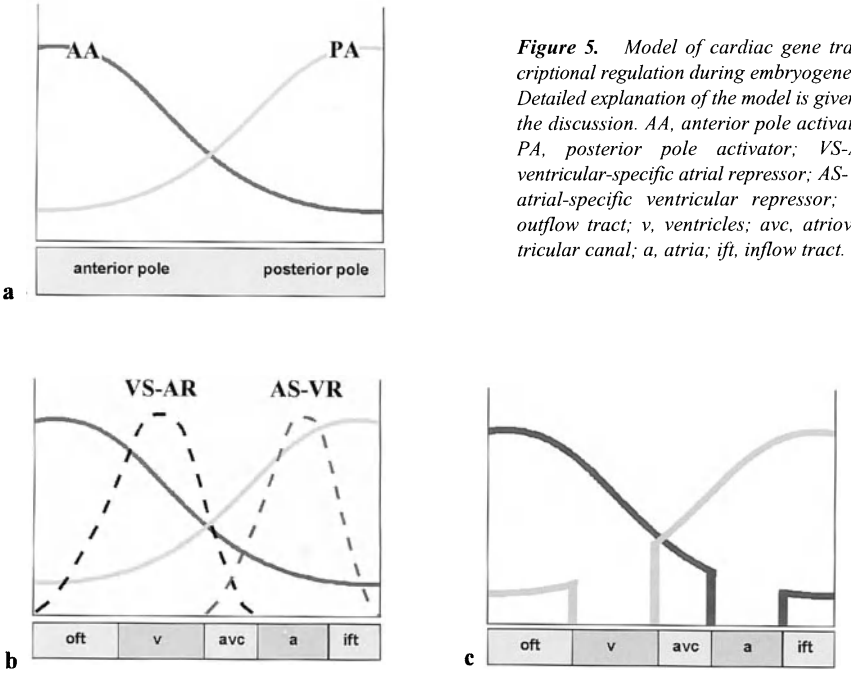

Figure 5. *Model of cardiac gene transcriptional regulation during embryogenesis. Detailed explanation of the model is given in the discussion. AA, anterior pole activator; PA, posterior pole activator; VS-AR, ventricular-specific atrial repressor; AS-VR, atrial-specific ventricular repressor; oft, outflow tract; v, ventricles; avc, atrioventricular canal; a, atria; ift, inflow tract.*

Conclusion

Within the adult heart, it is conventional to distinguish (atrial and ventricular) working myocardium and the conduction system, each characterized by distinct functional properties and patterns of gene expression. The embryonic heart also shows distinct myocardial components whereas a morphologically defined conduction system is not distinguishable, albeit the heart exerts an antero-posterior conductive polarity and an ECG similar to the adult one.

The expression pattern of endogenous myosin isoforms, in addition tot transgenic mice harboring regulatory sequences of the myosin light chain 1F/3F, permit seven different transcriptional compartments to be distinguished. This compartmentalization of the embryonic heart is entirely compatible with the model of cardiac segments of Moorman and Lamers (Trends Cardiovasc Med 1995;4:257) that explains how the embryonic heart can function without valves and without a morphologically distinct conduction system. In this model the sinoatrial node is derived from the inflow tract and the atrioventricular node from the atrioventricular channel.

In the present chapter we suggest that, based on the patterns of gene expression of myosin light chain and myosin heavy chain isoforms, atrial natriuretic factor, Gln2 antigen, creatine kinase isofroms and troponin isoforms, the ventricular conduction system is derived from the trabeculations. We show that the development of the conduction system is inextricably associated with the formation of the different transcriptional compartments without the need of an extra-cardiac origin of the conduction system.

Acknowledgements

This work has been supported by grants from NWO 902-16-219 and NHS 97206.

References

1. Moorman AFM, de Jong F, Denyn MFJ, and Lamers WH. Development of the conduction system. Circ Res 1998;82:629-44.
2. Moorman AFM, and Lamers WH. Molecular anatomy of the developing heart. Trends Cardiovasc Med 1994;4:257-64.
3. De Jong F, Moorman AFM, and Virágh S. Cardiac development: Prospects for a morphologically integrated molecular approach. In: Sipes, IG, McQueen, CA, and Gandolfi, AJ, eds. Comprehensive Toxicology. Cambridge: Cambridge University Press, 1997:5-26.
4. Franco D, Jing Y, Wagenaar GTM, Lamers WH, and Moorman AFM. The trabecular component of the embryonic ventricle. In: Ost'ádal, B, Nagano, M, Takeda, N, and Dhalla, NS, eds. The developing heart. New York: Lippincott Raven, 1996:51-60.
5. Kelly R, Alonso S, Tajbaksh S, Cossu G, and Buckingham M. Myosin light chain 3F regulatory sequences confer regionalised cardiac and skeletal muscle expression in transgenic mice. J Cell Biol 1995;129:383-96.
6. Ross RS, Navankasattusas S, Harvey RP, and Chien KR. An HF-1a/HF-1b/MEF-2 combinatorial element confers cardiac ventricular specificity and established an anterior-posterior gradient of expression. Development 1996;122:1799-1809.
7. Lyons GE. In situ analysis of the cardiac muscle gene program during embryogenesis. Trends Cardiovasc Med 1994;4:70-77.
8. Franco D, Lamers WH, and Moorman AFM. Patterns of expression in the developing myocardium: towards a morphologically integrated transcriptional model. Cardiovasc Res 1998;38:25-33.
9. Wessels A, Vermeulen JLM, Virágh S, Kálmán F, Morris GE, Man N, Lamers WH, and Moorman AFM. Spatial distribution of "tissue-specific" antigens in the developing human heart and skeletal muscle. I. An immunohistochemical analysis of creatine kinase isoenzyme expression patterns. Anat Rec 1990;228:163-76.
10. Wessels A, Vermeulen JLM, Verbeek FJ, Virágh S, Kálmán F, Lamers WH, Moorman AFM. Spatial distribution of "tissue-specific" antigens in the developing human heart and skeletal muscle, III: an immunohistochemical analysis of the distribution of the neural tissue antigen Gln2 in the embryonic heart: implications for the atrioventricular conduction system. Anat Rec 1992;232:97-111.
11. Franco D, Kelly R, Moorman AFM, and Buckingham M. Regionalised transcriptional domains of myosin light chain 3F transgenes in the embryonic mouse heart: morphogenetic implications. Dev Biol 1997;188:17-33.
12. Kubalak SW, Miller-Hance WC, O'Brien TX, Dyson E, and Chien KR. Chamber specification of atrial myosin light chain-2 expression precedes septation during murine cardiogenesis. J Biol Chem 1994;269:16961-70
13. O'Brien TX, Lee KJ, and Chien KR. Positional specification of ventricular myosin light chain 2 expression in the primitive murine heart tube. Proc Natl Acad Sci USA 1993;90:5157-61.
14. Seidman CE, Bloch KD, Klein KA, Smith JA, and Seidman JG. Nucleotide sequences of the human and mouse atrial natriuretic factor genes. Science 1984;226:1206-09.
15. Ausoni S, de Nardi C, Moretti P, Gorza L, and Schiaffino S. Developmental expression of rat cardiac troponin I mRNA. Development 1991;112:1041-51.
16. Moorman AFM, Vermeulen JLM, Koban MU, Schwartz K, Lamers WH, and Boheler KR. Patterns of expression of sarcoplasmic reticulum Ca2+ ATPase and phospholamban mRNAs durins rat heart development. Circ Res 1995;76:616-25.
17. Biben C, and Harvey RP. Homeodomain factor Nkx2-5 controls left/right asymmetric expression of bHLH gene *eHand* during murine heart development. Genes Dev 1997;11:1357-69.
18. Kimura S, Abe K, Suzuki M, Ogawa M, Yoshioka K, Kaname T, Miike T, and Yamamura

K-I. A 900 bp genomic region from the mouse dystrophin promoter directs *lacZ* reporter expression only to the right heart of transgenic mice. Dev Growth Differ 1997;39:257-65.

19. Van Kempen MJA, Fromaget C, Gros D, Moorman AFM, and Lamers WH. Spatial distribution of connexin-43, the major cardiac gap junction protein, in the developing and adult rat heart. Circ Res 1991;68:1638-51.
20. Van Kempen MJA, Vermeulen JLM, Moorman AFM, Gros DB, Paul DL, and Lamers WH. Developmental changes in connexin40 and connexin43 mRNA distribution patterns in the rat heart. Cardiovasc Res 1996;32:886-900.
21. De Jong F, Ophof T, Wilde AAM, Janse MJ, Charles R, Lamers WH, and Moorman AFM. Persisting zones of slow impulse conduction in the developing chicken hearts. Circ Res 1992;71:240-50.

3. A CARDIAC-SPECIFIC TROPONIN I PROMOTER. DISTINCTIVE PATTERNS OF REGULATION IN CULTURED FETAL CARDIOMYOCYTES, ADULT HEART AND TRANSGENIC MICE

Stefano Schiaffino, Simonetta Ausoni, Caterina Millino, Elisa Calabria, Claudia Sandri, and Raffaella Di Lisi

Introduction

Different types of regulatory genes are involved in cardiac muscle development and cardiac gene regulation, including ubiquitous factors, such as SRF, SP1 and TEF-1, and genes coding for specific transcription factors: MADS-box transcription factor genes, such as the MEF2 genes which are also involved in the specification of skeletal and smooth muscle, homeobox genes, such as Nkx2.5, zinc-finger genes of the GATA family, such as GATA 4-6, and bHLH genes, such as dHAND and eHAND [1,2]. Gene regulation seems to require combinatorial interactions between cardiac-specific and ubiquitous factors: for example a physical interaction between Nkx2.5 and SRF is involved in the activation of the cardiac α-actin gene [3]. The study of cardiac gene regulation is complicated by the specific pattern of transcription of each gene, both with respect to temporal specificity during development and spatial specificity in the various heart chambers, presumably reflecting a modular regulation via multiple cis-acting elements [4]. Multiple approaches, including promoter analyses in cultured cells, in adult heart and in transgenic mice, are required to dissect the activity in time and space of cardiac regulatory genes and their combinatorial interactions.

The cardiac troponin I gene

We have applied this multiple approach strategy to the study of the cardiac troponin I (cTnI) gene. The cTnI gene is one of the few myofibrillar protein genes that are selectively expressed in the myocardium. Most cardiac myofibrillar protein genes are in fact also expressed in skeletal muscle either transiently during development, e.g. the cardiac troponin T gene, or throughout postnatal life, e.g. the myosin heavy chain β-slow (MHC-β slow). To our knowledge there are only three myofibrillar protein genes

P.A. Doevendans et al. (eds.), Cardiovascular specific gene expression, 17-25.

which are expressed exclusively in the mammalian heart: cTnI [5], the atrial isoform of myosin light chain 2 (MLC-2a) [6], and the cardiac C protein or myosin binding protein C (cardiac MyBP-C) [7,8].

Another distinctive feature of the cTnI gene is the fact that this gene is poorly expressed at the earliest stages of heart development. In the rat the slow skeletal isoform of TnI (sTnI) is initially strongly expressed in the developing heart, then cTnI and sTnI are co-expressed during fetal and neonatal stages and sTnI is finally down-regulated during postnatal development [9,10,11,5]. A similar isogene switching occurs in the developing mouse [12] and human heart [13,14]. In situ hybridization analyses show that cTnI transcripts are present in atria and ventricles, but not in the distal outflow tract of the embryonic rat [15] and mouse heart (figure 1, see also [12]). In addition, cTnI protein can be detected by immunohistochemistry in rat atria but not in ventricles between day 11 and day 18, namely at stages when the corresponding mRNA is present in both atria and ventricles [15]. These findings point to the complexity of transcriptional and post-transcriptional regulation of the cTnI gene in the developing heart.

Figure 1. *Distribution of cTnI transcripts in the embryonic mouse heart as determined by in situ hybridization. Sections of formaldehyde-fixed, paraffin-embedded 10 day embryos were hybridized with a ^{35}S-labeled probe complementary to cTnI mRNA, then processed for autoradiography and viewed by dark-field microscopy. Note that transcripts are present in both atria (A) and ventricles (V) while they are poorly expressed in the proximal portion of the outflow tract and are absent in the distal outflow tract (OT).*

Promoter analysis of the cTnI gene in vitro and in vivo

The promoter elements and transcription factors responsible for tissue-specific and developmental stage-specific regulation of the cTnI gene were first investigated in vitro. A proximal positive regulatory region followed by an intermediate negative region and a distal positive regulatory region have been identified in the mouse cTnI gene promoter by transfection with deletion constructs in cultured cardiomyocytes [16]. A similar in vitro transfection approach has recently lead to the demonstration that a GATA element plays a crucial role in the rat cTnI gene promoter [17].

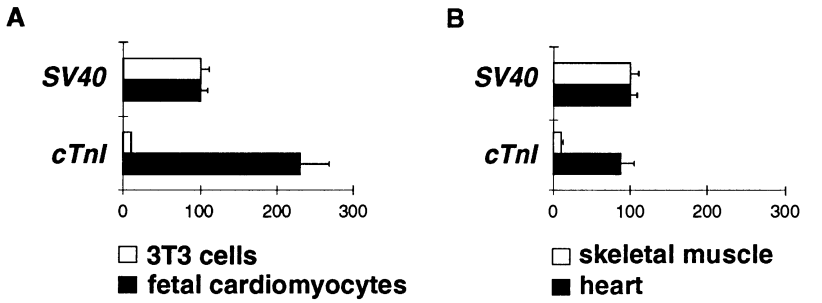

Figure 2. *A short fragment of the cardiac TnI promoter confers cardiac-specific expression to reporter genes after transient transfection in cultured fetal cardiomyocytes (A), and after DNA injection in adult heart (B). A: A -230/+16 fragment of the mouse cTnI gene linked to the CAT reporter is expressed at much higher levels in cultured fetal cardiomyocytes than in 3T3 cells. Note that the activity of the cTnI promoter is even higher than that of a viral SV40 promoter. B: The same -230/+16 fragment of the cTnI promoter is active after injection in the adult rat heart whereas it is poorly expressed after injection in regenerating rat skeletal muscle.*

We have now investigated in greater detail the regulatory properties of the proximal cTnI promoter in cultured cardiomyocytes, in the adult heart and in transgenic animals [18]. As shown in figure 2, a short (-230/+16) fragment of the cTnI promoter confers cardiac-specific expression to reporter genes after transient transfection in cultured fetal cardiomyocytes and in the adult heart. This region of the cTnI promoter contains several putative regulatory elements, including two GA-rich sequences highly homologous to the consensus binding site for the ubiquitous SP1 transcription factor, three GATA elements, and an A/T-rich sequence (figure 3). By electrophoretic mobility shift assays and supershift assays with specific antibodies we have established that the GA-rich sequences are target sites for SP1 and the A/T-rich sequence is a target site for MEF2 factors and the ubiquitous Oct-1 factor, while the GATA elements are target sites for GATA-4 and possibly for GATA-5 and -6. The role of these elements has been analyzed by transfecting deletion/mutation constructs in cultured cardiomyocytes and adult heart.

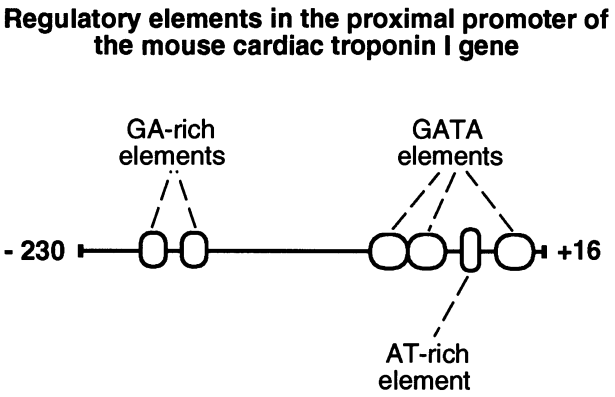

Figure 3. The proximal promoter of the mouse cardiac TnI gene contains several putative regulatory elements, including two GA-rich sequences which are target sites for SP1, three GATA elements which are target sites for GATA-4, and an A/T-rich sequence which is a target site for MEF2 and Oct-1.

As shown in figure 4, all three types of elements appear to be important for cTnI promoter regulation, however their relative contribution differs in cultured cardiomyocytes compared to adult myocardium. The most striking difference was observed with mutations of GATA elements that markedly reduce the activity of the promoter in cultured cells, but appear to have a minor effect in the adult heart. Interestingly, we have found that the level of factors binding to GATA elements present in the cTnI promoter is considerably reduced in nuclear extracts from adult heart compared to fetal cardiomyocytes. In addition, the distribution of the GATA 4-6 factors is known to change during development, e.g. GATA 5 is expressed in embryonic, but not in adult heart [19]. However, the relative role of the three GATA factors in the regulation of the cTnI gene remains to be established. In conclusion, the results of promoter analyses in vitro and in vivo indicate that the regulatory mechanisms responsible for the activation of the cTnI gene in differentiating fetal cardiomyocytes differ from those responsible for the maintenance of cTnI gene transcription in the mature heart; specifically, the results point to a much greater role of GATA factors in developing compared to adult heart.

Pattern of expression of the cTnI promoter in transgenic mice

In order to explore the role of the proximal promoter during early stages of cardiogenesis we have generated transgenic mice carrying a -230/+126 fragment of the cTnI gene linked to a LacZ reporter gene. Several lines of mice expressing the transgene have been obtained and are currently evaluated. Figure 5 illustrates two of these lines. In one line the cTnI promoter is strongly active throughout the embryonic heart (figure 5 A, B). In contrast, another transgenic line shows a regional pattern of expression, the transgene being mainly expressed in the right atrium and the left ventricle of the developing heart (figure 5 C, D). A different heterogeneous pattern is

seen in other lines in which the transgene is expressed in atria but not in ventricles (not shown). The variable pattern of expression is not related to transgene copy number, therefore presumably reflects an integration site-dependent effect. These findings indicate that a small sequence of the cTnI promoter contains regulatory elements that are able to direct cardiac-specific expression, however this transcriptional potential may vary in different heart compartments.

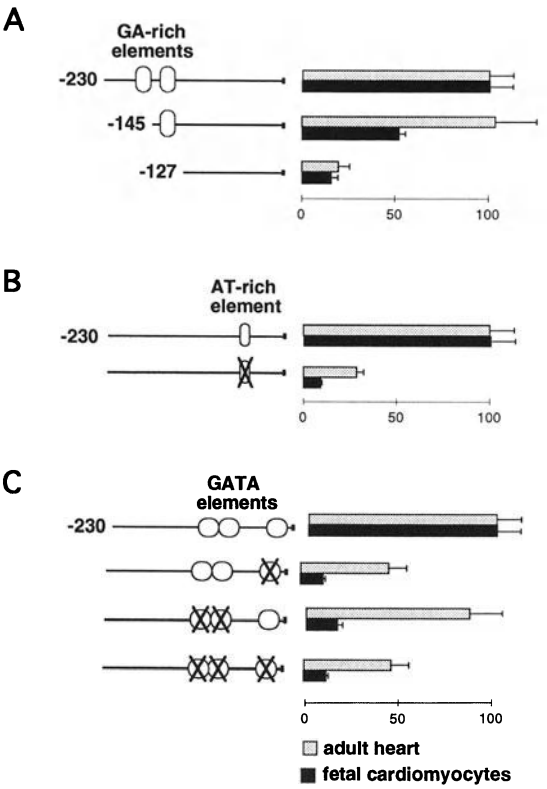

Figure 4. *Deletion and mutation of regulatory elements in the cardiac TnI promoter: differential effects in vitro and in vivo. Promoter analysis was carried out by transient transfection in cultured fetal cardiomyocytes (stippled bars) and in the adult heart (black bars). Note that mutations of GATA elements inactivate the cTnI promoter in cultured cells but have a minor effect in the adult heart.*

Other transgenes were previously found to display regionalized patterns of expression. Cardiac actin regulatory sequences direct LacZ transgene expression mainly in the left ventricle [20], whereas regulatory sequences from the MLC2v gene direct LacZ transgene expression in the right ventricle and outflow tract [21]. Some MLC3F-LacZ transgenes are expressed mainly in the right atrium and the left ventricle [22], whereas others are expressed in both atria and ventricles but not in the inflow and outflow tracts [23]. Transgenic mice may thus reveal differences between various heart compartments

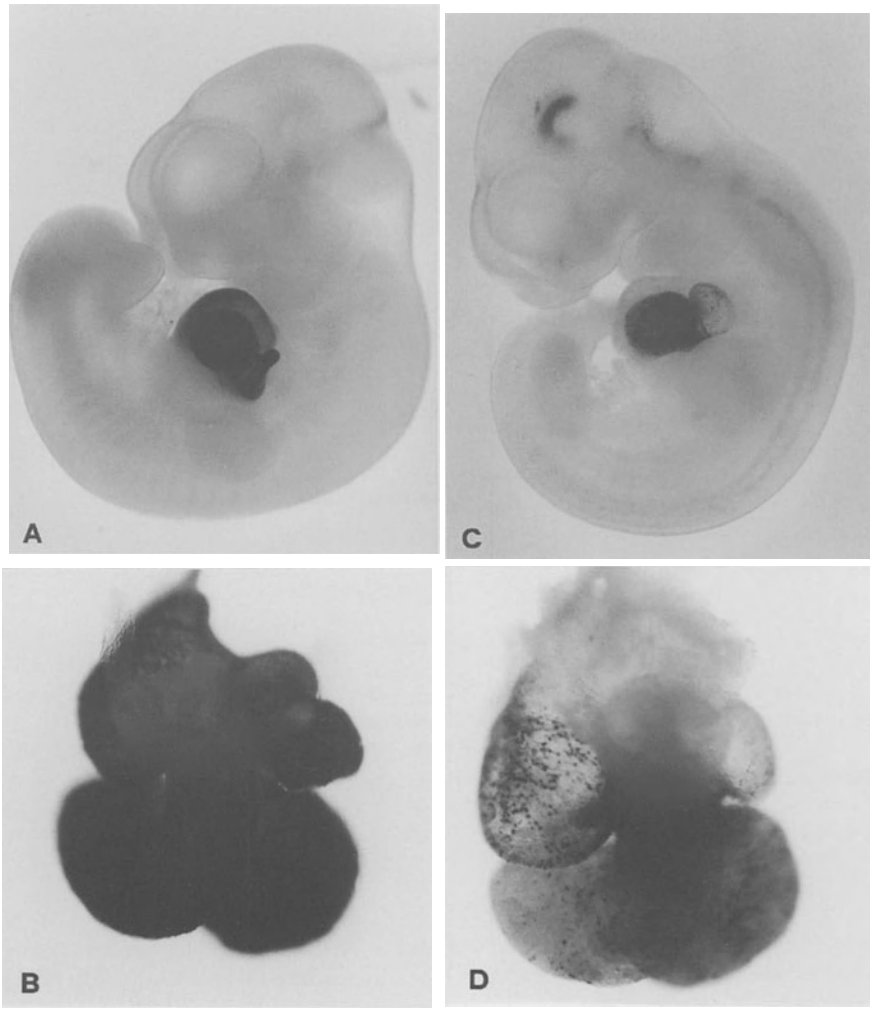

Figure 5. *A -230/+126 fragment of the cTnI gene promoter directs cardiac expression of a LacZ reporter gene in transgenic mice. Embryos were stained for* β*-galactosidase at day 10.5. In one transgenic line (A, B) the whole heart stains for the reporter, whereas in another line (C, D) the expression is stronger in the right atrium and left ventricle and there is some ectopic expression in the central nervous system.*

reflecting the existence of distinct transcriptional domains, which often are not revealed by the distribution of endogenous genes [24].
The problem now is to identify the specific factors responsible for the distinctive transcriptional potential of the various heart segments. One possibility is that cardiac-specific transcription factors are regionally distributed in the developing heart. For example, the bHLH transcription factors dHAND and eHAND show a divergent pattern of expression: dHAND is expressed in the right ventricle but only weakly in the left ventricle, wheras eHAND is expressed in the left but not in the right ventricle [25,26]. However, other transcription factors such as GATA4 and MEF2 seem to be expressed throughout the myocardium. It is possible that regional specificity within the heart reflects variations in the level of individual transcription factors and/or unique combinations of different factors. Selective alteration of cis-acting elements in transgenic mice could be used to identify the transcription factors responsible for regional specification.

Conclusions and perspectives

In conclusion, the cardiac-specific cTnI gene displays unique developmental and regional patterns of expression in the mammalian heart. Promoter analyses performed on differentiating and mature cardiomyocytes reveal a differential role of transcription factors, in particular GATA factors, in cTnI gene regulation. Transgenic mice often display heterogeneous pattern of cTnI transgene expression in heart compartments and will be useful to define the boundaries between transcriptional domains in the developing heart and the mechanisms that generate these domains.

Acknowledgments

This work was supported by Telethon Grant 928 (to S.A.), Biomed Contract BMH4-CT98-4004 (to S.S.), MURST (to S.S.), and the Giovanni Armenise-Harvard Foundation for Advanced Scientific Research.

References

1. Olson EN, Srivastava D. Molecular pathways controlling heart development. Science 1996;272:671-76.
2. Robbins J. Regulation of cardiac gene expression during development. Cardiovasc Res 1996;31:E2-12.
3 Chen CY, Schwartz RJ. Recruitment of the tinman homolog Nkx-2.5 by serum response factor activates α-actin gene transcription. Mol Cell Biol 1996;16:6372-84.
4. Firulli AB, Olson EN. Modular regulation of muscle gene transcription: a mechanism for muscle cell diversity. Trends Genet 1997;13:364-69.
5. Ausoni S, De Nardi C, Moretti P, Gorza L, Schiaffino S. Developmental expression of rat cardiac troponin I mRNA. Development 1991;112:1041-51.
6. Hailstones D, Barton P, Chan-Thomas P, Sasse S, Sutherland C, Hardeman E, Gunning P. Differential regulation of the atrial isoforms of the myosin light chains during striated muscle development. J Biol Chem 1992;267:23295-300.
7. Gautel M, Furst D, Cocco A, Schiaffino S. Isoform transitions of the myosin-binding protein C family in developing human and mouse muscles. Lack of isoform transcomplementation in cardiac muscle. Circ Res 1998;82:124-29.
8. Fougerousse F, Delezoide A.L., Fiszman MY, Scwhartz K, Beckmann JS, Carrier L. Cardiac myosin binding protein C gene is specifically expressed in heart during murine and human development. Circ Res 1998;82:130-33.
9. Saggin L, Gorza L, Ausoni S, Schiaffino S. Troponin I switching in the developing heart. J Biol Chem 1989;27:16299-302.
10. Sabry MA, Dhoot GK. Identification and pattern of expression of a developmental isoform of troponin I in chicken and rat cardiac muscle. J Muscle Res Cell Motil 1989;10:85-91.
11. Murphy AM, Jones L, Sims HF, Strauss AW. Molecular cloning of rat cardiac troponin I and analysis of troponin I isoform expression in developing heart. Biochemistry 1991;30:707-12.
12. Zhu L, Lyons GE, Juhasz O, Joya JE, Hardeman EC, Wade R. Developmental regulation of troponin I isoform genes in striated muscles of transgenic mice. Dev Biol 1995;169:487-503.
13. Bhavsar PK, Dhoot GK, Cumming DVE, Butler-Browne GS, Yacoub MH, Barton PJR. Developmental expression of troponin I isoforms in the fetal human heart. FEBS Lett 1991;292:5-8.
14. Hunkeler NM, Kullman J, Murphy AM. Troponin I isoform expression in human heart. Circ Res 1991;69:1409-14.
15. Gorza L, Ausoni S, Merciai N, Hastings KEM, Schiaffino S. Regional differences in troponin I isoform switching during rat heart development. Dev Biol 1993;156:253-64.
16. Ausoni S, Campione M, Picard A, Moretti P, Vitadello M, De Nardi C, Schiaffino S. Structure and regulation of the mouse cardiac troponin I gene. J Biol Chem 1994;269:339-46.
17. Murphy AM, Thompson WR, Peng LF, Jones II L. Regulation of the rat cardiac troponin I gene by the transcription factor GATA-4. Biochem J 1997;322:393-401.
18. Di Lisi R, Millino C, Calabria E, Altruda F, Schiaffino S, Ausoni S. Combinatorial cis-acting elements control tissue-specific activation of the cardiac tropinin I gene in vitro and in vivo. J Biol Chem 1998;273:25371-80.
19. Grépin C, Dagnino L, Robitaille L, Haberstroh T, Antakly T, Nemer M. A hormone-encoding gene identifies a pathway for cardiac but not skeletal muscle gene transcription. Mol Cell Biol 1994;14:3115-29.
20. Biben C, Hadchouel J, Tajbakhsh S, Buckingham M. Developmental and tissue-specific regulation of the murine cardiac actin gene in vivo depends on distinct skeletal and cardiac muscle-specific enhancer elements in addition to the proximal promoter. Dev Biol 1996;173:200-12.
21. Ross RS, Navankasattusas S, Harvey RP, Chien KR. A HF1a/HF1b/MEF-2 combinatorial

element confers cardiac ventricular specificity and establishes an anterior-posterior gradient of expression. Development 1996;122:1799-1809.

22. Kelly R, Alonso S, Tajbakhsh S, Cossu G, Buckingham M. Myosin light chain 3F regulatory sequences confer regionalized cardiac and skeletal muscle expression in transgenic mice. J Cell Biol 1995;129:383-96.
23. Franco D, Kelly R, Lamers WH, Buckingham M, Moorman AFM. Regionalized transcriptional domains of myosin light chain 3f transgenes in the embryonic mouse heart: morphogenetic implications. Dev Biol 1997;188:17-33.
24. Kelly R, Franco D, Moorman AFM, Buckingham M. Chamber-specific myofilament gene expression: implications for A/P patterning. In "Heart Development", Eds. Rosenthal N, Harvey R. Academic Press;1998:p.333-55.
25. Srivastava D, Cserjesi P, Olson EN. A subclass of bHLH proteins required for cardiac morphogenesis. Science 1995;270:1995-99.
26. Srivastava D, Thomas T, Lin Q, Kirby ML, Brown D, Olson EN. Regulation of cardiac mesodermal and neural crest development by the bHLH transcription factor, dHAND. Nature Genet 1997;16:154-60.

4. MICE DEFICIENT IN MUSCLE LIM PROTEIN (MLP) REVEAL A PATHWAY TO DILATED CARDIOMYOPATHY AND HEART FAILURE

Pico Caroni

Introduction

The striated muscle specific Lin 12, Islet 1, Mec 3 (LIM)-only protein MLP is a conserved positive regulator of myogenic differentiation associated with the actin-based cytoskeleton and the cell nucleus [1,2]. In the heart, MLP is expressed at high levels in atrial and ventricular myocytes during development and in the adult [1]. MLP consists of two LIM double-zinc fingers linked by a spacer of 58 residues. The LIM motif is a protein binding interface found in a diverse group of proteins [3]. MLP may promote myogenic differentiation by both acting as a molecular adapter to modulate protein assembly along the actin-based cytoskeleton, and by promoting muscle specific gene expression as a transcriptional co-factor. This hypothesis is supported by the demonstration that the second LIM motif of MLP can specifically target interacting proteins to the actin-based cytoskeleton [2], and the first LIM motif mediates the interaction of MLP with muscle-specific transcription factors [4].
Long-term cardiac and skeletal muscle performance is regulated through feedback mechanisms that link mechanical load to the expression of muscle genes, myofibrillar organization, and muscle fibre size [5,6]. In a clinically significant aspect of this process, the adult heart reacts to increased demands for mechanical work via the activation of an adaptive hypertrophic response that is associated with the induction of a defined subset of muscle genes, and expansion of the myofibrillar apparatus. Although compensatory in its nature, this reaction can lead to cardiac dysfunction and heart failure [7]. The molecular mechanisms that link mechanical load to striated muscle growth are poorly understood. Interestingly, like MLP, the LIM-only protein CRP (cysteine-rich protein), which is highly homologous to MLP and is expressed in smooth muscle cells and activated fibroblasts, also targets to the actin cytoskeleton. In muscle cells and activated fibroblasts, the possibility exists that mechanisms which involve the actin-based cytoskeleton may link mechanical stress to specific patterns of gene expression and cellular organization [8]. Accordingly, one possibility is that MLP may

P.A. Doevendans et al. (eds.), Cardiovascular specific gene expression, 27-33.

be involved in the linkage between tension and muscle growth through the organization of the myofibrillar apparatus and muscle cytoplasm along the actin cytoskeleton.

Severe postnatal dilated cardiac hypertrophy in MLP-deficient mice

To examine the role of MLP in muscle formation and growth we analyzed mice with a targeted disruption of the MLP gene [9]. Mice heterozygous for the disrupted MLP allele had no detectable phenotype. In contrast, although MLP (-/-) mice displayed no obvious defects at birth, 50-70% of them developed signs of fatigue between postnatal day 5 (P5) and P10, and died within 20-30 hours from the onset of these symptoms (early phenotype mice). MLP deficient mice that did not die during the second postnatal week developed to adulthood and were viable (adult phenotype mice). Second postnatal week mortality was higher in crosses between heterozygous (70-80%) than homozygous (50-55%) animals, suggesting that the penetrance of the early phenotype was affected by the genetic background of MLP (-/-) mice. In contrast, the adult phenotype was nearly 100% penetrant. It included severe defects in cardiac function and structure (see below). In addition, a marked impairment in sustained performance of the limb musculature was detected.

Closer examination of MLP (-/-) mice revealed selective defects in striated muscle structure and function. Although both skeletal and cardiac muscle lacked rigor, defects were most dramatic in the heart, which showed strikingly decreased tone and became obviously enlarged during postnatal life. At birth, MLP-deficient hearts were already deficient in rigor, but displayed no differences in heart/body weight ratios. Subsequently, mice with the early phenotype rapidly developed dramatically enlarged hearts, whereas cardiac growth was more gradual and less pronounced in the remaining MLP-deficient mice. Enlargement affected the four heart chambers to a similar extent. This finding and the fact that in wild-type mice MLP is expressed in all cardiomyocytes suggested that the phenotype was due to an intrinsic cardiac defect.

ANF mRNA was markedly elevated in the ventricles of early phenotype hearts. Strong induction was also detected for muscle ankyrin repeat protein (MARP) transcript, a novel hypertrophy-associated gene [10]. In contrast, no significant induction of MLC-2v or actin transcripts was detected. The hearts of adult MLP (-/-) mice had mRNA patterns characteristic of the cardiac hypertrophy response. In summary, all MLP deficient mice develop a marked cardiäc hypertrophy reaction, and the two subgroups of mice differ in their susceptibility to a massive and lethal response during the second postnatal week

Major defects in cyto-architectural organization in MLP deficient cardiac myocytes.

Ultrastructural analysis revealed a dramatic disruption of cardiac myofibrillar organization and a pronounced increase in non-myofibrillar space throughout the heart of MLP-deficient mice. Qualitatively similar alterations in ultrastructure have been described for the late phases of dilated cardiomyopathy in humans, albeit usually not

to such a dramatic extent [11,12]. Similarities between the two conditions also extend to characteristic alterations in the distribution of vinculin, a protein involved in the anchorage of the actin-based cytoskeleton to the cell membrane. In MLP-deficient mice vinculin immunoreactivity was consistently stronger and broader, and extended into the cytosol, and adherens junction. In further analogy to the human disease, the hearts of adult (but not early postnatal) phenotype mice had prominent signs of interstitial cell proliferation and fibrosis. These results indicate that MLP-deficient mice develop dilated cardiomyopathy with ultrastructural and histological features similar to those found in human patients. Alterations in the organization of the actin cytoskeleton and myofibrillar apparatus were already detectable in the hearts of newborn MLP-deficient mice [9], i.e. at a time when the heart tissue was already abnormally soft, but not obviously heavier. These findings suggest that in these mice some disorganization of cardiomyocyte cyto-architecture precedes an overt hypertrophic response.
To determine whether the cardiac phenotype of MLP (-/-) mice was intrinsic to heart muscle cells and cell autonomous, cultured newborn ventricular myocytes were analyzed. When compared to controls, cardiomyocytes from MLP (-/-) mice consistently spread over a larger area, and had unusually high numbers of pseudopodia. After 5 days in the presence of the β-adrenergic agonist isoproterenol, MLP-deficient cardiomyocytes had a lacerated appearance, suggestive of impaired resistance to mechanical stress. Significantly, similar irregular outlines were detected in freshly isolated adult cardiomyocytes from MLP (-/-) hearts [9], indicating that the overall organization of cardiomyocytes was severely perturbed in the absence of MLP, both in situ and in isolation. These findings indicate that the absence of MLP affects myofibril organization and overall cardiomyocyte cyto-architecture in a cell autonomous manner.

MLP accumulates at lateral anchorage sites of myofibrils, and promotes the cytoarchitectural organization of the cardiomyocyte

In adult ventricular cardiomyocytes in situ, MLP immunoreactivity was detected in a mainly striated cytosolic pattern and the signal was highest at vinculin-positive intercellular attachment sites [9], suggesting that it may be associated with the Z-line of myofibrils. Consistent with this interpretation, in cultured cardiomyocytes from newborn MLP (+/+) mice MLP accumulated in a 2μm-spaced double-band pattern along myofibrils in the vicinity of the Z-line [9]. Z-line-associated structures are responsible for the lateral allignment of myofibrils and their lateral anchorage at N-cadherin- and vinculin-containing costameres along the cell membrane [13]. In MLP-deficient cardiomyocytes connexin-43-positive gap junction structures at sites of cell-cell contact were consistently smaller and less well organized [9]. Similar deficits in connexin-43-positive structures at adherens junction sites were detected in freshly isolated cardiomyocytes from adult MLP (-/-) mice. These findings suggest that MLP may be a crucial component of the anchorage structures involved in the establishment and maintenance of cardiomyocyte cyto-architecture.
To determine whether MLP promotes proper cardiomyocyte cyto-architecture, MLP and related constructs were transfected in cultured cardiomyocytes from newborn MLP (-/-) mice. Expression of MLP led to significant organization and simplification of the

myofibril pattern in transfected cardiomyocytes [9]. MLP consists of the two LIM domains M1 and M2, linked by a 58 amino acid spacer region. Targeting to the actin cytoskeleton is due to the specific binding properties of the LIM domain M2 of MLP [2]. Consistent with the actin cytoskeleton properties of the Z-line region, the two-LIM construct M2M2 bound to Z-line structures, whereas the corresponding M1M1 construct did not. Interestingly, however, neither M2M2 nor M1M1 promoted myofibril organization in a manner comparable to that of MLP.

MLP-deficient mice reproduce the clinical features of cardiomyopathy and heart failure in man

To explore the possibility that MLP-deficient mice may reproduce the characteristic features of dilated cardiomyopathy in humans cardiac morphology and performance in adult MLP-deficient mice was analyzed in vivo utilizing miniaturized physiological technology [14,9]. Echocardiographic studies showed marked differences in cardiac morphology and function between MLP (-/-) and wild type (MLP (+/+) mice, and suggested the presence of depressed myocardial contractility (inotropic state) [9]. Retrograde catheterization of the left ventricle (LV) via the carotid artery in anesthetized, closed-chest mice revealed a marked reduction of the maximum first derivative of LV pressure in MLP (-/-) mice, clearly demonstrating depression of myocardial contractility. LV relaxation was also markedly impaired, and the LV end-diastolic pressure was elevated [9]. These features, together with elevated lung weights suggesting fluid accumulation, are consistent with left ventricular pump failure as seen in human dilated cardiomyopathy [15,16]. To determine if the MLP (-/-) mice displayed the decreased sensitivity of contractility and relaxation to β-adrenergic stimulation observed in human heart failure [17], the response of LV contractility and relaxation to graded doses of the β- adrenergic agonist dobutamine was measured. These experiments revealed that both normal responses to β-adrenergic stimulation were abolished in the MLP (-/-) mice [9].

Role of MLP in the organization of the actin-based cytoskeleton of striated muscle cells

How does MLP affect the organization of myofibrils and related cytosolic structures? One important clue comes from its accumulation at structures (Z-lines) that play a crucial role in the establishment and maintenance of cardiomyocyte cyto-architecture. Thus myofibrils get organized laterally at the Z-line, and their growth, organization and intercellular allignment involves anchorage sites of the Z-line to N-cadherin- and vinculin-positive costameres [13]. Our findings that: 1) myofibril organization, intercellular gap junction structures, and the overall structural compaction of cardiomyocytes in vivo and in vitro were impaired in the absence of MLP, and that 2) reintroduction of MLP in transfected cardiomyocytes from newborn MLP (-/-) mice attenuated the myofibril disorganization phenotype strongly support the notion that

MLP is a crucial component of the apparatus involved in the organization and maintenance of cardiomyocyte cytoarchitecture. Interestingly, addition of antibodies against N-cadherin to cardiomyocyte cultures induced myofibrillar and cytosolic disorganization comparable to that detected in MLP-deficient hearts, and these effects were also detected for cardiomyocytes that were not in contact with nearby cells [13,18]. Possibly, signals to the N-cadherin complex from both the outside and the inside (costamere complex, Z-line) of the cell regulate cardiomyocyte cytoarchitecture, and optimal signaling from the inside of the cardiomyocyte may require the presence of MLP.

Susceptibility to dilated cardiomyopathy in MLP-deficient mice

What drives the dramatic hypertrophic response in the early phenotype MLP (-/-) mice? Shortly after birth, the neonatal heart is confronted with an increase in mechanical workload. As a result, a physiological neonatal left ventricular hypertrophic response is activated about 3 days after birth. Remarkably, in MLP-deficient mice the massive hypertrophic response affected all four heart chambers. A possible explanation for these observations is that systemic, chamber wall stress, and local pressure signals may combine to induce and control the hypertrophic response in the heart. MLP may be directly involved in the mechanisms that couple tension to the hypertrophic response. Alternatively, it may play an essential role in the formation and maintenance of the structural substrate required for coupling. The etiology of dilated cardiomyopathy with hypertrophy in patients is poorly understood, but in some cases there is evidence for a previous viral myocarditis in otherwise healthy patients, with no apparent predisposition for heart disease [12,15,16]. The dilated cardiomyopathy that follows these infections appears to develop rapidly, and can involve several heart chambers. Although the hearts of newborn MLP-deficient mice were not enlarged, they were already soft with disorganization of actin-based structures. One possibility, therefore, is that dilated cardiomyopathy develops when the structural integrity of cardiomyocytes and their intercellular contact sites is compromised.

The morphological, functional and molecular features in MLP (-/-) adult mice are undistinguishable from those seen in human heart failure resulting from dilated cardiomyopathy of various etiologies. Dilated cardiomyopathy is the convergent phenotype of various diseases which cause loss or dysfunction of cardiomyocytes. The molecular mechanisms leading to the common phenotype of dilated cardiomyopathy are not known and of great interest. The striking properties of MLP (-/-) mice suggest that molecular pathways involving MLP may become dysfunctional during the transition to dilated cardiomyopathy and heart failure. It is anticipated that the principal value of the MLP-deficient model of genetic dilated cardiomyopathy will be for the identification of genes which are involved in the genesis and maintenance of heart failure [19-22], and the application of gene targeting/transgenic techniques to confirm the interactions of other genes with the MLP heart failure phenotype.

Conclusion

MLP is a LIM-only protein of terminally differentiated striated muscle cells, where it accumulates at actin-based structures involved in cytoarchitecture organization. To define the role of MLP in myogenic differentiation we generated MLP-deficient mice. Such mice have soft hearts, with disruption of cardiomyocyte cytoarchitecture at birth. Similar defects were detected in cultured newborn cardiomyocytes, where they could be reversed by forced expression of MLP. After birth, MLP-deficient mice consistently develop dilated cardiomyopathy with hypertrophy and heart failure. The results indicate that MLP plays an essential role for proper cardiomyocyte architectural organization, and suggest that dilated cardiomyopathy may involve intrinsic defects in the cytoarchitecture of cardiomyocytes. In addition, they provide an animal model for dilated cardiomyopathy with hypertrophy and heart failure in a genetically modifiable organism.

References

1. Arber S, Halder G, Caroni P. Muscle LIM protein, a novel essential regulator of myogenesis, promotes myogenic differentiation. Cell 1994;79:221-31.
2. Arber S, Caroni, P. Specificity of single LIM motifs in targeting and LIM/LIM interactions in situ. Genes Devel 1996;10:289-300.
3. Dawid IB, Toyama R, Taira M. LIM domain proteins. C R Acad Sci 1995;318:295-306.
4. Kong Y, Flick MJ, Kudla AJ, Konieczny SF. Muscle LIM protein promotes myogenesis by enhancing the activity of MyoD. Mol Cell Biol 1997;17:4750-60.
5. Chien KR, Knowlton KU, Zhu H, Chien S. Regulation of cardiac gene expression during myocardial growth and hypertrophy: Molecular studies of an adaptive physiologic response. FASEB J 1991;5:3037-46.
6. Yamazaki T, Komuro I, Yazaki Y. Molecular mechanism of cardiac cellular hypertrophy by mechanical stress. J Mol Cell Cardiol. 1995;27:133-40.
7. Keating MT, Sanguinetti MC. Molecular genetic insights into cardiovascular disease. Science 1996;272:681-85.
8. Grinnell F. Fibroblasts, myofibroblasts, and wound contraction. J Cell Biol 1994;124:401-04.
9. Arber S, Hunter JJ, Ross JJr, et al. MLP-deficient mice exhibit a disruption of cardiac cytoarchitectural organization, dilated cardiomyopathy, and heart failure. Cell 1997;88:393-403.
10. Baumeister A, Arber S, Caroni P. Accumulation of muscle ankyrin repeat protein transcript reveals local activation of primary myotube endcompartments during muscle morphogenesis. J Cell Biol 1997;139:1231-42.
11. Schaper J, Hein S. The structural correlate of reduced cardiac function in human dilated cardiomyopathy. Heart Failure 1993;9:95-115.
12. Olsen EGJ, Trotter SE. Pathology of dilated cardiomyopathy. In: Goodwin JF, Olsen EGJ, editors. Cardiomyopathies, realizations and expectations. Berlin: Springer Verlag, 1993:19-27.
13. Goncharova EJ, Kam Z, Geiger B. The involvement of adherens junction components in myofibrillogenesis in cultured cardiac myocytes. Development 1992;114:173-83.
14. Kubalak SW, Doevendans PA, Rockman HA, et al. Molecular analysis of cardiac muscle diseases via mouse genetics. In: Adolph KW, editor. Methods in molecular genetics. San Diego: Academic Press, 1996:470-87.
15. Dec GW, Fuster V. Idiopathic dilated cardiomyopathy. N Engl J Med 1994;331:1564-75.
16. Kasper EK, Agema WRP, Hutchins GM, et al. The causes of dilated cardiomyopathy: a clinicopathologic review of 673 consecutive patients. J Am Coll Cardiol 1994;23:586-90.
17. Bristow MR, Gisburg R, Minobe W, et al. Decreased catecholamine sensitivity and beta-adrenergic receptor density in failing human hearts. New Engl J Med 1982;307:205-11.
18. Peralta Soler A, Knudsen KA. N-cadherin involvement in cardiac myocyte interaction and myofibrillogenesis. Dev Biol 1994;162:9-17.
19. Hunter JJ, Tanaka N, Rockman HA, Ross JJr, Chien KR. Ventricular expression of a MLC-2v-Ras fusion gene induces cardiac hypertrophy and selective diastolic dysfunction in transgenic mice. J Biol Chem 1995;270: 23173-78.
20. Koch WJ, Rockman HA, Samama P, et al. Cardiac function in mice overexpressing the beta-adrenergic receptor kinase or a beta ARK inhibitor. Science 1995;268:1350-53.
21. Zhou MD, Sucov HM, Evans RM, Chien KR. Retinoid dependent pathways suppress myocardial cell hypertrophy. Proc Natl Acad Sci USA 1995;92:7391-95.
22. Chien KR. Genes and physiology: Molecular physiology in genetically engineered animals. J Clin Invest 1996;97:901-09.

5. REGULATION OF ENDOTHELIAL CELL SPECIFIC RECEPTOR TYROSINE KINASE GENE EXPRESSION DURING DEVELOPMENT AND DISEASE

Thorsten M. Schlaeger

Introduction

Endothelial cells and the development of the cardiovascular system

The cardiovascular system is the first organ system that forms during embryonic development. The early lethality of most of the gene mutations that affect the formation of the heart and blood vessels clearly demonstrates its importance for the growing embryo (see T.I. Koblizek *et al.*, chapter 17).

The normal development of the cardiovascular system starts at the mid-primitive streak stage in the extra-embryonic splanchnopleura, where hemangioblasts, proposed common precursors of endothelial and blood cells, are induced to differentiate by the adjacent endoderm (for review, see [1]). Aggregates of hemangioblasts are called blood islands, and cells in the center of each blood island will give rise to the primitive hematopoietic precursors, while those in the periphery will become angioblasts [2-4]. Angioblasts are the direct precursors of endothelial cells (ECs), which will line the walls of the heart as well those of all lymphatic and blood vessels.

The first vascular channels then form by the fusion of neighbouring blood island cavities. This *in situ*-formation of vessels is called vasculogenesis [5,6]. It is also the process by which the first intra-embryonic vessels arise, such as the dorsal aorta and the heart tube. However, most of the intra-embryonic angioblasts differentiate directly from the paraxial mesoderm, in the absence of hematopoiesis. Only the caudal splanchnopleura can give rise to embryonic hemangioblasts [7,8].

At later developmental stages, new vessels are mainly formed by angiogenesis, i.e. either by sprouting from a pre-existing vessel [9,10], or by the splitting of the lumen of a vessel (intussusception [11]). Angiogenesis is the only process by which those organs that lack endodermal components (e.g. brain and kidney) can be vascularized, while vasculogenesis is predominant at the beginning of the vascularization of the splanchnopleura and its derivatives (e.g. in liver, gut and lung) [12].

During the vascularization of a tissue, the number of vessels initially laid down usually

P.A. Doevendans et al. (eds.), Cardiovascular specific gene expression, 35-48.

exceeds the vascular density required, and pruning, i.e. the removal of excess and unperfused vessels, is involved in the modification of the vascular plexus. Other vessels acquire a stabilized phenotype, which is characterized by the strengthening of inter-endothelial cell junctions, the recruitment of pericytes and smooth muscle cells, and the deposition of a specialized extracellular matrix (for review, see [13,14]). In addition, some venous vessels give rise to lymphatic vessels by a process of sprouting [15,16]. Finally, organ-specific features of the blood vessels, such as the fenestrae of kidney glomerular ECs [17], and the unique characteristics of blood-brain barrier ECs [18], are induced by organ-specific paracrine cues.

In the adult, the vascular tree is very stable, with little turnover taking place [19]. However, during certain physiological and pathological situations, such as the tissue remodelling events associated with the female reproductive cycle, wound healing and the growth of solid tumors, the angiogenic program(s) become reactivated. Accordingly, the ECs have to be relieved from the constraints of the other components of the vessel wall [20,21], and switch from their previously differentiated and quiescent state to an invasive and proliferative phenotype [22].

Control of endothelial cell functions by receptor tyrosine kinases

The fate and function of a cell is in many cases determined at its surface, where the activity of a receptor molecule can be modulated by the corresponding ligand. Receptors of the large superfamily of receptor tyrosine kinases (RTKs) are key regulators of processes such as cell lineage establishment, differentiation, proliferation, survival, migration and cell-cell interaction. ECs express various RTKs, five of which are predominantly expressed in this cell type, namely *FLK1* [23], *FLT1* [24], *FLT4* [25], *TIE1* [26] and *TIE2* [27].

There are however some interesting qualitative and quantitative differences in the expression pattern of these genes in ECs. *FLK1* is the earliest marker known to be expressed on the presumptive hemangioblast (embryonic day 7.0 {E7.0} in the mouse; [28]). It stays up-regulated during vasculogenesis and virtually all forms of angiogenesis, in the embryo as well as in the adult. However, there is a strong down-regulation in vessels that become stabilized, and in the quiescent vessels of the adult animal *FLK1* expression is usually almost undetectable [29].

FLT1 expression also starts during gastrulation (E7.0) and reaches a peak at around the midsomite stage (E8.5), after which the level decreases and is maintained at a lower level. However, in contrast to *FLK1*-expression, *FLT1* down-regulation in the dorsal aorta (E18.5) and brain (adult) is less dramatic than that of *FLK1* (G. Breier, pers. comm.), while *FLT1* expression becomes more strongly reduced at other sites, such as in the endocardium and the mesenteric vessels (of the human embryo; [30]). In addition, *FLT1* in contrast to *FLK1* can be induced by hypoxia [31]. Interestingly, while the expression of *FLK1* and *FLT1* is generally low in the adult, their expression stays up-regulated in the kidney glomerular ECs, which are known to have a high rate of turnover and form characteristic fenestrations [32].

In vascular endothelial cells the initial transcription of the *FLT4* gene starts at E8.5. However, at later stages (E12.5) the expression becomes restricted to the ECs of veins, and later again to ECs of lymphatic vessels and high endothelial venules [25].

The earliest detection of *TIE2* in angioblasts and ECs is seen at E7.5 [33]. Of the five RTKs discussed here, *TIE2* is the most uniform marker for ECs, since its expression is retained throughout embryogenesis and in all vascular beds of the adult. However, *TIE2* expression is also up-regulated in ECs during angiogenesis [34], and levels of expression are significantly higher in arteries than in veins and capillaries ([35]; T.M. Schlaeger, unpublished observation).

Finally, *TIE1* gene activity is not observed before E8.0, i.e., only after a primitive vascular plexus has been laid down by the process of vasculogenesis [33]. Like the other RTKs, *TIE1* is highly expressed throughout embryogenesis and during angiogenesis in the adult. Interestingly, elevated *TIE1* expression levels have also been reported in arteriovenous malformations [36]. However, while *TIE1* expression is detectable in some organs of the adult (e.g., the kidney), it is strongly down-regulated in others (such as the brain), and in the liver the expression levels of *TIE1* are low even during development [37, 38].

However, it should be noted that all "endothelial specific" RTKs are also expressed in other tissues: *FLK1* is expressed by retinal progenitor cells [39], mesodermal cells of the amnion and trophoblasts [33], pancreatic duct epithelial cells [40] and hematopoietic precursor cells [23]; KDR (the human *FLK1* homologue) and *FLT1* are expressed by uterine smooth muscle cells [41]; *FLT1* is expressed by monocytes [42] and trophoblasts [33]; *TIE1* and *TIE2* are expressed by some hematopoietic cells [43], and *TIE2* also by mesodermal cells of the amnion [33].

Gene ablation studies have been valuable for our understanding of the function of the endothelial RTKs. Accordingly, we know that *FLK1* is required for hemangioblast differentiation and development [44], whilst *FLT1* function is necessary for the subsequent interactions leading to the assembly of the angioblasts into the walls of the primitive vessels [45]. In addition to these early functions in vascular development, *FLK1* and *FLT1* have also been implicated in EC survival [46], induction and maintainance of fenestrae [32,47], the control of vascular permeability [48] and normal and pathological angiogenesis [29,49]. A total of five members of the VEGF/PDGF gene family has been identified as physiological ligands for at least one of these two receptors, namely VEGF A, -B, -C, -D and PlGF (see also the chapter by T.I. Koblizek *et al.*).

In contrast to *FLK1* and *FLT1*, *TIE2* is dispensable for vasculogenesis but may be important for the interaction of ECs with the surrounding tissues, and for some organ-specific forms of angiogenesis [50-52]. *TIE2* has also been suggested to play a role in the "loosening of tight vascular structures" during angiogenesis in the adult animal [20, 21]. The ligands for *TIE2* are known as Angiopoietin-1 and -2, of which only the former is able to activate the receptor, while the latter can interfere with the binding of Angiopoietin-1 [21,53].

The ECs in mice that are homozygous null at the *TIE1*-allele are fragile and the vessels are leaky, suggesting a function of this gene in the stabilization of vessels and the integrity of ECs [51,54]. To date, the ligands for *TIE1* have not been described.

Finally, *FLT4* is a receptor for VEGF-C and VEGF-D [55,56], and may be involved in the sprouting of lymphatic ECs from venous vessels [15].

Taken together, these EC specific RTKs play pivotal roles during virtually all stages of

vascular development, from the differentiation of the hemangioblast through the assembly of the vessel wall and the expression of vascular bed-specific features, to angiogenesis in the adult animal.

Regulation of endothelial specific receptor tyrosine kinase gene expression during development and disease

The analysis of transcriptional regulatory elements of the EC specific RTKs should lead to a better understanding of the molecular mechanisms underlying vascular development in the embryo as well as physiological and pathological angiogenesis in the adult. In addition, it is critical to identify EC-specific promoters that allow for vascular bed-specific transcription in transgenic mice and which may help to design vectors that may be employed in gene therapy of various diseases.
However, given the great heterogeneity of ECs and the complexity of the three-dimensional structures they are integrated into, it is important to carefully choose the method of analysis, and to be aware of its limitations. Advantages and disadvantages of the different techniques that have been applied to study endothelial cell specific gene regulation are listed in Table 1.

Table 1. Methods applied to study endothelial cell specific gene regulation

Method	Advantages	Disadvantages
in vitro-methods	defined single cell-type system agents can be tested; cheap, no animals needed; live cells can be tested (GFP); easy to quantify	non-physiological cell culture conditions; cells tested are often of mono/oligo-clonal origin, or represent only one subtype of ECs; vascular bed specific features are lost
* transient transfection	easy, rapid	no chromosomal context; variability in transfection efficiency; tissue specificity difficult to assess; artifacts due to normalisation; cells must be proliferating;
* stable transfection	chromosomal context	integration site- and copy number artifacts; many clones must be screened
in vivo-methods	all cell types can be tested; cells are in an in vivo-context; mice can be crossed to "knockout"-mice, and tissues can be transplanted	tedious; expensive; animal work; agents cannot be tested easily; difficult to quantify
* transgene	routine if established; "sufficiency" of active regions can be defined	integrations-site and copy-number-dependent effects; activity can be very weak or integration site-dependent
* "knock-in"	direct analysis of the active transciptional control regions	heterozygocity effects; very labour- and time- intensive; only sequences that are "necessary" can be defined

In general, a combination of *in vitro*- and *in vivo*-studies should be most efficient and informative. In the following paragraphs a detailed analysis of the transcriptional regulation of the *TIE2* gene will be described and what is known about the regulation of the other EC specific RTKs will be summarized.

Regulation of TIE2 gene expression

We have started to analyze the transcriptional activity of genomic DNA-fragments from the putative promoter region of the *TIE2*-gene in transgenic mouse embryos using the bacterial β-galactosidase as a reporter gene. The first construct that showed an EC specific expression pattern at E10.5 was driven by a 1.6 kb PstI-HindIII fragment that included approximately 350 bp of the first exon and ended just upstream of the original translation initiation codon (see figure 1A). However, the reporter gene expression pattern reflected only the very early aspects of *TIE2* expression, i.e., the 1.6 kb promoter fragment was active only during vasculogenesis [57]. Angioblasts, early yolk sac vessels, dorsal aorta, vitelline vessels, endocardial and liver sinusoidal ECs were stained (see figure 1B). In contrast, vessels that have developed by "late vasculogenesis" in evolutionary younger structures, such as the allantois and the lung, or by angiogenesis from a primary vascular plexus, such as in the brain and in the late yolk sac, displayed only faint or no reporter gene activity. However, in mice in which the primitive vascular plexus of the yolk sac fails to undergo remodelling due to the lack of a functional allele of the RasGAP gene, *TIE2* promoter-driven reporter gene activity in the yolk sac stays at an elevated level [58].

The analysis of the EC specific activity of subfragments of the PstI-HindIII-fragment in transgenic mice revealed a modular structure of the *TIE2* promoter (see figure 1A): While sequences upstream of the SacI-site did not seem to play a significant role, the SacI-SphI fragment clearly had positive regulatory activity. However, the remaining SphI-HindIII promoter fragment was still only active in ECs, indicating that it contained sufficient information to restrict its activity to ECs. Deletion of the SphI-BamHI-fragment from the TIE2 promoter finally rendered the corresponding reporter gene construct completely inactive, as did the deletion of the StyI-HindIII-fragment, which lies entirely within the 5'-untranslated region (5'-UTR) of the first exon.

It is not clear which region within the 728 bp SphI-HindIII *TIE2* promoter fragment contains the elements that confer its EC specific activity during vasculogenesis, and whether the StyI-HindIII-fragment was necessary for transcription, RNA stability or translational efficiency. However, we have evidence that the BamHI-HindIII-fragment, although inactive on its own, can be activated by the addition of an enhancer, which defines this piece as the minimal or core promoter of the *TIE2* gene.

The observation of the incomplete activity of the PstI-HindIII fragment led us to hypothesize that there are regions not contained within the *TIE2* promoter which are necessary to drive *TIE2* gene expression at later stages of development, and also in the adult mouse. We therefore designed reporter gene constructs which contained additional genomic sequences from the *TIE2* gene to determine the capability of these sequences to achieve EC specific gene expression in transgenic embryos. One of these constructs incorporated an approximately 10 kb fragment from the 5' half of the large first intron of *TIE2* in addition to the promoter (see figure 1A).

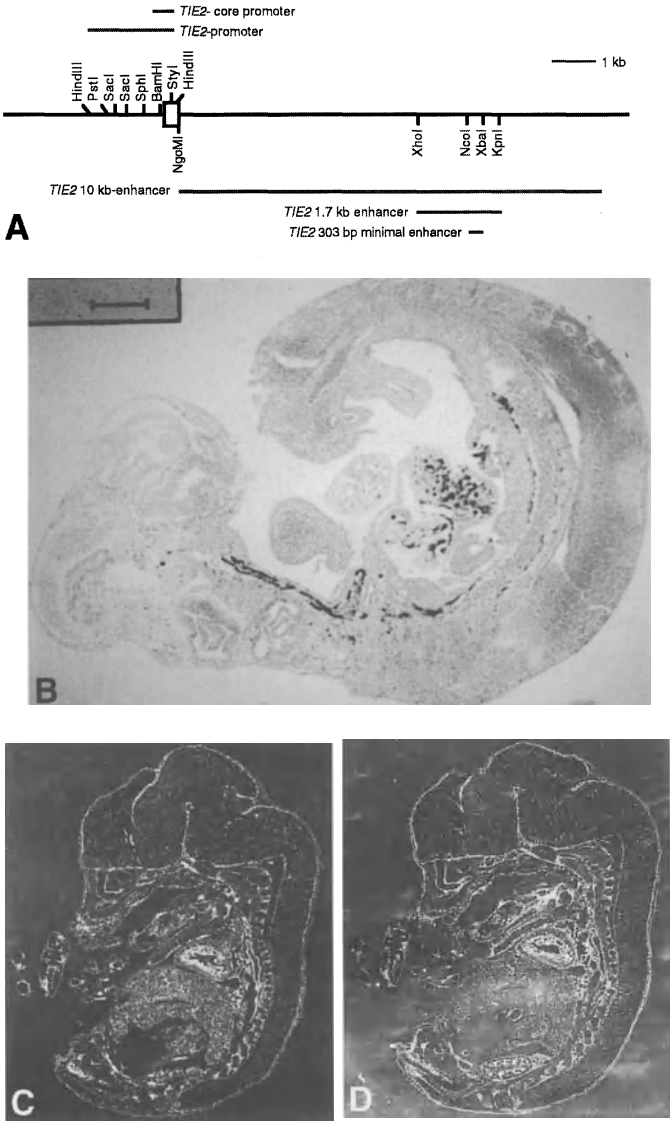

Figure 1. *A) Restriction map of the genomic locus of the murine TIE2 gene. The white box represents the first exon. The transcriptional active regions described in the text are indicated as grey lines. The SacI-site referred to in the text is the one proximal to the PstI-site. B) Sagittal section of an E11.5 embryo that was transgenic for the TIE2 promoter/lacZ construct and stained in toto for β-galactosidase activity. The reporter gene activity (= dark cells) is restricted to ECs of the liver, the yolk sac, the atrium, the dorsal aorta and the internal carotic artery. Note that there is virtually no staining detectable in regions where angiogenesis is taking place. C) LacZ mRNA in situ-hybridization of a sagittal sections of a 14.5 days old embryo transgenic for a β-galactosidase reporter gene driven by the TIE2 promoter and the TIE2 10 kb-enhancer. D) TIE2 mRNA in situ-hybridization of a section adjacent to the section shown in (C). The hybridization patterns are almost indistinguishable, with virtually all vascular ECs being positive for either mRNA.*

Staining of the corresponding transgenic embryos revealed a strong β-galactosidase activity in virtually all blood vessels [59]. Furthermore, all 13 mouse lines that were transgenic for this construct expressed the reporter gene specifically in ECs (see figure 1C), indicating that this 10 kb fragment also had the activity to protect the transgene from integration-site dependent effects that can lead to silencing or ectopic activation of transcription, as it had been observed with constructs that were driven by the *TIE2* promoter alone.

To directly compare the expression pattern of the *TIE2* promoter/10 kb enhancer reporter gene construct with that of the endogenous gene, LacZ- and *TIE2* mRNA *in situ* hybridizations were performed on adjacent sections of transgenic E14.5 embryos. The resulting signals were virtually indistinguishable, demonstrating the sufficiency of the promoter and the 10 kb intronic enhancer for the accurate recapitulation of the endogenous expression pattern of *TIE2* in the embryo (see figure 1 C and D). β-galactosidase stainings of sections of diverse tissues from adult mice transgenic for this reporter gene construct revealed that it was still active in nearly all vascular ECs, which contrasts with the reported down-regulation of *TIE2* gene expression at the mRNA level in the adult [33-35]. However, others have shown that low but significant amounts of *TIE2* mRNA as well as protein can still be detected in almost all vessels in the adult [60, 61], indicating that the expression cassette described above is also able to precisely recapitulate the endogenous expression pattern in the adult (also the stronger expression of endogenous *TIE2* seen in arteries versus veins and capillaries was mirrored by the activity of this construct).

In order to analyze the location of the transcriptionally active elements within the 10 kb enhancer from the first intron of the *TIE2* gene, we have performed transient transfection assays employing both primary bovine aortic endothelial (BAE) and polyoma middle T-immortalized murine brain capillary endothelioma cells (bEND5 cells, provided by S. Wizigmann-Voos). The activity of the promoter turned out to be much higher in the BAE-cells than in the bEND5-cells, which resembles the situation seen *in vivo*, where the promoter is similarly active in the (embryonic) aorta but down-regulated in the ECs of the vessels in the brain. However, in both BAE and bEND5 cells addition of the 10 kb intronic enhancer fragment to the reporter gene boosted the transcriptional activity, and the internal 1.7 kb XhoI-KpnI-fragment (see figure 1 A) turned out to be both necessary and sufficient for this effect. Further analysis of this 1.7 kb enhancer fragment resulted in the identification of the 303 bp NcoI-XbaI-"core enhancer"-fragment (see figure 1 A) that contained the complete EC specific activity. We then analyzed the shorter enhancer fragments for EC specific transcriptional activity in transgenic mice. These studies revealed that the 1.7 kb enhancer was specifically active in all vascular beds, even in the adult, similar to the 10 kb enhancer. However, the detected β-galactosidase expression levels were generally slightly reduced, and integration-site dependent effects occured occasionally. In addition, both the 1.7 kb enhancer and the 303 bp core enhancer were able to activate the heterologous thymidine kinase core promoter in an EC specific manner in transgenic embryos at E11.5, and this effect was independent of the position or orientation of the enhancer relative to that of the promoter.

The differences between the activities of the 10 kb and the 1.7 kb enhancer therefore

seem to be due to the lack of some general activating sequences in the 1.7 kb enhancer, which may be especially important in a chromosomal context; this can be inferred from the observation that there were no detectable differences between both enhancers in transient transfection analyses (see also table 1).
It has been shown that nuclear matrix attachment regions have such an activity [62], and we are now stably transfecting cultivated murine endothelial progenitor cells in order to investigate the position and function of these elements.
In addition, we are examining the DNA-protein interactions of the core enhancer, since it may contain regulatory elements that are necessary for *TIE2* gene expression after the promoter has become down-regulated during early development. The putative transcription factor binding sites within this enhancer fragment include motifs for GATA-2, Sp1, IKAROS-2, ATF/CREB, c-ets-1 and PEA3. However, we have also observed endothelial-cell specific protein binding to sequences that do not match known transcription factors binding sites, indicating that new factors may control this enhancer (T.M. Schlaeger, unpublished observation).
In a complementary approach, we are studying the *in vivo* function of these putative transcription factor binding sites by the analysis of reporter gene constructs containing specific mutations within the 303 bp enhancer in transgenic embryos. These experiments revealed the critical requirement of the 3'-half of the enhancer which contains the binding sites for the transcription factors ATF/CREB, c-ets-1 and PEA3, while for example the GATA-2 and the Sp1-sites can be mutated without a significant effect on the EC specific reporter gene expression. Similarly, an ATF/CREB- and an Ets-site have been shown to be important for the *in vitro*-activity of the *FLT1*-promoter (see below), and c-ets-1 has been shown to be selectively expressed in ECs, especially during angiogenesis [63]. In addition, PEA3-sites (which are also putative c-ets-1 binding sites) have been identified in conserved regions of the promoters of both *TIE1* (see below) and *TIE2*.
We are also interested in studying the mechanisms that modulate *TIE2* gene expression, as expression of this gene is up-regulated for example during tumor angiogenesis, and also in arteries versus veins and capillaries. To this end, we are currently crossing the *TIE2* reporter mice with diverse transgenic mouse lines that develop defined tumors or developmental abnormalities, such as those caused by the mutation of the genes coding for *TIE1* and *TIE2*, respectively (see above). Our preliminary data support the hypothesis [64, 65] that the *TIE2* receptor itself is necessary for a high activity of the *TIE2* promoter and enhancer during embryogenesis. In addition, we are testing the effect of different extracellular matrices, cytokines, conditioned media as well as hypoxia and shear stress to determine if any of these factors is able to modulate the activity of the *TIE2* promoter/enhancer *in vitro*.

Regulation of FLK1, FLT1 *and* TIE1 *gene expression*
The regulation of the other EC specific RTK genes is similarly an area of active investigation. To date, only *in vitro* analyses of the human and murine KDR and *FLK1* promoter, respectively, have been reported [66-68]. In both cases the single transcriptional start site lies around 300 bp upstream of the ATG start codon, and the promoter region lacks both TATA- and CAAT-boxes but contains sites for the

transcription factors Sp1, NFκB and AP-2. Both the *FLK1* and the KDR promoter had enhanced activities in ECs versus non-ECs. This EC specificity was conferred by two far upstream negative regulatory elements as well as one positively acting element in the 5'-UTR of the *FLK1*-promoter. In contrast, the 5'-UTR of the KDR-promoter were able to augment the reporter gene activity in both ECs and non-ECs, while EC specific positive enhancer elements were identified upstream of the transcriptional start site. Transcription factor protein binding to the Sp1-sites in the region upstream of the transcriptional start site of the KDR-promoter was observed to be specific to ECs *in vivo*, while negative regulatory regions far upstream were not identified.

In order to achieve reproducible EC specific gene expression in transgenic mice, it has been proposed that the *FLK1* promoter needs to be combined with an EC specific enhancer that, as is the case for the *TIE2* gene, lies within the first intron of the gene (A. Kappel, pers. comm.).

Analyses of the human *FLT1* promoter has led to the identification of a short fragment that is sufficient to confer EC specific gene expression *in vitro* [69,70]. This fragment includes a TATA-box which is located shortly upstream of the single transcriptional start site. Mutagenesis of either an ATF/CREB-motif or one out of five putative Ets-sites resulted in a severely reduced activity of the promoter [71], and a putative binding site for the hypoxia inducible transcription factor HIF1 has also been shown to be necessary for the responsiveness of this promoter to hypoxia [31]. In addition, there is evidence of there being several negative and positive regulatory elements upstream as well as downstream of the transcriptional start site. No EC specific transcriptional activity of a fragment derived from the *FLT1* gene *in vivo* has been reported to date. However, a small region downstream of the translational start site seems to be necessary for the expression of the murine *FLT1* gene in trophoblast cells [45].

In the *TIE1*-gene a short but highly conserved fragment has been shown to contain virtually all of the elements that are necessary to recapitulate *TIE1* gene expression in transgenic mice [72]. This 735 bp TATA-less promoter contains conserved sites for the transcription factors c-ets-1, AP2 and PEA3. Surprisingly, the activity of this fragment was not restricted to ECs *in vitro*.

An important observation concerning regulation of the *TIE1* gene comes from an experiment in which LacZ expression was driven by the endogenous gene regulatory elements in PDGF-B null-mice. In these mice lacZ-expression was not down-regulated in brain capillaries [73]. It will be important to elucidate how this relates to the reduced number of pericytes in the vessels of these "knock-out" mice, and via which cis-acting elements the effect is mediated. In contrast, endothelial β-galactosidase gene expression from the *TIE1* locus was reduced in *TIE1* nullizygous embryos, especially in the vessels which are leaky and hemorrhagic [54]. The elucidation of the underlying mechanisms could provide a paradigm for EC specific gene regulation by the cross-talk of these cells with the surrounding tissue.

Concluding remarks

The development of transgenic mouse technology has proven to be a powerful tool for

the investigation of mechanisms in mammalian development, especially in the case of the cardiovascular system. Although the analysis of the transcriptional regulation of EC specific RTK genes is still in its infancy, it has already yielded important data. For example, we are now able to distinguish ECs of different developmental origins, developmental stages and vascular beds at the transcriptional level. One important task is the elucidation of the mechanisms responsible for these differences in transcriptional activity. In addition, we are now able to investigate the function of virtually any gene in the cardiovascular system by its tissue-specific expression in transgenic mice [21,59]. Finally, by integrating all this information, we should gain a better understanding of the molecular mechanisms underlying the heterogeneous behaviour of ECs during development and disease. Such an understanding is a prerequisite for an attempt to manipulate the cardiovascular system during the various life-threatening congenital and acquired diseases in which this system is tightly entangled [74-76].

Conclusion

Endothelial cells are the first cellular component of the cardiovascular system that differentiates during early gastrulation. Endothelial cells also play a major role in intregrating the signals that lead to vascular remodeling, growth or regression at later stages of development as well as in the adult animal. In addition, endothelial cells exhibit a marked plasticity that depends on the developmental stage, size and nature of the vessels, and their function in the specific vascular beds of the different organs. So far, five members of the large receptor tyrosine kinase gene superfamily have been shown to be predominantly expressed in endothelial cells. The role of these genes in specific endothelial functions throughout vascular development, as well as during diseases that are associated with the vascular system, has been investigated during the last few years. Interestingly, the expression patterns of these endothelial receptor tyrosine kinases have been found to exhibit some differences indicative of their respective function(s), which has led to research in the analysis of the transcriptional control of these genes. These studies are challenging owing to the complexity of the transcriptional repertoire of endothelial cells and their dependence on cross-talk with the neighbouring cells. However, these studies are likely to provide important new insights into the molecular basis of the heterogeneous behavior of endothelial cell during development and disease. The aim of this review was to provide an overview of the current knowledge of endothelial receptor tyrosine kinase gene regulation.

Acknowledgements

I would like to thank Dr W. Risau and Dr T.N. Sato for giving me the opportunity to work in their labs at the RIMB, the MPI and the BIH, Dr U. Deutsch and the other colleagues for fruitful discussions and their support, and Dr C. Mitchell and Dr U. Deutsch for critically reviewing the manuscript.

References

1. Risau W, Flamme I. Vasculogenesis. Ann Rev Cell Developm Biol 1995;11:73-91.
2. Murray PDF. The development in vitro of the blood of the early chick embryo. Proc R Soc London Ser B III 1932;497-521.
3. His W. Lecithoblast und Angioblast der Wirbeltiere. Abhandl Math-Phys Ges d Wiss 1900;26:171-328.
4. Sabin FR. Studies on the origin of the blood vessels and of red blood corpuscles as seen in the living blastoderm of chick during the second day of incubation. Carnergie Contrib Embryol 1920;9:215-62.
5. von Schulte W. Early stages of vasculogenesis in the cat (Felis demestica) with special reference to the mesenchymal origin of endothelium. Anat Rec 1914;8:78-80.
6. Pardanaud L, Altmann C, Kitos P, Dieterlen-Lievre F, Buck CA. Vasculogenesis in the early quail blastodisc as studied with a monoclonal antibody recognizing endothelial cells. Development 1987;100:339-49.
7. Cumano A, Dieterlen-Lievre F, Godin I. Lymphoid potential, probed before circulation in mouse, is restricted to caudal intraembryonic splanchnopleura. Cell 1996;86:907-16.
8. Pardanaud L, Luton D, Prigent M, Bourcheix LM, Catala M, Dieterlen-Lievre F. Two distinct endothelial lineages in ontogeny, one of them related to hemopoiesis. Development 1996;122:1363-71.
9. Hertig AT. Angiogenesis in the early human chorion and in the primary placenta of the macaque monkey. Contrib Embryol Carnegie Inst Wash 1935;25:37-81.
10. Sabin FR. Origin and development of the primitive vessels of the chick and of the pig. Carnergie Contrib Embryol 1917;6:61-124.
11. Burri PH, Tarek MR. A novel mechanism of capillary growth in the rat pulmonary microcirculation. Anat Rec 1990;228:35-45.
12. Pardanaud L, Yassine F, Dieterlen-Lievre F. Relationship between vasculogenesis, angiogenesis and hematopoiesis during avian ontogeny. Development 1989;105:473-85.
13. Dejana E. Endothelial adherens junctions: implications in the control of vascular permeability and angiogenesis. J Clin Invest 1996;98:1949-53.
14. Risau W. Mechanisms of angiogenesis. Nature 1997;386:671.
15. Jeltsch M, Kaipainen A, Joukov V, et al. Hyperplasia of lymphatic vessels in Vegf-C transgenic mice. Science 1997;276:1423-25.
16. Kukk E, Lymboussaki A, Taira S, et al. Vegf-C receptor binding and pattern of expression with Vegfr-3 suggests a role in lymphatic vascular development. Development 1996;122(12):3829-37.
17. Milici AJ, Furie MB, Carley WW. The formation of fenestrations and channels by capillary endothelium in vitro. Proc Natl Acad Sci USA 1985;82:6181-85.
18. Stewart PA, Wiley MJ. Developing nervous tissue induces formation of blood-brain barrier characteristics in invading endothelial cells: A study using quail-chick transplantation chimeras. Dev Biol 1981;84:183-92.
19. Engerman RL, Pfaffenbach D, Davis MD. Cell turnover of capillaries. Lab Invest 1967;17:738-43.
20. Hanahan D. Signaling vascular morphogenesis and maintenance. Science 1997;277:48-50.
21. Maisonpierre PC, Suri C, Jones PF, et al. Angiopoietin-2, a natural antagonist for Tie2 that disrupts in vivo angiogenesis. Science 1997;277:55-60.
22. Yamagami I. Electron microscopic study on the cornea. I. The mechanism of experimental new vessel formation. Jap J Ophtalm 1970;14:41-58.
23. Matthews W, Jordan CT, Wiegand GW, Pardoll D, Lemischka IR. A receptor tyrosine

kinase specific to hematopoietic stem and progenitor cell-enriched populations. Cell 1991;65:1143-52.
24. Shibuya M, Yamaguchi S, Yamane A, et al. Nucleotide sequence and expression of a novel human receptor-type tyrosine kinase gene (flt) closely related to the fms family. Oncogene 1990;5:519-24.
25. Kaipainen A, Korhonen J, Mustonen T, et al. Expression of the fms-like tyrosine kinase 4 gene becomes restricted to lymphatic endothelium during development. Proc Natl Acad Sci USA 1995;92:3566-70.
26. Partanen J, Armstrong E, Makela TP, et al. A novel endothelial cell surface receptor tyrosine kinase with extracellular epidermal growth factor homology domains. Mol Cell Biol 1992;12:1698-707.
27. Dumont DJ, Yamaguchi TP, Conlon RA, Rossant J, Breitman ML. Tek, a novel tyrosine kinase gene located on mouse chromosome 4, is expressed in endothelial cells and their presumptive precursors. Oncogene 1992;7:1471-80.
28. Yamaguchi TP, Dumont DJ, Conlon RA, Breitman ML, Rossant J. Flk-1, an flt-related receptor tyrosine kinase is an early marker for endothelial-cell precursors. Development 1993;118:489-98.
29. Millauer B, Wizigmann-Voos S, Schnürch H, et al. High affinity VEGF binding and developmental expression suggest Flk-1 as a major regulator of vasculogenesis and angiogenesis. Cell 1993;72:835-46.
30. Kaipainen A, Korhonen J, Pajusola K, et al. The related FLT4, FLT1, and KDR receptor tyrosine kinases show distinct expression patterns in human fetal endothelial cells. J Exp Med 1993;178:2077-88.
31. Gerber HP, Condorelli F, Park J, Ferrara N. Differential transcriptional regulation of the two vascular endothelial growth factor receptor genes. Flt-1, but not Flk-1/KDR, is up-regulated by hypoxia. J Biol Chem 1997;272:23659-67.
32. Simon M, Grone HJ, Johren O, et al. Expression of vascular endothelial growth factor and its receptors in human renal ontogenesis and in adult kidney. Am J Physiol 1995;268:F240-50.
33. Dumont DJ, Fong GH, Puri MC, Gradwohl G, Alitalo K, Breitman ML. Vascularization of the mouse embryo: a study of flk-1, tek, tie, and vascular endothelial growth factor expression during development. Dev Dynam 1995;203:80-92.
34. Sato TN, Qin Y, Kozak CA, Audus KL. Tie-1 and tie-2 define another class of putative receptor tyrosine kinase genes expressed in early embryonic vascular system. Proc Natl Acad Sci USA 1993;90:9355-58.
35. Schnürch H, Risau W. Expression of tie-2, a member of a novel family of receptor tyrosine kinases, in the endothelial cell lineage. Development 1993;119:957-68.
36. Hatva E, Jaaskelainen J, Hirvonen H, Alitalo K, Haltia M. Tie endothelial cell-specific receptor tyrosine kinase is upregulated in the vasculature of arteriovenous malformations. J Neuropath Exp Neur 1996;55:1124-33.
37. Korhonen J, Polvi A, Partanen J, Alitalo K. The mouse tie receptor tyrosine kinase gene: expression during embryonic angiogenesis. Oncogene 1994;9:395-403.
38. Korhonen J, Partanen J, Armstrong E, et al. Enhanced expression of the tie receptor tyrosine kinase in endothelial cells during neovascularization. Blood 1992;80:2548-55.
39. Yang K, Cepko CL. Flk-1, a receptor for vascular endothelial growth factor (VEGF), is expressed by retinal progenitor cells. J Neurosci 1996;16:6089-99.
40. Rooman I, Schuit F, Bouwens L. Effect of vascular endothelial growth factor on growth and differentiation of pancreatic ductal epithelium. Lab Invest 1997;76:225-32.
41. Brown LF, Detmar M, Tognazzi K, Abu-Jawdeh G, Iruela-Arispe ML. Uterine smooth muscle cells express functional receptors (flt-1 and KDR) for vascular permeability factor/vascular endothelial growth factor. Lab Invest 1997;76:245-55.

42. Clauss M, Weich H, Breier G, et al. The vascular endothelial growth factor receptor Flt-1 mediates biological activities. Implications for a functional role of placenta growth factor in monocyte activation and chemotaxis. J Biol Chem 1996;271:17629-34.
43. Yano M, Iwama A, Nishio H, Suda J, Takada G, Suda T. Expression and function of murine receptor tyrosine kinases, TIE and TEK, in hematopoietic stem cells. Blood 1997;89:4317-26.
44. Shalaby F, Ho J, Stanford WL, et al. A requirement for Flk1 in primitive and definitive hematopoiesis and vasculogenesis. Cell 1997;89:981-90.
45. Fong GH, Klingensmith J, Wood CR, Rossant J, Breitman ML. Regulation of flt-1 expression during mouse embryogenesis suggests a role in the establishment of vascular endothelium. Dev Dynam 1996;207:1-10.
46. Alon T, Hemo I, Itin A, Peer J, Stone J, Keshet E. Vascular endothelial growth-factor acts as a survival factor for newly formed retinal-vessels and has implications for retinopathy of prematurity. Nat Med 1995;1:1024-28.
47. Roberts WG, Palade GE. Increased microvascular permeability and endothelial fenestration induced by vascular endothelial growth factor. J Cell Sci 1995;108:2369-79.
48. Senger DR, Galli SJ, Dvorak AM, Perruzzi CA, Harvey VS, Dvorak HF. Tumor cells secrete a vascular permeability factor that promotes accumulation of ascites fluid. Science 1983;219:983-85.
49. Plate KH, Breier G, Weich HA, Risau W. Vascular endothelial growth-factor is a potential tumor angiogenesis factor in human gliomas invivo. Nature 1992;359:845-48.
50. Dumont DJ, Gradwohl G, Fong GH, et al. Dominant-negative and targeted null mutations in the endothelial receptor tyrosine kinase, tek, reveal a critical role in vasculogenesis of the embryo. Gene Dev 1994;8:1897-909.
51. Sato TN, Tozawa Y, Deutsch U, et al. Distinct roles of the receptor tyrosine kinases Tie-1 and Tie-2 in blood vessel formation. Nature 1995;376:70-74.
52. Suri C, Jones PF, Patan S, et al. Requisite role of angiopoietin-1, a ligand for the TIE2 receptor, during embryonic angiogenesis. Cell 1996;87:1171-80.
53. Davis S, Aldrich TH, Jones PF, et al. Isolation of angiopoietin-1, a ligand for the TIE2 receptor, by secretion-trap expression cloning. Cell 1996;87:1161-69.
54. Puri MC, Rossant J, Alitalo K, Bernstein A, Partanen J. The receptor tyrosine kinase TIE is required for integrity and survival of vascular endothelial cells. EMBO J 1995;14:5884-91.
55. Joukov V, Pajusola K, Kaipainen A, et al. A novel vascular endothelial growth factor, VEGF-C, is a ligand for the Flt4 (VEGFR-3) and KDR (VEGFR-2) receptor tyrosine kinases. EMBO J 1996;15:290-98.
56. Achen M, Jeltsch M, Kukk E, et al. Vascular endothelial growth factor D (VEGF-D) is a ligand for the tyrosine kinases VEGF receptor 2 (Flk1) and VEGF receptor 3 (Flt4). Proc Natl Acad Sci USA 1998;95:548-53.
57. Schlaeger TM, Qin Y, Fujiwara Y, Magram J, Sato TN. Vascular endothelial cell lineage-specific promoter in transgenic mice. Development 1995;121:1089-98.
58. Henkemeyer M, Rossi DJ, Holmyard DP, et al. Vascular system defects and neuronal apoptosis in mice lacking ras GTPase-activating protein. Nature 1995;377:695-701.
59. Schlaeger TM, Bartunkova S, Lawitts JA, et al. Uniform Vascular-Endothelial-Cell-Specific Gene Expression In Both Embryonic and Adult Transgenic Mice. Proc Natl Acad Sci USA 1997;94:3058-63.
60. Wong AL, Haroon ZA, Werner S, Dewhirst MW, Greenberg CS, Peters KG. Tie2 expression and phosphorylation in angiogenic and quiescent adult tissues. Circ Res 1997;81:567-74.

61. Maisonpierre PC, Goldfarb M, Yancopoulos GD, Gao G. Distinct rat genes with related profiles of expression define a TIE receptor tyrosine kinase family. Oncogene 1993;8:1631-37.
62. McKnight RA, Shamay A, Sankaran L, Wall RJ, Hennighausen L. Matrix-attachment regions can impart position-independent regulation of a tissue-specific gene in transgenic mice. Proc Natl Acad Sci USA 1992;89:6943-47.
63. Wernert N, Raes MB, Lassalle P, et al. C-ets1 protooncogene is a transcription factor expressed in endothelial-cells during tumor vascularization and other forms of angiogenesis in humans. Am J Pathol 1992;140:119-27.
64. Merenmies J, Parada LF, Henkemeyer M. Receptor tyrosine kinase signaling in vascular development. Cell Growth Diff 1997;8:3-10.
65. Folkman J, D'Amore PA. Blood vessel formation: what is its molecular basis? Cell 1996;87:1153-55.
66. Patterson C, Wu Y, Lee ME, DeVault JD, Runge MS, Haber E. Nuclear protein interactions with the human KDR/flk-1 promoter in vivo. Regulation of Sp1 binding is associated with cell type-specific expression. J Biol Chem 1997;272:8410-16.
67. Patterson C, Perrella MA, Hsieh CM, Yoshizumi M, Lee ME, Haber E. Cloning and functional analysis of the promoter for KDR/flk-1, a receptor for vascular endothelial growth factor. J Biol Chem 1995;270:23111-18.
68. Rönicke V, Risau W, Breier G. Characterization of the endothelium-specific murine vascular endothelial growth factor receptor-2 (Flk-1) promoter. Circ Res 1996;79:277-85.
69. Ikeda T, Wakiya K, Shibuya M. Characterization of the promoter region for flt-1 tyrosine kinase gene, a receptor for vascular endothelial growth factor. Growth Factors 1996;13:151-62.
70. Morishita K, Johnson DE, Williams LT. A novel promoter for vascular endothelial growth factor receptor (flt-1) that confers endothelial-specific gene expression. J Biol Chem 1995;270:27948-53.
71. Wakiya K, Begue A, Stehelin D, Shibuya M. A cAMP response element and an Ets motif are involved in the transcriptional regulation of flt-1 tyrosine kinase (vascular endothelial growth factor receptor 1) gene. J Biol Chem 1996;271:30823-28.
72. Korhonen J, Lahtinen I, Halmekyto M, et al. Endothelial-specific gene expression directed by the tie gene promoter in vivo. Blood 1995;86:1828-35.
73. Lindahl P, Johansson BR, Leveen P, Betsholtz C. Pericyte loss and microaneurysm formation in PDGF-B-deficient mice. Science 1997;277:242-45.
74. Chien KR, Shimizu M, Hoshijima M, Minamisawa S, Grace AA. Toward molecular strategies for heart disease-past, present, future. Jap Circ J 1997;61:91-118.
75. Folkman J. Angiogenesis in cancer, vascular, rheumatoid and other disease. Nature Med 1995;1:27-31.
76. Shovlin CL, Scott J. Inherited diseases of the vasculature. Ann Rev Physiol 1996;58:483-507.

6. SMOOTHELINS: ONE GENE, TWO PROTEINS, THREE MUSCLE CELL TYPES .... SO FAR

Guillaume J.J.M. van Eys, Carlie J.M. de Vries, Sander S.M. Rensen, Victor L.J.L. Thijssen, Edward L.C. Verkaar, Gisela P.G.M. Coolen, Wiel M.H. Debie, Marco C. de Ruiter, and Sevilla D. Wadleigh-Detera

Introduction

Smooth muscle cells (SMCs) are found in a large variety of tissues. For years, SMCs have been divided into visceral and vascular SMCs, and into contractile and proliferative/ synthetic phenotypes. At present it is clear that such divisions are too simple. Vascular SMCs are in fact a collection of cells from various embryonic origins, with variations in morphology and gene expression patterns and with different functions [1,2,3,4,5]. Differences between SMC variants and modulations in phenotype can be monitored by marker proteins [1,6]. However, marker proteins for the subtle differences in SMC populations are hardly available. There are general markers for SMC, such as α-smooth muscle actin and calponin, but only a few proteins, such as smooth muscle myosin heavy chain and caldesmon, have been brought forward to discriminate between variants of SMCs [1,6,7,8,9]. Recently, characteristics of SM22α have been described that make this gene a promising candidate [3,10]. Marker proteins are not only important as molecules that allow a better definition of SMC variants, but also because they may provide promoter sequences that can be used as instruments to manipulate gene expression in SMCs and to 'hunt down' transcription factors involved in SMC-specific gene regulation. Gene therapy for hereditary or other diseases affecting particular smooth muscle tissues, requires promoters that are fine-tuned to the expression in one particular SMC variant and knowledge of transcription factors interacting with SMC-specific promoters.

The smooth muscle-specific smoothelin proteins have characteristics that make them candidates for markers that can discriminate between variants of SMCs. The proteins have been found almost exclusively in SMCs of the contractile phenotype [11]. So far, two isoforms have been reported, smoothelin A, a 59 kDa protein in visceral SMCs and smoothelin B, a larger 110 kDa isoform (previously described as a 94 kDa protein) in vascular SMCs [12,13]. Although we have made considerable progress in cloning and characterization of the smoothelins, the function of these proteins is largely unknown.

P.A. Doevendans et al. (eds.), Cardiovascular specific gene expression, 49-56.

Also, the SMC phenotype-specific expression of smoothelin isoforms needs further study. In this chapter we review the present state of knowledge on these proteins and discuss their function and tissue-specific expression, as well as future research.

Materials and methods.

Tissue samples and cell culture

Normal adult human tissues, obtained by autopsy, and tissues from various animals (pig, dog, cow, rabbit, rat, mouse, the toad *Xenopus laevis* and the fish *Oreochromus mossambicus*) were flash frozen in liquid nitrogen and stored at -80°C until use. SMCs were obtained from human iliac artery, uterine and mammary arteries, bovine aorta and embryonic chicken gizzard by enzymatic dispersion (collagenase/pancreatin: Life Technologies, Gaithesburg, MD, USA). Human SMCs were cultured on gelatin-coated plates in RPMI 1640/M199 (Life technologies) supplemented with 20% human serum and antibiotics (penicillin, streptomycin, fungizone). Embryonic chicken gizzard cells were cultured for 72 hours at high density on gelatin-coated cover slips. SMCs cultured for at least 5 passages were considered to be "long term cultures". The rat heart-derived myoblast cell line H9C2(2-1) [14] and COS7 cells [15] were purchased from ATCC. Cells were cultured in Dulbecco's Modified Essential Medium supplemented with 15% fetal calf serum (Life Technologies). For the myoma tissue explants 1 mm thick tissue slices were incubated as described for the cell cultures.

For immunohistochemistry tissues were mounted in Tissue-Tek (OCT-compound; Miles Inc. Elkhart, IN, USA), and 3 to 5 μm thick sections were cut at -25°C and air-dried overnight at 20°C or fixed with methanol (at -20°C for 5 min) followed by acetone (-20°C for 30 sec) and air-dried for 3 hours. Cells were grown on cover slips and also fixed in methanol/acetone.

Antibodies

Antibodies used in this study were:

1. The mouse monoclonal antibody R4A directed against smoothelin. Mice were immunized with the residue of a chicken gizzard preparation, extracted with high salt/Triton X-100. Fusion procedure and cloning of the hybridomas were performed according to standard protocols [16]. The monoclonal antibody R4A was selected on the basis of its specific reactivity pattern with a selection of human cardiac, skeletal and smooth muscle tissues. Only smooth muscle tissues showed a positive reaction. R4A is an antibody of the IgG1-subclass (Mouse Mab Isotyping kit; Life Technologies).
2. The mouse monoclonal antibody C6G directed against human smoothelin. Mice were immunized with recombinant human smoothelin-A. The smoothelin-A was produced as described previously [11]. Fusion procedure and cloning of the hybridomas were performed according to standard protocols [16]. Only human smooth muscle tissues displayed a positive reaction with C6G which is an antibody of the IgG1-subclass (Mouse Mab Isotyping kit; Life Technologies).
3. Monoclonal antibody E7 directed against β-tubulin [17].
4. Polyclonal rabbit antiserum (pDes) to chicken gizzard desmin [18].
5. Monoclonal antibody sm-1 specific for smooth muscle actin was purchased from Sigma Immuno Chemicals (St. Louis, MO, USA) [19].

In addition, rhodamine-labeled phalloidin (purchased from Molecular Probes Inc. Eugene, OR, USA) was used to stain actin stress-fibers.

Immunohistochemistry
Monoclonal antibodies R4A and C6G have been used in immunofluorescence as well as immunoperoxidase staining of a variety of tissues of different species. For colocalization studies R4A and C6G were combined with antibodies directed against desmin, tubulin and smooth muscle actin. The methods have been extensively described elsewhere [11].

Protein gel electrophoresis and Western blotting
Cultured cells (approximately 10^6) or about 40 cryostat sections (each 20 μm thick) of fresh frozen tissues were collected, washed and centrifuged (5 min at 12.000xg). After centrifugation the pellet was subjected to Triton X-100 extraction, a PBS wash and suspended in 1% Triton X-100, 5 mM ethylenedi-amino-tetraacetic acid disodium salt dihydrate (Merck), 0.4 mM phenylmethyl-sulfonyl-fluoride (Merck) in PBS, pH 7.4, and extracted for 5 min on ice. The method for gel electrophoresis and Western blotting has been described before [11].

Cloning of a human smoothelin cDNAs
A cDNA expression library was constructed with human colon smooth muscle derived polyA RNA using the Lambda ZAP-cDNA synthesis kit (Stratagene, La Jolla, California, USA). Total RNA was extracted by LiCl extraction [20]. PolyA RNA was purified by oligo(dT)-cellulose chromatography [21]. Synthesis of cDNA (by oligo(dT) priming) was performed as suggested by the manufacturer. After packaging the Uni-ZAP XR vector in phage (Gigapack II Packaging extract, Stratagene), clones containing cDNA inserts between 600 and 1600 bp were selected by immuno-screening with antibody R4A. After helper phage induced excision of plasmid vector pBluescript II pSK(-) (Stratagene) inserts were characterized by restriction analysis and sequencing, which was performed according to Sanger et al. [28]. To check whether the 1554 bp clone contained a full size cDNA, total RNA of human colon smooth muscle tissue was subjected to rapid amplification of cDNA ends (RACE) (5'RACE-kit, Life Technologies). The RACE products were amplified using Pwo DNA polymerase (Boeringer Mannheim, Germany), cloned into pUC19 and sequenced.
Since in vascular tissues on Western blots a prominent 110 kDa band was detected, reactive with R4A, the possibility of alternative splicing was investigated. RNA was extracted from human iliac artery derived SMCs by LiCl extraction [20]. Concentration and quality of RNA were evaluated by Northern blot analysis using a ^{32}P-labeled smoothelin cDNA. With primers based on the sequence of the human cDNA the possibility of alternative splicing was investigated by reverse transcription-polymerase chain reaction (RT-PCR). Rapid amplification of cDNA ends (5'RACE) on RNA derived from iliac artery was applied to investigate the possibility of a 5' extension of the mRNA. Using primers based on sequences of the 5' part of smoothelin-A cDNA in 5'RACE system (Life Technologies), PCR fragments were generated and cloned into pUC19. Colonies were screened by hybridization with a genomic smoothelin probe, containing the sequence from -200 to +60 of the start site of the smoothelin-A cDNA. Clones containing hybridizing inserts were mapped by restriction digestion and

sequenced. 5'RACE and primer extension [22] were performed with primers based on the longest vascular cDNA fragments. cDNA sequences were compared with genomic sequences. Searches for sequence homology were performed through the CAOS/EMBL data base (release 1995). Sequence comparison and structural analysis of the putative protein were performed on a UNIX computer using BLAST, BLAST-X algorithms (Altschul et al., 1990) and protein structure program PHD [24,25] and the program SOPMA [26,27].

Cloning and analysis of human smoothelin gene

Approximately 10^5 clones of a human placental cosmid genomic library (Stratagene, La Jolla, USA) were screened with the ^{32}P-dATP labeled smoothelin cDNA probe. Two positive clones were purified to homogeneity. Restriction analysis showed that the two clones had an approximately 30 kb overlap. One of the clones was found to contain the complete coding region of the smoothelin gene. In addition, 6 kb 5' flanking sequence was present. This clone was subcloned into pUC19 and exon containing subclones were identified by colony hybridization with cDNA fragments. A complete map of the cosmid clone was constructed and exons and their flanking sequences were sequenced. Sequencing was performed according to Sanger and coworkers [28] using either a Applied Biosytems AmpliTaq cycling kit for automatic sequencing in a Applied Biosystems 310, or a T7 sequencing kit (Pharmacia, Uppsalla, Sweden) for conventional ^{33}P-labeled sequencing.

Northern blot analysis

Total RNA of various tissues and from a variety of vertebrates (human, bovine, dog, rat, mouse) was extracted by LiCl [20] or Trizol (Life Technologies, Gaithesburgh, MD, USA). Ten μg of total RNA was separated on a 1,4% agarose formaldehyde denaturing gel [22]. RNA was transferred to nitrocellulose (S&S, Basel, Switzerland) and hybridized ^{32}P-labeled fragments of smoothelin cDNAs according to standard procedures [29]. Filters were washed in decreasing SSC (NaCl, Na-citrate) concentrations with a final concentration of 0.1x SSC/0.1% SDS. Probes were [^{32}P]-labeled by random priming, using a kit with a DNA polymerase Klenow fragment (Life Technologies) according to Feinberg [30].

Transfection of smoothelin cDNA into COS7 cells

The smoothelin cDNA was recloned in a pcDNA3 eukaryotic expression vector (Invitrogen, San Diego, USA) [this construct is further referred to as pcDNA3-SMO]. Isolated plasmid was purified by CsCl gradient centrifugation [22]. The procedure has been described in detail elsewhere [11].

Production of smoothelin protein in E.coli

For the generation of a new set of monoclonal antibodies against the smoothelins, cDNA fragments were inserted into prokaryotic expression vectors pQE9/10/11 (Qiagen, Kassel, Germany). Insertion in these vectors resulted in a fusion of the cDNA encoded protein to a 6-His peptide, allowing single-step purification of the protein by binding to Ni-agarose. Protein was synthesized during overnight induction with 1 μM IPTG (Life Technologies). Proteins produced in E.coli were obtained by guanidine/urea extraction and purified according to the protocol of the manufacturer (Qiagen). After

separation by SDS-PAGE proteins were blotted onto nitrocellulose and identified by antibody R4A as described above. PAGE-purified protein products were used for immunization of mice.

Results

Detection and identification of two smoothelin isoforms

The specificity of monoclonal antibody R4A, obtained after immunization of mice with chicken gizzard, was established by immunofluorescence assays and by Western blotting on a variety of tissues. This IgG1 type antibody was demonstrated by Western blotting of one- and two-dimensional gels and by immunohistochemical observations, to react exclusively with SMCs. Because of its restricted tissue distribution the antigen reacting with R4A has been designated 'smoothelin-A'. In visceral smooth muscle tissues (stomach, gut, uterus, prostate) the apparent molecular weight of the immunoreactive protein has been determined at 59 kDa. Smoothelin-A migrated slightly slower than desmin and, as observed in two-dimensional gel electrophoresis, appeared to have a pI between 8.0 and 8.5. After cloning of the human cDNA of smoothelin, a second monoclonal antibody, C6G, was generated by immunization with the recombinant protein. C6G reacted exclusively with human 59 kDa smoothelin. Epitopes for R4A and C6G have been established by deletion constructs of the human smoothelin-59 cDNA between amino acid 170-277 and 21-55, respectively. Reactions with breakdown products of about 40 kDa were occasionally observed. Immunocytochemical studies showed an equally strong reaction of R4A and C6G with visceral and vascular smooth muscle tissues. In vascular smooth muscle tissues the 59 kDa protein was represented by a minor band. Additional weak bands of about 70 and 40 kDa could be observed. However, the most prominent protein reacting with R4A was estimated to be 110 kDa. This protein was only found in vascular smooth muscle tissues or primary cell cultures derived of these tissues and has been denominated 'smoothelin-B'.

Molecular cloning and characterization of two smoothelins

A cDNA library was constructed from polyA RNA isolated from human colon smooth muscle tissue. The library was screened with the monoclonal antibody R4A. The size of the cDNA inserts varied between 600 and 1550 bp, due the position of the epitope of R4A (figure 1). The complete nucleotide sequence and deduced amino acid sequence was determined. To check whether the largest clone contained a full size cDNA, a 5'RACE reaction was performed on colon mRNA. No additional sequence was found, which indicates that the 1593 bp clone containes the full length cDNA for visceral smooth muscle tissues. Screening of a number of clones revealed that the 1593 bp cDNA contained a 1380 bp open reading frame that encodes a putative protein of 460 amino acids (figure 1). The calculated molecular weight of the protein, as deduced from the largests open reading frame of smoothelin-A, was about 50 kDa with a pI of 8.5. This open reading frame is larger than published previously [11]. Sequencing of additional clones resulted in two additions to the smoothelin cDNA at positions 164 (C) and 191 (G), which qualified the ATG at position 51 as a translation start codon. This resulted in a better agreement with the observed molecular weight and was later

confirmed by the positive C6G immunoreaction of smoothelin in visceral tissues {epitope of C6G is positioned between bp 215 and 300 of the smoothelin-A cDNA (1751 and 1848 of the smoothelin-B cDNA), as deduced from deletion fragment analysis}.

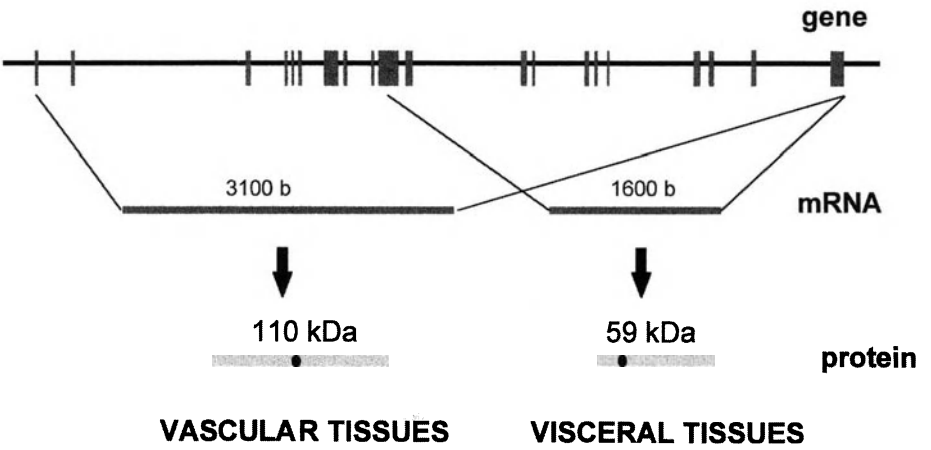

Figure 1. *The smoothelin gene (upper line) encodes for two transcripts (second line), a vascular specific 3000 nt and a visceral 1500 nt transcript. The two protein isoforms are denominated smoothelin-A and smoothelin-B (according to their molecular weights). In the gene the exons are represented by boxes. The transcription start of the 1600 nt transcript is in the middle of exon 10. The dots on bars representing the proteins is the epitope of monoclonal antibody R4A.*

After transfection of the smoothelin-A cDNA into COS7 cells Western blotting revealed a 59 kDa, R4A reactive protein, of the same size as the protein found in smooth muscle tissues such as colon. Transcription and translation of the full-size cDNA of smoothelin-A in a prokaryotic expression system gave an approximately 60 kDa, R4A immunoreactive molecule due to translation of 5' non-coding region and addition of 6His-tag. Further analysis showed that the putative smoothelin-A protein contains two Asn-X-Ser sequences (residues 151 and 277) (figure 2), which are required for asparagine-linked N-glycosylation [31]. Treatment of smooth muscle-derived smoothelin with neuramidase resulted in a reduction of the molecular weight by approximately 10 kDa.

Sequence homology at the nucleic acid and protein level with members of the spectrin superfamily, dystrophin, utrophin, β-spectrin and α-actinin was found for the region between amino acid residues 270 and 331 of smoothelin-A, and 815 and 876 for smoothelin-B. Even if conserved mutations are not included, this region of smoothelin showed 39% homology with human and mouse dystrophin, 46% homology with human and mouse β-spectrin, and 34% homology with human utropin. Homologies with α-actinin varied from 46% for human to 26% for D. discoideum. For the members of the spectrin family this region is located directly following the suggested core of the actin binding site of these molecules.

Both smoothelins have a relatively high number of serine, alanine, arginine and proline

residues. Neither positively nor negatively charged clusters could be found and no hydrophobic/transmembrane regions appear to be present in these proteins. The secondary structure of the putative protein was analysed by PHD, a neural network program [24,25] and by SOPMA [26,27]. Since no homologous sequences were available in the Swissprot databank the expected accuracy was estimated between 62 and 66% for PHD, and greater than 70% for SOPMA. Tertiairy structure analysis by these programs suggested that the amino terminal 130 aa of smoothelin-B may have an α-helical configuration. There are several smaller α-helical regions between residues 142 to 170, 549 to 610, and 733 to 791 and two minor helical structures at the carboxy terminal end (figure 2). Data base searches did not provide homologous sequences with exception of EST sequences. The obtained smoothelin cDNA sequence was checked by sequencing RT-PCR products generated with primers based on the obtained sequence and extensive restriction analysis.

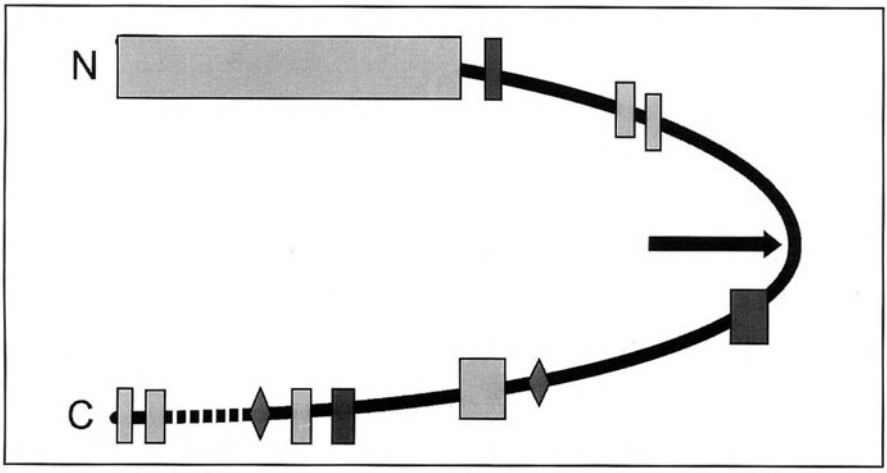

Figure 2. *Computer-assited structural analysis of the putative smoothelin proteins. Amino and carboxy termini are indicated by respectively N and C. Boxes represent potential α-helical (light gray) and β-sheet (dark gray) structures. The diamonds indicate glycosylation sites and the arrow the amino terminus of smoothelin-A. The potential actin-binding site is shown by the dashed interval of the protein close to the carboxy terminus.*

Cloning and analysis of the smoothelin gene

In situ hybridization with cDNA probes and radiation hybrid analysis demonstrated that the two smoothelin isoforms were coded for by a single copy gene located at chromosome 22q12.13 [32]. A human cosmid library was screened with a smoothelin-A cDNA probe. Two clones were selected. Hybridization experiments indicated that the whole smoothelin gene was present in the cosmid clone. A restriction map of the largest clone was constructed and used to subclone the cosmids in pUC19. It was demonstrated that the vascular specific sequence was encoded by the first nine exons and 5' half of

exon 10 of the smoothelin-B cDNA. The 3' half of exon 10 and the remaining ten exons are shared by both smoothelin isoforms. The twenty exons have been positioned. The first two rather small exons are separated from the other exons by a 5 kb intron. Exon 10 is the largest one comprising 526 bp. In the middle of this exon is the start point for the transcription of smoothelin-A. Exons 7 and 20 are also rather large, around 300 bp. All other exons are around 150 bp or smaller (figure 1). Most exon-intron bounderies have the AGGT recognition sequence. The intron between exons 16 and 17 contained a 50 bp TAAA repeat.

Since it was not clear whether the two smoothelin transcripts originate by alternative splicing or are induced through a dual promoter system, sequences directly 5' of the transcription initiation sites were screened for promoter/enhancer elements. The cosmid contains 6 kb upstream of the transcription initiation site of smoothelin-B. No TATA-box was found 5' of the smoothelin-A as well as the smoothelin-B putative promoter sites. However, a number of promoter/enhancer elements could be identified at both putative promoter sites. Amongst them are CarG(like), AP-2, SP-1, and GATA boxes.

Expression of smoothelin

Northern blotting analysis of RNA from several human visceral tissues containing smooth muscle cells, such as colon, stomach and uterus showed a band of approximately 1500 bases after hybridization with the smoothelin-A cDNA probe. However, a difference in smoothelin mRNA size was observed between visceral and vascular tissues. Northern blotting analysis on cultured vascular SMCs showed that the major transcript hybridizing to the previously described smoothelin cDNA was about 3000 nt, whereas the major transcript in visceral smooth muscle tissues was only about 1500 nt. Labeled smoothelin-A cDNA hybridized to the 3000 nt as well as to the 1500 nt mRNA, whereas the 5' half of smoothelin-B cDNA hybridized only to the 3000 nt mRNA. Northern blot analysis of RNA of smooth muscle containing tissues derived from different species such as mouse, rat, dog and cow showed a strong hybridization signal (under stringent hybridization conditions) and revealed no visible difference in mRNA size between these species. No such hybridization signal was found with RNA isolated from brain, adipose tissue, cardiac and skeletal muscle, and intestinal epithelium.

The results of the Northern blotting analysis confirmed the immunohistochemical screening on the presence of the two smoothelin isoforms in a number of different human tissues such as stomach, uterus, colon, prostate, aorta and other arteries (figure 3). Smooth muscle cells in all these tissues were positive whereas other tissue types, such as striated muscle, myoepithelium, myofibroblasts in Dupuytren's nodules, and several epithelia, neural and connective tissues, did not show staining with R4A. Analysis of different species evolutionary as distant as the teleost *Oreochromis mossambicus* and human showed that R4A reacted with smooth muscle cells of these species. In visceral tissues the amount of smoothelin is rather abundant, similar to the quantities found for desmin, indicating that smoothelin is an important constituent of visceral SMCs (figure 4). The amount of smoothelin-B found in blood vessels varies from little in elastic arteries (such as ascendent aorta) to rather abundant in muscular arteries (such as arteria iliaca and arteria femuralis) (figure 5), stressing the relation with contractility.

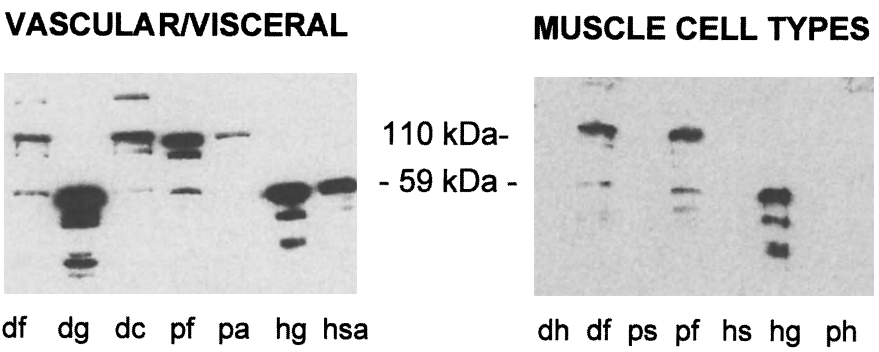

Figure 3. *Western blot analysis of the presence of smoothelin isoforms, as visualized by monoclonal antibody R4A, in a variety of muscle tissues. On the right panel striated muscle tissues are compared with smooth muscle tissues. A positive reaction is found in dog and pig femural artery (df and pf) and in human gut (hg). No reaction has been found in striated muscle such as dog and pig heart (dh and ph) and in human and pig skeletal muscle (hs and ps). The left panel shows that the smoothelin-A isoform has been found in dog and human gut (dg and hg) and in human leiosarcoma tissue, whereas the smoothelin-B isoform has been found in dog and pig femoral artery (df and pf) in dog carotid artery (dc) and in pig aorta (pa).*

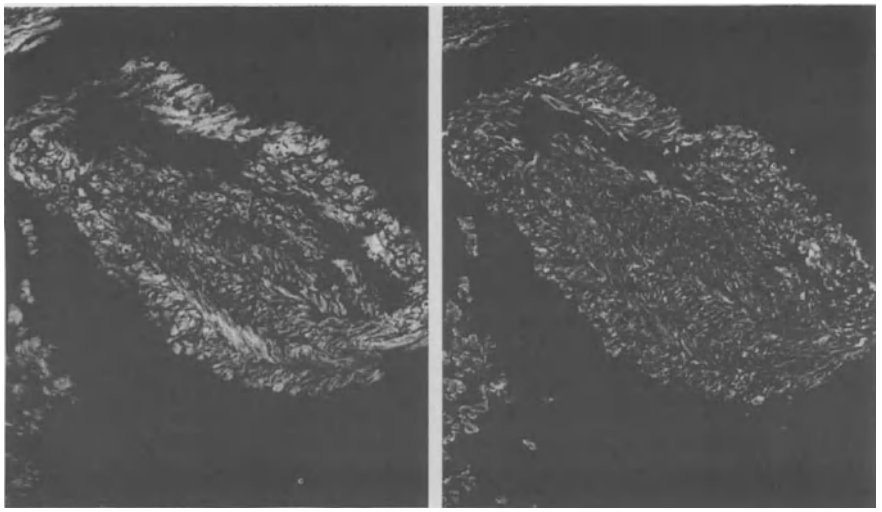

Figure 4. *Transverse section of human superficial circumflex iliac artery stained with R4A, anti-smoothelin, antibodies (left panel) and with pDes, anti desmin, antibodies (right panel).*

In smooth muscle tissue explants of uterine myoma the smoothelin-A mRNA concentration dropped sharply after transfer of tissue into culture medium. Smoothelin-A mRNA was no longer detectable by Northern blotting 12 h after removal of the tissue from the patients. However, immunohistochemical and Western blot analysis of these

tissue explants revealed that smoothelin protein remained present in the tissue up to 5 days after explantation (data not shown). The reduction in smoothelin-A mRNA and protein can not be attributed to degradation or necrosis of the tissue since GAPDH mRNA and proteins such as vimentin, desmin and α-smooth muscle actin did not diminish. No smoothelin mRNA could be detected in (primary) cultures of cells derived from smooth muscle tissue (human myoma, human colon, bovine aorta) or in long term cultured human vascular smooth muscle cells. In primary SMC cultures there is a gradual loss of immunoreactivity over subsequent passages. In SMC lines, so far, no reaction with R4A has been observed.

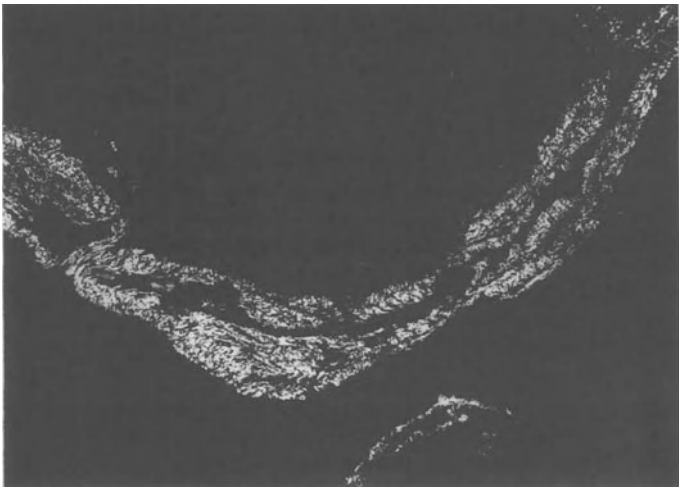

Figure 5. *Longitudinal section of human superficial circumflex iliac artery stained with R4A.*

Although in adult tissues smoothelin was only found in smooth muscle tissues, in chicken embryos the expression is more complicated. During early stages of embryonic development (Hamburger-Hamilton stages 17-36) smoothelin expression was found in the heart precursor and the somites (figure 6). The synthesis of smoothelin appeared to closely follow that of α-smooth muscle actin, as deduced from immunohistochemical staining of chicken embryos of consecutive stages. In stage 17 α-smooth muscle actin was already visible whereas smoothelin was not. At the later stages, smoothelin was present peaking around stage 25 and fading slowly after that stage to become invisible around hatching. Prelimenary data suggest that the smoothelin-B isoform is expressed in these early embryos.

Subcellular localization and organization of smoothelin

After homogenization and differential centrifugation smoothelin immunoreactivity was found in the Triton X-100 pellet, the same fraction in which cytoskeletal proteins such as desmin and actin were found [11]. Immunohistochemical analysis of several tissues revealed that smoothelin-A/B was abundantly present throughout smooth muscle

tissues, but close observation of individual cells indicated an uneven distribution over the cytoplasm. Confocal laser scanning microscropy (CSLM) of tissue sections of arteries, myoma and colon as well as primary cell cultures of human arterial and embryonic chicken gizzard cells with doubled-staining for either smoothelin/desmin or smoothelin/α-smooth muscle actin, indicated that smoothelin was organized in or was part of a filamentous structure. From the superposed pictures it was obvious that desmin and smoothelin showed no colocalization in both human and chicken primary SMCs. The pattern displayed after incubation of primary SMCs with R4A was similar in visceral- and vascular-tissue derived cells. In both SMC types smoothelin-A and smoothelin-B co-localized with the stress fibers of the primary cells.

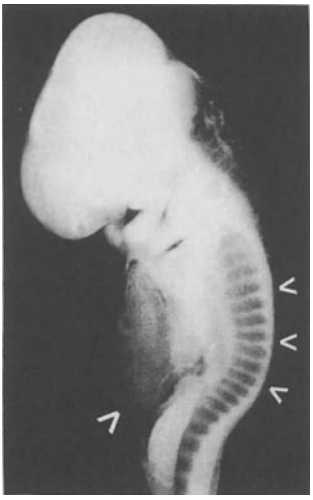

Figure 6. *Whole mount chicken embryo, HH stage 19, stained with R4A, anti-smoothelin monoclonal antibody. Staining of heart anlage and somites is indicated by arrowheads. (magnification 20x)*

In cultures from both tissues a number of cells did not react, most cells displayed a partial co-localization and a few cells showed a complete co-localization. Smoothelin often appeared to align with these fibers in a punctuated pattern. Smoothelin expression ceased in cultured SMCs, making them unsuited for localization studies. Transfections in SMCs were cumbersome. Transfection of the smoothelin-A cDNA driven by a CMV promoter (pcDNA3-SMO) into rat heart-derived myoblasts resulted in an abundant expression of smoothelin-A within 24 hours. Smoothelin-A appeared strongly to be associated with stress fibers. In addition, a relatively weak filamentous pattern was observed. A more clear filamentous pattern was observed in transfected COS7 cells. Extensive filamentous networks, reactive with R4A, were found. In time transient expression resulted in accumulation of R4A immunoreactive material in the cytoplasm. Double-immunostaining of the transfected COS7 cells showed that smoothelin does not colocalize with vimentin or keratin intermediate filaments nor with F-actin. Networks formed by tubulin and smoothelin-A differed considerably, which was most obvious for mitotic cells containing spindles. Transfections of CMV driven constructs showed an

abundant expression of smoothelin-A. An overproduction appeared to be likely since the fine punctated association, found in the cultured primary SMCs, could no longer be observed. Western blotting showed that pcDNA3-SMO transfection resulted in synthesis of a 59 kDa protein, reactive with R4A. In cells transfected with the pcDNA3 plasmid no R4A reactive material was found in immunohistochemical and Western blot assays.

Discussion

Three muscle cells types have been distinguished in vertebrates: skeletal, heart and smooth muscle cells. In structure and organization SMCs appear to be the most primitive. In SMCs, as compared to striated muscle cells, the organization of the contractile apparatus is less well structured (e.g. no sarcomeres), differentiation is not terminal, as is the case for heart and skeletal muscle cells, no fusion has been observed, and there is a resemblance with more primitive (non-vertebrate) muscle cells. This more primitive cell type is apparently well equiped for slow steady contraction, and evolution has selected this cell type for contraction in organs belonging to the digestive tract, the urogenital systems and blood vessels. On the other hand skeletal muscle, mostly dealing with abrupt and forceful movements, is found in organs of locomotion. The heart muscle shows a regular pattern of strong contractions and is in this and many other aspects an intermediate between skeletal and smooth muscle. At the cellular level structural differences between these three muscle cell types are related to their mode of action. During embryogenesis the defined positioning of the precursor cells and the straightforward way of differentiation of striated muscle cells have facilitated the elucidation of this process and many of the factors involved in differentiation of skeletal and heart muscle cells have been identified and characterized [33,34,35,36,37]. The situation for SMCs is quite different. Their embryonic origin is divers and their degree of differentiation depends on the role of these cells in the organs they belong to. Therefore, the elucidation of SMC differentiation and identification of factors involved in this process appears to be a considerably more complex task than for striated muscle. This research is strongly hampered by the lack of truly stage- and function-specific marker proteins.

The identification of two smoothelin isoforms and their expression in SMCs and in heart and somite cells during embryogenesis can contribute to our insight into the diversity of SMCs and the way these cells regulate their gene expression pattern in reaction to stimuli from the surrounding tissue. Although different isoforms have been found for such proteins as caldesmon and vinculin, no tissue-specificity could be established [1,7,38,39,40]. Also, it has been shown that the expression of SM22α promoter construct was phenotype related, although expression of the endogenous gene was not [3,10,37]. Thus, no protein has yet been identified with a specificity for the contractile SMC phenotype and with isoforms specific for visceral or vascular SMCs. The finding of vascular and visceral tissue-specific smoothelin isoforms, coded for by one gene, is valuable. One line of future research should focus on the mechanism that regulates the tissue specific expression of these two isoforms. Our present data are in favor of a dual promoter system, since no evidence for alternative splicing has been found. Different promoters for visceral and vascular expression may provide a way to

'pick up' transcription factors involved in this regulatory process. A complicating factor is that the smoothelins are only expressed in contractile SMCs, a characteristic that is rapidly lost during culturing, since proliferative SMCs soon will prevail. However, the utilization of immortalized SMC lines may offer a solution to this problem.

In adults smoothelin has been found solely in smooth muscle tissue. Extensive research on heart and skeletal muscle did not detect this protein in these muscle types [11]. Furthermore, comparison of vascular tissues and studies on tissue culture indicates that expression of smoothelin is restricted to actively contracting SMCs [41]. Results on cell cultures support these findings. Although it is possible to keep SMC in culture differentiated for a number of passages, it has become clear that the number of cells in which smoothelin expression ceases, increases with the number of passages. The contractility-related expression of smoothelin may be indicative of a function in the contractile process either by being part of the contractile apparatus or by involvement in signal transduction. A function in the contractile apparatus is in agreement with the actin-binding site that is located near the carboxy terminus of both smoothelin isoforms [42,43]. Also, co-localization of smoothelin-A and α-smooth muscle actin has been demonstrated in cultured cells [11,12]. More precise analysis of this co-localization reveals that both smoothelins are co-localizing in a dot-like fashion. This may indicate that smoothelins function as an intermediate between actin and another cytoskeletal or membrane component. This hypothesis is supported for smoothelin-B by the 140 amino acid helical structure at the amino terminal of the putative amino acid sequence predicted by computer supported modeling. Such helical structures are often employed for protein-protein interaction. A direct membrane association seems to be excluded by the absence of a hydrofobic region that could function as a membrane anchor.

A number of other proteins, such as SM22α, calponin and α-smooth muscle actin have been appointed as smooth muscle-specific proteins [1,5,8,40,44,45]. However, reports show that this specificity does not hold for all circumstances or stages of development [7,37,40,46,47,48]. Although expression of these proteins has been described in a number of tissues, the expression in striated muscle cells is developmentally and pathologically of particular interest. In early stages of embryonic development a number of smooth muscle-specific proteins are expressed in the precursor cells of striated muscle cells, e.g. in cells of the heart anlage and the somites [3,37,45]. Smoothelin shows an expression pattern similar to SM22α and calponin. Expression of these proteins appears to follow the expression of α-smooth muscle actin, underlining the association between these molecules and suggesting that α-smooth muscle actin is the driver in this developmental process. We hypothesize that the expression of smooth muscle-specific proteins in the early embryo is due to the inability of the muscle cells to directly organize into the complex sarcomeric structure of a striated muscle cell. In vitro studies have indicated that structures such as stress fibers are needed to position large structural molecules such as titin. In vivo the relative primitive SMC-like structure may be used as a starting point to build the sarcomeric structure [33,49,50,51]. This may be related to the low level of oxygen in embryonic tissues due to the lack of circulation. The precursor muscle cells adopt a more SMC-like, less oxygen-dependent organization which is used to get the circulation going [52,53]. Once circulation is sufficient to provide striated muscle cells with oxygen, the SMC-like expression pattern of the cells will be replaced by that of striated muscle cells and sarcomeric structures will build up.

A number of SMC proteins have been demonstrated to be expressed in diseased (often ischemic/hypoxic) striated muscle cells. A number of authors consider this to be a process of dedifferentiation, referring to expression of these proteins in striated muscle cells during embryonic development [54]. However, the dedifferentiation process never proceeds to a truly embryonic state, demonstrating that the terminal differentiation in striated muscle cells can not be completely nullified or overruled. Smoothelin expression has not been observed in ischemic or hibernating cardiac muscle, that expressed α-smooth muscle actin (J. Ausma/ M. Borgers, personal communication). Thus, although smoothelin and α-smooth muscle actin are co-expressed in early embryos, triggers for expression of smoothelin are absent in hibernating/ischemic myocardium, indicating differences in the transcription regulation of the two proteins. Although the structure of the gene has been largely dissolved, the regulation of expression of the gene and the generation of two isoforms is still unclear. Putative promoter sequences have been analysed. A TATA-box has been found neither 5' of smoothelin-A nor 5' of smoothelin-B coding sequences. Although more genes are known to lack this box, so far, all smooth muscle-specific genes have a TATA-box. A number of enhancer sequences have been found, but their impact on expression of both isoforms remains to be determined. The putative smoothelin-B promoter sequence does not show any homology with that of other SMC-specific genes such as SM22α and α-smooth muscle actin. Functional promoter analysis can only be performed in contractile SMCs. To our knowledge, there is no contractile SMC line and SMCs of primary cultures dedifferentiate within a limited number of passages to the synthetic phenotype. So, with the present SMC cultures a negative result in promoter studies may be attributed to the cell phenotype rather than to the promoter sequence. The advent of T-antigen carrying transgenic mice may provide opportunities to obtain SMC lines that can be employed in promoter studies necessary to establish the functioning of the smoothelin promoter(s).

Conclusion

Smoothelins are smooth muscle-specific proteins, which appear to be part of or associated with the cytoskeleton. An association with actin was demonstrated by immunohistochemical staining of cultured smooth muscle cells (SMCs) and transfected skeletal muscle cells. So far, two isoforms of smoothelin have been detected and characterized, a 59 kDa protein found in visceral SMCs, and a 110 kDa protein found in vascular tissues. The visceral isoform is denominated 'smoothelin-A', whereas the vascular isoform is denominated smoothelin-B'. Both proteins appear to be encoded by one gene, which consists of twenty exons. Smoothelin-A is the carboxy terminal half of smoothelin-B (exons 10 to 20 of the gene). It is not yet clear whether the two proteins are the result of alternative splicing or are generated through a dual promoter system. The putative promoter sequences do not contain a TATA box, but such enhancer sequences as CarG-boxes and E-boxes have been found. With exception of the actin-binding sequence, no major homologies with other genes have been established. Expression of both smoothelins in adults appears to be restricted to contractile SMCs. In early embryos smoothelin expression has been found in cells of the heart precursor and somites. The expression pattern is similar to the pattern

displayed by α-smooth muscle actin and SM22α. However, the specificity for contractile SMCs and differential expression of the two isoforms appear to be unique for the smoothelins.

Acknowledgements
The authors are indebted to Frank van der Loop and Erika Timmer for their contribution to this paper, and Mrs. Jeanette van Eys for checking the 'english'.

References

1. Owens GK. Regulation of differentiation of vascular smooth muscle cells. Physiol Rev 1995;75:487-517.
2. Gabbiani G, Schmid E, Winter S, Chaponnier C, Chastonay de C, Vandekerckhove J, Weber K, Franke WW. Vascular smooth muscle cells differ from other smooth muscle cells: predominance of vimentin filaments and a specific alpha-type actin. Proc Natl Acad Sci USA 1981;78:298-302.
3. Moessler H, Mericskay M, Li Z, Nagi S, Paulin D, Small JV. The SM22 promotor directs tissue-specific expression in arterial but not in venous or visceral smooth muscle cells in transgenic mice. Development 1996;122:2415-25.
4. Nanaev AK, Shirinsky VP, Birukov KG. Immunofluorescent study of heterogeneity in smooth muscle cells of human fetal vessels using antibodies to myosin, desmin, and vimentin. Cell Tissue Res 1991;266:535-40.
5. Campbell GR, Chamley-Campbell JH. Smooth muscle phenotypic modulation: Role in atherogenesis. Med Hypothesis 1981;7:729-35.
6. Campbell JH, Kocher O, Skalli O, Gabbiani G, Campbell GR. Cytodifferentiation and expression of alpha-smooth muscle actin mRNA and protein during primary culture of aortic smooth muscle cells: correlation with cell density and proliferative state. Atherosclerosis 1989;9:633-43.
7. Glukhova MA, Kabakov AE, Belkin AM, Frid MG, Ornatsky OI, Zhidkova NI, Koteliansky VE. Meta-vinculin distribution in adult human tissues and cultured cells. FEBS Lett 1986;207:139-41.
8. Haeberle JR, Hathaway DR, Smith CL. Caldesmon content of mammalian smooth muscles. J Muscle Res Cell Motil 1992;13:81-89.
9. Miano J, Cserjesi P, LigonP, Perisamy M, Olson EN. Smooth muscle myosin heavy chain marks exclusively the smooth muscle lineage during mouse embryogenesis. Circ Res 1994;75:803-12.
10. Li L, Miano JM, Mercer B, Olson E. Expression of the SM22α promotor in transgenic mice provides evidence for distinct transcriptional regulation programs in vascular and visceral smooth muscle cells. J Cell Biol 1996;132: 849-59.
11. Van der Loop FTL, Schaart G, Timmer EDJ, Ramaekers FCS, Van Eys GJJM. Smoothelin, a novel cytoskeletal protein specific for smooth muscle cells. J Cell Biol 1996;134:401-11.
12. Van der Loop FTL, Gabbiani G, Kohnen G, Ramaekers FCS, Van Eys GJJM. Differentiation of smooth muscle cells in human blood vessels as defined by smoothelin, a novel marker for the contractile phenotype. Arterioscl Thromb Vasc Biol 1996;1:665-71.
13. Wehrens XHT, Mies B, Gimona M, Ramaekers FCS, Van Eys GJJM, Small JV. Localization of smoothelin in avian smooth muscle and identification of a vascular-specific isoform. FEBS Lett 1997;405:315-20.
14. Kimes BW, Brandt BL. Properties of a clonal muscle cell line from rat heart. Exp Cell Res 1976;98:367-81.
15. Gluzman Y. SV40-transformed simian cells support the replication of early SV40 mutants. Cell 1981;23:175-82.
16. Köhler G, Milstein C. Continuous cultures of fused cells secreting antibody of predefined specificity. Nature 1975;256:495-97.
17. Chu DTW, Klymkowsky MW. Experimental analysis of cytoskeletal function in early Xenopus laevis embryos. Development 1987;8:140-42.
18. Ramaekers FCS, Moesker O, Huijsmans A, Schaart G, Westerhof G, Wagenaar SjSc, Herman CJ, Vooijs GP. Intermediate filament proteins in the study of tumor heterogeneity: an in-depth study of tumors of the urinary and respiratory tracts. Ann NY Acad Sci 1985;455:614-34.
19. Skalli O, Ropraz P, Trzeciak A, Benzonana G, Gillesen D, Gabbiani G. A monoclonal

antibody against alpha-smooth muscle actin: a new probe for smooth muscle differentiation. J Cell Biol 1986;103:2787-96.
20. Auffray C, Rougeon F. Purification of mouse immunoglobulin heavy chain messenger RNAs from total myeloma tumor RNA. Eur J Biochem 1980;107:393-414.
21. Aviv A, Leder P. Purification of biologically active globin messenger RNA by chromatography on oligothymidylic acid cellulose. Proc Natl Acad Sci USA 1972;69:1408-12.
22. Sambrook J, Fritsch EF, Maniatis T. Molecular cloning: A laboratory manual. Cold Spring Harbor, New York: 1989 Cold Spring Harbor Laboratory Press.
23. Altschul SF, Gish W, Miller W, Myers EW, Lipman DJ. Basic local alignment search tool. J Mol Biol 1990;215:403-10.
24. Rost B, Sander C. Prediction of protein secondary structure at better than 70% accuracy. J Mol Biol 1993;232:584-99.
25. Rost B, Sander C. Combining evolutionary information and neural networks to predict protein secondary structure. Proteins 1994;19:55-77.
26. Geourjon C, Deleage G. SOPMA: A self optimised prediction method for protein secondairy structure prediction. Prot Eng 1994;7:157-64.
27. Geourjon C, Deleage G. SOPMA: Significant improvements in protein secondairy structure prediction by prediction from multiple alignments. Comput Aplic Biosci 1994;11:681-84.
28. Sanger F, Coulson AR, Barrell BG, Smith AJH, Roe BA. Cloning a single stranded bacteriophage as an aid to rapid DNA sequencing. J Mol Biol 1980;143:161-78.
29. Church GM, Gilbert W. Genomic sequencing. Proc Natl Acad Sci USA 1984;81:1991-95.
30. Feinberg AP, Vogelstein B. A technique for radiolabeling DNA restriction endonuclease fragments to high specific activity. Anal Biochem 1983;132:6-12.
31. Pless DD, Lennarz WJ. Enzymatic conversion of proteins to glycoproteins. Proc Natl Acad Sci USA 1977;74:134-38.
32. Engelen JJM, Esterling LE, Albrechts JCM, Detera-Wadleigh SD, Van Eys GJJM. Assignment of the human gene for smoothelin (SMTN) to chromosome 22q12 by fluorescence in situ hybridization and radiation hybrid mapping. Genomics 1997;43:245-47.
33. Babai F, Musevi-Aghdam J, Schurch W, Royal A, Gabbiani G. Coexpression of alpha-sarcomeric, alpha-smooth muscle actin and desmin during myogenesis in rat and mouse embryos. Differentiation 1989;44:132-42.
34. Gunning P, Gordon M, Wade R, Gahlmann R, Lin CS, Hardeman E. Differential control of tropomyosin mRNA levels during myogenesis suggests the existence of an isoform competition-autoregulation compensation control mechanism. Dev Biol 1990;138:443-53.
35. McHugh KM, Crawford K, Lessard JL. A comprehensive analysis of the developmental and tissue-specific expression of the isoactin multigene family in the rat. Dev Biol 1991; 148:442-58.
36. Olson EN. MyoD family: A paradigm for development? Genes Dev 1990;4:1454-61.
37. Li L, Miano JM, Cserjesi P, Olson EN. SM22α, a marker of adult smooth muscle, is expressed in multiple myogenic lineage during embryogenesis. Circ Res 1995;78:188-95.
38. Frid MG, Shekhonin BV, Koteliansky VE, Glukhova MA. Phenotypic changes of human smooth muscle cells during development: late expression of heavy caldesmon and calponin. Dev Biol 1992;153:185-93.
39. Nagai R, Kuro-OM, Babij P, Periassamy M. Identification of two types of smooth muscle myosin heavy chain isoforms by cDNA cloning and immunoblot analysis. J Biol Chem 1989;264:9734-37.
40. Duband JL, Gimona M, Scatena S, Small JV. Calponin and SM22 as differentiation markers of smooth muscle markers: Spatiotemporal distribution during avian embryonic development. Differentiation 1993;55:1-11.
41. Van Eys GJJM, Voller MCW, Timmer EDJ, Wehrens XHT, Small JV, Schalken JA, Ramaekers FCS, Van der Loop FTL. Smoothelin expression characteristics: development of a smooth muscle cell in vitro system and identification of a vascular variant. Cell Struct Funct

1997;22:65-72.
42. Dhermy D. The spectrin super-family. Biol Cell 1991;71:249-54.
43. Karinch AM, Zimmer WE, Goodman SR. The identification and sequence of the actin-binding domain of human red blood cell beta-spectrin. J Biol Chem 1990;265:11833-40.
44. Lees-Miller JP, Heeley DH, Smillie LB. An abundant and novel protein of 22 kDa (SM22) is widely distributed in smooth muscle. Biochem J 1987;244:705-09.
45. Takahashi K, Hiwada K, Kokubu T. Vascular smooth muscle calponin: a novel T-like protein. Hypertension 1988;11:620-26.
46. Borrione AC, Zanellato AMC, Giurato L, Scannapieco G, Pauletto P, Sartore P. Non-muscle and smooth muscle myosin isoforms in bovine endothelial cells. Exp Cell Res 1990;190:1-10.
47. Li L, Liu Z, Mercer B, Overbeek P, Olson EN. Evidence for serum response factor-mediated regulatory networks governing SM22α transcription in smooth, skeletal, and cardiac muscle cells. Dev Biol 1997;187:311-21.
48. Takeuchi K, Takahashi K, Abe M, Nishida W, Hiwada K, Nabeya T, Maruyama K. Co-localization of immunoreactive forms of calponin with actin cytoskeleton in platelets, fibroblasts and smooth muscle. J Biochem 1991;109:311-16.
49. Bochaton-Piallat M-L, Ropraz P, Gabbiani G, Santeusanio G, Palmeiri G, Schiaroli S, Spagnoli LG. Actin isoforms and intermediate filament protein expression in human developing skeletal muscle. BAM 1992;2:83-87.
50. De Jong F, Geerts WJC, Lamers WH, Los JA, Moorman AHM. Isomyosin expression during formation of the tubular chicken heart: a three-dimensional immunohistochemical analysis. Anat Rec 1990;226:213-27.
51. Van der Loop FTL, Van Eys GJJM, Schaart G, Ramaekers FCS. Titin expression as an early indication of heart and skeletal muscle differentiation in vitro. Developmental re-organization in relation to cytoskeletal constituents. J Muscle Res Cell Mot 1996;17:23-36.
52. Chen Y-F, Durand J, Claycomb WC. Hypoxia stimulates atrial natriuretic peptide gene expression in cultured atrial cardiocytes. Hypertension 1997;29:75-82.
53. Schmedtje JF, Liu WL, Thompson TH, Runge MS. Evidence of hypoxia-inducible factor in vascular endothelial and smooth muscle cells. Biochem Biophys Res Comm. 1996;220:687-91.
54. Ausma J, Schaart G, Thoné F, Shivalkar B, Flameng W, Depré C, Vanoverschelde J-L, Ramaekers FCS, Borgers M. Chronic ischemic viable myocardium in man: Aspects of dedifferentiation. Cardiovasc Pathol 1995;4:29-37.

7. REGIONALIZATION OF TRANSCRIPTIONAL POTENTIAL IN THE MYOCARDIUM: 'CARDIOSENSOR' TRANSGENIC MICE

Robert G. Kelly, Peter S. Zammit, Diego Franco, Antoon F.M. Moorman, and Margaret E. Buckingham

Introduction

The vertebrate heart results from complex morphological interactions between different cardiac sub-compartments, including right and left atrial and ventricular chambers. Cardiac sub-domains originate in early heart development: cardiomyocytes differentiate in an anterior-posterior gradient in the anterior lateral mesoderm prior to the formation of a transiently linear heart tube. Studies in the chick have shown that the cardiac tube contains future sub-regions of the heart arranged in series along the anterior-posterior axis [1]. Subsequently the heart tube undergoes a process of rightward looping, and the caudal inflow region is displaced dorsally and anteriorally, resulting in an embryonic heart composed of a series of sub-compartments or segments: inflow tract (IFT), embryonic atrium, atrioventricular canal (AVC), embryonic left and right ventricles and outflow tract (OFT). Subsequent growth, septation, and remodelling of these distinct cardiac segments result in the development of separate right and left atrial and ventricular chambers with independent inlets and outlets. Morphological remodelling between different cardiac sub-domains is often perturbed in congenital heart defects in man.

Recent studies of endogenous and transgene markers in the developing mouse heart have demonstrated that different sub-units of the embryonic heart correspond to distinct domains of gene expression, each with their own transcriptional specificities [2]. Among the markers which have been demonstrated to exhibit left/right transcriptional differences in the mouse heart are myosin light chain (MLC) 3F transgenes [3]. MLC3F is transiently expressed at a low level in the embryonic ventricles and remains at a low level in the atria [3,4]. MLC3F-nlacZ transgenes reveal transcriptional differences between the right and left sides of the embryonic heart which persist throughout development and in the adult heart [3]. These transgenic mice provide informative markers with which to analyze the acquisition of regional expression domains in the

P.A. Doevendans et al. (eds.) Cardiovascular specific gene expression, 67-73.

early heart, and to follow normal and abnormal morphological remodelling of the heart as development proceeds.

Left and right transcriptional sub-domains in the mouse heart

The structure of the MLC1F/3F gene is illustrated in figure 1. The two promoters at this locus are differentially activated during skeletal muscle development in response to two enhancers which have been identified and analyzed in transgenic mice: one in the first intron active in fetal and adult skeletal muscle, and one 3' to the gene which is active in embryonic, fetal and adult skeletal muscle [5,6]. Transgenic analysis has also demonstrated that the MLC3F promoter is active in cardiomyocytes, independently of either skeletal muscle enhancer [3,4,7].

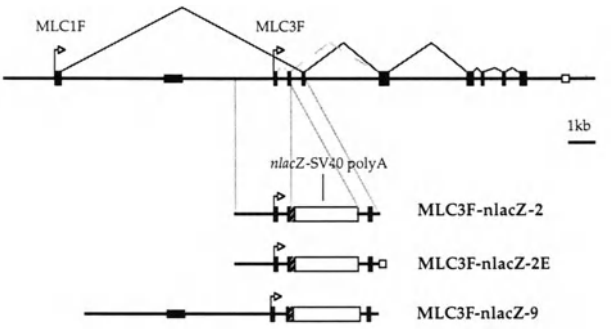

Figure 1. *Structure of the mouse MLC1F/3F locus and MLC3F-nlacZ transgenes, showing the exon (filled box), intron structure, splicing patterns and the positons of the intronic (shaded box) and 3' (empty box) skeletal muscle enhancers. In the transgene constructs the nlacZ reporter gene is positioned in frame in exon 3 (MLC3F specific).*

A β-galactosidase reporter gene, under transcriptional control of the MLC3F promoter, is regionally expressed in transgenic mouse hearts (constructs MLC3F-nlacZ-2 and MLC3F-nlacZ-2E [3,7]). X-gal treatment of isolated hearts reveals that β-galactosidase expression is strongest in the left ventricle and right atrium, with lower level expression in the left atrium and an exclusion from the right ventricle (figure 2). In situ hybridization analysis reveals that β-galactosidase transcripts accumulate in the left ventricular free-wall and interventricular septum, but not in the right ventricular free-wall, demonstrating that the regionalization of transgene expression results from transcriptional differences between the right and left sides of the heart [3]. Regionalization of MLC3F-nlacZ transgenes occurs very early during cardiac development, and the expression profile at embryonic day (E) 10.5 resembles the right atrial/left ventricular dominant expression pattern found in the adult heart (figure 2). Prior to looping, however, expression of the transgene appears symmetrically

distributed along the anterior-posterior and left-right axes of the heart tube (figure 2): regionalization of MLC3F transgene expression is therefore established concomitantly with looping [8].

Endogenous MLC3F transcripts accumulate to a low level in the mouse heart [3,5]. In situ hybridization analysis demonstrates that MLC3F transcripts are left/right regionalized in the embryonic heart at E10.5, but that subsequent modifications of MLC3F expression result in divergence between the endogenous and transgene expression patterns [7]. In particular endogenous MLC3F transcripts are down-regulated in the left ventricle and upregulated in the left atrium, modulations not observed for MLC3F transgenes. In addition, the myocardium of the caval veins is positive for endogenous MLC3F expression but negative for MLC3F transgenes. These results suggest that different cis-acting modules control the spatial and temporal distribution of MLC3F transcription in the mouse heart, and that those modules mediating regionalization at E10.5, but not those mediating subsequent modulation of MLC3F expression, are included on the MLC3F transgenes. Furthermore, these results demonstrate that MLC3F expression in atrial and caval vein myocardium is directed by distinct cis-acting modules, suggesting that the inflow region of the mouse heart is composed of sub-domains of differing transcriptional specificities [7].

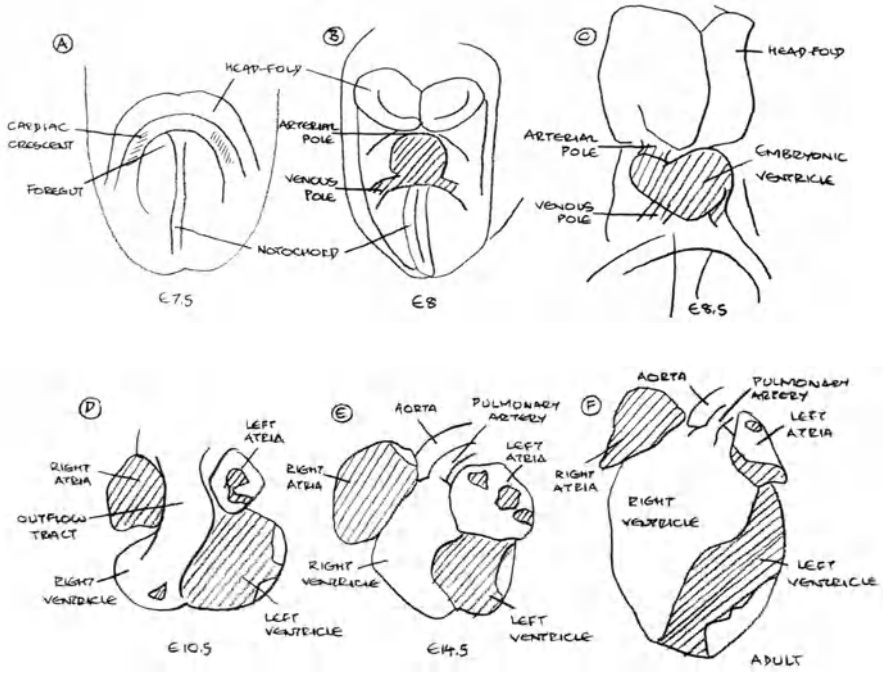

Figure 2. *Cartoon of MLC3F-nlacZ-2E transgene expression (shaded region) in the developing and adult mouse heart. Transgene regionalization emerges during cardiac looping and the resulting left ventricular/right atrial dominant expression profile is stable from E10.5 onwards.*

Other examples of transgenes regionalized to the left or right sides of the embryonic mouse heart have been reported recently. MLC2V-lacZ [9], and desmin-lacZ [10] transgenes, for example, are restricted to the right ventricle, in a complementary pattern to the MLC3F transgenes discussed above. These data suggest that the transcriptional control of many cardiac genes is organised on a modular basis. As in the case of MLC3F, the modules included on the respective transgenes are likely to be only a subset of those controlling temporal and spatial expression of the endogenous genes. Nevertheless, a number of endogenous genes have been demonstrated to be left/right regionalized in the developing heart, including atrial natriuretic factor [11] and MCK [12], which are transiently regionalized to the left and right ventricles respectively. The extent to which endogenous myocardial genes are regionalized is unknown, although initial results suggest that many genes, in particular those with dynamic expression profiles, exhibit left/right transcriptional differences at least transiently (PZ, RK, DF and MB, unpublished observations). The functional significance of extensive transcriptional sub-domains within the ventricular and atrial myocardium remains to be elucidated.

Myocardial gene expression appears to be controlled by the combinatorial activities of several families of transcription factors [13]. Candidate molecules which may play a role in mediating regionalization include the basic-helix-loop-helix factors e-hand and d-hand, MEF2 family members and Nkx homeodomain proteins. In the embryonic heart e-hand and d-hand are expressed in right and left ventricular domains respectively [14,15], and loss of d-hand results in deletion of the right ventricle [14]. MEF2 has been implicated in regionalization of right ventricular restricted MLC2V [9] and desmin [10] transgenes, and targeted mutation of MEF2C, like the d-hand null phenotype, results in deletion of the right ventricle [16]. Nkx2.5 null mice exhibit a block of cardiac looping [17] and loss of a subset of regionalized markers, including e-hand in the left ventricular domain [15]. Experiments are underway to identify the molecular mechanisms controlling left ventricular/right atrial dominant MLC3F expression.

Morphological implications of transcriptional regionalization in the heart: 'cardiosensor' transgenic mice

Mice carrying transgenes such as MLC3F-nlacZ which are stably regionalized in the myocardium ('cardiosensor' mice) allow analysis of the contribution of different regions of the embryonic heart to distinct structures of the definitive heart. Here we describe two examples of the use of stably regionalized MLC3F transgene markers to follow morphological processes during normal cardiogenesis. The MLC3F-nlacZ-2E transgene, the expression profile of which is illustrated in figure 2, has been used to follow the contribution of myocardial cells of the AVC (positive for transgene expression at E10.5) to atrial and ventricular structures during AVC septation. This analysis has shown that AVC myocytes contribute to the base of the atrial walls and to the right ventricle during AV junction remodelling [8]. In addition, a small population of β-galactosidase expressing myocardial cells contribute to the muscular component of the tricuspid valve leaflet [8].

Secondly a MLC3F-nlacZ-9 transgene, the expression domain of which is illustrated in figure 3, and which is more broadly expressed in the embryonic myocardium (right ventricle positive, but OFT negative), has been used to follow the contribution of the OFT myocardium to the definitive ventricles [8]. In figure 3 it can be seen that the negative myocardium of the embryonic OFT becomes incorporated into the ventricles during fetal growth and in the adult heart contributes to the infundibulum of the right ventricle and a small sub-aortic region of the left ventricle. The right ventricular outlet septum is β-galactosidase negative and may therefore also be derived from the embryonic OFT [8]. The use of regionalized transgene markers can therefore contribute significantly to analysis of the fate of different regions of the mouse heart. There are several advantages in using transgene over endogenous gene markers, including the facility of revelation of β-galactosidase activity and the extensive sub-compartmentalization picked up by transgenes compared to the broader temporal and spatial expression patterns of most endogenous cardiac genes. Critically, such 'lineage' analysis depends on transgene expression being static, ie providing a stable marker for a defined sub-population of myocytes. Stable expression can be established by detailed histological and whole-mount examination of intermediate steps [8].

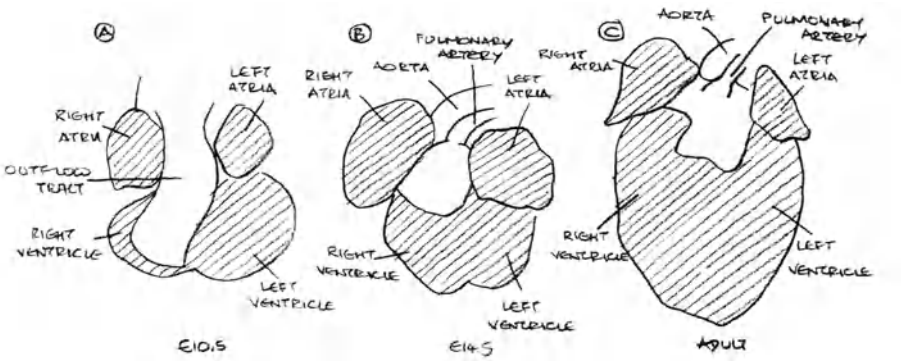

Figure 3. *Cartoon of MLC3F-nlacZ-9 transgene expression (shaded region) in the developing and adult mouse heart. A population of β-galactosidase negative myocardiocytes in the embryonic outflow tract becomes absorbed into the ventricles during fetal development. After Kelly et al., 1998 [2].*

Congenital heart disease in man frequently involves abnormalities at cardiac subcompartment boundaries, malformations of cardiac outlet connections, or abnormal chamber remodelling. An increasing number of mouse models of congenital heart disease have been described [18]; such mutant mice can be crossed with 'cardiosensor' transgenic mice to follow the contribution of different regions of the embryonic heart to particular malformed structures. For example, experiments are underway to analyse left and right atrial and ventricular specification in a mouse heterotaxy model, the iv/iv

mouse, by crossing the right atrial/left ventricular regionalized MLC3F-nlacZ-2E transgene into the iv genetic background. In these mice left/right positional information is lost and the direction of cardiac looping is randomized, with an associated increased frequency of abnormalities including atrial isomerism and outlet connection malformations [19]. Initial results show that transgene expression reveals defects in left-right specification of the atria before their morphological development [DF, RK, AFM, MB and Nigel Brown, unpublished observations]. Similarly, analysis of left/right regionalized transgene expression in mouse trisomy 16, a murine model for Down's syndrome, should reveal novel information about how different compartments of the embryonic heart contribute to atrioventricular septal defects. Gene targeting technology has greatly expanded the number of mutant mouse lines with cardiac malformations [14,17], and fine analysis of mutant phenotypes using selected 'cardiosensor' mice should provide insights into the mechanisms by which the early heart is patterned and the morphological interactions associated with subsequent cardiac remodelling.

Acknowledgements

M.B.'s laboratory is supported by grants from the Pasteur Institute, CNRS, AFM and EC Biomed Program (Grant CEE CT98-4004). RK and PZ were supported by Wellcome Postdoctoral Fellowships (PZ Grant No. 041522/Z/94). RK was subsequently supported by grants from the AFM and EC (including EC Biotechnology Grant PL 950228). DF acknowledges support of grants NWO (902-16-219) and NHS (97206).

References

1. De la Cruz MV, Sanchez-Gomez C, Palomino MA. The primitive cardiac regions in the straight tube heart (stage 9) and their anatomical expression in the mature heart: an experimental study in the chick embryo. J Anat 1989;165:121-31.
2. Kelly R, Franco D, Moorman AFM, Buckingham M. Chamber-specific myofilament gene expression: implications for A/P patterning. Chapter in "Heart Development", Eds. Rosenthal N, Harvey R. Academic Press;1998:p.333-55.
3. Kelly R, Alonso S, Tajbakhsh S, Cossu G, Buckingham M. Myosin light chain 3F regulatory sequences confer regionalized cardiac and skeletal muscle expression in transgenic mice. J Cell Biol 1995;129:383-96.
4. McGrew MJ, Bogdanova N, Hasegawa K, Hughes SH, Kitsis RN, Rosenthal N. Distinct gene expression patterns in skeletal and cardiac muscle are dependent on common regulatory sequences in the MLC1/3 locus. Mol Cell Biol 1996;16:4524-34.
5. Rosenthal N, Kornhauser JM, Donoghue M, Rosen KM, Merlie JP. Myosin light chain enhancer activates muscle-specific, developmentally regulated gene expression in transgenic mice. Proc Natl Acad Sci USA 1989;86:7780-84.
6. Kelly RG, Zammit PS, Schneider A, Alonso S, Biben C, Buckingham ME. Embryonic and fetal myogenic programs act through separate enhancers at the MLC1F/3F locus. Dev Biol 1997;187,183-99.
7. Kelly R, Zammit P, Mouly V, Butler-Browne G, Buckingham M. Dynamic left/right regionalization of endogenous myosin light chain 3F transcripts in the developing mouse heart. J Mol Cell Cardio 1998;30:1067-81.
8. Franco D, Kelly R, Lamers W, Buckingham M, Moorman AFM. Regionalized transcriptional domains of myosin light chain 3F transgenes in the embryonic mouse heart: morphogenetic implications. Dev Biol 1997;188:17-33.
9. Ross RS, Navankasattusas S, Harvey RP, Chien KR. An HF-1a/HF-1b/MEF-2 combinatorial element confers cardiac ventricular specificity and establishes an anterior-posterior gradient of expression. Development 1996;122:1799-809.
10. Kuisk IR, Li H, Tran D, Capetanaki Y. A single MEF2 site governs desmin transcription in both heart and skeletal muscle during mouse embryogenesis. Dev Biol 1996;174:1-13.
11. Zeller R, Bloch KD, Williams BS, Arceci RJ, Seidman CE. Localized expression of the atrial natriuretic factor gene during cardiac embryogenesis. Genes Dev 1987;1:693-98.
12. Lyons GE. In situ analysis of the cardiac muscle gene program during embryogenesis. Trends Cardiovasc Med 1994;4:70-77.
13. Olson EN, Srivastava D. Molecular pathways controlling heart development. Science 1996;272:671-76.
14. Srivastava D, Thomas T, Lin Q, Kirby ML, Brown D, Olson EN. Regulation of cardiac mesodermal and neural crest development by the bHLH transcription factor dHAND. Nat Genet 1997;16:154-60.
15. Biben C, Harvey RP. Homeodomain factor Nkx2-5 controls left/right asymmetric expression of bHLH gene eHand during murine heart development. Genes Dev 1997;11:1357-69.
16. Lin Q, Schwarz J, Bucana C, Olson EN. Control of mouse cardiac morphogenesis and myogenesis by transcription factor MEF2C. Science 1997;276:1404-07.
17. Lyons I, Parsons LM, Hartley L, Li R, Andrews JE, Robb L, Harvey RP. Myogenic and morphogenetic defects in the heart tubes of murine embryos lacking the homeobox gene Nkx2-5. Genes Dev 1995;9:1654-66.
18. Rossant, J. Mouse mutants and cardiac development: new molecular insights into cardiogenesis. Circ Res 1996;78:349-53.
19. Seo JW, Brown NA, Ho SY, Anderson RH. Abnormal laterality and congenital cardiac anomalies. Relations of visceral and cardiac morphologies in the iv/iv mouse. Circulation 1992;86:642-50.

8. HUMAN TROPONIN GENES: TRANSCRIPTIONAL REGULATION AND CHROMOSOMAL ORGANIZATION

Paul J.R. Barton, Pankaj K. Bhavsar, Kimberley A. Dellow, Philip J. Townsend, Magdi H Yacoub, and Nigel J. Brand

Introduction

The troponin complex forms the calcium-sensitive molecular switch which regulates striated muscle contraction in response to alterations in intracellular calcium concentration. It is located on the thin filament of the sarcomere and is composed of three subunits: troponin C, the calcium binding subunit; troponin T, which is involved in the attachment of the complex to tropomyosin; and troponin I, the inhibitory subunit. Multiple isoforms of each of these subunits have been identified (see table 1) which are expressed with distinct tissue-specificity and developmental regulation [1,2]. In the case of troponin I, three isoforms have been identified in vertebrate striated muscle and in the adult these are expressed in cardiac muscle, slow skeletal muscle and fast skeletal muscle respectively. In the adult heart, cardiac troponin I is the only troponin I isoform detected in the bulk of the myocardium. However, during development the predominant isoform expressed is slow skeletal troponin I [2]. We have previously documented aspects of troponin expression in the human heart [3-6] and demonstrated a developmental switch in troponin I expression during human development. Analysis of mRNA and protein levels suggests that the increase in expression of the cardiac troponin I gene seen in late fetal stages in man is due to an increase in transcription. Here, we present data on the basic machinery required for the expression of the human cardiac troponin I gene. In other studies we have analyzed the organization of the troponin gene families and revealed that the six human genes encoding the different troponin I and T isoforms are organized as paralogous pairs located at three different chromosomal sites. Analysis of the pair comprized of the cardiac troponin I and slow skeletal troponin T genes reveals that they are organized head to tail and lie within 3 kb of each other. Close physical linkage raises questions concerning the evolution of these two troponin gene families, for their regulation and for the analysis of mutations suspected to result in cardiomyopathy.

P.A. Doevendans et al. (eds.), Cardiovascular specific gene expression, 75-86.

Table 1. Chromosomal organization of Human troponin genes.

Protein	Isoform	Gene symbol	Chromosomal location
Troponin I	Slow skeletal	*TNNI1*	1q32
(TnI)	Fast skeletal	*TNNI2*	11q15.5
	Cardiac	*TNNI3*	19q13.4
Troponin T	Cardiac	*TNNT2*	1q32
(TnT)	Fast skeletal	*TNNT3*	11p15.5
	Slow skeletal	*TNNT1*	19q13.4
Troponin C	Cardiac /	*TNNC1*	3p14.3-p21.3
(TnC)	slow skeletal		
	Fast skeletal	*TNNC2*	20q12-q13.11

Data derived from the following references : TNNI1 [30]; TNNI2 [24,50]; TNNI3 [33]; TNNT2 [31,32]; TNNT1 [29]; TNNT1 [34]; TNNC1[1] [27,51]; TNNC2 [28,50]. [1] *Note that the cardiac troponin I gene has previously been described as TNNC1. The current human genome mapping project (HGMP) nomenclature of the troponin genes is that shown in table 1.*

Organization of the human cardiac troponin I gene promoter

In an attempt to determine the factors required for its expression we have isolated and characterized the human cardiac troponin I gene [7]. Analysis of 1.1 kb of proximal 5'-flanking sequence reveals the presence of a number of potentially important elements. These include putative M-CAT, MEF-3, CACC box, GATA (x2), AT-rich (MEF-2/TATA) and Initiator elements. In addition, eleven copies of a 36-38 bp, chromosome 19-specific, minisatellite sequence were identified. In order to investigate the function of the promoter and to test the importance of these elements we made a series of constructs containing varying lengths of flanking DNA. Transfection of these into neonatal rat cardiac myocytes, using standard procedures as previously described [7] suggested the possibility of both positive and negative regulatory regions within the first 6.5 kb of flanking region but showed that 98 bp of proximal sequence was sufficient to drive a significant level of transcription (data not shown). Within this region there is significant homology between rat, mouse and human genes and a number of the elements described above (figure 1). In all three genes the site of initiation of transcription is located within an Initiator (Inr) element [8] more commonly associated with genes which lack a TATA box. Overlapping the Inr is a consensus GATA element (WGATAR) [9] in reverse orientation and, further upstream, a conserved AT-rich region which forms a potential MEF-2 binding site [10] overlapping a consensus TATA box. A second consensus GATA sequence is located more distally in the human gene again in reverse orientation. In this case the sequence is not fully conserved in the rat or mouse. Finally, a CACC box, similar to that sequence described in myoglobin genes

[11] and cardiac troponin T enhancer [12], is located at the distal end of this region in the human gene. In both rat and mouse genes a more proximal and shorter CACC box is present (see below).

Figure 1. *Alignment of the proximal 98 bp promoter region of the human cardiac troponin I gene with the rat and mouse. The site of initiation of transcription (bold A) lies within an initiator element. Two GATA elements are present in reverse orientation with respect to the direction of transcription. Note that the proximal GATA element overlaps the initiator and that in the distal element the human sequence alone complies fully with the WGATAR consensus. CACC box and Sp1 elements are located at the distal end of the region in the human gene. In the rodent genes a related CACC box sequence is located more proximally (see text). Promoter sequences derived from published data [7,16,47].*

GATA, MEF-2 and CACC box elements are required for maximal expression

In order to further investigate the elements identified within the proximal 98 bp region, we conducted a series of experiments aimed at confirming their ability to bind specific transcription factors, assayed through electrophoretic mobility shift assay (EMSA), and their ability to influence transcription, assayed through transfection of constructs in which individual sites were mutated.

Two GATA elements are contained within the 98 bp proximal promoter region. The GATA family of factors have been implicated directly in cardiac gene regulation [9]: ablation of the GATA-4 gene in knock-out transgenic animals results in incomplete heart formation [13,14] and over-expression of GATA-4 in skeletal muscle can induce expression of cardiac-specific promoters [15]. Moreover, previous experiments have shown that GATA-4 acts as a positive transcriptional regulator of the rat troponin I gene [16]. We therefore examined the function of the GATA elements located in the proximal 98 bp of the human gene. EMSA analysis showed that both the proximal and distal GATA elements bound GATA-4 producing a single characteristic band the identity of which was further confirmed by supershift assay using a GATA-4-specific antibody (figure 2A). Furthermore, as this antibody resulted in a supershift of the majority of the band our data suggest that GATA-4 is the major GATA-binding activity present in neonatal cardiac myocytes. Site-directed mutagenesis of either of the GATA elements in a manner which abrogated DNA-binding activity resulted in a significant

reduction in promoter activity (see figure 3). These data indicate that both GATA elements are required in order to achieve maximal transcription of the 98 bp region although neither is essential for transcription to occur.

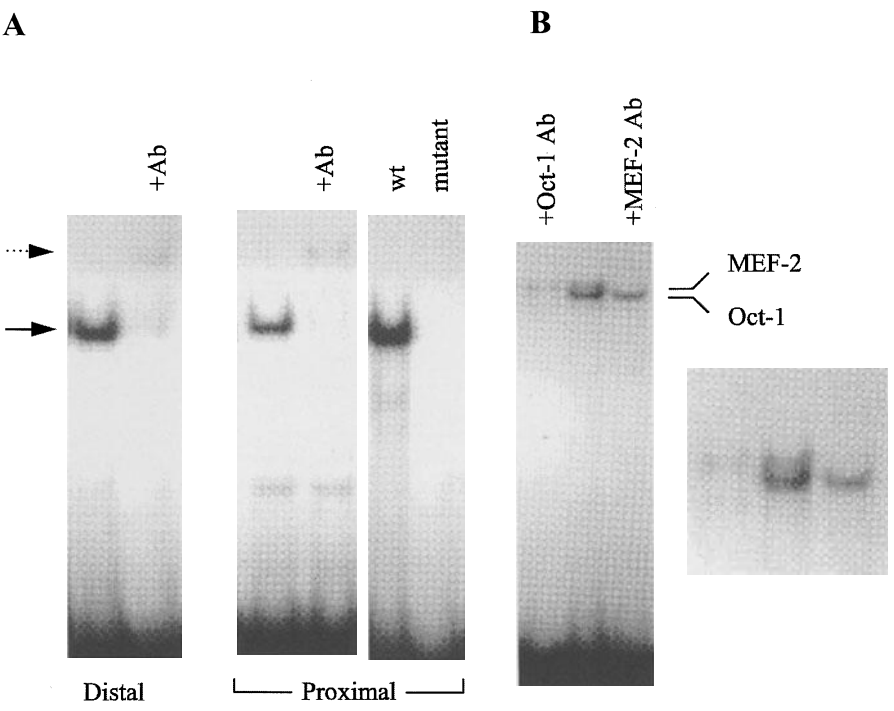

Figure 2. *Analysis of nuclear factors binding to GATA and AT-rich elements. A) EMSA analysis of the proximal and distal GATA elements in the human promoter using neonatal rat cardiac myocyte nuclear extracts. A single major band is identified (solid arrow) which is supershifted on addition of GATA-4 specific antibody (dotted arrow). Shown on the right is the loss of binding seen when the GATA element is mutated (AGATAA → ATCTAA on reverse strand). B) EMSA analysis of the AT-rich element using neonatal rat cardiac myocyte nuclear extracts. Two distinct binding activities of similar mobility are seen (centre track). Addition of antibody specific to MEF-2A/C (right track) or to Oct-1 (left track) results in a supershift of the upper or lower band respectively. A higher magnification is shown on the right.*

The AT-rich element lies in a region which is 100% conserved between the human and rodent genes. Analysis of the factors which bind to this element is complicated by the fact that this region was found to bind both Oct-1 and, more weakly, MEF-2 isoforms (figure 2B), and because it contains a canonical TATA box. Other AT-rich elements have been described with the potential to interact with multiple factors including a

region of the upstream enhancer of the muscle myosin creatine kinase (MCK) gene which can bind MHox, Oct-1 and MEF-2 [17] and the Xenopus MyoDa gene where MEF-2 and TATA box elements overlap [18]. In order to investigate the potential role of MEF-2 and TATA box elements in the cardiac troponin I gene we constructed mutants in which either the MEF-2 or TATA binding potential was ablated in such a way as not to compromize binding of the other factor [18]. Transfection of these constructs (figure 3) showed that ablating MEF-2 binding resulted in partial reduction of promoter activity (60% of wild type) whereas mutation of the TATA box alone had no detectable effect. These data suggest that it is the MEF-2 element and not a TATA box which is important for maximal activity. Further experiments are now required to determine how these contrasting activities may function in vivo and to determine the function of the initiator element in light of the apparent redundant nature of the TATA box. It is also of interest to note that the human slow skeletal muscle troponin I gene, which is expressed in cardiac muscle during development, also contains an initiator sequence [19]. In this case, however, there is no TATA box present upstream.

The human cardiac troponin I gene contains a sequence (CCCACCCC) which is similar to the CACC box present in the human myoglobin gene [11] and both the skeletal [20] and cardiac (CEF-2) [12] enhancers of the murine slow/cardiac troponin C gene [12]. This sequence is not present in the rat or mouse troponin I genes although a more proximal element, identical to the CACC box described in the ß-globin gene (CACACCC) [21], is present in both rat and mouse. It has previously been shown that mutation of either of the myoglobin or troponin C elements results in a significant drop in promoter activity [11,12] and that the myoglobin element can bind at least two factors: a 40kDa protein called CBF40 (for CACC box binding factor) and a winged-helix nuclear protein called MNF (for Myocyte Nuclear Factor) [22,23]. In our experiments, mutation of the CACC box results in a significant reduction in promoter activity (< 30% of control levels) confirming the importance of this element for maximal transcriptional activity of the human cardiac troponin I gene.

Genes for human striated muscle troponin I and T are organized in paralogous pairs

A total of eight troponin genes have been identified in the human genome as summarised in table 1. We recently defined the chromosomal location of the previously unassigned members of these gene families and this has revealed that the genes encoding troponin I and T are organized as paralogous pairs at three chromosomal sites [24]. Chromosomal assignments were made based on PCR amplification of DNA from a 'monochromosomal' somatic cell hybrid panel [25] and from the Genebridge4 radiation hybrid panel [26]. Results of Genebridge4 analysis show the cardiac/slow skeletal muscle troponin C gene (TNNC1) between D3S3118 and GCT4B10 on the short arm of chromosome 3 [27], the fast skeletal muscle troponin C gene (TNNC2) to map between D20S721 and GCT10F11 on chromosome 20 [28] and the fast skeletal muscle troponin I gene (TNNI2) to map to chromosome 11, coincident with D11S922, a marker previously assigned to 11p15.5 [24].

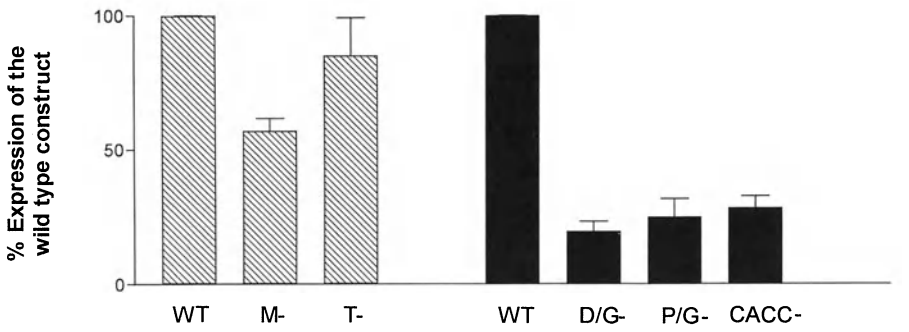

Figure 3. *Analysis of the function of GATA, AT-rich and CACC box elements.* ***Left panel****: Effect of mutation of the AT-rich element to ablate MEF-2 binding (M-: GTATATTTAG → GTATATTAGC) or the TATA-box (T: GTATATTTAG → GTAAATTTAG) compared to the control parental construct (wt) containing 531 bp of proximal promoter linked to the CAT reporter gene in pBLCAT3+.* ***Right panel****: Effect of mutation of the distal (D/G-) and proximal (P/G-) GATA elements (both AGATAA → AGAATT on reverse strand) and CACC element (CCCACCCC → CCCGGTAC) compared to the parental construct. The results show the average of at least 4 independant duplicate transfections into neonatal rat cardiac myocytes (± SEM). All transfections were normalized against a ß-galactosidase control plasmid.*

The fast skeletal muscle troponin T (TNNT3) gene has been previously assigned to 11p15.5 by in situ hybridization [29] and our data therefore demonstrate that the fast skeletal troponin I and T genes map to the same chromosomal region. We therefore sought to investigate linkage between other troponin I and troponin T genes. The slow skeletal muscle troponin I (TNNI1) and cardiac troponin T (TNNT2) genes have both been assigned to 1q32 [30,31] and the cardiac troponin T gene has been identified as the CMH2 (familial hypertrophic cardiomyopathy) locus [32]. A search based on sequence alignment with the sequence tagged site (STS) database revealed matches between the STS elements WI-9272 (100% sequence identity) and exon 1 of the slow skeletal troponin I gene [19], and between D1S1723 (98% sequence identity) and the mRNA sequence of cardiac troponin T [5]. Further analysis of the genome database revealed that these STS elements had been independently located within a single, 370 kb yeast artificial chromosome (YAC) recombinant (970-H-3) contained within contig WC1.18, thereby demonstrating close physical linkage of these genes. Close physical linkage was further confirmed by isolating two independent P1 artificial chromosome (PAC) genomic recombinants (Genome Systems Inc) which both contain the whole of both genes as determined by hybridization with oligonucleotides corresponding to their respective 5' and 3' exons (data not shown). The slow skeletal troponin I and cardiac troponin T genes therefore lie within the 150-170 kb region contained in these PAC

recombinants.

A search using available sequence data failed to identify other mapped STS elements within published troponin gene sequences. However, the cardiac troponin I (TNNI3) and slow skeletal muscle troponin T (TNNI1) genes have been independently localized, in both cases to chromosome 19q13.4 [33,34]. We recently determined the genomic structure of the cardiac troponin I gene [7] and have subsequently analyzed two independent P1 genomic recombinant clones which we have shown to contain the whole of both the cardiac troponin I and slow skeletal troponin T genes by hybridization using oligonucleotides corresponding to their respective 5' and 3' ends. Preliminary analysis of one of these P1 clones reveals that the genes are organized head to tail (in the order cardiac troponin I - slow skeletal troponin T) and lie within 3 kb of each other (figure 4).

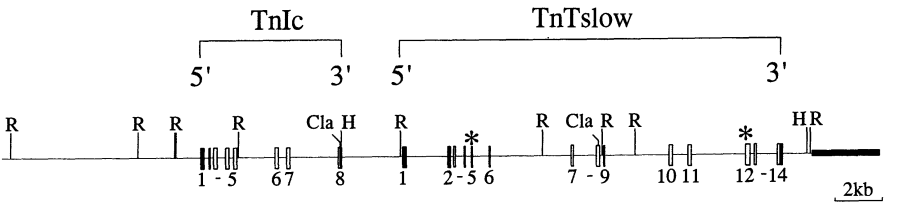

Figure 4. *Structure of the cardiac troponin I and slow skeletal troponin T gene locus. The organization of the locus is based on restriction mapping and sequence analysis of a P1 recombinant clone. Approximate positions of coding exons are shown as open boxes. Filled boxes are non-coding exons. The structure of the cardiac troponin I (TnIc) gene is derived from previous studies [7]. The structure of the slow skeletal troponin T (TnTs) gene is based on preliminary mapping and sequence analysis. Exon sequences were identified by reference to published mRNA sequence [48]. * Denotes exons in the slow skeletal troponin T gene subject to alternative splicing [48,49]. R, H and Cla are restriction sites for EcoR1, HindIII, and ClaI respectively.*

While all sarcomeric proteins, including isoforms of actin, myosin light chain and tropomyosin, are encoded by multigene families, only the myosin heavy chain genes have been previously identified as being linked. These are grouped at two loci, one containing the α- and β- cardiac genes MYH6 and MYH7 [35] the other containing the skeletal muscle genes MYH1-MYH5 [36,37] and probably originated through tandem gene duplication. The functional significance of myosin gene clustering remains unclear but the organisation of the skeletal muscle cluster does not correlate directly with their developmental order of expression [37] as is seen, for example, with the globin [38] and homeobox [39] gene clusters. For the troponin I and T genes the situation is different as pairing is between members of two different gene families where the observed linkage is not easily related to their pattern of expression. For example, while the fast skeletal troponin I and T genes are co-expressed and could, therefore, be co-regulated by a single locus control region, the closely linked cardiac troponin I and slow skeletal

troponin T share no common site of expression in the adult or the embryo.
Their organisation suggests that the troponin genes are derived from triplication of a locus containing an ancestral troponin I/troponin T gene pair resulting in three paralogous chromosomal regions [40]. This raises the possibility that other closely linked genes may exist at each of these three sites as has been demonstrated in other cases [41]. Current data is limited for most other species, but we note that in both Drosophila and C. elegans the single troponin I and troponin T genes are located on the same chromosome [42-44]. A further possibility is that the ancestral locus may have contained a single gene with combined functions of both troponin I and troponin T. In this respect we note that smooth muscle caldesmon acts as the allosteric regulator of actin-myosin interaction and combines functional features of both troponin I and T [45]. If there were a single ancestral gene, separation of two distinct transcription units would have preceded triplication of the locus and the subsequent divergence of the independent patterns of regulation seen in the current human gene pairs. Consistent with this, our data show that the cardiac troponin I and slow skeletal troponin T genes are organized head to tail and are in very close proximity. The third component of the complex, troponin C, is derived from the family of proteins containing the calcium-binding 'EF' hand and has evolved independently in so far as the genes encoding the cardiac/slow skeletal muscle isoform (TNNC2) and the fast skeletal muscle isoform (TNNC1) are located at separate sites on chromosome 20 [28] and 3p [27], respectively. Detailed structural analysis of the troponin I/T gene pairs is now required to determine their precise organisation and whether linkage may be important for their regulation. In particular, close physical linkage has implications for the analysis of mutations involved in familial hypertrophic cardiomyopathy. A large number of mutations in the cardiac troponin T gene have been described which result in this disease. A recent report has described mutations in the cardiac troponin I gene raising the possibility that further troponin genes may also be involved [46]. Close physical linkage will result in co-segregation of both members of each gene pair and any structural rearrangement of the locus could affect expression of both genes. Exclusion of the second troponin gene as possible cause of inherited disease may therefore be a necessary precaution when analysing troponin mutations causing familial hypertrophic cardiomyopathy.

Conclusion

In summary, a total of eight troponin genes have been identified in the human genome and these show distinct patterns of temporal and spatial expression. We have chosen to analyse the human cardiac troponin I gene as a model of developmentally-regulated cardiac-specific gene expression. Functional studies using a series of promoter deletion constructs indicate that a minimal promoter containing 98 bp is sufficient to drive transcription in cardiac myocytes. This region includes an Initiator element, an AT-rich (TATA/MEF-2) element, CACC box and two GATA elements. DNA-binding assays and site-directed mutagenesis demonstrate that each of these elements is important for efficient transcription of the promoter. In parallel studies we have defined the

organization of the troponin gene families and revealed that the six human genes encoding the different troponin I and T isoforms are organized as paralogous pairs located on three different chromosomes. Analysis of the pair comprising the cardiac troponin I and slow skeletal troponin T genes reveals that they are organized head to tail and lie within 3 kb of each other. The functional significance of this linkage remains unclear but is of interest as these genes share no common site of expression in the adult or the embryo.

Acknowledgements

This work was supported by the British Heart Foundation (FS297, PG/93139, PG/96186 and FS/96010). We thank Richard Treisman for the gift of MEF-2A/C antibody, Stephen Orr for assistance with subcloning, Una Sahye for cardiac myocyte preparations, Antony Mullen for PCR cloning and Martin Cullen for assistance with genomic sequence analysis of the slow troponin T gene.

References

1. Parmacek MS, Leiden JM. Structure, function, and regulation of troponin C. Circulation 1991;84:991-1003.
2. Schiaffino S, Gorza L, Ausoni S. Troponin isoform switching in the developing heart and its functional consequences. Trends Cardiovasc Med 1993;3:12-17.
3. Bhavsar PK, Dhoot GK, Cumming DVE, Butler-Browne GS, Yacoub MH, Barton PJR. Developmental expression of troponin I isoforms in the fetal human heart. FEBS Lett 1991;292:5-8.
4. Sasse S, Brand NJ, Kyprianou P, et al. Troponin I gene expression during human cardiac development and in end-stage heart failure. Circ Res 1993;72:932-38.
5. Townsend PJ, Farza H, MacGeoch C, et al. Human cardiac troponin T: identification of fetal isoforms and assignment of the TNNT2 locus to chromosome 1q. Genomics 1994;21:311-16.
6. Townsend PJ, Barton PJR, Yacoub MH, Farza H. Molecular cloning of human cardiac troponin T isoforms: expression in developing and failing heart. J Mol Cell Cardiol 1995;27:2223-36.
7. Bhavsar PK, Brand NJ, Yacoub MH, Barton PJR. Isolation and characterisation of the human cardiac troponin I gene. Genomics 1996;35:11-23.
8. Smale ST, Baltimore D. The "initiator" as a transcription control element. Cell 1989;57:103-13.
9. Evans T. Regulation of cardiac gene expression by GATA-4/5/6. Trends Cardiovasc Med 1997;7:75-83.
10. Brand NJ. Myocyte enhancer factor 2 (MEF2). Int J Biochem Cell Biol 1997;29:1467-70.
11. Bassel-Duby R, Grohe CM, Jessen ME, et al. Sequence elements required for transcriptional activity of the human myoglobin promoter in intact myocardium. Circ Res 1993;73:360-66.
12. Parmacek MS, Vora AJ, Shen T, Barr E, Jung F, Leiden JM. Identification and characterization of a cardiac-specific transcriptional regulatory element in the slow/cardiac troponin C gene. Mol Cell Biol 1992;12:1967-76.
13. Kuo CT, Morrisey EE, Anandappa R, et al. GATA4 transcription factor is required for ventral morphogenesis and heart tube formation. Genes Devel 1997;11:1048-60.
14. Molkentin JD, Lin Q, Duncan SA, Olson EN. Requirement of the transcription factor GATA4 for heart tube formation and ventral morphogenesis. Genes Devel 1997;11:1061-72.
15. Molkentin JD, Kalvakolanu DV, Markham BE. Transcription factor GATA-4 regulates cardiac muscle-specific expression of the α-myosin heavy-chain gene. Mol Cell Biol 1994;14:4947-57.
16. Murphy AM, Thompson WR, Peng LF, Jones II L. Regulation of the rat cardiac troponin I gene by the transcription factor GATA-4. Biochem J 1997;322:393-401.
17. Cserjesi P, Lilly B, Hinkley C, Perry M, Olson EN. Homeodomain protein MHox and MADS protein myocyte enhancer-binding factor-2 converge on a common element in the muscle creatine kinase enhancer. J Biol Chem 1994;269:16740-45.
18. Leibham D, Wong MW, Cheng TC, et al. Binding of TFIID and MEF2 to the TATA element activates transcription of the Xenopus MyoDa promoter. Mol Cell Biol 1994;14:686-99.
19. Corin SJ, Juhasz O, Zhu L, Conley P, Kedes L, Wade R. Structure and expression of the human slow twitch skeletal muscle troponin I gene. J Biol Chem 1994;269:10651-59.
20. Parmacek MS, Ip HS, Jung F, et al. A novel myogenic regulatory circuit controls slow/cardiac troponin C gene transcription in skeletal muscle. Mol Cell Biol 1994;14:1870-85.
21. Myers RM, Tilly K, Maniatis T. Fine structure genetic analysis of a beta-globin promoter. Science 1986;232:613-18.
22. Bassel-Duby R, Hernandez MD, Gonzalez MA, Krueger JK, Williams RS. A 40-kilodalton protein binds specifically to an upstream sequence element essential for muscle-specific transcription of the human myoglobin promoter. Mol Cell Biol 1992;12:5024-32.

23. Bassel-Duby R, Hernandez MD, Yang Q, Rochelle JM, Seldin MF, Williams RS. Myocyte nuclear factor, a novel winged-helix transcription factor under both developmental and neural regulation in striated myocytes. Mol Cell Biol 1994;14:4596-605.
24. Barton PJR, Townsend PJ, Brand NJ, Yacoub MH. Localization of the fast skeletal muscle troponin I gene (TNNI2) to 11p15.5: Genes for troponin I and T are organized pairs. Ann Hum Genet 1997;61:519-23.
25. Kelsall DP, Rooke L, Warne D, et al. Development of a panel of monochromosomal somatic cell hybrids for rapid gene mapping. Ann Hum Genet 1995;59:233-41.
26. Gyapay G, Schmitt K, Fizames C, et al. A radiation hybrid map of the human genome. Hum Mol Genet 1996;5:339-46.
27. Townsend PJ, Yacoub MH, Barton PJR. Assignment of the human cardiac/slow skeletal muscle troponin C gene (TNNC1) between D3S3118 and GCT4B10 on the short arm of chromosome 3 by somatic cell hybrid analysis. Ann Hum Genet 1997;61:375-77.
28. Townsend PJ, Yacoub MH, Barton PJR. Assignment of the human fast skeletal muscle troponin C gene (TNNC2) between D20S721 and GCT10F11 on chromosome 20 by somatic cell hybrid analysis. Ann Hum Genet 1997;61:457-59.
29. Mao C, Baumgartner AP, Jha PK, Huang TH, Sarkar S. Assignment of the human fast skeletal troponin T gene (TNNT3) to chromosome 11p15.5: Evidence for the presence of 11pter in a monochromosome 9 somatic cell hybrid in NIGMS mapping panel 2. Genomics 1996;31:385-88.
30. Eyre HJ, Akkari PA, Meredith C, et al. Assignment of the human slow skeletal muscle troponin gene (TNNI1) to 1q32 by fluorescence in situ hybridisation. Cytogenet Cell Genet 1993;62:181-82.
31. Mesnard L, Logeart D, Taviaux S, Diriong S, Mercadier J, Samson F. Human cardiac troponin T: Cloning and expression of new isoforms in the normal and failing heart. Circ Res 1995;76:687-92.
32. Thierfelder L, Watkins H, MacRae C, et al. Alpha-tropomyosin and cardiac troponin T mutations cause familial hypertrophic cardiomyopathy: a disease of the sarcomere. Cell 1994;77:701-12.
33. Bermingham N, Hernandez D, Balfour A, Gilmour F, Martin JE, Fisher EMC. Mapping TNNC1, the gene that encodes cardiac troponin I in the human and the mouse. Genomics 1995;30:620-22.
34. Samson F, de Jong PJ, Trask BJ, et al. Assignment of the human slow skeletal troponin T gene to 19q13.4 using somatic cell hybrids and fluorescence in situ hybridization analysis. Genomics 1992;13:1374-75.
35. Saez LJ, Gianola KM, McNally EM, et al. Human cardiac myosin heavy chain genes and their linkage in the genome. Nuc Acids Res 1987;15:5443-59.
36. Soussi-Yanicostas N, Whalen RG, Petit C. Five skeletal myosin heavy chain genes are organized as a multigene complex in the human genome. Hum Mol Genet 1993;2:563-69.
37. Yoon SJ, Seiler SH, Kucherlapati R, Leinwand L. Organization of the human skeletal myosin heavy chain gene cluster. Proc Natl Acad Sci USA 1992;89:12078-82.
38. Crossley M, Orkin SH. Regulation of the beta-globin locus. Curr Opin Genet Dev 1993;3:232-37.
39. Krumlauf R. Evolution of the vertebrate Hox homeobox genes. BioEss 1992;14:245-52.
40. Lundin LG. Evolution of the vertebrate genome as reflected in paralogous chromosomal regions in man and the house mouse. Genomics 1993;16:1-19.
41. Katsanis N, Fitzgibbon J, Fisher EMC. Paralogy mapping: identification of a region in the human MHC triplicated onto human chromosomes 1 and 9 allows the prediction and isolation of novel PBX and NOTCH loci. Genomics 1996;35:101-08.
42. Barbas JA, Galceran J, Krah Jentgens I, et al. Troponin I is encoded in the haplolethal region of the Shaker gene complex of Drosophila. Genes Devel 1991;5:132-40.

43. Fyrberg E, Fyrberg CC, Beall C, Saville DL. Drosophila melanogaster troponin-T mutations engender three distinct syndromes of myofibrillar abnormalities. J Mol Biol 1990;216:657-75.
44. Myers CD, Goh P, Allen TS, Bucher EA, Bogaert T. Developmental genetic analysis of troponin T mutations in striated muscle and nonstriated muscle cells of Caenorhabditis elegans. J Cell Biol 1996;132:1061-77.
45. Marston S. Ca^{2+}-dependent protein switches in actomyosin based contractile systems. Int J Biochem Cell Biol 1995;27:97-108.
46. Kimura A, Harada H, Park J, et al. Mutations in the cardiac troponin I gene associated with hypertrophic cardiomyopathy. Nat Genet 1997;16:379-82.
47. Ausoni S, Campione M, Picard A, et al. Structure and regulation of the mouse cardiac troponin I gene. J Biol Chem 1994;269:339-46.
48. Gahlmann R, Troutt AB, Wade RP, Gunning P, Kedes L. Alternative splicing generates variants in important functional domains of human slow skeletal troponin T. J Biol Chem 1987;262:16122-26.
49. Samson F, Mesnard L, Mihovilovic M, et al. A new human slow skeletal troponin T (TnTs) mRNA isoform derived from alternative splicing of a single gene. Biochem Biophys Res Com 1994;199:841-47.
50. Tiso N, Rampoldi L, Pallavicini A, et al. Fine mapping of five human skeletal muscle genes: alpha-tropomyosin, beta-tropomyosin, troponin-I slow-twitch, troponin-I fast-twitch, and troponin-C fast. Biochem Biophys Res Com 1997;230:347-50.
51. Song WJ, Vankeuren ML, Rabkin HA, Cypser JR, Gemmill RM, Kurnit DM. Assignment of the human slow twitch skeletal muscle/cardiac troponin C gene (TNNC1) to human chromosome 3p21.3 -> 3p14.3 using somatic cell hybrids. Cytogenet Cell Genet 1997;75:36-37.

9. RETINOID SIGNALING: INSIGHT FROM GENETICALLY ENGINEERED MICE

Pilar Ruiz-Lozano, and Kenneth R. Chien

Introduction

To dissect the complex molecular and positional cues which guide various states of cardiac morphogenesis, a number of laboratories have employed gene-targeting approaches and examined the physiological role of putative cardiogenic candidate genes. Various of these candidate genes were selected by virtue of their temporal and spatial pattern of expression during cardiogenesis [1], by their functional effects in vitro and in vivo [2,3], or by their ability to control the cardiac gene program [4-11]. A wide variety of defects have been reported that range from abnormalities in the aortic arch/aortic sac, conotruncal, and outflow tract, individual defects in the right and left ventricle, defects in trabeculation, and in the atrioventricular cushions [for review, see 12].

The RXRα model

In particular, the retinoid family of nuclear receptors appear to play an important role in cardiac function. Among the two related families of nuclear retinoid receptors, RARs (encoded by 3 different genes α, β and γ) and RXRs (α, β and γ), both of which are members of the superfamily of ligand-inducible transcriptional regulators. A single mutation of RXRα is necessary and sufficient to yield profound defects in cardiac morphogenesis while RAR receptors have synergistic effects to mutations in RXRα, thus suggesting that RXR/RAR are the physiologically active partners [13,14]. RXRα null mutant mice display malformations in the eye, defects in the ventricular compact zone, and abnormalities in cushion tissue mesenchyme [9,15-16], and die around embryonic day 14.5 from heart failure [17]. Due to the ability of retinoid receptors to regulate transription in a ligand (vitamin A deriatives)-dependent manner, these defects presumably arise as a consequence of individual deficiencies in the cellular mRNA content of particular RXRα target genes. Relatively little is known regarding the downstream target genes which are essential for these steps in cardiac morphogenesis and function, and which must ultimately be under the control of vitamin A signaling pathways.

P.A. Doevendans et al. (eds.), Cardiovascular specific gene expression, 87-97.

Strategies to analyze downstream target genes

Several strategies have been described to search for components of the retinoid signaling pathway, including in vitro studies on retinoic acid responsive cells [16] and direct examination of candidate genes [17]. Via the isolation of in vivo targets of RXRα by subtractive hybridization, we have systematically analyzed the mRNA population that is downregulated in the mutant versus the wild type embryos. To our knowledge, this study provides one of the first reported comprehensive analyses on gene expression based on a genetically modified mouse model and supports the utility of this approach toward the analysis of the growing list of mice which harbor a deficiency in a specific transcription factor. This could be of particular value in the analysis of the diverse pathways regulated by transcription factors and the molecular dissection of the physiological alterations of the growing number of null mutant animal models.

Isolation of RXRα downstream target genes via a directional tag subtraction cloning strategy with cDNA libraries derived from RXRα -/- and wild type embryos

To isolate putative RXRα downstream target genes, we used a subtractive hybridization method to generate a cDNA library of clones that were enriched in the wild type versus the RXRα mutant embryos [18]. Two independent strategies were employed based upon either the generation of whole embryo cDNA (eWpT7 and eKpG) or embryonic cardiac ventricle (vWpT7 or vKpG) libraries derived from wild type and RXRα -/- day 13.5 embryos [18]. Subtraction was performed either through eWpT7 *minus* eKpG, or by vWpT7 *minus* vKpG. Purified single stranded fractions corresponding to mRNAs enriched in the wild type were separated, PCR amplified, and cloned to yield the wild-type subtracted libraries (eSpT7 and vSpT7), where 96% of the input target was removed (figure 1A). Subsequently, we picked and arrayed 432 clones randomly from the subtracted cDNA libraries and hybridized replica filters with the subtracted, the unsubtracted wild type whole embryo (target) and the unsubtracted mutant whole embryo (driver) cDNA probes. These cDNA clones, enriched in the subtracted probe and non detectable with the driver probe, were selected as candidates for RXRα downstream mRNAs (figure 1B). We determined the cDNA sequence of 115 selected clones, which resulted in the identification of three classes of cDNAs (table 1). A portion of the subtracted clones represented novel sequences, which displayed both ubiquitous and tissue-restricted pathways of expression

Differential expression pattern of selected cDNAs during embryonic development of wild type versus RXRα-/- embryos

We analyzed the differential expression of a group of subtracted clones from the wild-type mouse embryo day 13.5 and compared this to the expression pattern in RXRα null mutant littermates by either in situ hybridization (ISH) on paraffin-embedded embryos or Northern blot analysis of total RNA samples. A summary of validated clones is

shown in table 1 and several examples are provided in figure 2. In particular, clone G1, encoding the 14.5b subunit of the NADH-ubiquinone oxidoreductase (mitochondrial Complex I), was ubiquitously expressed in the wild-type and showed a markedly reduced expression in the RXRα -/- embryo (figure 2A). Atrial myosin light chain-2 (MLC-2a) was persistently expressed in the RXRα mutant ventricles (figure 2), as previously described [17].

A significant number of the subtracted cDNAs (50%; 61/115) encoded known enzymes involved in energy metabolism. For instance, clone G1 encodes the 14.5b subunit of the NADH-ubiquinone oxidoreductase complex [19], and appeared 33 times in the subtracted library. Other clones involved in energy metabolism were also found in the subtracted library, including NADH-I , Fructose 1,6 bisphosphate aldolase [20]; and the glucagon receptor [21,22].

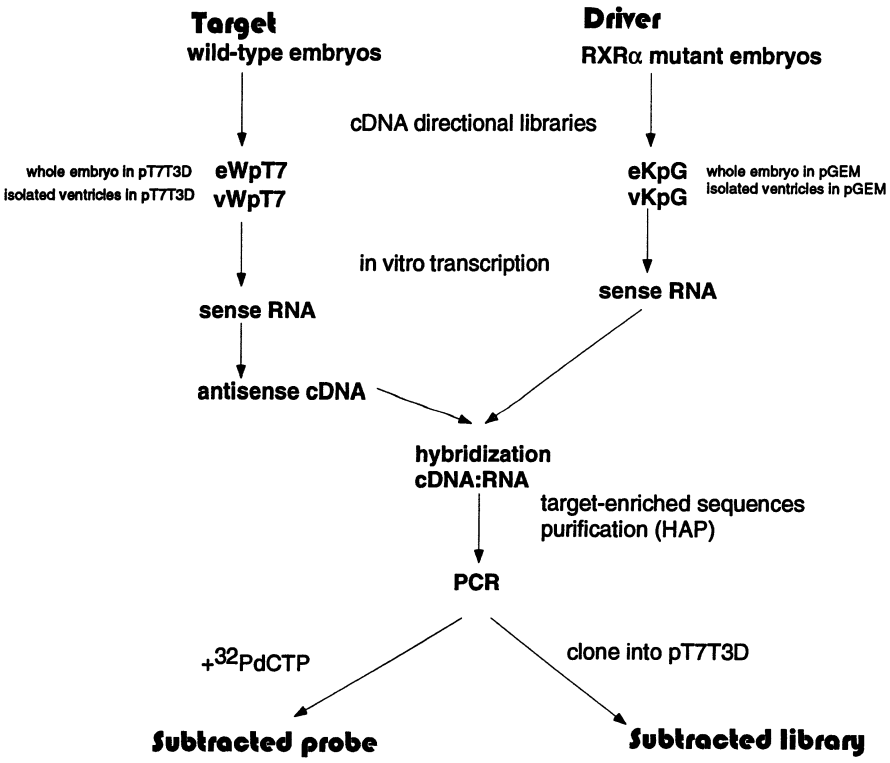

Figure 1A. *Differential screening of the subtracted RXRα cDNA library. Strategy of subtraction: Directional cDNA libraries from either whole embryo or isolated cardiac ventricles were generated in two different phagemid vectors. Inserts were in vitro transcribed and antisense target cDNA was hybridized to sense driver cRNA. Target-enriched sequences were purified by HAP chromatography and used to generate either the subtracted probe or the wild type subtracted library.*

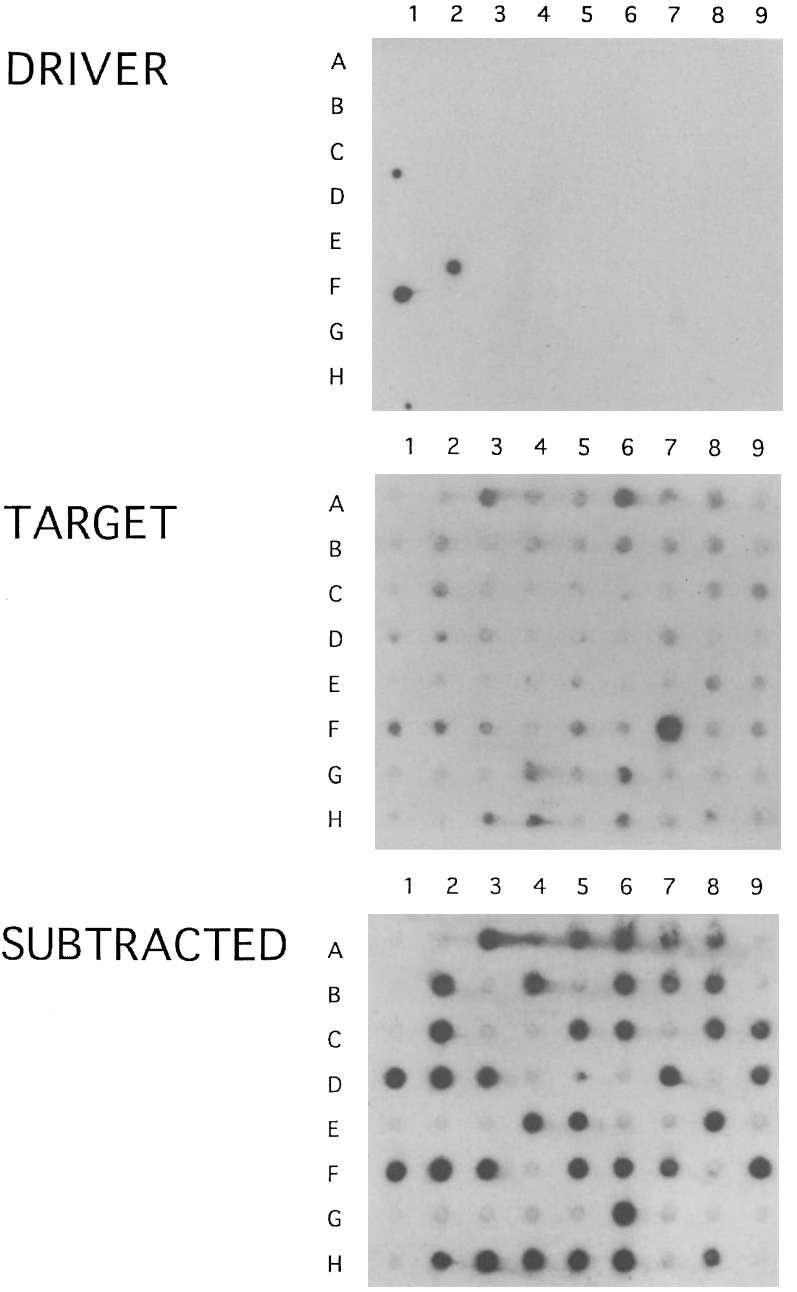

Figure 1B. *Differential screening of the subtracted RXRα cDNA library. Clones from the RXRα+/+ minus RXRα-/- subtracted libraries were picked and arrayed to make replica filters. Each filter was hybridized with unsubtracted RXRα -/- cDNA probe (DRIVER), unsubtracted RXRα +/+ cDNA probe (TARGET), or RXRα +/+-minus-RXRα -/- SUBTRACTED cDNA probe.*

Selective energy deprivation in the embryonic hearts of RXRα -/- embryos

To initially assess energy status in the RXRα mutant, we determined the ATP content in different embryonic tissues. ATP content in skeletal muscle and fetal liver was similar in the three RXRα genotypes. In contrast, a 60% reduction of the ATP content per milligram of total protein was observed in the isolated ventricles of RXRα null mutant embryos. Heterozygotes displayed an ATP concentration similar to wild-type samples in every tissue measured (figure 3). These data were reproduced in three independent experiments, using a total of 20 embryos (6 wild-type, 9 heterozygous, 5 homozygous). These results suggest that mutations affecting mitochondrial oxidative systems have pronounced effects in organs, such as heart, that are more reliant on oxidative energy production. In the systematic examination of putative downstream target genes by this subtraction cloning strategy, we have found that a high proportion of the subtractive clones encode proteins involved in energy metabolism. For example, bovine heart Complex I is composed of 41 different subunits and is the largest proton-translocating oxidoreductase in the mitochondria respiratory chain [23,24]. This complex catalyzes the transfer of electrons from NADH to ubiquinone which is coupled with a vectorial transfer of protons across the mitochondrial membrane, thereby driving ATP formation (for a review, see [25]). Interestingly, in the RXRα-deficient embryos, there was a virtual complete deficiency in the subunit 14.5b of Complex I. Since subunit 14.5b of Complex I (clone G1) was present at a 50% level in the RXRα heterozygous deficient embryos, this relationship supports the concept that this gene may indeed be a direct target of RXRα during the course of cardiac development in a manner dependent on RXRα gene dosage. G1 mRNA mis-expression in retinoid-deficient rat embryos further supports a direct role of ligand-activated retinoid receptors on the regulation of metabolic genes.

Subclass	Sequence Homology /Motif	Embryonic expression pattern	Frequency	Downregulation, as per in situ hybridization
Metabolic genes				
G1	14.5bNADH-Q DH	Ubiquitous	33	Yes
w85	NADH-I	Tongue, pituitary	7	Yes
3v12	Glucagon receptor	Ubiquitous	7	Yes
3v11	F1,6 bP aldolase	Ubiquitous	10	Yes
3v16	Phosphorylase	Ubiquitous	4	Yes
Novel genes				
C8	Novel	Fetal liver	12	Yes
3v2	Novel	Ubiquitous	3	Yes
B2	Novel	Fetal liver	8	Yes
10v2v5	Novel	Heart	1	No
B8	Novel	Skeletal muscle	2	No
Other				
w70	CARP *	Cardiac muscle	4	Yes
v17	PSD-95	Ubiquitous	2	Yes
3v9	Rhodopsin	Skeletal, brain, neural	7	Yes
4G6	Mitochondrial DNA		15	ND
		TOTAL	115	

Table 1. *Subclassification of subtracted cDNA clones isolated from wild type versus RXRα -/- mouse embryos 13.5. Name of the subtracted clones, sequence homology and frequency of a determined sequence among isolated clones are indicated. Individual clones were analyzed independently by in situ hybridization. Whether they were differentially expressed (downregulated) in the mutant RXRα compared to the wild-type embryos is indicated in the right column. (ND; not determined) (From [18], with permission).*

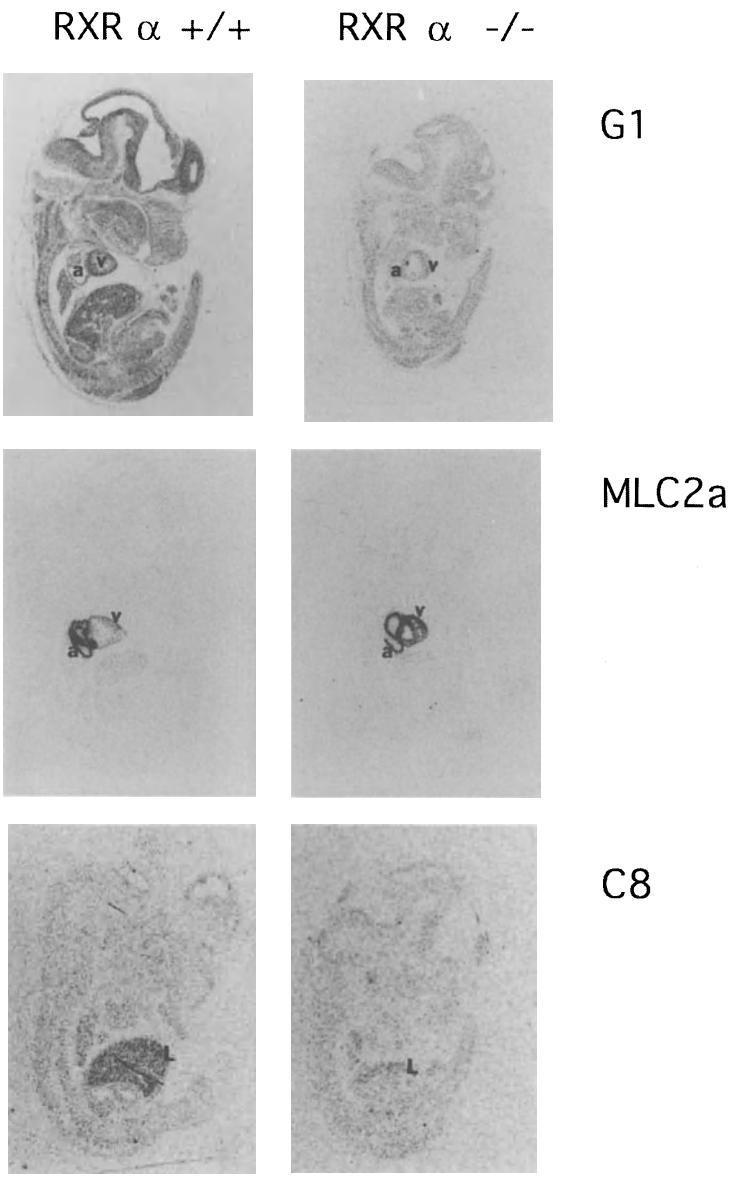

Figure 2. *Differential expression of mRNAs in RXRα targeted embryos, as revealed by in situ hybridization. A Midsagittal sections through wild type (RXRα +/+) or null mutant (RXRα -/-) embryonic day 13.5 littermates were hybridized with riboprobes for the selected subtracted clones, G1 (NADH:ubiquinone oxidoreductase), or the novel cDNA clone C8, displayed a reduced but detectable expression in the mutant animal. Note the persistent ventricular expression of MLC-2a in the mutant heart. The atrial myosin light chain (MLC-2a) antisense riboprobe was used as a control for the integrity of the RNA in both embryos, as well as a control for the aberrant expression in the RXRα mutant null embryo (as reported in Dyson et al., 1995). The name of each probe is shown in the right panel. v, ventricle; a, atria; L, liver. (From [18], with permission).*

A severe deficiency in this component would be expected to act in the mitochondrial respiratory chain in a manner analogous to the delivery of respiratory inhibitors that work at the ubiquinone step, such as synthetic capsaicin analogs [26]. Therefore, ATP depletion would be expected to be particularly prominent in organ systems which are highly dependent on high energy phosphates for the maintenance of normal function. Since the heart requires ATP for the maintenance of its normal contractility, and displays a high degree of ATP utilization to maintain this function [27], it would be expected that any impairment in this process might first appear in cardiac tissues. Consistent with this notion, the ATP levels in the ventricles of RXRα-deficient embryos were significantly lower than control, and approached levels that are consistent with marked energy deprivation. Thus, associated with this deficiency in the mitochondria respiratory chain, there is clear evidence of energy deprivation. This effect appeared to be selective for the heart, as ATP content in other tissues within the mutant embryo were maintained at control levels. The specific decrease in ATP content in the mutant heart may imply a metabolic deficiency for which the heart is a more sensitive tissue.

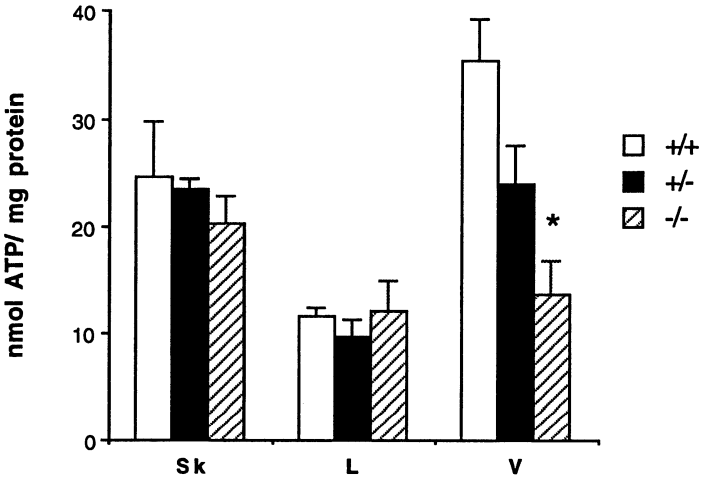

Figure 3. *ATP content. ATP content was measured in different embryonic tissues of various RXRα embryos (+/+, wild type; +/-, heterozygote and -/-, null mutant). Tissues were: Skeletal muscle (Sk), liver (L) and ventricle (V). ATP measures were normalized as nmol of ATP per milligrams of total protein. Data are plotted as mean values and standard error. *: Value statististically significant from control as per one factor ANOVA analysis (p <0.05) (From [18], with permission).*

The RXRα cardiac phenotype may represent a secondary effect of RXRα on metabolic pathways and consequent dilated cardiomyopathy

The phenotype seen in RXRα deficient hearts is mimicked by a diversity of mice that harbor deficiencies in a wide variety of transcriptional factors and other signaling molecules, including WT-1, βARK-1, myc, and TEF-1 (reviewed in [12]). This phenotype, known as the "thin myocardial wall syndrome" [28], has been thought to be due to a maturational arrest in ventricular lineages, reflecting an inherent defect in

myocardial proliferation and/or to be an index of relative hypoplasia of the ventricular wall. However, given that the current study shows direct evidence for severe energy deprivation and down-regulation of genes associated with cardiomyopathy in the human setting, a distinct alternative possibility exists that the RXRα phenotype, and perhaps the other phenotypes as well, actually represent the process of chamber dilation that is seen in the setting of adult heart failure. This view is supported by the recent finding that the requirement for RXRα in preventing "thin wall myocardial" syndrome is not in ventricular muscle cells per se [29].

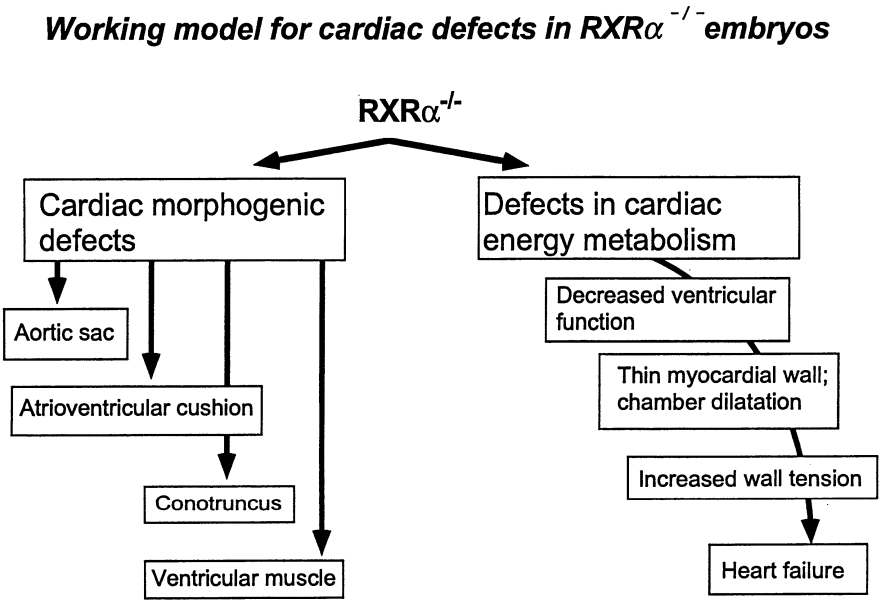

Figure 4. *Working model for the onset of ventricular chamber dysmorphogenesis in RXRα -/- embryos. RXRα deficiency affects the expression of genes responsible for morphogenesis and genes that regulate embryonic metabolism. A severe energy deprivation exists due to the down-regulation of metabolic target genes associated with cardiomyopathy . Subsequent to a decrease in ventricular function, the chamber dilation, thinning of the ventricular wall, and ultimately heart failure ensue as a secondary event.*

In the mouse, and in other species, including man, heart failure is associated with cardiac chamber dilatation and a thinning of the ventricular wall. This phenotype is also seen in MLP-deficient mice (see Chapter 4), which display cardiac chamber dilation during the onset of cardiomyopathy and heart failure [30]. The finding of embryonic heart failure, as documented by a decrease in cardiac contractility [17], in combination with the current study which identifies downstream metabolic target genes for RXRα, are suggestive of a mechanistic model in which RXRα regulates at least two separate sets of genes: genes responsible for morphogenesis and genes that control energy status. Alterations in the expression of cardiac morphogenetic genes would result in defects in the aortic sac, atrioventricular cushion, conotruncus or ventricular muscle. A deficiency

in maintaining energy status of cardiac muscle would result in a decrease in ventricular chamber function [31], concomitant dilatation and thinning of the myocardial wall, leading to increased wall tension and finally heart failure (figure 4). Our studies [18] underscore the importance of the maintenance of mouse cardiac function in the course of cardiac chamber morphogenesis, even though we can not rule out the possibility of a certain degree of cross-talk between both pathways. Taken together, we propose a model whereby the relative thinning of the ventricular wall and dysmorphogenesis of the ventricular chamber in the RXRα deficient mice may represent a secondary effect at the onset of a dilated cardiomyopathy due to energy deprivation as a result of dysregulation of a panel of metabolic target genes. Further studies on the mechanistic role of both the morphological and metabolic target genes in specific cardiac morphogenic defects are required to critically test this model.

Conclusion

We have used subtracted hybridization to investigate the molecular basis of retinoid associated cardiomyopathy and have identified a collection of metabolic genes that suggest an intriguing relationship between cardiac morphogenesis and cardiac performance. This type of form and function linkage has not been previously described and may have broader applications to other developmental systems.

Acknowledgments

P.R-L is a recipient of a F32 INSRA. K.R.C. is a recipient of NIH grants, HL46345, HL53773, HL51549, and HL55926.

References

1. Lints T J, Parsons LM, Hartley L, Lyons I, Harvey R P. Nkx2.5, a novel murine homeobox expressed in early heart progenitor cells and their myogenic descendants. Development 1993;119:419-31.
2. Srivastava D, Cerjesi P, Olson EN. New subclass of bHLH proteins required for cardiac morphogenesis. Science 1995;270,1995-99.
3. Srivastava D, Thomas T, Lin Q, Kirby ML, Brown D, Olson EN. Regulation of cardiac mesodermal and neural crest development by the HLH transcription factor dHAND. Nat Genet 1997;16:154-60.
4. Jiang Y, Evans T. The Xenopus GATA-4,5,6 genes are associated with cardiac specification and can regulate cardiac-specific transcription during embryogenesis. Dev Biol 1996;174:258-70.
5. Murphy AM, Thompson WR, Peng LF, Jones L. Regulation of the rat cardiac troponin I gene by the transcription factor GATA-4. Biochem J 1997;322:393-401.
6. Lyons GE, Micales BK, Schwarz J, Martin JF, Olson EN. Expression of Mef2 genes in the mouse central nervous system suggests a role in neuronal maturation. J Neurosci 1995;15;5727-38.
7. Kuo CT, Morrisey EE, Anandappa R, Sigrist K, Lu MM, Parmacek MS, Soudais C, Leiden JM. GATA-4 transcription factor is required for ventral morphogenesis and heart tube formation. Genes Dev 1997;11:1048-60.
8. Molkentin JD, Lin Q, Duncan SA, Olson EN. Requirement of the trancription factor GATA-4 for heart tube formation and ventral morphogenesis. Genes Dev 1997;11:1061-72.
9. Sucov HM, Dyson E, Gumeringer CL, Price J, Chien KR, Evans RM. RXRα mutant mice establish a genetic basis for vitamin A signaling in heart morphogenesis. Genes Dev 1994;8:1007-18.
10. Moens CB, Stanton BR, Parada LF, Rossant J. Defects in heart and lung development in compound heterozygotes for two different targeted mutations at the N-myc locus. Development 1993;119:485-99.
11 Chen Z, Friedrich GA, Soriano P. Transcriptional enhancer factor 1 disruption by a retroviral gene trap leads to heart defects and embryonic lethality in mice. Genes Dev 1994;8:2293-2301.
12. Fishman MC, Chien KR. Fashioning the vertebrate heart: the earliest embryonic decisions. Development 1997;124:2099-117.
13. Kastner P, Mark M, Ghysenlicck N, Krezel W, Dupe V, Grondona JM, Chambon P. Genetic evidence that the retinoid signal is transduced by heterodimeric RXR/RAR functional units during mouse development. Development 1997;124:313-26.
14. Lee RY, Luo J, Evans RM, Giguere V, Sucov HM. Compartment-selective sensitivity of cardiovascular morphogenesis to combinations of retinoic acid receptor gene mutations. Circ Res 1997;80:757-64.
15. Kastner P, Grondona J, Mark M, Gansmuller A, LeMeur M, Decimo D, Vonesch JL, Dolle P, Chambon P.Genetic analysis of RXRα developmental function: convergence of RXR and RAR signaling pathways in heart and eye morphogenesis. Cell 1994;78:987-1003.
16. Jonk LJ, Jonge ME, Vervaat JM, Wissink S, Kruijer W. Isolation and developmental expression of retinoic-acid induced genes. Dev Biol 1994;161:604-14.
17. Dyson E, Sucov HM, Kubalak SW, Schmid-Schönbein G, Delano FA, Evans RM, Ross J Jr, Chien KR. Atrial-phenotype is associated with embryonic ventricular failure in retinoid X receptor α -/- mice. Proc Natl Acad Sci USA 1995;92:7386-90.
18. Ruiz-Lozano P, Smith SM, Perkins G, Kubalak SW, Boss GR, Sucov HM, Evans RM, Chien KR. Energy deprivation and a deficiency in downstream metabolic genes during the onset of embryonic heart failure in RXRα-/- embryos. Development 1998;125:533-44.
19. Arizmendi JM, Sketel JM, Runswich MJ, Fearnley IM, Walker JE. Complementary cDNA

sequences of two 14.5 kDa subunits of NADH:ubiqunone oxidoredusctase from bovine heart mitochondria. Completion of the primary structure of the complex? FEBS Lett 1992;313:80-84.

20. Buono P, Paolella G, Mancini FP, Izzo P, Salvatore F. The complete nucleotide sequence of the gene coding for the human aldolase C. Nucleic Acids Res 1998;16:4733.
21. MacNeil DJ, Occi JL, Hey PJ, Strader CD, Graziano MP. Cloning and expression of a human glucagon receptor. Biochem Biophys Res Commun 1994;198:328-34.
22. Lok S, Kuijper JL, Jelinek LJ, Kramer JM, Whitmore TE, Sprecher CA, Mathewes S, Grant FJ, Biggs SH, Rosenberg GB. The human glucagon receptor encoding gene : structure, cDNA sequence and chromosomal localization. Gene 1994;140:203-09.
23. Walker JE, Skenel JM, Buchanan SK. Structural analysis of NADH;ubiquinone oxidoreductase from bovine heart mitochondria. Methods Enzymol 1995;260:14-34.
24. Pilkington SJ, Arizmendi JM, Fearnley IM, Runswich MJ, Skehel JM, Walker JE. Structural organization of complex I from bovine mitochondria. Biochem. Society Transaction 1993;21:26-31.
25. Ohnishi T. NADH-Quinone oxidoreductase, the most complex Complex. J. Bioenerg Biomembr 1993;25:325-29.
26. Satoh T, Miyoshi M, Sakamoto K, Iwamura H. Comparison of the inhibitory action of synthetic capsaicin analogues with various NADH:ubiquinone oxidoreductases. Biochem Biophys Acta 1996;1273:21-30.
27. Kelly DP, Strauss AW. Inherited cardiomyopathies. New Engl J Med 1994;330:913-19.
28. Rossant J. Mouse mutants and cardiac development: new molecular insights into cardiogenesis. Circ Res 1996;78:349-53.
29. Chen J, Kubalak SW, Chien KR. Ventricular muscle-restricted targeting of the RXRα gene reveals a non-cell autonomous requirement in cardiac chamber morphogenesis. Development 1998;125:1943-49.
30. Arber S, Hunter JJ, Ross J Jr, Hongo M, Sansig G, Borg J, Perriard J-C, Chien KR, Caroni P. MLP-deficient mice exhibit a disruption of cardiac myofibrillar organization, dilated cardiomyopathy, and heart failure. Cell 1997;88:393-403.
31. Neubauer S, Horn M, Cramer M, Harre K, Newell JB, Peters W, Pabst T, Ertl G, Hahn D, Ingwall JS, Kochsiek K. Myocardial phosphocreatine-to-ATP ratio is a predictor of mortality in patients with dilated cardiomyopathy Circulation 1997;96:2190-96.

10. VENTRICULAR EXPRESSION OF THE ATRIAL REGULATORY MYOSIN LIGHT CHAIN GENE

Pieter A. Doevendans, Ronald Bronsaer, Pilar Ruiz-Lozano, Jan Melle van Dantzig, and Marc van Bilsen

Introduction

The techniques of molecular biology have opened new diagnostic pathways in clinical cardiology. These pathways include the molecular genetic analysis of families with cardiac diseases like hypertrophic cardiomyopathy and dilated cardiomyopathy (DCM). Although four chromosomal loci are associated with the inherited form of DCM, the genes involved are still unknown [1]. In most patients with dilated cardiomyopathy inheritance appears less important and the etiology remains obscure.

To assess the clinical value of changes in gene expression, in unraveling mechanisms of cardiac failure, molecular diagnostic routes are being evaluated. These techniques include *in situ* hybridization to detect viral RNA and Northern blotting to unmask changes in gene expression associated with the development of DCM. In addition, Western blotting and immunohistochemistry can be used to evaluate changes at the protein level. These studies can be conducted in human tissue samples either obtained by endomyocardial biopsy, or from explanted hearts. As the availability of human tissue is limited, initial studies have been conducted in animal models. Specific questions concerning transcription can be addressed *in vitro* in cultured neonatal rat ventricular myocytes (NRVM). Under these artificial circumstances myocyte hypertrophy can be induced by hormonal and cytokine stimuli.

Recent studies reported distinctive morphological changes in hypertrophic NRVM mediated by alternative gene programs. For instance, stimulation of cardiomyocytes by cardiothrophin-1 through a Gp130 signaling pathway leads to elongation of cells, and the induction of atrial natriuretic protein (ANP), while the α-skeletal actin level is unaffected [2]. In contrast, phenylephrine stimulation leads to broadening of the myocytes through G-protein signaling activation and induction of both ANP and α-skeletal actin [3]. In hypertrophic transgenic mice overexpressing Ras (a central intracellular signaling protein), ANP and brain natriuretic peptide (BNP) are upregulated, without changes in the levels of sarcomeric proteins. The changes in gene expression depend on the inducing stimuli and subsequent activation of signaling

P.A. Doevendans et al. (eds.), Cardiovascular specific gene expression, 99-116.

pathways [2-4]. These studies suggest that different hypertrophic conditions resulting in changes in myocyte morphology and function are associated with different molecular fingerprints. Whether evaluation of the molecular fingerprint will be helpful to determine the cause of cardiac disease remains to be determined. The molecular make up of cardiomyocytes could potentially be used as a prognostic marker, as has been demonstrated for excreted peptides like BNP [5-7].

The myosin light chains (MLC) present an interesting family of genes as they can be used as molecular markers for chamber specification during cardiogenesis. In addition, mutations in the MLC genes can give rise to familial hypertrophic cardiomyopathy. The essential (MLC-1) and regulatory (MLC-2) proteins are part of the hexameric myosin complex (figure 1). Different cell types express related isoforms derived from distinct genes (table 1). The usefulness of the cardiac MLC-2 genes, as markers for chamber formation during murine embryonic development was demonstrated in several studies[8,9]. The ventricular isoform (MLC-2v) is expressed from day 8 post coitum (pc) initially in ventricular cardiomyocytes and later in slow skeletal muscle. In contrast the atrial isoform (MLC-2a) is active in the entire heart tube including the ventricular prechamber, and becomes restricted to atrial cardiomyocytes around day 10 (figure 2). In homozygous retinoid X receptor α (RXR-α) deficient mice, persistent expression of the MLC-2a gene in ventricular cardiomyocytes was found. The maturation of the ventricular tissue was impaired leading to a thin wall, diminished trabeculation and septal defects. The murine embryos died around day 14-15 pc, due to cardiac failure[10, 11].

Table 1. Mammalian regulatory, phosphorylatable myosin light chains.

Gene	Nomenclature	Expression
MLC-2 fast	MLC-2f	Fast skeletal muscle [45]
MLC-2 slow/ventricular	MLC-2s, MLC-2v	Slow skeletal/ventricle muscle [9]
MLC-2 mandibular	MLC-2m, MYL5	Mandibular muscle, fetal skeletal muscle [46]
MLC-2 atrial	MLC-2a	Atrium [8]
MLC-2 sm	MLC- C20	Smooth muscle and non-muscle [47]

The pattern of the MLC-2a gene during embryonic development makes the gene an interesting molecular target to study. Potentially under pathologic conditions MLC-2a could be re-expressed in ventricular myocytes under hypertrophic or failing conditions as part of a re-activated fetal gene program.

In this study we report the identification of the MLC-2a promoter. The behavior of the endogenous MLC-2a gene in cultured and stimulated NRVM and hypertrophic adult rat ventricular tissue was studied. In addition, deletion fragments of the MLC-2a promoter driving luciferase were used to analyze the activity of the MLC-2a promoter in transfected NRVM under various hypertrophy stimuli.

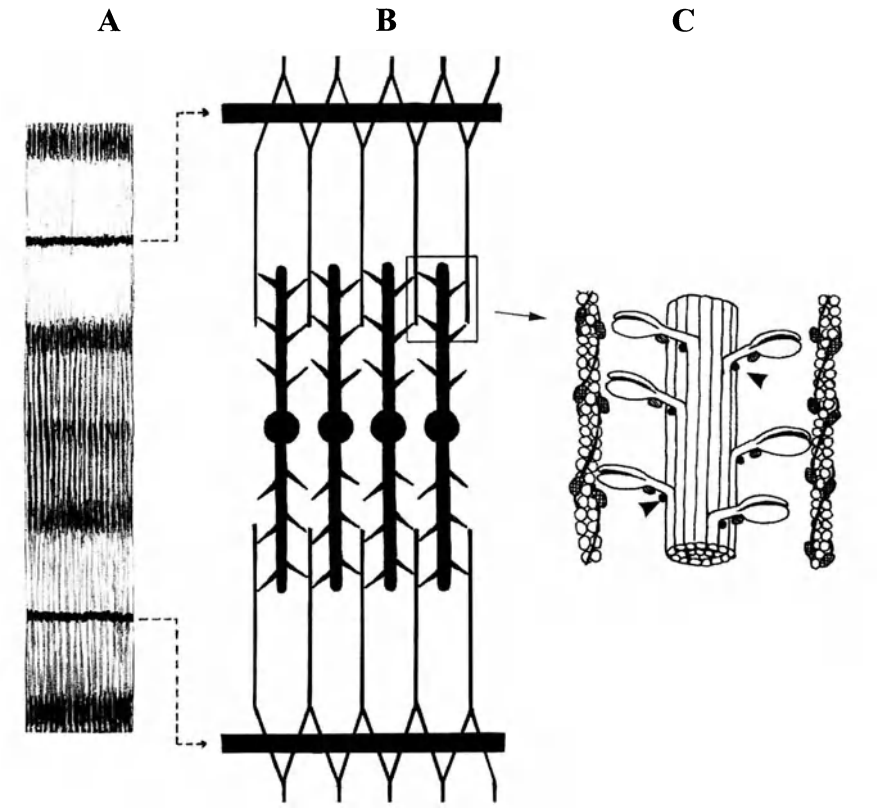

Figure 1. *Schematic representation of striated muscle. A) The microscopic aspect of the cross striations and the various structural units composing the sarcomere in a relaxed state. B) Schematic drawing showing the thin and thick filament and their position at the same magnification as panel A. C) Proteins assembled in the sarcomere with the myosin crossbridges interacting with actin. The position of the MLC-2 is indicated at the neck of the myosin molecules (arrow). Note the position of the regulatory myosin light chain at the hinge of the tail and neck of the myosin heavy chain.*

Methods

Isolation of genomic clones of the murine MLC-2a gene

The murine clone of the MLC2a gene was isolated from the 129SVJ mouse-liver genomic library in Lambda FIX ®II Vector (Stratagene, La Jolla Ca). This library has an average insert size varying form 9.0 to 22.0 Kb. In brief, the cloning procedure wa as follows: Y1090 R^- *E. coli* bacteria were grown overnight in the presence of 0.2% maltose and incubated with a dilution of the library at 20.000 pfu per 600 µl cells for each 90 mm NZY plate. From each plate duplicate filters (Hybond-N, Amersham, Buckinghamshire UK) were lifted. The filters were treated by alkaline solutions to denature DNA, and were UV cross linked at a wave length of 312 nm for 3 minutes. Filters were prehybridized for 30 minutes in SSPE, (0.9M NaCl, 0.05M Sodium

Phosphate, 5mM EDTA), Denhardt's solution (0.1% bovine serum albumine, 0.1% Ficoll™, 0.1% Polyvinylpyrrolidone) and 0,5% SDS. Hybridization was performed using 400 bp of the murine MLC-2a cDNA as a probe [8]. For the hybridization 500.000 cpm/ml of heat denatured probe was added with 100 µg/ml of sonicated denatured salmon sperm DNA. Hybridization was performed overnight at 65°C and followed by high stringency washes going to 0.1x SSPE and 0.1% SDS at 65°C. The filters were wrapped in SaranWrap and positioned in a cassette with Kodak X-Omat (Rochester, NY) film for autoradiography. After three rounds of screening pure phage colonies could be selected and amplified

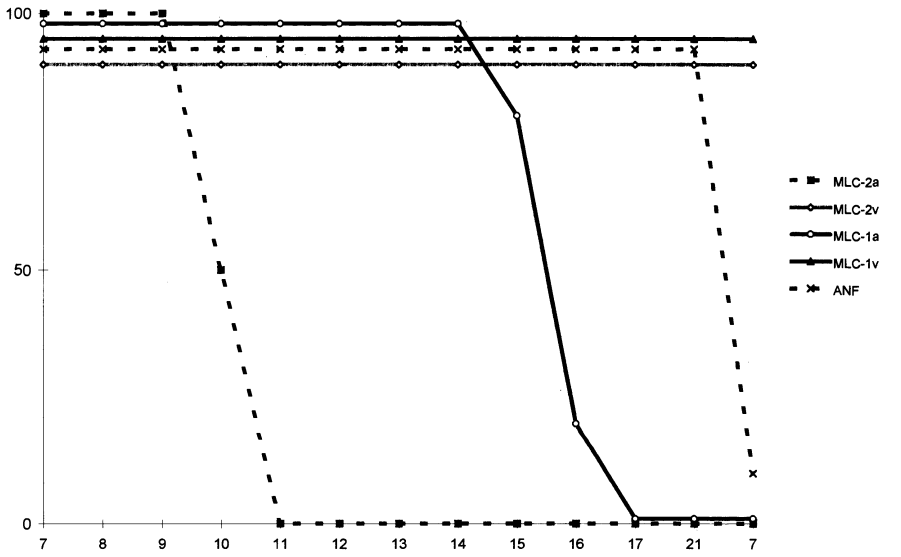

Figure 2. *Relative expression levels of ventricular (MLC-1v and 2v) and atrial (MlC-1a and 2a) myosin light chain genes and atrial natriuretic peptide in ventricular myocytes during embryonic development (days post coitum) and one week post partum (pp). Data are based on visual interpretation of in situ hybridization and northern blot results (semiquantitative).*

Characterization of genomic clones of the MLC-2a gene

All the primers listed in the methods section are shown in the 5'-3' orientation.

Candidate clones were characterized by restriction analysis. The restriction fragments were size fractionated by gel electrophoresis and transferred to a Hybond-N (Amersham) filter by capillary transfer. Filters were subsequently used for Southern analysis. To identify the 5' end of the cDNA an oligonucleotide was generated complimentary to GTTGTGCCTGCTTGGT (39-55), and for the 3' end the oligonucleotide GGCTCACCTCAATAAA (545-566) [8]. In order to identify the transcription initiation site of the MLC-2a gene, primer extension and the 5' rapid amplification cDNA ends (RACE, GibcoBRL, Gaithersburg MD) kit was used. The

template for these reactions was poly A purified murine mRNA from adult mouse atrial tissue. RNA was isolated by the RNAzol method (Cinna Biotecx, New York, NY) and poly A selected by using a poly-T column. Of the isolated mRNA 1 μg was used for the 5' RACE reaction to identify the transcription start site.
Sequencing was carried out according to the method of Sanger et al. [12]. Cycle sequencing was performed with ABI Prism Dye Terminator Cycle Sequence Ready Reaction kit (Perkin Elmer, Norwalk CT).

Neonatal Rat Ventricular Myocyte culture
Animals were handled according to the guidelines of the Animal Welfare Committee of the University of Maastricht. Cultured NRVM were prepared as previously described [13]. In brief, myocytes were isolated from the ventricles of 1-2 day old Wistar Kyoto rats by digestion with Collagenase II (Worthington, Lakewood NJ) and pancreatin (GibcoBRL, Paisley UK) at 37°C in a spinner flask. Purification of the cell suspensions was performed on a discontinuous Percoll gradient (Sigma Chemical Co, St Louis MO). The myocytes were plated in gelatinized 60 mm culture dishes at low density ($3.5x10^4$ cells/cm^2), in Dulbecco's modified Eagle Medium (DMEM) (Gibco BRL, cat no: 42430-025) and medium 199 (Gibco BRL, cat no: M199, 31153-026) 4:1 (v/v) supplemented with 10% horse serum and 5% fetal calf serum, (Sera-lab, Sussex England) and antibiotics (100 units/ml penicillin and 100 μg/ml streptomycin, GibcoBRL). Following overnight attachment in this medium the cells were washed twice with DMEM, and incubated with DMEM/medium199 (4:1; v/v) supplemented with glutamine and antibiotics. For myocyte stimulation studies the cells were incubated for 48 h in serum-free DMEM, containing glutamine and antibiotics in the presence of either 10^{-5} M phenylephrine (PE; Sigma), 10^{-8} M endothelin-1 (ET-1; Bachem, Bubendorf Switzerland), or β-estradiol 10^{-8} M (ICN pharmaceuticals, Costa Mesa CA). To evaluate the effects of serum, cells were maintained in 0%, 1%, or 10 % (v/v) new born calf serum (Sera-lab).

Plasmid constructs and transfection by calcium phosphate precipitation
Using convenient restriction sites in the 5' untranslated region of the MLC-2a gene deletion fragments were generated. (Pvu II: 1.8 Kb, Bam HI 0.2 Kb). Additional constructs containing 0.45 and 1.0 Kb of the MLC-2a regulatory DNA were generated by PCR and subcloning. All constructs were sequenced either at the ends to check for correct positioning or sequenced completely to exclude PCR-induced mutations. The fragments were cloned into the pXP1[14]or pGL2 (Promega, Madison WI) promoterless luciferase vector. Transient transfection of the myocytes was performed by the calcium phosphate precipitation method [15]. Each 60 mm culture dish of myocardial cells was transfected using 8 μg of a luciferase reporter vector and 2 μg of a cytomegalovirus-ß-galactosidase expression vector. One day after transfection cells were washed twice with DMEM and were stimulated with PE, ET-1 or ß-estradiol. The cells were harvested 48 h later. To control for transfection efficiency the CMV-galactosidase (pON 249) [16] was used, while RSV-luciferase [17] served as a positive control. Data represent at least six experiments using three distinct cesiumchloride purified plasmid preparations.

Luciferase and ß-galactosidase Assays
Cells were lysed in buffer containing (100 mM K_2HPO_4:KH_2PO_4 (92:8 vol.), pH 7.9, 0.5% Triton x-100, 1mM dithiothreitol) and assayed for ß-galactosidase and luciferase activity. The final composition of the ß-galactosidase reaction was 100 mM sodium phosphate, pH 7.3, 0.1 mM magnesium chloride, 2 mM magnesium sulfate, 40 mM ß-mercaptoethanol and 4 mg/ml Ortho-Nitrophenyl-ß-D-Galactopyranoside. ß-Galactosidase activity in 20μl of cell extract was measured in triplicate at 420 nm in a Pharmacia-LKB Ultrospec-III spectrophotometer (Pharmacia Biotech AB, Uppsala Sweden). The final composition of the luciferase reaction medium was 67 μM D-Luciferin, 2 mM ATP, in 300 μl of KTME (100 mM Tricine, 10 mM $MgSO_4$, 2 mM EDTA, pH 7.8). Luciferase activity in 10 μl cell extract was measured in triplicate in a Perkin Elmer Luminesence Spectrometer LS 50 B (Perstorp Analytical Lumac, Landgraaf, the Netherlands). Data are presented as relative luciferase activity based on the luciferase/ galactosidase ratio.

Abdominal aortic banding in rats
Wistar rats weighing 150-200 g were anesthetized with sodium pentobarbital (60mg/kg). The aorta was approached transperitoneally through a right lateral abdominal incision. The aorta was subsequently clipped above the renal arteries, and narrowed to a diameter of 0.25 mm. Thereafter the abdomen was closed in three layers. After surgery the rats were treated with Temgesic® subcutaneously to relieve postoperative pain. The rats were harvested 4 weeks after surgery and left ventricular free wall tissue was used for RNA isolation.

RNA isolation and Northern Blotting
RNA was isolated from NRVM and left ventricular tissue using the TRIzol reagent (Gibco). The quality of the RNA was routinely assessed by size fractionation on formaldehyde-agarose gels followed by ethidium bromide staining. Northern blot hybridizations were performed by minor modifications of a previously described method[18]. Briefly, the RNA (10 μg) was size fractionated by formaldehyde-agarose gel electrophoresis and transferred to nylon membranes (Hybond-N, Amersham Buckinghamshire UK) by capillary transfer. Filters were baked at 80°C for 30 minutes followed by a UV cross-linking of the RNA at 0.4 J/cm^2. Filters were prehybridized for 30 minutes at 65°C using a RapidHyb Buffer (Amersham). Subsequently, a 450 bp fragment of the MLC-2a cDNA, random labeled with α^{32}P dCTP (Dupont de Nemours NV, Brussels Belgium) was added to the hybridization-solution and incubated for 2 h at 65°C. Stringent posthybridization wash conditions were used (0.1 x SSC, 0.1% SDS at 65°C). Expression of the MLC-2a gene was detected by autoradiography and phosphor imaging. As a control, for loading and transfer efficiency, the filters were routinely stained with methylene blue to visualize the 18 S and 28 S RNA bands. In addition hybridizations were performed using randomly labeled 18 S and ANF cDNA as probes. Quantification of Northern blot data based on three independent myocyte isolations.

rt-PCR

First-Strand cDNA synthesis using 5 μg total RNA was performed using a poly-dT primer and the enzyme Reverse Transcriptase (Gibco) in a volume of 20 µl. Following termination of the first-strand synthesis reaction, the samples were incubated with RNase H at 37° for 20 minutes. The same first-strand preparation was used for analyzing each of the gene products by PCR. PCR was performed with 2.5 µl of the first strand reaction, 1 unit of *Taq* polymerase (GibcoBRL) and 50 pmol of the appropriate primers in a reaction volume of 25 µl. The primers used for MLC-2a detection were sense 5'-GCATGTTCGACCCCAG-3' and antisense 5'-AGTTCAGGCACAGAG TTTATT-3' giving a PCR product of 240 bp. Quality of the First Strand cDNA was checked by PCR with murine GAPDH specific primers [19], giving yield to a PCR product of 300 bp. Primer sequence antisense 5'TTATTATAGGGTCTGGGATG 3' and sense 5'-ACACTGAGGACCAGGTTGTC-3'.

Data analysis

Luciferase\Galactosidase ratio was calculated to correct for differences in transfection efficiency within one experiment. To correct for variation in consecutive experiments the Luc\Gal ratios are expressed as relative to the Luc\Gal ratio of the 0.2 Kb MLC-2a promoter fragment, which was arbitrarily set at 1.0. The other results are represented as calculated activities relative to the 0.2 Kb fragment. For statistical analysis the non-parametric Kruskal Wallis test was applied. P-values of <0.05 were considered to be statistically significant.

Results

Genomic structure of MLC-2a

Two different phage colonies (AM1, AM2) were selected after 3 rounds of plaque purification. The phage genomic DNA insert size turned out to be 14 (AM1) and 13 Kb (AM2). For restriction analysis the purified phage DNA was incubated with BamH I, Bstx I, EcoR I, Hind III, Not I, Pst I and Sst I. Restriction analysis revealed a major overlap between the inserts of AM1 and AM2. Accordingly clone AM1 was used for further analysis. By Southern blotting the localization of the MLC-2a cDNA on the AM1 clone was confirmed. The genomic structure of the MLC-2a gene is shown in figure 3. The sequence and position of the 5' end of the cDNA and 5' untranslated region were identified through primer extension and the 5' RACE method. An antisense oligonucleotide was made complimentary to MLC-2a cDNA (ATGAGAAGC TGCTTGAATC, 390-407) [8]. Primer extension failed to present the complete cDNA end, as the extension product terminated repeatedly in the first coding ATG triplet. Therefore 5'-RACE was performed and the amplified DNA was cloned into TA-cloning vector (Invitrogen, San Diego CA) and sequenced. The first exon was identified, and the start of the coding region was designated as +1 (figure 3). The first exon appeared to be 22 basepairs (bp) long and terminated in ATG, providing the first triplet of the coding region.

Following determination of the transcription start site over 3.0 Kb of the 5' flanking region was sequenced. Sequence comparison with known sequences in GenBank release 83.0 (1994) using the nblast NIH program, revealed a 96% homology of the region -2.5 to -2.0 Kb to cDNA (exon 11) of the rat glucokinase gene [20]. More recently the sequence of the murine glucokinase gene was reported and as expected homology to exon 11 was 100% [21]. The mouse glucokinase gene has been mapped to mouse chromosome 11, and therefore, by inference the MLC-2a gene must be on the same chromosomal locus. Low homology (< 10%) to several genes was found by the nblast computer algorithm for the 5' flanking region of the MLC-2a gene close to the transcription initiation site. These findings indicate that the 5' flanking region of the MLC-2a gene spans 2045 bp. In addition the sequence of the 3' flanking region and the introns was determined (figure 3). AM1 contained approximately 700 bp of 3' flanking region. By sequence analysis of the genomic clone and comparison to the cDNA sequence the intron-exon boundaries were defined. The coding region of the MLC-2a gene encompasses 7 exons.

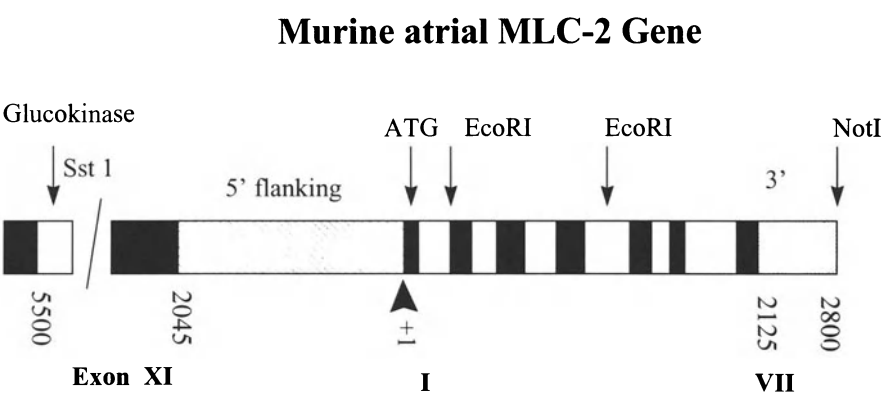

Figure 3. *Schematic representation of the genomic structure of the regulatory atrial myosin light chain. Exons are shown as black, introns white and flanking region as shaded boxes. Indicated is the position of exon 11 of the mouse glucokinase gene. The 5' flanking region is 2045 bp in length. Seven exons were identified, together with the introns the length of the genomic fragment is 2125 bp. The shaded box labeled 3' indicates the part of the 3' flanking region of which the DNA sequence is known.*

Endogenous atrial MLC-2 expression in ventricular myocytes in vitro

The expression of the MLC-2a gene in cultured ventricular cardiomyocytes was determined by Northern blotting (not shown) and rt-PCR (figure 4). The effect of various serum conditions on the level of expression was assessed. Even in the absence of serum (0%), expression of the MLC-2a gene was detected both by rt-PCR and Northern blotting. The highly sensitive rt-PCR approach did not reveal the presence of any MLC-2a message in total RNA from adult mouse ventricular tissue, thereby validating the specificity of the PCR-conditions applied. The quality of the extracted RNA and rt-PCR reaction was comparable for the different conditions tested, as shown

by the expression of the housekeeping gene (glyceraldehyde-3-phosphate dehydrogenase: GAPDH). Stimulation of NRVM with PE and ET-1 showed a significant increase in the message for the MLC-2a gene. These findings indicate activation of the endogenous promoter of the MLC-2a gene in NRVM. The endogenous ANF signal showed a similar pattern of induction at 1 and 10% serum addition and after PE, ET-1 and β-estradiol treatment. There was no marked change in the level of expression of ribosomal RNA (18S) detected by Northern blotting.
Marked differences in myocyte appearance were observed under different experimental conditions. Cardiomyocytes maintained in the absence of serum or treated with β-estradiol became small and cornered. Whereas myocytes kept in medium with 10% serum showed no marked changes going from plating medium to the experimental conditions. ET-1 caused a marked increase in cardiomyocyte size compared to serum and PE treated myocytes.

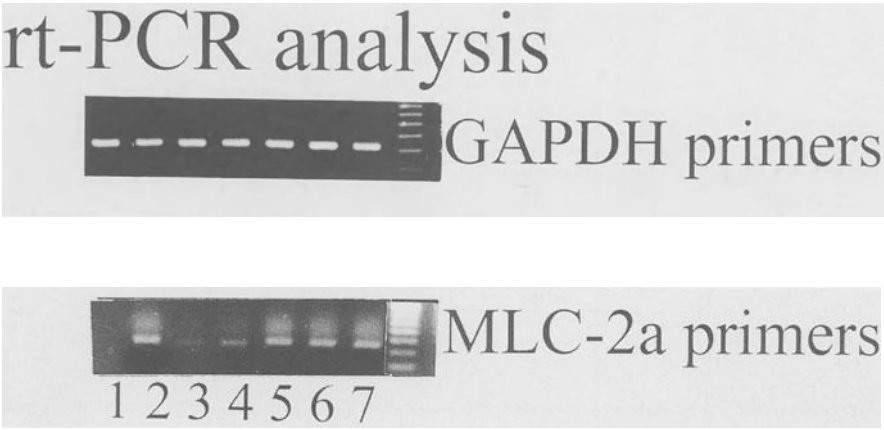

Figure 4. *rt-PCR for MLC-2a and GAPDH. No PCR product was generated with adult mouse ventricular RNA (lane 1). Total RNA from murine atrial tissue was used as a positive control (lane 2). Expected 250 bp PCR bands were found when using RNA from cultured ventricular myocytes, in the absence of serum (3), 10% serum (4), ET-1 (5), PE (6) and β-estradiol (7). The rt-PCR was applied here as a qualitative assay. The amount of PCR product does not necessarily correlates with the amount of mRNA template. The 300 bp murine GAPDH fragment was amplified to check the quality of the isolated total RNA.*

Exogenous atrial MLC-2 promoter activity in ventricular cardiomyocytes in vitro
Deletion fragments of the MLC-2a promoter driving luciferase were transfected in NRVM. Cells were maintained in the absence of serum and treated with either β-estradiol, PE or ET-1 or untreated. Transfection with the 0.2 Kb MLC-2a promoter fragment showed no significant differences in relative luciferase activity comparing treatment versus non-treatment. Relative to the 0.2 Kb fragment, the 0.45 Kb fragment showed higher expression levels. No increased luciferase activity was measured upon stimulation experiments with the promoter fragments < 1.8Kb. In contrast, PE stimulation resulted in approximately threefold increase in relative luciferase activity in the 1.8 Kb construct (figure 5). The induction by ET-1 was comparable,

approximately 2.5-fold for the 1.8 Kb fragment. β-Estradiol treatment of the cells resulted in a marked induction of relative luciferase activity, when the cells were transfected with the 1.8 Kb promoter fragment (10-fold). The stimulatory effect of ß-estradiol was not observed with promoter fragments of 1.0 Kb or less. The increase of luciferase activity of the 1.8Kb fragment upon β-estradiol, PE or ET-1 stimulation was statistically significant compared to the 0.2 Kb fragment (figure 5).

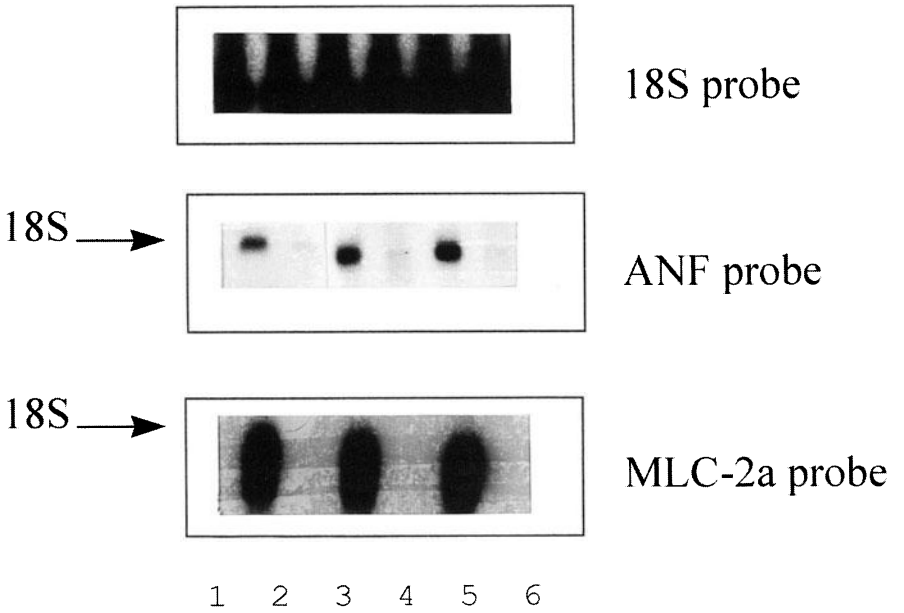

Figure 5. *Results of transient transfection experiments in cultured rat neonatal ventricular cardiomyocytes. Different deletion fragments of the MLC-2a promoter were used varying in size form 0.2 to 1.8 Kb. Following transfection cells were incubated with medium in the absence of serum (0%), endothelin-1 (10^{-8} M), phenylephrine (10^{-5} M) or β-estradiol (10^{-8}M). There was a significant increase in the level of promoter activities of the 0.45 Kb fragment without treatment and for the 1.8 Kb fragment after treatment (*, $p < 0.05$ Kruskal Wallis). The relative luciferase activity for the 0.2 Kb fragment were (mean ±sd): no treatment, 2209 (±1102); endothelin-1, 2110 (±738); phenylephrine, 2359 (±978); β-estradiol, 1903 (±473).*

Endogenous atrial MLC-2 expression in ventricular tissue in vivo

Rat cardiac tissue was analyzed by Northern blotting. Four weeks after aortic banding cardiac hypertrophy was shown as an increase in heart to body weight ratio (not shown). Atrial and ventricular tissue from untreated and ventricular tissue from sham operated rats was included as a control. As anticipated the atrial tissue of all mice was positive for both ANF and MLC-2a. In control ventricular tissue the signal remained below the detection level (figure 6). In ventricular tissue of aortic banded rats the re-expression of ANF and MLC-2a was demonstrated. After 12 hours of blot exposure a marked expression of the MLC-2a gene was seen relative to the ANF level.

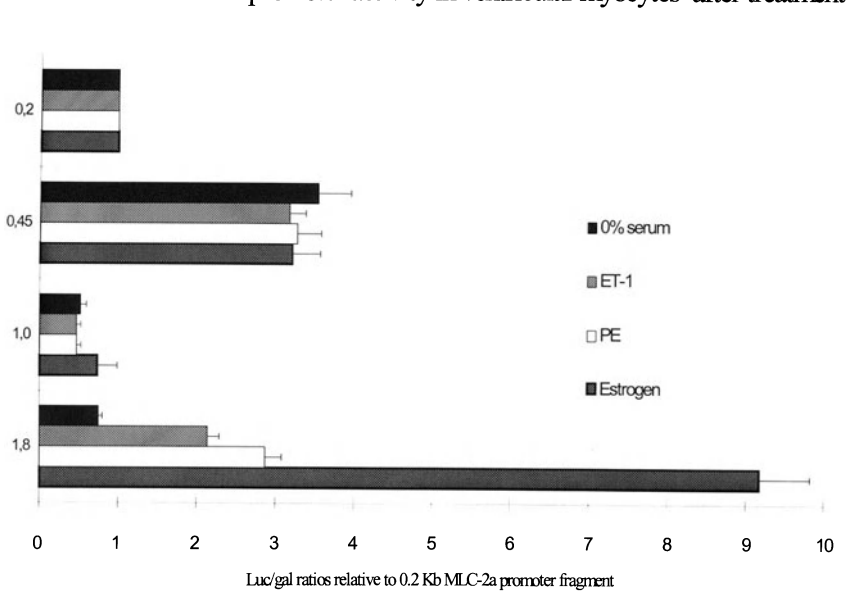

Figure 6. *Representative Northern analysis showing the re-expression of MLC-2a and ANF in ventricular tissue from aortic banded rats. Hybridization signal with 18S shows equal amounts of RNA per lane. Lane 1 is rat atrial tissue representing a positive control sample. Lane 2 is ventricular tissue from an untreated rat. Lanes 3 and 5 show the hybridization signals of MLC-2a and ANF in ventricular tissue from two different rats following aortic banding. Lane 4 and 6 contain ventricular tissue samples of sham operated rats.*

Discussion

Genomic clones containing the complete MLC-2a cDNA and >6.0Kb of the 5' flanking region were isolated and characterized. The MLC-2a gene contains 7 exons which is consistent with the genomic structure of related family members [8,22].
The MLC-2a gene is re-expressed in cultured NRVM. The MLC-2a mRNA is detectable when the cells are maintained in the absence of serum and levels increase further when either 10% serum, ET-1, PE or ß-estradiol is added to the medium. Transient transfection studies with deletion fragments of the MLC-2a 5' flanking region reveal that the region spanning from -1.0 to -1.8 Kb is responsible for upregulating reporter gene (luciferase) activity upon treatment of myocytes with ET-1, PE and ß-estradiol. In left ventricular tissue of aortic banded rats expression of the MLC-2a gene was demonstrated at the mRNA level.

Re-expression of MLC-2a in cultured NRVM
The endogenous MLC-2a gene is expressed in NRVM in defined serum-free medium, whereas in neonatal rats expression of MLC-2a is exclusively found in atrial myocytes. The re-expression of the MLC-2a gene shown in this study suggests that the procedure of isolating and culturing ventricular cardiomyocytes in itself provides the stimulus for

re-expression. Several factors could be important for the induction of MLC-2a expression under these conditions. Myocyte isolation is traumatic as the myocytes are separated from neighboring cells and the extracellular matrix becomes degraded. The cardiomyocytes are plated at a relative low density, so that there is basically no restoration of cell/cell contact. In addition, the cells will require attachment to the culture dishes to survive the procedure. In theory each of these factors could be responsible for the induction of MLC-2a expression indicating dedifferentiation. The re-expression of fetal genes in cultured cardiomyocytes in the absence of serum, was shown by Wollert et al. [2] for the ANF and α skeletal actin gene. Their study, total RNA from neonatal rat cardiomyocytes was analyzed after a 48 hour incubation period in serum free medium.

Re-expression of the MLC-2a gene after ET-1 and PE treatment

Treatment of cultured NRVM with PE and ET-1 increased MLC-2a expression concordant with morphological signs of hypertrophy. ET-1 and PE cardiomyocyte treatment resulted in expression of immediate early genes, the induction of contractile protein synthesis [23] and the reactivation of a fetal gene program [24-29]. Different receptor-signaling pathways in ventricular cardiomyocytes are involved in sensing hypertrophic stimuli [30]. Endothelin receptor A is the predominant receptor isoform found in cardiomyocyte membranes [25], and PE activates the α-adrenergic receptors. Endothelin receptor A and α-adrenergic receptors have been shown to interact with G-proteins. For both hormones signaling involves activation of the Ras/Raf pathway, while several other routes of intracellular signaling can be used [31]. In general the signal transduction pathways connecting the receptor for a hypertrophic stimulus to transcriptional regulation are diverse and highly complex through cross-talk between the pathways involved (review [32]).

Although there are many similarities in the hypertrophic response induced by ET-1 and PE, several reports indicate that different fetal gene expression programs exist and morphologic signs of hypertrophy can vary. This has been underscored by a prolonged versus transient ANF expression in NRVM after PE and ET-1 treatment, respectively [26]. Furthermore, Fuller et al. [33]showed that the expression of fetal genes can be blocked without attenuation of the morphological signs of hypertrophy, by over-expressing a phosphatase (Mitogen-activated protein kinase phosphatase 1). MKP1 can inactivate mitogen activated protein kinase, a key protein in the Ras/Raf signaling pathway [31]. In our experiments treatment of cardiomyocytes with β-estradiol showed a high level of MLC-2a expression without overt cell enlargement, suggesting different pathways of morphological cardiomyocyte hypertrophy and reactivation of a fetal gene program, generally associated with hypertrophy. This effect of estrogen treatment on sarcomeric gene expression in cardiomyocytes has not been reported previously.

Cardiotrophin-1 (CT-1) treatment of cardiomyocytes induces specific hypertrophic morphologic changes. The CT-1 protein belongs to a family of cytokines requiring the receptor protein gp-130 to mediate its effect. CT-1 induces expression of ANF but not skeletal α-actin. In contrast stimulation by PE showed elevated levels of both ANF and skeletal α-actin. PE treatment gave widening and lengthening of cardiomyocytes, whereas the CT-1 induced hypertrophy was characterized only by lengthening of the

cells [2].

The situation *in vivo* is more complex. Ventricular myocyte selective overexpression of the constitutively active Ras gene (dominant positive) in transgenic mice resulted in a hypertrophic phenotype with intracavitary flow obstruction [4]. Molecular analysis of this mouse model of hypertrophic obstructive cardiomyopathy showed a selective upregulation of atrial and brain natriuretic factor, without increased levels of contractile protein expression (including MLC-2a) [4]. These findings are in line with the *in vitro* results with CT-1 stimulation. In contrast, re-expression of MLC-2a in the ventricles of aortic banded wild type mice was demonstrated by RNA analysis. Despite the role of the Ras/Raf pathway in mediating ET-1 and PE responses, the results in the transgenic mice and aortic banded mice indicate that the Ras/Raf signaling cascade may not be directly responsible for ventricular re-expression of the endogenous MLC-2a in mice *in vivo*. All these studies show differences in the genes activated down stream of the signaling cascade upon hypertrophic stimuli. It is likely that determination of the hypertrophic molecular fingerprint can be helpful in determining the signal pathway activation and potential cause of cardiac disease.

Exogenous MLC-2a promoter activation in ventricular myocytes

The 0.45 Kb promoter fragment contains several E-boxes, one GATA and one retinoic acid responsive element in addition to the conserved *cis* elements of the 0.2 Kb fragment. The relatively strong promoter activity of this fragment can be important for future transgenic experiments [34]. The unstimulated 1.0 and 1.8 Kb constructs are less active compared with the 0.2 Kb. This repressive effect is not dependent on serum conditions or neurohormonal stimulation and suggestive for the presence of a transcriptional silencer in the region between 0.45 Kb to 1.0 Kb. The MLC-2a promoter fragments of 1.8 and 3.0 Kb are strongly activated by ET-1 and PE treatment, as assessed by the increased luciferase activity. The transfection data indicate the presence of *cis* elements responsible for ET-1 and PE induction between position -1.0 Kb to -1.8 Kb. Sequence comparison revealed, amongst others, two AT-rich elements within this promoter fragment that may act as potential myocyte enhancer factor (MEF2) binding sites.

The *cis* element of the MLC-2v promoter involved in PE-induced upregulation has been mapped to the HF1B site, also an AT- rich element with which MEF2 can interact [35]. The transgenic experiment with the constitutively active RAS gene shows that the behavior of the endogenous complete MLC-2v promoter is different from the *in vitro* results, as no upregulation of MLC-2v transcription was documented [4]. The role of the AT-rich element in the MLC-2a promoter will need to be addressed in future studies.

Estrogen activation of the MLC-2a promoter

β-Estradiol treatment of NRVM, transfected with the 1.8 Kb promoter fragment, resulted in a 10-fold increase in relative luciferase activity. The DNA site required for estrogen induction has been mapped to the fragment from -1.0 to -1.8 Kb of the MLC-2a promoter, as shown in this study.

Functional estrogen receptors in ventricular myocytes were demonstrated by Grohe et

al. [36]. Estrogen receptors belong to the superfamily of nuclear receptors or more specifically to the steroid hormone receptors (Class 1) [37,38]. The activated receptors translocate to the nucleus and homodimerize after ligand (estrogen) binding. The ligand-receptor complex binds to a palindromic sequence AGGTCA with a spacing of three nucleotides. After ligand-receptor interaction with the *cis* element of the target gene an interaction with the transcription initiation complex has been shown to occur. Through this interaction the level of transcription can be upregulated [38]. Sequence comparison of the MLC-2a promoter fragment from -1.0 to -1.8 Kb revealed a conserved hormone responsive element. The physiological significance of this finding is unclear. So far the effect of estrogens has been studied epidemiologically [39], and in oncology and vascular biology. It has been shown that estrogen treatment has beneficial effects on vascular tone, vascular resistance and cardiac output in monkeys [40,41]. Whether estrogen treatment induces the expression of MLC-2a in ventricular tissue *in vivo* is presently unknown. The behavior of the transfected MLC-2a promoter is very interesting and provides a unique tool to unravel the signaling pathway involved in estrogen-
receptor interaction and DNA binding in cardiomyocytes.

Conclusion and future perspective

MLC-2a as a molecular marker

Previous studies have shown the value of the MLC-2v and MLC-2a genes as molecular markers during chamber formation in cardiogenesis. The expression pattern of the two genes is unique, where the ventricular isoform is ventricular specific. In contrast the MLC-2a gene is initially active throughout the complete heart tube similar to ANF and MLC-1a. The MLC-2a has however a short lasting expression in cardiomyocytes differentiating into the ventricular phenotype. This makes the gene a valuable tool in unraveling the molecular process of ventricular chamber formation. Another interesting feature is the expression of the MLC-2a gene in transcription factor knock-out experiments leading to embryonic lethality at day 8 (GATA 4, [42]), 10 (MEF2c [43], Nkx2.5 [44]), 11 (TEF-1 [45]), 14 (RXRα [10]). Apparently yet unidentified transcription factors are crucial for cardiogenesis and the MLC-2a promoter contains the clues to identification of these potentially dominant factors.

This study demonstrates the value of MLC-2a as a molecular marker in cardiac hypertrophy. Furthermore, the results presented show that it is important to distinguish direct promoter mediated changes in gene expression from a general induction of a so called fetal gene program. MLC-2a and ANF can be upregulated in cardiomyocytes without morphological signs of hypertrophy. The lack of MLC-2a expression in constitutively active Ras overexpressing mice points to the value of the MLC-2a gene as a molecular marker in hypertrophy.

Atrial specific gene therapy

Several genes have been described that are expressed exclusively in atrial tissue. For instance, the MLC-1a, MLC-2a and ANF promoters can be used for atrial specific gene

expression. The ANF promoter has already been used successfully in transgenic experiments [46,47]. All three genes are re-expressed in ventricular tissue under pathologic conditions. The short lasting expression of MLC-2a in ventricular tissue makes the promoter valuable for early transient genetic interventions during cardiogenesis. The value of the MLC-2a promoter is currently being evaluated in transgenic mice.

Acknowledgments

The authors are indebted to Ming Dong Zhou and Monique Lacorbiere for their technical support. We are grateful to Monique Jansens and Aisha Knoop for assistance in preparing this chapter.

References

1. Doevendans PA, van Dantzig J, Meijer H, Schaap C. Molecular genetics of human cardiomyopathies. In: Peters R, Piek J, eds. Molecular cardiology in clinical perspective. 1 ed. Amsterdam: Knoll; 1997:33-53.
2. Wollert KC, Taga T, Saito M, et al. Cardiotrophin-1 activates a distinct form of cardiac muscle cell hypertrophy. Assembly of sarcomeric units in series VIA gp130/leukemia inhibitory factor receptor-dependent pathways. J Biol Chem 1996;271:9535-45.
3. Knowlton KU, Baracchini E, Ross RS, et al. Co-regulation of the atrial natriuretic factor and cardiac myosin light chain-2 genes during alpha-adrenergic stimulation of neonatal rat ventricular cells. Identification of cis sequences within an embryonic and a constitutive contractile protein gene which mediate inducible expression. J Biol Chem 1991;266:7759-68.
4. Gotschall K, Hunter JJ, Tanaka N, et al. Ras-dependent pathways induce obstructive hypertrophy in echo-selected transgenic mice. Proc Natl Acad Sci USA 1997;94:4710-15.
5. Leskinen H, Vuolteenaho O, Ruskoaho H. Combined inhibition of endothelin and angiotensin II receptors blocks volume load-induced cardiac hormone release. Circ Res 1997;80:114-23.
6. Wallen T, Landahl S, Hedner T, Nakao K, Saito Y. Brain natriuretic peptide predicts mortality in the elderly. Heart 1997;77:264-67.
7. Yamamoto K, Burnett-JC J, Jougasaki M, et al. Superiority of brain natriuretic peptide as a hormonal marker of ventricular systolic and diastolic dysfunction and ventricular hypertrophy. Hypertension. 1996;28:988-94.
8. Kubalak SW, Miller-Hance W, O'Brien T, Dyson E, Chien K. Chamber-specification of atrial myosin light chain-2 expression precedes septation during mouse cardiogenesis. J Biol Chem 1994;269:16961-70.
9. O'Brien TX, Lee KJ, Chien KR. Positional specification of ventricular myosin light chain 2 expression in the primitive murine heart tube. Proc Natl Acad Sci USA 1993;90:5157-61.
10. Dyson E, Sucov HM, Kubalak SW, et al. Atrial-like phenotype is associated with embryonic ventricular failure in retinoid X receptor alpha -/- mice. Proc Natl Acad Sci USA 1995;92:7386-90.
11. Kubalak S, Doevendans PA, Rockman H, et al. Molecular analysis of cardiac muscle diseases based on mouse genetics. In: Adolph KW, ed. Human molecular genetics, 1st ed. Orlando: Academic Press; 1996:470-87.
12. Sanger F, Coulson AR. A rapid method for determining sequences in DNA by primed synthesis and DNA polymerase. J Mol Biol 1975;94:444-48.
13. De Vries JE, Vork MM, Roemen THM, De Jong YF, Van der Vusse GJ, van Bilsen M. Saturated, but not mono-unsaturated fatty acids induce apoptotic cell deathnin neonatal rat ventricular myocytes. J Lipid Res 1997;38:1384-94.
14. Nordeen SK. Luciferase reporter gene vectors for analysis of promoter and enhancers. Biotech 1988;6:454-57.
15. Chen C, Okayama H. High-efficiency transformation of mammalian cells by plasmid DNA. Mol Cell Biol 1987;7:2745-52.
16. Cherrington JM, Mocarski ES. Human cytomegalovirus transactivates the α promoter-enhancer via an 18-base pair repeat element. J Virol 1989;63:1435-40.
17. de Wet JR, Wood KV, DeLuca M, Helinski D, Subramani S. Firefly luciferase gene: structure and expression in mammalian cells. Mol Cell Biol 1986;7:725-37.
18. Iwaki K, Sukhatme VP, Shubeita HE, Chien KR. Alpha- and beta-adrenergic stimulation induces distinct patterns of immediate early gene expression in neonatal rat myocardial cells. fos/jun expression is associated with sarcomere assembly; Egr-1 induction is primarily an alpha 1-mediated response. J Biol Chem 1990;265:13809-17.
19. Sabath DE, Broome HE, Prystowsky MB. Glyceraldehyde-3-phosphate dehydrogenase mRNA is a major interleukin 2 induced transcript in a cloned T-helper lymphocyte. Gene

1990;91:185-91.
20. Andreone TL, Printz RL, Pilkis SJ, Magnuson MA, Granner DK. The amino acid sequence of rat liver glucokinase deduced from cloned cDNA. J Biol Chem 1989;264:363-69.
21. Postic C, Niswender KD, Decaux JF, et al. Cloning and characterization of the mouse glucokinase gene locus and identification of distal liver-specific DNase I hypersensitive sites. Genomics 1995;29:740-50.
22. Barton PJ, Cohen A, Robert B, et al. The myosin alkali light chains of mouse ventricular and slow skeletal muscle are indistinguishable and are encoded by the same gene. J Biol Chem 1985;260:8578-84.
23. Shubeita HE, McDonough PM, Harris AN, et al. Endothelin induction of inositol phospholipid hydrolysis, sarcomere assembly, and cardiac gene expression in ventricular myocytes. A paracrine mechanism for myocardial cell hypertrophy. J Biol Chem 1990;265:20555-62.
24. Brown LA, Nunez DJ, Brookes CI, Wilkins MR. Selective increase in endothelin-1 and endothelin A receptor subtype in the hypertrophied myocardium of the aorto-venacaval fistula rat. Cardiovasc Res 1995;29:768-74.
25. Hilal Dandan R, Merck DT, Lujan JP, Brunton LL. Coupling of the type A endothelin receptor to multiple responses in adult rat cardiac myocytes. Mol Pharmacol 1994;45:1183-90.
26. McDonough PM, Brown JH, Glembotski CC. Phenylephrine and endothelin differentially stimulate cardiac PI hydrolysis and ANF expression. Am J Physiol 1993;264:H625-30.
27. Sei CA, Glembotski CC. Calcium dependence of phenylephrine-, endothelin-, and potassium chloride-stimulated atrial natriuretic factor expression form long term primary neonatal rat atrial cardiocytes. J Biol Chem 1990;265:7166-72.
28. Shubeita HE, Martinson EA, van Bilsen M, Chien KR, Brown JH. Transcriptional activation of the cardiac myosin light chain 2 and atrial natriuretic factor genes by protein kinase C in neonatal rat ventricular myocytes. Proc Natl Acad Sci USA 1992;89:1305-09.
29. Soonpaa MH, Field LJ. Assessment of cardiomyocyte DNA synthesis in normal and injured adult mouse hearts. Am J Physiol 1997;272:H220-26.
30. Lembo G, Hunter JJ, Chien KR. Signaling pathways for cardiac growth and hypertrophy. Recent advances and prospects for growth factor therapy. Ann NY Acad Sci 1995;752:115-27.
31. Thorburn A, Thorburn J, Chen SY, et al. HRas-dependent pathways can activate morphological and genetic markers of cardiac muscle cell hypertrophy. J Biol Chem 1993;268:2244-49.
32. van Bilsen M. Signal transduction revisited. Cardiovasc Res 1997;36:310-22.
33. Fuller SJ, Davies EL, Gillespie Brown J, Sun H, Tonks NK. Mitogen-activated protein kinase phosphatase 1 inhibits the stimulation of gene expression by hypertrophic agonists in cardiac myocytes. Biochem J 1997;323:313-19.
34. Doevendans PA, Hunter JJ, Lembo G, Wollert KC, Chien KR. Strategies for studying cardiovascular diseases in transgenic mice and gene-targeted mice. In: Monastersky GM, Robl JM, eds. Strategies in transgenic animal science. 1st ed. Washington: American Society For Microbiology; 1995:107-44.
35. Thorburn J, Carlson M, Mansour SJ, Chien KR, Ahn NG, Thorburn A. Inhibition of a signaling pathway in cardiac muscle cells by active mitogen-activated protein kinase kinase. Mol Biol Cell 1995;6:1479-90.
36. Grohe C, Kahlert K, Briesemeister G, Stimpel M, Vetter H, Neyses L. Myocardial and myogenic cells contain functional estrogen recepotors. Circulation 1994;90:2898.
37. Mangelsdorf DJ, Evans RM. The RXR heterodimers and orphan receptors. Cell 1995;83:841-50.
38. Beato M, Herrlich P, Schutz G. Steroid hormone receptors: many actors in search of a plot.

Cell 1995;83:851-57.
39. Grodstein F, Stampfer MJ, Colditz GA, et al. Postmenopausal hormone therapy and mortality. N Engl J Med 1997;336:1769-75.
40. Pelzer T, Shamim A, Neyses L. Estrogen effects in the heart. Mol Cell Biochem 1996;160-161:307-13.
41. Williams JK, Kim YD, Adams MR, Chen MF, Myers AK, Ramwell PW. Effects of estrogen on cardiovascular responses of premenopausal monkeys. J Pharmacol Exp Ther 1994;271:671-76.
42. Molkentin JD, Lin Q, Duncan SA, Olson EN. Requirement of the transcription factor GATA 4 for heart tube formation and ventricular morphogenesis. Genes Dev 1997;11:1061-72.
43. Lin Q, Schwarz J, Bucana C, Olson EN. Control of mouse cardiac morphogenesis and myogenesis by transcription factor MEF2C. Science 1997;276:1404-08.
44. Lyons I, Parsons LM, Hartley L, Li R, Andrews JE, Robb L, Harvey RP. Myogenic and morphogenetic defects in the heart tubes of murine embryos lacking the homeo box gene Nkx2-5. Genes Dev 1995;9:1654-66.
45. Chen Z, Glenn A, Soriano P. Transcriptional enhancer factor 1 disruption by a retroviral gene trap leads to heart defects and embryonic lethality in mice. Genes Dev 1994;8:2293-301.
46. Field LJ. Atrial-natriuretic factor-SV40 large T antigen transgenes produce atrial tumors and cardiac arrhythmias in mice. Science 1988;239:10029-33.
47. Knowlton KU, Rockman HA, Itani M, Vovan A, Seidman CE, Chien KR. Divergent pathways mediate the induction of ANF transgenes in neonatal and hypertrophic ventricular myocardium. J Clin Invest 1995;96:1311-18.

11. EXPRESSION OF RAT GAP JUNCTION PROTEIN CONNEXIN 40 IN THE HEART

W. Antoinette Groenewegen

Introduction

Cells of the myocardium are electrically coupled through gap junction channels. They allow ions and small molecules to pass from one cell to the next and in this way conduct the cardiac action potential. This results in synchronized activation of the cardiac cells and allows coordinated contraction of the heart. Gap junction channels (for a review see [1]) consist of two hemi-channels and these in turn are made up of 6 protein subunits, connexins. At least fifteen different, but highly homologous mammalian connexins genes have been cloned. In the heart, connexin(Cx)43 (where 43 indicates the predicted molecular weight from the cDNA in KiloDaltons) is the most widely expressed connexin, while other cardiac connexins, Cx40 and Cx45, show a much more restricted pattern of expression. By immunostaining, Cx43 protein is detected throughout the heart but cannot be detected in the SA-node, the AV-node, the top of the AV-bundle and the top of the bundle branches. This is true for both neonatal and adult rat heart. By contrast, Cx40 exibits a clearly different expression pattern [2]. During embryonic development, Cx40 expression is widespread throughout the myocardium, but is gradually down-regulated in a region-specific manner towards birth. By the neonatal stage, Cx40 can still be detected in the atrium and, in addition, is clearly expressed in the ventricular conduction system. In the adult rat heart, Cx40 can only be detected in the ventricular conduction system including the top of the AV-bundle. Thus in the adult rat, Cx40 appears associated with fast conducting tissue and it is interesting to note in this context that the single channel conductance for Cx40 gap junction channels is about 3 times larger than that for Cx43 gap junction channels [1]. In addition, Cx40 hemi-channels can not form electrically functioning channels with Cx43 hemi-channels from neighbouring cells. How the spatio-temporal expression of the Cx40 gene is regulated is largely unknown. In order to begin to understand the regulation of the Cx40 gene at the transcriptional level, we set out to identify the Cx40 promoter sequence.

P.A. Doevendans et al. (eds.), Cardiovascular specific gene expression, 117-24.

Methods

5'-RACE (Rapid amplification of cDNA ends) was performed using a kit from Gibco/BRL according to the manufacturers protocols. cDNA was synthezised using anti-sense primer A (5'-TTCCTGCATGCGCACAGTGT-3'), basepaire (bp) 303-322 [3]. The first PCR was performed with anti-sense primer B (5'-CAACCAGGCTGAATGGTATC-3'), bp 173-192 [3] and the anchor primer provided with the 5'-RACE kit. The nested PCR was performed with anti-sense primer C (5'-CCATCTTGCCAAGTGTTGGA-3', figure 1, bp -16 to 4) and the universal amplification primer provided with the kit. PCR products were cloned into pGEM-T (Promega) for sequencing. Genomic clones were isolated from a λEMBL3 rat genomic library using a BglII/XhoI fragment of the rat Cx40 cDNA (kindly provided by Dr D.L. Paul, Harvard Medical School, Boston, U.S.A.) according to standard protocols.
The putative promoter sequence upstream of exon 1 was obtained by long distance(LD)-PCR mediated genomic walking [4] using GenomeWalker (formerly PromoterFinder) Libraries from Clontech. Briefly, the kit provides five separate rat genomic DNA library-digests that were prepared by cutting each with a different blunt cutting restriction enzyme. Special DNA adaptors were then added to the blunt DNA fragments. Nested PCR reactions with gene-specific primers and primers that anneal to the adaptors were then performed in our laboratory according to the manufacturers protocols. The size of the PCR product that is obtained depends on the distance between the gene-specific primer and the restriction enzyme with which the DNA had been digested to prepare the library-digest. We performed two genome walks, one in the anti-sense direction using primers E and F (see figure 1) and one in the sense direction with primer G (5'-AAGGGGTGGAGAGAGAAAGAGGA-3') and primer H (5'-GAGGAGGGAGGGCGATGGGATA-3') that anneal to the sequence identified by the anti-sense genomic walk. Selected PCR products were cloned into pGEM-T vector for sequencing. Primer extension was carried out as described [5] using primer I (figure 1, bp -73 to -34 cDNA sequence). RNase protection was performed using the RPA II system from Ambion.

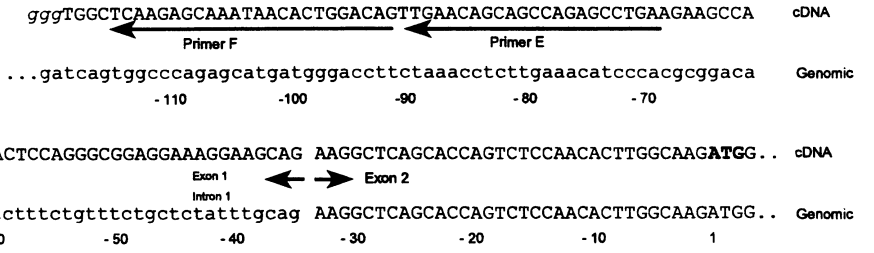

Figure 1. *5'-end DNA sequences from Cx40 cDNA isolated by 5'-RACE and from genomic Cx40 DNA from a λEMBL3 clone. Capital letters indicate exon 1 and 2 sequences, lower case letters indicate intron sequence, italics indicate bases of the tail sequence. The translation initiation signal ATG is in bold type. The sequence for the anti-sense primers E and F are indicated by the arrows, the complement was synthesized. These sequences can be accessed in the Genbank database with accession numbers AF025765 (cDNA sequence) and AF025767 (genomic sequence).*

Results and discussion

Isolation of 5'-end sequences for Cx40

The genomic organization of several other connexin genes consist of 2 exons, the complete coding sequences being contained in the second exon [1]. A small untranslated exon, exon 1, is situated several Kb upstream of the coding sequences. We assumed the genomic organization of the rat Cx40 gene to be similar and since the 5'-untranslated exon 1 sequences for the Cx40 mRNA were unknown [3], we first needed to identify this sequence in order to subsequently isolate the Cx40 promoter sequence. The PCR method 5'-RACE was used to amplify the unknown 5'-end sequences from both lung and adult heart RNA. Sequencing of the cloned PCR products revealed approximately 110 bp new 5'-end sequence which was identical in the PCR products amplified from both tissues (figure 1; Genbank accession number: AF025765).

Genomic Cx40 clones were isolated from a λEMBL3 library using a probe derived from the coding sequences. Figure 2 shows a restriction enzyme map of the genomic region around the coding sequences. The 9 Kb HindIII fragment was subcloned and the sequence upstream of the coding region was obtained. Comparison of this genomic sequence (figure 1; Genbank accession number: AF025767) to that obtained by 5'-RACE from lung and heart mRNA showed that these sequences diverged ~34 bp upstream of the ATG translation start codon (figure 1), which indicated the presence of an intron. The additional Cx40 cDNA sequence we designated exon 1. Southern blotting with oligonucleotide probes from exon 1 against the ~7.0 Kb SmaI fragment digested from one of the genomic clones (figure 2) did not give a hybridization signal and it was therefore concluded that exon 1 is located more than 5.5 Kb upstream of the coding sequences in genomic DNA. Together our data indicate that Cx40 gene structure is similar to that of the other connexin genes and consisted of two exons, a small untranslated exon 1, separated by a large intron from exon 2.

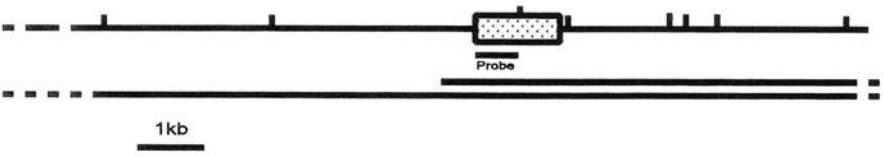

Figure 2. *Partial restriction enzyme map of genomic DNA flanking the Cx40 coding sequence (dotted box) obtained from two overlapping genomic clones. Probe indicates the part of the coding region DNA that was used as a probe to screen the λEMBL3 library. S: SmaI; H: HindIII; Xh: XhoI; Xb: XbaI; E: EcoRI; the lines underneath the map indicate the position of the two λEMBL3 clones. Dotted lines indicate that the clone extends beyond this part of the map.*

5'-untranslated sequences for Cx40 mRNA from other tissues

The gene for the gap junction protein Cx32 has been shown to contain several alternative exon 1 sequences, which are expressed in a tissue-specific manner [6,7]. Expression of these alternative Cx40 mRNAs, which only differ in their 5'-untranslated sequences, is presumably driven by alternative promoters. We investigated whether the 5'-untranslated sequence described above was also present in some other tissues of the cardiovascular system in which Cx40 is known to be expressed.

Cx40 cDNA from neonatal rat heart, the rat aortic smooth muscle cell line A7r5 and again from adult rat heart were analysed. PCR was performed using forward primer D (figure 1, bp -115 to -94 cDNA sequence) which anneals to the most 5'-untranslated sequence of the Cx40 mRNA identified above and anti-sense primer B which anneals in the coding region (see Methods). The expected band of ~300 bp was obtained in each tissue, while control reactions were negative (not shown). From these results we conclude that the 5'-end sequence is also present in Cx40 mRNA from neonatal rat heart and A7r5 cells, and we confirmed its presence in adult rat heart.

Isolation of genomic DNA upstream of the Cx40 gene

We first performed an anti-sense PCR walk using two anti-sense primers E and F (see figure 1) that were designed to anneal to the 5'-end of exon 1. Figure 3 schematically shows the PCR products obtained in all five library-digests, ranging in size from ~ 350 bp to ~ 6 Kb. No product was obtained in the water control reaction while the positive control reaction gave the expected size fragment (not shown). Two products, the 350 bp product from the PvuII library-digest and the 3 Kb product from the SspI library-digest were cloned into pGEM-T vector and the sequences at the 3'-end of these fragments were found to be identical. This suggested that the sequence obtained was upstream of exon 1. However, since there was no overlap between the newly identified, putative promoter sequence and exon 1 sequence, we needed to confirm that this new upstream sequence is linked to the Cx40 gene. Therefore, sense primers G and H, based on the upstream sequence identified by the anti-sense walk, were synthesized and PCR was performed in the sense direction. In three out of the five library-digests, specific PCR products were obtained (lower part figure 3). Two products (from PvuII and SspI library-digests) were cloned and sequenced at their 5'-ends. The sequences from both clones were identical thus confirming that the putative promoter sequence is upstream of the Cx40 gene. In addition, the data confirmed the cDNA sequence of exon 1 in genomic DNA.

Transcription start site mapping

We mapped the transcription start site for Cx40 mRNA more precisely by primer extension and RNase protection assays in RNA from different tissues. By primer extension with primer I, the same two bands were obtained in each tissue of 85 and 84 bp (figure 4). Because reverse transcriptase does not always extend to the very end of the mRNA molecule, these two bands probably only represent one transcription start site, and indicates that exon 1 is 85 bp. For other tissues, 20 μg of total RNA was analyzed in each case.

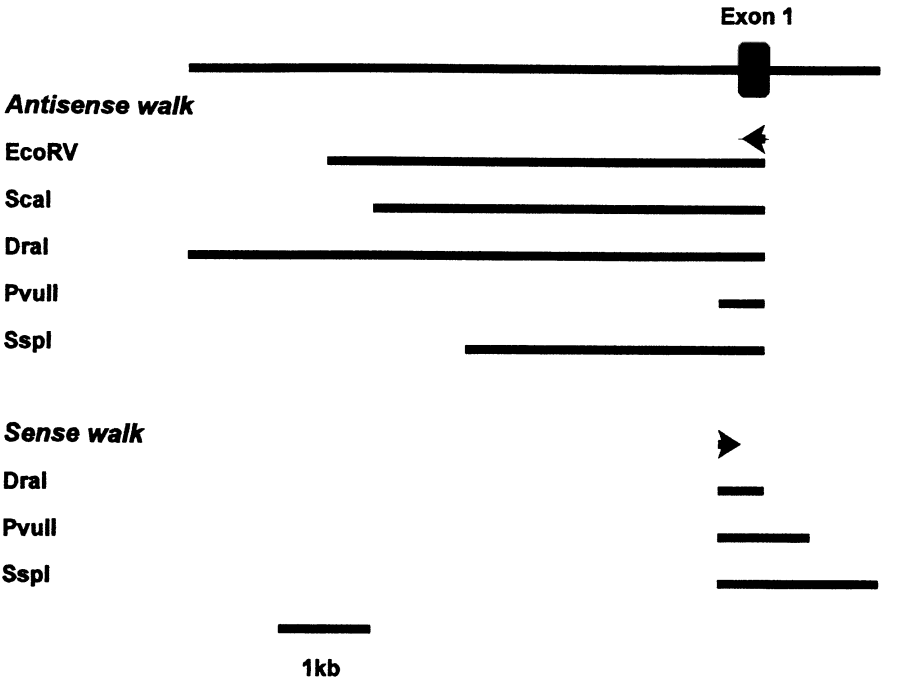

Figure 3. *Schematic representation of the PCR products amplified in the LD-PCR genomic walking experiments. The sequences for the anti-sense primers E and F used in the anti-sense walk (represented by the arrow pointing left in the upper part of the figure) are indicated in figure 1. PCR products were obtained in all five library-digests. The blunt cutting enzymes used to produce the genomic DNA digests are indicated on the left. Thus, a DraI site is present ~6 Kb upstream of exon 1. Similarly, the position of the other enzyme sites upsteam or downstream of exon 1 can be inferred from the size of the PCR products. In the sense walk (lower part), products were obtained in three of the library-digests. The sequences for the sense walk primers G and H (represented by the arrow pointing right in the lower part of the figure) are given in Methods.*

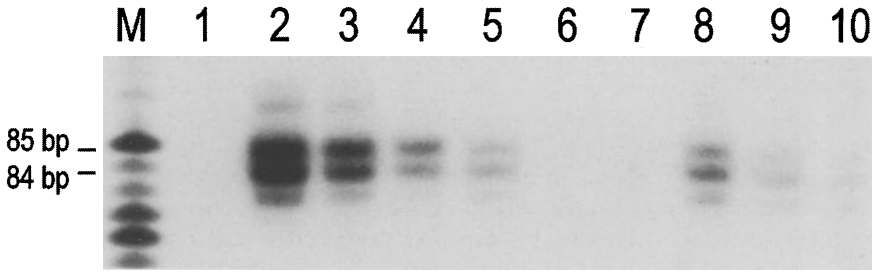

Figure 4. *Transcription start site mapping of Cx40 mRNA in different tissues by primer extension analysis: Lane 1 probe only; lanes 2, 3 and 4: A7r5 RNA (20, 10 and 5 μg respectively); lane 5, adult lung; lane 6, adult atrium; lane 7, adult ventricle; lane 8, neonatal lung; lane 9, neonatal atrium, lane 10, neonatal ventricle, 20 μg total RNA/lane; lane M: a sequencing reaction was used as size marker, only one lane of the reaction is shown.*

The data show that Cx40 mRNA levels varied between tissues, with A7r5 cells expressing the highest level of Cx40 mRNA, followed by neonatal and adult lung RNA expressing reasonably high levels of Cx40 mRNA. In neonatal atrium and ventricle Cx40 mRNA levels were still detectable, but, in adult atrium and ventricle no bands could be detected by this method. These relative levels agree with published data on Cx40 distribution in these different tissues and developmental stages [2,3,8]. In addition, RNase protection analysis was performed on RNA from the same tissues as above using the 350 bp PCR product obtained in the anti-sense walk (see above) as a probe for exon 1. In A7r5 cells, two bands of 85 and 87 bp were obtained (results not shown). On prolonged incubation of 10 μg total RNA from A7r5 cells with RNase A/T1 mixture or with a higher concentration of the RNase mixture to digest unhybridized cRNA probe, the upper of the two bands disappeared, indicating that the 87 bp band was an incomplete RNase digestion product. Therefore, we conclude that RNase protection analysis also indicates one transcription start site and that the size of exon 1 is 85 bp. Thus the size of exon 1 deduced by these experiments is in agreement with that obtained by 5'-RACE. The relative levels of Cx40 mRNA detected by the RNase protection assay in 20 μg total RNA from the different tissues (not shown) were similar to those detected by the primer extension assay.
While the possibility of alternative exon 1 sequences cannot be ruled out completely, our data do not indicate their existence. Since the levels of Cx40 mRNA detected by both primer extension and RNase protection using exon 1 probes are in agreement with what is known about Cx40 distribution. This also argues against any significant contribution in Cx40 expression from alternative promoters in the tissues at the developmental stages examined in this study. It therefore seems likely that the upstream sequence that we have isolated by LD-PCR controls the transcription of the Cx40 gene in these different tissues.

Analysis of the putative promoter sequence for transcription factor binding sites
The sequence of ~1000 bp upstream of the transcription start site was determined and figure 5 schematically shows the putative transcription factor binding sites that are present in this region (Genbank accession number AF025766). We noticed the TATA-like sequence TTAAAAA at -29 bp. There is a Sp1 binding site just upstream of the transcription start site that overlaps with an AP2 site. In addition, potential binding sites for AP1, several E-boxes, an NFκB site and Nkx-2.5 site are present. E-box sequences are associated with muscle specific gene expression [9] and they bind the bHLH family of transcription factors. In the heart two bHLH proteins dHAND and eHAND are essential for cardiac development and their expression coincides with Cx40 expression [10]. Also the binding site for the homeobox Nkx-2.5 is interesting. This transcription factor is expressed during embryonic development as well as in the adult stage of the mouse heart. Interestingly, the gene for Atrial Natriuretic Factor, another developmentally and region-specifically regulated gene, is a target for Nkx-2.5 [11]. Future studies in which parts of this upstream region will be analyzed for promoter activity in reporter-gene constructs will detail the activity of the Cx40 promoter.

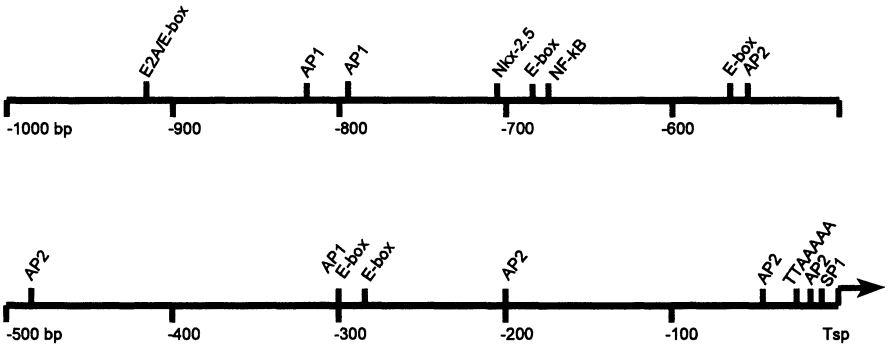

Figure 5. *Schematic representation of the transcription factor binding sites in the DNA sequence upstream of the transcription start site (Tsp) indicated by the arrow. The sequence TTAAAAA is a TATA-like element at -29 bp. The sequence can be accessed in the Genbank database with accession number AF025766.*

Summary and conclusions

We have isolated the 5'-end sequences for rat Cx40 mRNA. Cx40 mRNA from lung, adult and neonatal heart and A7r5 cells all contain the same 5'-end sequence. We have shown that the Cx40 gene consist of two exons separated by a large intron of at least 5.5 Kb. Genomic DNA upstream and downstream of exon 1 was amplified by LD-PCR mediated genomic walking. Fine mapping of the transcription start site by primer extension and RNase protection analysis indicated one transcription start site in a number of tissues examined, showing that exon 1 is 85 bp long. The same primer extension/RNase protection analyses revealed that Cx40 mRNA level was highest in A7r5 cells, followed by neonatal and adult lung, neonatal atria and ventricle. The upstream region of the connexin gene was analysed for the presence of consensus sequences for transcription factor binding sites. It contains a TATA-like sequence and a number of potential binding sites for Sp1, AP2, AP1, NFκB, NKx-2.5 and E-box sequences. Our data suggests that the same region of upstream DNA regulates Cx40 gene transcription in the different tissues examined. Therefore spatio-temporal control of Cx40 gene expression may be due to different transcription factors or differences in the level of transcription factors.

Acknowledgements

I wish to thank my co-workers Dr H.J. Jongsma, Dr H. M.W. v.d. Velden, A.A.B. van Veen, Dr M.J. van Kempen and Dr F. Coenjaerts for their helpful discussions and contributions to this work. This study was supported by the Netherlands Heart Foundation, grant numbers M93.002 and M96.001.

References

1. Gros DB, Jongsma HJ. Connexins in mammalian heart function. Bioessays 1996;18:719-30.
2. Van Kempen MJ, Vermeulen JL, Moorman AF, Gros D, Paul DL, Lamers WH. Developmental changes of connexin40 and connexin43 mRNA distribution patterns in the rat heart. Cardiovasc Res 1996;32:886-900.
3. Haefliger JA, Bruzzone R, Jenkins NA, Gilbert DJ, Copeland NG, Paul DL. Four novel members of the connexin family of gap junction proteins. Molecular cloning, expression, and chromosome mapping. J Biol Chem 1992;267:2057-64.
4. Siebert PD, Chenchik A, Kellogg DE, Lukyanov KA, Lukyanov SA. An improved PCR method for walking in uncloned genomic DNA. Nucleic Acids Res 1995;23:1087-88.
5. Ausubel FM, Brent R, Kingston RE, Moore DD, Seidman JG, Smith JA, et al. Current Protocols in Molecular Biology. 1997.
6. Neuhaus IM, Dahl G, Werner R. Use of alternate promoters for tissue-specific expression of the gene coding for connexin32. Gene 1995;158:257-62.
7. Sohl G, Gillen C, Bosse F, Gleichmann M, Muller HW, Willecke K. A second alternative transcript of the gap junction gene connexin32 is expressed in murine Schwann cells and modulated in injured sciatic nerve. Eur J Cell Biol 1996;69:267-75.
8. Beyer EC, Reed KE, Westphale EM, Kanter HL, Larson DM. Molecular cloning and expression of rat connexin 40, a gap junction protein expressed in vascular smooth muscle. J Membr Biol 1992;127:69-76.
9. Mably JD, Liew CC. Factors involved in cardiogenesis and the regulation of cardiac-specific gene expression. Circ Res 1996;79:4-13.
10. Delorme B, Dahl E, Jarry-Guichard T, Brand J, Willecke K, Gros D, et al. Expression pattern of connexin gene products at the early developmental stages of the mouse cardiovascular system. Circulation Research 1997;81:423-37.
11. Durocher D, Chen CY, Ardati A, Schwartz RJ, Nemer M. The atrial natriuretic factor promoter is a downstream target for Nkx-2.5 in the myocardium. Mol Cell Biol 1996;16:4648-55.

12. SYMPATHETIC REGULATION OF CARDIAC DELAYED RECTIFICATION: RELATIONSHIP TO CARDIAC ARRHYTHMIAS

Robert S. Kass

Introduction

Electrical impulses control the frequency, strength, and duration of contraction of the heart. During the normal cardiac cycle, a regular rhythmic pattern must be established of time-dependent changes in cellular permeability to maintain the cardiac cycle that underlies normal cardiac function. Impulses, which originate in the sinoatrial (SA) node, are conducted by the myocardium throughout the atria until they converge at the atrioventricular (AV) node, pass through the bundle of His and the Purkinje fiber conducting system, and eventually excite the working myocardial cells in the ventricles. As the heart is a dynamic organ and must adjust its output with changes in physiological demand, control of electrical activity by neurohormones is essential in the maintenance of proper cardiovascular function. Recent work has linked defects in several ion channel proteins to at least two forms of inherited cardiac arrhythmias: the Long QT Syndrome (LQTS) [1] and the Brugada Syndrome [2]. In the cases of these diseases identified mutations in ion channel structure have been shown to cause functional changes in channel properties using heterologous expression of the channel proteins [3]. The data obtained to date indicate that the inherited changes (mutations) in channel structure change channel activity in a manner that is consistent with most disease phenotypes, but by themselves, are not sufficient to account for fatal cardiac events and sudden cardiac death (SCD). Other factors must be considered. Here one factor, the regulation of a key potassium current, the slow delayed rectifier channel I_{Ks}, will be discussed in the context of a possible link to fatal events in one form of the long QT syndrome: LQT1 as this form of LQTS is most likely to lead to fatal arrhythmias in the face of sympathetic stimulation [4].

P.A. Doevendans et al. (eds.), Cardiovascular specific gene expression, 125-37.

Slow Potassium Channel Activity in Heart

Noble and Tsien [5] provided the first quantitative investigation of time-dependent outward currents that activate over the voltage range of and with a time course similar to the action potential of the cardiac ventricles. Because the underlying conductance(s) of these currents activate slowly and with a delay compared to the rapidly activating sodium and calcium channel currents, the currents were referred to as "delayed rectifier" conductances. Several very important characteristics of cardiac delayed rectification emerged from this study. Two components of potassium-sensitive current were found to be activated during prolonged depolarization to voltages positive to -50 mV in the sheep cardiac Purkinje fiber. Although the currents were sensitive to the external potassium ion concentration, they were not perfectly potassium-selective as judged by the equilibrium potentials of the two current components. Consequently, the names I_{x1}, and I_{x2}, were chosen to identify the components. The dominant permeant ion, based on equilibrium potential measurements, was indeed found to be potassium [5,6]. Key properites of these currents were established early on. The first component, I_{x1}, activated with time constants that were voltage-dependent and on the order of 0.05 to 0.5 second, depending on membrane potential (figure 1). The current activated at voltages positive to - 50 mV, a voltage range important to plateau voltages. The second component, I_{x2} was characterized by extremely slow activation kinetics, less potassium selectivity, and a relatively linear instantaneous current-voltage relationship. Both current components were used to successfully reconstruct the measured currents [5] as well as the Purkinje fiber action potential [7]. After this pioneering work, other groups reported similar slowly activating and non-inactivating potassium-sensitive currents in a wide variety of cardiac preparations [8,9]. In most cases, the kinetics of activation and deactivation of these currents was complex, and the interpretation of the data as representative of two individual current components was preserved. Because of the unique relationhip between the time course of the gating of these channels and the action potential duration of the ventricle, it was thought very early on that changes in this current induced by epinephrine might be important in controlling action potential duration in the face of elevated sympathetic tone [6,7,10].

Pharmacological Dissection: Discovery of Novel Components

Sanguinetti and Jurkiewicz [10], in an attempt to resolve the mechanism of action of the drug E4031, a putative class III agent, found that currents measured during depolarizing test pulses appeared to be less sensitive to this compound than tail currents measured after termination of the test pulses. They reasoned that this effect could be due to either [1] voltage-dependent block of the drug or [2] specific inhibition of a current component that rectifies during depolarization but is measurable as a decaying tail current after termination of the depolarizing test pulse. They concluded that delayed rectification in ventricular cells consists of two components: one that activates rapidly but then spontaneously inactivates with depolarization (I_{Kr}); and a second, approximately ten-fold larger component, which is lanthanum- and E-4031-insensitive

and does not inactivate, which was labeled I_{Ks} because of its slow kinetics. I_{Ks} is the dominant component of I_K recorded positive to voltages of + 20 mV in the ventricle, and importantly it is the component that is sensitive to catecholamines [12].

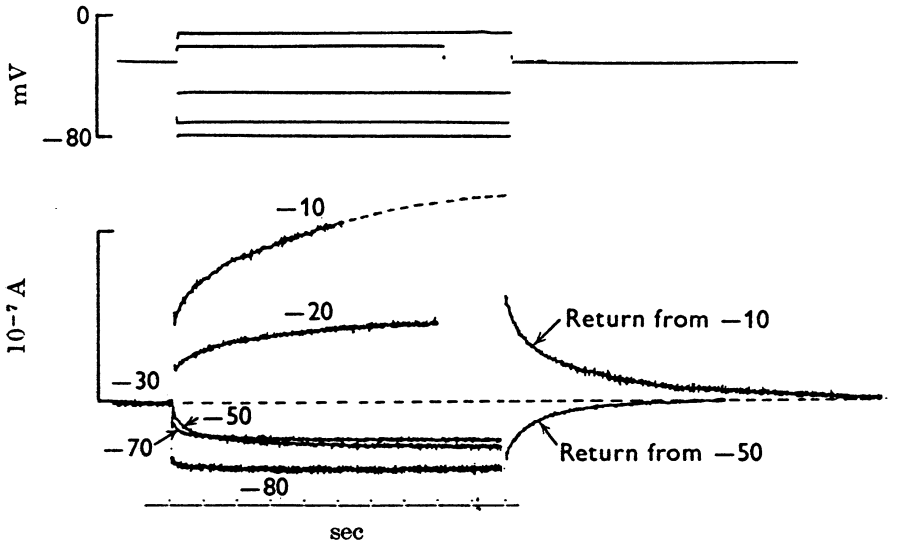

Figure 1. *Membrane currents in response to step potential changes from a holding potential (-30 mV) in the plateau range. The currents in response to steps -10, -20, -50, -70 and -80 mV are shown. Large slow current changes occur in response to positive steps. The current changes in response to negative steps are smaller and at -80 mV there is virtually no slow current change. The records of recovery of current following returns from -10 and -50 mV are also shown. Note that the time courses are not symmetric and that time course of current following return from -10 mV contains a slow component which is almost absent in the case of recovery from -50 mV [5].*

Neuromodulation of delayed rectification in the heart

Cardiac electrical and mechanical activity is modulated extensively by the neuroendrocrine system. Key to this control is the regulation of K^+ currents in different anatomical regions of the heart. Changes in heart rate must be accompanied by concomitant control of the action potential durations to ensure a proper temporal relationship between diastolic filling and systolic ejection. Because delayed rectifier channels are such major determinants of action potential duration (APD), their neurohomonal regulation, which has been shown to be closely linked to control of APD_{50} [10] is key to cardiac function.

β-*Adrenergic Stimulation*

Stimulation of the sympathetic nerves releases norepinephrine from nerve terminals that extensively innervate the heart. This causes marked increases in heart rate, as well as the strength of contraction, and a shortening of the cardiac action potential. Closely

linked to changes in heart rate and contractile activity are the well-known stimulatory effects of β-adrenergic stimulation not only on L-type calcium channel activity, which has been investigated extensively by many groups, but also on one component of delayed rectification in the heart (I_{Ks}). Sympathetic regulation of this K^+ channel is not linked directly to stimulation of L-type calcium channel activity nor to enhanced entry of calcium ions through modulated L-type channels [13].

Tsien et al. [14] first showed that cAMP can increase I_K in isolated calf Purkinje fibers and since that work, many groups have shown that β-adrenergic agonists, cAMP and its analogues, and phosphodiesterase inhibitors increase I_{Ks}, in Purkinje fibers and other multicellular preparations [10,15,16] as well as in isolated cardiac myocytes [17,18]. The effects of β-stimulation are dramatic: four- to six-fold increases in current amplitude have been measured (figure 2). Thus, the importance of I_{Ks} regulation to control of the action potential duration should not be underestimated.

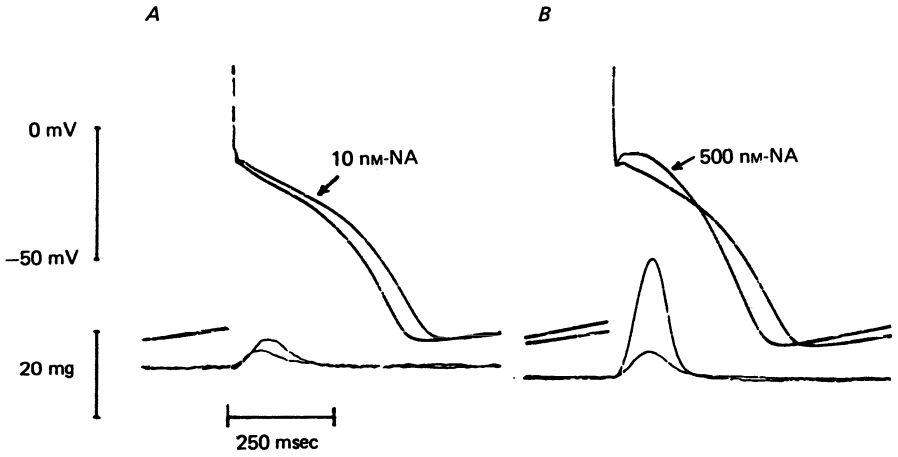

Figure 2. *Concentration-dependent actions of noradrenaline on the Purkinje fibre action potential and twitch. Storage oscilloscope records of membrane potential and tension obtained during a continuous microelectrode impalement. A, prolongation of the action potential duration by 20 nM-noradrenaline. B, reduction of action potential duration by 500 nM-noradrenaline. Twitch height is increased by both concentrations.*

Studies of I_{Ks} in single cells have provided evidence that β-adrenergic enhancement of I_K is associated with phosphorylation of an intracelluar protein by protein kinase A (PKA), although this remains to be proven directly. Support for the hypothesis that I_K is regulated by a cytoplasmic, cAMP-dependent signaling pathway has been obtained from experiments performed using isolated cardiac myocytes. I_K has been shown to be increased by extracellular application of β-adrenergic agonists or membrane-permeable cAMP analogues, as well as by direct intracellular application of cAMP or the catalytic subunit of cAMP-dependent protein kinase [17,19,20,21]. Forskolin stimulates I_K in the absence of agonist, whereas dialysis with either the regulatory subunit or a specific inhibitor of the enzyme prevents agonist-induced enhancement of I_K. These results, reviewed in more detail by Anumonwo et al. and Hartzell [22,23] all are consistent with

the hypothesis that β-adrenergic enhancement of I_K is associated with phosphorylation of an intracellular protein by protein kinase A, and all support the key view that regulation of I_K by cAMP-dependent phosphorylation is crucial to normal heart function.

Molecular genetics: Identification of Delayed Rectifier Genes

Molecular genetic and biochemical approaches to the study of ion channel proteins have revealed remarkable conservation of channel structure that spans species and tissues. Key to identification of the molecular basis of electrical activity in native cells is the correlation of functional properties of native and recombinant channels as well as other means of identification such as immunological identification of native and recombinant proteins.

Most voltage-gated K^+ channels have structural similarity to a class of channels first isolated from experiments with the fruit fly *Drosophila* by both the Jan [24] and Pongs [25] laboratories. Powerful structural evidence for this conservation has recently been provided by crystalization of a K^+ channel from a bacterium [26,27]. These channels, the so-called *Shaker* A-type channels, are characterized by rapid activation followed by voltage-dependent inactivation. The derived protein sequences of the *Shaker* channels were found to have remarkable similarities to previously cloned Na^+ and dihydropyridine-sensitive Ca^{2+} channels [28]. The hydropathy profile of the K^+ channel proteins indicates six transmembrane-spanning hydrophobic segments (S1, S2, S3, S4, S5, and S6). The fourth segment, S4, is positively charged and proposed to be the voltage sensor of the channel that controls voltage-dependent gating. Na^+ and Ca^{2+} channel proteins contain four regions of internal repeats. Thus, each K^+ channel is very similar to one quarter of a Na^+ or Ca^{2+} channel. Because *Shaker-type* K^+ channels consist of only one region of internal repeats, it was thought that K^+ channels are multimers with four subunits required to assemble a functioning channel-a hypothesis supported by elegant experimental data of MacKinnon [27,29].

Molecular Genetics of Potassium channels and the Long QT Syndrome

The molecular identity of I_{Kr} and I_{Ks} had remained unknown until revealed by molecular genetic analysis of an inherited disease, the long QT syndrome, because the predicited sequence of a key subunit, minK [30,31,32], was distinct from other voltage-gated K^+ channels.

The familial form of long QT syndrome is predominantly an autosomal dominant disorder associated with recurrent syncope and a propensity to polymorphous ventricular tachycardia (torsade de pointes) and sudden death [33,34]. As the name implies, the disease phenotype is caused by inherited defects in the cardiac repolarization process. In 1995 major breakthroughs in our understanding of this disease were achieved as defects in ion channels were discovered to be linked and then shown to be causally responsible for two forms of the disease: LQT-2 (chromosome 7) [35] and LQT-3 (SCN5A, chromosome 3) [36].

SCN5A surprisingly encodes the subunit of the human heart voltage-gated Na^+ channel. Functional analysis of the discovered mutations indicated that the mutant channels failed to inactivate complete upon maintained depolarization and hence contributed directly to prolongation of the ventricular action potential [3,37-39]. Analysis of the LQT-2 linked gene indicated that it was a member of the ether-a-go-go (EAG) channel family, originally cloned by screening a hippocampal library [40,41] and later cloned from the human heart and named HERG (Human Ether-a-go-go Related Gene) [41]. Importantly, expression of the cRNA encoding this gene product elicited membrane currents with voltage-dependent kinetic and pharmacologic profiles almost identical to that of I_{Kr} [35]. Like I_{Kr}, the HERG gene product activates over a more negative range of voltages than I_{Ks} and shows rectification at more positive potentials characterized by a negative slope conductance at voltages positive to 0 or +10 mV. More recent studies [42] have shown that this apparent inward rectification is caused by rapid C-type inactivation and could be abolished by mutation of one amino acid residue (S631A) in the outer mouth of the pore of HERG [43]. C-type inactivation involves movement of conserved core domain residues that result in closure of the external mouth of the channel pore. Unlike C-type inactivation in other channels, HERG appears to be unique in possessing voltage-dependent inactivation [42,44].

Subsequent analysis of the functional consequences of LQT-2 mutations have indicated that, in most cases, the mutations acted as dominant negative mutations causing a net reduction in outward current during the critical plateau period and hence prolongation of repolarization [45]. These data which correlate clinical recordings with biophysical changes in expressed channel activity provide direct experimental proof of the functional importance of specific potassium channel activity to human heart electrophysiology.

KvLQT1, another novel K^+ channel gene, was subsequently discovered by positional cloning and linkage to chromosome 11 from molecular genetic studies of another form of the long QT syndrome, LQT-1 [46]. The initial report of the KvLQT-1 gene revealved only a partial clone with high homology with the pore (p) region of other voltage-gated K channels. Functional data were lacking. However, once the full length clone was obtained, two very important studies revealed that KvLQT1 encodes a subunit of the slowly-activating and non-inactivating delayed potassium current I_{Ks} which was first characterized by Noble and Tsien [47].

I_{Ks} and the Long QT syndrome: identification of molecular properties based on analysis of human disease

Importantly, the structural and functional role of a second subunit, minK, was revealed recently by studies which clearly showed that expression of I_{Ks} channels requires co-assembly of minK along with KvLQT1 subunits [45,48,49]. Until the discovery of this link between I_{Ks} and KvLQT1, the molecular basis of this important current had been a matter of considerable controversy because it had been most closely associated solely with minK. MinK is a gene cloned from cardiac tissue including human and encodes a protein containing 129-130 amino acids, which contains only one membrane spanning domain and no homology with other cloned voltage-gated K channels [50-53]. It is now

clear that minK, by itself, does not form functional K^+ channels, but is an essential subunit that co-assembles with the KvLQT1 gene product to form channels that underlie I_{Ks}. This work strongly suggested that mutations in either the KvLQT1 or minK genes may affect biophysical, regulatory, or pharmacological properties of expressed I_{Ks} and hence repolarization (figure 3). Not surprisingly, subsequent studies confirmed this prediction by linking LQT-1 to mutations in minK as well as KvLQT-1 [54]. Hence the importance of I_{Ks} and thus minK and KvLQT1 in regulating repolarization of the human ventricle is validated by these findings.

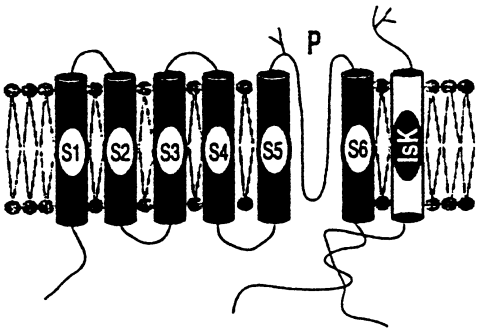

Figure 3. *The molecular architectures of KvLQT1 and IsK [48].*

Sympathetic Stimulation and LQT

LQT syndrome patients are particularly prone to develop serious ventricular arrhythmias under sympathetic activation [33,34,55,56], and recent clinical data strongly suggest that for carriers of LQT-1 gene defects adrenergic factors are more likely to trigger cardiac events than carriers of LQT-3 or LQT-2 gene defects [57]. Because I_{Ks} is regulated by norepinephrine (see below) and is a key factor in control of action potential duration in the face of elevated sympathetic stimulation [10,50,58]. It is very likely that suppressed activity of I_{Ks} in carriers of KvLQT-1 gene defects underlies, at least in part, sympathetic nervous system exacerbation of cardiac arrhythmias in LQT-1 patients. Similarly, in other cardiac disorders in which sympathetic modulation is altered such as congestive heart failure [59], it is now clearly important to consider possible contributions of KvLQT-1 and minK gene products to rhythm disturbances. Thus an understanding of the molecular basis of the regulation of delayed rectification by neurohormones is key to understanding and treating these disorders of cardiac rhythm.

Molecular basis of neuro-modulation of I_{Ks}

In considering the molecular basis of I_{Ks} regulation by PKA several factors must be considered. First, because it is now clear that both minK and KvLQT1 subunits assemble to form functional I_{Ks} channels, potential phosphorylation sites on both

channel subunits must be considered. Initial attempts to identify the molecular basis of I_{Ks} regulation relied on expression of membrane current in Xenopus oocytes injected with minK cRNA. In these initial experiments, expressed currents were demonstrated to be enhanced by PKA [60] indicating that it is possible to reconstruct the native channel PKA enhancement. However, identification of specific sites on KvLQT-1 and minK proteins that are targets of PKA phosphorylation remains to be established. A putative role of minK in regulation of channels has been clearly shown by mutagenesis experiments that first focused on PKC-dependent channel modulation. Initial experiments indicated that protein kinase C (PKC) inhibited I_{Ks} expressed in Xenopus oocytes and that this inhibition could be prevented by mutation of a specific minK residue [61]. Subsequent studies showed that species variation in minK could account for differences in PKC regulatory actions [61-63]. These data provide the strongest evidence that minK is an important regulator of I_{Ks} activity and that the minK protein is a likely target of regulatory enzymes. Recent work has shown that the KvLQT1 protein itself can be the target of cAMP [64] (figure 4), and hence the molecular basis of I_{Ks} regulation is, no doubt, due to a combination of modulation of the two molecular targets: minK and KvLQT1. Further work is needed to clarify putative roles of the KvLQT1 protein as another target and further, how phosphorylation of these proteins increases the magnitude of the expressed currents, the ultimate physiological response.

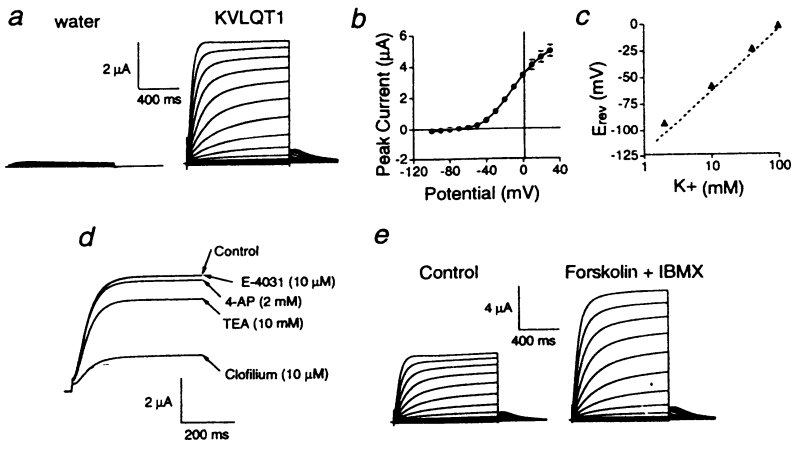

Figure 4. *Functional and pharmacologic characterization of KvLQT1 currents in Xenopus oocytes.(a) Families of currents from water- and KvLQT1-injected oocytes were elicited by 1-sec voltage steps from a holding potential of -80 mV to test potentials ranging from -100 to +40 mV in 10 mV increments. (b) Peak current-voltage (I-V) relationship for 12 oocytes expressing KvLQT1. Currents were recorded using the protocol in a. (c) Dependence of tail current reversal potential (E_{rev}) on the K^+ concentration. Tail currents were elicited at potentials of -110 to +10 mV after a pulse to +20 mV(n=6 oocytes), while the external K^+ concentration varied between 2, 10, 40, and 98 mM. (d) Effects of E-4031, 4-aminopurine, tetrathylammonium, and clofilium on KvLQT1 current. Superimposed currents were recorded during 500-ms steps to +30 mV, from -80 mV, during the same experiment. (e) Effects of cAMP on KvLQT1 currents. Currents were recorded using the protocol in a before and 10 min after the simultaneous addition of 10 μM foskolin and 100 μM IBMX to the bath [64].*

Targeting of modulatory enzymes: selective regulation of ion channels by singaling cascades

Identification of the molecular components that underlie regulation of cardiac delayed rectification very likely will require studies of both target proteins and molecules that direct the modulating enzymes. Recent studies of the molecular basis of the regulation of cardiac L-type calcium channels (I_{Ca}) have revealed that for this very well-studied pathway, reconstitution of PKA-dependent enhancement of I_{Ca} has required heterologous expression of multiple channel subunits, but in addition, anchoring proteins that have been shown to direct the posphorylating (PKA) enzyme to the target protein (L-type calcium channel) [65-72]. Initial studies of the modulation of I_{Ks} in mouse heart engineered to overexpress the human β2-adrenergic receptor have shown that, in cells isolated from these hearts, cAMP appears to be preferentially increased in regions surrounding the L-type calcium channel vs the I_{Ks} channels [73] strongly suggesting that distinct targeting proteins are associated with these two channel types. Elucidation of these targeting molecules will be an important contribution in unraveling the molecular basis of regulation of cardiac ion channels. It should provide key new information for the development of novel therapeutic tools to manage electrical disturbances that result from an imbalance of the β-adrenergic control of heart electrical activity.

Summary and conclusions

Although the LQTS is a rare inherited disorder, the information that has been revealed by studying the molecular genetics of this disease has already made a profound impact on our understanding of the molecular genetics of human heart function. Emerging from these investigations is the picture that ion channel regulation, studied in *in vitro* cellular biophysical experiments can reveal crucial factors that are needed for proper physiological function of the human heart. The exciting combination of *in vitro* electrophysiological studies with genetically-altered animal models will allow further and specific testing of the roles of channel and signaling molecule mutations in the genesis of cardiac arrhythmias. The linkage of Brugada's syndrome to a mutation in the human heart Na^+ channel is the first step in extending the lessons learned from LQTS to inherited disorders that are more widespread and, perhaps, more likely to be lethal. The role of the minimal potassium channel protein minK, will no doubt emerge to be important in multiple disorders where there is linkage between sympathetic stimulation and cardiac dysfunction.

References

1. Kass RS, Davies MP. The roles of ion channels in an inherited heart disease: molecular genetics of the long QT syndrome. Cardiovasc Res 1996;32:443-54.
2. Chen Q, Kirsch GE, Zhang D, Brugada R, Brugada R, Brugada J, et al. Genetic basis and molecular mechanism for idiopathic ventricular fibrillation. Nature 1998;392:293-96.
3. An RH, Bangalore R, Rosero SZ, Kass RS. Lidocaine block of LQT-3 mutant human Na channels. Circ Res 1996;79:103-08.
4. Moss AJ. Management of patients with the hereditary long QT syndrome. J Cardiovasc Electrophysiol 1998;9:668-74.
5. Noble D, Tsien R. Outward membrane currents activated in the plateau range of potentials in cardiac Purkinje fibres. J Physiol 1969;200:205-31.
6. Hauswirth O, Noble D, Tsien RW. The mechanism of oscillatory activity at low membrane potentials in cardiac Purkinje fibres. J Physiol (Lond) 1969;200:255-65.
7. McAllister RE, Noble D, Tsien RW. Reconstruction of the electrical activity of cardiac Purkinje fibres. J Physiol 1975;251:1-59.
8. McDonald TF, Trautwein W. Membrane currents in cat myocardium: Separation of inward and outward components. J Physiol 1978;274:193-216.
9. Noma A, Irisawa H. A time and voltage-dependent potassium current in the rabbit sinoatrial node cell. Pflüg Arch 1976;366:251-58.
10. Kass RS, Wiegers SE. The ionic basis of concentration-related effects of noradrenaline on the action potential of calf cardiac Purkinje fibres. J Physiol 1982;322,541-58.
11. Sanguinetti MC, Jurkiewicz NK. Two components of cardiac delayed rectifier K+ current. Differential sensitivity to block by class III antiarrhythmic agents. J Gen Physiol 1990;96:195-215.
12. Sanguinetti MC, Jurkiewicz NK, Scott A, Siegle PK. Isoproterenol antagonizes prolongation of refractory period by the class III antiarrhythmic agent E-4031 in guina pig myocytes. Circ Res 1993;68:77-84.
13. Kass RS. Delayed Rectification in the Cardiac Purkinje Fiber is not activated by intracellular calcium. Biophys J 1984;45:837-39.
14. Tsien RW, Giles W, Greengard P. Cyclic AMP mediates the effects of adrenaline on cardiac Purkinje fibers. Nature 1972;240:181-83.
15. Carmeliet E, Mubagwa K. Changes by acetylcholine of membrane currents in rabbit cardiac Purkinje fibres. J Physiol 1986;371:201-17.
16. Umento T. β-actions of catecholamines on the K-related currents of the bullfrog atrial muscle. Jap J Physiol 1984;34:513-28.
17. Walsh KB, Kass RS. Regulation of a heart potassium channel by protein kinase A and C. Science 1988;242:67-69.
18. Duchatelle-Gourdon I, Hartzell HC, Lagrutta AA. Modulation of the delayed rectifier potassium current in frog cardiomyocytes by β-adrenergic agonists and magnesium. J Physiol 1989;415:251-74.
19. Harvey RD, Hume JR. Autonomic regulation of delayed rectifier K+ current in Mammalian heart involves G proteins. Am J Phys 1987;257:H818-23.
20. Yazawa K, Kameyama M. Mechanism of receptor-mediated modulation of the delayed outward potassium current in guinea-pig ventricular myocytes. J Physiol 1990;421:135-50.
21. Bennett PB, Begenisich T. Catecholamines modulate the delayed rectifying potassium current (I_K) in guinea pig ventricular myocytes. Pflug Arch 1987;410:217-19.
22. Anumonwo JM, Freeman LC, Kwok WM, Kass RS. Potassium channels in the heart: electrophysiology and pharmacologcial regulation. Cardiovasc Drug Rev 1991;9:299-316.
23. Hartzell HC. Regulation of cardiac ion channels by catecholamines, acetylcholine, and second messenger systems. Prog Biophys Molec Biol 1987;52:165-247.

24. Papazian DM, Schwarz TL, Tempel BL, Jan YN, Jan LY. Cloning of genomic and complementary DNA from Shaker, a putative potassium channels gene from Drosophila. Science 1987;237:749-53.
25. Pongs O, Kecskemethy N, Muller R, Krah-Jentgens I, Baumann A, Kiltz HH, et al. Shaker encodes a family of putative potassium channel proteins in the nervous system of Drosophila. EMBO J 1988;7:1087-96.
26. MacKinnon R, Cohen SL, Kuo A, Lee A, Chait BT. Structural conservation in prokaryotic and eukaryotic potassium channels. Science 1998;280:106-09.
27. MacKinnon R. Determination of the subunit stoichiometry of a voltage-activated potassium channel. Nature 1991;350: 232-35.
28. Catterall WA. Ion channels in plasma membrane signal transduction. J Bioenerg Biomembr 1996;28:217-18.
29. Mackinnon R. Pore loops: an emerging theme in ion channel structure. Neuron 1995;14:889-92.
30. Pragnell M, Snay KJ, Trimmer JS, Maclusky NJ, Naftolin F, Kaczmarek LK, Boyle MB. Estrogen induction of a small, putative K^+ channel mRNA in rat uterus. Neuron 1990;4:807-12.
31. Goldstein SA, Miller C. Site-specific mutations in a minimal voltage-dependent K^+ channel alter ion selectivity and open-channel block. Neuron 1991;7:403-08.
32. Busch AE, Kavanaugh MP, Varnum MD, Adelman JP, North RA. Regulation by second messengers of the slowly activating, voltage-dependent potassium current expressed in Xenopus oocytes. J Physiol 1992;450:491-502.
33. Moss A, Schwartz PJ, Crampton RS, Tzivoni D, Locati EH, Maccluer J, et al. The long QT syndrome: prospecitve longitudinal study of 328 families. Circulation 1991;84:1136-44.
34. Schwartz PJ, Periti M, Malliani A. The long Q-T syndrome. Am Heart J 1975;89:378-90.
35. Sanguinetti MC, Jiang C, Curran ME, Keating MT. A mechanistic link between an inherited and an acquired cardiac arrhythmia: HERG encodes the I_{Kr} potassium channel. Cell 1995;81:299-307.
36. Wang Q, Shen J. Splawski I, Atkinson D, Li Z, Robinson JL, Moss AJ, Towbin JA, Keating MT. SCN5A mutations associated with an inherited cardiac arrhythmia, long QT syndrome. Cell 1995;80:805-11.
37. Bennett PB, Yazawa K, Matika N, George AL. Molecular mechanism for an iniherited cardiac arrhythmia. Nature 1995;376:683-685.
38. Priori SG, Napolitano C, Cantu F, Brown AM, Schwarz PJ. Differential response to Na^+ channel blockade, β-adrenergic stimulation and rapid pacing in a cellular model mimicking the SCN5A and HERG defects present in the long-QT syndrome. Circ Res 1996;78:1009-15.
39. Wang DW, Yazawa K, Makita N, George AL, Bennett PB. Pharmacological targetting of long QT mutant sodium channels. J Clin Invest 1997;99:1714-20.
40. Warmke J, Drysdale R, Ganetzky B. A distinct potassium channel polypeptide encoded by the Drosophila eag locus. Science 1991;252:1560-62.
41. Warmke JW, Ganetzky B. A family of potassium channel genes related to eag in Drosophila and mammals. Proc Natl Acad Sci USA 1994;91:3438-42.
42. Schonherr R, Heinemann SH. Molecular determinants for activation and inactivation of HERG, a human inward rectifier potassium channel. J Physiol 1996;493:635-42.
43. Zou A, Xu QP, Sanguinetti MC. A mutation in the pore region of HERG K^+ channels expressed in xenopus oocytes reduces rectification by shifting the voltage dependence of inactivation. J Physiol 1998;509:129-37.
44. Ho WK, Kim I, Lee CO, Earm YE. Voltage-dependent blockade of HERG channels expressed in Xenopus oocytes by external Ca^{2+} and Mg^{2+}. J Physiol 1998;507:631-38.
45. Sanguinetti MC, Curran ME, Zou A, Shen K, Spector PS, Keating MT. Coassambly of K(v)LQT1 and minK (IsK) proteins to form cardiac Iks potassium channel. Nature

1996;384:80-83.
46. Wang Q, Curran ME, Splawski I, Burn TC, Millholland JM, Vanraay TJ, et al. Positional cloning of a novel potassium channel gene - KVLQT1 mutations cause cardiac arrhythmias. Nat Gen 1996;12:17-23.
47. Noble D, Tsien R. The kinetics and rectifier properties of the slow potassium current in cardiac Purkinje fibres. J Physiol (Lond) 1968;195:185-214.
48. Barhanin J, Lesage F, Guillemare E, Fink M, Lazdunski M, Romey G. K(v)LQT1 and IsK (MinK) proteins associate to form the Iks cardiac potassium current. Nature 1996;384:78-80.
49. Sanguinetti MC, Curran ME, Spector PS, Keating MT. Spectrum of HERG K channel dysfunction in an inherited cardiac arrhythmia. Proc Natl Acad Sci USA 1996;93:2208-12.
50. Folander K, Smith JS, Antanavage J, Bennett C, Stein RB, Swanson R. Cloning and expression of the delayed-rectifier IsK channel from neonatal rat heart and diethylstilbestrol-primed rat uterus. Proc Natl Acad Sci USA 1990;87:2975-79.
51. Murai T, Kazikuza A, Takumi T, Ohkubo H, Nakanishi S. Molecular cloning and sequence analysis of human genomic DNA encoding a novel membrane protein which exhibits a slowly activating potassium channel activity. Biochem Biophys Res Comm 1989;161:176-81.
52. Folander K, Douglass J, Swanson R. Confirmation of the assignment of the gene encoding K(V)1.3, a voltage-gated potassium channel (KCNA3) to the proximal short arm of human chromosome 1. Genomics 1994;23:295-96.
53. Busch AE, Herzer T, Takumi T, Krippeitdrews P, Waldegger S, Lang F. Blockade of human IsK channels expressed in Xenopus oocytes by the novel class III antiarrhythmic drug NE-10064. Eur J Pharmacol 1994;264:33-37.
54. Splaswski I, Tristani-Firouzi M, Lehmann MH, Sanguinetti MC, Keating MT. Mutations in the hminK gene cause long QT syndrome and suppress IKs function. Nat Genet 1997;17:338-40.
55. Defferrari GM, Locati EH, Priori SG, Schwarz PJ. Left cardiac sympathetic denervation in long QT syndrome patients. J Intervent Cardiol 1995;8:776-81.
56. Schwartz PJ, Locati EH, Napolitano C, Priori SB. The long QT syndrome. In : Cardiac Electrophysiology: From Cell to Bedside. Eds. Zipes DP, Jalife J. (Philadelphia: W.B. Saunders Co) 1995;788-811.
57. Hajj-Ali R, Zareba W, Rosero SZ, Moss AJ, Schwartz PJ, Benhorin J, Priori SG, Robinson JL, Locati EH. Adrenergic triggers and non-adrenergic factors associated with cardiac events in long QT syndrome patients. PACE 1997;20:1072 [Abstract].
58. Walsh KB, Begenisich TB, Kass RS. β-adrenergic modulation of cardiac ion channels: differential temperature-sensitivity of potassium and calcium currents. J Gen Physiol 1989;93:841-54.
59. Walsh KB, Kass RS. Distinct voltage-dependent regulation of a heart delayed IK by protein kinases A and C. Am J Physiol 1991;261:C1081-90
60. Blumenthal EM, Kaczarek LK. Modulation by cAMP of a slowly activating potassium channel expressed in Xenopus oocytes. J Neurosci 1992;12:290-96.
61. Busch AE, Maylie J. MinK channels: A minimal channel protein with a maximal impact. Physiol Biochem 1993;3:270-76.
62. Varnum MD, Busch AR, Bond CT, Maylie J, Adelman JP. The min K channel underlies the cardiac potassium current I_{Ks} and mediates species-specific reponses to protein kinase C. PNAS 1993;90:11528-32.
63. Busch AE, Varnum MD, North RA, Adelman JP. An amino acid mutation on a potassium channel that prevents inhibition by protein kinase C. Science 1992;255:1705-07.
64. Yang WP, Levesque PC, Little WA, Conder ML, Shalaby FY, Blanar MA. KvLQT1, a voltage-gated potassium channel responsible for human cardiac arrhythmias. Proc Natl Acad Sci USA 1997;94:4017-21.
65. Gao T, Yatani A, Dell'acqua ML, Sako , Green SA, Dascal N, Scott JD, Hosey MM. cAMP-

dependent regulation of cardiac L-type Ca^{2+} channels requires membrane targeting of PKA and phosphorylation of channel subunits. Neuron 1997;19:185-96.

66. Puri TS, Gerhardstein BL, Zhao XL, Ladner MB, Hosey MM. Differential effects of subunit interactions on protein kinase A- and C-mediated phosphorylation of L-type calcium channels. Biochem 1997;36:9605-15.
67. Zhao XL, Gutierrez LM, Chang CF, Hosey MM. The alpha 1-subunit of skeletal muscle L-type Ca channels is the key target for regulation by A-kinase and protein phosphatase-1C. Biochem Biophys Res Comm 1994;198:166-73.
68. Ahlijalian MK, Westenbroek RE, Catterall WA. Subunit structure and localization of dihydropyridine-sensitive calcium channels in mammalian brain, spinal cord, and retina. Neuron 1990;4:819-32.
69. Gray PC, Tibbs VC, Catterall WA, Murphy BJ. Identification of a 15-kDa cAMP-dependent protein kinase- anchoring protein associated with skeletal muscle L-type calcium channels. J Biol Chem 1997;272:6297-302.
70. Gurevich VV, Dion SB, Onorato JJ, Ptasienski K, Kim CM, Sterne-Marr R, Hosey MM, Benovic JL. Arrestin interactions with G protein-coupled receptors. Direct binding studies of wild type and mutant arrestins with rhodopsin, β2-adrenergic, and m2 muscarinic cholinergic receptors. J Biol Chem 1995;270:720-31.
71. Rotman EI, Murphy BJ, Catterall WA. Sites of selective cAMP-dependent phosphorylation of the L-type calcium channel alpha-1 subunit from intact rabbit skeletal muscle myotubes. J Biol Chem 1995;270:16371-77.
72. Scultoreanu A, Scheuer T, Catterall WA. Voltage-dependent potentiation of L-type Ca2+ channels due to phosphorylation by cAMP-dependent protein kinase. Nature 1993;364:240-43.
73. An RH, Heath B, Koch WJ, Lefkowitz RJ, Kass RS. Targeting of cAMP-dependent increases in L-type Ca (I_{Ca}) over delayed K channel (I_{Ks}) activity by overexpression of the β2 adrenergic receptor in the developing mouse heart. Biophys J 1998;74:A35 [Abstract].
74. Bristow MR, Feldman AM. Changes in the receptor-G protein-adenylyl cyclase system in heart failure from various types of heart muscle disease. Basic Res Cardiol 1992;87:15-35.

13. THE SARCO(ENDO)PLASMIC RETICULUM Ca^{2+} PUMPS IN THE CARDIOVASCULAR SYSTEM

Anne-Marie Lompré, Olivier Vallot, Marielle Anger, and Anne Ozog

Introduction

The sarcoplasmic reticulum (SR) is of major importance in the electrochemical coupling in striated muscle. In the heart, approximately 80% of the Ca^{2+} used for the contraction-relaxation cycle is released from SR through the Ca^{2+}-induced Ca^{2+}-release mechanism. In smooth muscle, SR is essential in the pharmacochemical coupling. The effect on contraction of many agonists which act through the activation of the phospholipase C cascade and production of inositol 1,4,5-trisphosphate (IP3) is dependent on the release of Ca^{2+} from internal stores. On the other hand, entry of Ca^{2+} from the extracellular space induces local increases in Ca^{2+} concentration sufficient to release Ca^{2+} from the SR/ER of cardiac and smooth muscle cells by the Ca^{2+}-induced Ca^{2+}-release mechanism activated by the ryanodine receptor (RyR). Calcium plays a role in endothelial cell signaling as a messenger for the release of endothelial factors regulating vascular smooth muscle and cardiac contractility. Both transsarcolemmal Ca^{2+} flux and release from internal stores are responsible for the agonists-induced increase in cytoplasmic Ca^{2+} concentration. In endothelial cells, the IP_3-induced Ca^{2+}-release is the major mechanism in the Ca^{2+} signaling pathway but the existence of the Ca^{2+}-induced Ca^{2+}-release mechanism and the presence of ryanodine receptors were also demonstrated [1].
Restoration of a low cytosolic Ca^{2+} concentration after cell activation is due to efflux of Ca^{2+} to the extracellular space by the plasmamembrane Ca^{2+}-ATPase and the $Na+/Ca^{2+}$ exchanger and refilling of the Ca^{2+} stores by the sarco(endo)plasmic reticulum Ca^{2+}-ATPases (SERCA). We will review some of the recent data on the SERCA isoforms and their regulation in the cardiovascular system.

The Sarco(Endo)plasmic Reticulum Ca^{2+} ATPase isoforms.

The sarco(endo)plasmic reticulum Ca^{2+}-ATPase, SERCA, is composed of a single polypeptide of 100 kD and is a member of an important family of homologous enzymes, the P-type transport ATPases which catalyze the active transport of cations

P.A. Doevendans et al. (eds.), Cardiovascular specific gene expression, 139-50.

across cell membranes. This family comprises the plasma membrane Ca^{2+}-ATPases, the Na^+/K^+-ATPases, and the H^+-ATPases. They are characterized by the formation of a covalent aspartylphosphate intermediate, intimately linked to the translocation process. For SERCA, ATP hydrolysis and enzyme phosphorylation result in translocation of two Ca^{2+} ions into the lumen of the SR.

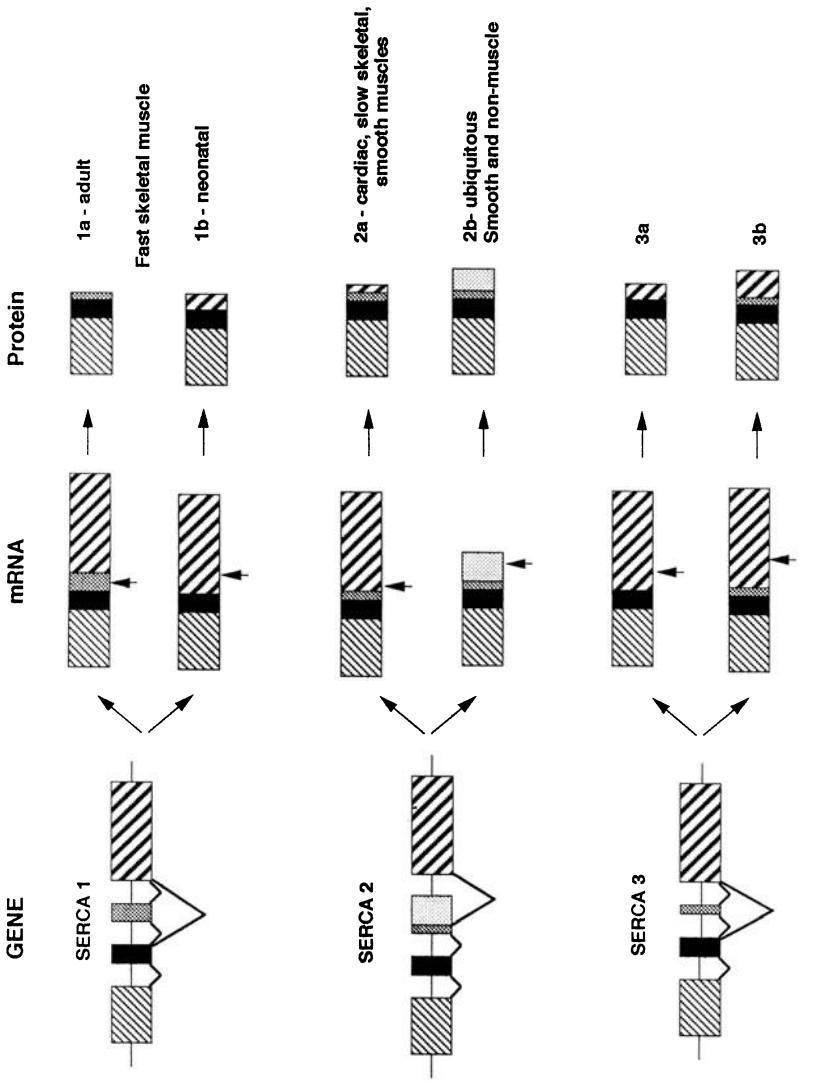

Figure 1. *Schematic representation of the 3' portion of the SERCA genes showing the alternative splicing mechanisms leading to the generation of two different transcripts for each gene. The arrows indicate the position of the stop codon.*

The first SERCA was cloned by MacLennan et al. [2] and since then many more sequences have been published. Six distinct SERCA isoforms encoded by three different genes have been described (figure 1). The SERCA 1 gene encodes SERCA 1a, present in adult fast skeletal muscle, and SERCA 1b, detected transiently in neonatal fast skeletal muscle. The C-terminal 8 amino acids of the neonatal isoform are replaced in the adult isoform by a single glycine residue. The SERCA 2 gene also encodes two alternatively spliced isoforms expressed in a tissue-specific manner: In the adult, SERCA 2a is present in heart, slow-skeletal muscles and some smooth muscle containing tissues such as the aorta. SERCA 2a is also present in embryonic skeletal muscle. SERCA 2b is a housekeeping isoform which is present at low levels in all cell types and is abundant in smooth and some non-muscle cell types. Both SERCA 2a and SERCA 2b are coexpressed in the media of the vasculature (figure 2). SERCA 2b differs from SERCA 2a by the replacement of the last four C-terminal amino acids by a peptide of 49 amino acids. Another isoform, SERCA 3, encoded by an independent gene, was found in a wide variety of tissues [3]. More recently we and others have shown that, in fact, it is coexpressed with SERCA 2b in specific cell types, mainly endothelial cells (figure 2), the megakaryocyte cell lineage, platelets and epithelial cells from trachea, intestine and salivary glands [4-7], the T-lymphoblastoid Jurkat cell line and mast cells [8] and neuronal purkinje cells [9]. In salivary glands, SERCA 3 is localized at the basal pole, whereas SERCA 2b is present at the luminal pole [6].

At early developmental stages SERCA 3 is present in the heart tube and later on, its expression in the cardiovascular system is restricted to the arterial endothelial cells, but we have not been able to detect SERCA 3 mRNA, either in veins or endocardium [10]. In the meantime, two distinct SERCA 3 sequences have been submitted to genebank. The two proteins differ by the replacement of the last 6 C-terminal amino acids of SERCA 3a by a 45-amino-acid peptide in SERCA 3b [11]. Their tissue distribution has not yet been determined.

The functional differences between the various SERCA isoforms have been investigated *in vitro* by transfecting the different cDNAs into Cos-1 cells. Analysis of the proteins produced indicates that SERCA 1 and SERCA 2a translocate Ca^{2+} with the same rate, whereas SERCA 2b transports Ca^{2+} more slowly and hydrolyzes ATP with a slower turnover rate. The affinity for Ca^{2+} of the different enzymes varies in the following order: 2b > 2a = 1 >> 3a [12,13]. Moreover, SERCA 3a has a higher apparent affinity for vanadate and a different pH-dependence than the other isoforms, suggesting a different function for this enzyme [12]. Up to now, no data are available concerning the biochemical properties of SERCA 3b.

The physiological importance of each isoform *in vivo* is not clearly established, but the use of transgenic animals has provided new insight into the understanding of SERCA 2a and SERCA 3 function. Overexpression of SERCA 2a in neonatal cardiomyocytes in culture by adenoviral vector [14,15] or in transgenic mice [16] confirms the central role of SERCA 2a in contractile function. Indeed SR Ca^{2+} uptake, the rate of decline of the intracellular calcium transient and of the myocyte relenghtening, reflecting the cytoplasmic Ca^{2+} lowering, were accelerated by 20 to 30% in cells overexpressing SERCA 2a. This was associated with accelerated relaxation of the heart. Furthermore, the rate of myocyte shortening and the rate of left ventricular pressure development

were increased suggesting greater Ca^{2+} release [16]. Post-rest contractions and the force-frequency relationship reflects SR loading capacity. In muscles from the SERCA 2a-overexpressing mice, the time to half maximum post-rest potentiation was significantly shorter than in the wild type littermates, suggesting that SR Ca^{2+} loading in the rest interval is faster in trangenic animals. In transgenic animals or normal isolated cardiomyocytes only limited amounts (20-30%) of SERCA 2a can be incorporated into the SR membrane, despite very high levels of SERCA 2a mRNA. However, expression of a SERCA 2a transgene in cardiomyocytes with abnormally low SERCA 2 levels can rescue depressed cardiomyocyte SERCA 2 levels and intracellular Ca^{2+} transients [15].

The respective role of SERCA 2b and SERCA 3 in single endothelial or epithelial cells was difficult to assign. To test the hypothesis that SERCA 3 plays a particular role in Ca^{2+} signaling, the group of G. Shull has generated SERCA 3 (a+b) deficient mice [17]. Homozygous mutant mice were viable, fertile and did not display an overt disease phenotype. Because SERCA 3 is highly expressed in endothelial cells, they studied the effect of null mutation on the vascular tone. The contractile response of aortic rings to phenylephrine or KCl, as well as the relaxation properties in the presence of NO donors were similar in wild type and mutant mice. However, the acetylcholine-induced endothelium-dependent relaxation of precontracted vessels was significantly reduced in homozygous mutants, suggesting that SERCA 3 is important in the Ca^{2+} signaling involved in nitric-oxide mediated vasorelaxation. Surprisingly, the mutant mice were not hypertensive as expected for NO-deficient mice.

Regulation of SERCA activity

In vivo, only SERCA 2 is regulated by phospholamban (PLB), since there is no PLB in fast skeletal muscle where SERCA 1 is expressed. However, in Cos-1 cells the activities of SERCA 1, SERCA 2a and SERCA 2b were all inhibited when they were coexpressed with PLB, whereas SERCA 3 was unaffected by the presence of PLB [12,13,18]. The PLB binding site is similar in SERCA 1 and 2, but this sequence is absent in SERCA 3 [18]. *In vitro*, PLB can be phosphorylated by the cAMP-dependent protein kinase (PKA), the SR membrane-bound Ca^{2+}/calmoduline-dependent protein kinase (SR CaM kinase), the cGMP-dependent protein kinase (PKG) and the protein kinase C (PKC). PKA and SR CaM kinase are involved in mediating the β-adrenergic response by phosphorylation of PLB on serine 16 and threonine 17, respectively, whereas PKG and PKC do not phosphorylate PLB in beating hearts. In smooth muscle, several studies have demonstrated that cGMP is more effective than cAMP in decreasing cytosolic Ca^{2+}. Moreover, in membrane preparations from aorta, phosphorylation of PLB is higher in the presence of cGMP than cAMP. Finally, phosphorylation of PLB has been observed *in vivo,* associated with increased Ca^{2+}-ATPase activity, in conditions where cGMP levels are increased [19,20 for review].

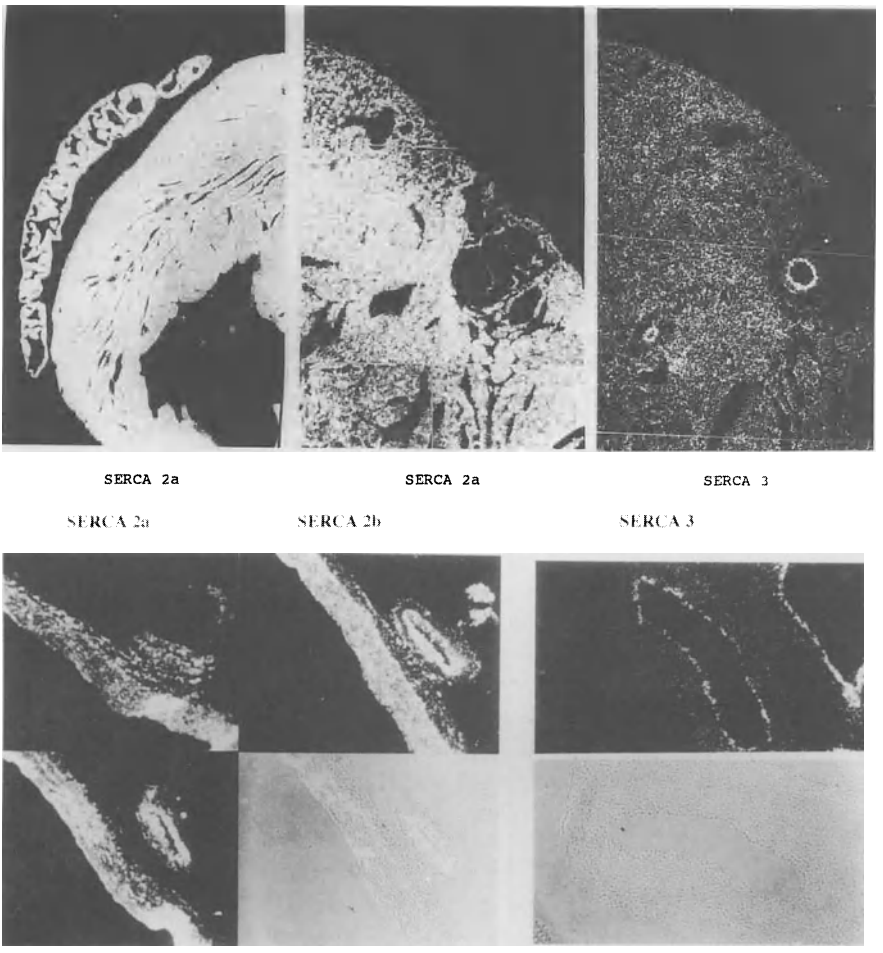

Figure 2. *A: In situ hybridization of sections from adult rat heart with SERCA 2a and SERCA 3 probes. SERCA 2a is present in the cardiomyocytes in both atria and ventricles, the left atrium and ventricle are presented. Higher magnification shows that SERCA 3 is present only in the endothelial layer of the coronary arteries. B: hybridization of rat aorta with SERCA 2a, SERCA 2b, SERCA 3 and α-Smooth muscle actin probes. SERCA 2a and 2b are coexpressed in the media whereas SERCA 3 is in the intimal layer.*

Modulation of SERCA expression in the heart

During ontogenic development

SERCA 2a was shown to be present at early developmental stages and turned out to be the main isoform expressed in cardiomyocytes throughout development [10,21]. In addition, we have shown that SERCA 2a mRNA was coexpressed with SERCA 3 mRNA [a + b probe] in the rat heart tube at embryonic day (ED) 10, whereas SERCA 2b mRNA was not present in the heart, but was highly expressed in the mesenteric area. Later on, ED 14-16, SERCA 2a mRNA was present in the heart and in the developing skeletal muscles, and SERCA 3 in the endothelium of arteries and in the hemopoietic cells in the liver [10]. In the adult, SERCA 2a was present in atrial and ventricular myocytes, but higher expression was observed in the inflow tract and atria than in the outflow tract and ventricles [10,21,22]. Furthermore, the ventricular part of the conductive tissue was also almost devoid of SERCA 2 mRNA [21,23] and the other isoforms were not upregulated in this region [23]. PLB mRNA was detected only at ED 12 and its pattern of distribution is reverse of that of SERCA 2a [21].

These data indicate that, as development proceeds, SERCA 2a remains the major SERCA isoform present in cardiomyocytes. However, quantitative modulation of the SERCA 2a mRNA level was observed during development and aging: the amount of SERCA 2a mRNA is increased at birth [23, 24] and decreased during senescence [25-27].

In cardiac hypertrophy

In 1989-90 three independent groups have demonstrated that, in animal models, severe compensated hypertrophy secondary to pressure overload was accompanied by a large relative decrease in the level of SR Ca^{2+}-ATPase mRNA and protein associated with a decreased SR Ca^{2+}-uptake rate [24,28,29]. In moderate cardiac hypertrophy the expression of SERCA 2 is unchanged [29] or even slightly increased [30]. Since then, numerous studies were published on the subject. The data obtained in animal models of pressure overload are generally in agreement with these previous results [20,30 for review]. A relation was observed between changes in SR activity or Ca^{2+} pump protein level and SERCA mRNA level, suggesting that regulation of SR activity occurs at a pre-translational level. Furthermore, the decrease in SERCA mRNA level correlated with that of ryanodine receptor mRNA level [30]. These data favor the idea that alterations in SERCA expression lead to changes in the SR Ca^{2+} uptake and Ca^{2+} release properties and that changes in SERCA expression levels account for the reduced Ca^{2+} transient and the reduced contractile properties of the hypertrophic hearts [31,32]. However, despite significant changes in myocardial relaxation and depressed SERCA 2 gene expression [31], no differences in SR Ca^{2+} load and amount of SR Ca^{2+} released were observed between cardiocytes isolated from control and hypertrophied hearts when normalized to cell volume [33]. Furthermore, reduced contractility and altered Ca^{2+} transients without changes in the properties of the RyRs, with regard to density and sensitivity to Ca^{2+}, as well as unaltered ability of SR to store Ca^{2+} as defined by the amount of Ca^{2+} released by caffeine, was recently reported in a strain of spontaneously hypertensive rats (DahlSS/Jr) and in SH-HF rats in heart failure [34]. The ability of the

voltage-gated Ca^{2+} current, I_{ca}, to trigger Ca^{2+} release from SR was reduced in both hypertrophied and failing hearts. Because I_{Ca} density and RyRs were normal, the authors suggested that the defect in the excitation-contraction coupling resides in a change in the positional relation between RyRs and the plasmamembrane Ca^{2+} channels. Experiments are now needed to prove that the plasmamembrane Ca^{2+} channels and the Ca^{2+} release channels are more distant in hypertrophied than in control hearts and that this phenomenon is not specific to this particular type of hypertrophy. In some studies [31,35] reduction in SERCA mRNA level was observed only 4 to 5 months after imposition of the load and was considered as a marker of impaired cardiac performance during the transition from compensated hypertrophy to failure. In other experiments [29,30], decrease in SERCA 2 expression was observed earlier in compensated hypertrophy. Thus, both duration and severity of the load are important factors in determining relative changes in SERCA expression.

The results obtained on human failing versus non failing hearts are much more conflicting. Either decreased or unchanged SERCA mRNA and protein level and decreased or unchanged SR activity have been reported [36,37 for review]. Moreover, in some studies no relation was observed between changes in SR function and SERCA protein level [36], whereas in others these two variables were correlated [38]. Similarly, the amount of SERCA mRNA was not correlated with the level of SERCA protein [36,37]. These data are very difficult to interpret; regulation at the translational level might occur or, alternatively, some of the discrepancies in the results may also be accounted for by regional and cellular heterogeneity in the distribution of the SERCA pump in hypertrophied hearts. In fact, changes in the architecture of the dyad, alteration in the expression of the genes coding for the Ca^{2+} pumps and Ca^{2+} release channels, regional and cell to cell heterogeneity in the expression of SERCA are likely to reflect different stages of the progression from compensated hypertrophy to heart failure .

The sarcoplasmic reticulum in vessels

In hypertensive animals

Several lines of evidence indicate that diminished Ca^{2+} pump activity contributes to elevation of $[Ca^{2+}]$ in the hypertensive state [39, for review]. We measured SR activity and the expression of the SR Ca^{2+} pumps in the aorta from spontaneous hypertensive rats (SHR) and wistar kyoto (WKY) rats [40,41]. The data indicate that 1) at 5 weeks, before any increase in blood pressure in the SHR, the rate of oxalate-supported Ca^{2+} uptake and the SERCA 2a/SERCA 2b ratio were similar in thoracic aortas from SHR and WKY rats. 2) From 5 to 17 weeks in both SHR and WKY rats SERCA 2a mRNA level was increased in parallel to the increase in α-smooth muscle actin mRNA, suggesting differentiation toward a more differentiated smooth muscle phenotype. The SERCA 2b mRNA level was unchanged. 3) When increase in blood pressure was significant in SHRs, the oxalate-supported Ca^{2+}-uptake rate was higher in SHR than in WKY. 4) In the abdominal aorta, the increase in activity was accompanied by an increase in SERCA 2a and SERCA 2b at the mRNA level, but in the thoracic aorta the increase in activity was less pronounced and not associated with an increase in SERCA

mRNA levels [41]. High SERCA 2 mRNA and plasmamembrane Ca^{2+}ATPase mRNA levels were also found in thoracic aorta from 10-week-old SHR compared to WKY rats [42]. Our data suggest that Ca^{2+} transport is regulated at the pretranslational level, but do not exclude that other mechanisms, such as alteration of the SERCA/phospholamban ratio, also contribute to the alteration of SR activity in the aorta of SHR. To our opinion, the increased intracellular Ca^{2+} level in vascular smooth muscle cells (VSMC) from SHR cannot be attributed to a decrease in SR activity, but rather to an increase in the amount of SR which may contribute to elevating vascular tone through Ca^{2+} release mechanisms. In agreement with this, Côrtes et al. [43] have shown that, in Ca^{2+} free medium, Ca^{2+} release induced by thapsigargin (which represents release from SR/ER) was twice as high as in rat aortic SMCs from SHR than in those from WKY rats. In addition, they showed that the ryanodine-sensitive Ca^{2+} release induced by angiotensin II is enhanced in VSMC from SHR. Thus, the ryanodine-sensitive, thapsigargin-sensitive pool is greater in SHR than in WKY rats. SERCA 3 is a major isoform in platelets, and the level of expression of the SERCA 3 gene was shown to be higher in platelets from SHR compared to WKY rats [8]. The data on SR activity are conflicting and in many other studies SR activity has been shown to be diminished in SHR. The explanation for this discrepancy is unclear at present; strain differences may be one of the explanations.

A point mutation of the SERCA 2 gene leading to restriction fragment length polymorphisms was found in the SERCA 2 gene from SHR. A cosegregation analysis of SERCA 2 genotype, systolic blood pressure and platelet intracellular Ca^{2+} concentration in SHR suggests that the SERCA 2 gene contributes to increased thrombin and intraplatelet Ca^{2+} concentrations and that SERCA 2 is not identical to *ht*, a major locus of rat chromosome 12 involved in hypertension [44]. Interesting results may be obtained from a similar study performed on the SERCA 3 gene which, in humans, is localized on chromosome 17p13.3.

The phenotype of the VSMCs and of platelets are different, but the mechanisms involved in alteration of expression of the SERCA genes in SHR are the same since in both cell types, the cell-specific SERCA gene is upregulated. Although the same SERCA 2 gene is expressed in cardiac and VSMC, chronic hemodynamic overload has opposite effects on expression of this gene in the two tissues: up-regulation in aorta and down-regulation in heart.

In proliferating VSMCs

Proliferation and dedifferentiation of SMCs is observed in atherosclerosis and hypertension and can be reproduced in tissue culture. When VSMCs proliferate they undergo a transition from a contractile to a proliferative phenotype and this is associated with major alterations in gene expression. Alteration in the response to caffeine, ryanodine and angiotensine II has been reported in VSMC in culture and the data are compatible with disappearance of the ryanodine-sensitive pool with proliferation [43,45]. Which molecular events cause the changes in these pharmacological properties remains to be elucidated.

Conclusion

In conclusion, at least three different SERCAs are expressed in the cardiovascular system, SERCA 2a in the cardiomyocytes, 2a and 2b in the vascular myocytes and SERCA 3 in the endothelial cells. SERCA 2a and 2b have very similar functions, but SERCA 3 has a much lower affinity for Ca^{2+} and is not regulated by PLB phosphorylation. Expression of SERCA 2a in the cardiomyocytes is regulated during development and in several pathological states, in particular in cardiac hypertrophy consecutive to pressure overload. A decrease in SERCA 2 expression is likely to be a major determinant in alteration of contractility of the hypertrophied heart. Expression of SERCA 2a and 2b in vessels is regulated during hypertension and proliferation. Less is known concerning SERCA 3 in endothelial cells but recent data tend to indicate that it may play a key role in the Ca^{2+} signaling involved in NO-mediated vasorelaxation.

References

1. Lesh RE, Marks AR, Somlyo AV, Fleischer S, Somlyo AP. Anti-ryanodine receptor antibody binding sites in vascular and endocardial endothelium. Circ Res 1993;72:481-88.
2. MacLennan DH, Brandl CJ, Korczak B, Green NM. Amino-acid sequence of a Ca^{2+}+ Mg^{2+}-dependent ATPase from rabbit muscle sarcoplasmic reticulum, deduced from its complementary DNA sequence. Nature 1985;316:696-700.
3. Burk SE, Lytton J, MacLennan DH, Shull GE. cDNA cloning, functional expression, and mRNA tissue distribution of a third organellar Ca^{2+} pump. J Biol Chem 1989;264:18561-68.
4. Anger M, Samuel JL, Marotte F, Wuytack F, Rappaport L, Lompré AM. The sarco(endo)plasmic reticulum Ca^{2+}-ATPase mRNA isoform, SERCA 3, is expressed in endothelial and epithelial cells in various organs. FEBS Lett 1993,334:45-48.
5. Dode L, Wuytack F, Kools PFJ, Baba-Aïssa F, Raeymaekers L, Briké F, Van De Ven WJ, Casteels R. cDNA cloning, expression and chromosomal localization of the human sarco/endoplasmic reticulum Ca^{2+}-ATPase 3 gene. Biochem J 1996;318:689-99.
6. Lee MG, Xu X, Zeng W, Diaz J, Wojcikiewicz RJH, Kuo TH, Wuytack F, Raeymaekers l, Muallem S. Polarized expression of Ca^{2+} channels in pancreatic and salivary gland cells. Correlation with initiation and propagation of [Ca^{2+}] waves. J Biol Chem 1997;272:15765-70.
7. Bobe R, Bredoux R, Wuytack F, Quarck R, Kovàcs T, Papp B, Corvazier E, Magnier C, Enouf J. The rat platelet 97-kDa Ca^{2+}-ATPase isoform is the sarcoendoplasmic reticulum Ca^{2+}-ATPase 3 protein. J Biol Chem 1994;269:1417-24.
8. Wuytack F, Papp B, Verboomen H, Raeymaekers L, Dode L, Bobe R, Enouf J, Bokkala S, Authi KS, Casteels R. A SERCA3-type Ca^{2+} pump is expressed in platelets, in lymphoid cells and in mast cells. J Biol Chem 1994;269:1410-16.
9. Wu K-D, Lee W-S, Wey J, Bungard D, Lytton J. Localization and quantification of endoplasmic reticulum Ca^{2+}-ATPase isoform transcripts. Am J Physiol 1995;269:C775-84.
10. Anger M, Samuel JL, Marotte F, Wuytack F, Rappaport L, Lompré AM. *In situ* mRNA distribution of sarco(endo)plasmic reticulum Ca^{2+}-ATPase isoforms during ontogeny in the rat. J Mol Cell Cardiol 1994;26:101-12.
11. Tokuyama Y, Chen X, Roe MW, Bell GI. Sarcoendoplasmic reticulum Ca^{2+} ATPase SERCA 3a and SERCA 3b. Genebank 1996; Accession U43393 and U49394.
12. Lytton J, Westlin M, Burk SE, Shull GE, MacLennan DH. Functional comparisons between isoforms of the sarcoplasmic or endoplasmic reticulum family of calcium pumps. J Biol Chem 1992;267:14483-89.
13. Verboomen H, Wuytack F, de Smedt H, Himpens B, Casteels R. Functional difference between SERCA2a and SERCA2b Ca^{2+} pumps and their modulation by phospholamban. Biochem J 1992;286:591-96.
14. Hajjar RJ, Kang JX, Gwathmey JK, Rosenzweig A. Physiological effects of adenoviral gene transfer of sarcoplasmic reticulum calcium ATPase in isolated rat myocytes. Circulation 1997;95:423-29.
15. Giordano FJ, He H, McDonough P, Meyer M, Sayen MR, Dillmann WH. Adenovirus-mediated gene transfer reconstitutes depressed sarcoplasmic reticulum Ca^{2+}-ATPase levels and shortens prolonged cardiac myocyte Ca^{2+} transients. Circulation 1997; 96:400-03.
16. He H, Giordano FJ, Hilal-Dandan R, Choi D-J, Rockman HA, McDonough P, Bluhm WF, Meyer M, Sayen MR, Swanson E, Dillmann WH. Overexpression of the rat sarcoplasmic reticulum Ca^{2+}ATPase gene in the heart of transgenic mice accelerates calcium transients and cardiac relaxation. J Clin Invest 1997;100:380-89.
17. Liu LH, Paul RJ, Sutliff RL, Miller Ml, Lorenz JN, Pun RYK, Duffy JJ, Doetschman T, Kimura Y, MacLennan DH, Hoying JB, Shull GE. Defective endothelium-dependent relaxation of vascular smooth muscle and endothelial cell Ca^{2+} signaling in mice lacking sarco(endo)plasmic reticulum Ca^{2+}-ATPase isoform 3. J Biol Chem 1997;272:30538-45.

18. Toyofuku T, Kurzydlowski K, Tada M, MacLennan DH. Identification of regions in the Ca^{2+}-ATPase of sarcoplasmic reticulum that affect functional association with phospholamban. J Biol Chem 1993;268:2809-15.
19. Raeymaekers L and Wuytack F. Ca^{2+} pumps in smooth muscle cells. J Muscle Res Cell Motil. 1993;14:141-57.
20. Lompré A-M, Anger M, Levitsky D. Sarco(endo)plasmic reticulum calcium pumps in the cardiovascular system: function and gene expression. J Mol Cell Cardiol 1994;26:1109-21.
21. Moorman AFM, Vermeulen JLM, Koban MU, Schwartz K, Lamers WH, Boheler KR. Patterns of expression of sarcoplasmic reticulum Ca^{2+}-ATPase and phospholamban mRNAs during rat heart development. Circ Res 1995;76:616-25.
22. Minajeva A, Kaasik A, Paju k, Seppet E, Lompre A-M, Veksler V, Ventura-Clapier R. Sarcoplasmic reticulum function in determining atrioventricular contractile differences in rat heart. Am J Physiol 1997;273:H2498-H2507.
23. Gorza L, Vettore S, Volpe P, Sorrentino V, Samuel J-L, Anger M, Lompré A-M. Cardiac myocytes differ in mRNA composition for sarcoplasmic reticulum Ca^{2+} channels and Ca^{2+} pumps. In *Cardiac growth and Regeneration*. Annal NY Acad Sci 1995;752:141-48.
24. Komuro I, Kurabayashi M, Shibazaki Y, Takaku F, Yazaki Y. Molecular cloning and characterization of a Ca^{2+} + Mg^{2+} -dependent Adenosine Triphosphatase from rat cardiac sarcoplasmic reticulum. Regulation of its expression by pressure overload and developmental stage. J Clin Invest 1989;83:1102-08.
25. Lompré AM, Lambert F, Lakatta EG, Schwartz K. Expression of sarcoplasmic reticulum Ca^{2+}-ATPase and calsequestrin genes in rat heart during ontogenic development and aging. Circ Res 1991;69:1380-88.
26. Maciel LMZ, Polikar R, Rohrer D, Popovich BK, Dillmann WH. Age-induced decreases in the messenger RNA coding for the sarcoplasmic reticulum Ca^{2+} ATPase of the rat heart. Circ Res 1990;67:230-34.
27. Assayag P, Charlemagne D, de Leiris J, Boucher F, Valère P-E, Lortet S, Swynghedauw B, Besse S. Senescent heart compared with pressure overload-induced hypertrophy. Hypertension 1997;29:15-21.
28. Nagai R, Zarain-Herzberg A, Brandl CJ, Fuji J, Tada M, MacLennan DH, Alpert NR, Periasamy M. Regulation of myocardial Ca^{2+}-ATPase and phospholamban mRNA expression in response to pressure overload and thyroid hormone. Proc Natl Acad Sci USA 1989;86: 2966-70.
29. De la Bastie D, Levitsky D, Rappaport L, Mercadier JJ, Marotte F, Wisnewsky C, Brovkovich V, Schwartz K, Lompré AM. Function of the sarcoplasmic reticulum and expression of its Ca^{2+}-ATPase gene in pressure overload-induced cardiac hypertrophy in the rat. Circ Res 1990;66:554-64.
30. Arai M, Suzuki T, Nagai R. Sarcoplasmic reticulum genes are upregulated in mild cardiac hypertrophy but downregulated in severe cardiac hypertrophy induced by pressure overload. J Mol Cell Cardiol 1996;28:1583-90.
31. Qi M, Shannon TR, Euler DE, Bers DM, Samarel AM. Downregulation of sarcoplasmic reticulum Ca^{2+}-ATPase during progression of left ventricular hypertrophy. Am J Physiol 1997;272:H2416-24.
32. Tsutsui H, Ishibashi Y, Imanaka-Yoshida K, Yamamoto S, Yoshida T, Sugimachi M, Urabe Y, Takeshita A. Alterations in sarcoplasmic reticulum calcium-storing proteins in pressure-overload cardiac hypertrophy. Am J Physiol 1997;272:H168-75.
33. Delbridge L, Satoh H, Yuan W, Bassani JWM, Qi M, Ginsburg KS, Samarel AM, Bers DM. Cardiac myocyte volume, Ca^{2+} fluxes, and sarcoplasmic reticulum loading in pressure-overload hypertrophy. Am J Physiol. 1997;272:H2425-35.
34. Gomez AM, Valdivia HH, Cheng H, Lederer MR, Santana LF, Cannell MB, McCune SA, Altschuld RA, Lederer WJ. Defective excitation-contraction coupling in experimental cardiac

hypertrophy and failure. Science 1997;276:800-06.
35. Feldman AM, Weinberg EO, Ray PE, Lorell BH. Selective changes in cardiac gene expression during compensated hypertrophy and the transition to cardiac decompensation in rats with chronic aortic banding. Circ Res 1993;73:184-92.
36. Schwinger RHG, Böhm M, Schmidt U, Karczewski p, Bavendick U, Flesch M, Krause EG, Erdmann E. Unchanged protein levels of SERCA II and phospholamban but reduced Ca^{2+} uptake and Ca^{2+}-ATPase activity of cardiac sarcoplasmic reticulum from dilated cardiomyopathy patients compared with patients with nonfailing hearts. Circulation 1995;92:3220-28.
37. Linck B, Bobnik P, Eschenhagen T, Müller FU, Neumann J, Nose M, Jones LR, Schmitz W, Scholz H. Messenger RNA expression and immunological quantification of phospholamban and SR Ca^{2+}-ATPase in failing and nonfailing human hearts. Cardiovasc Res 1996;31:625-32.
38. Hasenfuss G, Reinecke H, Studer R, Meyer M, Pieske B, Holtz J, Holubarsch C, Posival H, Just H, Drexler H. Relation between myocardial function and expression of sarcoplasmic reticulum Ca^{2+}-ATPase in failing and nonfailing human myocardium. Circ Res 1994;75:434-42.
39. Kwan CY. Dysfunction of calcium handling by smooth muscle in hypertension. Can J Physiol Pharmacol 1985;63:366-74.
40. Le Jemtel TH, Lambert F, Levitsky DO, Clergue M, Anger M, Gabbiani G, Lompré A-M. Age-related changes in sarcoplasmic reticulum Ca^{2+}-ATPase and α-smooth muscle actin gene expression in aortas of normotensive and spontaneously hypertensive rats. Circ Res 1993;72: 341-48.
41. Levistky DO, Clergue M, Lambert F, Souponitskaya MV, Le Jemtel TH, Lecarpentier Y, Lompré A-M.. Sarcoplasmic reticulum calcium transport and Ca^{2+}-ATPase gene expression in thoracic and abdominal aortas of normotensive and spontaneously hypertensive rats. J Biol Chem 1993;268:8325-31.
42. Monteith GR, Kable EPW, Kuo TH, Roufogalis BD. Elevated plasma membrane and sarcoplasmic reticulum Ca^{2+} pump mRNA levels in cultured aortic smooth muscle cells from spontaneously hypertensive rats. Biochem Biophys Res Commun 1997;230:344-46.
43. Côrtes SF, Soares Lemos V, Stoclet J-C. Alterations in calcium stores in aortic myocytes from spontaneously hypertensive rats. Hypertension 1997;29:1322-28.
44. Ohno Y, Matsuo K, Suzuki H et al. Genetic linkage of the sarco[endo]plasmic reticulum Ca^{2+}-dependent ATPase II gene to intracellular Ca^{2+} concentration in the spontaneously hypertensive rat. Biochem Biophys Res Commun 1996;227: 789-93.
45. Masuo M, Toyo-oka T, Shin WS Sugimoto T, Growth-dependent alterations of intracellular Ca^{2+}-handling mechanisms of vascular smooth muscle cells. PDGF negatively regulates functional expression of voltage-dependent, IP3-mediated, and Ca^{2+}-induced Ca^{2+}-release channels. Circ Res 1991;69:1327-39.

14. POTASSIUM CHANNELS; GENES, PROTEINS, AND PATIENTS

Connie Alshinawi, and Arthur A.M. Wilde

Introduction

Potassium (K^+) channels play a major role in generating cardiac electrical activity. Cardiac action potentials are characterized by a long duration which is pivotal for proper contraction. In physiological conditions the repolarization process is largely determined by several potassium channels with different time and voltage characteristics. These channels are distributed heterogeneously over different parts of the heart. In addition, developmental changes in channel diversity are pertinent. Furthermore, under the influence of a variety of stimuli, which include metabolic changes, neurohumoral influences and disease, the set of expressed potassium channels may change. In pathophysiological conditions such as cardiac hyperthrophy and/or heart failure, altered characteristics of potassium channels usually lead to prolonged repolarization. Arrhythmias ensue, based on either dispersion in repolarization or reexcitation during the course of the action potential (afterdepolarizations and triggered activity).
In recent years molecular techniques have significantly increased our understanding of structure-function relationship of ion channels. Potassium channels were among the first to be studied. Indeed, the structure of several families of potassium channels has been elucidated and individual amino-acids, pivotal to specific characteristics of channel function, have been identified. Moreover, since specific aberrations in genes encoding for potassium channels seem to be associated with a specific phenotype ('experiments of nature'), genotype-phenotype comparisons in patients with K^+ channelopathies also shed light on domains or residues of structural or functional importance. In this paper we will track the way from gene to patient and emphasize those experimental data pertinent to potassium channel function in pathophysiological conditions.

Genes and proteins

Shaker-type channels

Potassium channels consist of an assembly of at least 4 channel proteins (α-subunits)

P.A. Doevendans et al. (eds.), Cardiovascular specific gene expression, 151-60.

around a central ion conduction pore and a number of ancillary subunits which are capable of modifying function and properties of the channel. The first voltage dependent potassium channel (Kv) cDNA was cloned from *Drosophila melanogaster*. Subsequently various mammalian homologues of *Shaker* subfamilies *Shaker* (Kv1), *Shab* (Kv2), *Shaw* (Kv3) and *Shal* (Kv4) have been described. Each α-subunit contains six putative transmembrane segments (S1-S6) flanked by cytoplasmically located N- and C-terminal domains (figure 1). A pore loop between S5 and S6, designated H5 or P loop, which contains the potassium channel signature sequence, forms the external vestibule of the pore, while the S4-S5 linker and the C-terminal end of S6 appear to form the intracellular mouth of the pore. The fourth transmembrane domain (S4) which contains positively charged residues at every third position, functions as a voltage sensor which slides across the membrane in response to changes in the transmembrane potential, bringing about a conformational change in the channel, thereby mediating gating. The N-terminus may function as an inactivation particle, occluding the cytoplasmic end of the channel pore by a 'ball and chain" mechanism. Residues in H5 and S6 are also thought to be involved in inactivation presumably by bringing about a conformational change that narrows the extracellular mouth of the pore ('C-type inactivation', named after the involvement of residues in or near the C-terminus of the protein; structure-function relation reviewed in [1,2]). Ancillary cytoplasmic subunits associate with the Kv1 and Kv2 subfamilies and modify gating [3] and membrane expression [4,5]. No such subunits have been described for Kv3 and Kv4.

Only one member within Shaker subfamilies Kv5, Kv6, and Kv8 has hitherto been identified. Although they possess the structural hallmarks of functional subunits, Kv5.1, Kv6.1 [6] and Kv8.1 [7] are unable to express currents as homomultimers, but appear to modify behavior of other Kv channel subunits from other subfamilies upon heteromultimerization [8,9]. A similarly electrically silent subunit, jShal1 [10], has been cloned from *Polyorchis* jellyfish and shown to produce a similar effect.

The diversity of *Shaker*-type channel mRNA in the heart is extensive. Northern analysis, RNase protection assays and *in situ* hybridisation studies have detected transcripts encoding members of the Kv1 through Kv6 sub-families of the Kv superfamily [11-13]. The potential number of expressed K^+ currents is also high. The fact that members within one sub-family and between different subfamilies are able to form heteromultimers [8-10,14], increases the number of potential phenotypes. Moreover, further diversity can be introduced by association with modulatory (β-) subunits. Hence, finding the molecular correlates for native cardiac currents is not an easy task. Additional confounding factors include variations in K^+ channel expression in different anatomical regions of the heart [12] and variation of expression at different stages of development [15]. Furthermore, variations attributable to species differences do not allow direct extrapolation of findings in an animal model to what effectively occurs in the human heart. In addition, channel phenotype in simple expression systems can not always be related to channel properties in native tissues.

At present, Kv1.5 is thought to encode the ultrarapidly activating delayed rectifier current, I_{Kur}, in mammalian atria, Kv4.2 and/or Kv4.3 probably produce the transient outward current, I_{To1}, while Kvs' 1.2, 1.4, and 2.1 contribute in as yet undetermined ways to outward currents (reviewed by Brown [16]; figure 1).

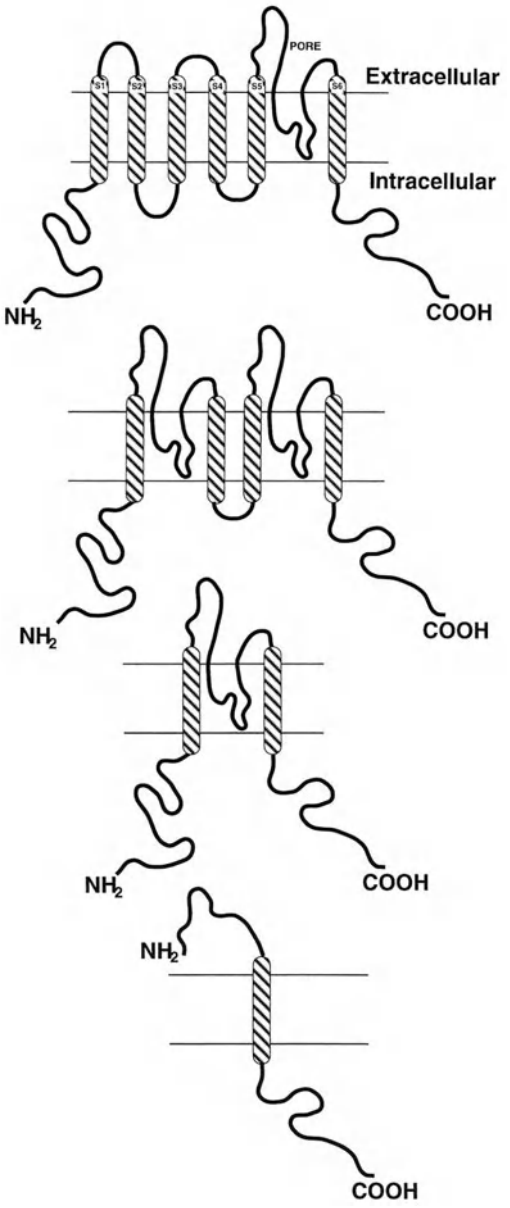

GENE	CURRENT
KCNQ1	I_{Ks} (with minK)
HERG	I_{Kr}
Kv1.4	I_{TO1}?
Kv1.5	I_{Kur}
Kv4.x	I_{TO1}
Kv2.1	?
Kir2.x	I_{K1}
Kir3.1	$I_{K.ACh}$?
Kir3.4	$I_{K.ACh}$
Kir6.2	$I_{K.ATP}$
TWIK	I_{Kp}?
ORK1	I_{Kp}?
minK	I_{sK}

Figure 1. *Schematic representation of K+ channel structure (left panels). Representative members of each family are given in the right columns (gene product and the putative current generated). The upper left panel depicts the six membrane spanning segment channel with a pore (indicated) and the S4 domain acting as the voltage sensor. Four of these proteins (alpha-subunits) assemble together, with or without modulatory β-subunits, to form functional K+ channels. In the middle left panels twin pore channels and 2 membrane spanning segments channels are presented (TWIK and its drosophila homolog ORK1 may encode for a background potassium current I_{Kp}). The lower left panel indicates the minK structure which for example interacts with KCNQ1 to from functional (I_{Ks}) channels.*

HERG

The human *ether-a-go-go* (EAG) related gene (HERG) was cloned from a hippocampal cDNA library by homology to the *Drosophila EAG* gene [17-18]. Other homologes of HERG [19-23], have since been identified, demonstrating that the ERG potassium channel genes constitute a distinct subfamily of the *EAG* family which is closely related to the cyclic nucleotide-gated family in the potassium channel phylogenetic tree [24]. By PCR analysis of a somatic cell hybrid panel Warmke and Ganetzky [18] localised HERG to human chromosome 7 and later, Curran et al. [25] mapped HERG by linkage and physical mapping to 7q35-36, and showed that mutations in this gene are associated with Long QT syndrome (LQTS2).

Like the α-subunits of the *Shaker*-type K^+ channels, HERG has six putative membrane-spanning domains and a conserved putative pore domain. Despite this architectural similarity, HERG subunits form inward-rectifier K^+ channels [26,27], which are generally made up of a different class of K^+ channel subunits possessing two membrane-spanning segments (K_{ir} channels; see below). Inward rectification of HERG is thought to be mediated by a C-type inactivation mechanism similar to that of the *Shaker*-type channels but which in HERG proceeds much faster than transition of the channel from closed to open state [27].

Heterologous expression of HERG in *Xenopus* oocytes [26,28] produced currents with biophysical properties described for the native cardiac rapidly activating K^+ current (I_{Kr}), except that the kinetics of activation and deactivation were slower. Increased I_{Kr} current density is observed after coexpression with a small transmembrane modulatory protein, minK or IsK encoded by the KCNE1 gene [29]. Lees-Miller et al. [22] and London et al. [23] cloned N-terminal isoforms of mouse ERG (MERG) and demonstrated that coexpression of full-length MERG (which corresponds to HERG) and one of the N-terminal isoforms in *Xenopus* oocytes produced currents with deactivation kinetics that were faster than those for MERG alone and matched the physiological profile of I_{Kr} for mouse myocytes. This, coupled with the overlapping distribution of the two isoforms in the mouse [22,23], supports the hypothesis that these isoforms coassemble *in vivo* to form the channel responsible for I_{Kr} in mouse.

KvLQT1

KvLQT1 (gene now renamed KCNQ1) was identified by positional cloning in a family with LQTS1 [30]. It is a member of a family of voltage-gated K^+ channels for which very recently two other members, KCNQ2 [31,32] and KCNQ3 [33], have been identified in man. This family shares the same general topology with the *Shaker*-type channels. It is estimated that mutations in KCNQ1 account for >50% of inherited LQTS.

KvLQT1 associates with IsK to generate the channel responsible for the slowly activating delayed rectifier K^+ current (I_{Ks}) in the heart [34,35]. It has more recently been suggested that the characteristics of the native IKs current also depend on the relative expression of an N-terminal truncated isoform of KvLQT1 (isoform 2 in [36]) which lacks the N-terminus and the initial part of the first transmembrane domain [37,38]. This isoform which has an overlapping expression with the full-length KvLQT1 isoform in the major anatomic regions of the heart is a strong negative-

dominant of full-length KvLQT1 [37,38].
The current conducted by KvLQT1 and IsK is not limited to the heart. This assembly is also expressed in the *stria vascularis* of the inner ear [39,40], where it is responsible for a key secretory role in the control of endolymph homeostasis associated with normal hearing. Heterozygous mutations in either KCNQ1 [30] or KCNE1 [41] have been associated with the dominantly inherited, Romano-Ward (RW) LQT syndrome [42,43], whereas homozygosity for mutations in either of the two genes [40, 44] have been associated with the recessive Jervell-Lange-Nielsen syndrome (JLNs) [45], which is also associated with congenital sensorineural deafness. The involvement of KCNE1 mutations in JLNS is in accordance with the fact that mice with a null mutation of this gene display inner ear defects very similar to those of JLN patients [46]. However, contrary to expectations this transgenic mouse did not have a prolonged QT interval. This illustrates, as indicated before, the complexity of K^+ channel physiology and pathophysiology in particular with regard to species variability.

The inward rectifiers
The most important inward rectifying K^+ channels present in the heart are I_{K1} ('the inward rectifier'), the ATP-sensitive potassium channel $I_{K.ATP}$ and the acethylcholine-sensitive potassium channel $I_{K.ACh}$. Secondary to its high conductance, I_{K1} is responsible for a stable resting membrane potential, at least in physiological conditions. In the absence of their physiological blockers (i.e. magnesium and polyamines) these channels lack any voltage dependence and display an Ohmic current-voltage relationship. At the molecular level this is reflected by the absence of the S4 transmembrane domain described above.
$I_{K.ATP}$ channels couple the metabolic state of the cell to its electrical activity [47]. Regulation is accomplished by metabolic factors, among which, the intracellular ATP, ADP and lactate concentrations. The sensitivity to sulphonylureas, for a long time in use for the treatment of diabetes mellitus, laid the way towards cloning of the channel. Hence, the β-cell sulfonylurea receptor was the first to be purified and cloned [48]. It appeared that the sulfonylurea receptor (named SUR1) did not possess ion-conducting properties, but together with an inwardly rectifying K^+ channel (called Kir 6.2), K^+ channels were formed with characteristics closely resembling functional pancreatic $I_{K.ATP}$ channels [49]. Closely related proteins (SUR2A and SUR2B) were shown to reconstitute with Kir 6.2 functional $I_{K.ATP}$ channels of the cardiac and skeletal type [50] and the smooth muscle type respectively [51].
Finally, the muscarinic K^+ channel ($I_{K.ACh}$) is an inward rectifying K^+ channel with similar two membrane spanning segments (figure 1). Kir3.1 (or in the older terminology GIRK1) is likely to encode $I_{K.ACh}$ [52]. The channel is coupled via G-proteins to an extensive intracellular signal transduction pathway. It is likely that a number of subunits are involved in regulation of the channel. Obviously their role is directly related to the parasympathetic activation of the heart.

Genes, proteins, and patients

The paradigm to study the role of potassium channels in clinical cardiac arrhythmias is the congenital long QT-interval syndrome (cLQTS). The syndrome which occurs as an autosomal dominant or recessive trait, is characterized by QT-interval prolongation on the ECG and polymorphic ventricular arrhythmias (torsade de pointes), which often occur in relation to exercise or emotion and which may give rise to recurrent syncope or sudden cardiac death. Linkage analysis of the autosomal dominant inherited cLQTS (Romano-Ward syndrome) indicated genetic heterogeneity with at least 5 loci and 4 genes identified [53,54]. These genes all encode for proteins which form (part of) ion channels. The slowly activating delayed rectifier (I_{Ks}) and the rapidly activating delayed rectifier (I_{Kr}) are involved by mutations in KvLQT1 (11p15.5, LQTS1) and HERG (7q35-36, LQTS2), respectively. MinK mutations (21q21.1-22.2, LQTS5) also affect the characteristics of I_{Ks} [41] and because the minK protein may also coassemble with HERG proteins [29] I_{Kr} may also be affected. In LQTS3 the Na^+ channel α-subunit (encoded by the gene SCN5A on 3p21-24) is involved while the gene in LQTS4 (4q25-27) has not been identified yet. As indicated above the recessive inherited cLQTS (Jervell and Lange-Nielsen syndrome), associated with congenital deafness, is caused by either (homozygous) mutations in minK or KvLQT1 (see above).

Based on the time and voltage characteristics of the involved currents one may anticipate the phenotype of a particular gene defect. The trigger for arrhythmic events may in particular be genotype-specific. I_{Ks} is presumably the main K^+ current in conditions of high sympathetic activity particularly at shorter cycle lengths. Indeed, exercise-related events dominate the clinical picture in LQTS1 and in JLN syndrome [55]. In LQTS2 patients arrhythmic events occur both during exercise and at rest.

In heterologous expression studies KvLQT1 mutations associated with the Romano Ward syndrome exert dominant-negative suppression of KvLQT1 function [56,57]. KvLQT1 mutations associated with the JLN type have a less severe dominant-negative effect [57] or no dominant-negative effect [58], thereby accounting for the different mode of inheritance of the two syndromes. Clinically, one would expect a less malignant phenotype in carriers of the mutants with no or only a mild dominant-negative effect. Indeed, QT-intervals in the parents of JLN patients, in which the mutation is heterozygously present since the affected patient is homozygous for the mutation, are only marginally prolonged [59]. A strong dominant-negative effect has been described for one of the IsK mutations associated with the Romano Ward syndrome [41].

Mutated HERG proteins also exert a dominant negative effect with resultant less outward (potassium) current [60]. There are also mutations with a complete loss of function [60]. Once again one would anticipate on a clinically less malignant phenotype in carriers of the former mutants, but studies relating genotype to phenotype are not (yet) available in LQTS2 patients.

Genotype-specific ECG's have also been described [61]. T-waves in LQTS1 patients are wide with a relatively high amplitude whereas T-waves of low amplitude are present in LQTS2 patients. The T-wave differences may be based on the (transmural) distribution of mutated and normal proteins [62].

Apart from the congenital LQTS, no other K^+ channelopathies have been recognized in cardiovascular diseases thusfar. We antipate however, that more entities will be described in which the above mentioned or other K^+ channel are causally involved.
As indicated in the introduction section, ion channel function and expression may also be altered by environmental factors. A variety of cardiac diseases, including myocardial ischemia and cardiac hypertrophy, and altered hemodynamic states can modify the characteristics of ionic currents. QT-interval alterations and/or prolongation and sudden cardiac death are common findings in these syndromes [63]. It is likely that the synthesis and assembly of ionic channels in the sarcolemma is altered and/or the regulatory units are affected in these conditions. Indeed, it has been shown that mRNA transcripts of K^+ channel proteins are altered in experimental models of chronic infarction [64] and in failing human myocardium [65]. We have shown the potential importance of regulating proteins since different isoforms of KvLQT1 may interact in a dominant negative way [38]. In this respect it is for example well conceivable that different factors pertinent to these diseases may provoke alternative splicing of the KvLQT1 gene with resultant increased expression of the isoforms which reduce the magnitude of I_{Ks}.

Conclusion

In conclusion, the molecular biology of K^+ channels has unraveled a variety of K^+ channels genes encoding different K^+ channel families which all play a distinguished role in cardiac electrophysiology. This increasing knowledge has proven to be of benefit for patients and families in which K^+ channelopathies exist. It is anticipated that more common cardiac disorders are also associated with altered gene expression leading to altered K^+ channel distribution throughout the myocardium. This will undoubtly underlie the clinical electrophysiological changes in diseased patients.

References

1. Kukuljan M, Labarca P, Latorre R. Molecular determinants of ion conduction and inactivation in K^+ channels. Am J Physiol 1995;268:C535-56.
2. Jan LY, Jan YN. Voltage-gated and inwardly rectifying potassium channels. J Physiol 1997;505:267-82.
3. Wang Z, Kiehn J, Yang Q, Brown AM, Wible BA. Comparison of binding and block produced by alternatively spliced Kv1 subunits. J Biol Chem 1996;271:28311-17.
4. Rhodes KJ, Monaghan MM, Barrezueta NX, et al. Voltage-gated K+ channel beta subunits: expression and distribution of Kv beta 1 and Kv beta 2 in adult rat brain. J Neurosci 1996;16:4846-60.
5. Fink M, Duprat F, Lesage F, et al. A new K^+ channel beta subunit to specifically enhance Kv2.2 (CDRK) expression. J Biol Chem 1996;271:26341-48.
6. Drewe JA, Verma S, Frech G, Joho RH. Distinct spatial and temporal expression patterns of K^+ channel mRNA from different subfamilies. J Neuroscience 1992;12:538-48.
7. Hugnot JP, Salinas M, Lesage F, et al. Kv8.1, a new neuronal potassium channel subunit with specific inhibitory properties towards Shab and Shaw channels. EMBO J 1996;15:3322-31.
8. Post MA, Kirsch GE, Brown AM. Kv2.1 and electrically silent Kv6.1 potassium channel subunits combine and express a novel current. FEBS Lett 1996;399:177-82.
9. Salinas M, de Weille J, Guillemare E, Lazdunski M, Hugnot JP. Modes of regulation of shab K^+ channel activity by the Kv8.1 subunit. J Biol Chem 1997;272:8774-80.
10. Jegla T, Salkoff L. A novel subunit for shal K+ channels radically alters activation and inactivation. J Neuroscience 1997;17:32-44.
11. Dixon JE, McKinnon D. Quantitative analysis of potassium channel mRNA expression in atrial and ventricular muscle of rats. Circ Res 1994;75:252-60.
12. Brahmajothi MV, Morales MJ, Rasmusson RL, Campbell DL, Strauss HC. Heterogeneity in K^+ channel transcript expression detected in isolated ferret cardiac myocytes. PACE 1997;20:388-96.
13. Dixon JE, Shi W, Wang H-S, et al. Role of the Kv4.3 K^+ channel in ventricular muscle. A molecular correlate for the transient outward current. Circ Res 1996;79:659-68.
14. Isacoff EY, Jan YN, Jan LY. Evidence for the formation of heteromultimeric potassium channels in Xenopus oocytes. Nature 1990;345:530-34.
15. Xu H, Dixon JE, Barry DM, et al. Developmental analysis reveals mismatches in the expression of K^+ channel subunits and voltage-gated channel currents in rat ventricular myocytes. J Gen Physiol 1996;108:405-19.
16. Brown AM. Cardiac potassium channels in health and disease. Trends Cardiovasc Med 1997;7:118-24.
17. Warmke J, Drysdale R, Ganetzky B. A distinct potassium channel polypeptide encoded by the Drosophila EAG locus. Science 1991;252:1560-2.
18. Warmke JW, Ganetzky B. A family of potassium channel genes related to EAG in Drosophila and mammals. Proc Natl Acad Sci 1994;91:3438-42.
19. Titus SA, Warmke JW, Ganetzky B. The Drosophila ERG K^+ channel polypeptide is encoded by the seizure locus. J Neuroscience 1997;17:875-81.
20. Shi WM, Wymore RS, Wang HS, Pan ZM, Cohen IS, Mckinnon D, Dixon JE. Identification of two nervous system-specific members of the erg potassium channel gene family. J Neuroscience 1997;17:9423-32
21. Wang XJ, Reynolds ER, Deak P, Hall LM The seizure locus encodes the Drosophila homologe of the HERG potassium channel. J Neuroscience 1997;17:882-90.
22. Lees-Miller JP, Kondo C, Wang L, Duff HJ. Electrophysiological characterization of an alternatively processed ERG K^+ channel in mouse and human hearts. Circ Res 1997;81:719-26.

23. London B, Trudeau MC, Newton KP, et al. Two isoforms of the mouse ether-a-go-go-related gene coassemble to form channels with properties similar to the rapidly activating component of the cardiac delayed rectifier K^+ current. Circ Res 1997;81:870-8.
24. Guy HR, Durell SR, Warmke J, Drysdale R, Ganetzky B. Similarities in amino acid sequences of Drosophila EAG and cyclic nucleotide-gated channels. Science 1991;254:730.
25. Curran ME, Splawski I, Timothy KW, Vincent GM, Green ED, Keating MT. A molecular basis for cardiac arrhythmia: HERG mutations cause long QT syndrome. Cell 1995;80:795-803.
26. Trudeau MC, Warmke JW, Ganetzky B, Robertson GA. HERG, a human inward rectifier in the voltage-gated potassium channel family. Science 1995;269:92-95.
27. Smith PL, Baukrowitz T, Yelle G. The inward rectification mechanism of the HERG cardiac potassium channel. Nature 1996;379:833-36.
28. Sanguinetti MC, Jiang C, Curran ME, Keating MT. A mechanistic link between an inherited and an acquired cardiac arrhythmia: HERG encodes the I_{Kr} potassium channel. Cell 1995;81:299-307.
29. McDonald TV, Yu Z, Ming Z, et al. A minK-HERG complex regulates the cardiac potassium current I_{Kr}. Nature 1997;388:289-92.
30. Wang Q, Curran ME, Splawski I, et al. Positional cloning of a novel potassium channel gene: KvLQT1 mutations cause cardiac arrhythmias. Nat Genet 1996;12:17-23.
31. Biervert C, Schroeder BC, Kubisch C, et al. A potassium channel mutation in neonatal human epilepsy. Science 1998;279:403-06.
32. Singh NA, Charlier C, Stauffer D, et al. A novel potassium channel gene, KCNQ2, is mutated in an inherited epilepsy of newborns. Nat Genet 1998;18:25-29.
33. Charlier C, Singh NA, Ryan SG, et al. A pore mutation in a novel KQT-like potassium channel gene in an idiopathic epilepsy family. Nat Genet 1998;18:53-55.
34. Barhanin J, Lesage F, Guillemare E, Fink M, Lazdunski M, Romey G. K(V)LQT1 and lsK (minK) proteins associate to form the I(Ks) cardiac potassium current. Nature 1996;384:78-80.
35. Sanguinetti MC, Curran ME, Zou A, et al. Coassembly of K(V)LQT1 and minK (IsK) proteins to form cardiac I(Ks) potassium channel. Nature 1996;384:80-83.
36. Lee MP, Hu R-J, Johnson LA, Feinberg AP. Human KVLQT1 gene shows tissue-specific imprinting and encompasses Beckwith-Wiedemann syndrome chromosomal rearrangements. Nat Genet 1997;15:181-85.
37. Jiang M, Tseng-Crank J, Tseng GN. Suppression of slow delayed rectifier current by a truncated isoform of KvLQT1 cloned from normal human heart. J Biol Chem 1997;272:24109-12.
38. Demolombe S, Baro I, Pereon Y, et al. A negative dominant isoform of the long QT syndrome 1 gene product. J Biol Chem 1998;273:6837-43.
39. Sakagami M, Fukazawa K, Matsunaga T, et al. Cellular localization of rat Isk protein in the stria vascularis by immunohistochemical observation. Heart Res 1991;56:168-72.
40. Neyroud N, Tesson F, Denjoy I, et al. A novel mutation in the potassium channel gene KVLQT1 causes the Jervell and Lange-Nielsen cardioauditory syndrome. Nat Genet 1997;15:186-89.
41. Splawski I, Tristani-Firouzi M, Lehmann MH, Sanguinetti MC, Keating MT. Mutations in the hminK gene cause long QT syndrome and suppress I_{Ks} function. Nat Genet 1997;17:338-40.
42. Romano C. Congenital cardiac arrhythmia. Lancet 1965;1:658-59.
43. Ward OC. A new familial cardiac syndrome in children. J Ir Med Assoc 1964;54:103-06.
44. Tyson J, Tranebjaerg L, Bellman S, et al. IsK and KvLQT1: mutation in either of the two subunits of the slow component of the delayed rectifier potassium channel can cause Jervell and Lange-Nielsen syndrome. Hum Mol Genet 1997;6:2179-85.

45. Jervell A, Lange-Nielsen F. Congenital deaf mutism, functional heart disease with prolongation of the QT interval, and sudden death. Am Heart J 1957;54:59-78.
46. Vetter DE, Mann JR, Wangemann P, et al. Inner ear defects induced by null mutation of the isk gene. Neuron 1996;17:1251-64.
47. Wilde AAM, Janse MJ. Electrophysiological effects of ATP-sensitive potassium channel modulation: Implications for arrhythmogenesis. Cardiovasc Res 1994;28;16-24.
48. Aquilar-Bryan L, Nichols CG, Wechsler SW, et al. Cloning of the β-cell high-affinity sulfonylurea receptor: a regulator of insulin secretion. Science 1995;268:423-26.
49. Inagaki N, Gonoi T, Clement IV JP, et al. Reconstitution of $I_{K.ATP}$: an inward rectifier subunit plus the sulphonylurea receptor. Science 1995;270:1166-70.
50. Inagaki N, Gonoi T, Clement IV JP, et al. A family of sulphonylurea receptors determines the pharmacological properties of ATP-sensitive K^+ channels. Neuron 1996;16:1011-17.
51. Isomoto S, Kondo C, Yamada M, et al. A novel sulphonylurea receptor form with BIR (Kir 6.2) a smooth muscle type ATP-sensitive K^+ channel. J Biol Chem 1996;271:24321-24.
52. Krapivinsky G, Gordon EA, Wickman K, et al., The G-protein-gated atrial K^+ channel $I_{K.ACh}$ is a heteromultimer of two inwardly rectifying K^+ channel proteins. Nature 1995;374:135-41.
53. Kass RS, Davies MP. The roles of ion channels in an inherited heart disease: molecular genetics of the long QT syndrome. Cardiovasc Res 1996;32:443-54.
54. Roden DM, Lazzara R, Rosen M, et al. Multiple mechanisms in the long QT syndrome. Current knowledge, gaps, and future directions. Circulation 1996;94:1996-2012.
55. Schwartz PJ, Matteo PS, Moss AJ, et al. Gene-specific influence on the triggers for cardiac arrest in the long QT syndrome (abstract). Circulation 1997;96:I-212.
56. Shalaby FY, Levesque PC, Yang WP, et al. Dominant-negative KvLQT1 mutations underlie the LQT1 form of long QT syndrome. Circulation 1997;96:1733-36.
57. Chouabe C, Neyroud N, Guicheney P, Lazdunski M, Romey G, Barhanin J. Properties of KvLQT1 K^+ channel mutations in Romano-Ward and Jervell and Lange-Nielsen inherited cardiac arrhythmias. EMBO J 1997;16:5472-79.
58. Wollnik B, Schroeder BC, Kubisch C, Esperer HD, Wieacker P, Jentsch TJ. Pathophysiological mechanisms of dominant and recessive KVLQT1 K^+ channel mutations found in inherited cardiac arrhythmias. Hum Mol Genet 1997;6:1943-49.
59. Fraser GR, Froggatt P, James TN. Congenital deafness associated with electrocardiographic abnormalities. Ann Hum Genet 1964;28:133-57.
60. Sanguinetti MC, Curran ME, Spector PS, Keating MT Spectrum of HERG K^+-channel dysfunction in an inherited cardiac arrhythmia. Proc Natl Acad Sci USA 1996;93:2208-12.
61. Moss AJ, Zareba W, Benhorin J, et al. ECG T-wave patterns in genetically distinct forms of the heriditary Long QT syndrome. Circulation 1995;92:2929-34.
62. Wilde AAM, Veldkamp MW. Ion channels, the QT-interval and arrhythmias. PACE 1997;20:2048-51.
63. Tomaselli GF, Beuckelmann DJ, Calkins HG, et al. Sudden cardiac death in heart failure. The role of abnormal repolarization. Circulation 1994; 90: 2534-39.
64. Choy AMJ, Kupershmidt S, Lang CC, et al. Regional expression of HERG and KvLQT1 in heart failure (abstract). Circulation 1996; 94, suppl I: I-164.
65. Gidh-Jain M, Huang B, Jain P, El-Sherif N. Differential expression of voltage-gated K^+ channel genes in left ventricular remodeled myocardium after experimental myocardial infarction. Circ Res 1996; 79: 669-75.

15. EXPRESSION OF CX43 IN CARDIAC AND AORTIC MUSCLE CELLS OF HYPERTENSIVE RATS

Jacques-Antoine Haefliger, and Paolo Meda

Introduction

Gap junctions are seen at sites where the plasma membranes of two adjacent cells become closely apposed [1,2], reducing the intercellular space, which is usually about 200 nm wide, to a narrow gap of 2 nm (figures 1 and 2). In these regions, the two interacting membranes feature specialized microdomains characterized by the concentration of uniformely large protein assemblies named connexons (figures 1 and 2). These structures provide the wall of intercellular channels, that allow for the passage of ions as well as for the exchange from one cell to another of metabolites and second messengers up to 1kDa [3,4]. Such a direct cell-to-cell exchange of molecules can be visualized using exogenous tracers, such as Lucifer Yellow [5]. After microinjection into individual cells, the intercellular diffusion of this tracer, which cannot cross the cell membrane, can be directly observed under a fluorescence microscope (figure 2). Gap junction channels are formed by the hexameric assembly of membrane-spanning proteins (figures 1 and 2), known as connexins, which in mammals belong to a family of 13 members [2]. Five of these proteins, referred to as Cx43, Cx45, Cx46, Cx40 and Cx37 have been identified in the cardiovascular system [6,7]. As yet, little is known about their physiological role and their possible changes in cardiovascular diseases.
Gap junctions ensure the electrical and mechanical coupling of different types of muscle cells [8]. Such a role is critical in the heart, since proper propulsion of blood in the circulation, obligatory depends on the coordinated contraction of both atrial and ventricular cardiomyocytes [9,10]. This contraction in turn is mediated by the rapid propagation of action potentials to multiple cells, that should depolarize in coordination. These events are dependent on gap junctional communications, whereby adjacent cardiomyocytes exchange current-carrying ions. By diffusing from one cell to the next, these ions synchronize the electrical and mechanical activity of neighbor cells [9]. Coordination of smooth muscle cells of the vascular wall is also critical to the local modulation of vasomotor tone, thus contributing to the proper function of large vessels. The aortic media, which is a sparsely innervated and electrically quiescent tissue, is likely to be particulary dependent on gap junctional communication for coordinating

P.A. Doevendans et al. (eds.), Cardiovascular specific gene expression, 161-69.

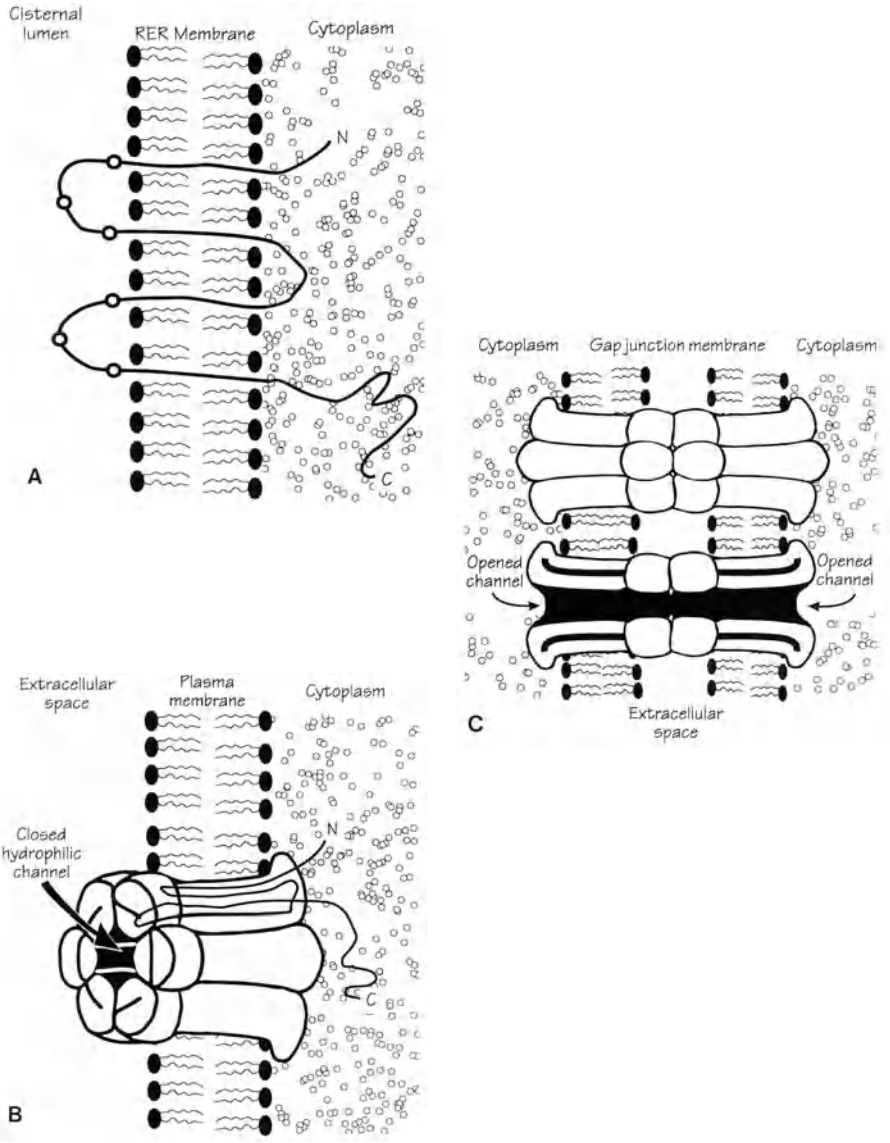

Figure 1. *Topography of a connexin channel. A) During biosynthesis, connexin proteins are inserted in the membrane of rough endoplasmic reticulum (RER), which they cross four times. This arrangement provides for two loops in the cisternal lumen, and for the location of both C-and N-termini in the cytoplasm. All connexins feature three cysteine residues (open circles) in the two intracisternal loops. The C-terminus varies in sequence and length in different connexins. B) During their intracellular transport, connexins arrange as hexamers to form a tubular structure (called connexon) around a hydrophilic space of 2 nm diameter that extends across the entire thickness of the membrane. C) At gap junctions, connexons of one cell dock with those made by an adjacent cell. The alignement of two apposed connexons forms the wall of a channel, which directly links the cytoplasms of two neighbour cells. Modified with permission from [5].*

the responses of smooth muscle cells to diverse neural and endothelial signals [11-15]. Thus, conditions perturbing the function of the aortic wall, as observed during chronic hypertension, are expected to be associated with alterations of connexins, gap junctions or coupling.

To assess whether conditions perturbing the function of heart and aorta are associated with alterations of connexins, gap junctions or coupling, we have studied the expression of Cx43, the physiologically predominant connexin of myocardial and aortic smooth muscle cells [9,14,16], during chronic hypertension. To this end, we have first investigated two rat models that are characterized by a similar degree of hypertension and of hypertrophy of both aorta and heart, but differ markedly in the mechanism which causes these changes. In the two kidney, one-clip model (2K,1C) hypertension was produced by clipping one renal artery, leading to stimulation of renin secretion and to an angiotensin II-dependent elevation of blood pressure [17,18]. In the mineralocorticoid-salt induced model (DOCA-salt) hypertension resulted from increased retention of sodium, in the presence of suppressed renin secretion [19,20]. In a second step, we have investigated a third model, in which rats were made hypertensive by inhibiting nitric oxyde synthase with N-nitro-L-arginine-methyl ester (L-NAME) [21].

Results

Blood pressure levels were elevated 1.4-1.6 fold over that of normotensive controls in all 2K,1C, DOCA-salt and L-NAME animals.

Effects of hypertension on heart

Hypertensive rats of the 2K,1C and DOCA-salt models showed a 30% increase in heart index compared to normotensive controls (figure 3A). In agreement with this change, Northern blot analysis showed a two fold increase in the expression of α-skeletal actin mRNA in the two groups of hypertensive rats and histology revealed a thickening of the left ventricular wall [22]. Hypertensive rats of the L-NAME showed a smaller increase (18%) in heart index (figure 3A), and a lesser thickening of the left ventricular wall, in spite of a three fold increase in the expression of α-skeletal actin mRNA (Haefliger et al., unpublished results). Quantitative assessment by Northern blot analysis showed that Cx43 expression was similar in the hypertrophied hearts of hypertensive rats of the three models studied, and in those of normotensive controls (figure 4). This finding correlated with the absence of significant differences in the amount of Cx43, which was immunolabelled in heart muscle of 2K,1C and DOCA-salt animals [22].

Effects of hypertension on aorta

The thickness of the intima plus media layers of the aorta was significantly larger in hypertensive than in normotensive animals, resulting in a 40% increase of the vessel cross-sectional area (figure 3B), in spite of a constant lumen radius [22]. In the 2K,1C and DOCA-salt hypertensive rats, these changes were due to an enlargment of smooth

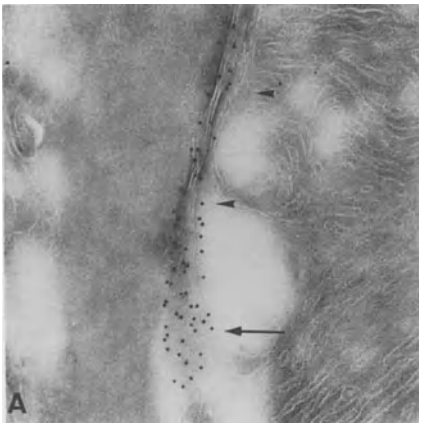

Figure 2. *Connexins, gap junctions and coupling. A) Immunostaining with antibodies and protein A-gold particles reveals the plaque arrangement of connexins (arrow) in regions where two plasma membranes are closely apposed, reducing the intercellular space to a gap of 2 nm (arrowheads). B) By freeze-fracture electron microscopy, gap junctions are identified as intramembrane aggregates of proteic particles, each representing a connexon, on the protoplasmic face (p) of the membrane. The imprints of connexons which are observed on the exoplasmic face of the membrane (e) indicate that gap junction channels entirely cross the plasma membranes of two adjacent cells. C) Microinjection of one cell with Lucifer Yellow, is immediately followed by the passage of this vital tracer in neighbouring cells connected by gap junctions channels. This event is referred to as intercellular or junctional coupling. The microelectrode used to inject the dye is labelled (m). Bar represents 190 nm in A and B, and 22 µm in C. Reproduced from [5].*

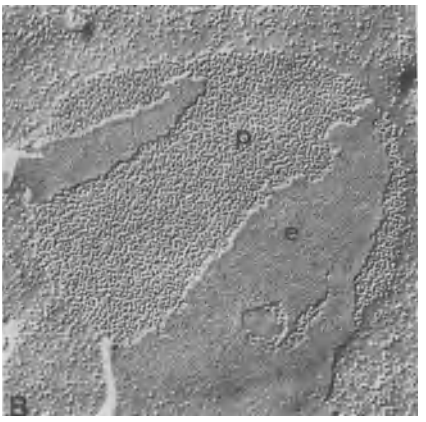

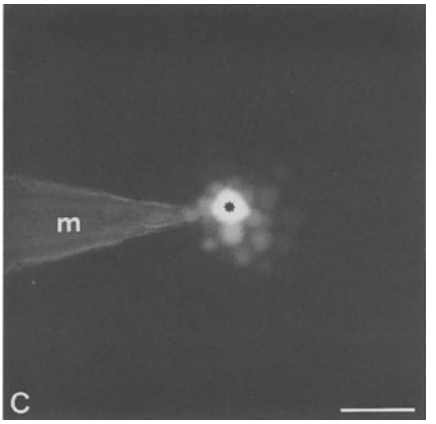

muscle cells, whose numerical density was slightly reduced. Quantitative assessment of Cx43 gene expression by Northern blotting of total RNA, showed significantly higher values in the aorta of the 2K,1C and DOCA-salt hypertensive rats than in that of normotensive rats (figure 4). These changes were paralleled by a modest but sizeable increase in the amount of Cx43, as monitored by immunolabelling of aorta cryosections [22].

In contrast with these findings, the aortas of the L-NAME treated animals featured a decreased level of Cx43 mRNA (figure 4), when compared to untreated controls, in spite of a 25% increase of the vessel cross-sectional area (figure 3B).

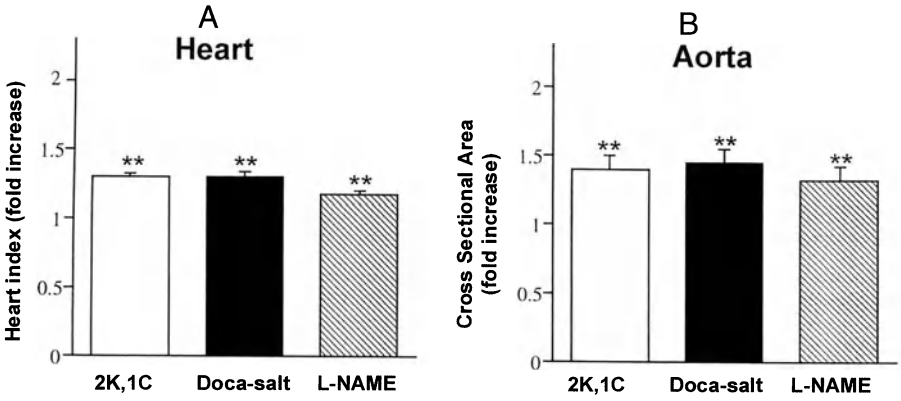

Figure 3. *Thickening of cardiac and aortic walls in hypertensive rats. A) As compared to normotensive animals (whose heart index was scored 1), the 2K,1C and DOCA-salt hypertensive rats showed a similar 30% increase in heart index. In contrast, the L-NAME hypertensive rats showed only a 17% increase in this parameter, which gives the weight of myocardium per unit animal weight. Values are expressed as mean ± SEM. Asterisks denote a difference significant at the p <.01 level. B) After four weeks of hypertension, the aorta of 2K,1C and DOCA-salt hypertensive animals showed a thickened wall, resulting in a 40% increase in the cross-sectional area (control value was set to 1), despite of a similar internal diameter. The aorta of L-NAME hypertensive rats was thickened to a lesser extent, resulting in a 25% increase in cross sectional area. Asterisks denote a difference significant at the p <.01 level.*

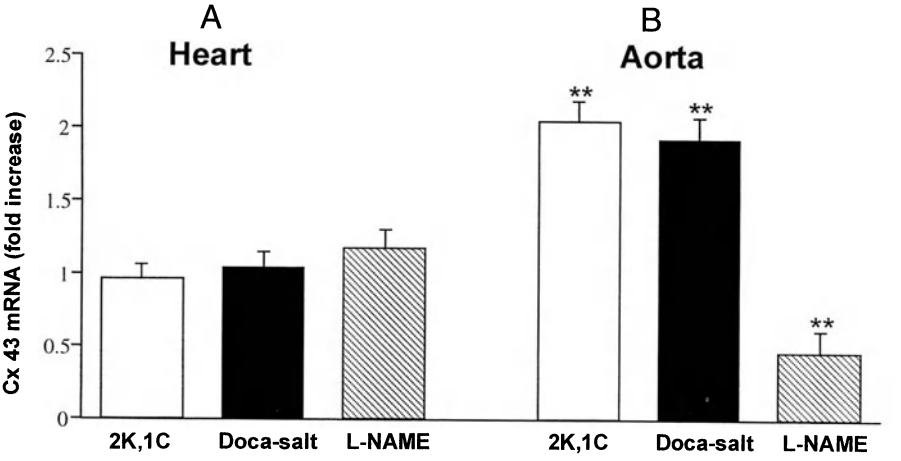

Figure 4. *Expression of Cx43 in heart and aorta of hypertensive rats. A) Analysis of heart RNA revealed that the levels of the Cx43 transcript, which was mostly contributed to by cardiomyocytes, were not altered in the three types of hypertensive rats we investigated.*

B) Analysis of aorta RNA revealed that the transcript for Cx43, which was mostly contributed to by smooth muscle cells, was increased about two fold in the hypertensive rats of the 2K,1C and DOCA-salt models. In contrast, the hypertensive rats treated with L-NAME showed a 50% reduction of the Cx43 transcript compared to control value (which was set to 1 in all groups). Data of the 2K,1C and DOCA-salt animals are modified from [22].

Discussion

We have examined the effects of chronic hypertension on the expression of Cx43, the major native connexin of the cardiovascular system [23], in three different experimental rat models.

After one month, the increase in blood pressure achieved in the three models was comparable. We have found that hypertensive animals feature cardiac hypertrophy [22] in the absence of differences in the levels of Cx43 connecting myocardial cells. This finding suggests that Cx43 is not involved in the myocardial adaptation that accompanies a hypertension-induced increase in heart load. This conclusion does not rule out that other connexins (Cx45, Cx40, Cx37), which colocalize with Cx43 at myocardial gap junctions [7,24], could participate in the cardiac changes during hypertension. Indeed, the inactivation of the Cx43 gene in transgenic mice suggests that, at least under certain conditions, Cx43 may be functionally replaced by other connexins [25,26].

Under the conditions studied, the 2K,1C and the DOCA-salt hypertensive animals exhibited a similar degree of thickening of the aortic wall, which was mostly accounted for by the hypertrophy of smooth muscle cells and the accumulation of extracellular materials. The hypertensive rats from these two groups also featured a comparable two fold increase in the level of Cx43 that was expressed by the smooth muscle cells of the aortic media. This change could not be related to the circulating levels of angiotensin II, which were increased in the 2K,1C [27-29] but unchanged in the DOCA-salt model [19]. Hence, the change in the expression of aortic Cx43 is likely to be associated with the increase in blood pressure.

The molecular mechanism leading to the pressure-induced increase in the expression of the Cx43 gene remains to be elucidated. The presence of multiple promoters in the 5'-untranslated region of this gene [30,31] raises the possibility that the regional regulation of this increase, is controlled by tissue-specific transcription factors [32,33]. Interestingly, transcription of Cx43 may be promoted by increased expression of *c-fos* [34], a transcription factor which accumulates in smooth muscle cells of rat aortas following exposure to angiotensin II [35,36]. Cx43 may be implicated in modulating the vasomotor tone of the aortic wall by providing an intercellular pathway for the synchronous contraction of smooth muscle cells, through the propagation of gap junction-permeant second messengers [12-15].

The finding that Cx43 was decreased in the aortic smooth muscle cells of rats treated with L-NAME, in spite of the fact that this drug increased mean blood pressure as in the 2K,1C and DOCA-salt models, further suggest that the Cx43-mediated cell-to-cell communication is somehow related to the distensibility characteristics of conduits arteries. Carotid distensibility is increased in the 2K,1C model but not in the L-NAME model ([21,37] and Haefliger et al., unpublished results).

Conclusion

We have found that the expression of Cx43 is differentially regulated in the hypertrophic muscle cells of heart and aorta, and that this tissue-specific regulation takes place in rats made similarly hypertensive by different mechanisms. Although, further studies are needed to understand how the changes in Cx43 expression participate in the adaptative response of the aorta to high blood pressure, our data indicate that Cx43 may represent a suitable tissue-specific marker to monitor hypertension-induced changes in the vasculature.

Acknowledgements

Dr. Haefliger is supported by a career award from the Max Cloétta Foundation. This work was supported by grants from the Swiss National Science Foundation (31-46770.96 to Dr. Haefliger, 32-53720.98 to Dr. Meda), the European Union (BMH4-CT96-1427 to Dr. Meda), and the Foundation De Reuter (to Dr. Meda).

References

1. Meda P. Molecular biology of gap junction proteins. Mol Biol of Diabetes, Part I 1994;14:333-56.
2. Bennett MVL, Barrio LC, Bargiello TA, Spray DC, Hertzberg E, Saez JC. Gap junctions: new tools, new answers, new questions. Neuron 1991;6:305-20.
3. Beyer EC, Goodenough DA, Paul DL. Herzberg EL, Johnson RG, editors.Gap Junction. New-York: Alan R. Liss, 1988; The connexins, a family of related gap junction proteins. p. 167-75.
4. Loewenstein WR. Junctional intercellular communication. The cell-to-cell membrane channel. Physiol Rev 1981;61:829-913.
5. Haefliger J-A, Waeber G, Meda P. Communication intercellulaire par les canaux jonctionnels "GAP": Rôle en endocrinologie. Méd Hyg 1997;55:270-74.
6. Haefliger J-A, Bruzzone R, Jenkins NA, Gilbert DJ, Copeland NG, Paul DL. Four novel members of the connexin family of gap junction proteins: molecular cloning, expression and chromosome mapping. J Biol Chem 1992;267:2057-64.
7. Kanter HL, Laing JG, Beyer EC, Green KG, Saffitz JE. Multiple connexins colocalize in canine ventricular myocyte gap junctions. Circ Res 1993;73:344-50.
8. Christ GJ. Modulation of a1-adrenergic contractility in isolated vascular tissue by heptanol: A functional demonstration of the potential importance of intercellular communication to vascular response generation. Life Sci 1995;56:709-21.
9. Severs NJ. Pathophysiology of gap junctions in heart disease. J Cardiovasc Electrophys 1994;5:462-75.
10. Peters NS. Gap Junctions and Clinical Cardiology: from Molecular Biology to Molecular Medicine. Eur Heart J 1997;18:1697-702.
11. Segal SS. Cell-to-Cell communication coordinates blood flow control. Hypertension 1994;23:1113-20.
12. Segal SS, Duling BR. Flow control among microvessels coordinated by intercellular conduction. Science 1986;234:868-70.
13. Larson DM, Haudenschild CC, Beyer EC. Gap junction messenger RNA expression by vascular wall cells. Circ Res 1990;66:1074-80.
14. Christ GJ, Brink PR, Zhao W, Moss J, Gondré CM, Roy C, Spray DC. Gap junctions modulate tissue contractility and alpha adrenergic agonist efficacy in isolated rat aorta. J Pharmacol Exp Ther 1993;266:1054-65.
15. Christ GJ, Spray DC, El-Sabban M, Moore LK, Brink PR. Gap junction in vascular tissues. Evaluating the role of the intercellular communication in the modulation of vasomotor tone. Circ Res 1996;79:631-46.
16. Bruzzone R, Haefliger J-A, Gimlich RL, Paul DL. Connexin40, a component of gap junctions in vascular endothelium, is restricted in its ability to interact with other connexins. Mol Biol Cell 1993;4:7-20.
17. Goldblatt H, Lynch J, Hanzal RF, Summerville WW. Studies on experimental hypertension: production of persistent elevation of systolic blood pression by means of renal ischemia. J Exp Med 1934;59:347-79.
18. Leenen FHH, De Jong W, De Wied D. Renal venous and peripheral plasma renin activity in renal hypertension. Am J Physiol 1973;225:1513-18.
19. Gavras H, Brunner HR, Larah JH, Vaughn ED, Koss M, Cote LJ, Gavras I. Malignant hypertension resulting from deoxycorticosterone acetate and salt excess. Circ Res 1975;36:300-09.
20. Liu DT, Birchall I, Hewitson T, Kincaid-Smith P, Whitworth JA. Effect of dietary calcium on the development of hypertension and hypertensive vascular lesions in DOCA-salt and two-kidney, one clip hypertensive rats. J Hypert 1994;12:145-53.

21. Delacrétaz E, Zanchi A, Nussberger J, Hayoz D, Aubert J-F, Brunner HR, Waeber B. Chronic nitric oxyde synthase inhibition and carotid artery distensibility in renal hypertensive rats. Hypertension 1995;26:332-36.
22. Haefliger J-A, Castillo E, Waeber G, Bergonzelli GE, Aubert J-F, Sutter E, Nicod P, Waeber B, Meda P. Hypertension increases connexin43 in a tissue-specific manner. Circulation 1997;95:1007-14.
23. Beyer EC, Kistler J, Paul DL, Goodenough DA. Antisera directed against connexin43 peptides react with a 43-KD protein localized to gap junctions in myocardium and other tissues. J Cell Biol 1989;108:595-605.
24. Bastide B, Neyses L, Ganten D, Paul M, Willecke K, Traub O. Gap Junction Protein Connexin40 is preferentially expressed in vascular endothelium and conductive bundles of rat and is increased under hypertensive conditions. Circ Res 1993;73:1138-49.
25. Reaume AG, de Sousa PA, Kulkarni S, Langille BL, Zhu D, Davies TC, Juneja SC, Kidder GM, Rossant J. Cardiac malformation in neonatal mice lacking connexin43. Science 1995;267:1831-34.
26. Gros DB, Jongsma HJ. Connexins in mammalian heart function. Bioessays 1996;18:719-30.
27. Haefliger J-A, Bergonzelli G, Waeber G, Aubert J-F, Nussberger J, Gavras H, Nicod P, Waeber B. Renin and angiotensin II receptor gene expression in kidneys of renal hypertensive rats. Hypertension 1995;26:733-37.
28. Levy BI, Michel J-B, Salzmann J-L, Azizi M, Poitevin P, Safar M, Camilleri J-P. Effects of chronic inhibition of converting enzyme on mechanical and structural properties of arteries in rat renovascular hypertension. Circ Res 1988;63:227-39.
29. Morishita R, Higaki J, Miyazaki M, Ogihara T. Possible role of the vascular renin-angiotensin system in hypertension and vascular hypertrophy. Hypertension 1992;19:62-67.
30. Yu W, Dahl G, Werner R. The connexin43 gene is responsive to oestrogen. Proc R Soc Lond B Biol Sci 1994;255:125-32.
31. Chen Z-Q, Lefebvre DL, Bai X-H, Reaume A, Rossant J, Lye SJ. Identification of two regulatory elements within the promoter region of the mouse Cx-43 gene. J Biol Chem 1995;270:3863-68.
32. Petrocelli T, Lye SJ. Regulation of transcripts encoding the myometrial gap junction protein, connexin-43, by estrogen and progesterone. Endocrinology 1993;133:284-90.
33. Piersanti M, Lye SJ. Increase in messenger ribonucleic acid encoding the myometrial gap junction protein, connexin-43, requires protein synthesis and is associated with increased expression of the activator protein-1, c-fos. Endocrinology 1995;136:3571-78.
34. Lefebvre DL, Piersanti M, Bai X-H, Chen Z-Q, Lye SJ. Myometrial transcriptional regulation of the gap junction gene, connexin-43. Reprod Fertil Devel 1996;7:603-11.
35. Taubman MB, Berk BC, Izumo S, Tsuda T, Alexander RW, Nadal-Ginard B. Angiotensin II induces c-fos mRNA in aortic smooth muscle. J Biol Chem 1989;264:526-30.
36. Naftilan AJ, Pratt RE, Eldridge CS, Lin HL, Dzau VJ. Angiotensin II induces c-fos expression in smooth muscle via transcriptional control. Hypertension 1989;13:706-11.
37. Delacrétaz E, Hayoz D, Osterheld MC, Genton CY, Brunner HR, Waeber B. Long-term nitric oxyde synthase inhibition and distensibility of carotid artery in intact rats. Hypertension 1994;23:967-70.

16. GENETIC ENGINEERING AND CARDIAC ION CHANNELS

Andrew A. Grace, Richard C. Saumarez, and Jamie I. Vandenberg

Introduction

In recent years there have been significant advances in our understanding of the molecular basis of the electrical activity of the heart with the cloning of many ion channel sub-units [1] and descriptions of their patterns of expression [2,31]. The situation now is such that our knowledge of individual ion channels considerably exceeds that of how they function *in vivo* and how their activities are co-ordinated to ensure normal cardiac activity. One important impetus to changing this state-of-affairs is the need for improved understanding of cardiac arrhythmias. Abnormalities of cardiac ion channel expression and function are known to contribute to the genesis of arrhythmias although it is not known precisely how [4].

Arrhythmogenic substrates can be divided into complex and discrete subsets. Most arrhythmias arise in patients with structural cardiac diseases where electrophysiological phenotypes are complex and are not easily open to molecular dissection [4,5]. Conversely, the identification of discrete, relatively simple and therefore experimentally amenable arrhythmogenic substrates in the long-QT [4,6,7] and Brugada [8,9] syndromes offer great opportunities for improving the understanding of mechanisms that may be of broad applicability. In combination with *in vivo* techniques of genetic manipulation [7,10] and the development of refined methods of physiological assessment [4,11-14] it seems likely that knowledge of arrhythmia mechanisms will now have molecular underpinning. The purpose of this short review is to consider the problems inherent in these approaches and suggest some ways forward.

Ion channel Expression and Complex Arrhythmogenic Substrates

Heart failure, an example of a complex arrhythmogenic substrate, is usually associated with scar formation following myocardial infarction with half of reported deaths caused by ventricular arrhythmias due to re-entry of waves of excitation [5]. Under these circumstances, structural (e.g. fibrosis), cellular (e.g. myofibrillar disarray, myocyte

P.A. Doevendans et al. (eds.), Cardiovascular specific gene expression, 171-78.

hypertrophy) and gene expression (e.g. structural proteins, ion channel) changes contribute to arrhythmogenic substrates both in animal models [15] and clinically [5,16]. These changes together alter the electrophysiological properties of myocardium and predispose to reentry.

The few studies of ion channel gene expression in heart failure have generally shown decreased expression of potassium channel genes consistent with the patterns of delayed repolarization that have been observed [5,16-18]. Delayed repolarization is also likely to modify refractoriness setting up conditions for reentry [4,5]. Complex cardiac disease may therefore best be regarded as being due to quantitative, and polygenic, changes in ion channel expression associated with complex phenotypes that are not easily open to complete functional molecular dissection.

Ion Channel Function and Discrete Arrhythmogenic Substrates

The long-QT and Brugada syndromes may present with syncope, seizures or sudden cardiac death as a result of ventricular arrhythmias [8,19] and arise directly as a result of specific ion channel mutations [6,9]. Indeed, the elucidation of the molecular genetics of these conditions has had an important impact on our thinking by showing how discrete changes in ion channel function may have profound electrophysiological consequences. Several genes have been implicated in monogenic long-QT syndromes. In LQT1, LQT2 and LQT5 there are mutations in potassium channel genes (*KvLQT1*, *HERG* and *KCNE1,* respectively) that normally contribute to repolarization [6,20]. These mutations impair function. By contrast, in LQT3 there is a gain-in-function with mutations in *SCN5A* resulting in destabilization of the inactivation gate of the fast inward sodium channel, prolonging the inward current and hence delaying repolarization of the action potential [21,22]. Mutations in *SCN5A* also result in the Brugada syndrome although here the underlying mechanisms are likely to be very different [9]. Specifically, it appears that a mis-sense mutation leads to more rapid recovery from sodium channel inactivation and that a frame-shift mutation causes the channel to be non-functional [9].

The pathogenesis of arrhythmias in the long-QT and Brugada syndromes is however unresolved [4,19,23]. *In vitro* studies in models of long-QT syndrome suggest that delayed repolarization leads to secondary depolarizations which could hypothetically initiate re-entry [4,19,24]. Notwithstanding, the electrophysiological phenotype is likely to be more complex. For example, electrogram fractionation has been observed in high-risk patients with both long-QT syndrome [14,24] and primary ventricular fibrillation [25].

The relation between such monogenic conditions and arrhythmias raises several questions. For example, do individual ion channel mutations lead to arrhythmias via distinct or similar mechanisms? How relevant is the analysis of these rare monogenic conditions to genetically complex cardiac diseases? The development of animal models with mutations introduced into ion channel genes, comparisons to other animal models of heart disease and the development of electrophysiological measurements for use both in these models and clinically is likely to help to resolve such issues [4,17].

Electrophysiological Analysis of Arrhythmogenic Substrates

It is not possible to predict with any precision which patients may be at risk of arrhythmias [26]. Programmed stimulation and the induction of arrhythmias is used to guide management in patients with previous myocardial infarction but has little value in the assessment of cardiomyopathies [27,28], the long-QT syndromes [14,29] or primary ventricular fibrillation [25]. An ideal method of assessment would reflect those features likely to mediate reentry. Accordingly, new techniques are required to quantify the relationship between intraventricular conduction, repolarization and refractoriness [23] to estimate the likelihood of re-entry [4,28].

In the normal heart electrograms are usually composed of single bipolar voltage deflections. In abnormal tissue, however, electrograms are often composed of multiple discrete components and this abnormal response is termed fractionation (see figure 1; [28,30]). The quantitative analysis of electrogram fractionation in response to premature stimuli was developed, on an empiric basis, as a method for detecting the multiple electrical pathways presumed to occur in the disordered myocardium of patients with hypertrophic cardiomyopathy [27,28]. Analyzing fractionation patterns is reasonably successful in detecting patients at apparently high risk of developing arrhythmias [27,28] and is now undergoing prospective assessment in large-scale multi-centre studies (supported by the British Heart Foundation and Biomed II). The relationship between the quantitative analysis of electrogram fractionation and prognosis suggests an assay of the ability of hypertrophic myocardium to support re-entry [27,28]. Electrogram fractionation in response to premature stimulation has also been detected in patients with primary ventricular fibrillation [25] and the long-QT syndrome [14].

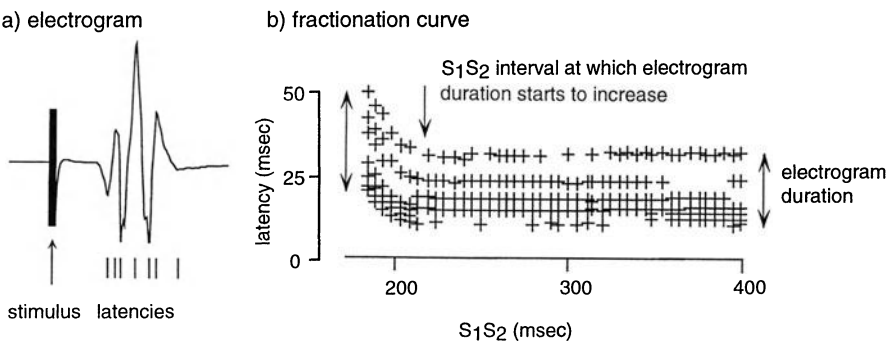

Figure 1. *Principles of electrogram fractionation. Electrograms recorded from normal ventricular myocardium in response to premature stimuli are usually composed of single bipolar voltage deflections. Conversely, abnormal tissue is characterized by electrograms composed of multiple components; a pattern termed fractionation [28]. The multiple components of such fractionated electrograms are thought to reflect multiple pathways or wavelets of excitation in the region of the recording electrode [28]. The number of components, the electrogram duration and the induction of fractionation at longer coupling intervals are all thought to reflect a greater propensity to develop re-entry circuits. a) An electrogram recorded at an S_1S_2 coupling interval of 170 msec in a normal rabbit heart. b) An intraventricular conduction (fractionation) curve showing the latency to each component, duration of the electrogram and the S_1S_2 coupling interval at which the electrogram duration started to increase.*

Pharmacological Manipulation of Cardiac Ion Channels

The application of electrogram fractionation to animal models provided an opportunity to directly link the changes in individual ion channels to clinically obtained measures of arrhythmia risk. As a first step to realizing this aim we have recently developed a model of long-QT syndrome to see whether measurements of electrogram fractionation could be obtained in hearts from small animals [14]. Langendorff-perfused ferret hearts, prepared as previously described [31], with platinum electrodes placed at 8 epicardial sites have been used with computer-driven stimulation performed at 4 sites with applied decremental sequences similar to those used in man. Electrograms are recorded from the remaining 7 electrodes and analyzed using clinical protocols (see figure 2) [27,28]. Anthopleurin-A (AP-A) which inhibits the open-to-inactivated state transition (O⇒I) of the sodium current has been used to model LQT3 [24,32,33] and LQT2 has been reproduced using quinidine, *d,l*-sotalol or dofetilide. The addition of these agents reproduce the abnormalities in repolarization, refractoriness, conduction delay and electrogram fractionation observed in high-risk long-QT syndrome patients (see figure 2).

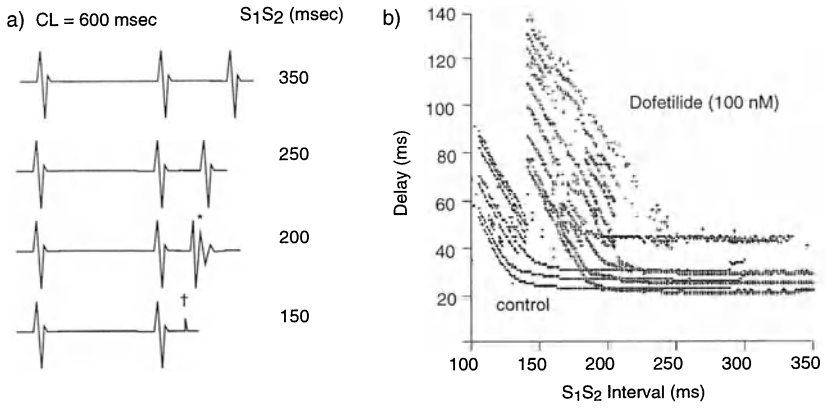

Figure 2. *Electrogram fractionation in response to premature stimulation in perfused ferret heart. a) Cartoon illustrating electrograms with decreasing S_1-S_2 coupling intervals. Pulses delivered with a S_1-S_2 of 200 msec lead to electrogram fractionation (*) with an effective refractory period (ERP) at 150 msec. The pattern of intraventricular conduction is characterized by determining the delay in each potential following the pacing stimulus [28]. Electrograms are then analyzed as a set of delays which are plotted against the coupling interval of the premature stimulus (S_1S_2) to give an intraventricular conduction curve [28]. b) Intraventricular conduction curve. The delays for each electrogram potential are measured at a single electrode in response to progressive shortening of S_1-S_2 delivered by a distant electrode. Dofetilide (100 nM) caused an increase in both the S_1S_2 at which delayed conduction occurs (S_1S_2D) and the maximum duration of the fractionated electrocardiogram (IED) with patterns that entirely reproduce the clinical data obtained from patients with long-QT syndrome.*

These results confirm that the quantitative analysis of electrogram fractionation is transferable between patients and experimental models; that there is a direct link between the electrophysiological consequences of single ion channel mutations and clinical risk in long-QT syndrome; and probably most importantly the electrophysiological features of the long-QT syndrome arrhythmogenic substrate can be reproduced in an animal model.

Genetic Manipulation of Cardiac Ion Channels

Gene-targeting should allow the relationship between single gene mutations and electrophysiological phenotypes to be defined [4,13]. For complex cardiac disease several transgenic and gene-targeted mouse models are available [7]. However, in order to study how specific gene mutations provide arrhythmogenic substrates requires the manipulation of ion channel genes directly [4,10]. The mouse is the most appropriate system for genetic manipulation although many experimental problems need to be addressed if these models of disordered cardiac electrophysiology are to be exploited [4,13].

Human long-QT syndrome mutations provide a series of candidates for genetic manipulation to produce potentially informative electrophysiological phenotypes [4,17]. These mutations do however pose problems in that the mouse myocardium expresses a different complement of ion channels to humans. For example, the expression of delayed rectifier potassium channel homologues (e.g. of *HERG* and *KvLQT1*) appear notably different to humans [34] and in adult mouse the expression is low [35,36].

There are already some mice available with mutations that may be relevant to long-QT syndrome [37]. For example, homozygous *minK* deletion results in a mouse with inner ear defects due to impaired endolymph production and shaker-waltzer behavior and may enable the contribution of *minK* to normal cardiac electrophysiology to be determined [38].

Mouse Cardiac Electrophysiology

Several groups have demonstrated the feasibility of making electrophysiological measurements in intact mouse heart [13,37,39]. The approach we are using is to miniaturize the techniques needed to record and analyze electrograms and apply these to the mouse. Langendorff-perfused mouse hearts are prepared using similar protocols to those applied to ferret hearts (see above) and in recent experiments we have demonstrated that these hearts can remain stable at 37°C and can be used to record monophasic action potentials (not shown) and electrogram fractionation (see figure 3). Gene targeting can then be used to manipulate individual ion channel function allowing several questions to be addressed and specifically examine the relationship between repolarization duration and refractoriness, the mechanisms leading to arrhythmias, the interactions with other ion channels and the identification of modifier genes.

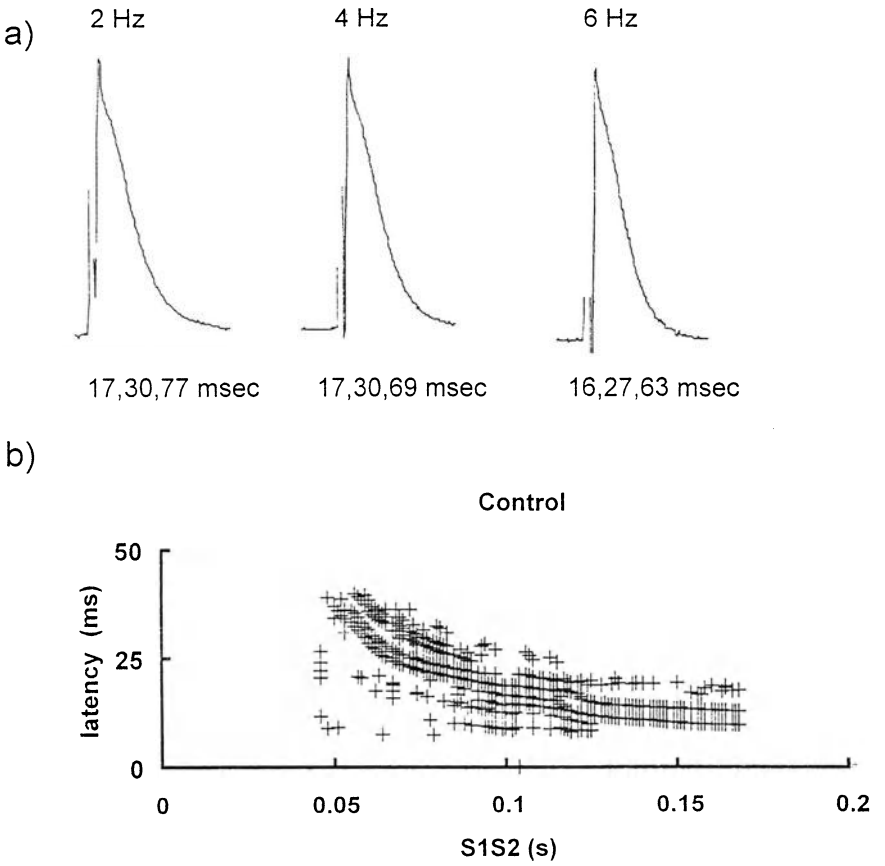

Figure 3. *Cardiac monophasic action potentials (mAPs) and electrogram fractionation in perfused mouse heart. a) mAPs recorded at 2, 4 and 6 Hz. Action potentials are recorded using suction electrodes and digitized using a CED 1401-plus analogue-digital converter operated using Spike 2 software (Cambridge Electronic Design Ltd.) and PC-based programs have been written to allow rapid automated analysis which includes: action potential duration (APD) at 10, 30, 50 and 90% repolarization; latency between trigger spike and the action potential upstroke and the velocity of action potential upstroke (V_{max}). b) Electrogram fractionation curve obtained in perfused mouse heart. The general pattern of response to premature stimulation is similar pattern to that seen both clinically and in ferret heart (see figure 2).*

Conclusions

Genetic manipulation of cardiac ion channels in the mouse is now absolutely straightforward using available technologies [7,10]. The challenge will come with the physiological assessment of these models [13] and the critical analysis of any data obtained against a background of improved knowledge of the patterns of ion channel expression and function in health and disease.

References

1. Barry DM, Nerbonne JM. Myocardial potassium channels: electrophysiological and molecular diversity. Annu Rev Physiol 1996;58:363-94.
2. Takimoto K, Li D, Hershman KM, Li P, Jackson EK, Levitan ES. Decreased expression of Kv4.2 and novel Kv4.3 K^+ channel subunit mRNAs in ventricles of renovascular hypertensive rats. Circ Res 1997;81:533-39.
3. Gidh-Jain M, Huang B, Jain P, El-Sherif N. Differential expression of voltage-gated K^+ channel genes in left ventricular remodeled myocardium after experimental myocardial infarction. Circ Res 1996;79:669-75.
4. Grace AA, Chien KR. Congenital long QT syndromes. Toward molecular dissection of arrhythmia substrates. Circulation 1995;92:2786-89.
5. Tomaselli GF, Beuckelmann DJ, Calkins HG, Berger RD, Kessler PD, Lawrence JH, et al. Sudden cardiac death in heart failure. The role of abnormal repolarization. Circulation 1994;90:2534-39.
6. Keating MT, Sanguinetti MC. Molecular genetic insights into cardiovascular disease. Science 1996;272:681-85.
7. Chien KR, Grace AA. Principles of cardiovascular molecular and cellular biology. In: Braunwald E, editor. Heart Disease. 5th ed. Philadelphia: W B Saunders, 1997:1626-49.
8. Brugada J, Brugada P. Further characterization of the syndrome of right bundle branch block, ST segment elevation, and sudden cardiac death. J Cardiovasc Electrophys 1997;8:325-31.
9. Chen Q, Kirsch GE, Zhang D, Brugada R et al. Genetic basis and molecular mechanism for idiopathic ventrcialr fibrillation. Nature 1998;392:293-96.
10. Colledge WH, Abella BS, Southern KW, Ratcliff R, Jiang C, Cheng SH, et al. Generation and characterization of a delta F508 cystic fibrosis mouse model. Nat Genet 1995;10:445-52.
11. Berul CI, Aronovitz MJ, Wang PJ, Mendelsohn ME. In vivo cardiac electrophysiological studies in the mouse. Circulation 1996;94:2641-48.
12. Restivo M. Animal models of the long QT syndrome. J Cardiovasc Electrophys 1997;8:1159-62.
13. James JF, Hewett TE, Robbins J. Cardiac physiology in transgenic mice. Circ Res 1998;82:407-15.
14. Saumarez RC, Vandenberg JI, Lowe MD, Taylor PJ, Ward DE, Camm AJ, et al. Electrogram fractionation in the long QT syndrome and as modelled in perfused heart by inhibition of inactivation of SCN5A-encoded ion channels. Submitted 1998.
15. Hart G. Cellular electrophysiology in cardiac hypertrophy and failure. Cardiovasc Res 1994;28:933-46.
16. Nabauer M, Beuckelmann DJ, Erdmann E. Characteristics of transient outward current in human ventricular myocytes from patients with terminal heart failure. Circ Res 1993;73:386-94.
17. Roden DM, George AL, Jr. The cardiac ion channels: relevance to management of arrhythmias. Annu Rev Med 1996;47:135-48.
18. Beuckelmann DJ, Nabauer M, Erdmann E. Alterations of K^+ currents in isolated human ventricular myocytes from patients with terminal heart failure. Circ Res 1993;73:379-85.
19. Schwartz PJ, Locati EH, Napolitano C, Priori SG. The long QT syndrome. In: Zipes DP, Jalife J, editors. Cardiac Electrophysiology: from cell to bedside. Philadelphia: WB Saunders Co., 1995:788-811.
20. Duggal P, Vesely MR, Wattanasirichaigoon D, Villafane J, Kaushik V, Beggs AH. Mutation of the gene for IsK associated with both Jervell and Lange-Nielsen and Romano-Ward forms of Long-QT syndrome. Circulation 1998;97:142-46.
21. Wang Q, Shen J, Splawski I, Atkinson D, Li Z, Robinson JL, et al. SCN5A mutations associated with an inherited cardiac arrhythmia, long QT syndrome. Cell 1995;80:805-11.

22. Bennett PB, Yazawa K, Makita N, George AL, Jr. Molecular mechanism for an inherited cardiac arrhythmia. Nature 1995;376:683-85.
23. Miller C. The inconstancy of the human heart. Nature 1996;379:767-68.
24. El Sherif N, Caref EB, Yin H, Restivo M. The electrophysiological mechanism of ventricular arrhythmias in the long QT syndrome. Tridimensional mapping of activation and recovery patterns. Circ Res 1996;79:474-92.
25. Saumarez RC, Heald S, Gill J, Slade AK, de Belder M, Walczak F, et al. Primary ventricular fibrillation is associated with increased paced right ventricular electrogram fractionation. Circulation 1995;92:2565-71.
26. Domanski MJ, Zipes DP, Schron E. Treatment of sudden cardiac death. Current understandings from randomized trials and future research directions. Circulation 1997;95:2694-99.
27. Saumarez RC, Slade AK, Grace AA, Sadoul N, Camm AJ, McKenna WJ. The significance of paced electrogram fractionation in hypertrophic cardiomyopathy. A prospective study. Circulation 1995;91:2762-68.
28. Saumarez RC, Slade AKB, McKenna WJ. Arrhythmias in hypertrophic cardiomyopathy. In: Podrid P, Kowey P, editors. Cardiac Arrhythmia: mechanisms, diagnosis and management. Baltimore: Williams and Wilkins, 1995:1095-1109.
29. Bhandari AK, Shapiro WA, Morady F, Shen EN, Mason J, Scheinman MM. Electrophysiologic testing in patients with the long QT syndrome. Circulation 1985;71:63-71.
30. Gardner PI, Ursell PC, Fenoglio JJ, Jr., Wit AL. Electrophysiologic and anatomic basis for fractionated electrograms recorded from healed myocardial infarcts. Circulation 1985;72:596-611.
31. Bethell HWL, Vandenberg JI, Smith GA, Grace AA. Changes in ventricular repolarization during acidosis and low-flow ischemia. Am J Physiol 1998;275:H551-61.
32. Priori SG, Napolitano C, Cantu F, Brown AM, Schwartz PJ. Differential response to Na+ channel blockade, beta-adrenergic stimulation, and rapid pacing in a cellular model mimicking the SCN5A and HERG defects present in the long-QT syndrome. Circ Res 1996;78:1009-15.
33. Hanck DA, Sheets MF. Modification of inactivation in cardiac sodium channels: ionic current studies with Anthopleurin-A toxin. J Gen Physiol 1995;106:601-16.
34. Nuss HB, Marban E. Electrophysiological properties of neonatal mouse cardiac myocytes in primary culture. J Phys Lond 1994;479:265-79.
35. Wang L, Feng Z, Kondo CS, Sheldon RS, Duff HJ. Developmental changes in the delayed rectifier K+ channels in mouse heart. Circ Res 1996;79:79-85.
36. Wang L, Duff HJ. Identification and characteristics of delayed rectifier K+ current in fetal mouse ventricular myocytes. Am-J-Physiol 1996;270:H2088-93.
37. London B, Jeron A, Zhou J, Buckett P, Han X, Mitchell GF, et al. Long QT and ventricular arrhythmias in transgenic mice expressing the N terminus and first transmembrane segment of a voltage-gated potassium channel. Proc Natl Acad Sci USA 1998;95:2926-31.
38. Vetter DE, Mann JR, Wangemann P, Liu J, McLaughlin KJ, Lesage F, et al. Inner ear defects induced by null mutaion of the isK gene. Neuron 1996;17:1251-64.
39. Guerrero PA, Schuessler RB, Davis LM, Beyer EC, Johnson CM, Yamada KA, et al. Slow ventricular conduction in mice heterozygous for a connexin43 null mutation. J Clin Invest 1997;99:1991-98.

17. RECEPTOR TYROSINE KINASE SIGNALING IN VASCULOGENESIS AND ANGIOGENESIS

Thomas I. Koblizek, Werner Risau, and Urban Deutsch

Introduction

The formation of the vascular system is an important process during embryonic development and several pathological situations. Knowledge of the molecular mechanisms may lead to the development of therapies for pathological processes involving both endothelial cell proliferation and new blood vessel formation as well as those characterized by insufficient nutrient and oxygen supply of tissues. An example for abnormal vessel growth are solid tumors, whose unlimited growth is absolutely dependent on the formation of new vessels. The tumor vasculature allows for nutrient supply and the formation of metastases [1]. Of similar negative influence is vessel growth in several non neoplastic conditions like rheumathoid arthritis, diabetic retinopathy and psoriasis [2,3]. In contrast, the growth of new vessels during collateral formation in the ischemic limb or the ischemic heart would be highly desirable [4,5]. The formation of the vascular system starts early in embryonic development with the generation of a primitive vascular plexus in the yolk sac by a process termed vasculogenesis [6]. It describes the fusion of endothelial cell precursors called angioblasts that have differentiated from mesodermal cells. While most organs of endodermal origin like the lung are vascularized by vasculogenesis, tissues of mesodermal and ectodermal origin like the kidney and brain are thought to be vascularized mostly by a different process called angiogenesis [7]. Angiogenesis is the generation of new vessels by budding and sprouting from already formed vessels or by subdivision of larger vessels (also called non-sprouting angiogenesis or intussusception). The newly formed vascular system is then reorganized by complex and poorly understood processes according to the tissue requirements. Tissue oxygen as well as glucose concentration are important regulators as low tissue levels induce the expression of factors that can induce vessel growth. The reorganization includes not only the formation of additional vessels but also the removal of excessive vessels, called pruning. The mediators of vessel regression are not known. Also, there is no direct evidence for programmed cell death (apoptosis) of endothelial cells during embryonic development. This may reflect either the limitations of the methodology applied or the

P.A. Doevendans et al. (eds.), Cardiovascular specific gene expression, 179-91.

rapid disappearance of apoptotic cells [8]. However, at least during certain phases endothelial cells seem to be dependent on survival factors [9].

Both intra- and extraluminal factors are involved in the further maturation of blood vessels, which mature or regress along with the tissue or organ they supply. In the developing vascular beds, the direction of flow can change, with arterioles becoming venules and vice versa. Non-perfused blood vessels regress. Better perfusion of a tissue may lead to hyperoxygenation and thus to vessel regression. Although initially laid down independent of the circulation, the vascular system is than shaped by forces generated by the circulation. Shear stress, for example, strongly affects endothelial cells, inducing modification of cell-cell as well as cell-extracellular matrix junctions and upregulating factors chemotactic for mesenchymal cells [10,11]. Simultaneously, the vascular wall matures: the basal lamina is modified, pericytes and smooth muscle cells differentiate and elastogenesis begins in elastic arteries.

Table 1. Genes important for the development of the cardiovasular system

Gene	Lethal at day	Vascular knock-out phenotype	Ref.
Cytokines (ligands)			
VEGF	E11	impaired vasculogenesis and angiogenesis	[17, 18]
Ang-1	E12	reduced heart trabeculation, remodelling and pericyte recruitment	[39]
Neuregulin	E11	reduced trabeculation of the heart	[51]
TGFβ1	E10.5	variable defects during vasculogenesis	[52]
Receptors			
Flk1	E10	absence of endothelial differentiation and vasculogenesis	[14]
Flt1	E9.5	formation of disorganized vessels during vasculogenesis	[16]
ErbB2/4	<E11	reduced trabeculation of the heart	[53, 54]
Tie-1	E13.5	edema formations and hemorrhages	[28, 29]
Tie-2	E10	reduced heart trabeculation, pericyte recruitment, remodelling, sprouting	[28, 35]
TGFβRII	<E13.5	defective vasculogenesis	[55]
Signalling molecules			
B-Raf	<E13.5	enlarged vessels, endothelial apoptosis	[56]
RasGAP	E10	impaired remodelling (yolk sac), aberrant sprouting (dorsal aorta)	[57]
SOS1	E12	hemorrhaging, and reduced trabeculation in the heart	[58]
Gα13	E10	absence of tube formation (yolk sac); disorganized vessels (head)	[59]
Transcription factors			
TEL	E11	defective angiogenesis in the yolk sac	[46]
LKLF	E13.5	impaired tunica media formation and aneurysms	[47]

Candidate molecules for the regulation of cardiovascular development have been identified in the past years and their in vivo role has been established by targeted gene inactivation in mice (table 1). These include cytokines, their receptors, signaling molecules, transcription factors and extracellular matrix proteins. In this article, we will concentrate on the processes mediated by paracrine signals via protein ligands that bind and modulate the activity of receptor tyrosine kinases (RTKs) expressed almost exclusively on endothelial cells and how endothelial cells integrate the different signals. The model for the key steps in the formation of new vessels is outlined in figure 1. So far, there are two families of tyrosine kinase receptors that are expressed predominantly on endothelial cells: the vascular endothelial growth factor receptors (VEGFR) and the receptor tyrosine kinases with Ig and endothelial growth factor (EGF) homology (Tie, figure 2).

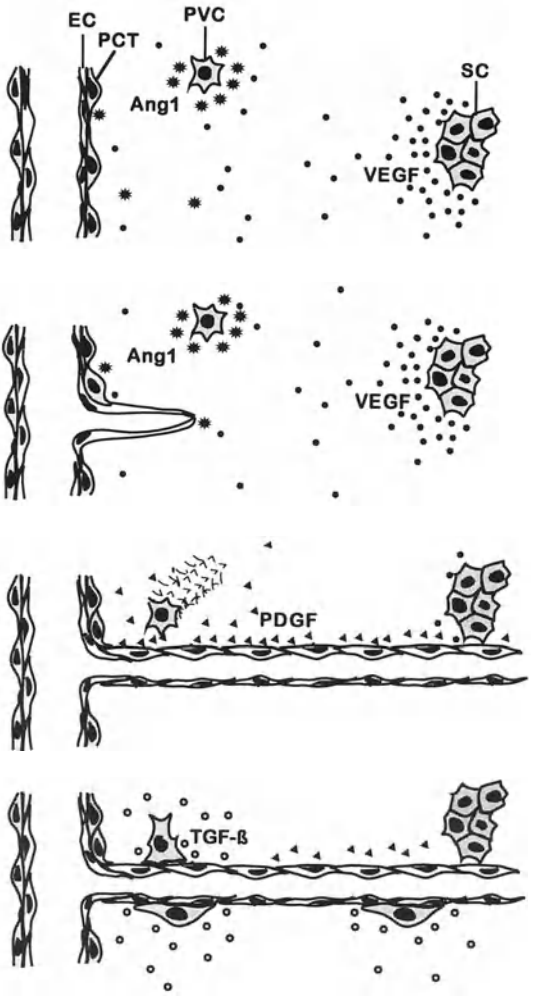

Figure 1. *Schematic drawing of the regulation of new blood vessel formation. Insufficient nutrient and oxygen supply induces VEGF expression (filled circles) in stromal cells (SC). Ang1 (stars) is expressed in perivascular cells (PVC) closer to the existing vessel. Sprouting starts by invasion of endothelial cells (EC) after degradation of the basement membrane. Following a phase of migration and proliferation of endothelial cells a lumen is formed. As soon as blood flow starts in the newly formed capillary, flow forces and shear stress induce expression of PDGF (filled triangles) in the endothelial cells. PDGF recruits perivascular cells to migrate to the capillary. Increased oxygen concentration leads to a decrease of VEGF expression in the neighbouring stromal cells. TGF-β (open circles), activated by the contact between endothelial and perivascular cell, induces perivascular cell differentiation into a vascular smooth muscle cell or pericyte (PCT), extracellular matrix deposition and inhibits endothelial cell proliferation.*

Their crucial importance for vessel growth has been shown not only in transgenic mice, but also during tumor vascularization. By the use of dominant negative VEGFR2 or soluble Tie2-Ig fusion proteins tumor growth could be drastically inhibited, suggesting that VEGFR2 as well as Tie2 receptor signaling is required for tumor angiogenesis [12,13].

Vascular Endothelial Growth Factor (VEGF) and its Receptors

The VEGFs are a family of disulphide-linked dimeric glycoproteins related to platelet-derived growth factor (PDGF). It includes VEGF, also called VEGF-A, placenta growth factor (PlGF), VEGF-B, VEGF-C and VEGF-D. Besides VEGF-A (here referred to as VEGF), only VEGF-B has been reported to be a growth factor for endothelial cells. Numerous studies have shown that VEGF has several properties expected of a candidate regulator of angiogenesis: it is secreted by normal and tumor cell lines; its expression can be strongly induced by hypoxia; it is an endothelial cell specific mitogen; it is angiogenic in in vivo test systems such as the chorioallantoic membrane and the rabbit cornea; it is chemotactic for endothelial cells and monocytes; and it induces in endothelial cells the production of plasminogen activators which are presumably involved in the proteolytic degradation of the extracellular matrix during capillary sprouting.

VEGF receptors are transmembrane receptor tyrosine kinases characterized by an extracellular domain with seven immunoglobulin-like domains and an intracellular split tyrosine kinase domain. Both receptors for VEGF-A, VEGFR1 (also called Flt-1) and VEGFR2 (also called Flk-1/KDR) are coexpressed on endothelial cells, but it is not known whether they interact functionally or form heterodimers like the PDGF receptors. VEGFR1, in addition to its binding to PlGF and VEGF-B, is also a functional receptor for VEGF-A on human monocytes which do not express VEGFR2.

During embryogenesis, VEGF and VEGFR2 are crucial for the differentiation of the lateral mesoderm to form both the endothelial cell precursors (angioblasts) and may be indirectly the hematopoietic cells [14]. In at least the erythroid lineage, VEGFR2 activity appears not to be cell-autonomously required as these cells can develop from VEGFR2 deficient progenitors in chimeric embryos [15]. After differentiation, VEGFR2 is rapidly downregulated in hematopoietic cells but is maintained in endothelial cells. The other receptor for VEGF, VEGFR1, is also necessary for blood vessel formation but at a later time. In VEGF-R1-/- mice, angioblast differentiation occurs normally but the assembly of angioblasts into functional blood vessels is impaired and intraluminal endothelial cells are observed in blood islands and the dorsal aorta [16]. VEGF, the cognate ligand, acts in a paracrine manner as it is produced by the endoderm, while VEGF receptors are expressed by mesoderm-derived angioblasts. A threshold activity of VEGF seems to be necessary for endothelial cell differentiation and blood vessel maturation because mice lacking a single allele of the normal VEGF gene die in utero [17,18]. In these mice, angioblast differentiation is not affected initially, but subsequent blood vessel formation in the yolk sac and in the embryo, e.g. the dorsal aorta, is aberrant. Thus, it is apparent that the VEGF receptors and a

sufficiently high concentration of their cognate ligand are necessary for the first steps in blood vessel development, i.e. vasculogenesis. The results are consistent with the hypothesis that VEGFR2 induction is the first step in angioblast differentiation and that angioblast survival depends on the quantity and activity of the VEGF ligands.

During later stages of development, the localization of VEGF receptors in endothelium and of VEGF mRNA in adjacent tissues indicates that VEGF also stimulates angiogenesis in a paracrine manner. For example, VEGF is expressed transiently in the ventricular zone of the developing mouse brain and appears to form a concentration gradient that stimulates the ingrowth of capillaries from the perineural vascular plexus [19]. Similarly, VEGF produced by astrocytes may guide capillary growth in the developing retina [20].

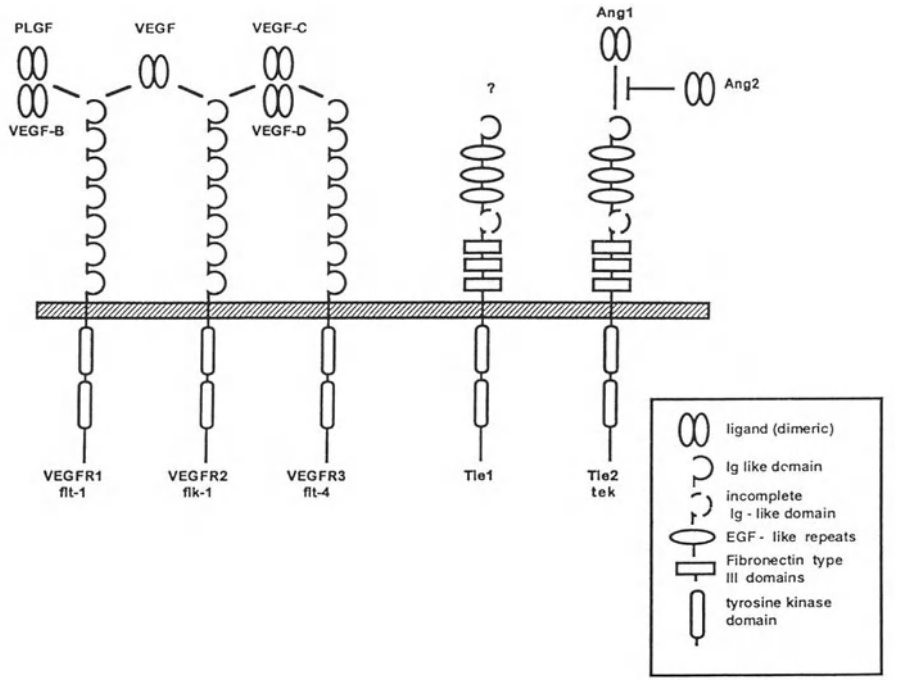

Figure 2. *Receptor tyrosine kinases in endothelial cells. VEGF and the related proteins, placenta growth factor (PlGF), VEGF-B, VEGF-C and VEGF-D are the ligands of the VEGF receptor family members (VEGFR1, VEGFR2, VEGFR3). Ang1 and Ang2 are ligands of the Tie2 receptor. Whereas Ang1 activates the Tie2 receptor, Ang2 inhibits this activation [37, 38]. A ligand for the Tie1 receptor has not been published. VEGF and Tie receptors are transmembrane receptor tyrosine kinases with an extracellular domain (shown at the top), a single transmembrane domain and a split intracellular tyrosine kinase domain (shown at the bottom). VEGFR1 (also known as Flt-1) binds VEGF with higher affinity than VEGFR2 (also known as the mouse Flk-1 or the human KDR receptor). VEGFR1 is also a receptor for PlGF, an angiogenic factor that is expressed abundantly in the placenta and VEGF-B, an endothelial cell mitogen which is expressed during mouse fetal development [48]. VEGFR3 (also known as Flt-4) is activated by VEGF-C, a chemotactic factor for endothelial cells [49] and VEGF-D, an endothelial cell mitogen with structural and functional similarities to VEGF-C [50]. VEGFR-3 is expressed in early vascular development of the mouse, but becomes restricted to the lymphatic endothelium later in development. The promiscuity of receptors and of ligands may result in a complex pattern of receptor-ligand interactions among the various family members, but the specific functions of the new VEGF family members have not been elucidated.*

The specific role of VEGF as an embryonic angiogenesis factor is further supported by experiments in which VEGF is overexpressed in the limb bud of chick embryos, resulting in hypervascularization without alteration of limb morphogenesis [21]. Application of exogenous VEGF also induced hyperfusion of the dorsal aorta [22]. These results underline the critical dose-dependency of VEGF function.

The Tie Receptor Family and the Angiopoietins

Two other RTKs have been found to be expressed predominantly on endothelial cells. With their unique extracellular domain composition, containing Ig-like loops, fibronectin-like domains and EGF-like repeats, Tie1 and Tie2/tek constitute a distinct class of RTKs [23-27]. Generation of mice deficient in Tie1 or Tie2 has demonstrated an essential role for these receptors during mouse embryonic development. Tie1-/- embryos exhibit marked subcutaneous and internal edema formation as well as local hemorrhages and die between E13.5 and birth [28,29]. In these mice, the vascular integrity is impaired such that intercellular junctions appear to be unaffected, as revealed by ultrastructural analysis, while red blood cells can extravasate through "electron-light" endothelial cells. To assess the ability of Tie1-/- EC to contribute to the vasculature, chimaeras were created from wildtype morulae and embryonic stem cells in which lacZ had been inserted into the Tie1 locus thus disrupting the Tie1 allele [30]. Whereas at E10.5 Tie1 deficient EC contributed to all vessels, at E15.5 Tie1-/- cells were underrepresented in angiogenesis-derived vessels such as those in the midbrain and the kidney. These results suggest a different requirement for Tie1 in vascular beds derived by vasculogenesis versus those established by angiogenesis.

Although Tie1 has also been found to be expressed on a subpopulation of hematopoietic stem cells and B cells [31,32] analysis of the hematopoietic stem cells in Tie1 deficient mice has not revealed any distinct defect [33] and the function of Tie1 in these cells remains obscure.

Tie2 is the second member of this family of receptor tyrosine kinases. The expression of both Tie receptors and VEGFR during embryonic development is almost indistinguishable, except for the fact that VEGFR2 is the first to be detected at E7.0, followed by Tie2 expression starting at E7.5 and Tie1 commencing at E8.0 in the extraembryonic mesoderm [34]. In spite of their almost identical embryonic expression pattern, Tie2 deficient mice show a very different vascular phenotype from those of VEGFR2 deficient mice [28,35,36]. The Tie2-/- mice die at E10.5 and show aberrant heart development lacking trabeculae as well as persisting, primitive vessels in the yolk sac and simple dilated vessels in the perineural plexus in contrast to the differentiated vascular system in wildtype mice at the same stage. The latter defect may reflect a function of Tie2 in vascular remodeling. Tie2 is also necessary for sprouting as capillary sprouts in Tie2 deficient mice fail to invade into the neural tube.

Ligands for the Tie2 receptor have been identified and named angiopoietins 1 and 2 (Ang1 and Ang2 [37,38]). While Ang1 activates the Tie2 receptor (i.e., promotes receptor phosphorylation) Ang2 antagonizes this activation. Ang1 deficient mice show the same qualitative defects in heart development and vascular remodeling as the Tie2 deficient mice but survive until E12.5 [39]. The delayed lethality of the Ang1 phenotype suggests either a basal ligand-independent activity of the Tie2 receptor or the

presence of another as yet unidentified ligand. In addition, ultrastructural analysis of capillaries in Ang1 deficient mice revealed a vastly reduced number of pericytes and SMC integrated in the vessel walls that was also observed in Tie2 deficient mice. This suggests a role of Ang1 in the process of vessel maturation, however a direct effect of Ang1 in recruitment of perivascular cells remains to be shown. Although only a weak mitogen for EC, Ang1 induces capillary sprout formation in an in vitro angiogenesis assay [61]. In this assay, Ang1 and VEGF induce sprouting synergistically.
Ang2, the second ligand specifically binding the Tie2 receptor, inhibits Ang1 induced Tie2 receptor autophosphorylation in endothelial cells. Interestingly, Ang2 itself can induce Tie2 activation in transfected non-endothelial cells [38]. The mechanism of this cell-type specific receptor activity is not known. Overexpression of Ang2 in all endothelial cells in transgenic mice using Tie2 transcriptional regulatory elements leads to a phenotype resembling those of Ang1 or Tie2 deficient mice, e.g. heart defects, growth retardation and detachment of the endothelium from the underlying mesenchyme. Interestingly, some aspects of these defects, like widespread vessel discontinuities and loss of normal dentritic patterns seemed more severe suggesting an additional role for Ang2 apart from blockage of Ang1 induced Tie2 activation.

Signaling Downstream of Endothelial Receptor Tyrosine Kinases
In spite of their largely overlapping expression patterns, each of the receptor mutants described exhibit a surprisingly different phenotype, indicating that the different receptors have separate and unique functions during vascular development. Cellular responses like sprouting and tube formation are limited to only a few cell types in vivo and may utilize a cell type-specific molecular signaling machinery. Therefore, it appears likely that these processes can not be assessed in transfected cells expressing just one or a subset of these EC-specific proteins. Nevertheless, several of the more general signaling pathways have been found to be activated by endothelial RTKs. These cell surface molecules exert their biological functions by ligand induced oligomerization and consecutive autophosphorylation. Tyrosine phosphorylation is followed by binding and phosphorylation of intracellular signaling molecules, leading to either modulation of their own enzymatic activity or their ability to bind yet other downstream molecules. One well-studied pathway activated by VEGF is the hydrolysis of phosphatidylinositol 4,5-bisphosphat (PIP2) catalyzed by phospholipase C-γ (PLC-γ) which binds to both VEGFR1 and 2 in response to VEGF stimulation [40,41]. The reaction product diacylglycerol (DAG) activates protein kinase C (PKC). A second essential signaling molecule considered to be activated by VEGFR1 upon ligand stimulation is the phosphatidylinositol-3-kinase (PI3K, [42]). This enzyme has been shown to be essential for various cellular responses like proliferation, motility, cell shape changes and inhibition of apoptosis. One other direct response to PI3K, the elevation of free intracellular Ca^{2+} has also been observed after VEGF stimulation. A third pathway leading to the activation of mitogen activated protein kinase (MAPK) is initiated presumably by binding and activation of the adapter molecules Shc and/or Grb2 to VEGFR2 after VEGF stimulation. Also, phosphorylation of GTPase activating protein (GAP) has been described, but this activation does not seem to be sufficient to initiate VEGF dependent MAPK phosphorylation in transfected NIH3T3 cells like it

is seen in endothelial cells [40]. Activation of the Src family members Fyn and Yes in response to VEGF has also been described [43]. Recently, binding of another adaptor molecule, Nck and two SH2-domain containing protein tyrosine phosphatases (PTPs) SHP1 and SHP2 to VEGFR2 has been reported [44].
The Tie2 receptor has so far only been described to bind Grb2 and SHP2 but not to PI3K or PLC-γ [45]. Whether activation of Tie2 modulates MAPK activity remains to be shown. It is also unclear, if the Tie1 receptor contributes to the celltype-specific effects of Ang2 on endothelial cells vs. transfected cells. Molecules binding to the Tie1 receptor have not been identified yet.

Table 2. Signaling molecules binding to intracellular domains of endothelial receptor tyrosine kinases.

Receptor:	**VEGFR1**	**VEGFR2**	**VEGFR3**	**Tie1**	**Tie2**
Signaling molecules:	PLCγ [40, 41] GAP [40] p85/PI3K [42]	Grb2 [44] Nck [44] PLCγ [41, 44] Shc [44] SHP1 [44] SHP2 [44]	Grb2 [60] Shc [60]	?	Grb2 [45] SHP2 [45]

Potential nuclear targets of endothelial cell signaling
Ultimately, ligand induced tyrosine kinase receptor activation can result in induction or repression of transcription of specific genes, the products of which exert functions required for EC differentiation, proliferation and morphogenesis. Thus, cell type or differentiation-specific transcription factors are the final mediators of RTK signaling. As indicated by the specific vascular phenotypes of knock-out mouse embryos, TEL, an ets-family member and LKLF, a zinc finger transcription factor, are candidate target proteins of Tie receptors [46,47]. Both proteins seem to be required for the maintainance and stabilization of blood vessel, similar to certain aspects of the Tie1 and Tie2 receptor deficiencies. As the expression of Tie1 and Tie2 remains unaltered, it appears possible that these proteins are functionally regulated by Tie receptors.

Concluding remarks

There has been a tremendous increase of research interest and consequently also insight into the mechanisms of the formation of the vascular system. Now that some of the players have been identified, it should be possible to study how these molecules act in concert to create the appropriate signals for the EC to produce the complex and perfectly adapted vascular tree of the adult organism. One major open question in the field is the function of the orphan receptor Tie1. Also, heterodimer formation of both the VEGF receptor family members as well as the Tie receptors has not been demonstrated yet. This would give a possible hint to the EC-specificity of the signaling

of these kinases. Another possible explanation would be signaling molecules specific for EC. Adequate in vitro test systems could help to elucidate the importance of the diverse signaling pathways for the numerous activities necessary to establish, maintain and regulate the many diverse functions of the complex vascular system.

References

1. Folkman J. Tumor angiogenesis. Adv Cancer Res 1985;43:175-203.
2. Adamis AP, Miller JW, Bernal MT, D'Amico DJ, Folkman J, Yeo TK, Yeo KT. Increased vascular endothelial growth factor levels in the vitreous of eyes with proliferative diabetic retinopathy. Am J Ophthalm 1994;118:445-50.
3. Peacock DJ, Banquerigo ML, Brahn E. Angiogenesis inhibition supresses collagen arthritis. J Exp Med 1992;175:1135-38.
4. Colville-Nash PR, Willoughby DA. Growth factors in angiogenesis: current interest and therapeutic potential. Mol Med Today 1997;vol:14-23.
5. Folkman J. Angiogenesis in cancer, vascular, rheumatoid and other disease. Nat Med 1995;1:27-31.
6. Risau W, Flamme I. Vasculogenesis. Annu Rev Cell Dev Biol 1995;11:73-91.
7. Pardanaud L, Yassine F, Dieterlen-Lièvre F. Relationship between vasculogenesis, angiogenesis and hemopoiesis during avian ontogeny. Development 1989;105:473-85.
8. Augustin HG, Braun K, Telemenakis I, Modlich U, Kuhn W. Ovarian angiogenesis - phenotypic characterization of endothelial-cells in a physiological model of blood-vessel growth and regression. Am J Pathol 1995;147:339-51.
9. Alon T, Hemo I, Itin A, Pe'er J, Stone J, Keshet S. Vascular endothelial growth factor acts as a survival factor for newly formed retinal vessels and has implications for rethinopathy of prematurity. Nat Med 1995;1:1024-28.
10. Franke RP, Grafe M, Schnittler H, Seiffge D, Mittermayer C, Drenckhahn D. Induction of human vascular endothelial stress fibres by fluid shear stress. Nature 1984;307:648-49.
11. Resnick N, Gimbrone MA. Hemodynamic forces are complex regulators of endothelial gene expression. FASEB J 1995;9:874-82.
12. Millauer B, Longhi MP, Plate KH, Shawver LH, Risau W, Ullrich A, Strawn LM. Dominant-negative inhibition of Flk-1 suppresses the growth of many tumor types in vivo. Cancer Res 1996;56:1615-20.
13. Lin P, Polverini P, Dewhirst M, Shan S, Rao PS, Peters K. Inhibition of tumor angiogenesis using a soluble receptor establishes a role for Tie2 in pathologic vascular growth. J Clin Invest 1997;100:2072-78.
14. Shalaby F, Rossant J, Yamaguchi TP, Gertsenstein M, Wu XF, Breitman ML, Schuh AC. Failure of blood-island formation and vasculogenesis in Flk-1-deficient mice. Nature 1995;376:62-66.
15. Shalaby F, Ho J, Stanford WL, Fischer KD, Schuh AC, Schwartz L, Bernstein A, Rossant J. A requirement for Flk1 in primitive and definitive hematopoiesis and vasculogenesis. Cell 1997;89:981-90.
16. Fong GH, Rossant J, Gertsenstein M, Breitman ML. Role of the Flt-1 receptor tyrosine kinase in regulating the assembly of vascular endothelium. Nature 1995;376:66-70.
17. Carmeliet P, Ferreira V, Breier G, Pollefeyt S, Kieckens L, Gertsenstein M, Fahrig M, Vandenhoeck A, Harpal K, Eberhardt C, Declercq C, Pawling J, Moons L, Collen D, Risau W, Nagy A. Abnormal blood vessel development and lethality in embryos lacking a single VEGF allele. Nature 1996;380:435-39.
18. Ferrara N, Carver-Moore K, Chen H, Dowd M, Lu L, O'Shea K, Powell-Braxton L, Hillan KJ, Moore MW. Heterozygous embryonic lethality induced by targeted inactivation of the VEGF gene. Nature 1996;380:439-42.
19. Breier G, Clauss M, Risau W. Coordinate expression of vascular endothelial growth factor receptor-1 (flt-1) and its ligand suggests a paracrine regulation of murine vascular development. Dev Dynamics 1995;204:228-39.
20. Stone J, Itin A, Alon T, Pe'er J, Gnessin H, Chang-Ling T, Keshet E. Development of retinal vasculature is mediated by hypoxia-induced vascular endothelial growth factor (VEGF)

expression by neuroglia. J Neurosci 1995;15:4738-47.
21. Flamme I, von Reutern M, Drexler HCA. Overexpression of vascular endothelial growth factor in the avian embryo induces hypervascularization and increased vascular permeability without alterations of embryonic pattern formation. Dev Biol 1995;171:399-414.
22. Drake CJ, Little CD. Exogenous vascular endothelial growth factor induces malformed and hyperfused vessels during embryonic neovascularization. Proc Natl Acad Sci USA 1995;92:7657-61.
23. Dumont DJ, Yamaguchi TP, Conlon RA, Rossant J, Breitman ML. Tek, a novel tyrosine kinase gene located on mouse chromosome 4, is expressed in endothelial cells and their presumptive precursors. Oncogene 1992;7:1471-80.
24. Runting AS, Stacker SA, Wilks AF. Tie2, a putative protein tyrosine kinase from a new class of cell surface receptor. Growth Factors 1993;9:99-105.
25. Schnürch H, Risau W. Expression of tie-2, a member of a novel family of receptor tyrosine kinases, in the endothelial cell lineage. Development 1993;119:957-68.
26. Sato TN, Qin Y, Kozak CA, Audus KL. Tie-1 and tie-2 define another class of putative receptor tyrosine kinase genes expressed in early embryonic vascular system. Proc Natl Acad Sci USA 1993;90:9355-58.
27. Ziegler SF, Bird TA, Schneringer JA, Schooley KA, Baum PR. Molecular cloning and characterization of a novel receptor protein tyrosine kinase from human placenta. Oncogene 1993;8:663-70.
28. Sato TN, Tozawa Y, Deutsch U, Wolburg-Buchholz K, Fujiwara Y, Gendron-Maguire M, Gridley T, Wolburg H, Risau W, Qin Y. Distinct roles of the receptor tyrosine kinases Tie-1 and Tie-2 in blood vessel formation. Nature 1995;376:70-74.
29. Puri MC, Rossant J, Alitalo K, Bernstein A, Partanen J. The receptor tyrosine kinase TIE is required for integrity and survival of vascular endothelial cells. EMBO J 1995;14:5884-91.
30. Partanen J, Puri MC, Schwartz L, Fischer KD, Bernstein A, Rossant J. Cell autonomous functions of the receptor tyrosine kinase TIE in a late phase of angiogenic capillary growth and endothelial cell survival during murine development. Development 1996;122:3013-21.
31. Hashiyama M, Iwama A, Ohshiro K, Kurozumi K, Yasunaga K, Shimizu Y, Masuho Y, Matsuda I, Yamaguchi N, Suda T. Predominant expression of a receptor tyrosine kinase, TIE, in hematopoietic stem cells and B cells. Blood 1996; 87:93-101.
32. Batard P, Sansilvestri P, Scheinecker C, Knapp W, Debili N, Vainchenker W, Buhring HJ, Monier MN, Kukk E, Partanen J, Matikainen MT, Alitalo R, Hatzfeld J, Alitalo K. The Tie receptor tyrosine kinase is expressed by human hematopoietic progenitor cells and by a subset of megakaryocytic cells. Blood 1996;87:2212-20.
33. Rodewald HR, Sato TN. Tie1, a receptor tyrosine kinase essential for vascular endothelial cell integrity, is not critical for the development of hematopoietic cells. Oncogene 1996;12:397-404.
34. Dumont DJ, Fong GH, Puri MC, Gradwohl G, Alitalo K, Breitman ML. Vascularization of the mouse embryo - a study of flk-1, tek, tie, and vascular endothelial growth factor expression during development. Dev Dynam 1995;203:80-92.
35. Dumont DJ, Gradwohl G, Fong GH, Puri MC, Gertsenstein M, Auerbach A, Breitman ML. Dominant-negative and targeted null mutations in the endothelial receptor tyrosine kinase, tek, reveal a critical role in vasculogenesis of the embryo. Genes Develop 1994;8:1897-909.
36. Saccani G, Gherardi S, Trifiro A, Bordini CS, Calza M, Freddi C. Use of ion chromatography for the measurement of organic acids in fruit juices. Journal of Chromatography 1995;706:395-403.
37. Davis S, Aldrich TH, Jones PF, Acheson A, Compton DL, Jain V, Ryan TE, Bruno J, Radziejewski J, Maisonpierre PC, Yancopoulos GD. Isolation of angiopoietin-1, a ligand for the TIE2 receptor, by secretion-trap expression cloning. Cell 1996;87:1161-69.
38. Maisonpierre PC, Suri C, Jones PF, Bartunkova S, Wiegand SJ, Radziejewski C, Compton

D, McClain J, Aldrich TH, Papadopoulos N, Daly TJ, Davis S, Sato TN, Yancopoulos GD. Angiopoietin-2, a natural antagonist for Tie2 that disrupts in vivo angiogenesis. Science 1997;277:55-60.

39. Suri C, Jones PF, Patan S, Bartunkova S, Maisonpierre PC, Davis S, Sato TN, Yancopoulos GD. Requisite role of angiopoietin-1, a ligand for the TIE2 receptor, during embryonic angiogenesis. Cell 1996;87:1171-80.
40. Seetharam L, Gotoh N, Maru Y, Neufeld G, Yamaguchi S, Shibuya M. A unique signal transduction from FLT tyrosine kinase, a receptor for vascular endothelial growth factor VEGF. Oncogene 1995;10:135-47.
41. Cunningham SA, Arrate MP, Brock TA, Waxham MN. Interactions of Flt-1 and KDR with phospholipase C gamma - identification of the phosphotyrosine binding sites. Bioch Bioph Res Comm 1997;240:635-39.
42. Cunningham SA, Waxham MN, Arrate PM, Brock TA. Interaction of the Flt-1 tyrosine kinase receptor with the p85 subunit of phosphatidylinositol 3-kinase. Mapping of a novel site involved in binding. J Biol Chem 1995;270:20254-57.
43. Waltenberger J, Claesson Welsh L, Siegbahn A, Shibuya M, Heldin CH. Different signal transduction properties of KDR and Flt1, two receptors for vascular endothelial growth factor. J Biol Chem 1994;269:26988-95.
44. Kroll J, Waltenberger J. The vascular endothelial growth factor receptor KDR activates multiple signal transduction pathways in porcine aortic endothelial cells. J Biol Chem 1997;272:32521-27.
45. Huang L, Turck CW, Rao P, Peters KG. GRB2 and SH-PTP2: potentially important endothelial signaling molecules downstream of the TEK/TIE2 receptor tyrosine kinase. Oncogene 1995;11:2097-103.
46. Wang LC, Kuo F, Fujiwara Y, Gilliland DG, Golub TR, Orkin SH. Yolk sac angiogenic defect and intra-embryonic apoptosis in mice lacking the Ets-related factor TEL. EMBO J 1997;16:4374-83.
47. Kuo CT, Veselits ML, Barton KP, Lu MM, Clendenin C, Leiden JM. The LKLF transcription factor is required for normal tunica media formation and blood vessel stabilization during murine embryogenesis. Gene Dev 1997;11:2996-3006.
48. Olofsson B, Pajusola K, Kaipainen A, von Euler G, Joukov V, Saksela O, Orpana A, Pettersson RF, Alitalo K, Eriksson U. Vascular endothelial growth factor B, a novel growth factor for endothelial cells. Proc Natl Acad Sci USA 1996;93:2576-81.
49. Joukov V, Pajusola K, Kaipainen A, Chilov D, Lahtinen I, Kukk E, Saksela O, Kalkkinen N, Alitalo K. A novel vascular endothelial growth factor, VEGF-C, is a ligand for the Flt4 (VEGFR-3) and KDR (VEGFR-2) receptor tyrosine kinases. EMBO J 1996;15:290-98.
50. Achen MG, Jeltsch M, Kukk E, MõkinenE, Vitali A, Wilks AF, Alitalo K, Stacker SA. Vascular endothelial growth factor D (VEGF-D) is a ligand for the tyrosine kinases VEGF receptor 2 (Flk1) and VEGF receptor 3 (Flt4). Proc Natl Acad Sci USA 1998;95:548-53.
51. Meyer D, Birchmeier C. Multiple essential functions of neuregulin in development. Nature 1995;378:386-90.
52. Dickson MC, Martin JS, Cousins FM, Kulkarni AB, Karlsson S, Akhurst RJ. Defective hematopoiesis and vasculogenesis in transforming growth factor-β1 knock-out mice. Development 1995;121:1845-54.
53. Gassmann M, Casagranda F, Orioli D, Simon H, Lai C, Klein R, Lemke G. Aberrant neural and cardiac development in mice lacking the ErbB4 neuregulin receptor. Nature 1995;378:390-94.
54. Lee KF, Simon H, Chen H, Bates B, Hung MC, Hauser C. Requirement for neuregulin receptor erbB2 in neural and cardiac development. Nature 1995;378:394-98.
55. Oshima M, Oshima H, Taketo MM. TGF-α receptor type II deficiency results in defective yolk sac hematopoiesis and vasculogenesis. Dev Biol 1996;179:297-302.

56. Wojnowski L, Zimmer AM, Beck TW, Hahn H, Bernal R, Rapp UR, Zimmer A. Endothelial apoptosis in Braf-deficient mice. Nat Genet 1997;16:293-97.
57. Henkemeyer M, Rossi DJ, Holmyard DP, Puri MC, Mbamalu G, Harpal K, Shih TS, Jacks T, Pawson T. Vascular system defects and neuronal apoptosis in mice lacking ras GTPase-activating protein. Nature 1995;377:695-701.
58. Wang DZ, Hammond VE, Abud HE, Bertoncello I, McAvoy JW, Bowtell DD. Mutation in Sos1 dominantly enhances a weak allele of the EGFR, demonstrating a requirement for Sos1 in EGFR signaling and development. Genes Dev 1997;11:309-20.
59. Offermanns S, Mancino V, Revel JP, Simon MI. Vascular system defects and impaired cell chemokinesis as a result of G [alpha]13 deficiency. Science 1997;275:533-36.
60. Fournier E, Dubreuil P, Birnbaum D, Borg JP. Mutation at tyrosine residue 1337 abrogates ligand-dependent transforming capacity of the FLT4 receptor. Oncogene 1995;11:921-31.
61. Koblizek TI, Weiss C, Yancopoulos GD, Deutsch U, Risau W. Angiopoietin-1 induces sprouting angiogenesis *in vitro.* Curr Biol 1998;23:529-32.

18. MOLECULAR ANALYSIS OF VASCULAR DEVELOPMENT AND DISORDERS

Peter Carmeliet, and Désiré Collen

Introduction

Blood vessels are among the first organs to develop during embryogenesis and are essential for organogenesis and nutrition of the embryo. Although formation of blood vessels most actively occurs during embryonic development, tissue vascularization proceeds after birth in the retina, in the heart, and, cyclically, in the reproductive organs. In addition, abnormal vessel growth importantly contributes to the pathogenesis of several disorders with high morbidity and mortalitiy. Excessive vessel growth has been implicated in the pathogenesis of retinopathies, cancer and inflammation. In contrast, insufficient vessel growth may lead to tissue ischemia and failure. Although formation of new blood vessels has typically been associated with endothelial cells, the periendothelial mural pericytes (smaller vessels) or smooth muscle cells (larger vessels) are equally important for normal and pathological vessel formation. Recent studies have highlighted the importance of endothelial <--> periendothelial cell crosstalk during normal and pathological blood vessel formation. Accordingly, integrated research into the molecular mechanisms that regulate the development and function of both endothelial and pericyte/smooth muscle cells has become a major focus in vascular biology. A number of candidate molecules (growth factors, matrix component, adhesion molecules, and proteinases) has been identified that stimulate or inhibit these processes. Recently, remarkable progress in their molecular analysis has been achieved through targeted manipulation of the mouse genome. The role of some of these molecules will be discussed in this chapter.

Assembly of endothelial cells in embryonic blood vessels

Distinct cellular processes mediate blood vessel formation during embryogenesis [1-5]. Initially, mesodermal cells differentiate in situ into early hemangioblasts and form cellular aggregates (blood islands), in which the inner cell population develops into hematopoietic precursors and the outer cell population gives rise to the primitive

P.A. Doevendans et al. (eds.), Cardiovascular specific gene expression, 193-225.

endothelial cells. In vitro findings suggest that basic fibroblast growth factor (bFGF or FGF2) may participate in angioblast differentiation via induction of a cellular receptor for vascular endothelial growth factor (VEGF-A) [6].

The second stage involves "vasculogenesis", during which endothelial cells fuse and form a primordial vascular network. The larger vessels of the embryo and the primary vascular plexus in the lung, the pancreas, the spleen, the heart and the yolk sac arise by this process [1]. Lumen formation of the primitive capillaries, an essential aspect of vasculogenesis, may result from endothelial vacuolization (intracellular lumen formation), or from a continuation of a preexisting lumen through joining of distal endothelial cells (intercellular lumen formation). Gene inactivation studies in mice indicate that these processes are controlled by VEGF-A [7,8], fibronectin [9], the α_5-integrin receptor [10], VE-cadherin [11], transforming growth factor (TGF)-β1 [12], and possibly FGF2 (see below). Whereas the VEGF-A receptor FLK1 may be involved in positive regulation [13], another VEGF-A receptor FLT1 may antagonistically inhibit this process [14]. In addition, immunoneutralization studies in the avian embryo indicate that the $\alpha_v\beta_3$ integrin is involved in endothelial spreading and in the formation of endothelial protrusions, required for lumen formation and vessel patterning [15].

During the third phase, a primitive vascular plexus develops into a complex organized and interconnecting network. One mechanism involves intussusceptive microvascular growth, whereby a preexisting vessel is split into two daughter vessels by formation of transcapillary pillars and by invagination by surrounding pericytes and extracellular matrix [16-18]. This process, whereby sinusoidal capillaries generate loops that remain constantly perfused, seems to be of special importance in the lung, but is probably more widespread than originally considered. It is also the predominant mechanism for VEGF-induced vascular growth in the chicken allantoic membrane [16,19]. Although its molecular mechanisms remain largely unknown, VEGF-A [7,8], the angiopoietins (ANG), and the TIE receptors [20-24], and several extracellular matrix components [9] may be implicated. A second mechanism of network expansion involves sprouting of new blood vessels from a preexisting blood vessel ("angiogenesis"), such as occurs in the brain, the kidney and the intersomitic vessels. In order for endothelial (or pericyte) cells to emigrate from their preexisting site, they first need to proteolytically degrade the surrounding basement membrane (plasminogen activators and matrix metalloproteinases [25]), to loosen their interendothelial cell contacts (VE-cadherin [11]), and to relieve the periendothelial cell support (ANG2 [23]). The endothelial cells need to proliferate, to change their shape, to protrude extensions and to migrate towards the angiogenic stimulus (VEGF-A [7,8]; the $\alpha_v\beta_3$ integrin [15]) (initiation step). Subsequently, the endothelial cells are assembled in cords which form a lumen (VEGF-A [7,8]; the $\alpha_v\beta_3$integrin [15]), and fuse with other vessels (fibronectin [9]; VCAM-1 [26,27]; α_4 integrin [28]). As the endothelial tubes mature, they become surrounded by periendothelial mural cells (ANG1 and TIE2 [22]; tissue factor [29]; PDGF-B [30,31]; TGF-β [112]) (maintenance and termination steps). Somewhat surprisingly, certain extracellular matrix components (vitronectin [32]) and proteinases [25] did not affect this process. This may suggest that several mechanisms of embryonic vascular development are redundant or that they are compensated. It is conceivable that angiogenesis inhibitors are involved in the termination of sprouting, but insights in their

biological role awaits future study.

A third mechanism involves the intercalated growth of blood vessels ("non-sprouting angiogenesis"), whereby preexisting capillaries merge, or additional endothelial cells fuse into existing vessels to increase their diameter and length. This process is important for vessel growth in the heart, and during healing of endothelial wounds [16,19], but its molecular mechanisms remain enigmatic.

Hypoxia and metabolic stress are somehow important for these early steps of embryonic vascularization, as evidenced by the vascular defects in embryos lacking the arylhydrocarbon-receptor nuclear translocator (ARNT) [33,34], the hypoxia-inducible factor (HIF)-1 (unpublished observations), or the von Hippel-Lindau (VHL) gene product [35]. Although distinct tissues have been proposed to be vascularized by either vasculogenic or angiogenic processes, more recent evidence challenges such a dogmatic classification, as primary angioblasts with resultant vasculogenesis have also been observed in the neural tube, the kidney and the somites [1, 36].

After the onset of circulation (e.g. during the organogenetic period; fourth phase), this emerging vascular plexus becomes remodeled and pruned into a tree of veins, capillaries and arteries, the expansion of which is matching the metabolic demands of the growing embryo. It involves fusion and regression of blood vessels, changes in lumen diameter and vessel wall thickness, and the deposition of specialized extracellular matrix components (elastin, fibrillins) which provide the vessel novel properties (viscoelasticity). Metabolic, hydrodynamic, hypoxic or rheologic factors, and the interaction between endothelial and mural cells may determine these processes. Vessel regression may result from endothelial cell emigration, transdifferentiation or death [1]. Both the loss of endothelial survival signals [37,38], and the production of death factors could mediate the latter process.

Another characteristic of this phase of blood vessel development is that endothelial cells acquire particular heterogeneity due to specialized differentiation, which appears to be dependent on interactions with local parenchymal cells [1,39]. For example, astrocytes appear responsible for the induction of the blood-brain-barrier, whereas choroidal epithelial cells induce the formation of fenestrated capillaries. Although the molecular mechanisms of such organ-specific differentiations remain largely unknown, the different VEGF-A splice forms have been suggested to be involved in the formation and the maintenance of a fenestrated endothelium [1,39].

The vascular endothelial growth factor family

Vascular endothelial growth factor

VEGF-A, unlike other known angiogenic factors, has a unique combination of properties: (i) it is produced by cells in close vicinity of endothelial cells, suggesting paracrine regulation of blood vessel formation [40,41]; (ii) it is secreted and exerts a direct and largely restricted effect on endothelial cells via interaction with cellular receptors FLK1 (VEGF receptor-2) and FLT1 (VEGF-receptor-1) [42]; (iii) it induces a pleiotropic response allowing endothelial cells to proliferate, to migrate, to assemble into tubes, to survive, and is one of the most potent permeability factors [43,44]; (iv) its expression is highly regulated by hypoxia, providing a physiological feedback

mechanism to accomodate insufficient tissue oxygenation by promoting blood vessel formation [45]; and (v) it is a potent growth factor since its over- or under-expression significantly affects blood vessel formation *in vivo* [7,8,46]. The pattern of expression of the VEGF-ligands and their receptors during embryogenesis suggests a role for these molecules in vascular development. VEGF-A is produced by cells in close vicinity to the developing endothelial cells [40]. The VEGF receptors FLT1 and FLK1 (see below) have distinct but overlapping temporo-spatial expression patterns during embryogenesis [41,47]. In contrast to the minimal levels of VEGF-A gene expression in most adult tissues, VEGF-A expression is detectable in the adult kidney, possibly implicating a role in the maintenance of endothelial cell homeostasis and/or in their fenestration [43,44].

Targeted inactivation of a single VEGF-A allele resulted in haploinsufficiency with embryonic lethality due to abnormal blood vessel development around 9.0-10.0 days of gestation [7,8,48]. The dorsal aorta had a much smaller lumen. In addition, sprouting of the vessels was reduced, and connections of the large blood vessels with the heart (in the outflow region) appeared abnormal. In the yolk sac, large vitello-embryonic blood vessels were absent, and only an irregular plexus of enlarged capillaries was present. Significant vascular defects were also present in the placenta, but hematopoiesis appeared normal [8]. Blood vessel development was more affected in homozygous VEGF-A deficient embryos, generated by aggregation of homozygous VEGF-A deficient embryonic stem cells with tetraploid embryos, than in heterozygous VEGF-A deficient embryos. These data suggest a tight gene dosage-dependent relationship and production of only minimally required VEGF-A levels during embryonic development. Indeed, at 8.5 days post coitum, there were only some scattered endothelial cells within the homozygous VEGF-A deficient embryo that failed to organize into a pair of dorsal aortas. Taken together, VEGF-A is not essential for initiating the differentiation of angioblasts to early endothelial cells, but affects further blood vessel formation at different levels. Treshold levels of VEGF-A appear to be required for the continued differentiation or, possibly, the survival of endothelial cells, and for their fusion into a vessel around a large lumen. In addition, VEGF-A affects sprouting (and probably also other forms of) angiogenesis, and controls remodeling of emerging vessels into an interconnected network (as for example evidenced by the abnormal yolk sac vasculature in heterozygous VEGF-A deficient embryos).

Hypoxia is an important regulator of angiogenesis and of the expression of VEGF-A [45]. Hypoxic regulation of VEGF-A gene expression is mediated by hypoxia-inducible factors (HIFs). To date, HIF-1α, HIF2α (also named EPAS-1, HRF or HLF [49-51]), and HIF-1β (or ARNT) [49, 52] have been identified, which bind an enhancer HIF-response element in the promoter region of VEGF-A. In addition, hypoxia stabilizes the VEGF-A mRNA through interaction of RNA binding proteins with sequences in the 3' untranslated region [45]. The VHL gene product has been implicated in the latter process [53]. We and others have embarked on targetedly inactivating these hypoxia-inducible factors that regulate VEGF-A gene expression. Embryos deficient in the ARNT die around 10.5 days of gestation due to defective vascular development, similar to that in VEGF-A deficient embryos [33]. However, different from the latter, vascular defects were observed in the yolk sac and in some, but not in all regions within

the embryo proper. Somatic ARNT deficient cells also had an impaired hypoxic induction of gene expression and failed to develop higly vascularized tumors in vivo [54]. In another ARNT inactivation study, ARNT deficient embryos died around 10 days of gestation due to placental hemorrhaging, delayed and abnormal neurogenesis and visceral arch development [34]. Despite seemingly normal chorio-allantoic fusion, the chorionic capillary plexus was underdeveloped. The yolk sac vasculature appeared, however, normal. Deficiency of the VHL gene resulted in embryonic lethality around 10.5 to 12.5 days of gestation due to abnormal vascularization in the placenta [35]. Both mutant embryo and placenta developed normally until 9.5 days of gestation. At the time of chorioallantoic fusion and expansive growth of the placental labyrinth, VHL deficient embryos lacked embryonic blood vessels in the placental labyrinth, but presumably, the embryo proper appeared normal. The trophoblasts failed to develop into syncytiotrophoblasts, and by 11.5 to 12.5 days, the placental labyrinth showed great disruption, loss of normal structure, necrosis and hemorrhage. In addition, the yolk sac in some embryos appeared atrophic and had reduced numbers of blood islands. An intriguing question is whether VEGF-A mRNA expression in VHL deficient embryos is affected. Analysis of embryonic stem cells lacking HIF-1 reveals that hypoxic or hypoglycemic induction of several target genes (VEGF-A, phosphoglycerokinase, lactate dehydrogenase) is significantly reduced to absent when cells were cultured as embryoid bodies or monolayers in vitro [55]. In addition, HIF-1 deficient teratocarcinoma's were significantly more avascular when grown in nude mice in vivo. Taken together, these data imply important roles for hypoxia-inducible mechanisms in control of angiogenic factors and blood vessel formation in vivo.

VEGF-homologues

More recently, other VEGF-related factors with a conserved pattern of 8 cysteine residues have been identified. Homo- or heterodimerization of these ligands may determine their biological specificity [56-58]. Placental growth factor (PlGF) is expressed in the placenta and, to a lesser extent, in the heart, the lung and the thyroid gland [59]. Although the role of PlGF homodimers on endothelial cell proliferation is controversial, it may, via interaction with VEGF-A, modulate the mitogenic, chemotactic and vascular permeability-inducing properties of the latter [56-58,60-62]. Deficiency of PlGF in transgenic mice did not compromize development, feritility or placentation (G. Persico et al., personal communication). This was not anticipated in view of the presumed role of PlGF in establishing vascular connections in the placenta. However, initial analysis suggests that healing of skin wounds, formation of granulation tissue, and vascular permeability after topical VEGF-A application are abnormal.

VEGF-B has similar endothelial mitogenic potency as VEGF-A, and is primarily expressed in the heart, the skeletal muscle, the brain and the kidney [63]. VEGF-A and VEGF-B are co-expressed in many tissues and are able to heterodimerize with each other. VEGF-B remains largely cell-associated, possibly providing spatial cues to outgrowing endothelial cells, or acting as a releasable pool to induce endothelial cell regeneration after injury. Recent data suggest that VEGF-B deficient mice develop normally and are healthy (U. Ericksson et al., personal communication).

VEGF-C (also called VEGF-related protein: VRP; or VEGF-2) stimulates migration

and proliferation of endothelial cells, although with a lower potency than VEGF-A [64-67]. At high doses, VEGF-C is able to interact with the VEGF receptor-2 or FLK1 [64,67]. In the adult, it is most abundantly expressed in the heart, the placenta, the lung, the kidney, the muscle, the ovary and the small intestine. During embryonic development, VEGF-C and FLT4 may initially be involved in the development of the venous system, whereas at later periods, they colocalize in the perinephric, mesenterial and jugular regions where the first lymphatic vessels sprout from venous sac-like structures. Mice overexpressing VEGF-C in the skin specifically develop hyperplasia of lymphatic vessels [68]. Since VEGF-C binds to both FLK1 and FLT4, the specific effect of VEGF-C on lymphatic and not on endothelial cell function may relate to a requirement for heterodimerization of both receptors.
FIGF (also called VEGF-D) is a VEGF homologue [69]. *In vivo*, VEGF-D is expressed abundantly in the lung, the heart, the small intestine, and the fetal lung. It was also expressed at lower levels in skeletal muscle, in the colon and the pancreas [70]. Although the structural similarities between VEGF-C and VEGF-D suggest similar functions, their expression patterns differ [70]. VEGF-D is able to induce proliferation and morphological transformation of fibroblasts [69], but its possible effects on endothelial cells, and its regulation by hypoxia remain unknown to date.

VEGF receptors
Three receptor tyrosine kinases with seven immunoglobulin domains, that bind the VEGF family members with different specifity and affinity, have thus far been identified [42]: the VEGF receptor-1 (VEGFR-1or FLT1) binds VEGF-A and PlGF [58,60], the VEGF receptor-2 (VEGFR-2 or FLK1) binds VEGF-A and VEGF-C (possibly with a lower affinity, although controversial) [64,71], and the VEGF receptor-3 (VEGFR-3 or FLT4) binds VEGF-C [64,72]. In addition, low-affinity surface-associated receptors that selectively bind VEGF-A165 via the exon 7-encoded domain have been identified in certain tumor cells [73]. A receptor for VEGF-D has not been characterized yet, but because of its structural similarities to VEGF-C, FLT4 may be a candidate. Deficiency of the VEGF receptor FLK1 resulted in embryonic lethality around day 10 of gestation due to abnormal vascular development [13]. Histological examination revealed complete absence of organized blood vessels and necrosis in the mutant embryo proper. More recent analysis of chimeric wild type <-> homozygous FLK1 null mutant mice indicated that endothelial cells were always wild type, demonstrating a cell-autonomous requirement for FLK1 in endothelial cell differentiation [74]. Targeting of the FLT1 gene also resulted in embryonic lethality around 10 days of gestation [14]. Staining for LacZ (expressed by the targeted FLT1 promoter) revealed the presence of numerous differentiated endothelial cells, which, however, failed to form an organized vascular network. These vascular structures were abnormally large and fused, and contained enclosed LacZ positive endothelial cells. These findings suggest a possible role of FLT1 in contact inhibition of endothelial cell growth, or in endothelial cell assembly via controlling adhesion between endothelial cell precursors.

Role of extracellular matrix proteinases in endothelial biology

Movement of endothelial cells involves proteolysis of the extracellular matrix. Two families of matrix degrading proteinases, the plasminogen activator (PA) and the matrix metalloproteinase (MMP) system, can, in concert, degrade most extracellular matrix proteins. The plasminogen system is composed of an inactive proenzyme plasminogen that can be converted to plasmin by either of two plasminogen activators (PA), tissue-type PA (t-PA) or urokinase-type PA (u-PA) [75]. This system is controlled at the level of plasminogen activators by plasminogen activator inhibitors (PAIs), of which PAI-1 is believed to be physiologically the most important [76], and at the level of plasmin by alpha2-antiplasmin [75]. Due to its fibrin-specificity, t-PA is primarily involved in clot dissolution [75]. u-PA binds a cellular receptor (u-PAR), and has been implicated in pericellular proteolysis during cell migration and tissue remodelling during angiogenesis, atherosclerosis and restenosis [77]. Plasmin is able to degrade fibrin and extracellular matrix proteins directly or, indirectly, via activation of other proteinases (such as the metalloproteinases) [78-80]. Plasmin can also activate or liberate growth factors from the extracellular matrix including latent TGB-β1, FGF2, IGF-1 and VEGF-A [43,78,81].

Matrix metalloproteinases (MMPs) constitute a family of proteinases able to degrade most extracellular matrix components in the vessel wall [82-84]. In the mouse, MMP-13 (collagenase 3) is the primary interstitial collagenase, whereas MMP-2 (gelatinase A) and MMP-9 (gelatinase B) degrade collagen type IV, V, VII and X, elastin and denatured collagens. The stromelysins-1 and -2 (MMP-3 and MMP-10) and matrilysin (MMP-7) break down the proteoglycan core proteins, laminin, fibronectin, elastin, gelatin and non-helical collagens, while the macrophage metalloelastase (MMP-12) primarily degrades insoluble elastin in addition to collagen IV, fibronectin, laminin, entactin and proteoglycans. The membrane-type metalloproteinases (MT1-MMP and MT2-MMP) activate gelatinase-A. Control of MMP activity is mediated by tissue inhibitors of MMPs (TIMPs) in a tissue- and substrate-specific manner. Since MMPs are secreted as zymogens, they require extracellular activation. u-PA-generated plasmin is a likely pathological activator of several zymogen MMPs [80].

Quiescent endothelial cells constitutively express t-PA, MMP-2 and minimal MMP-1 [75,84]. Net proteolysis is, however, prevented by coincident expression of PAI-1, TIMP-1 and TIMP-2 [76,85]. In contrast, when endothelial cells migrate, they significantly upregulate u-PA, u-PAR, and, to a lesser extent, t-PA at the leading edge of migration [84,86-88]. Although PAI-1 is also increased, its expression at different locations and times allows a net increase in fibrinolytic activity [89,90]. A variety of cytokines and growth factors with angiogenic activity modulate the expression of these proteinases. VEGF-A and FGF2 (synergistically) induce expression of u-PA, t-PA and u-PAR [78,91,92], whereas TNF- and interleukin-1 upregulate expression of MMP-1, MMP-3 and MMP-9. TGF-β1 downregulates u-PA, and induces PAI-1, constituting thereby a negative feedback for FGF2 and VEGF-A [78].

Although immunoneutralization or chemical inhibition of PAs and MMPs reduce endothelial cell migration *in vitro* [84], surprisingly, mice deficient in u-PA and/or t-PA [88], PAI-1 [89,93,94], u-PAR [95,96], Plg [97,98] or alpha$_2$-antiplasmin (unpublished

observations) develop normally without overt vascular anomalies. This is also true for mice deficient in MMP-3, MMP-7, MMP-9, MMP-11, MMP-12 or TIMP-1. In the adult, reendothelialization alongside denuded vessels was not different in mice deficient in t-PA, u-PA, u-PAR, PAI-1 and Plg [80,89,96,97]. In contrast, hemangioblastoma formation after Polyoma middle-T retroviral infection was dependent on generation of u-PA-mediated plasmin [99]. These data suggest that migration of endothelial cells alongside a denuded vessel does not require u-PA-generated plasmin, whereas invasion of endothelial cells through an anatomic barrier of extracellular matrix requires plasmin proteolysis.

Developmental regulation of smooth muscle cell assemby

Developmental regulation of smooth muscle cell assembly. In contrast to the vast literature on endothelial cell function during blood vessel formation, relatively little is known about the role of the periendothelial cells during this process [100]. Nevertheless, endothelial tubes are encapsulated by mural cells, e.g. pericytes in the microvasculature, smooth muscle cells around larger vessels, and cardiomyocytes surrounding the endocardium. They play important roles not only during the initial sprouting and remodeling of the emerging vascular bed, but in addition are essential for the stabilization and maturation of the vasculature via the production of specialized extracellular matrices (elastin fibers). The biology of pericytes and smooth muscle cells has been reviewed previously [101-106]. Pericytes associate abluminally with endothelial cells, protruding processes parallel to the long axis of midcapillaries, or encircling the wall of pre- and postcapillary venules and arterioles. They produce several matrix components (collagen I, III, IV, fibronectin, tenascin, laminin, glycosaminoglycans, osteolcalcin), and are "intramurally" embedded within a basement membrane which they share with the endothelium [104]. The characteristics of the midcapillary pericytes gradually change over a "transitional" phenotype to those of "true" smooth muscle cells surrounding terminal arterioles, venules and larger vessels. Although tissues differ widely in the number of pericytes or in their endothelial coverage (retina > lung > skeletal muscle > cardiac muscle > adrenal gland etc), the functional consequences of these differences during quiescent or angiogenic conditions remain largely unknown [104].

Pericytes have heterogeneous functions in different tissues, suggesting tissue-specific regulation [107, 108]. They may regulate capillary blood flow by vasomotor regulation [101] and have been implicated in the maintenance of a selective permeability barrier for plasma constituents [101,109]. Another property of pericytes is their plasticity to differentiate into smooth muscle cells, which could be relevant for the transition of midcapillary pericytes to smooth muscle cells when the vascular network expands and capillaries develop into arterioles, such as for example during hypoxia in the lung [110]. Pericytes may also control endothelial cell growth and differentiation (see below), and their responsiviness to hypoxia may be relevant in this context [111]. Intriguingly, pericytes are among the few cell types thriving under hypoxic conditions.

Pericytes/smooth muscle cells in different locations differ in their embryonic origin.

The mural cells of blood vessels proximal to the heart are derived from cardiac neural crest cells (neuroectodermal origin), whereas those of vessels more distal to the heart are derived from mesenchymal cells (mesodermal origin). Although the mechanisms of pericyte and smooth muscle cell recruitment and differentiation remain largely unknown, similarities between endothelial and pericyte growth have been recognized. One mechanism may involve their in situ differentiation from mural precursors, similar to the "vasculogenic" differentiation of angioblasts. Such differentiation of mesodermally derived cells to smooth muscle α-actin expressing cells may occur in the developing aorta, initially in the ventral vicinity and progressing distantly from the endothelium [112,113]. Another mechanism of pericyte and smooth muscle recruitment involves their (longitudinal) migration alongside a preexisting parent vessel to more distal sites, such as occurs during hypoxic pulmonary hypertension [110]. A third mechanism involves "pericyte sprouting". Indeed, when endothelial cells (perpendicularly) emigrate from their preexisting site during sprouting angiogenesis, pericytes also "sprout" from their parental vessels.

Endothelial cells are believed to recruit and organize mural cells through intercellular communication, presumably via candidate signals such as PDGF-B [31,114,115], the angiopoietins [22,23], tissue factor [29,116,117], and possibly FGF2. Once in contact with endothelial cells, pericytes may inhibit endothelial proliferation, as evidenced by the increased number of endothelial cells in PDGF-B deficient microvessels lacking pericytes [31]. In addition, they induce endothelial differentiation (including for example the intracellular distribution of actin fibers), and prevent tearing of endothelial cells by production of extracellular matrix. TGF-β1, which only becomes activated when endothelial and pericyte cells make close contacts, appears to mediate these effects [12,101,118]. Plasmin, generated from plasminogen by plasminogen activators, that are produced by endothelial, pericyte or epithelial cells, controls the activation of the latent TGF-β1. Once the initial pericyte recruitment phase is over, the prenatal blood vessels undergo another phase of development (maturation), characterized by deposition of specialized extracellular matrix components such as collagen, elastin and fibrillin. These matrix components provide the developing arteries viscoelastic properties (elastin and fibrillin-2) [119] and strength (collagen and fibrillin-1) [120].

The tyrosine receptor kinase TIE2 and its angiopoietin ligands

Recently, two ligands for the TIE2 receptor, e.g. angiopoietin-1 (ANG1) and angiopoietin-2 (ANG2) were identified. ANG1 specifically induced tyrosine phosphorylation of TIE2 in endothelial cells, but, surprisingly, failed to induce endothelial cell proliferation, migration or tube formation in collagen gels [121]. Targeted disruption of the ANG1 gene resulted in embryonic lethality around 11.0 to 12.5 days of gestation due to abnormal cardiovascular development [22]. Vascular defects included a less complex and immature vascular network, characterized by more dilated, and almost syncitial appearance of the vessels, much less distinction in size between large and small vessels, and fewer and straighter branches. In addition, certain vessels, such as the intersomitic vessels, appeared to regress beyond 11 days of

gestation. Together, these findings suggest that remodeling of the initially homogeneous capillary network into both large and small vessels is defective by a failure in recruitment of periendothelial cells, possibly because endothelial cells fail to transmit a recruiting signal (PDGF-BB) for mesenchymal cells in the absence of ANG1. ANG2 is a negative TIE2 ligand which blocks the action of ANG1 in recruiting and sustaining periendothelial support cells [23, 122]. In the presence of VEGF-A, ANG2 may promote angiogenic sprouting by loosening the periendothelial cell support and basement membrane encapsidation, whereas, in the absence of the VEGF-A survival signal, it may induce vessel regression. Not surprisingly, transgenic mice overexpressing ANG2 also die during embryogenesis, with similar vascular defects as mice lacking ANG1 or TIE2. Interference with tie2 gene function was accomplished by generation of transgenic mice with a dominant negative TIE2 mutant due to lysine-to-alanine mutation of codon 853 (TIE2-L853A) in the intracellular domain, which abolished (auto)phosphorylation [123]. In addition, tie2 gene function was disrupted via homologous recombination in embryonic stem cells (tie2-/-) [20]. TIE2-L853A and tie2-/- embryos displayed immature dilated blood vessels without distinction between large and small vessels, which were more fragile and ruptured, inducing hemorrhaging in diverse cavities of the body.

Transforming growth factor-β1

Transforming growth factor-β1 (TGF-β1) is a multifunctional cytokine capable of affecting blood vessel formation [124-127]. It can bind to several cellular receptors on endothelial cells of which the receptor serine/threonine kinases type I and II have been identified as signal transducing TGF-β1 receptors. In addition, TGF-β1 interacts with other molecules such as betaglycan and endoglin, and combinatorial interactions between these TGF-β binding molecules may modulate its biological role. TGF-β1 inhibits macrovascular endothelial cell proliferation, induces apoptotic endothelial cell death, impairs endothelial cell migration, and reduces their proteolytic activity in vitro [118,125]. However, TGF-β1 exerts pleiotropic and bimodal effects on endothelial cells in vitro, which largely depend on its concentration, on the type and the density of endothelial cells, on the nature of extracellular matrix components, and on the interaction with other growth factors such as FGF2 and VEGF-A [125,128]. In fact, TGF-β1 has also been shown to promote proliferation of angiogenic endothelial cells, to induce formation of capillary-like tubes, and to increase expression of endothelial PECAM, fibronectin and tight cell junctions *in vitro* [125,129]. The latter properties may explain why TGF-β1 is angiogenic *in vivo*. However, TGF-β1 may induce blood vessel formation in vivo indirectly via affecting inflammatory or connective tissue cells which in turn can produce angiogenic molecules such as VEGF-A, PDGF, FGF2, etc. [125,130-133].

Besides a possible direct endothelial cell effect, TGF-β1 may control blood vessel formation via an effect on peri-endothelial mesenchymal cells by inhibiting their growth and migration, by promoting their differentiation (for example of α-actin production), and by inducing their production of extracellular matrix [134-136]. However, the role

of TGF-β1 on smooth muscle cell function remains controversial, as TGF-β1 gene transfer to the arterial wall or prolonged administration of TGF-β1 protein stimulate intimal thickening [137-139], whereas neutralizing anti-TGF-β1 antibodies reduce this process [140]. Its effect to increase extracellular matrix production appears to be the most consistent mechanism of action. Part of the apparently contradictory roles of TGF-β1 may be attributable (at least in part) to the bimodal effect of TGF-β1 on smooth muscle cell proliferation via complex control of an autocrine PDGF-AA loop [141,142].

Alternatively, the cellular response to TGF-β1 may depend on the cell type (embryonic versus adult smooth muscle cell phenotype, pericytes versus smooth muscle cells etc), or depend on the contextual presence of other signaling molecules [132]. Endothelial and smooth muscle cells secrete TGF-β1 in a biologically inactive form which can be activated by plasmin, but only when both cell types make close contact with each other [118]. TGFβ-1 has been implicated in pathological vessel development, restenosis, hypertensive remodeling and atherosclerosis [143]. Targeted inactivation of the TGF-β1 gene resulted in embryonic lethality in approximately 50% of homozygous TGF-β1 deficient embryos around 9.5 days post coitum [12]. Analysis of TGF-β1 deficient embryos revealed vascular defects in the yolk sac ranging from delay in vasculogenesis, development of small, disorganized and fragile vessels to regional absence of yolk sac vessel formation, inducing wasting of the embryos. There were frequently no contacts in the yolk sac between the endothelial cell layers and the apposed visceral endoderm and mesothelial cells, respectively, suggesting that these contacts had either not formed or were disrupted. As a result, the immature vitelline vessels were fragile, lacking the structural support, and ruptured with leakage of blood in the yolk sac. Deficiency of the TGF-β receptor type II similarly resulted in embryonic lethality due to defects in hematopoiesis and vasculogenesis [144]. These results suggest that TGF-β1 is essential for the early steps of blood vessel formation (vasculogenesis). Impaired terminal endothelial differentiation may also play a role. In addition, TGF-β1 appears to be essential for vascular integrity and maturation of the vascular bed, possibly by impairing differentiation of mesenchymal cells to pericytes, or by reducing their production of extracellular matrix.

Platelet-derived growth factor and its receptor

The PDGF family includes three dimeric ligands, PDGF-AA, PDGF-AB and PDGF-BB, encoded by two different genes [125,145-147]. As for TGF-β1, PDGFs have pleiotropic actions on both endothelial and mural cells, but since the evidence for an effect on pericytes and smooth muscle cells is more convincing, its role is discussed in this section. The PDGF receptor type-alpha (PDGFR-α) binds the A- or the B-chain of the PDGF dimers with high affinities, whereas the PDGF receptor type-β (PDGFR-β) only binds the B-chain. PDGFs are abundantly detected in the -granules of platelets, but also in smooth muscle cells, leukocytes and endothelial cells. PDGF-BB is angiogenic *in vivo* [148-150]. However, it is not clear whether PDGF-BB acts directly on endothelial cells, or elicits these effects by recruitment of inflammatory cells

and mesenchymal cells, which produce angiogenic factor such as VEGF-A, TGF-β1 or FGF2 [125,130-132]. *In vivo*, angiogenic microcapillary endothelial cells coexpress PDGF-BB and PDGFR-β [115], whereas regenerating macrovascular endothelial cells coexpress PDGF-A and PDGFR-α [151], suggesting autocrine endothelial growth control by PDGF. In vitro, PDGF-BB induces proliferation and tube formation via interaction with PDGF-β receptors but only of developing angiogenic endothelial cell cords [125,152]. In contrast, macrovascular endothelial cells maintain expression of PDGF-BB but lack expression of PDGFR-β and fail to proliferate in response to PDGF-BB.

Apart from an effect on endothelial cells, endothelial PDGF-BB appears to affect blood vessel formation by inducing migration and proliferation of PDGFR-β expressing pericytes in a paracrine loop. Smooth muscle PDGF-AA may stimulate growth of smooth muscle cells in an autocrine loop [101,115,125,145,147,151,153]. Notably, PDGF-BB appears to induce a migratory rather than a contractile differentiation, as evidenced by the reduced levels of α-actin levels in PDGF-stimulated cells [154]. This suggests that other factors (TGF-β1, tissue factor?) are required to induce a contractile differentiation state, once mural cells have been recruited to the endothelium. Application of the PDGF-B protein [155], or enhancement of PDGF-B expression in the vessel wall [156] induces neonitima formation, whereas inhibition of PDGF activity [157] or of PDGFR-β production *in vivo* [158] suppresses arterial remodeling and initimal thickening.

Targeted disruption of the PDGF-B gene resulted in defective development of the vascular smooth muscle cell lineage [30]. In kidney development, it is possible that PDGF-BB, initially expressed by the differentiating glomerular epithelium, recruits mesangial progenitor cells and subsequently, when PDGF-BB and PDGF-β receptor are expressed by mesangial cells, stimulates proliferation of mesangial cells in an autocine loop [159]. Lack of pericytes throughout the entire microvascular bed, due to impaired recruitment (and proliferation) of PDGFR-β positive vascular wall progenitors, also explains why PDGF-B-deficient capillaries were tortuous, variable in diameter and aneurysmal, ultimately contributing to perinatal death owing to generalized hemorrhaging [31]. Interestingly, naked endothelial tubes at sites of pericyte loss contained increased numbers of endothelial cells, suggesting inhibitory control by pericytes. It is currently unclear which signals (tissue factor, ANG1?) stimulate induction of these vascular wall progenitors.

Loss of PDGF-B gene function also caused other defects of the smooth muscle lineage development [30]. Indeed, the large arteries of the mutant embryos were markedly dilated. However, since the number of smooth muscle cell layers appeared normal, deficiency of PDGF-B resulted in dysfunction rather than hypoplasia or hypotrophy of the smooth muscle cells, possibly related to the vasoconstrictor properties of PDGF [145]. Similar defects in kidney development and hematopoiesis were observed in mice lacking the PDGFR-β [160], suggesting that these processes result from signaling of PDGF-BB through the PDGFR-β. Analysis of wild type <-> PDGFR-β deficient chimeric mice reveals the absence of differentiated smooth muscle cells in the aortic wall, suggesting that the PDGFR-β plays an essential cell-autonomous role in smooth muscle cell development (Bowen-Pope et al, personal communication). Taken together,

PDGF-BB is not critical for endothelial tube formation, but appears to play a central role in the structural integrity of the endothelial tubes via an effect on recruitment of pericytes. PDGF-A may also be crucial for the development of the heart and blood vessels, as Patch mice (lacking PDGFR-α) contain fewer smooth muscle cells around their normal endothelial tubes, as well as a thinned myocardium [161].

Extracellular matrix proteinases I: The coagulation system

Initiation of the plasma coagulation system is triggered by tissue factor (TF), which functions as a cellular receptor and cofactor for activation of the serine proteinase factor VII (FVII) to factor VIIa (FVIIa) [162,163]. The TF FVIIa complex activates factor X either directly, or indirectly via activation of factor IX, resulting in the activation of prothrombin to thrombin and in the conversion of fibrinogen to fibrin. Because of an efficient FXa-dependent feedback inhibition of TF FVIIa by the Kunitz domain-type inhibitor TF pathway inhibitor (TFPI), which is synthetized primarily by and bound to the endothelium of microvessels, coagulation is initiated but rapidly shut off. Therefore, sustained progression of the coagulation has been proposed to depend on a positive feedback stimulation by thrombin and factor Xa, which activate factor XI, factor VIII and factor V (the latter two serving as membrane-bound receptors/cofactors for the proteolytic enzymes factor IXa and factor Xa, respectively) [164]. Apart from antithrombin III, anticoagulation results from interaction of thrombin with thrombomodulin, activating thereby protein C which, together with protein S, inactivates factor Va and factor VIIIa in a negative feedback loop [165]. Evidence has been provided that the coagulation system may be involved in other functions beyond fibrin-dependent hemostasis including cellular migration and proliferation, immune response, metastasis and brain function [162,163,166,167]. The following evidence suggests that TF participates in processes beyond initiation of fibrin formation: (i) it is a member of the immunoglobulin superfamily and expressed as an immediate early gene during inflammation and immune challenge [162,163]; (ii) its intracellular domain mediates signaling during metastasis, cellular activation or growth factor production [163]; (iii) it may participate in tumor neovascularization, possibly via an effect on VEGF expression [168-170], and (iv) it is expressed in a varitey of embryonic tissues including the visceral endoderm cells in the yolk sac (which surround the endothelium), and at later stages, in the smooth muscle cells of larger blood vessels [171,172]. Its precise role and relevance in these processes in vivo remains, however, largely unknown.

Targeted inactivation of the TF gene resulted in increased fragility of endothelial cell-lined channels in the yolk sac in 80 to 100% of the mutant embryos [29,173-175]. At a time when the blood pressure increased during embryogenesis (day 9 of gestation), the immature TF deficient blood vessels ruptured, formed micro-aneurysms and 'blood lakes', and failed to sustain proper circulation between the yolk sac and embryo [29]. Since these are essential for transferring maternally derived nutrients from the yolk sac to the rapidly growing embryo, the embryo became wasted and died due to generalized necrosis. Similar observations were made when TF deficient embryos were cultured in

vitro, suggesting that the observed vascular defects in the yolk sac were not merely due to a possible defect in feto-maternal exchange [29]. Visceral endoderm cell function appeared normal, suggesting that they were not responsible for the vascular defects. In contrast, defective development and/or recruitment of periendothelial mesenchymal cells (primitive smooth muscle cell or pericytes) appeared to be a likely reason for the vascular defects. These cells surround the endothelium in yolk sac vessels, form a primitive "muscular" wall and provide structural support by their close physical association and their increasing production of extracellular matrix proteins. Microscopic and ultrastructural analysis revealed that deficiency of tissue factor resulted in a 75% reduction of the number of mesenchymal cells, and a diminished amount of extracellular matrix [29]. Immunocytochemical analysis further revealed a reduced level of smooth muscle α-actin staining in these cells, suggesting impaired differentiation and/or accumulation. Because these primitive smooth muscle cells provide structural support for the endothelium, the vessels in the mutant embryos are too fragile and break open.

In contrast to the severe TF deficient embryonic lethality, deficiency of FVII did not compromize embryonic development and only caused fatal bleeding after birth [176]. Differences in genetic background did not appear to explain the different phenotypes since deficiency of TF, when generated in a similar mixed C57Bl/6J x 129/SvJ background as FVII, still caused 85% embryonic lethality [175]. Transfer of maternal FVII did not appear to rescue the FVII deficient embryos as it was minimally detectable, even at supraphysiological maternal FVII plasma levels [176]. In addition, it should be noticed that FVII mRNA levels in the yolk sac at 9.5 days of gestation were minimal, and that FVII plasma levels in wild type embryos at 11.5 days of gestation were only ~0.2% of those present in adult mice. In order to investigate the mechanism of action of embryonic TF, its presumed hemostatic role in fibrin formation during embryogenesis was studied [176]. Surprisingly, fibrin deposits in the visceral yolk sac were not observed in our ultrastructural and immunocytochemical analysis of wild type embryos, as would be expected in case TF deficient embryos would die secondarily to a fibrin-dependent hemostatic defect. These findings raise some critical questions about the presumed role of TF and FVII during early embryonic hemostasis. We cannot exclude that minimal transfer of maternal FVII (undetectable by the present techniques) rescues FVII deficient embryos. However, such minimal FVII transfer did not appear to induce detectable fibrin formation, possibly suggesting that early embryonic hemostasis may be less dependent on fibrin formation than anticipated. In fact, generation of the coagulation factors Xa or thrombin (or others) may be also (or even more) important for vascular development, as they affect proliferation and migration of vascular cells directly [166,167,177], or indirectly via release of PDGF [145]. The abnormal embryonic development in embryos lacking the thrombin receptor (PAR-1) [178] or factor V [179], in contrast to the normal development of fibrinogen deficient embryos [180] may underscore the important role of thrombin during embryonic hemostasis. TF may also directly be mitogenic or chemotactic for smooth muscle cells via intracellular signaling [116]. Intracellular TF-signaling has also been implicated in the production of growth factors such as VEGF (DeProst et al, personal communication), which could increase the permeability of embryonic vessels (and

thereby the availability of other plasma molecules to the periendothelial space), or modulate the function of smooth muscle cells (see above). Whatever the molecular mechanism, TF appears to be play a central role in vessel wall integrity.

More than half (60%) of the embryos, expressing a mutant TFPI without the first Kunitz domain (which impairs interaction with factor VIIa but not with factor Xa), die around a similar time as the TF deficient embryos because of impaired vascular integrity and bleeding, with remarkable phenocopying of the TF deficient vascular defects [181]. The remainder of the TFPI deficient embryos develop untill birth but suffer fatal consumptive coagulopathy around birth. However, in contrast to the marked intravascular thrombosis in TFPI deficient neonates, surprisingly little fibrin was observed in 9.5 day old TFPI deficient embryos. It is at present undetermined whether bleeding in early TFPI deficient embryos was due to exhausted fibrin formation, or due to abnormal vascular integrity, for example caused by depletion of morphogenic coagulation factors (factor Xa or thrombin). In addition, alternative roles of TFPI might be considered such as inhibition of trypsin, or yet unknown functions. Thrombin has been implicated in processes beyond hemostasis. Indeed, it is mitogenic for fibroblasts and vascular smooth muscle cells, chemotactic for monocytes and activates endothelial cells [167]. Many of the cell signaling activities of thrombin appear to be mediated by the currently identified thrombin receptors, PAR-1 and PAR-3 [182]. Expression studies have suggested that the PAR-1 participates in inflammatory, proliferative or reparative responses such as restenosis, atherosclerosis, neovascularization and tumorigenesis 167. In addition, in situ analysis indicated that this receptor is expressed during early embryogenesis in the developing heart and blood vessels, in the brain and in several epithelial tissues [171]. Targeting of PAR-1 resulted in a block of embryonic development in approximately 50 % of the homozygous deficient embryos around a similar developmental stage as in TF deficient embryos, presumably resulting from abnormal yolk sac vascular development [178,183]. Although the cellular defect was not characterized in detail, vitelline vessels appeared to be abnormal, resulting in increased fragility of blood vessels with secondary rupture, blood leakage and pallor of the embryo. Similarly enlarged pericardial cavities in PAR-1 deficient embryos suggested compromized vitello-embryonic blood circulation. Other coagulation factors might also appear to be involved in morphogenic processes during early embryogenesis, possibly in blood vessel formation. Deficiency of factor V resulted in embryonic lethality in approximately half of the homozygously deficient embryos, possibly due to vascular defects in the yolk sac [179]. Thrombomodulin deficient embryos also die during early gestation but the precise cause of lethality remains unclear [184]. Notably, fibrin deposits were not observed.

Taken together, hemostasis in the early embryo (e.g. around 9 days of gestation) may be less dependent on fibrin formation and platelet function (thrombocytopenic embryos develop normally and bleed only postnatally [185]) than anticipated. Later during embryogenesis, probably around midgestation, when the embryo produces larger quantities or a more complete set of coagulation factors, hemostasis appears to become typically dependent on fibrin formation as during adulthood. Indeed, embryos expressing a mutant factor V Leiden (D. Ginsburg, personal communication), TFPI or lacking protein C (in collaboration with L. Jalbert, E. Rosen and F. Castellino, Notre

Dame, USA) progressively develop fibrin deposits before birth (beyond 12 days of gestation in mutant TFPI embryos). It is therefore not surprising that postnatal bleeding occurs in (the surviving fraction of) mice deficient of factor V [179], factor VII [176], factor VIII [186], factor IX and fibrinogen [180] due to defective clot formation following trauma of normally developed blood vessels (see below).

Proteinases II: The plasminogen and matrix metalloproteinases

Cell migration requires proteolysis of the extracellular matrix. Somewhat surprisingly, proteinases of the plasminogen activator (PA) or of the matrix metalloproteinase (MMP) system are not required for mural cell migration during embryogenesis. In contrast, gene targeting studies have revealed that they play a significant role during pathological smooth muscle cell migration, as well as in vessel wall integrity.

Arterial stenosis

Vascular interventions for the treatment of atherothrombosis induce "restenosis" of the vessel within three to six months in 30 to 50 % of treated patients [187,188]. The risk and costs associated with reinterventions represent a significant medical problem, mandating a better understanding at the molecular level of this process. Arterial stenosis may result from remodelling of the vessel wall (such as occurs predominantly after balloon angioplasty) and/or from accumulation of cells and extracellular matrix in the intimal layer (such as occurs predominantly after intraluminal stent application) [189,190]. Several candidate molecules have been identified based on correlative expression studies, but their in vivo role has frequently remained obscure. Although the availability of transgenic mice offers a novel opportunity to study the role of candidate genes in this process, the lack of feasible and appropriate mouse models of arterial stenosis has limited such progress. We and others have developed models of arterial injury in the mouse and, although they may not represent an ideal model of human restenosis, they allow to study the biological role and mechanism of the candidate genes, and to assemble a molecular analysis of the underlying mechanisms.

Proteinases participate in the proliferation and migration of smooth muscle cells, and in the matrix remodelling during arterial wound healing [25,83,191]. Two proteinase systems have been implicated, the plasminogen (or fibrinolytic) system and the metalloproteinase system, which in concert can degrade most extracellular matrix proteins. PAI-1 is expressed by uninjured vascular smooth muscle cells [76,85]. u-PA, t-PA and (to a lesser degree) PAI-1 activity in the vessel wall are significantly increased after injury, coincident with the time of smooth muscle cell proliferation and migration [86,88,89,192,193]. Of the MMPs, only MMP-2 appears to be expressed in the quiescent smooth muscle cells, whereas expression of MMP-3, MMP-7, MMP-9, MMP-12 and MMP-13 is induced in injured, transplanted or atherosclerotic arteries [194-199].

Two experimental models of arterial injury were used, one based on the application of an electric current [200] and the other on an intraluminal guidewire [88,89] to examine the molecular mechanisms of neointima formation in mice deficient in fibrinolytic

system components. The electric current injury model differs from mechanical injury models in that it induces a more severe injury across the vessel wall resulting in necrosis of all smooth muscle cells. This necessitates wound healing to initiate from the adjacent uninjured borders and to progress into the central necrotic region, allowing to quantitate the migration of smooth muscle cells. Microscopic and morphometric analysis revealed that the rate and degree of neointima formation and the neointimal cell accumulation after injury were similar in wild type, t-PA deficient and u-PAR deficient arteries [88,96]. However, neointima formation in PAI-1 deficient arteries occurred earlier after injury [89]. In contrast, both the degree and the rate of arterial neointima formation in u-PA deficient, Plg deficient and combined t-PA:u-PA deficient arteries was significantly reduced until 4 to 6 weeks after injury [88,97]. Infiltration of the media by leukocytes was also significantly reduced in Plg deficient mice [97]. Similar genotypic differences were obtained after mechanical injury [88,89], which more closely mimics the balloon-angioplasty injury in patients.

Evaluation of the mechanisms responsible for these genotype-specific differences in neointima formation revealed that proliferation of medial and neointimal smooth muscle cells was only marginally different between the genotypes [88,89,96,97]. Impaired migration of smooth muscle cells is a likely cause of reduced neointima formation in mice lacking u-PA-mediated plasmin proteolysis since smooth muscle cells migrated over a shorter distance from the uninjured border into the central injured region in Plg deficient than in wild type arteries [88,97]. In addition, migration of u-PA deficient smooth muscle cells, but not of t-PA deficient or u-PAR deficient smooth muscle cells, cultured in the presence of serum, was impaired after scrape wounding [88].

Notably, when smooth muscle cells were cultured without serum, u-PA was essential for migration induced by FGF2, wheres t-PA was required for migration induced by PDGF-BB [201]. The requirement of u-PA is consistent with the more than 100-fold increased expression levels of u-PA mRNA, immunoreactivity and zymographic activity by migrating smooth muscle and inflammatory cells. Besides the genotypic effects on the media and intima, adventitial remodeling with infiltration of leukocytes and myofibroblasts was also severely impaired, whereas intravascular thrombosis (albeit transient) was more frequent and extensive in mice lacking u-PA or Plg. Although our results demonstrate that migration of smooth muscle cells requires plasmin proteolysis, it is possible that PAI-1 may also influence cellular migration by affecting vitronectin-dependent cell adhesion through interaction with the $a_v\beta_3$-integrin receptor [202]. However, vitronectin and PAI-1 poorly colocalized in the murine healing arteries [89]. That u-PAR deficient arteries developed a similar degree of neointima was not due to lack of u-PAR expression in wild type arteries as revealed by the expression of functional u-PAR by smooth muscle cells *in vitro* and *in vivo* [96]. Instead, immunogold labeling of u-PA in injured arteries revealed that u-PA was present on the cell surface of wild type smooth muscle cells and accumulated in the pericellular milieu (associated with extracellular matrix components such as collagen fibers) around u-PAR deficient cells [96]. In fact, u-PA accumulated to slightly increased levels in the pericellular milieu. Degradation of ^{125}I-labeled fibrin after 8 hrs or activation of proMMP-9 and proMMP-13 was similar by wild type as u-PAR

deficient cells. Taken together, these data suggest that sufficient pericellular plasmin proteolysis is present in the absence of binding of u-PA to its cellular receptor. Possibly, the role of u-PAR in particular biological processes may depend on its topographical and temporo-spatial expression pattern. Somewhat surprisingly, no genotypic differences were observed in reendothelialization [88,89,96,97] suggesting a cell-type specific requirement of plasmin proteolysis for cellular migration.

More recently, the role of MMPs was investigated. Only low levels of MMP-2 were detected in a quiescent artery. In contrast, following injury, significantly induced expression levels of MMP-2, MMP-3, MMP-9, MMP-12 and MMP-13 were observed across the entire injured vessel wall [203]. Similar levels of proMMP-2 and active MMP-2 were observed in arterial extracts of wild type and Plg deficient mice, confirming that activation of proMMP2 is not dependent on plasmin (see also below). In contrast, significantly lower levels of active MMP-9 were present in Plg deficient than in wild type arteries. Since MMP-9 is primarily expressed by leukocytes, and leukocytes are involved in the healing of the injured arteries, the lower active MMP-9 levels may contribute to the impaired medial and adventitial remodeling and to the reduced neointima formation.

The involvement of plasmin proteolysis in neointima formation was supported by intravenous injection in PAI-1 deficient mice of a replication-defective adenovirus expressing human PAI-1 [89]. This resulted in preferential infection of hepatocytes and in more than 100- to 1000-fold increased plasma PAI-1 levels. Although the injured arterial segment was not infected, PAI-1 immunnoreactivity was detected in the developing neointima, presumably due to deposition of plasma PAI-1. This resulted in a similar degree of inhibition of neointima formation as observed in u-PA deficient mice without noticeable toxic liver necrosis or intravascular thrombosis. Proteinase-inhibitors have been suggested as anti-restenosis drugs, and recent studies indicate that seeding of retrovirally transduced smooth muscle cells, expressing high levels of PAI-1, inhibits balloon angioplasty induced arterial stenosis (Clowes et al, personal communication). In addition, use of a viral PAI-1 like serpin (SERP-1) reduces lesion formation in cholesterol-fed injured rabbits [204]. Our studies suggest that strategies aimed at reducing u-PA-mediated plasmin proteolysis may be beneficial for reduction or prevention of restenosis. However, antifibrinolytic strategies should be targeted at inhibiting plasmin proteolysis and not at preventing the interaction of u-PA with its receptor. In addition, PAI-1 gene therapy should be balanced since excessive inhibition of u-PA may prevent healing of the injured vessel wall, possibly rendering it more susceptible to rupture.

Allograft transplant stenosis

More recently, studies have started to analyze the role of the plasminogen system in a mouse model of transplant arteriosclerosis, that mimics in many ways the accelerated arteriosclerosis in coronary arteries of transplanted cardiac allografts in man [205]. In this model, host-derived leukocytes adhere to and infiltrate beneath the endothelium and form a predominantly leukocyte-rich neointima within 15 days after transplantation, whereas, at later times, smooth muscle cells, derived from the donor graft, accumulate in the neointima. Since previous targeting studies have shown that migration of

leukocytes and smooth muscle cells is dependent on plasmin proteolysis [88,89,96,97,206], carotid arteries from B.10A(2R) wild type mice were transplanted in C57Bl6:129 Plg deficient mice. Such analysis revealed that neointima formation within 15 days was not significantly different, although significantly more leukocytes infiltrated into the media in wild type than in Plg deficient mice. In addition, adventitial infiltration by leukocytes and accumulation of myofibroblasts was markedly greater in wild type than in Plg deficient mice. Within 45 days after transplantation, the neointima was, however, much smaller and 10-fold fewer α-actin positive smooth muscle cells were present in Plg deficient than in wild type mice. In addition, media necrosis was less pronounced whereas fragmentation of the elastic laminae and neoadventitia formation were more severe in wild type than in Plg deficient mice. Graft thrombosis was, however, much more frequent and extensive in Plg deficient mice. Expression of u-PA, t-PA, MMP-2, MMP-3, MMP-9, MMP-12 and MMP-13 were significantly increased within 15 days after transplantation, when cells actively migrate. Notably, the reverse transplantation of Plg deficient arteries into wild type recipients did not affect the development of the neointima, indicating that plasminogen circulating in the plasma is essential.

Taken together, it appears that plasmin is not essential for leukocytes to adhere and to migrate beneath the endothelium. However, plasmin mediates lysis of arterial thrombi, and is required for leukocytes to fragment the elastic laminae and to infiltrate into the media. Similar to the atherosclerotic aorta (see below), destruction of the medial stroma was conditional on prior elastic lamina degradation by macrophages. Since plasmin is unable to degrade elastin, collagen and other matrix components in the media, it presumably activates other matrix degrading proteinases, likely of the MMP family (see also below). Subsequently, medial smooth muscle cells proliferate and migrate into the intima, a process which is also mediated by plasmin.

Atherosclerosis

Atherosclerotic lesions initially consist of subendothelial accumulations of foamy macrophages (fatty streaks) which subsequently develop into fibroproliferative lesions by infiltration of myofibroblasts and accumulation of extracellular matrix [143]. A fibrous cap rich in smooth muscle cells and extracellular matrix overlies a central necrotic core containing dying cells, calcifications and cholesterol crystals. As long as these lesions do not critically limit blood flow, they may grow insidiously. However, clinical syndromes of myocardial or peripheral tissue ischemia due to occluding thrombosis are frequently triggered by rupture of unstable plaques, and constitute the primary cause of cardiovascular morbidity and mortality in Western societies. In addition, the atherosclerotic wall may become thinner due to media necrosis, ultimately resulting in aneurysm formation and fatal bleeding. Aneurysm formation is the 13th cause of mortality, responsible for more than 15,000 deaths annually in the United States only [207-209]. The pathogenetic mechanisms of atherosclerotic aneurysm remain, however, largely undefined.

Epidemiologic, genetic and molecular evidence suggests that impaired fibrinolysis resulting from increased PAI-1 or reduced t-PA expression, or from inhibition of plasminogen activation, may contribute to the development and/or progression of

atherosclerosis [210-212]. Presumably, this results from increased thrombosis and matrix deposition, which promote plaque growth. Indeed, PAI-1 plasma levels are elevated in patients with ischemic heart disease, angina pectoris and recurrent myocardial infarction [213]. Recent genetic analyses revealed a link between polymorphisms in the PAI-1 promoter and the susceptibility of atherothrombosis [211]. Adipocytes may significantly contribute to the increased plasma PAI-1 levels in obese patients prone to ischemic heart disease. A possible role for increased plasmin proteolysis in atherosclerosis is, however, suggested by the enhanced expression of t-PA and u-PA in plaques [214, 215]. Plasmin proteolysis might indeed participate in plaque neovascularization, induction of plaque rupture, or in ulceration and formation of aneurysms [214,215].

Therefore, atherosclerosis was studied in mice deficient in apolipoprotein E (apoE) [216], singly or combined deficient in t-PA, u-PA or PAI-1, and fed a cholesterol-rich diet for 5 to 25 weeks [80]. No differences in the size or the predilection site of early fatty streaks and more advanced plaques were observed between mice with a single deficiency of apoE or with a combined deficiency of apoE and t-PA, or of apoE and u-PA, suggesting that plasmin is not essential for subendothelial infiltration by macrophages. Apparently, deficiency in apoE and Plg results in accelerated atherosclerosis [217]. Whether this is due to a direct effect of plasminogen deficiency on matrix deposition (fibrin deposition did, however, not appear to be different), or another effect, was not elucidated. Indeed, the poor general health of the Plg deficient mice with their associated generalized state of increased inflammatory stress, as well as their significantly lower levels of high density lipoproteins may have contributed to the accelerated atherosclerosis [217].

Significant genotypic differences were observed in the integrity of the atherosclerotic aortic wall [80]. Indeed, destruction of the media with resultant erosion, transmedial ulceration, necrosis of medial smooth muscle cells, aneurysmal dilatation and rupture of the vessel wall were more prevalent and severe in mice lacking apoE or apoE:t-PA than mice lacking apoE:u-PA. At the ultrastructural level, elastin fibers were eroded, fragmented and completely degraded, whereas collagen bundles and glycoprotein-rich matrix were disorganized and scattered in apoE deficient and apoE:t-PA deficient mice, whereas apoE:u-PA deficient mice were virtually completely protected. Mac3 immunostaining and ultrastructural analysis revealed that macrophages were absent in the media of uninvolved arteries, that they were only able to infiltrate into the media of atherosclerotic arteries after they degraded the elastin fibers, and that media destruction progressed in an intima-to-adventitial gradient. Plaque macrophages (and especially those infiltrating into the media) expressed abundant amounts of u-PA mRNA, antigen and activity at the base of the plaque, similar as in patients [214,215]. In contrast, t-PA and PAI-1 were confined to the more apical regions within the plaque. Thus, a dramatic increase of free u-PA activity (which is minimal in quiescent arteries) was generated by the infiltrating plaque macrophages. Since plasmin by itself is unable to degrade insoluble elastin or fibrillar collagen, it most likely activated other matrix proteinases. Because of their well-described increased expression in atherosclerotic plaques and aneurysms, matrix metalloproteinases (MMPs) constituted likely candidates. Macrophages in murine atherosclerotic plaques abundantly expressed MMP-3, MMP-9,

MMP-12 and MMP-13 [80]. Furthermore, cultured peritoneal macrophages derived from wild type mice, or mice deficient in t-PA, MMP-3, MMP-7 and MMP-9 degraded 3H-elastin in a plasminogen-dependent manner, whereas u-PA deficient or MMP-12 deficient macrophages were unable to do so. In addition, wild type and t-PA deficient but not u-PA deficient cultured macrophages activated secreted proMMP-3, proMMP-9, proMMP-12 and proMMP-13 but only in the presence of plasminogen, indicating that u-PA-generated plasmin was responsible for activation of these proMMPs. These plasmin-activatable metalloproteinases colocalized with u-PA in plaque macrophages. Another possible mechanism of action of plasmin is that it mediates the degradation of glycoproteins in the stroma of the aortic wall, thereby exposing the highly insoluble elastin to elastases and facilitating elastolysis *in vivo* [218]. Taken together, these results implicate an important role of u-PA in the structural integrity of the atherosclerotic vessel wall, likely via triggering activation of matrix metalloproteinases. Direct proof whether and which MMPs are involved in media destruction and aneurysm formation has to await a similar analysis in mice that are combined deficient of apoE and each of these MMPs.

Myocardial ischemia

Acute myocardial infarction due to the occlusion of coronary arteries is a leading cause of morbidity and mortality in Western societies. Despite the therapeutic benefits of trombolysis, coronary angioplasty and bypass surgery, myocardial performance is severely disabled and the associated arrhythmias and ventricular wall rupture represent a significant cause of sudden death [219,220]. In addition, chronic heart failure frequently results from infarct expansion, mitral valve insufficiency and left ventricular aneurysm formation. Therefore, a better understanding of the pathophysiological mechanisms leading to ventricular wall rupture and myocardial scar formation are mandated.

Sudden death due to ventricular wall rupture or infarct expansion usually occurs within five days after myocardial infarction in human patients, coincident with the invasion of inflammatory cells and endothelial cells, and the diffuse myocytolysis. Infarct expansion (characterized by a disproportional regional thinning and dilatation of the ventricular wall due to stretching and slippage of myocytes in the ischemic area) is a frequent complication of transmural infarcts and associated with heart failure, cardiac rupture and increased mortality. Excessive degradation of fibrillar collagen I and III (the most abundant cardiac interstitial matrix components) by infiltrating leukocytes and endothelial cells (which produce significant amounts of PAs and MMPs) may cause infarct expansion and heart rupture.

Within one to two weeks after myocardial ischemia, a highly vascularized granulation tissue rich in infiltrating fibroblasts removes the cellular debris and mediates collagen deposition, which ultimately leads to scar formation [221]. Aneurysms cause expansive paradoxical ventricular wall motion and can be complicated by congestive heart failure, arterial embolism, and arrhythmia's. Myofibroblasts mediate this process since they produce increased levels of TIMP within one week after ischemia, and produce abundant amounts of collagen I and III. Fibronectin and laminin may bridge the myocyte cell surface with the collagen fibers in the pericellular matrix and may be

involved in cell adhesion, migration and proliferation during cardiac wound healing. Apart from their role in cardiac remodeling, proteinases may also be involved in collateral growth of the ischemic myocardium (see above). Untill today, little is, however, known about the role of the PA and MMP proteinases, and their interaction, in myocardial infarction and scar formation.

Recently, a modified mouse model of chronic myocardial infarction has been used to evaluate the role of the plasminogen system in cardiac healing. Initial studies reveal that the plasminogen system is importantly involved in this process (in collaboration with M. Daemen and J. Smits, Maastricht, the Netherlands). Indeed, following ligation of the left anterior descending coronary artery, wild type or t-PA deficient mice heal their ischemic myocardium within two weeks via scar formation. In a fraction of these mice, rupture of the ischemic myocardium occurs shortly after infarction, possibly related to excessive u-PA-generated plasmin proteolysis by infiltrating wound cells. In sharp contrast, mice lacking u-PA or Plg are protected against ventricular wall rupture, but fail to heal the ischemic myocardium which remains largely devoid of infiltrating leukocytes, endothelial cells and fibroblasts. Mural thrombosis in the ventricular cavity occurred, however, more frequently in Plg and u-PA deficient mice than in wild type mice. How these morphologic observations correlate with expression of fibrinolytic or matrix metalloproteinase enzymes and whether cardiac function is affected differently in the various genotypes remains to be determined. Nevertheless, the data show that u-PA-generated plasmin proteolysis is required for healing, but needs to be carefully balanced to avoid tissue destruction and ventricular wall rupture. Studies are underway to investigate the role of the various MMPs in the respective knockout mice.

Conclusion

Gene targeting studies are useful to obtain novel insights into the role and relevance of a gene during normal or pathological biological processes *in vivo*. New insights into the role of growth factors and proteinases in the formation of a normal blood vessel and in its pathologic progression to disorders such as thrombosis, restenosis and atherosclerosis have recently been obtained. Members of the VEGF family and hypoxia-inducible regulators play essential roles in development of endothelial networks, whereas other growth factors (TGF-β, PDGF-B, angiopoietin) are involved in establishment of a mural coat around these endothelial tubes. Several coagulation factors appear to play an unanticipated role in the formation of the primitive muscular wall of blood vessles, indicating a role for these coagulation factors beyond mere controle of hemostasis. Urokinase-mediated plasmin proteolysis plays a significant role in the migration of smooth muscle cells and tissue remodeling during neointima formation after vascular injury or transplantation, in the destruction of the media and aneurysm formation during atherosclerosis, and in cardiac rupture and healing after acute myocardial infarction. The insights from these gene targeting studies have fostered initiatives aimed at preventing neointima formation of cardiac rupture. Whether inhibition of plasmin proteolysis is a feasible means to prevent aneurysm formation during atherosclerosis, remains to be determined.

Acknowledgements

The authors are grateful to the members of the Center for Transgene Technology and Gene Therapy and to all external collaborators who contributed to these studies.

List of abbreviations

ANG	= angiopoetin
ARNT	= arylhydrocarbon-receptor nuclear translocator
bFGF	= basic fibroblastic growth factor
HIF	= hypoxia-inducible factor
IGF	= insulin-like growth factor
MMP	= matrix metalloproteinase
PA	= plasminogen activator
PAI	= plasminogen activator-inhibitor
PAR	= plasminogen activator receptor
PDGF	= platelet-derived growth factor
PDGFR	= platelet-derived growth factor receptor
PECAM	= platelet/ endothelial cell adhesion molecule
PlGF	= placental growth factor
TF	= tissue factor
TFPI	= tissue factor pathway inhibitor
TGF	= transforming growth factor
TIMP	= tissue inhibitors of matrix metalloproteinase
t-PA	= tissue-type plasminogen activator
u-PA	= urokinase-type plasminogen activator
u-PAR	= urokinase-type plasminogen activator receptor
VCAM	= vascular cell adhesion molecule
VEGF	= vascular endothelial growth factor
VRP	= VEGF-related protein

References

1. Wilting J, Christ B. Embryonic angiogenesis: a review. Naturwissenschaften 1996;83:153-64.
2. Risau W. Mechanisms of angiogenesis. Nature 1997;386:671-74.
3. Folkman J, D'Amore PA. Blood vessel formation: what is its molecular basis? Cell 1996;87, 1153-55.
4. Carmeliet P, Collen D. Genetic analysis of blood vessel formation. Role of endothelial versus smooth muscle cells. Trends Cardiovasc Med 1997;7:271-81.
5. Noden DM. Embryonic origins and assembly of blood vessels. Ann Rev Respir Dis 1989;140:1097-103.
6. Flamme I, Risau W. Induction of vasculogenesis and hematopoiesis *in vitro*. Development 1992;116:435-39.
7. Carmeliet P *et al.* Abnormal blood vessel development and lethality in embryos lacking a single vascular endothelial growth factor allele. Nature 1996;380:435-439.
8. Ferrara N *et al.* Heterozygous embryonic lethality induced by targeted inactivation of the VEGF gene. Nature 1996;380:439-42.
9. George EL, Georges Labouesse EN, Patel King RS, Rayburn H, Hynes RO. Defects in mesoderm, neural tube and vascular development in mouse embryos lacking fibronectin. Development 1993;119:1079-91.
10. Yang JT, Rayburn H, Hynes RO. Embryonic mesodermal defects in alpha5 integrin-deficient mice. Development 1993;119:1093-1105.
11. Vittet D, Buchou T, Schweitzer A, Dejana E, Huber P. Targeted null-mutation in the vascular endothelial-cadherin gene impairs the organization of vascular-like structures in embryoid bodies. Proc Natl Acad Sci USA 1997;94:6273-78.
12. Dickson MC *et al.* Defective haematopoiesis and vasculogenesis in transforming growth factor-beta 1 knock out mice. Development 1995;121:1845-54.
13. Shalaby F *et al.* Failure of blood-island formation and vasculogenesis in Flk-1-deficient mice. Nature 1995;376:62-66.
14. Fong GH, Rossant J, Gertsenstein M, Breitman ML. Role of the Flt-1 receptor tyrosine kinase in regulating the assembly of vascular endothelium. Nature 1995;376:66-70.
15. Drake CJ, Cheresh DA, Little CD. An antagonist of integrin $a_v\beta_3$ prevents maturation of blood vessels during embryonic neovascularization. J Cell Sci 1995;108:2655-61.
16. Patan S, Haenni B, Burri PH. Implementation of intussusceptive microvascular growth in the chicken chorioallantoic membrane (CAM): 1. Pillar formation by folding of the capillary wall. Microvasc Res 1996;51:80-98.
17. Patan S, Alvarez MJ, Schittny JC, Burri PH. Intussusceptive microvascular growth: a common alternative to endothelial sprouting. Arch Histol Cytol 1992;55:65-75.
18. Patan S, Haenni B, Burri PH. Implementation of intussusceptive microvascular growth in the chicken chorio-allantoic membrane (CAM). 2. Pillar formation by capillary fusion. Microvasc Res 1997;53:33-52.
19. Wilting J *et al.* VEGF121 induces proliferation of vascular endothelial cells and expression of flk-1 without affecting lymphatic vessels of chorioallantoic membrane. Dev Biol 1996;176:76-85.
20. Sato, T.N. et al. Distinct roles of the receptor tyrosine kinases Tie-1 and Tie-2 in blood vessel formation. Nature 1995;376:70-74.
21. Puri MC, Rossant J, Alitalo K, Bernstein A, Partanen J. The receptor tyrosine kinase TIE is required for integrity and survival of vascular endothelial cells. Embo J 1995;14:5884-91.
22. Suri C *et al.* Requisite role of angiopoietin-1, a ligand for the TIE2 receptor, during embryonic angiogenesis. Cell 1996;87:1171-80.
23. Maisonpierre PC, Suri C, Jones PF, *et al.* Angiopoeitin-2, a natural antagonist for Tie2 that disrupts in vivo angiogenesis. Science 1997;277:55-60.
24. Patan S. TIE1 and TIE2 receptor tyrosine kinases inversely regulate embryonic angiogenesis

by the mechanism of intussusceptive microvascular growth. Microvasc Res 1998;56:1-21.
25. Carmeliet P, Collen D. Gene manipulation and transfer of the plasminogen system and coagulation system in mice. Sem Thromb Hemost 1996;22:525-542.
26. Gurtner GC *et al.* Targeted disruption of the murine VCAM1 gene: essential role of VCAM-1 in chorioallantoic fusion and placentation. Genes Dev 1995;9:1-14.
27. Kwee L, Baldwin S, Stewart C, Buck C,Labow M. Defective development of the embryonic and extraembryonic circulatory system in vascular cell adhesion molecule (VCAM-1) deficient mice. Development 1995;121:489-503.
28. Yang JT, Rayburn H, Hynes RO. Cell adhesion events mediated by alpha4 integrins are essential in placental and cardiac development. Development 1995;121:549-60.
29. Carmeliet P *et al.* Role of tissue factor in embryonic blood vessel development. Nature 1996;383:73-75.
30. Levéen P *et al.* Mice deficient for PDGF B show renal, cardiovascular, and hematological abnormalities. Genes Dev 1994;8:1875-87.
31. Lindahl P, Johansson BR, Levéen P, Betsholtz C. Pericyte loss and microaneurysm formation in PDGF-BB deficient mice. Science 1997;277:242-45.
32. Zheng X, Saunders TL, Camper SA, Samuelson LC, Ginsburg D. Vitronectin is not essential for normal mammalian development and fertility. Proc Natl Acad Sci USA 1995;92:12426-30.
33. Maltepe E, Schmidt JV, Baunoch D, Bradfield CA, Simon CM. Abnormal angiogenesis and responses to glucose and oxygen deprivation in mice lacking the protein ARNT. Nature 1997;386:403-07.
34. Kozak KR, Abbott B, Hankinson O. ARNT-deficient mice and placental differentiation. Developmental Biology 1997;191:247-306.
35. Gnarra JR *et al.* Defective placental vasculogenesis causes embryonic lethality in VHL-deficient mice. Proc Natl Acad Sci USA 1997;94:9102-07.
36. Robert B, St John PL, Hyink DP, Abrahams DR. Evidence that embryonic kidney cells expressing flk-1 are intrinsic, vasculogenic angioblasts. Am J Physiol 1996;271:F744-53.
37. Benjamin LA, Keshet E. Conditional switching of vascular endothelial growth factor (VEGF) expression in tumors: induction of endothelial cell shedding and regression of hemangioblastoma-like vessels by VEGF withdrawal. Proc Natl Acad Sci USA 1997;94:8761-66.
38. Alon T *et al.* Vascular endothelial growth factor acts as a survival factor for newly formed retinal vessels and has implications for retinopathy of prematurity. Nat Med 1995;1:1024-28.
39. Risau W. Differentiation of endothelium. FASEB J 1995;9:926-33.
40. Breier G, Clauss M, Risau W. Coordinate expression of vascular endothelial growth factor receptor-1 (flt-1) and its ligand suggests a paracrine regulation of murine vascular development. Dev Dyn 1995;204:228-39.
41. Dumont DJ *et al.* Vascularization of the mouse embryo: a study of flk-1, tek, tie, and vascular endothelial growth factor expression during development. Dev Dyn 1995;203:80-92.
42. Terman BI, Dougher Vermazen M. Biological properties of VEGF/VPF receptors. Cancer Metastasis Rev 1996;15:159-63.
43. Ferrara N, Davis-Smyth T. The biology of vascular endothelial growth factor. Endocrine Rev 1997;18:4-25.
44. Dvorak HF, Brown LF, Detmar M, Dvorak AM. Vascular permeability factor/vascular endothelial growth factor, microvascular hyperpermeability, and angiogenesis. Am J Pathol 1995;146:1029-39.
45. Dor Y, Keshet E. Ischemia-driven angiogenesis. Trends Cardiovasc Med 1997;7:289-94.
46. Drake CJ, Little CD. Exogenous vascular endothelial growth factor induces malformed and hyperfused vessels during embryonic neovascularization. Proc Natl Acad Sci USA 1995;92:7657-61.
47. Yamaguchi TP, Dumont DJ, Conlon RA, Breitman ML, Rossant J. Flk-1, an flt-related receptor tyrosine kinase is an early marker for endothelial cell precursors. Development 1993;118: 489-98.

48. Carmeliet P, Collen D. Insights into vascular biology via targeted gene inactivation and adenovirus-mediated gene transfer of the plasminogen system. In: Coronary Restenosis. From Genetics to Therapeutics (Ed. Feuerstein GZ; Marcel Dekker Inc, New York);1997:225-40.
49. Wenger RH, Gassmann M. Oxygen(es) and the hypoxia-inducible factor-1. Biol Chem 1997;378:609-16.
50. Ema M *et al.* A novel bHLH-PAS factor with close sequence similarity to hypoxia-inducible factor 1 alpha regulates VEGF expression and is potentially involved in lung and vascular development. Proc Natl Acad Sci USA 1997;94:4273-78.
51. Tian H, McKnight SL, Russell DW. Endothelial PAS domain protein 1 (EPAS1), a transcription factor selectively expressed in endothelial cells. Genes Dev 1997;11:72-82.
52. Semenza GL. Transcriptional regulation by hypoxia-inducible factor-1. Trends Cardiovasc Med 1996;6:151-57.
53. Levy AP *et al.* Regulation of vascular endothelial growth factor by hypoxia and its modulation by the von Hippel-Lindau tumor suppressor gene. Kidn Intern 1997;51:575-78.
54. Wood SM, Gleadle JM, Pugh CQ, Hankinson O, Ratcliffe P. The role of the aryl hydrocarbon receptor nuclear transporter (ARNT) in hypoxic induction of gene expression. J Biol Chem 1996;271:15117-23.
55. Carmeliet P *et al.* Role of HIF-1alpha in hypoxia-mediated apoptosis, cell proliferation, and tumor angiogenesis. Nature 1998;394:485-90.
56. DiSalvo J *et al.* Purification and characterization of a naturally occurring vascular endothelial growth factor.placenta growth factor heterodimer. J Biol Chem 1995;270:7717-23.
57. Birkenhager R *et al.* Synthesis and physiological activity of heterodimers comprising different splice forms of vascular endothelial growth factor and placenta growth factor. Biochem J 1996;316:703-07.
58. Park JE, Chen HH, Winer J, Houck KA, Ferrara N. Placenta growth factor. Potentiation of vascular endothelial growth factor bioactivity, *in vitro* and *in vivo*, and high affinity binding to Flt-1 but not to Flk-1/KDR. J Biol Chem 1994;269:25646-54.
59. Maglione D, Guerriero V, Viglietto G, Delli Bovi P, Persico MG. Isolation of a human placenta cDNA coding for a protein related to the vascular permeability factor. Proc Natl Acad Sci USA 1991;88:9267-71.
60. Sawano A, Takahashi T, Yamaguchi S, Aonumura M, Shibuya M. Flt-1 but not KDR/Flk-1 tyrosine kinase is a receptor for placenta growth factor, which is related to vascular endothelial growth factor. Cell Growth Differ 1996;7:213-21.
61. Cao Y, Linden P, Shima D, Browne F, Folkman J. *In vivo* angiogenic activity and hypoxia induction of heterodimers of placenta growth factor/vascular endothelial growth factor. J Clin Invest 1996;98:2507-11.
62. Hauser S, Weich H. A heparin-binding form of placenta growth factor (PlGF-2) is expressed in human umbilical vein endothelial cells and in placenta. Growth Factors 1993;9:259-68.
63. Oloffson B *et al.* Vascular endothelial growth factor B, a novel growth factor for endothelial cells. Proc Natl Acad Sci USA 1996;93:2576-81.
64. Joukov V *et al.* A novel vascular endothelial growth factor, VEGF-C, is a ligand for the Flt4 (VEGFR-3) and KDR (VEGFR-2) receptor tyrosine kinases. Embo J 19996;15:290-98.
65. Lee J *et al.* Vascular endothelial growth factor-related protein: a ligand and specific activator of the tyrosine kinase receptor Flt4. Proc Natl Acad Sci USA 1996;93:1988-92.
66. Jing-Shan H *et al.* A novel regulatory function of proteolytically cleaved VEGF-2 for vascular endothelial and smooth muscle cells. FASEB J 1997;11:498-504.
67. Kukk E *et al.* VEGF-C receptor binding and pattern of expression with VEGFR-3 suggests a role in lymphatic vascular development. Development 1996;122:3829-37.
68. Jeltsch M *et al.* Hyperplasia of lymphatic vessels in VEGF-C transgenic mice. Science 1997;276:1423-25.
69. Orlandini M, Marconcini L, Ferruzzi R, Oliviero S. Identification of a c-fos-induced gene that

is related to the platelet-derived growth factor/vascular endothelial growth factor family. Proc Natl Acad Sci USA 1996;93:11675-80.
70. Yamada Y, Nezu J, Shimane M, Hirate Y. Molecular cloning of a novel vascular endothelial growth factor, VEGF-D. Genomics 1997;42:483-88.
71. Quinn TP, Peters KG, De Vries C, Ferrara N, Williams LT. Fetal liver kinase 1 is a receptor for vascular endothelial growth factor and is selectively expressed in vascular endothelium. Proc Natl Acad Sci USA 1993;90:7533-37.
72. Galland F *et al.* The FLT4 gene encodes a transmembrane tyrosine kinase related to the vascular endothelial growth factor receptor. Oncogene 1993;8:1233-40.
73. Soker S, Fidder H, Neufeld G, Klagsbrun M. Characterization of novel vascular endothelial growth factor (VEGF) receptors on tumor cells that bind VEGF165 via its exon 7-encoded domain. J Biol Chem 1996;271:5761-67.
74. Shalaby F, Ho J, Stanford WL *et al.* A requirement for Flk-1 in primitive and definitive hematopoiesis and vasculogenesis. Cell 1997;89:981-90.
75. Collen D, Lijnen HR. Basic and clinical aspects of fibrinolysis and thrombolysis. Blood 1991;78:3114-24.
76. Schneiderman J, Loskutoff DJ. Plasminogen activator inhibitors. Trends Cardiovasc Med 1991;1:99-102.
77. Blasi F *et al.* The urokinase receptor: structure, regulation and inhibitor-mediated internalization. Fibrinolysis 1994;8:182-88.
78. Saksela O, Rifkin D. Cell-associated plasminogen activation: regulation and physiological function. Annu Rev Cell Biol 1988;4:93-126.
79. Chapman HA Jr, Stone OL. Co-operation between plasmin and elastase in elastin degradation by intact murine macrophages. Biochem J 1984;222:721-28.
80. Carmeliet P *et al.* Urokinase-generated plasmin is a candidate activator of matrix metalloproteinases during atherosclerotic aneurysm formation. Nat Genet 1994;17:439-46.
81. Keyt BA *et al.* The carboxyl-terminal domain (111-165) of vascular endothelial growth factor is critical for its mitogenic potency. J Biol Chem 1996;271:7788-95.
82. Murphy G. Matrix metalloproteinases and their inhibitors. Acta Orthop Scand 1995;66:55-60.
83. Dollery CM, McEwan JR, Henney AM. Matrix metalloproteinases and cardiovascular disease. Circ Res 1995;77:863-68.
84. Mignatti P, Rifkin DB. Plasminogen activators and matrix metalloproteinases in angiogenesis. Enzyme Protein 1996;49:117-37.
85. Simpson AJ, Booth NA, Moore NR, Bennett B. Distribution of plasminogen activator inhibitor (PAI-1) in tissues. J Clin Pathol 1991;44;139-43.
86. Clowes AW, Clowes MM, Au YP, Reidy MA, Belin D. Smooth muscle cells express urokinase during mitogenesis and tissue-type plasminogen activator during migration in injured rat carotid artery. Circ Res 1990;67:61-67.
87. Bacharach E, Itin A, Keshet E. *In vivo* patterns of expression of urokinase and its inhibitor PAI-1 suggest a concerted role in regulating physiological angiogenesis. Proc Natl Acad Sci USA 1992;89:10686-90.
88. Carmeliet P *et al.* Urokinase-type but not tissue-type plasminogen activator mediates arterial neointima formation in mice. Circ Res 1997;81:829-39.
89. Carmeliet P *et al.* Inhibitory role of plasminogen activator inhibitor-1 in arterial wound healing and neointima formation. A gene targeting and gene transfer study in mice. Circulation 1997;96:3180-91.
90. Pepper MS, Sappino AP, Montesano R, Orci L, Vassalli J-D. Plasminogen activator inhibitor-1 is induced in migrating endothelial cells. J Cell Physiol 1992;153:129-39.
91. Pepper MS, Ferrara N, Orci L, Montesano R. Vascular endothelial growth factor induces plasminogen activators and plasminogen activator inhibitor-1 in microvascular endothelial cells. Biochem Biophys Res Comm 1991;181:902-06.

92. Pepper MS, Ferrara N, Orci L, Montesano R. Potent synergism between vascular endothelial growth factor and basic fibroblast growth factor in the induction of angiogenesis in vitro. Biochem Biophys Res Comm 1992;189:824-31.
93. Carmeliet P *et al.* Plasminogen activator inhibitor-1 gene-deficient mice. I. Generation by homologous recombination and characterization. J Clin Invest 1993;92:2746-55.
94. Carmeliet P *et al.* Plasminogen activator inhibitor-1 gene-deficient mice. II. Effects on hemostasis, thrombosis and thrombolysis. J Clin Invest 1993;92:2756-2760.
95. Dewerchin M *et al.* Generation and characterization of urokinase receptor-deficient mice. J Clin Invest 1996;97:870-78.
96. Carmeliet P *et al.* Receptor-independent role of urokinase-type plasminogen activator in arterial wound healing and intima formation in mice. J Cell Biol 1998;140:233-45.
97. Carmeliet P, Moons L, Ploplis V, Plow EF, Collen D. Impaired arterial neointima formation in mice with disruption of the plasminogen gene. J Clin Invest 1997;99:200-08.
98. Ploplis VA *et al.* Effects of disruption of the plasminogen gene on thrombosis, growth, and health in mice. Circulation 1995;92:2585-93.
99. Sabapathy KT *et al.* Polyoma middle-T induced vascular tumor formation: the role of the plasminogen activator/plasmin system. J Cell Biol 1997;137:953-63.
100. Katoh Y, Periasamy M. Growth and differentiation of smooth muscle cells during vascular development. Trends Cardiovasc Med 1996;6:100-06.
101. Hirschi KK, d'Amore PA. Pericytes in the microvasculature. Cardiovasc Res 1996;32:687-98.
102. Nehls V, Drenckhahn D. The versatility of microvascular pericytes: from mesenchyme to smooth muscle? Histochemistry 1993;99:1-12.
103. Owens GK. Regulation of differentiation of vascular smooth muscle cells. Phys Rev 1995;75:487-517.
104. Shepro D, Morel NML. Pericyte physiology. FASEB J 1993;7:1031-38.
105. Sims DE. Recent advances in pericyte biology. Implications for health and disease. Can J Cardiol 1991;7:431-43.
106. Diaz-Flores L, Gutierrez R, Varela H, Rancel N, Valladares F. Microvascular pericytes: a review of their morphological and functional characteristics. Histol Histopathol 1991;6:269-86.
107. Krause D, Kunz J, Dermietzel R. Cerebral pericytes-a second line of defense in controlling blood-brain barrier peptide metabolism. Adv Exp Med Biol 1993;331:149-52.
108. Nehls V, Denzer K, Drenckhahn D. Pericyte involvement in capillary sprouting during angiogenesis in situ. Cell Tissue Res 1992;270:469-74.
109. Peters A, Josephson K, Vincent SL. Effects of aging on the neuroglial cells and pericytes within area 17 of the rhesus monkey cerebral cortex. Anat Rec 1991;229:384-98.
110. Crocker DJ, Murad TM, Geer JC. Role of pericytes in wound healing. An ultrastructural study. Exp Mol Pathol 1970;13:51-65.
111. Nomura M *et al.* Possible participation of autocrine and paracrine vascular endothelial growth factors in hypoxia-induced proliferation of endothelial cells and pericytes. J Biol Chem 1995;270:28316-24.
112. Nakamura H. Electron microscopic study of the prenatal development of the thoracic aorta in the rat. Am J Anat 1988;181:406-18.
113. Jostereau FV, LeDouarin NM. The developmental relationship between osteocytes and osteoclasts: A study using the quail-chick nuclear marker in endochondral ossification. Dev Biol 1978;63:253-65.
114. Zerwes HG, Risau W. Polarized secretion of platelet-derived growth factor-like chemotactic factor by endothelial cesll in vitro. J Cell Biol 1987;105:2037-41.
115. Holmgren L, Glaser A, Pfeifer-Ohlsson S, Ohlsson R. Angiogenesis during human extraembryonic development involves th spatiotemporal control of the PDGF ligand and receptor gene expression. Development 1991;113:749-54.
116. Sato Y, Asada Y, Marutsuka K, Hatakeyama K, Sumiyoshi A. Tissue factor induces migration

of cultured aortic smooth muscle cells. Thromb Haemost 1996;75:389-92.
117. Marmur JD *et al.* Tissue factor is rapidly induced in arterial smooth muscle after balloon injury. J Clin Invest 1993;91:2253-59.
118. Nunes I *et al.* Structure and activation of the large latent transforming growth factor-beta complex. Int J Obes Relat Metab Disord 1996;20:S4-8.
119. Davis EC. Elastic lamina growth in the developing mouse aorta. J Histochem Cytochem 1995;43:1115-23.
120. Adachi E, Hopkinson I, Hayashi T. Basement-membrane stromal relationships: interactions between collagen fibrils and the lamina densa. Int Rev Cytol 1997;173:73-156.
121. Davis S *et al.* Isolation of angiopoietin-1, a ligand for the TIE2 receptor, by secretion-trap expression cloning. Cell 1996;87:1161-69.
122. Hanahan D. Signaling vascular morphogenesis and maintenance. Science 1997;277:48-50.
123. Dumont DJ *et al.* Dominant-negative and targeted null mutations in the endothelial receptor tyrosine kinase, tek, reveal a critical role in vasculogenesis of the embryo. Genes Dev 1994;8:1897-1909.
124. Kingsley DM. The TGF-beta superfamily: new members, new receptors, and new genetic tests of function in different organisms. Genes Dev 1994;8:133-46.
125. Battegay EJ. Angiogenesis: mechanistic insights, neovascular diseases, and therapeutic prospects. J Mol Med 1995;73:333-46.
126. Akhurst RJ, Lehnert SA, Faissner A, Duffie E. TGF beta in murine morphogenetic processes: the early embryo and cardiogenesis. Development 1990;108:645-56.
127. Pepper MS. Transforming growth factor-beta: vasculogenesis, angiogenesis and vessel wall integrity. Cytokine Growth Factor Res 1997;8:21-43.
128. Pepper MS, Vassalli JD, Orci L, Montesano R. Biphasic effects of transforming growth factor-beta 1 on *in vitro* angiogenesis. Exp Cell Res 1993;204:356-63.
129. Iruela-Arispe ML, Sage EH. Endothelial cells exhibiting angiogenesis *in vitro* proliferate in response to TFG-beta1. J Cell Biochem 1993;52:414-30.
130. Sunderkotter C, Steinbrink K, Goebeler M, Bhardwaj R, Sorg C. Macrophages and angiogenesis. J Leukoc Biol 1994;55:410-22.
131. Pertovaara L *et al.* Vascular endothelial growth factor is induced in response to transforming growth factor-β in fibroblastic and epithelial cells. J Biol Chem 1994;269:6271-74.
132. Waltenberger J. Modulation of growth factor action. Implications for treatment of cardiovascular diseases. Circ 1997;96:4083-94.
133. Koh GY *et al.* Targeted expression of transforming growth factor-β1 in intracardiac grafts promotes vascular endothelial cell DNA synthesis. J Clin Invest 1995;95:114-21.
134. Antonelli Orlidge A, Saunders KB, Smith SR, D'Amore PA. An activated form of transforming growth factor beta is produced by cocultures of endothelial cells and pericytes. Proc Natl Acad Sci USA 1989;86:4544-48.
135. D'Amore PA., Smith SR. Growth factor effects on cells of the vascular wall: a survey. Growth Factors 1993;8:61-75.
136. Metcalfe JC, Grainger DJ. TGF-β: implications for vascular disease. J Hum Hypertens 1995;9:679-683.
137. Nabel EG *et al.* Direct transfer of transforming growth factor beta 1 gene into arteries stimulates fibrocellular hyperplasia. Proc Natl Acad Sci USA 1993;90:10759-63.
138. Kanazaki T *et al. In vivo* effect of TGF-β1: enhanced intimal thickening by administration of TGF-β1 in rabbit arteries injured with a balloon catheter. Arterioscl Thromb Vasc Biol 1995;15:1951-57.
139. Majesky MW, Lindner V, Twardzik DR, Schwartz SM, Reidy MA. Production of transforming growth factor β1 during repair of arterial injury. J Clin Invest 1991;88:904-10.
140. Wolf YG, Rasmussen LM, Ruoslahti E. Antibodies against transforming growth factor-β1 suppress intimal hyperplasia in a rat model. J Clin Invest 1994;93:1172-78.

141. Battegay EJ, Raines EW, Seifert A, Bowen-Pope DF, Ross R. TGF-β induces bimodal proliferation of connective tissue cells via complex control of an autocrine PDGF loop. Cell 1990;63:515-24.
142. Stouffer GA, Owens GK. TGF-β promotes proliferation of cultured smooth muscle cells via both PDGF-AA-dependent and PDGF-AA-independent mechanisms. J Clin Invest 1994;93:2048-55.
143. Ross R. The pathogenesis of atherosclerosis: a perspective for the 1990s. Nature 1993;362:2844-50.
144. Oshima M, Oshima H, Taketo MM. TGF-beta receptor type II deficiency results in defects of yolk sac hematopoiesis and vasculogenesis. Dev Biol 1996;179:297-302.
145. Ross R, Raines EW, Bowen Pope DF. The biology of platelet-derived growth factor. Cell 1996;46:155-69.
146. Heldin CH, Westermark B. Platelet-derived growth factor: three isoforms and two receptor types. Trends Genet 1989;5:108-11.
147. Klagsbrun M, Dluz S. Smooth muscle cell and endothelial cell growth factors. Trends Cardiovasc Med 1993;3:213-17.
148. Risau W *et al.* Platelet-derived growth factor is angiogenic *in vivo*. Growth Factors 1992;7:261-66.
149. Martins RN, Chleboun JO, Sellers P, Sleigh M, Muir J. The role of PDGF-BB on the development of the collateral circulation after acute arterial occlusion. Growth Factors 1994;10:299-306.
150. Brown DM, Hong SP, Farrell CL, Pierce GF, Khouri RK. Platelet-derived growth factor BB induces functional vascular anastomoses in vivo. Proc Natl Acad Sci USA 1995;92:5920-24.
151. Lindner V, Reidy MA. Platelet-derived growth factor ligand and receptor expression by large vessel endothelium *in vivo*. Am J Pathol 1995;146:1488-97.
152. Battegay EJ, Rupp J, Iruela Arispe L, Sage EH, Pech M. PDGF-BB modulates endothelial proliferation and angiogenesis in vitro via PDGF beta-receptors. J Cell Biol 1994;125:917-28.
153. Grotendorst GR, Chang T, Seppa HE, Kleinman HK, Martin GR. Platelet-derived growth factor is a chemoattractant for vascular smooth muscle cells. J Cell Physiol 1982;113:261-66.
154. Corjay MH, Thompson MM, Lynch KR, Owens GK. Differential effect of platelet-derived growth factor versus serum-induced growth on smooth muscle alpha-actin and nonmuscle β-actin mRNA expression in cultured rat aortic smooth muscle cells. J Biol Chem 1989;264:10501-06.
155. Jawien A, Bowen-Pope DF, Lindner V, Schwartz SM, Clowes AW. Platelet-derived growth factor promotes smooth muscle migration and intimal thickening in a rat model of balloon angioplasty. J Clin Invest 1992;89:507-11.
156. Nabel EG, Plautz GE, Nabel GJ. Recombinant growth factor gene expression in vascular cells in vivo. Ann N Y Acad Sci 1994;714:247-52.
157. Ferns GAA *et al.* Inhibition of neointimal smooth muscle accumulation after angioplasty by an antibody to PDGF. Science 1991;253:1129-32.
158. Sirois MG, Simons M, Edelman ER. Antisense oligonucleotide inhibition of PDGFR-β subunit expression directs suprresion of intimal thickening. Circulation 1997;95:669-76.
159. Alpers CE, Seifert RA, Hudkins KL, Johnson RJ, Bowen-Pope DF. Developmental patterns of PDGFB-chain, PDGF receptor and alpha-acti expression in human glomerulonogenesis. Kidney Int 1992;42:390-99.
160. Soriano P. Abnormal kidney development and hematological disorders in PDGF beta-receptor mutant mice. Genes Dev 1994;8:1888-96.
161. Schatteman GC, Motley ST, Effman EL, Bowen-Pope D.F. Platelet-derived growth factor receptor alpha subunit deleted patch mouse exhibits severe cardiovascular dysmorphogenesis. Teratology 1995;51:351-66.
162. Edgington TS, Mackman N, Brand K, Ruf W. The structural biology of expression and function of tissue factor. Thromb Haemost 1991;66:67-79.

163. Camerer E, Kosto AB, Prydz H. Cell biology of tissue factor, the principal initiator of blood coagulation. Thromb Res 1996;81:1-41.
164. Broze GJ Jr. Tissue factor pathway inhibitor and the revised theory of coagulation. Annu Rev Med 1995;46:103-12.
165. Esmon CT. The protein C anticoagulant pathway. Arterioscler Thromb 1992;12:135-45.
166. Altieri DC. Xa receptor EPR-1. FASEB J 1995;9:860-65.
167. Coughlin SR. Molecular mechanisms of thrombin signaling. Semin Hematol 1994;31:270-77.
168. Zhang Y *et al.* Tissue factor controls the balance of angiogenic and antiangiogenic properties of tumor cells in mice. J Clin Invest 1994;94:1320-27.
169. Zhang Y *et al.* Intravenous somatic gene transfer with antisense tissue factor restores blood flow by reducing tumor necrosis factor-induced tissue factor expression and fibrin deposition in mouse Meth-A sarcomas. J Clin Invest 1996;97:2213-24.
170. Contrino J, Hair G, Kreutzer DL, Rickles FR. In situ detection of tissue factor in vascular endothelial cells: correlation with the malignant phenotype of human breast disease. Nat Med 1996;2:209-15.
171. Soifer SJ, Peters KG, O'Keefe J, Coughlin SR. Disparate temporal expression of the prothrombin and thrombin receptor genes during mouse development. Am J Pathol 1994;144:60-69.
172. Luther T *et al.* Tissue factor expression during human and mouse development. Am J Pathol 1996;149:101-13.
173. Bugge TH *et al.* Fatal embryonic bleeding events in mice lacking tissue factor, the cell-associated initiator of blood coagulation. Proc Natl Acad Sci USA 1996;93:6258-63.
174. Toomey JR, Kratzer KE, Lasky NM, Stanton JJ, Broze GJ Jr. Targeted disruption of the murine tissue factor gene results in embryonic lethality. Blood 1996;88:1583-87.
175. Toomey JR, Kratzer KE, Lasky NM, Broze GJJ. Effect of tissue factor deficiency on mouse and tumor development. Proc Natl Acad Sci USA 1997;94:6922-26.
176. Rosen E *et al.* Factor VII deficient mice develop normally but suffer fatal perinatal bleeding. Nature 1997;390:290-94.
177. Gasic GP, Arenas CP, Gasic TB, Gasic GJ. Coagulation factors X, Xa, and protein S as potent mitogens of cultured aortic smooth muscle cells. Proc Natl Acad Sci USA 1992;89:2317-20.
178. Connolly AJ, Ishihara H, Kahn ML, Farese RV Jr, Coughlin SR. Role of the thrombin receptor in development and evidence for a second receptor. Nature 1996;381:516-19.
179. Cui J, O'Shea KS, Purkayastha A, Saunders TL, Ginsburg D. Fatal haemorrhage and incomplete block to embryogenesis in mice lacking coagulation factor V. Nature 1996;384:66-68.
180. Suh TT *et al.* Resolution of spontaneous bleeding events but failure of pregnancy in fibrinogen-deficient mice. Genes Dev 1995;9:2020-33.
181. Huang ZF, Higuchi D, Lasky N, Broze GJJ. Tissue factor pathway inhibitor gene disruption produces intrauterine lehtality in mice. Blood 1997;90:944-51.
182. Ishihara H *et al.* Protease-activated receptor 3 is a second thrombin receptor in humans. Nature 1997;386:502-06.
183. Darrow AL *et al.* Biological consequences of thrombin receptor deficiency in mice. Thromb Haemost 1996;76:860-66.
184. Healy AM, Rayburn HB, Rosenberg RD, Weiler H. Absence of the blood-clotting regulator thrombomodulin causes embryonic lethality in mice before development of a functional cardiovascular system. Proc Natl Acad Sci USA 1995;92:850-54.
185. Shivdasani RA *et al.* Transcription factor NF-E2 is required for platelet formation independent of the actions of thrombopoietin/MGDF in megakaryocyte development. Cell 1995;81:695-704.
186. Bi L *et al.* Targeted disruption of the mouse factor VIII gene produces a model of haemophilia A. Nat Genet 1995;10:119-21.
187. Libby P, Schwartz D, Brogi E, Tanaka H, Clinton SK. A cascade model for restenosis. A

special case of atherosclerosis progression. Circulation 1992;86:III47-52.
188. Clowes AW, Reidy MA. Prevention of stenosis after vascular reconstruction: pharmacologic control of intimal hyperplasia-a review. J Vasc Surg 1991;13:885-91.
189. Schwartz SM, Reidy MA, O'Brien ER. Assessment of factors important in atherosclerotic occlusion and restenosis. Thromb Haemost 1995;74:541-51.
190. Kakuta T, Currier JW, Haudenschild CC, Ryan TJ, Faxon DP. Differences in compensatory vessel enlargement, not intimal formation, account for restenosis after angioplasty in the hypercholesterolemic rabbit model. Circulation 1994;89:2809-15.
191. van Leeuwen RT. Extracellular proteolysis and the migrating vascular smooth muscle cell. Fibrinolysis 1996;10:59-74.
192. Reidy MA, Irvin C, Lindner V. Migration of arterial wall cells. Expression of plasminogen activators and inhibitors in injured rat arteries. Circ Res 1996;78:405-14.
193. Fearns C, Samad F, Loskutoff DJ. Synthesis and localization of PAI-1 in the vessel wall. in Advances in vascular biology (Ed. van Hinsbergh, V.W.M.; Gordon and Breach Publishers, Camberwell, Victoria, Australia). 1996;207-27.
194. Newman KM *et al.* Cellular localization of matrix metalloproteinases in the abdominal aortic aneurysm wall. J Vasc Surg 1994;20:814-20.
195. Galis ZS, Sukhova GK, Kranzhöfer R, Clark S, Libby P. Macrophage foam cells from experimental atheroma constitutively produce matrix-degrading proteinases. Proc Natl Acad Sci USA 1995;92:402-06.
196. Galis ZS *et al.* Cytokine-stimulated human vascular smooth muscle cells synthesize a complement of enzymes required for extracellular matrix digestion. Circ Res 1994;75:181-89.
197. Halpert I *et al.* Matrilysin is expressed by lipid-laden macrophages at sites of potential rupture in atherosclerotic lesions and localizes to areas of versican deposition, a proteoglycan substrate for the enzyme. Proc Natl Acad Sci USA 1996;93:9748-53.
198. Irizarry E *et al.* Demonstration of interstitial collagenase in abdominal aortic aneurysm disease. J Surg Res 1993;54:571-74.
199. Sakalihasan N, Delvenne P, Nusgens BV, Limet R, Lapiere CM. Activated forms of MMP2 and MMP9 in abdominal aortic aneurysms. J Vasc Surg 1996;24:127-33.
200. Carmeliet P *et al.* A model for arterial neointima formation using perivascular electric injury in mice. Am J Pathol 1997;150:761-777.
201. Herbert JM, Lamarche I, Carmeliet P. Urokinase- and tissue-type plasminogen activator are required for the mitogenic and chemotactic effects of bovine fibroblast growth factor and platelet-derived growth factor-BB for vascular smooth muscle cells. J Biol Chem 1997;272:23585-91.
202. Stefansson S, Lawrence DA. The serpin PAI-1 inhibits cell migration by blocking integrin alpha V beta3 binding to vitronectin. Nature 1996;383:441-43.
203. Lijnen R *et al.* Function of the plasminogen/plasmin and matrix metalloproteinase systems after vascular injury in mice with targeted inactivation of fibrinolytic genes. Arterioscl Thromb Vasc Biol 1998;18:1035-45.
204. Lucas A *et al.* Virus-encoded serine proteinase inhibitor SERP-1 inhibits atherosclerotic plaque development after balloon angioplasty. Circulation 1996;94:2890-900.
205. Shi C, Russell ME, Bianchi C, Newell JB, Haber E. Murine model of accelerated transplant arteriosclerosis. Circ Res 1994;75:199-207.
206. Ploplis V, French E, Carmeliet P, Collen D, Plow E. Plasminogen deficiency differentially affects recruitment of inflammatory cell populations in mice. Blood 1998;91:2005-9.
207. Belkin M, Donaldson MC, Whittemore AD. Abdominal aortic aneurysms. Curr Opin Cardiol 1994;9:581-90.
208. Ernst CB. Abdominal aortic aneurysm. N Engl J Med 1993;328:1167-72.
209. Halloran BG, Baxter BT. Pathogenesis of aneurysms. Semin Vasc Surg 1995;8:85-92.
210. Juhan-Vague I, Collen D. On the role of coagulation and fibrinolysis in atherosclerosis. Ann

Epidemiol 1992;2:427-438.
211. Hamsten A, Eriksson P. Fibrinolysis and atherosclerosis: an update. Fibrinolysis 1994;8:253-62.
212. Schneiderman J *et al.* Increased type 1 plasminogen activator inhibitor gene expression in atherosclerotic human arteries. Proc Natl Acad Sci USA 1992;89:6998-7002.
213. Hamsten A *et al.* Plasminogen activator inhibitor in plasma: risk factor for recurrent myocardial infarction. Lancet 1987;2:3-9.
214. Schneiderman J *et al.* Expression of fibrinolytic genes in atherosclerotic abdominal aortic aneurysm wall. A possible mechanism for aneurysm expansion. J Clin Invest 1995;96:639-645.
215. Lupu F *et al.* Plasminogen activator expression in human atherosclerotic lesions. Arterioscler Thromb Vasc Biol 1995;15:1444-55.
216. Plump AS *et al.* Severe hypercholesterolemia and atherosclerosis in apolipoprotein E-deficient mice created by homologous recombination in ES cells. Cell 1992;71:343-53.
217. Xiao Q *et al.* Plasminogen deficiency accelerates vessel wall disease in mice predisposed to atherosclerosis. Proc Natl Acad Sci USA 1997;94:10335-40.
218. Chapman HA Jr, Stone OL, Vavrin Z. Degradation of fibrin and elastin by intact human alveolar macrophages in vitro. Characterization of a plasminogen activator and its role in matrix degradation. J Clin Invest 1984;73:806-15.
219. Libby P. Molecular basis of the acute coronary syndromes. Circulation 1995;91:2844-50.
220. Fuster V. Mechanisms leading to myocardial infarction: insights from studies of vascular biology. Circulation 1994;90:2126-46.
221. Hudlicka O, Brown MD. Postnatal growth of the heart and its blood vessels. J Vasc Res 1996;33:266-87.

19. CROSSTALK BETWEEN THE ESTROGEN RECEPTOR AND THE INSULIN-LIKE GROWTH FACTOR (IGF-1) RECEPTOR. IMPLICATIONS FOR CARDIAC DISEASE

Christian Grohé, Rainer Meyer, and Hans Vetter

Introduction

There are significant gender-based differences in cardiac diseases such as cardiac hypertrophy and hypertensive heart disease [1-3]. As the incidence of cardiac disease in women increases after the menopause [1], it has been postulated that estrogen plays a role in the morbidity of heart disease. The mechanisms how estrogen affects this process is currently under investigation [4,5]. Recent findings have demonstrated that estrogen exerts a large array of non-genomic and genomic effects on the myocardium [4-7]. In this context, we have previously shown that cardiac myocytes and cardiac fibroblasts contain functional estrogen receptors (ER) which activate a subset of cardiac target genes i.e connexin 43 [4]. The ER belongs to a class of steroid hormone receptor which are activated upon ligand binding, however recent observations demonstrate that the ER is also activated through phosphorylation-dependent signaling pathways [8,9]. These signaling pathways are shared with a variety of different growth factors i.e. the insulin-like growth factor (IGF-1). Growth factors like IGF-1 activate intracytoplasmic signal transduction cascades through binding of specific plasma-membrane bound receptor-tyrosine kinases [10]. The level of IGF-1 has been associated with cardiac disease i.e. hypertrophic cardiomyopathy in human patients has been linked with overexpression of IGF-1 in cardiac tissue [11]. Furthermore, the specific overexpression of the IGF-1 cDNA in mice leads to cardiac hypertrophy and reveals gender-based differences [10]. Interestingly, IGF-1 has also been shown to activate the ER in tumor cell lines like human breast cancer cells [12]. Therefore, we hypothesized that the signaling pathway of IGF-1 and estrogen might also interact in myogenic growth and differentiation and that this interaction may well play a role in the pathogenesis of cardiac disease. To further elucidate these mechanisms we investigated the expression of ERs and the influence of IGF-1 on ER activation in an estrogen-responsive myogenic cell model (L6 rat skeletal myoblasts) [13].

P.A. Doevendans et al. (eds.), Cardiovascular specific gene expression, 227-35.

Materials and methods

All chemicals were obtained from Merck (Darmstadt, Germany) unless otherwise specified.

Cell culture techniques
L6 rat skeletal myoblasts were obtained from American Type Culture Collection, and maintained in 10% fetal calf serum (FCS) in Dulbecco's modified eagle medium (DMEM) as described before [13]. Phenol red-free medium was used throughout all experiments as phenol red is known to act as a weak estrogen.

Immunofluorescent staining of the ER
Cells were grown on uncoated glass coverslips for immunofluorescent staining as described before [13]. Cells were fixed with 2% paraformaldehyde and phosphate buffered saline. Immunofluorescent studies of ER α were performed with a 1:20 dilution of a polyclonal rabbit antibody (kind gift of K. Yoshinaga, NIH, Bethesda, Maryland). Studies in which the primary antibody was omitted served as negative controls. Cells were studied following 24 hrs incubation in the absence or presence of 10^{-9} M 17β-estradiol (E2).

Immunoblot analysis
L6 cells were cultured in serum free DMEM without phenol red for 24 hrs prior to stimulation with E2 (10^{-9} M) for 24 hrs. Myoblasts were lysed in 1 ml of the following buffer: 50 mM NaCl, 20 mM Tris (pH 7.4), 50 mM NaF, 50 mM EDTA, 20 mM sodium pyrophosphate ($Na_4P_2O_7$), 1 mM sodium orthovanadate (Na_3VO_4), 1% triton X-100, 1 mM PMSF, 0.6 mg/ml leupeptin and 10 μg/ml aprotinin. Protein content was measured with a standard Bradford assay. Protein measurement was controlled by coomassie brilliant blue G-colloidal (Sigma Biochemical, St. Louis) staining of a similar SDS-PAGE as used for immunoblotting. ER α and β were detected with a monoclonal ER α antibody (Bio-mol, Hamburg, Germany, SRA-1000, 1:500) and a polyclonal ER β antibody (Dianova, Hamburg, Germany, PA1-310 1:500), respectively. Detection was performed with the Enhanced Chemiluminescence technique (ECL, Amersham, Braunschweig, Germany). Total cellular lysates (40μg/lane) were separated by SDS-PAGE in a 7.5% gel and transferred to nitrocellulose membranes (Hybond C, Amersham).

Transfection assay
Cells were grown to a density of 60–70% confluency and transfected using a liposome-conjugated transfection technique according to the manufacturer's instructions (DOTAP, Boehringer-Mannheim, Mannheim, Germany) as described before [13]. Cells were transfected with ERE-*LUC* a reporter containing three copies of an estrogen-responsive element from the vitellogenin-promoter driving expression of the firefly Luciferase cDNA (kind gift of C. Glass). After 24 hours, the transfection medium was removed and cells were maintained in phenol red-free DMEM with and without E2 and/or ICI 182780, a pure estrogen antagonist (kind gift of Dr. A. Wakeling,

Zeneca Pharmaceuticals). The specific IGF-1 analogue H 1356 (Bachem, Heidelberg, Germany) was added in a subset of transfection studies to investigate IGF-1 receptor inhibition on the experimental results. An equal volume of vehicle alone (0.1% ethanol) was added to control cells. Following 24 hrs of incubation, cells were harvested and luciferase activity was determined on a luminometer (C-Gem, Optocom 1). In a subset of each transfection series, cells were transfected with pL7RH-βGal (SV-40 promoter including a nuclear localization signal driving the β-galactosidase cDNA) to determine the transfection efficiency (data not shown).

Statistical analysis

All reported values are mean ±SEM. Statistical comparisons were made by Student t-test. Statistical significance was assumed if a null hypothesis could be rejected at the $p<0.05$ level.

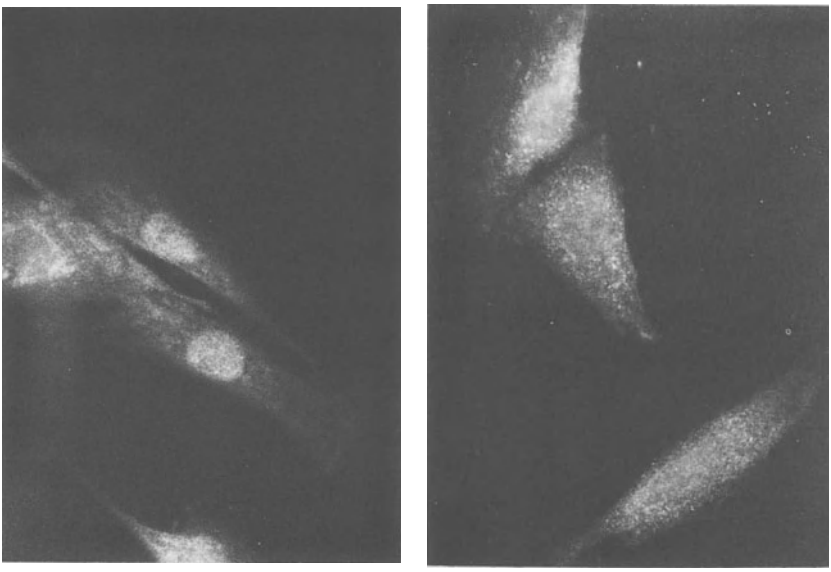

Figure 1. *L6 skeletal myoblasts express ER protein. Unstimulated (a) and E2 (10^{-6} M) stimulated (b) cells grown on glass cover slips were immunostained with an anti-ER α primary antibody and a DTAF-conjugated secondary antibody. In the absence of E2 (a), a mixed cytoplasmatic and nuclear distribution of the ER could be demonstrated. After treatment with E2 the majority of the ER protein was found in the nucleus (b). Magnification 1200X.*

Results

To further elucidate the mechanisms underlying the influence of estrogen on myogenic growth, we investigated the expression pattern of ERs α and β in L6 skeletal myoblasts. As shown in figure 1, ER α is detectable by immunofluorescent staining in this cell line. In the absence of estrogen, ER α is evenly distributed in the cytoplasm and in the nucleus (figure 1a). After stimulation with estrogen (10^{-9} M E2), the immunofluorescent signal translocates to the nucleus (figure 1b). This suggests that the ER translocates to the nucleus after binding its specific ligand in this myogenic cell model and appears to be funcionally competent.

In a next step, we investigated by immunoblotting whether ERs of both isoforms are expressed in L6 skeletal myoblasts. As shown in figure 2, ER α and ER β protein could be detected in cellular lysates obtained from L6 cells. The protein content of both receptors increased after stimulation with 10^{-9} M E2 for 24 hours revealing a positive autoregulation of ERs of both isoforms. Coincubation with the pure anti-estrogen ICI 182780 inhibited the upregulation of the ER protein demonstrating the specifity of the stimulation by E2. Interestingly, coincubation with the IGF-1 antagonist H1356 revealed that activation of the ER was inhibited in experiments where the IGF-1 antagonist H1356 was added to E2 stimulated cells.

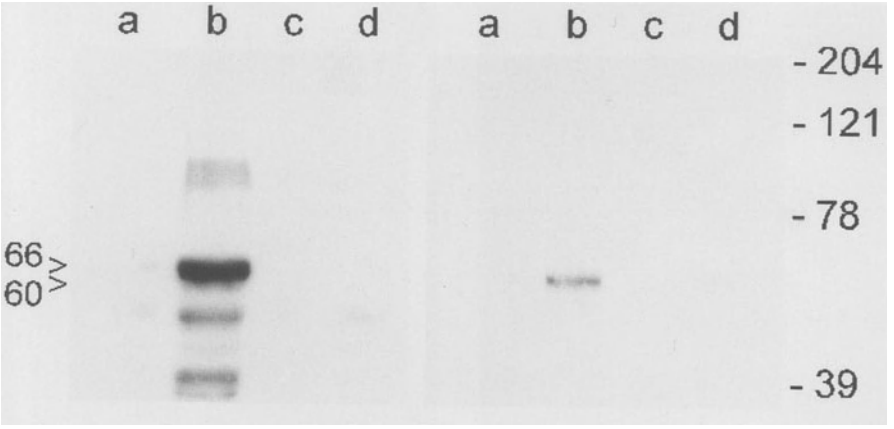

Figure 2. *L6 skeletal myoblasts express ER α and β protein. Total cellular lysates of rat L6 skeletal myoblasts were subjected to SDS-PAGE, immunoblotted with an anti-ER α (left panel) and β (right panel) primary antibody and visualized by a chemiluminescence technique. In the absence of estrogen (a), only a very weak signal could be detected. The amount of protein increased after stimulation with E2 (10^{-9} M) (b). Experiments with the anti-estrogen ICI 182780 (10^{-7} M) (c) or the IGF-1 receptor antagonist H1356 (10^{-7} M) (d) showed that coincubation of these compounds with E2 (10^{-9} M) inhibited the activation of the respective receptor protein . One of three similar studies is shown.*

To further elucidate the influence of IGF-1 on ER activation in L6 cells, a series of transfection assays was carried out. IGF-1 activated the expression of the estrogen-responsive reporter plasmid (ERE-*LUC*) as shown in figure 3. These data show that IGF-1 stimulates the expression of ERE-*LUC*. Again, coincubation experiments with the specific IGF-1 receptor antagonist H1356 revealed that IGF-1 receptor blockade inhibited this stimulation. These data suggest that IGF-1 induced activation of ERE-*LUC* is mediated through the IGF-1 receptor. In control experiments where the estrogen antagonist ICI 182780 was added to the media in the presence of estrogen, no activation of the estrogen-responsive reporter construct was observed demonstrating the specificity of this activation. Taken together these data demonstrate that IGF-1 stimulates an estrogen-responsive reporter construct and that this effect is likely to be mediated through the IGF-1 receptor.

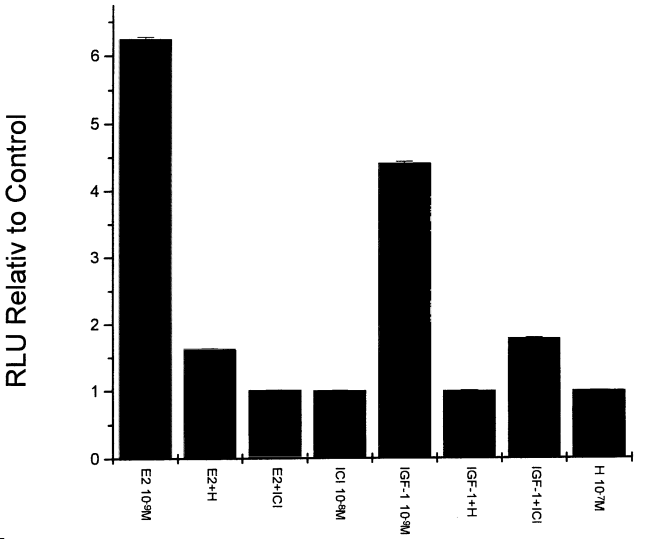

Figure 3. *E2 and IGF-1 activate a estrogen-responsive reporter in L6 skeletal myoblasts. Bar graph shows activation of an estrogen-responsive reporter plasmid in L6 skeletal myoblasts. Cells were transfected and grown in the absence or presence of 17β-estradiol (E2) (10^{-9} M) or IGF-1 (10^{-9} M) and harvested after 24 hours. Experiments with the IGF-1 receptor antagonist H1356 (10^{-7} M) (H) or the anti-estrogen ICI 182780 (ICI, 10^{-7} M) showed that coincubation of these compounds with E2 (10^{-9} M) inhibited the activation of the estrogen-responsive luciferase reporter plasmid. Luciferase activity is shown relative to control cells that were not exposed to hormones. Bars represent the mean luciferase activity with SEM (n=9, *p<0.01).*

Discussion

Recent observations suggest that estrogen may well play a role in the pathogenesis of cardiac disease [1-5]. The incidence of a large array of cardiac diseases such as cardiac hypertrophy and hypertensive heart disease shows a significant increase in postmenopausal women and the role of estrogen in this process is currently under investigation. The steroid hormone family of estrogens binds to a specific cytoplasmatic receptor, which belongs to the class of nuclear receptors. After ligand binding, the ER

translocates to the nucleus and regulates the transcription of downstream target genes. A variety of rapid non-genomic mechanisms by which estrogen influences its cellular targets, however, remain to be elucidated. Recently, a second ER called ERβ has been identified [14,15]. This second ER can form heterodimers with the classic ER now designated ERα. ERα and ERβ, however, respond differentially to ligand binding of estrogenic hormones [16]. In addition, the expression pattern of ERβ appears to be different from ERα [17]. The identification of a second ER has extended our understanding of the complex regulatory network involved in estrogenic effects. The fact, that at least two different isoforms of the ER exist raises the question if these two isofroms serve different functions in their respective cellular context. We here show that skeletal myoblasts contain functional ERs of both isoforms and that these receptors are functionally competent. The expression of the different ERs may help to identify the mechanisms involved in these processes i.e. the characterization of non-genomic effects seen upon incubation with estrogen in the cytoplasm [6-9]. In this context, it was shown that growth factors like IGF-1 activate the ERα [12,18-20], but the mechanisms underlying these observations are poorly understood.

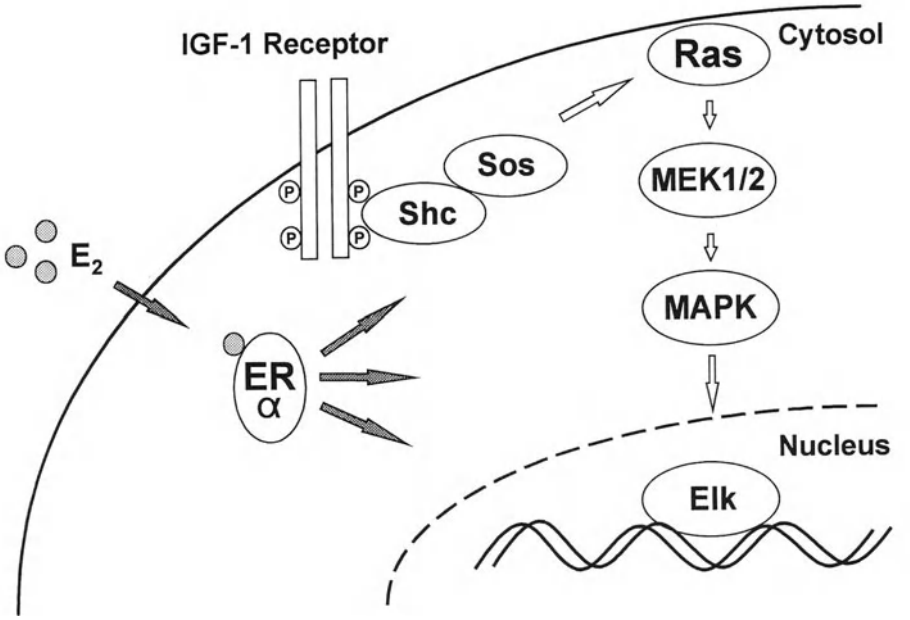

Figure 4. *IGF-1 receptor and ER signal cascades from plasma membrane to nucleus. Diagram shows the intracellular signal cascades which are involved in IGF-1 and estrogen induced intracytoplasmic transduction pathways. Activation of downstream targets by IGF-1 and estrogen and potential interactions are indicated by arrows.*

Previously, it has been shown that the IGF-1 receptor and the downstream adaptor protein insulin receptor substrate (IRS) are phosphorylated by estrogen [19]. This observation suggests a possible interaction between the signaling pathways and mode of activation of both the ER and the IGF-1 receptor. We here show that in a myogenic

cell model inhibition of IGF-1 receptor autophosphorylation (IGF-1 antagonist H1356) modulates the activation of an estrogen-responsive reporter plasmid by IGF-1. This suggests that activation of the ER by IGF-1 can be blocked at the plasma membrane level. The IGF-1 antagonist (H1356) is a peptide analogue which specifically inhibits the autophosphorylation of the relevant receptor tyrosine kinase, the IGF-1 receptor. Inhibition of the receptor tyrosine kinase ultimately leads to inactivation of the respective downstream signaling cascade in the cytoplasm. The extracellular receptor kinases (ERK 1/2 also known as Mitogen Activated Protein Kinases) are likely candidates of this cascade as IGF-1 has been shown to phosphorylate these kinases and the ER is phosphorylated by these kinases [8]. We have shown that estrogen activates the ERK 1/2 kinases in adult cardiac myocytes and that these phosphorylation-dependent kinases stimulate downstream nuclear targets such as ELK-1 [21].

Conclusion

It is likely that the intracellular signaling cascades which are involved in the regulation of both growth relevant stimuli, i.e. IGF-1 and hormonal stimuli, i.e. estrogen, may be shared by these agonists (see figure 4). This mode of action may help to explain the cellular network involved in the regulation of estrogenic effects at the non-genomic level. It has been a longstanding controversy whether estrogen binds to a potential membrane receptor as described by Pappas et al. [22]. However, the genomic structure of this membrane receptor has yet to be determined. It appears to be a feasible hypothesis that estrogen directs its plasma membrane bound effects through the activation of specific receptor tyrosine kinases as earlier reports show autophosphorylation of the IGF-1 receptor by estrogen [19]. The role of plasma membrane bound receptors in the regulation of estrogenic effects deserves further attention and is critical for the understanding of rapid non-genomic effects of estrogen. Taken together our data show an interaction between the signaling pathway of the IGF-1 receptor and the ER in a myogenic cell model. The observation that growth factors like IGF-1 and estrogen share identical signaling pathways in a myogenic cell model may help to explain the rapid non-genomic effects of estrogen on myogenic growth and differentiation. The understanding of these processes will finally lead to a better understanding of the beneficial effects of estrogen on the cardiovascular system.

Acknowledgements

This work was supported by a grant from the Deutsche Forschungsgemeinschaft. The authors would like to thank Kerstin Löbbert, Simone Nüdling and Stefan Kahlert for their expertise and contribution to this work. The authors would also like to thank Dr. A. E Wakeling (Zeneca Pharmaceuticals, Cheshire, UK) for sharing the pure anti-estrogen ICI 182780.

References

1. Marcus R, Krause L, Weder AB, Dominguez-Mejia AN, Schork D, Julius S. Sex-specific determinants of increased left ventricular mass in the Tecumseh blood pressure study. Circulation 1994;90:928–36.
2. Gardin, JM, Wagenknecht LE, Anton-Culver H, Flack J, Gidding S, Jurosaki T, Wong ND, Manolio TA. Relationship of cardiovascular risk factors to echocardiographic left ventricular mass in healthy young black and white adult men and women. Circulation 1995;92:380–87.
3. Dahlberg ST. Gender difference in the risk factors for sudden cardiac death. Cardiology 1990;77:S31–40.
4. Grohé C, Kahlert S, Löbbert K, Karas RH, Stimpel M, Vetter H, Neyses L. Cardiac myocytes and cardiac fibroblasts contain functional estrogen receptors. FEBS Lett 1997;416:107–12.
5. Grohé C, Kahlert S, Löbbert K, van Eickels M, Stimpel M, Vetter H, Neyses L. Effects of moexiprilat on estrogen-stimulated cardiac fibroblast growth. Br J Pharm 1997;121:1350–54
6. Morley P, Whitfield JF, Vanderhyden BC, Tsang BK, Schwartz JL. A new, nongenomic estrogen action: the rapid release of intracellular calcium. Endocrinology 1992;131:1305–12
7. Jiang C, Poole-Wilson PA, Sarrel PM., Mochizuki S, Collins P, Mcleod KT. Effect of 17β-oestradiol on concentration, Ca^{2+} current and intracellular free Ca^{2+} in guinea-pig isolated cardiac myocytes. Br J Pharm 1992;106:739-45.
8. Kato S, Endoh H, Masuhiro Y, Kitamoto T, Uchiyama S, Sasaki H, Masushige S, Gotoh Y, Nishida E, Kawashima H, Metzger D, Chambon P. Activation of the estrogen receptor through phosphorylation by mitogen-activated protein kinase. Science 1995;270:1491–94.
9. Migliaccio A, Di Domenico M, Castoria G , deFalco A, Bontempo P, Nola, E, Auricchio F.Tyrosine kinase/p21ras/MAP-kinase pathway activation by estradiol-receptor complex in MCF-7 cells. EMBO J 1996;15:1292–300.
10. Reiss K, Wie C, Ferber A, Kajstura J, Li P, Li B, Olivetti G, Homcy CJ, Baserga R, Anversa P. Overexpression of insulin-like growth factor-1 in the heart is coupled with myocyte proliferation in transgenic mice. Proc Natl Acad Sci 1996;93:8630–35.
11. Li R, Li G, Mickle D, Weisel RD, Merante F, Luss H, Rao V, Christakis GT, Williams WG. Overexpression of transforming growth factor-β1 and insulin-like growth factor-1 in patients with idiopathic hypertrophic cardiomyopathy. Circulation 1997;96:874–81.
12. Lee AV, Weng C N, Jackson JG, Yee D. Activation of estrogen receptor-mediated gene transcription by IGF-1 in human breast cancer cells. J Endocrinol 1997;152:39–47.
13. Kahlert S, Grohé C, Karas RH, Löbbert K, Neyses L, Vetter H. Effects of estrogen on skeletal myoblast growth. Biophys Biochem Res Comm 1997;232:373–78.
14. Kuiper GGJM, Enmark E, Pelto-Huikko M, Nilsson S,Gustafsson JA. Cloning of a novel estrogen receptor expressed in rat prostrate and ovary. Proc Natl Acad Sci 1996;93:5925–30.
15. Mosselman S, Polman J, Dijkema R. ERβ: identification and chracterization of a novel human estrogen receptor. FEBS Lett 1997;392:49–53.
16. Paech K, Webb P, Kuiper GGJM, Nilsson S, Gustaffson JA, Kushner PJ, Scanlan TS. Differential ligand activation of estrogen receptors ERα and ERβ at AP 1 sites. Science 1997;277:1508–10.
17. Saunders PTK, Maguire SM, Gaughan J, Milar MR. Expression of oestrogen receptor beta (ERβ) in multiple rat tissues visualised by immunohistochemistry. J Endocrinol 1997;154:R13–R16
18. Sahlin L, Norstedt G., Eriksson H. Estrogen regulation of the estrogen receptor and insulinlike growth factor-I in the rat uterus: a potential coupling between effects of estrogen and IGF-1. Steroids 1994;59:421–30.
19. Richards RG, Diaugustine RP, Petrusz P, Clark GC, Sebastian J. Estradiol stimulates tyrosine phosphorylation of the insulin-like growth factor-1 receptor and insulin receptor substrate-1 in the uterus. Proc Natl Acad Sci USA 1996;93:12002–07.

20. Kleinman D, Karas M, Roberts CT, Leroith D, Philip M, Segev Y, Levy J, Sharoni Y. Modulation of insulin-like growth factor I (IGF-1) receptors and membrane-associated IGF-binding proteins in endometrial cancer cells by estradiol. Endocrinology 1995;140:2531-37.
21. Grohé C, Kahlert S, Nüdling S, Vetter H, Meyer R. Oestrogen activates the MAPK and JNK signal transduction pathway in rat cardiac myocytes. J Physiol (abstract) 1997;11:821.
22. Pappas TC, Gametchu B, Watson CS. Membrane estrogen receptors identified by multiple antibody labeling and impeded-ligand binding. FASEB J 1995;9:404–10.

20. EXPRESSION OF BASIC HELIX-LOOP-HELIX PROTEINS AND SMOOTH MUSCLE PHENOTYPE IN THE ADULT RAT AORTA

Paul R. Kemp, and James C. Metcalfe

Introduction

Smooth muscle cells play a major role in the formation of the vascular lesions found in atherosclerosis and restenosis injury after angioplasty [1,2]. The smooth muscle cells found in such lesions show reduced levels of many markers of the differentiated state of smooth muscle (e.g. SM22α, smooth muscle-myosin heavy chain {SM-MHC} and smooth muscle α-actin {Smα-actin} [3,4]). In some instances the smooth muscle-specific isoforms of contractile proteins (e.g. SM-MHC) are replaced by their non-muscle equivalents. In addition to loss of expression of smooth muscle-specific genes, intimal vascular smooth muscle cells (VSMCs) express genes that are associated with calcium metabolism in bone tissue (e.g. matrix GLA protein and osteopontin [5-8]). There has been significant progress towards identifying the factors involved in promoting or inhibiting smooth muscle cell proliferation in these pathologic conditions. However, little is known about the mechanisms that regulate the differentiated state of this cell type or the factors involved in defining smooth muscle phenotype [9]. Given the phenotypic changes seen in VSMC in pathological conditions, the systems which control the differentiated state of smooth muscle may play a significant role in lesion formation.

Transcription regulation in vascular smooth muscle cells

There are several approaches to defining the factors important in determining the phenotype of the VSMCs in the adult vessel wall. We and others have isolated and characterized the promoter regions of genes whose expression is restricted to smooth muscle in adult animals [10-12]. These promoters contain binding sites for several families of transcription factors, members of which are important in the expression of tissue-specific genes. For example the SM-MHC, SMα-actin and SM22α promoters contain multiple CArG and E-boxes which bind the MADS box transcription factor

P.A. Doevendans et al. (eds.), Cardiovascular specific gene expression, 237-44.

SRF and members of the bHLH family of transcription factors respectively. Analysis of the SMα-actin gene has shown that the CArG boxes in the proximal promoter region are important for the expression of this gene, suggesting that SRF or an SRF-like factor plays a major role in determining the level of expression of this gene in smooth muscle [11]. CArG boxes have also been shown to be important in the expression of SM22α in vascular but not visceral smooth muscle [13]. Whilst these studies have defined the factors that directly activate a smooth muscle-specific gene, they do not necessarily identify the hierarchy of factors which determine the overall phenotype of VSMCs under normal or pathological conditions.

Another approach to identifying the factors important in defining adult VSMC phenotype is to determine which transcription factors are expressed in smooth muscle and whether the expression of these factors correlates with smooth muscle phenotype. Several studies have screened for members of transcription factor families known to be involved in the determination of phenotype in other systems. One study by Miano et al. [14] showed that neonatal smooth muscle cells express a variety of Hox genes including HoxA5, HoxA11, HoxB1, HoxB7, and HoxC9, whereas screening an adult smooth muscle cell library in the same manner did not detect any of these genes. Using a similar screening approach Gorski et al. identified Gax (growth associated homeobox) [15], the expression of which is restricted to the cardiovascular system. Gax is expressed in the non-proliferating cells of the normal vessel wall and Gax expression is markedly reduced following balloon angioplasty. Over-expression of Gax has also been shown to inhibit VSMC proliferation and induce apoptosis. Another cardiovascular specific Hox gene, Hox 1.11, was identified by a similar screening method [16]. VSMCs have been shown to express all four known MEF-2 genes [17]. In skeletal muscle MEF-2 genes are important in driving the expression of muscle-specific genes. However, in spite of the presence of MEF-2 binding sites in the SM-MHC and SM22α promoters and the observation that MEF-2B can bind one of these binding sites, MEF-2 gene expression is not detectable in the normal adult vessel wall. Furthermore, following balloon angioplasty of the rat carotid artery MEF-2 expression increases even though the cells de-differentiate [17]. These data suggest that unlike the skeletal muscle system, MEF-2 genes do not play an important role in the adult VSMC phenotype. Another family of genes which is known to play an important role in determining a number of cell phenotypes is the bHLH family of transcription factors. We have examined the expression of Id1 and Id2 in rat aortic VSMCs as they de-differentiate *in vitro*. Id expression correlated with serum stimulation rather than SM-MHC content implying that it was not involved in the de-differentiation process [18]. Furthermore, whilst antisense Id expression promoted the formation of myotubes in MyoD transfected smooth muscle cells, it did not induce the expression of SM-MHC in a clone of neonatal VSMCs *in vitro* [19,20]. However, Id3 has recently been shown to be expressed in intimal VSMCs following balloon angioplasty but not in the VSMCs of the uninjured vessel wall [21].

The set of transcription factors which defines the adult VSMC phenotype may overlap with those involved in commitment to the VSMC lineage during development. Therefore a further approach to identifying genes involved in the adult is to look for genes which are restricted in their expression to the embryonic vasculature. To date

there are no reports of transcription factor genes which are expressed exclusively in embryonic vascular smooth muscle. However, many transcription factors expressed in the developing heart are also expressed in the developing vasculature. For example, the bHLH transcription factors dHand and eHand are expressed in the developing heart and aorta as well as in other cell populations derived from the neural crest and in the developing gut [22-24]. Targeted deletion of one of these genes in mice, dHand, resulted in embryonic lethality at embryonic day 10.5 with a failure of heart development [25]. In addition to the loss of right ventricle formation the aortic sac did not form properly and analysis of the expression of SM22α showed a failure in VSMC development [25].

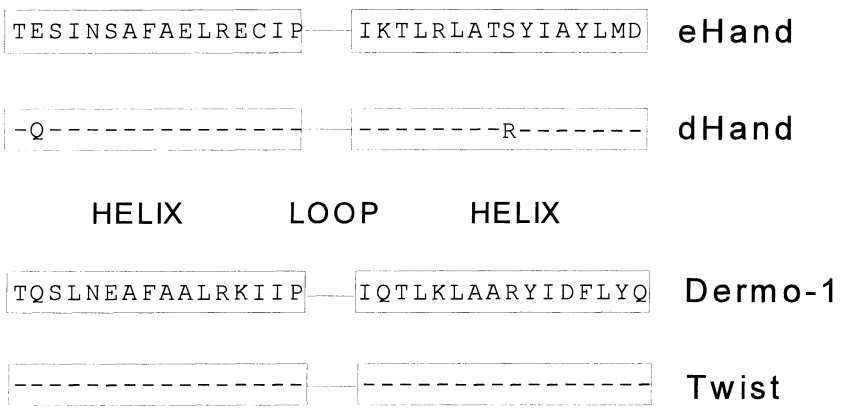

Figure 1. *Alignment of the helix-loop-helix domains of dHand, eHand, Twist and Dermo-1.*

The role of helix-loop-helix transcription factors in VSMC differentiation

Since expression of eHand was also found in the gut smooth muscle of adult mice, we decided to use degenerate primers to the HLH domain of eHand for a PCR screen for bHLH transcription factors in adult rat aortic smooth muscle. This screen isolated sequences consistent with the presence of four bHLH proteins and we have used PCR from specific primers to confirm the identity of these genes as dHand, eHand, Twist and Dermo-1. Comparison of the HLH domains of the four genes allows them to be grouped into two pairs. The two Hand genes have almost identical HLH domains (one amino acid difference in each helix, figure 1) and the HLH domains of Twist and Dermo-1 are identical. The HLH regions of the two pairs, however, are substantially different (figure 1). The Hand gene proteins are 48% identical overall but over an 80 amino acid region covering the bHLH regions the identity is 80%. The structure of the genes for these proteins are also similar with the mRNA encoded by two exons. In addition to these structural similarities, there appear to be functional similarities between the two Hand genes. In the chick, for example, dHand and eHand appear to play redundant roles in cardiac looping [24,26]. In the mouse the expression patterns

of dHand and eHand are not identical, in that dHand is expressed throughout the developing heart but predominantly in the right ventricle and aortic sac, whereas eHand is expressed in the developing left ventricle and aortic sac but not in the developing right ventricle.

```
Dermo-1 ---------- ---------G SPSAQSFEEL QSQRILANVR ERQRTQSLNE
                           *   * ** *** * **  **** **********
Twist   GGGGGGAGGG GGGGGGSSSG GGSPQSYEEL QTQRVMANVR ERQRTQSLNE

        AFAALRKIIP TLPSDKLSKI QTLKLAARYI DFLYQVLQSD EMDNKMTSCS
        ********** ********** ********** ********** * * ** ***
        AFAALRKIIP TLPSDKLSKI QTLKLAARYI DFLYQVLQSD ELDSKMASCS

        YVAHERLSYA FSVWRMEGAW SMSASH
        ********** ********** ******
        YVAHERLSYA FSVWRMEGAW SMSASH
```

Figure 2. *Comparison of the C-terminal regions of Twist and Dermo-1 proteins showing the three arginine residues required for the inhibition of MyoD in bold.*

A similar analysis of the Twist and Dermo-1 proteins shows that they are 64% identical overall. The C-terminal 100 amino acids of Dermo-1 and Twist are 93% identical (with the N-termini being much less conserved). Twist also contains a polyglycine tract which is not present in Dermo-1. In *Drosophila*, Twist protein is a transcription activator and can act synergistically with the NF-αB homologue, Dorsal [27,28]. Amongst the target genes for Twist in *Drosophila* are Tinman, the homologue of Nkx 2.5 and D-MEF-2 [29, 30]. In mammalian systems, however, the available data are consistent with an inhibitory role for Twist in myogenesis. For example, Twist is expressed throughout the epithelial somite and is subsequently excluded from the myotome. Furthermore, overexpression of Twist inhibits myogenesis by binding to E-proteins and preventing their association with the myogenic bHLH proteins [31]. In addition to titrating E-proteins, Twist inhibits the myogenic bHLH function by interacting directly with the basic domain of these proteins and inhibits trans-activation by MEF-2 [31]. The region of Twist required for the interaction with the myogenic bHLH proteins is the basic N-terminus of the HLH domain and includes three arginine residues which are essential for this activity (figure 2). Both of these inhibitory functions reside within the region of Twist which is conserved in Dermo-1 and includes the three arginine residues required for the inhibition of the myogenic bHLH proteins (figure 2). Although little is currently known about the function of Dermo-1, a comparison with Twist suggests that it may act as a functional inhibitor of both MEF-2 and tissue-specific bHLH proteins. It is notable therefore, that whilst Dermo-1 can bind to an E-box with E12 protein, this complex does not appear to stimulate but to inhibit the transcriptional activity of the myogenic proteins.

The above data prompted us to propose a model in which the phenotypic plasticity of the VSMC phenotype in the vessel wall of adult animals is governed, at least in part,

by two pairs of bHLH transcription factors with opposing activities (figure 3). In this model the differentiated VSMC phenotype is driven by the two Hand genes and antagonized by Twist and Dermo-1. To evaluate this model we have examined whether the expression of these bHLH genes reflects the differentiation state of VSMCs, as defined by the expression of three markers of the differentiated VSMC phenotype (SM-MHC, SM22α and SMα-actin) using RNA extracted from three different VSMC cell sources.

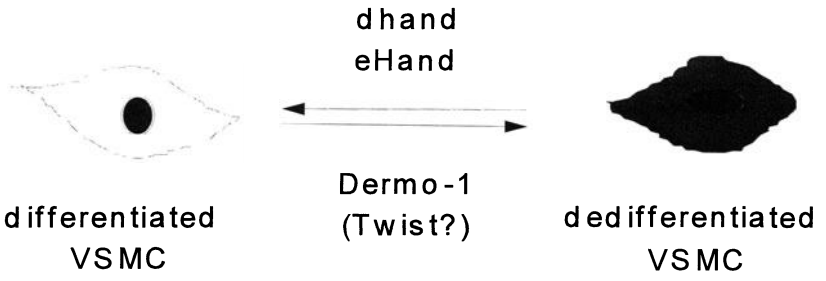

Figure 3. *Proposed model for the control of vascular smooth muscle phenotype by bHLH proteins.*

The most differentiated cell type in our study, VSMCs in the intact aorta, was prepared by removing the aorta from an adult rat then removing the connective tissue. These cells expressed significant amounts of SM-MHC, SM22α and SMα-actin mRNA. Adult rat aortic VSMCs which had been dispersed into culture and passaged were less differentiated since they did not express detectable amounts of SM-MHC and expressed less SM22α and SMα-actin than the cells of the aorta. The least differentiated cells were a clone of neonatal aortic VSMCs which did not express SM-MHC and expressed the lowest amounts of SM22α and SMα-actin. To determine the amount of dHand, eHand and Dermo-1 expressed by the cells we have used a semi-quantitative PCR approach in which the accumulation of amplified product for each of the components is measured by Southern analysis. In these experiments the expression of eHand and dHand is highest in the most differentiated cell type whereas the expression of Dermo-1 is highest in the least differentiated cell type. Such observations, whilst consistent with the hypothesis, are only associations and do not demonstrate a causal relationship between the expression of these bHLH genes and the phenotype of the cells. To investigate this relationship we have examined the effect of overexpressing Hand genes in a multipotential cell type, P19 embryonal carcinoma cells. These cells differentiate into a variety of cell types in response to different treatments. For example, in the presence of low concentrations of retinoic acid (10nM) some cells differentiate into cardiac myocytes and start to beat. In the presence of a high concentration of retinoic acid (1 μM) the cells start to differentiate into neural cells with a small percentage of cells differentiating into smooth muscle cells. The proportion of cells differentiating into smooth muscle cells can be increased by expression of an antisense RNA to the transcription factor Brn-2 [33]. By contrast, transfection of P19 cells with an expression

vector for the bHLH protein Stra13 causes the cells to follow a neural differentiation pathway. Our preliminary experiments show expression of SM22α following transfection of P19 cells with a dHand expression vector and are consistent with a role for dHand in the expression of the smooth muscle gene SM22α. These data are also consistent with the observations of Srivastava et al. that SM22α gene expression is reduced in the VSMCs of dHand null embryos [25].

Conclusion

The data presented show that adult VSMCs express at least four bHLH genes (ehand, dHand, Twist, and Dermo-1) in addition to those previously reported. Furthermore, the expression of the two Hand genes correlates directly with VSMC phenotype *in vitro* whereas the expression of Twist and Dermo-1 is inversely correlated with VSMC phenotype *in vivo* in the balloon injured rat carotid artery. Taken together, the data are consistent with a model in which VSMC phenotype in the adult is controlled at least in part by the opposing actions of these bHLH transcription factors.

Acknowledgements

This work was supported by the British Heart Foundation. PRK is a British Heart Foundation Basic Sciences Lecturer.

References

1. Schwartz SM, Campbell GR, Campbell JH. Replication of smooth muscle cells in vascular disease. Circ Res 1986;58:427-44.
2. Ross R. The pathogenesis of atherosclerosis-an update. N Engl J Med 1986;314:488-500.
3. Rovner AS, Murphy RA, Owens GK. Expression Of Smooth-Muscle and Nonmuscle Myosin Heavy-Chains In Cultured Vascular Smooth-Muscle Cells. J Biol Chem 1986;261:4740-45.
4. Shanahan CM, Cary NRB, Metcalfe JC, Weissberg PL. High Expression Of Genes For Calcification-Regulating Proteins In Human Atherosclerotic Plaques. J Clin Invest 1994;93:2393-402.
5. Giachelli CM, Bae N, Almeida M, Denhardt DT, Alpers CE, Schwartz SM. Osteopontin is elevated during neointima formation in rat arteries and is a novel component of human atherosclerotic plaques. J Clin Invest 1993;92:1686-96.
6. Giachelli C, Bae N, Lombardi D, Majesky M, Schwartz S. Molecular cloning and characterization of 2B7, a rat mRNA which distinguishes smooth muscle cell phenotypes in vitro and is identical to osteopontin (secreted phosphoprotein I, 2aR). Biochem Biophys Res Commun 1991;177:867-73.
7. Grainger DJ, Kemp PR, Liu AC, Lawn RM, Metcalfe JC. Activation of transforming growth-factor-beta is inhibited in transgenic apolipoprotein(a) mice. Nature 1994;370:460-62.
8. Shanahan CM, Weissberg PL, Metcalfe JC. Isolation of gene markers of differentiated and proliferating vascular smooth-muscle cells. Circ Res 1993;73:193-204.
9. Owens GK. Regulation Of Differentiation Of Vascular Smooth-Muscle Cells. Physiol Revs 1995;75:487-517.
10. Kallmeier RC, Somasundaram C, Babij P. A novel smooth muscle-specific enhancer regulates transcription of the smooth muscle myosin heavy chain gene in vascular smooth muscle cells. J Biol Chem 1995;270:30949-57
11. Shimizu RT, Blank RS, Jervis R, Lawrenzsmith SC, Owens GK. The Smooth-Muscle Alpha-Actin Gene Promoter Is Differentially Regulated In Smooth-Muscle Versus Nonsmooth Muscle-Cells. J Biol Chem 1995;270:7631-43.
12. Kemp PR, Osbourn JK, Grainger DJ, Metcalfe JC. Cloning and analysis of the promoter region of the rat SM22-alpha gene. Biochem J 1995;310:1037-43.
13. Kim S, Ip HS, Lu MM, Clendenin C, Parmacek MS. A serum response factor-dependent transcriptional regulatory program identifies distinct smooth muscle cell sublineages. Mol Cell Biol 1997;17:2266-78.
14. Miano JM, Firulli AB, Olson EN, Hara P, Giachelli CM, Schwartz SM. Restricted Expression Of Homeobox Genes Distinguishes Fetal From Adult Human Smooth-Muscle Cells. Proc Natl Acad Sci USA 1996;93:900-05.
15. Gorski DH, Lepage DF, Patel CV, Copeland NG, Jenkins NA, Walsh K. Molecular-Cloning Of a Diverged Homeobox Gene That Is Rapidly Down- Regulated During the G(0)/G(1) Transition In Vascular Smooth-Muscle Cells. Mol Cell Biol 1993;13:3722-33.
16. Patel CV, Gorski DH, Lepage DF, Lincecum J, Walsh K. Molecular-Cloning Of a Homeobox Transcription Factor From Adult Aortic Smooth-Muscle. J Biol Chem 1992;267:26085-90.
17. Firulli AB, Miano JM, Bi WZ, et al. Myocyte Enhancer-Binding Factor-Ii Expression and Activity In Vascular Smooth-Muscle Cells - Association With the Activated Phenotype. Circ Res 1996;78:196-204.
18. Kemp PR, Grainger DJ, Shanahan CM, Weissberg PL, Metcalfe JC. The Id gene is activated by serum but is not required for dedifferentiation in rat vascular smooth-muscle cells. Biochem J 1991;277:285-88.
19. Kemp PR, Grainger DJ, Metcalfe JC, Weissberg PL. Id gene-expression antagonizes MyoD-induced myotube formation in vascular smooth-muscle cells. J Cell Biochem 1993;17A:938.
20. Kemp PR, Metcalfe JC, Grainger DJ. Id - a dominant-negative regulator of skeletal-muscle

differentiation - is not involved in maturation or differentiation of vascular smooth-muscle cells. FEBS Lett 1995;368:81-86.
21. Matsumura ME, Lobe DR, Jeon C, McNamara CA. Id3 and a novel isoform are involved in the response to vascular injury. Circulation 1997;96:1274.
22. Hollenberg SM, Sternglanz R, Cheng PF, Weintraub H. Identification of a new family of tissue-specific basic helix-loop- helix proteins with a 2-hybrid system. Mol Cell Biol. 1995;15:3813-22.
23. Cserjesi P, Brown D, Lyons GE, Olson EN. Expression Of the Novel Basic Helix-Loop-Helix Gene Ehand In Neural Crest Derivatives and Extraembryonic Membranes During Mouse Development. Dev Biol 1995;170:664-78.
24. Srivastava D, Cserjesi P, Olson EN. A Subclass Of bHLH Proteins Required For Cardiac Morphogenesis. Science 1995;270:1995-99.
25. Srivastava D, Thomas TK, Olson EN, Hill S, Yamagishi H. The bHLH transcription factor dHAND is required for normal vascular development. Circulation 1997;96:1681.
26. Srivastava D, Olson EN. Knowing in your heart what's right. Trends Cell Biol 1997;7:447-53.
27. Leptin M. Twist and Snail As Positive and Negative Regulators During Drosophila Mesoderm Development. Gene Dev 1991;5:1568-76.
28. Shirokawa JM, Courey AJ. A direct contact between the dorsal rel homology domain and Twist may mediate transcriptional synergy. Mol Cell Biol 1997;17:3345-55.
29. Lilly B, Galewsky S, Firulli AB, Schulz RA, Olson EN. D-MEF2: a MADS box transcription factor expressed in differentiating mesoderm and muscle cell lineages during Drosophila embryogenesis. Proc Natl Acad Sci USA 1994;91:5662-66.
30. Lee YM, Park T, Schulz RA, Kim Y. Twist-mediated activation of the NK-4 homeobox gene in the visceral mesoderm of Drosophila requires two distinct clusters of E-box regulatory elements. J Biol Chem 1997;272:17531-41.
31. Spicer DB, Rhee J, Cheung WL, Lassar AB. Inhibition Of Myogenic bHLH and MEF-2 Transcription Factors By the bHLH Protein Twist. Science 1996;272:1476-80.
32. Bain G, Ray WJ, Yao M, Gottlieb DI. From embryonal carcinoma cells to neurons: the P19 pathway. Bioessays 1994;16:343-48.
33. Suzuki T, Kim HS, Kurabayashi M, et al. Preferential Differentiation Of P19 Mouse Embryonal Carcinoma-Cells Into Smooth-Muscle Cells - Use Of Retinoic Acid and Antisense Against the Central Nervous System-Specific Pou Transcription Factor Brn-2. Circ Res 1996;78:395-404.

21. EXPRESSION OF THE IGF SYSTEM IN ACUTE AND CHRONIC ISCHEMIA

Elisabeth Deindl, René Zimmermann, and Wolfgang Schaper

Introduction

The insulin-like growth factors (IGFs) are potent anabolic agents, structurally related to insulin, that can influence function and growth processes in almost every organ of the body [1]. Unlike insulin these peptides associate with distinct binding proteins (IGFBPs) present in serum or other biological fluids [2]. The expression of the IGFs is regulated by various hormones, oncogenes and other growth factors and signal transduction is mediated by specific transmembrane receptors.
Because of the wide range of their biological effects and their therapeutic potential in a variety of clinical disorders, the IGFs have become a focus of research during the last few years.
Recent observations in neuronal models suggest trophic and protective actions of the IGFs in settings of ischemia and reperfusion [3-7]. Like adult myocytes, neurons are terminally differentiated cells that exhibit pathways of endogenous protection similar to ischemic preconditioning in the heart [8-12]. In skeletal muscle, it was demonstrated that the IGFs stimulate glucose uptake by their insulin-like activity [13,14]. It is therefore tempting to speculate that in times of metabolic stress, as in ischemia, the heart expresses "its own insulin" by making use of the metabolic properities of the IGFs.
The most important strategy of the ischemic myocardium to ensure its survival is the formation of new blood vessels. Previous studies our lab demonstrated that myocardial angiogenesis is associated with the appearance of monocytes/macrophages [15], potent suppliers of growth factors, among them the IGFs. To characterize the role of the IGFs in ischemia we analyzed the expression of these growth factors, their binding proteins and receptors in our porcine models of acute and chronic ischemia.

The IGF system

The three peptide hormones insulin, IGF-I and IGF-II have approximately 50% of their

P.A. Doevendans et al. (eds.), Cardiovascular specific gene expression, 245-55.

amino acids in common. Insulin, having a half live in the range of minutes, is synthesized in the beta cells of the pancreas and circulates at picomolar concentrations in the blood. The IGFs, which are synthesized primarily in the liver, circulate at much higher concentrations (nanomolar) and are largely bound to one of the six known high affinity binding proteins [16]. These IGFBPs, which bind the IGFs with a 2 - 50-fold higher affinity than the IGF receptors, modulate the biological activity of the growth factors via regulating their bioavailability. The IGFBPs are primarily synthesized in the liver, but are also produced locally by most tissues like the IGFs proper. Both types of gene products, the IGFs and their binding proteins are modified; the IGFs post-transcriptionally via splicing - resulting in a variety of splice products - and the IGFBPs post-translationally, exerting profound effects on the structure and function of the binding proteins and hence on the actions of the IGFs.

Insulin acts primarily on the liver, muscle and adipose tissue [17], whereas the IGFs are important for the function of almost every organ of the body by acting in an autocrine or paracrine manner [1,18]. The signal transduction of insulin, IGF-I and IGF-II proceeds via two high affinity membrane-associated tyrosine kinase receptors [19]. A third receptor, the IGF-II-mannose-6-phophate receptor, binds IGF-I as well as IGF-II, but leads to no known intracellular signal actions (figure 1). Activation of either the insulin receptor or the IGF-I receptor evokes similar initial respones within the cell [20]. However, since insulin regulates metabolic functions and the IGFs modulate growth and differentiation, the final pathway these hormones activate within the cell must be separate and distinct.

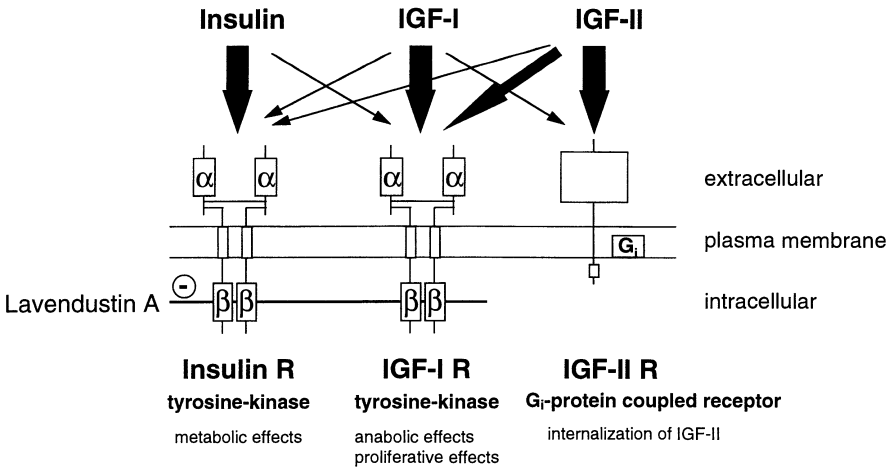

Figure 1. *Signal transduction pathway of the insulin/IGF system. Insulin, IGF-I and IGF-II bind to their own receptors with high (bold arrows) and to the other receptors with lower (thin arrows) affinity. Insulin does not bind to the IGF-II receptor. The insulin and the IGF-I receptor are homodimers consisting of extracellular (α), transmembrane and intracellular (β) domains. The intracellular domains have protein tyrosine kinase activity that can be blocked by lavendustin A. In general, the insulin receptor mediates metabolic effects whereas anabolic and proliferative effects are transmitted by the IGF-I receptor. The exact function of the IGF-II receptor, which is a G-protein coupled receptor, remains to be elucidated.*

Acute ischemia

To analyze the expression of the transcripts of the IGF-system during acute ischemia we used our porcine model of stunning [21]. Short periods of occlusion and reperfusion render the affected myocardium for a limited period of time (about 1h) more tolerant to the untoward effect of a subsequent long period of occlusion. This phenomenon, defined as ischemic preconditioning [3,22,23], implies the existence of molecular mechanisms which induce cardioprotection. In parallel, these coronary occlusions lead to myocardial stunning, i.e, a long lasting but reversible contractile dysfunction in the absence of cell necrosis [24,25]. The long duration of the contractile dysfunction (hours to days) indicates molecular damage which requires repair processes at the transcriptional and translational level.

To achieve preconditioning/stunning the left anterior descending artery (LAD) was occluded twice for 10 min separated by 30 min of reperfusion. After a second occlusion, the myocardium was reperfused for up to 210 min. Tissue samples were collected at distinct points of time (figure 2) from the ischemic region and from the non-ischemic left circumflex coronary artery region of the same heart (control values). Furthermore we used cardiac biopsies from sham operated animals and from slaughterhouse pigs as separate controls. Throughout the whole experimental protocol systolic wall thickening was measured as a parmeter for contractile function (data not shown).

In order to characterize the expression of the members of the IGF-system we performed in situ hybridization studies [26]. The results revealed that IGF-I as well as IGF-II are mainly transcribed in myocytes and, to a lesser extent, in fibroblasts of the interstitium. Northern blot and slot blot analysis showed that IGF-I, the IGF-I and the insulin receptor as well as the IGFBPs 2 - 6, but not IGFBP-1, are constitutively expressed in the porcine myocardium, but are not induced by repetitive cycles of ischemia [26]. However, repetitive cycles of ischemia and reperfusion led to an early and significant increase of the IGF-II mRNA (4 - 5 fold) compared to the corresponding mRNA level of slaughterhouse pigs, but not in comparison to sham operated animals or the IGF-II mRNA level of the control tissue of the same animal (figure 2) [26] . These results led to our postulation that at least in our model IGF-II is a stress inducible gene, the expression of which is further enhanced under conditions of acute ischemia. For the IGFBP-5 we also found increased mRNA levels in the ischemic as well as the normally perfused region of the same heart compared to slaughterhouse pigs or sham operated animals (figure 2) [26]. The IGFBP-5 mRNA is only upregulated by ischemia/reperfusion but not by the surgical stress (sham operated animals), which implies an ischemia specific response. The reason for the increased mRNA level of this specific transcript in the non-ischemic region of the hearts remains to be elucidated. Interestingly the mRNA level of the IGFBP-5 peaks about 30 min later compared to that of IGF-II.

These results led us to the hypothesis that the stress inducible IGF-II may also have cardioprotective functions. IGF-II does not only support protein synthesis but also suppresses protein degradation [27]. It appears possible that IGF-II exerts a protective role in the myocardium by aiding the survival of myocytes after damage by stress in analogy to its trophic functions in the brain, an organ that is terminally differentiated

like the heart. The IGFBP-5, on the other hand, could in part account for the limited time frame of the cardioprotection, as its expression is delayed compared to that of IGF-II.

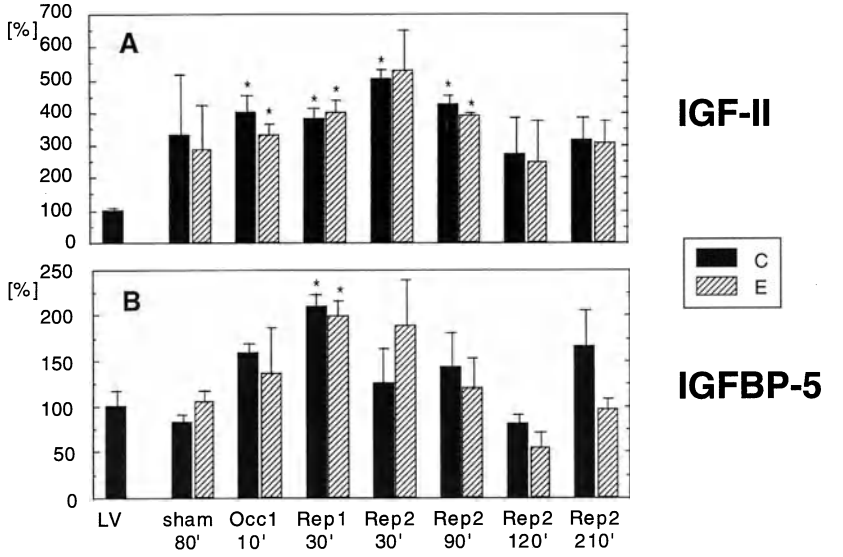

Figure 2. *Bar graph representing the mRNA expression of IGF-II (A) and IGFBP-5 (B) during repetitive cycles of ischemia and reperfusion. Changes in the experimental ischemic/reperfused (E) and normal perfused control heart regions (C) are shown. Error bars = SEM. The average of the values obtained for the left ventricle (LV) of non-sham control pigs was defined as 100%. Levels of significance are shown for control and experimental heart tissue respectively.*

To verify our hypothesis human recombinant IGF-II (0.25mg/ml) was applied by means of direct intramyocardial infusion for 60 min prior to a 60 min LAD occlusion and infarct size was measured [28]. We found a significant reduction of infarct size of the area at risk of about 20%. To further elucidate the underlying mechanisms, we infused an equipotent concentration of recombinant human insulin (0.02 IU/ml) in a second group and found a comparable degree of cardioprotection [28]. The receptors involved were characterized by simultaneous infusion of lavendustin A (100mM), a potent and selective inhibitor of protein tyrosine kinases [29], to block either the enzymatically active domain of the IGF-I or the insulin receptor. The co-infusion of lavendustin A abolished the cardioprotective effect of IGF-I as well as that of insulin (table 1), indicating that either the insulin or the IGF-I receptor is involved in signal transduction [29]. Little knowledge is available about the physiological functions of the IGFBPs. Recent investigations demonstrated that physiological actions of the IGFs (i.e., cellular glucose uptake) can be inhibited by their binding proteins [13,30]. Due to the good correlations of the time courses of the appearance of the IGFBP-5 mRNA and the vanishing protection of ischemic preconditioning we tested the effect of IGFBP-5 on the action of IGF-II. Our results displayed that the cardioprotective effect of IGF-II was neutralized when equimolar concentrations of IGFBP-5 were co-infused.

Table 1. Myocardial protection in the different experimental groups (each consisting of 4 animals) using a nominal scale.

group	protection
control	0/4
IGF-II	4/4
insulin	4/4
IGF-II + lavendustin A	0/4
insulin + lavendustin A	0/4
IGF-II + IGFBP-5	0/4

Our studies displayed that IGF-II is a stress inducible gene which has the potency to delay the progression of an experimental infarct just like ischemic preconditioning. IGFBP-5, whose expression is somewhat delayed, inhibits the cardioprotection afforded by IGF-II and may thus account for the limited protective time frame of ischemic preconditioning. The protective effect of IGF-II could be either mediated by the insulin or the IGF-I receptor but not by the IGF-II receptor, although IGF-II can bind to all three types of receptors. The cardioprotective effect of IGF-II is abolished when lavendustin A, a specific tyrosine kinase inhibitor, is co-infused, which accounts for the insulin or the IGF-I receptor as the signaling receptor, as the IGF-II receptor is a G coupled but not a tyrosine kinase receptor (figure 1). The fact that insulin shows the same cardioprotective effect as IGF-II and insulin does not bind to the IGF-II receptor and only weakly to the IGF-I receptor makes it likely that the signal transduction is mediated via the insulin receptor. It is furthermore conceivable that the effect of IGF-II is either a mitogenic or a metabolic one and not an anabolic one, proposing the insulin receptor as the signaling part. The cardioprotection afforded by IGF-II is probably due to its insulin-like action on glucose uptake. During the repetitive cycles of ischemia and reperfusion, the heart circumvents its inability to synthesize its own insulin via upregulating IGF-II. In the heart, influencing glucose metabolism has been shown to be benefical in ischemia/reperfusion settings [31-33]. Preliminary experiments of our group with positron emission tomography (together with Schwaiger, unpublished) showed increased focal glucose uptake after intramyocardial IGF-II infusion, from which we conclude that this was one of the underlying mechanisms responsible for the increased ischemia resistance of the myocardium.

Chronic ischemia

Short periods of ischemia and reperfusion are an appropriate methode to induce preconditioning/stunning. However, to reach chronic ischemia we had to develop another model, the microembolized porcine myocardium [34]. Microembolization was

achieved by injecting polystyrene microspheres (25 µm diameter) into the left circumflex artery (LCx) with (n=5) or without (n=12) thoracotomy via a coronary artery catheter. Using this method we have been able to induce chronic ischemia resulting in focal necrosis and inflammation linked angiogenesis. The hearts were excised after 3 to 168h of microembolization and tissue collected from the ischemic left circumflex perfused embolized region and from the non-ischemic intraventricular septum (control) was analyzed as mentioned above. Our in situ hybridization studies revealed that, in contrast to normal control myocardial tissue, the microembolized myocardium (necrotic tissue) at 72h of chronic ischemia was characterized by invading monocytes and macrophages transcribing IGF-I mRNA. Northern blot results revealed a significant increase (1.8 fold) of the IGF-I mRNA after 72h of chronic ischemia and to a lesser extend at 168h (figure 3) [35]. The IGF-II mRNA displayed increased amounts under conditions of acute ischemia, but we did not detect altered mRNA levels during chronic ischemia [35]. However, for the IGFBP-5, being upregulated in the preconditioned myocardium, we found significantly decreased mRNA amounts (2.7 fold) in the microembolized myocardium at the same point of time where we found increased IGF-I levels (figure 3) [36]. The induction of the IGFBP-3 (3 to 24h of microembolization) preceeded that of IGF-I, but was also detectable at a lesser extent after 72h of chronic ischemia (figure 3) [36]. For the IGFBP-6 we found significantly increased levels at all points of time analyzed.

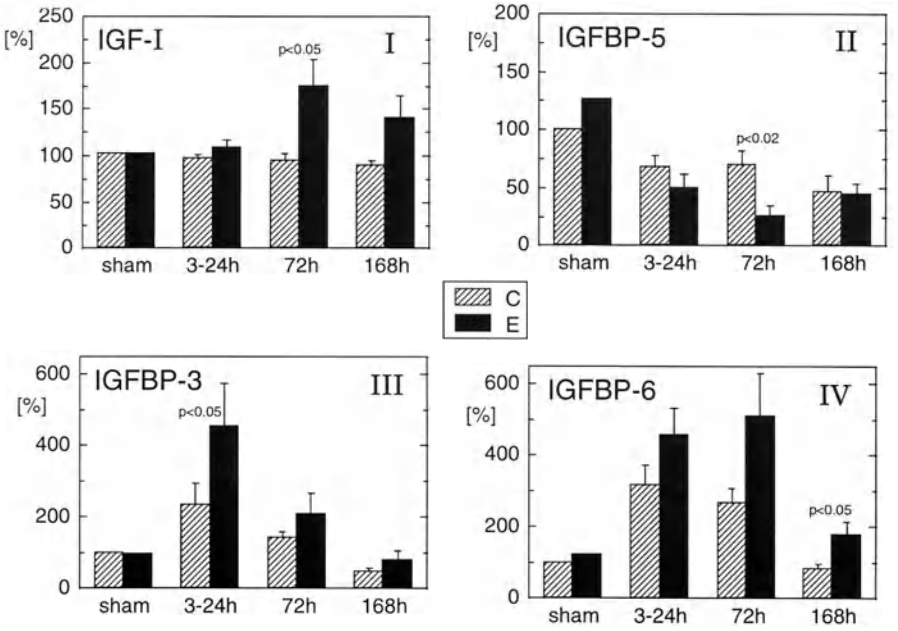

Figure 3. *Bar graph representing the mRNA expression of IGF-I (I), IGFBP-5 (II), IGFBP-3 (III) and IGFBP-6 (IV) in chronic ischemia. Changes in the experimental microembolized (E) and normal control heart (C) are shown. Error bars = SEM. The average of the values obtained for cardiac control tissue of the sham operated animals was defined as 100%. *P < 0.05 v control.*

Although our results displayed that chronic ischemia does not influence the mRNA expression of IGF-II, the IGF-I receptor, the insulin receptor and the IGFBPs 2 and 4, we cannot exclude that these binding proteins possess a regulatory function, as the binding proteins might experience a modulation of their activity via post-translational modifications.
Microembolization of the porcine myocardium leads to capillary sprouting in and around areas of focal necrosis, induced by microspheres [15,34]. After 72h of chronic ischemia we observed in those areas infiltrates consisting mainly of monocytes/ macrophages. Additionally endothelial cell mitosis, a requirement for the formation of new blood vessels, was frequently observed in the proximity to monocytes and macrophages. As we have previously shown these mononuclear cells, which are involved in microembolization associated angiogenesis, produce angiogenic mitogens [37,38]. Our results displayed at 72h of chronic ischemia a significantly increased level of the IGF-I mRNA and our in situ data showed that this potent mitogen is produced by invading monocytes and macrophages. So our data suggest that IGF-I, supplied by mononuclear cells, is involved in inflammation linked angiogenesis. Furthermore our data revealed that the IGFBPs-3, -5 and -6 are involved in this inflammation linked angiogenesis via modulating the action of the IGFs. Which specific functions the IGFBPs have we can only speculate upon.

Summary and conclusion

The insulin like growth factors IGF-I and IGF-II are constitutively expressed in myocytes of different species (human [39], pig [40], rat [41]) but also in endothelial cells [42], smooth muscle cells [43] and fibroblasts [44]. By our in situ hybridization experiments we showed that the IGFs are mainly transcribed by myocytes in the porcine myocardium. Cardiac myocytes are terminally differentiated cells and even non-myocyte cells of the normal myocardium rarely proliferate. For a mitogen like IGF-I, there seems no requirement in the heart. We therefore postulate that in the normal porcine myocardium IGF-I may be involved in the maintainance of basic functions of myocytes. It may, like IGF-II, which is regarded as a trophic factor in the brain, exert its insulin-like metabolic functions or act as a positive inotropic agent [45].
Different types of ischemia cause different reactions of the affected myocardium. Whereas acute ischemia renders the affected myocardium more tolerant towards subsequent periods of longer ischemia, chronic ischemia induces myocardial angiogenesis. These two distinct reactions obey two distinct molecular mechanisms. This is reflected by the coordinate expression of the members of the IGF system. Thus, in the porcine myocardium, repetitive cycles of acute ischemia and reperfusion led to the expression of the stress inducible IGF-II gene which displayed cardioprotective functions - presumably by increasing the glucose uptake of myocytes. Interestingly, increased myocardial glycogen content is a characteristic feature of the "hibernating human myocardium" [46]. It is likely that the heart circumvents its inability to synthesize insulin via increasing its IGF-II production, "the heart´s own insulin", as a self-defense mechanism to repeated episodes of ischemia.

Chronic ischemia on the other hand was characterized by an increased expression of IGF-I in invading monocytes and macrophages, resulting in inflammation linked angiogenesis. The action of the IGFs is more modulated by their specific binding proteins and not by their receptors. This is not only reflected by the fact that the IGFBPs bind the IGFs with a much higher affinity than the receptors do, but also by their distinct RNA expression during acute and chronic ischemia. Acute ischemia was shown to induce the expression of the IGFBP-5 30 min later compared to that of IGF-II. This binding protein presumably accounts for the limited protective time frame afforded by IGF-II. Chronic ischemia in contrast did not influence the expression of IGF-II and caused a downregulation of IGFBP-5. At first glance this may be somehow astonishing as chronic ischemia is nothing else but a prolonged acute ischemia. But as already mentioned IGF-II is a stress inducible gene, the expression of which is influenced by the surgical stress during the stunning procedure being absent in microembolization (achieved without thoracotomy). The expression of the IGFBP-5 on the other hand is presumably induced by the repetitive cycles of reperfusion in acute ischemia not occuring in the procedure of chronic ischemia. The coordinate expression of the IGFBP-3 and -6 (upregulated) and -5 in chronic ischemia accounts for the involvement of these binding proteins in regulating the actions of the IGFs. However, there is little knowledge available about the concrete functions of the distinct binding proteins, and their actions are very complex. We therefore can only speculate about the distinct regulatory functions these proteins may exert during acute ischemia. We also can not exclude that the other binding proteins, not displaying altered gene expression due to ischemia, are involved in modulating the actions of the IGFs, as their functions might be modulated on a post-translational level.

Acknowledgement

We thank the Steinkopff Verlag, Darmstadt, Germany for giving us the permission to reproduce a diagram [47] and Elsevier Science, New York, USA to give us the permission to reproduce a table and diagrams [28,35,36].

References

1. Daughaday WH, Rotwein P. Insulin-like growth factors I and II. Peptide, messenger ribonucleic acid and gene structures, serum, and tissue concentrations. Endocr Rev 1989;10:68-91.
2. Conover CA. Regulation and physiological role of the insulin-like growth factor binding proteins. Endocr J 1996;43:43-48.
3. Murry CE, Jennings RB, Reimer KA. Preconditioning with ischemia: a delay of lethal cell injury in ischemic myocardium. Circulation 1986;74:1124-36.
4. Zhu CZ, Auer RN. Intraventricular administration of insulin and IGF-1 in transient forebrain ischemia. J Cereb Blood Flow Metab 1994;14:237-42.
5. Zhu CZ, Auer RN. Centrally administered insulin and IGF-1 in transient forebrain ischemia in fasted rats. Neurol Res 1994;16:116-20.
6. Strong AJ, Fairfield JE, Monteiro E, et al. Insulin protects cognitive function in experimental stroke. J Neurol Neurosurg Psychiatry 1990;53:847-53.
7. Hamilton MG, Tranmer BI, Auer RN. Insulin reduction of cerebral infarction due to transient focal ischemia. J Neurosurg 1995;82:262-68.
8. Aoki M, Abe K, Kawagoe J, Nakamura S, Kogure K. Acceleration of HSP70 and HSC70 heat shock gene expression following transient ischemia in the preconditioned gerbil hippocampus. J Cereb Blood Flow Metab 1993;13:781-88.
9. Aoki M, Abe K, Kawagoe J, Nakamura S, Kogure K. The preconditioned hippocampus accelerated HSP70 heat shock gene expression following transient ischemia in the gerbil. Neurosci Lett 1993;155:7-10.
10. Liu Y, Kato H, Nakata N, Kogure K. Temporal profile of heat shock protein-70 synthesis in ischemic tolerance induced by preconditioning ischemia in rat hippocampus. Neuroscience 1993;56:921-27.
11. Gidday JM, Fitzgibbons JC, Shah AR, Park TS. Neuroprotection from ischemic brain injury by hypoxic preconditioning in the neonatal rat. Neurosci Lett 1994;168:221-24.
12. Kato H, Liu Y, Kogure K, Kato K. Induction of 27-kDa heat shock protein following cerebral ischemia in a rat model of ischemic tolerance. Brain Res 1994;634:235-44.
13. Bevan SJ, Parry-Billings M, Opara E, Liu CT, Dunger DB, Newsholme EA. The effect of insulin-like growth factor II on glucose uptake and metabolism in the rat skeletal muscle in vitro. Biochem J 1992;286:561-65.
14. Burguera B, Elton CW, Tapscott EB, Pories WJ, Dimarchi R, Sakano K. Stimulation of glucose uptake by insulin-like growth factorII/mannose6-phosphate receptor. Biochem J 1994;300:781-85.
15. Schaper J, Weihrauch D. Collateral vessel development in the porcine and canine heart. In: Schaper W, Schaper J, ed. Collateral Circulation - Heart, Brain, Kidney, Limbs. Boston, Dordrecht, London: Kluwer Academic Publishers, 1993: 65-102.
16. Jones JI, Clemmons DR. Insulin-like growth factors and their binding proteins: biological actions. Endocr Rev 1995;16:3-34.
17. Kahn CR. The molecular mechanism of insulin action. Annu Rev Med 1985;36:429-51.
18. LeRoith D, Adamo M, Werner H, Roberts CTJ. Insulin-like growth factors and their receptors as growth regulators in normal physiology and pathological states. Trends Endocrinol Metab 1991;2:134-39.
19. Ruderman N, Moses AC, Moller DE. Insulin, insulin-like growth factors, and their receptors. In : Arias IM, ed. The liver: biology and pathobiology, 3rd Ed. New York , Raven Press 1994:969-96
20. LeRoith D, Werner H, Beitner-Johnson D, Roberts CTJ. Molecular and cellular aspects of the insulin-like growth factor I receptor. Endocr Rev 1995;16:143-63.
21. Brand T, Sharma HS, Fleischmann KE, et al. Proto-oncogene expression in porcine

myocardium subjected to ischemia and reperfusion. Circ Res 1992;71:1351-60.
22. Sack S, Mohri M, Arras M, Schwarz ER, Schaper W. Ischaemic preconditioning - time course of renewal in the pig. Cardiovasc Res 1993;27:551-55.
23. Schott RJ, Rohmann S, Braun ER, Schaper W. Ischemic preconditioning reduces infarct size in swine myocardium. Circ Res 1990;66:1133-42.
24. Heyndrickx GR, Millard RW, McRitchie RJ, Maroko PR, Vatner SF. Regional myocardial, functional, and electrophysiological alterations after brief coronary occlusion in conscious dogs. J Clin Invest 1975;56:978-85.
25. Ito B, Tate H, Kobayashi M, Schaper W. Reversibly injured, post-ischemic canine myocardium retains normal contractile reserve. Circ Res 1987;61:834-46.
26. Kluge A, Zimmermann R, Münkel B, Verdouw PD, Schaper J, Schaper W. Insulin-like growth factor II is an experimental stress inducible gene in a porcine model of brief coronary occlusions. Cardiovasc Res 1995;29:708-16.
27. Ewton DZ, Falen SL, Florini JR. The type II insulin-like growth factor (IGF) receptor has low affinity for IGF-1 analogs: pleiotropic actions of IGFs on myoblasts are apparenty mediated by the type I receptor. Endocrinology 1987;120:115-23.
28. Vogt A, Htun P, Kluge A, Zimmermann R, Schaper W. Insulin-like growth factor-II delays myocardial infarction in experimental coronary artery occlusion. Cardiovasc Res 1997;33:469-77.
29. Burke Tj. Protein-tyrosine kinases: potential targets for anticancer drug development. Stem Cells Dayt 1994;12:1-6.
30. Hellenius M, Brismar K, Gerglund B, De Faire U. Effects on glucose tolerance insulin secretion, insulin-like growth factor 1 and its binding protein, IGFBP-1, in a randomized controlled diet and exercise study in healthy, middle aged men. J Intern Med 1995;238:121-30.
31. Apstein C, Gravino F, Haudenschild C. Determinants of a protective effect of glucose and insulin on the ischemic myocardium. Circ Research 1983;52:515-26.
32. Maroko PR, Kjekshus JK, Sobel BE, et al. Factors influencing infarct size following experimental coronary artery occlusion. Circulation 1971;43:67-82.
33. Opie L, Bruyneel K, Owen P. Effects of glucose, insulin and potassium infusion on tissue metabolic changes within first hour of myocardial infarction in baboon. Circulation 1975;52:49-57.
34. Mohri M, Schaper W. Angiogenesis in porcine hearts with coronary microembolization. In: Schaper W, Schaper J, ed. Collateral Circulation - Heart, Brain, Kidney, Limbs. Boston, Dordrecht, London: Kluwer Academic Publishers, 1993: 103-21.
35. Kluge A, Zimmermann R, Münkel B, Mohri M, Schaper J, Schaper W. Insulin-like growth factor I is involved in inflammation linked angiogenic processes after microembolization in porcine heart. Cardiovasc Res 1995;29:407-15.
36. Kluge A, Zimmermann R, Weihrauch D, et al. Coordinate expression of the insulin-like growth factor system after microembolisation in porcine heart. Cardiovasc Res 1997;33:324-31.
37. Arias M, Mohri M, Sack S, Schwarz ER, Schaper J, Schaper W. Macrophages accumulate and release tumor necrosis factor-alpha in the ischemic porcine myocardium. In: Circulation 1992;86(Suppl I):0129 [Abstract].
38. Zimmermann R, Schaper J, Münkel B, Mohri M, Schaper W. In situ hybridization studies of acidic fibroblast growth factor (aFGF) in ischemic porcine myocardium. In: J Mol Cell Cardiol 1993;25(Suppl I):IX P3 [Abstract].
39. Han VKM, D'Ercole AJ, Lund PK. Cellular localisation of somatomedin (insulin-like growth factor) messenger RNA in human fetus. Science 1987;88:193-97.
40. Leaman DW, Simmen FA. Insulin-like growth factor-I and II messenger RNA expression in muscle, heart, and liver of streptozotocin-diabetic swine. Endocrinology 1990;126:2850-57.

41. Engelmann GL, Boehm KD, Haskell JF, Khairallah PA, Ilan J. Insulin-like growth factors and neonatal cardiomyocyte development: ventricular gene expression and membrane receptor variations in normotensive and hypertensive rats. Mol Cell Endocrinol 1989;63:1-14.
42. Kern PA, Svoboda ME, Eckel RH, Van Wyk JJ. Insulin-like growth factor action and production in adipocytes and endothelial cells from human adipose tissue. Diabetes 1989;38:710-17.
43. Gloudemans T, Pospiech I, Vanderven LTM, et al. Expression and CpG methylation of the insulin-like growth factor-II gene in human smooth muscle tumors. Cancer Res 1992;52:6516-21.
44. Gartner MH, Benson JD, Caldwell MD. Insulin-like growth factors I and II expression in the healing wound. J Surg Res 1992;52:389-94.
45. Froesch ER, Schmid C, Schwander J, Zapf J. Actions of insulin-like growth factors. Annu Rev Physiol 1985;47:443-67.
46. Elsässer A, Schlepper M, Klövekorn W-P, et al. Hibernating myocardium - an incomplete adaptation to ischemia. Circulation 1997;96:2920-31.
47. Zimmermann R, Andres J, Brand T, et al. Kardiale Genexpression nach kurzen Koronarverschlüssen. Z Kardiol 1995;84 (Suppl 4):159-65.

22. LONG-CHAIN FATTY ACIDS AND SIGNAL TRANSDUCTION IN THE CARDIAC MUSCLE CELL

Marc van Bilsen, Karin A.J.M. van der Lee, and Ger J. van der Vusse

Introduction

Long-chain fatty acids have various important biological functions in mammalian cells. First, they provide building blocks for phospholipids, the major constituents of cellular membranes. Fatty acids also play a central role in cellular energy metabolism, being an energy source for various tissues. The latter is especially true for the heart which has a clear preference for fatty acids as substrate. Moreover, evidence is accumulating that, in addition to other lipidic compounds, like diacylglycerol and lysophospholipids, long-chain fatty acids per se are involved in cellular signal transduction. In this chapter the use of primary cultures of rat neonatal ventricular myocytes as a model system to explore various issues relating to the effects of long-chain fatty acids on the cardiomyocyte are presented. Emphasis is put on the effects of different fatty acid species on cell viability and on their effect on gene expression, especially on the expression of genes involved in fatty acid uptake and metabolism. Finally the implications of these findings for cardiac function under physiological and pathophysiological conditions are briefly discussed.

Fatty acids and cellular signalling

At present there is ample evidence to support the notion that fatty acids per se may act as modulators of a variety of biological processes. For instance, using modern electrophysiological techniques, fatty acids have been shown to affect the activity of a number of cardiac ion-channels, including K^+-channels, the L-type Ca^{2+}-channel and the Na^+-channel [1-3]. Based on these observations Kang and Leaf [3,4] have speculated on the role of fatty acids in the development of arrhythmias. In this respect it is noteworthy that already in 1968 Oliver and Kurien [5] reported a relation between elevated serum levels of free fatty acids and the incidence of arrhythmias in patients with acute myocardial infarction.
Although the role of fatty acids in signal transduction is being acknowledged, relatively

P.A. Doevendans et al. (eds.), Cardiovascular specific gene expression, 257-68.

little is known about the mechanism of their action [6,7]. In this respect the role of protein acylation deserves attention. It has been demonstrated that myristoylation at the N-terminal end of α-subunits of GTP-binding proteins is an irreversible process occurring co-translationally, whereas palmitoylation of G-proteins appears to be post-translational and under dynamic control [8]. It is generally believed that palmitoylation of G_α facilitates the anchoring of the heterotrimeric G-proteins to the cell membrane and that receptor-stimulated depalmitoylation mediates the translocation of G_α to the cytosolic compartment [9]. Other components of signaling cascades thought to be modulated through reversible palmitoylation are G-protein coupled receptors, p21 Ras, and members of the Src-family of proteins [8]. In view of the important roles of p21 Ras and Src in signal transduction the significance of this type of protein modification certainly deserves attention. The same holds for the interaction between fatty acids and PKC. A substantial body of evidence indicates that long-chain fatty acids, acting as substitutes for diacylglycerol, affect the activity of certain PKC isoforms. This is of special interest as the activation of PKC, like that of p21 Ras, has been shown to be part of signalling cascades involved in the development of cardiomyocyte hypertrophy [10].

Finally, it was shown that fatty acids, directly or indirectly, influence gene expression in various cell types. The differentiation of fat cells was promoted when fatty acids were added to the culture medium [11]. In contrast, the administration of fatty acids to skeletal myoblasts inhibited their differentiation into myotubes, and actually induced the expression of adipocyte-specific genes [12]. Collectively these studies suggest that long-chain fatty acids, in addition to being an important metabolic fuel, are likely to affect cellular processes within the context of the cardiomyocyte. To explore this possibility primary cultures of neonatal rat ventricular myocytes were chosen as a cellular model system. This model system has been used extensively to study the mechanisms of the development of cardiac hypertrophy [13]. However, as it has been shown that the long-term incubation of various cell types with fatty acids, especially with saturated fatty acid species, may compromise cell function and viability [14-16], it was first investigated if fatty acids affect cardiomyocyte viability.

Fatty acids and cell viability

The oxidation of fatty acids provides most of the energy for the beating heart. In the circulating blood palmitic acid (C16:0) is abundantly present and therefore, from a quantitative point of view, one of the most important fatty acid species for the heart [17]. Indeed, the vast majority of studies on cardiac fatty acid metabolism, using isolated hearts or isolated myocytes, have employed this fatty acid species as representative of all fatty acids. Another feature of this type of studies is that they are of relatively short duration (in the order of hours).

To explore the long-term effect of fatty acids on neonatal myocyte viability, the cells were exposed to physiological concentrations of various fatty acid species, complexed to bovine serum albumin (BSA) for up to 48 hours. First, the effects of palmitic acid (C16:0) were investigated. To elucidate whether possible effects could be ascribed to

chain length or the degree of saturation, cells were also exposed to palmitoleic acid (C16:1), stearic acid (C18:0) or oleic acid (C18:1), and to combinations of saturated and mono-unsaturated fatty acids. Cellular viability was assessed morphologically and by the release of cytosolic proteins. Surprisingly, C16:0 at all concentrations tested (500, 250, and 125 μM, keeping the BSA concentration at 150 μM) was highly toxic for the cardiomyocytes. Morphological analysis of the cardiomyocytes incubated with C16:0 showed severe cell damage, the first signs of which were already apparent after 8 hours of incubation. In line with these morphological observations the appearance of cytoplasmic proteins, such as lactate dehydrogenase (LDH) and heart-type fatty acid-binding protein (H-FABP), in the culture medium started after 8-12 hours. After 48 hours the release of cytosolic proteins into the medium was almost complete (>90% of cell contents).

In the presence of C18:0, the culture medium also severely compromised cell viability (figure 1). In contrast, the addition of mono-unstaturated fatty acids had no effect on cellular protein release and was not associated with marked changes in cell morphology, except for the cellular accumulation of substantial amounts of triacylglycerols as visualized by Oil Red O staining and as determined by capillary gas chromatography (not shown). Interestingly, the combined administration of C18:1 and C16:0 (250 μM each) completely abolished the otherwise harmful effects of C16:0 (250 μM), when present as the sole fatty acid species.

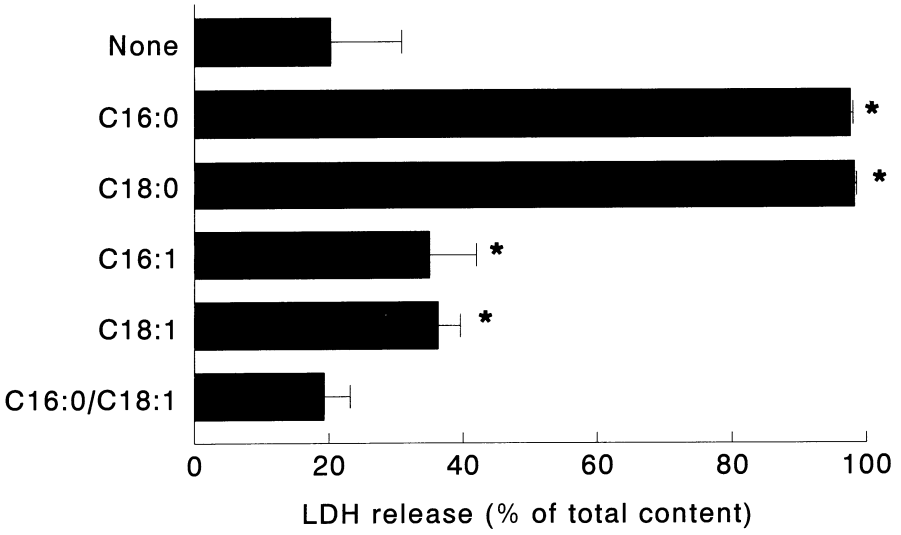

Figure 1. *Effect of fatty acids on the percentage release of lactate dehydrogenase (LDH) from neonatal cardiomyocytes. Cells were cultured in the presence of different fatty acids species (500 μM) or combinations of fatty acids (250 μM each) complexed to BSA (150 μM) for 48 hours. * indicates significant difference from cells cultured in the absence of fatty acids ('none'). (From: de Vries et al. J Lip Res 38, 1384-1394, 1997, with permission).*

These observations clearly indicate that saturated fatty acids have a dramatic impact on cardiomyocyte viability. Next, it was questioned whether the fatty acid-mediated cell death was due to necrosis or apoptosis. A hallmark of apoptosis is the development of numerous cleavages in genomic DNA, specifically in between nucleosomes, leading to a typical DNA-fragmentation pattern of multiples of approximately 200 base pairs. DNA-laddering was observed in cardiomyocytes exposed to either 500 μM or 250 μM C16:0, but not when the cardiomyocytes were cultured with a mixture of C16:0/C18:1 (250 μM each). The DNA-laddering pattern was most prominent in cells exposed to C16:0 for 16 hours. In support of the DNA-laddering assay, was the in situ detection of DNA strand breaks by means of the TUNEL (terminal transferase-mediated dUTP-biotin nick end labeling) assay. The percentage TUNEL positive cells was markedly increased under those conditions where DNA-laddering was apparent (data not shown).

Putative mechanisms of fatty acid-induced apoptosis

It has been shown that the mere absence of serum factors is already sufficient to initiate apoptosis in cultured cells, including primary cultures of neonatal cardiac myocytes [18]. The present findings indicate that apoptosis is further enhanced when saturated fatty acids are present in the culture medium. It remains to be determined, however, why the apoptotic response is confined to specific fatty acid species.

Analysis of the fatty acid composition of the phospholipid pool showed that each type of fatty acid supplied was incorporated in the cellular phospholipid pool to an appreciable extent. Accordingly, the cytotoxic effects of saturated fatty acids may relate to their relative enrichment in the phospholipid fraction. A substantial increase in the mol % of saturated fatty acyl chains in the phospholipid pool in neonatal myocytes will diminish membrane fluidity and, hence, compromise cell function. Indeed, loss of cellular viability was demonstrated in cardiac cells following the incorporation of either C16:0 or C18:0 (melting points 63 °C and 70 °C, respectively), but not of cis-C16:1 or cis-C18:1 (m.p. 0.5 °C and 13 °C, respectively), in their membrane lipids. Singh and coworkers [19] provided evidence that an increase in the mol % of saturated fatty acids in the phospholipid pool represents a crucial part of the apoptotic process. Alterations in the phospholipid composition of cellular membranes have been shown to initiate apoptosis. For instance, a genetic defect in the synthesis of phosphatidylcholine was found to trigger apoptosis in CHO cells [20]. Also, the pharmacological inhibition of arachidonate redistribution between the various phospholipid classes was demonstrated to induce apoptosis in a promyelocytic cell line [21]. These considerations support the notion that a relative excess of saturated fatty-acyl chains in the phospholipid pool, and the associated effects on membrane fluidity, drive the cardiomyocytes into apoptosis.

Alternatively, recent studies indicate that signal transduction through the sphingomyelin-ceramide pathway activates apoptosis in various cell types, among which neonatal myocytes [22]. Within cardiac tissue this special type of phospholipid is relatively abundant. In the rat heart it comprises approximately 3% of the total

phospholipid pool and only saturated acyl-moieties, with chain lengths ranging from 16 to 24 C-atoms, are attached to the sphingosine core structure via an amide bond [23]. Through the activity of the enzyme sphingomyelinase, which catalyzes a phospholipase C-like reaction, sphingomyelin is hydrolyzed yielding phosphocholine and ceramide as products. In recent studies some of the biological effects of tumor necrosis factor-α (TNFα) have been attributed to its activation of the sphingolipid signaling cascade [22,24]. The negative inotropic effect of TNFα on adult cardiomyocytes appeared to be due to an increase in the cellular sphingosine level [24]. TNFα-induced apoptosis of neonatal cardiomyocytes also involved sphingosine production [22]. Furthermore, addition of long-chain saturated fatty acids like palmitate (C16:0) or stearate (C18:0), precursors of sphingolipid synthesis, to the culture medium resulted in the de novo synthesis of ceramide and induced apoptosis in hematopoietic cell lines [25]. Interestingly, also in the present study saturated, but not mono-unsaturated, fatty acids induced apoptosis. However, the detrimental effects of saturated fatty acids were absent when mono-unsaturated fatty acids were also included. The latter observation seems hard to reconcile with the idea that the mere availability of C16:0 is sufficient to induce ceramide-mediated apoptosis in neonatal cardiomyocytes.

Long-term exposure of neonatal cardiomyocytes to fatty acids

As the long-term incubation with equimolar amounts of C16:0 and C18:1 was well-tolerated by neonatal rat cardiomyocytes and the fact that this combination shows resemblance to the in vivo situation (together C16:0 and C18:1 comprise approximately 60% of the circulating fatty acids) this combination was chosen to investigate the long-term effects of fatty acids on gene expression in more detail. The response of neonatal rat ventricular cardiomyocytes to exogenous fatty acids on the expression of a selection of genes was investigated at the mRNA level. The cells were incubated in the presence of either glucose only (10 mM), fatty acids only (combination of C16:0 and C18:1, 250 μM each), or a combination of glucose and fatty acids. After 48 hours of incubation the cells were harvested and total RNA was isolated for Northern blot analysis. The exposure of neonatal cardiomyocytes to fatty acids, either as the single substrate or in combination with glucose, led to a 2- to 4-fold increase of the mRNA level of genes involved at various levels of cellular fatty acid handling (figure 2). First of all Fatty Acid Translocase (FAT), one of the integral membrane proteins that are supposed to be involved in the transport of long-chain fatty acids across the sarcolemma [26,27], was induced. Second, the mRNA level of the cytosolic protein H-FABP was elevated. This protein mediates the transfer of the water-insoluble fatty acids from the sarcolemma to the mitochondria [28]. Furthermore, the mRNA of long-chain Acyl-CoA dehydrogenase (LCAD) increased 3.5-fold. The latter enzyme participates in the mitochondrial-oxidation of fatty acids. In contrast, in cells cultured in the presence of fatty acids the mRNA level of the insulin-responsive glucose transporter GLUT4 tended to decrease. Together, these observations indicate that long-term exposure of cardiac myocytes to fatty acids evokes a selective and coordinated induction of genes involved in fatty acid handling. It may seem trivial that

upon exposure to fatty acids, the cardiomyocyte responds with an increase in the expression levels of genes involved in fatty acid uptake and metabolism, thereby increasing its capacity to handle fatty acids. However, the corollary of this finding is that the cardiac myocyte is capable of sensing changes in substrate supply.

As mentioned earlier, under normal conditions glucose and fatty acids are the major substrates for the cardiac muscle [29,30]. However, cardiac substrate preference alters during development. Carbohydrates are the main substrates for the fetal heart, whereas in the postnatal period the heart rapidly switches to fatty acids as its main energy source [31]. It is generally believed that the alterations in substrate utilization and concordant changes in the activity of enzymes involved in fatty acid utilization are primarily caused by the postnatal changes in circulating levels of hormones, such as insulin, glucagon, and thyroid hormone [32]. The present findings, however, suggest that in addition to hormonal regulation, the mere change in nutrient supply around birth (from glucose present in maternal blood to fatty acids in lipid-rich milk) could directly be responsible for some of these in vivo changes.

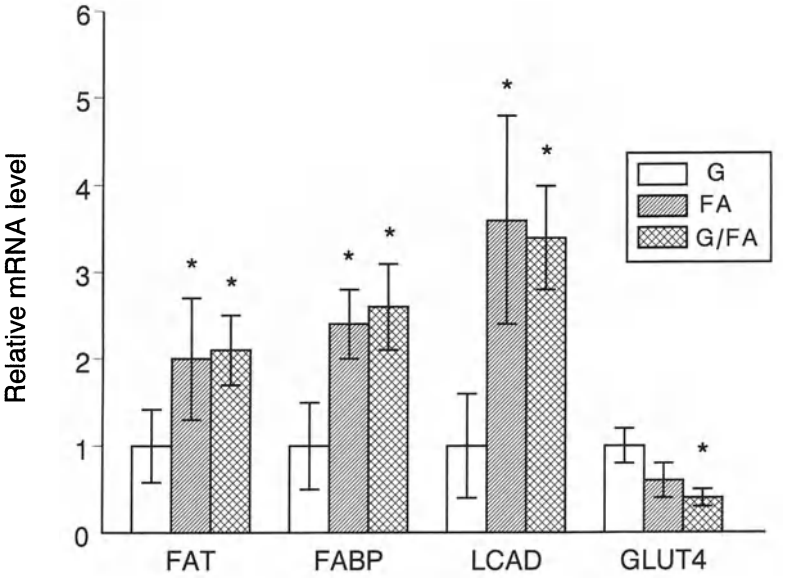

Figure 2. *Effects of substrate of on mRNA levels of Fatty Acid Translocase (FAT), heart-type fatty acid-binding protein (H-FABP), long-chain acyl-CoA dehydrogenase (LCAD), and the GLUT4 glucose transporter. Neonatal myocytes were cultured in the presence of either 10 mM glucose (G), 250 μM each of C16:0 and C18:1 (FA), or a combination thereof (G/FA). mRNA signals were first normalized to the corresponding 18S signal. Subsequently the mRNA/18S ratios were normalized to the glucose group. * Indicates $p<0.05$ versus glucose group.*

Putative mechanism of fatty acid-mediated gene expression

At this moment no conclusive answer can be given as far as the mechanism involved in fatty acid-mediated gene expression. As opposed to poly-unsaturated fatty acids,

C16:0 and C18:1 do not function as precursors of eicosanoids. This implies that the observed effects on gene expression are due to the fatty acids themselves, or to intracellular metabolites like long-chain acyl-CoA, rather than to the formation of biologically active cyclooxygenase or lipoxygenase products. Effects of fatty acids on gene expression have been reported for other cell types, such as adipocytes, hepatocytes, and skeletal myocytes [12,33,34]. As far as the mechanism is concerned, the results obtained with these cell types have provided evidence for the existence of a direct pathway through which fatty acids may modulate transcriptional regulation. First, it was shown that various genes involved in lipogenesis contained a consensus DNA-sequence that conferred fatty acid-responsiveness to these genes. Later it was shown that transcription factors of the nuclear hormone superfamily, the so-called Peroxisome Proliferator-Activated Receptors (PPAR), binds to this regulatory element in conjunction with their dimerization partner the Retinoic-X-Receptor (RXR). By now three PPAR isoforms (α,β,γ) have been cloned. PPAR α and β are expressed in the heart, albeit at different levels. For a long time the natural ligand of PPAR has remained unidentified. However, recent findings indicate that both prostaglandins and long-chain fatty acids act as ligands for the PPAR's [35,36]. It is noteworthy that for a number of genes involved in cardiac lipid metabolism, among which, medium-chain acyl-CoA dehydrogenase and H-FABP, it has been shown that they contain putative PPAR-responsive elements in their 5'-untranslated regions [37,38]. Accordingly, it seems worth investigating whether PPAR's also play a role in fatty acid-mediated regulation of gene transcription in the heart.

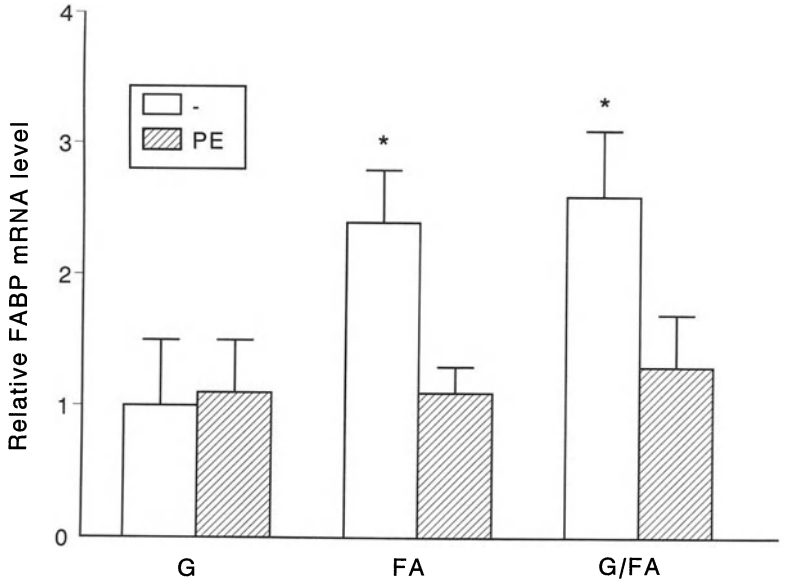

Figure 3. *Changes in H-FABP mRNA level in non-stimulated (open bars) and phenylephrine-stimulated (10 μM; hatched bars) neonatal myocytes cultured in serum-free medium containing either 10 mM glucose (G), 500 μM of C16:0/C18:1 (FA), or a combination of glucose and fatty acids (G /FA) as substrates for 48 hours. To allow comparison H-FABP signals were normalized to the corresponding 18S signal. * Indicates $p<0.05$ versus non-stimulated glucose group (open bar, G).*

Cardiac hypertrophy and fatty acid utilization

Under various pathophysiological conditions, including diabetes and cardiac hypertrophy, it has been shown that cardiac metabolism changes quite dramatically. In the setting of diabetes cardiac energy metabolism becomes even more dependent on the oxidation of fatty acids [39]. In contrast, during cardiac hypertrophy the opposite takes place, i.e., the utilization of carbohydrates increases at the expense of fatty acids. This phenomenon has been observed in in vivo models of pressure overload-induced cardiac hypertrophy, using radiolabeled glucose and fatty acid analogues [40], as well as in studies with ex vivo perfused hypertrophic hearts [41]. Recently, Sack and coworkers [42] showed that this reduction in fatty acid oxidation might be secondary to a downregulation of the expression of genes involved in mitochondrial-oxidation in hypertrophic hearts. Furthermore, various studies have shown that inborn errors in fatty acid metabolism are associated with cardiomyopathy [43]. These observations point to a causal relationship between alterations in fatty acid metabolism and changes in cardiac phenotype.

To investigate the possible interplay between fatty acid-mediated processes and hypertrophy, cardiomyocytes were cultured in the absence or presence of fatty acids and stimulated with the α_1-adrenergic agonist phenylephrine (PE, final concentration 10 μM), a well-established stimulus for neonatal cardiomyocyte hypertrophy [44]. Northern blot analysis of total RNA isolated from neonatal myocytes cultured in the presence of different (combinations of) substrates revealed that the mRNA level of H-FABP was affected by fatty acids. In the presence of C16:0/C18:1, irrespective of the presence of glucose, a 2- to 3-fold increase in the cellular H-FABP mRNA content was observed in non-stimulated cells after 48 hours (figure 3). Interestingly, in line with the notion that cardiac hypertrophy is associated with a decline in the utilization of fatty acids, the fatty acid-induced rise in H-FABP mRNA level was abrogated in PE-stimulated hypertrophic cardiomyocytes.

Concluding remarks

Current findings indicate that the neonatal ventricular myocyte presents a valuable model system to unravel the long-term effects of fatty acids on cardiomyocyte phenotype. As reviewed in this paper, various aspects of fatty acid-mediated signal transduction can be studied. This is exemplified by showing that in cardiomyocytes apoptosis can be selectively induced by saturated, but not by mono-unsatutrated fatty acid species. Moreover, it is shown that exposure of cardiac muscle cells to fatty acids evokes a coordinated up-regulation of the expression of a set of genes involved in lipid metabolism, strongly suggesting the existence of a common signalling pathway through which alterations in lipid metabolism are conveyed to the transcriptional machinery of the cardiomyocyte. Finally, it is demonstrated that following induction of hypertrophy by means of the α_1-adrenergic agonist phenylephrine the fatty-acid mediated upregulation of H-FABP is completely abolished. The latter observation is in line with the notion that hypertrophy is associated with a shift from fatty acid to glucose

oxidation. Although the presence of the substrate shift is well-established, the biological significance of this phenomenon remains open to discussion. Nonetheless current findings indicate that the cardiomyocyte responds to changes in substrate supply through transcriptional regulation and suggest that there may be some type of cross-talk between fatty acid metabolism and the phenotypical alterations that accompany cardiac hypertrophy.

Acknowledgements

The technical assistance of PHM Willemsen, ThM Roemen, and Y de Jong was greatly appreciated. The research of MvB has been made possible by a fellowship of the Royal Netherlands Academy of Arts and Sciences.

References

1. Honore E, Barhanin J, Attali B, Lesage F, Lazdunski M. External blockade of the major cardiac delayed-rectifier K+ channel (Kv1.5) by polyunsaturated fatty acids. Proc Natl Acad Sci USA 1994;91:1937-41.
2. Huang JMC, Xian H, Bacaner M. Long-Chain Fatty Acids Activate Calcium Channels in Ventricular Myocytes. Proc Natl Acad Sci USA 1992;89:6452-56.
3. Kang JX, Leaf A. Evidence that free polyunsaturated fatty acids modify Na+ channels by directly binding to the channel protein. Proc Natl Acad Sci USA 1996;93:3542-46.
4. Kang JX, Leaf A. The cardiac antiarrhythmic effects of polyunsaturated fatty acid. Lipids 1996;31 Suppl:S41-44.
5. Oliver MF, Kurien VA, Greenwood TW. Relation between serum-free-fatty acids and arrhythmias and death after acute myocardial infarction. Lancet 1968;1:710-14.
6. Khan WA, Blobe GC, Hannun YA. Arachidonic acid and free fatty acids as second messengers and the role of protein kinase C. Cell Signal 1995;7:171-84.
7. Van Bilsen M, Van der Vusse GJ. Phospholipase-A2-dependent signalling in the heart. Cardiovasc Res 1995;30:518-29.
8. Bouvier M, Moffett S, Loisel TP, Mouillac B, Hebert T, Chidiac P. Palmitoylation of G-protein-coupled receptors: a dynamic modification with functional consequences. Biochem Soc Trans 1995;23:116-20.
9. Iiri T, Backlund PS, Jr., Jones TL, Wedegaertner PB, Bourne HR. Reciprocal regulation of Gs alpha by palmitate and the beta gamma subunit. Proc Natl Acad Sci USA 1996;93:14592-97.
10. Shubeita HE, Martinson E, Van Bilsen M, Chien KR, Brown JH. Expression of a constitutively active protein kinase C gene activates the transcription of the ANF and MLC-2 genes in cultured myocardial cells. Proc Natl Acad Sci USA 1992;89:1305-09.
11. Grimaldi PA, Knobel SM, Whitesell RR, Abumrad NA. Induction of aP2 gene expression by nonmetabolized long-chain fatty acids. Proc Natl Acad Sci USA 1992;89:10930-34.
12. Teboul L, Gaillard D, Staccini L, Inadera H, Amri E-Z, Grimaldi PA. Thiazolidinediones and fatty acids convert myogenic cells into adipose-like cells. J Biol Chem 1995;270:28183-87.
13. Van Bilsen M, Chien KR. Growth and hypertrophy of the heart: towards an understanding of cardiac specific and inducible gene expression. Cardiovasc Res 1993;27:1140-49.
14. Rosenthal MD. Accumulation of neutral lipids by human skin fibroblasts: differential effects of saturated and unsaturated fatty acids. Lipids 1981;16:173-82.
15. Zhang CL, Lyngmo V, Nordoy A. The effects of saturated fatty acids on endothelial cells. Thromb Res 1992;65:65-75.
16. Doi O, Doi F, Schroeder F, Alberts AW, Vagelos PR. Manipulation of fatty acid composition of membrane phospholipid and its effects on cell growth in mouse LM cells. Biochim Biophys Acta 1978;509:239-50.
17. Van der Vusse GJ, Roemen THM, Flameng W, Reneman RS. Serum-myocardium gradients of non-esterified fatty acids in dog, rat and man. Biochim Biophys Acta 1983;752:361-70.
18. Sheng ZL, Knowlton K, Chen J, Hoshijima M, Brown JH, Chien KR. Cardiotrophin 1 (Ct 1) Inhibition of Cardiac Myocyte Apoptosis Via a Mitogen Activated Protein Kinase Dependent Pathway: Divergence From Downstream Ct 1 Signals For Myocardial Cell Hypertrophy. J Biol Chem 1997;272:5783-91.
19. Singh JK, Dasgupta A, Adayev T, Shahmehdi SA, Hammond DA, Banerjee P. Apoptosis is associated with an increase in saturated fatty acid containing phospholipids in the neuronal cell line, HN2-5. Biochim Biophys Acta 1996;1304:171-78.
20. Cui Z, Houweling M, Chen MH, et al. A genetic defect in phosphatidylcholine biosynthesis triggers apoptosis in chinese hamster ovary cells. J Biol Chem 1996;271:14668-71.
21. Surette ME, Winkler JD, Fonteh AN, Chilton FH. Relationship between

arachidonate-phospholipid remodeling and apoptosis. Biochemistry 1996;35:9187-96.
22. Krown KA, Page MT, Nguyen C, et al. Tumor Necrosis Factor Alpha Induced Apoptosis in Cardiac Myocytes: Involvement of the Sphingolipid Signaling Cascade in Cardiac Cell Death. J Clin Invest 1996;98:2854-65.
23. Van Bilsen M, Van der Vusse GJ, Willemsen PHM, Roemen THM, Coumans WA, Reneman RS. Lipid alterations during ischemia and reperfusion of isolated rat hearts: Its relation to myocardial damage. Circ Res1989;64:303-14.
24. Oral H, Dorn GW, Mann DL. Sphingosine Mediates the Immediate Negative Inotropic Effects of Tumor Necrosis Factor Alpha in the Adult Mammalian Cardiac Myocyte. J Biol Chem 1997;272:4836-42.
25. Paumen MB, Ishida Y, Muramatsu M, Yamamoto M, Honjo T. Inhibition of Carnitine Palmitoyltransferase I Augments Sphingolipid Synthesis and Palmitate Induced Apoptosis. J Biol Chem 1997;272:3324-29.
26. Abumrad NA, El-Maghrabi MR, Amri E-Z, Lopez E, Grimaldi PA. Cloning of a rat adipocyte membrane protein implicated in binding or transport of long-chain fatty acids that is induced during preadipocyte differentiation. J Biol Chem 1993;268:17665-68.
27. Ibrahimi A, Sfeir Z, Magharaie H, Amri E-Z, Grimaldi P, Abumrad NA. Expression of the CD36 homolog (FAT) in fibroblast cells: Effects on fatty acid transport. Proc Natl Acad Sci USA 1996;93:2646-51.
28. Glatz JF, van der Vusse GJ. Cellular fatty acid-binding proteins: their function and physiological significance. Prog Lipid Res 1996;35:243-82.
29. Neely JR, Morgan HA. Relationship between carbohydrate and lipid metabolism and the energy balance of heart muscle. Annu Rev Physiol 1974;36:413-59.
30. Van der Vusse GJ, Glatz JFC, Stam HCG, Reneman RS. Fatty acid homeostasis in the normoxic and ischemic heart. Physiol Rev 1992;72:881-940.
31. Lopaschuk GD, Collins-Nakai RL, Itoi T. Developmental changes in energy substrate use by the heart. Cardiovasc Res 1992;26:1172-80.
32. Girard J, Ferré Pé Pégorier J-P, Duée PH. Adaptations of glucose and fatty acid metabolism during perinatal period and suckling-weaning transition. Physiol Rev 1992;72:507-62.
33. Amri EZ, Ailhaud G, Grimaldi P. Regulation of adipose cell differentiation. II. Kinetics of induction of the aP2 gene by fatty acids and modulation by dexamethasone. J Lipid Res 1991;32:1457-63.
34. Jump DB, Ren B, Clarke S, Thelen A. Effects of fatty acids on hepatic gene expression. Prostagl Leuk Essent Fatty Acids 1995;52:107-11.
35. Schoonjans K, Staels B, Auwerx J. Role of the peroxisome proliferator-activated receptor (PPAR) in mediating the effects of fibrates and fatty acids on gene expression. J Lipid Res 1996;37:907-25.
36. Forman BM, Tontonoz P, Chen J, Brun RP, Spiegelman BM, Evans RM. 15-Deoxy-delta 12, 14-prostaglandin J2 is a ligand for the adipocyte determination factor PPAR. Cell 1995;83:803-12.
37. Raisher BD, Gulick T, Zhang Z, Strauss AW, Moore DD, Kelly DP. Identification of a novel retinoid-responsive element in the promoter region of the medium chain acyl-coenzyme A dehydrogenase gene. J Biol Chem 1992;267:20264-69.
38. Treuner M, Kozak CA, Gallahan D, Grosse R, Muller T. Cloning and characterization of the mouse gene encoding mammary-derived growth inhibitor/heart-fatty acid-binding protein. Gene 1994;147:237-42.
39. Wall SR, Lopaschuk GD. Glucose Oxidation Rates in Fatty Acid-Perfused Isolated Working Hearts from Diabetic Rats. Biochim Biophys Acta 1989;1006:97-103.
40. Kagaya Y, Kanno Y, Takeyama D, et al. Effects of long-term pressure overload on regional myocardial glucose and free fatty acid uptake in rats. Circulation 1990;81:1353-61.
41. Allard MF, Schonekess BO, Henning SL, English DR, Lopaschuk GD. Contribution of

oxidative metabolism and glycolysis to ATP production in hypertrophied hearts. Am J Physiol 1994;267:H742-50.
42. Sack MN, Rader TA, Park S, Bastin J, McCune SA, Kelly DP. Fatty acid oxidation enzyme expression is downregulated in the failing heart. Circulation 1996;94:2837-42.
43. Strauss AW, Powell CK, Hale DE, et al. Molecular basis of human mitochondrial very-long-chain acyl-CoA dehydrogenase deficiency causing cardiomyopathy and sudden death in childhood. Proc Natl Acad Sci USA 1995;92:10496-500.
44. Chien KR, Knowlton KU, Zhu H, Chen S. Regulation of cardiac gene expression during myocardial growth and hypertrophy: molecular studies of an adaptive physiologic response. FASEB J 1991;5:3037-46.

23. REDUCTION OF KIDNEY RENIN EXPRESSION BY RIBOZYMES

Matthew G. F. Sharp, Jörg Peters, and John J. Mullins

Introduction

The renin-angiotensin system is involved in the regulation of fluid volume and salt homeostasis, and it is now clear that renin is a major moderator of fluid and salt balance, and may be important in human disease. The introduction of antisense RNA sequences complementary to the gene of interest, and catalytic RNA (ribozymes), can be used experimentally to probe molecular events in physiological processes. However, strategies involving antisense RNA are prone to several limiting factors. For example, complementary sequences must be accessible for hybridization, and a large molar excess of antisense molecules is often required before significant gene inhibition is observed. We have attempted to improve the efficiency of antisense RNA-mediated gene inhibition by the inclusion of catalytic domains, specific for the mouse renin genes, into a gene encoding the ubiquitous small nuclear RNA (snRNA) U1, which is involved in intron recognition and pre-mRNA processing. This approach confers several advantages: (i) high level expression of the ribozyme, (ii) twin ribozyme domains cleave target mRNA twice, improving ribozyme: product dissociation rates, and (iii) use of the U1 splicing factor to co-localize the ribozyme to the cellular compartment where transcription of the target pre-mRNA occurs. Ribozyme RNA was highly expressed in transgenic mice, and a significant ($P<0.01$) reduction in renal active renin was achieved. This study explores the use of modified U1 snRNA as a vector system for antisense and ribozyme inhibition studies, and indicates how further refinements of this strategy may be applied in the future.

Background

Renin is an aspartyl protease which cleaves the plasma protein angiotensinogen to produce the decapeptide angiotensin I (AngI), which may then be converted into the potent octapeptide pressor hormone, angiotensin II (AngII). Known physiological effects of AngII include increased peripheral resistance directly via vasoconstriction, and increased salt and water retention by stimulating aldosterone release. The renin gene is a candidate in the genetic predisposition to cardiovascular diseases and

P.A. Doevendans et al. (eds.), Cardiovascular specific gene expression, 269-83.

hypertension, and the experimental control of its expression level would be an useful tool in physiologically relevant model systems. It is now possible to introduce mutations into any gene in mice, and we have recently shown that inactivation of one of the mouse renin genes (*Ren-1^d*), but not the other gene (*Ren-2*, [1]) results in a significant fall in blood pressure in female mice [2]. Aberrant expression of renin in transgenic animals has shown that high levels of the zymogen (prorenin) in the circulation can cause extreme hypertension [3] and vascular and cardiac hypertrophy [4]. Further studies of renin gene expression in physiological model systems is required before the role of this protein in the integrated control of cardiovascular homeostasis is completely understood.

Renin is synthesized principally in the kidney juxtaglomerular (JG) cells, a group of modified smooth muscle cells located at the distal end of the renal afferent arteriole of the kidney cortex [5], although all species studied have extrarenal sites of renin biosynthesis. Most mammals possess a single renin gene, some laboratory mouse strains and all wild *Mus musculus* subspecies possess two renin genes, *Ren-1^d* and *Ren-2*, which are expressed at similar levels in JG cells [6,7]. These genes encode highly homologous but distinct proteins, renin-1^d and renin-2, which have different glycosylation potential, and different patterns of gene expression [8]. For example, the *Ren-2* gene is highly expressed in the granular convoluted tubule cells of the submandibular gland. It is unclear, at present, what the function of this extrarenal renin-2 is in mouse strains which carry two renin genes, as targeted mutation of the *Ren-2* gene has no effect on renal histology or blood pressure [1]. The tissue-specific interference of renin gene expression would aid in investigating this area.

Gene inhibition

The ability to control gene expression in animal models, both positively and negatively, is a powerful tool for delineating the molecular events in the initiation and progression of disease states. It is possible to inhibit processes such as splicing, polyadenylation, nuclear export and translation of a gene product by co-expressing an RNA sequence complementary to the gene under study. Antisense RNA has been used with some success in unicellular systems, in cultured cells and in transgenic animals and plants to down-regulate the expression of a gene of interest [9,10].

Short oligonucleotides [11-14] targeted against the transcripts of the angiotensinogen and AT1a receptor genes can significantly reduce gene expression and blood pressure in whole animal studies. Retrovirus vectors expressing antisense to AngII receptor type 1 in neuronal cultures from SHR [15], and systemically in young SHR rats [16] have demonstrated the importance of AngII signalling in the setting up and maintenance of basal blood pressure levels. Transgenic mice have been used by Pedrazzini et al. [17] to develop an inducible antisense model which would allow the controlled regulation of angiotensinogen levels, but in this system gene inhibition was transitory.

It is known that RNA can possess several enzymatic activities, including the cleavage of the phosphodiester chain of nucleic acids. These active structures, called ribozymes, require only a divalent cation, and there is no requirement for an external energy source, nor any other cofactor [18]. Hammerhead ribozymes were first isolated from plant pathogen RNA viruses and virusoids. These molecules normally cleave in cis, but it is

clear that these enzymes can be manipulated to cleave separate target RNA molecules (i.e. in trans) at the sequence UH (where H is A, U or C). The specificity of the reaction is defined by the base pairing between sequences flanking the catalytic core of the ribozyme and the target RNA molecule. These new tools have many potential applications in the investigation of genetic pathways and in the treatment of human diseases, such as viral diseases, which are caused by a characterized genetic pathogen [19]. There is a growing body of experimental data to show that ribozymes can be effective in inhibiting gene expression in many cell types, including mammalian cells and whole organisms [10]. This technology offers an improvement over antisense RNA strategies due to the fact that the target RNA is cleaved catalytically by the ribozyme, and the ribozyme RNA survives this reaction and is able to interact subsequently with more target RNA molecules. This, in turn, means that the level of antisense RNA required is no longer stoichiometric, and gene inhibition is possible with reduced levels of antisense RNA.

In this chapter, we describe our attempts to increase the effectiveness of ribozyme and antisense expression constructs, targeting renin, in transgenic mice. We have attempted to co-localize inhibitory and target RNAs through the incorporation of ribozymes into the splicing machinery. In transgenic mice, a reduction was seen in the level of kidney renin mRNA and renal renin protein. We show that engineered U1 RNAs have the capacity for use as highly efficient ribozyme vectors, but the rules of ribonucleoprotein particle assembly need to be clearly understood if the full potential of this approach is to be realized in the future.

Materials and Methods

Construction of ribozyme expression vectors

Synthetic oligodeoxynucleotides (figures 1 and 2) were annealed in a thermal cycler by oscillating the temperature between 60°C and a maximum temperature which began at 94°C, and reduced by 2°C per 30 second cycle, for 13 cycles. The annealed duplex was cloned into the human U1 genomic clone HSD2 [20], which had been digested with both BglII and BclI (figure 1A). This results in the replacement of five nucleotides of the 5' end of the U1 snRNA with novel sequences. Two plasmids were made, incorporating a region of renin complementary sequences, either with or without ribozyme sequences, and were named pU1AS43 and pU1RZ43 (see figure 1). The same oligos were cloned in plasmid pSP71 (Promega) in a similar way (and named pSPAS43 and pSPRZ43), to facilitate in vitro transcription of ribozyme RNA. Constructs were checked by DNA sequencing.

Ribozyme cleavage assay

RNA was transcribed from plasmids pSPRZ43 and pSPAS43 in vitro using T3 and T7 RNA polymerases (Ribomax, Promega) and the yield was measured spectrophometrically. Substrate for ribozyme action was 1200 bp of the mouse *Ren-2* mRNA [21] , cloned in pBluescript II KS, transcribed as above. Pure RNA molecules were mixed on ice in a buffer containing 10 mM Tris-HCl and 12 mM MgCl2, and then

incubated at 39°C. The reaction was stopped by the addition of EDTA to >10 mM, and the products resolved on 4% polyacrylamide gels, fixed in 12% methanol-10% acetic acid and dried. Autoradiography was at room temperature with Kodak XAR5 film.

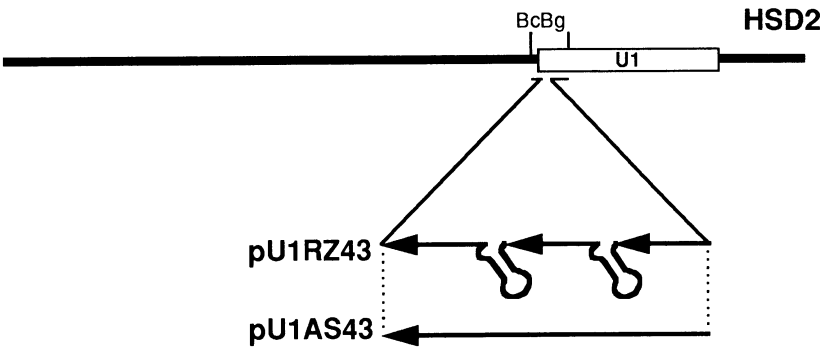

Figure 1. *Design of ribozyme expression vectors. Clone HSD2, which has 3.3kb of human genomic DNA (solid line) containing a gene for the U1 snRNA (open box), is shown (U1 gene is not to scale). Bc, BclI; Bg, BglII. Constructs pU1AS43 and pU1RZ43 were made by cloning either double-stranded oligonucleotide into the sites indicated in HSD2. pU1AS43 has 41 nucleotides complementary to the mouse renin sequences which replace nucleotides 3-12 of the human U1 coding region. pU1RZ43 has the same region of renin complementary sequences, interrupted by two copies of the hammerhead ribozyme motif.*

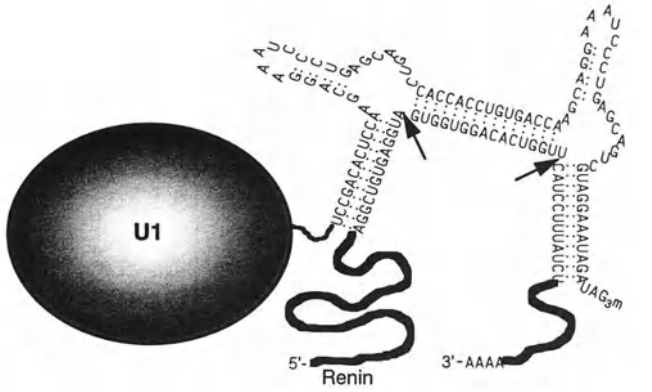

Figure 2. *Proposed interaction of ribozyme U1RZ43 with the target renin mRNA. The bulk of the U1 RNA, complexed with snRNP proteins (grey oval), and the major part of the renin mRNA (thick line), are shown schematically. The twin hammerhead domains are shown paired to the renin substrate mRNA. Sites of cleavage are indicated by arrows.*

Filter hybridization analysis

Genomic DNA (10 μg) was digested with restriction enzyme and separated on 1% agarose slab gels in 0.5 x TAE buffer containing 0.5μg/ml ethidium bromide, and capillary blotted onto positively charged nylon membrane (Boehringer Mannheim) according to the manufacturer's instructions.

For preparation of RNA, tissues were homogenized in guanidinium isothiocyanate/ phenol as described [22]. Quality of RNA was checked by agarose gel electrophoresis and spectrophotometry. RNA was purified as above from nuclear and cytoplasmic fractions from cultured cells after detergent-mediated partial lysis and centrifugation. RNA was denatured using glyoxal, and separated on 1.2% agarose gels in MOPS buffer as described [23] , and capillary-transferred onto charged nylon membrane, according to the manufacturer's instructions (Boehringer Mannheim). Hybridization [24] of ^{32}P-labelled, random-primed DNA probes was followed by washing filters in 0.2 M SSC, 0.1% SDS, at 68°C. Autoradiography was performed with intensifying screens and Kodak XAR5 or Fuji film at -70°C, or with a PhosphoImager (Molecular Dynamics).

Renin measurements

To measure renin levels in mouse tissues, animals were sacrificed by CO_2 anesthesia, and tissues snap frozen in liquid nitrogen. Tissue renin concentrations were assayed as described [25]. The AngI generated by the tissue active renin was measured by radioimmunoassay [26]. Statistical significance was assessed using the non-parametric Mann-Whitney U test.

Cell culture

The human hepatoma cell line HepG2 was cultured in Dulbecco's modified Eagle's medium (DMEM): Ham's F12 (1:1) with 10% foetal calf serum in a hydrated atmosphere of 7% CO_2. Cells were passaged at 70-90% confluence and were split 1:5 except for cloning experiments. DNA constructs were introduced using the $CaCl_2$ co-precipitation method. HepG2 cells were co-transfected with a plasmid containing the hygromycin-resistance gene hpt under the control of the mouse PGK-1 promoter, and with one of the ribozyme- or antisense-containing constructs pU1RZ43 and pU1AS43, or with the human U1 gene alone as a control.

Immunoprecipitation

HepG2 cells stably expressing modified U1 RNAs were seeded at 2.2 x 10^6 cells per 60 mm dish (80% confluence), and grown overnight in phosphate-free MEM, without serum, supplemented with 250 μCi of $^{32}PO_4$. Cells were then harvested, and Sm-complexed material immunoprecipitated with the Sm antigen-specific monoclonal antibody Y-12 (a gift from Dr. J. A. Steitz), as described [27,28]. Radiolabelled RNA purified in this way was separated on 10% polyacrylamide, 7.3 M urea sequencing gels and imaged using a PhosphoImager (Molecular Dynamics).

Preparation of Transgenic Mice

Plasmid DNAs were digested to remove vector sequences and microinjected into C57BL/6 x CBA/Ca F2 mouse eggs as described [3]. Transgenic offspring were identified by DNA blotting using the transgene as a hybridization probe, and back crossed to CBA/Ca mice. All animal husbandry was in accordance with the Animals (Scientific Procedures) Act, 1986.

Results

Design of Ribozyme Expression Vectors

A 3.3 kb human genomic clone (HSD2) containing a structural gene for the U1 snRNA, and its promoter and transcription termination signal sequences [20,29], was modified by the inclusion of antisense and ribozyme sequences (figure 1). Using existing genomic restriction endonuclease recognition sites, oligonucleotides were cloned which replaced the excised U1 gene sequences, except for nucleotides (nts) +3 to +12 of the human U1 snRNA. These nucleotides were replaced with sequence complementary to nucleotides 877 to 917 of the mouse *Ren-2* sequence (GenBank Accession Number V00845) (pU1AS43; figure 1), or with the same antisense region punctuated by two catalytic ribozyme domains derived from the satellite RNA of subterranean clover mottle virus (sSCMV) designed to cleave the *Ren-2* mRNA after positions 888 and 904 (pU1RZ43; figure 1). These ribozyme cleavage sites are conserved in both the *Ren-1*^{d} and *Ren-2* mouse renin genes. Two catalytic domains were built into pU1RZ43 such that the initial interaction between *Ren-2* and ribozyme RNAs was over 41 nts, which is then reduced to three short regions (12+15+12 nts) after cleavage by both ribozymes (see figure 2). These short regions of complementarity should then be less able to form a stable duplex after the ribozyme cleavage reaction. Thus the products of the reaction should dissociate from the ribozyme RNA, allowing further cycles of substrate annealing and catalysis to take place. The modification of this region of the U1 snRNA was not expected to interfere with the normal assembly of U1 snRNP complexes or association with Sm antigen, as the 5' terminus of this RNA is located on a protuberance originating from the main body of the particle [30], and is accessible for base pairing with intron-exon splice junctions [31].

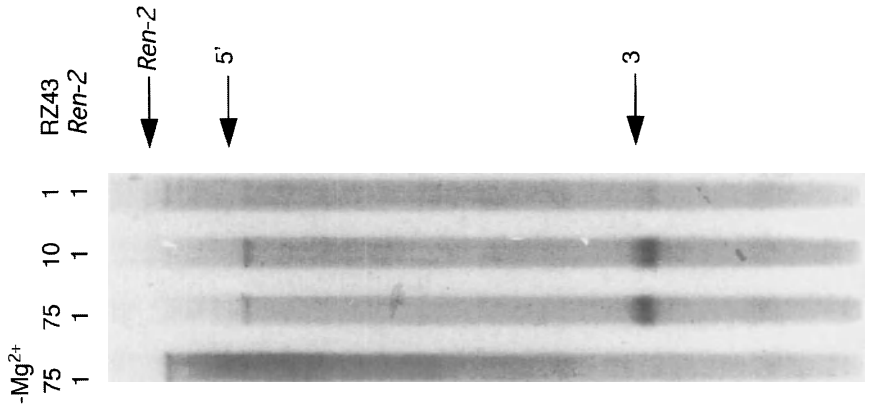

Figure 3. *In vitro analysis of the Ren-2 ribozymes. Different molar ratios of RZ43 ribozyme RNA and renin mRNA, ranging from 75:1 to 1:1, were mixed in the presence (or absence: -Mg^{2+}) of 12mM $MgCl_2$, and incubated for 2 hours at 39°C. Samples were then analyzed by electrophoresis through 4% polyacrylamide/7.3M urea gels. Positions of full-length renin substrate RNA (Ren-2), and 5' and 3' cleavage products are shown (arrows).*

In vitro activity of ribozymes

The cleavage activity of the ribozyme RZ43 was confirmed by mixing a renin substrate RNA transcribed from a plasmid containing the mouse *Ren-2* cDNA with RZ43 RNA transcribed in vitro. This assay system allowed an estimation of the efficacy of cleavage of a substrate which is almost full length. The assay conditions do not fully reflect the in vivo environment inside mammalian cells, although conditions were kept within the physiological range of Mg^{2+} concentration and temperature. Cleavage of the *Ren-2* mRNA occurred efficiently at the predicted site with ribozyme RZ43 using a 10:1 molar ratio of RNAs (figure 3), and some cleavage was visible with equimolar ratios of ribozyme and substrate RNAs. Cleavage products were easily detected from this relatively complex target molecule, which contained the whole *Ren-2* coding region, after only two hours incubation. Many ribozymes show optimal activity only at higher temperatures and with very short model substrate RNAs, and so the activity of RZ43 may be even higher in these conditions. The activity of the RZ43 RNA was dependent upon the presence of Mg^{2+} ions (figure 3).

Expression of Ribozymes in Hepatoma cells

The human hepatoma cell line HepG2 was used to test the expression and efficacy of pU1RZ43 and pU1AS43 in cultured cells. Pools of cells stably transfected with either the pU1RZ43 or pU1AS43 gene were expanded, and the expression level and nuclear localization of modified snRNAs assessed. Figure 4A shows that the U1RZ43 ribozyme RNA is expressed abundantly in HepG2 cells, and that this transcript is more abundant in the nuclear rather than cytoplasmic compartment, as is observed with the endogenous human U1 RNA.

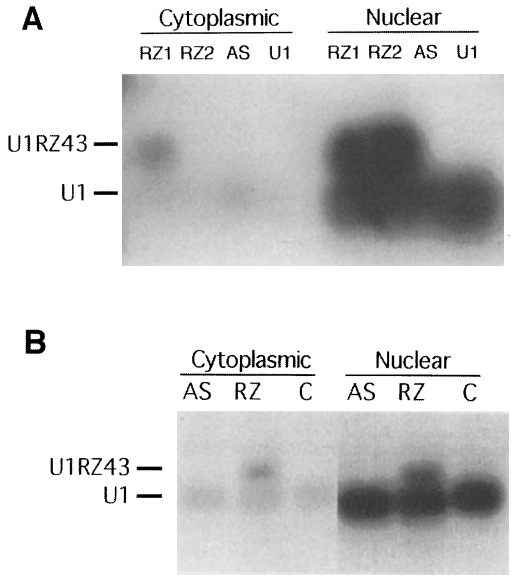

Figure 4. *Expression of ribozymes in cultured hepatoma cells. A, RNA blot analysis of 10 μg of total RNA purified by crude nuclear and cytoplasmic fractionation of stably transfected hepatoma cells (HepG2). RZ, U1RZ43-containing cells; AS, U1AS43-containing cells; U1, cells transfected with the parental human U1 gene only. B, RNA blot analysis of 10 μg of total RNA from cells transiently transfected with pU1AS43 (AS) and pU1RZ43 (RZ) plasmids in HepG2 cells. C, control mock transfected HepG2 cells. Filters were probed with ^{32}P-labelled cRNA transcript complementary to the RZ43 ribozyme, which also cross-hybridizes with the AS43 RNA and the endogenous U1 RNA. Sizes of bands are in nucleotides.*

Transient expression of these constructs in HepG2 cells (figure 4B) demonstrates only very low level expression from the U1RZ43 expression cassette, suggesting that transient expression experiments are not feasible with this promoter. Significant expression of pU1AS43 was not observed in these cells, which may suggest that the antisense sequence introduced into the U1 RNA is destabilizing in vivo. The ribozyme-containing RNAs do accumulate, however, which may be because of the highly structured nature of the hammerhead domain, conferring stability to the engineered transcript.

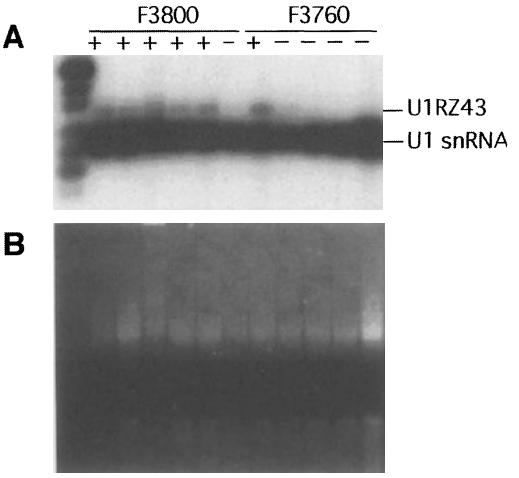

Figure 5. *Transgene expression in transgenic mice. A) Kidney RNA (30μg) blot from transgenic U1RZ43 mice of lines F3800 and F3760 was hybridized to a ^{32}P-labelled cRNA probe from pSPRZ43, specific for the ribozyme RZ43 and the endogenous mouse U1 snRNA. Transcript sizes are in nucleotides. B) agarose gel before transfer, stained with ethidium bromide. Markers are plasmid pUC19 digested with Hpa II.*

Ribozyme activity in transgenic mice

Based on the abundant expression and apparent subcellular localization of the modified U1 RNAs in HepG2 cells, both the antisense (U1AS43) and the ribozyme (U1RZ43) constructs were microinjected into fertilized mouse oocytes to generate transgenic mice. Five founder transgenic mice carrying the U1RZ43 gene and five founders transgenic for the U1AS43 gene were characterized by DNA (Southern) blot analysis. Transgene expression was analyzed in all founders, and two representative mouse lines transgenic for the U1RZ43 gene are shown in figure 5. Transgenic mice all demonstrated expression in the kidney of a transcript of 248 nt, the expected size for the U1RZ43 RNA, in addition to the cross-hybridizing 165 nt transcript of the mouse U1 genes which is also present in non-transgenic littermates. The RZ43 RNA is easily detectable, and is present at lower levels than the highly abundant U1 RNA. The level of U1AS43 transgene expression in all five founders was analyzed by RNA blotting of submandibular gland RNA. Very low levels of U1AS43 expression were detected in these mice (M. G. F. S., unpublished observations), which perhaps reflects a lower stability of this RNA, as discussed above.

Efficiency of ribozymes expressed in snRNAs

A ribonuclease protection assay was used to analyze the level of renin mRNA in kidneys of transgenic mice (the principal site of renin biosynthesis). Repeated analysis showed that expression of the U1RZ43 ribozyme in mouse kidney results in a small reduction in renin gene expression, and that mice transgenic for the antisense gene U1AS43 had renin mRNA levels within the normal range (M. G. F. S. and J. J. M., unpublished observations). RNA (northern) blot analysis of kidney RNA from lines F3754, which expresses the U1RZ43 ribozyme, and F3846, which expresses the U1AS43 antisense, show moderate levels of renin gene inhibition (figure 6A). The levels of active renin protein in kidney tissue of transgenic mice were measured, and the results are shown graphically in figure 6B. There is a significant decrease in the level of active renin in U1RZ43 transgenic mouse kidneys to approximately 65% of the levels in non-transgenic mice. However, this decrease is not reproduced in SMG (data not shown). Mice transgenic for the renin antisense gene U1AS43 show no significant differences from non-transgenic controls (figure 6B).

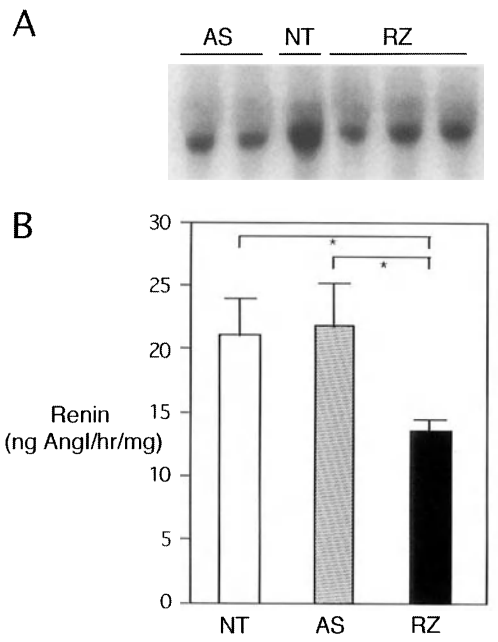

Figure 6. *Renin gene inhibition in transgenic mice. A) RNA blot of 30μg of kidney RNA from male mice from lines F3846 (U1AS43) and F3754 (U1RZ43) hybridized with a renin probe shows some reduction of renin mRNA levels in transgenic mice (AS, RZ) compared with non-transgenic mice. B) tissue renin activity in kidneys of mice transgenic for U1RZ43 (solid bars) shows a significant reduction in active renin protein (*P<0.01), when compared with either non-transgenic (open bars) or U1AS43 (hatched bars) mice. Data are mean+SE. One outlier was excluded from the U1RZ43 kidney renin group, as it was >2 standard deviations above the mean for the group.*

Compositional analysis of modified snRNPs

The low efficiency of renin gene inhibition in transgenic mice expressing modified U1 transcripts prompted us to analyze further the composition of the particles which contained antisense and ribozyme RNA in vivo. This was done by immunoprecipitation of all snRNP complexes containing the Sm antigen, using the specific monoclonal

antibody Y-12. HepG2 cells, stably transfected with either U1AS43 or U1RZ43, were grown in the presence of $^{32}PO_4$ in order to label all newly synthesized RNA molecules. Cells were then lysed, and the immunoprecipitating material separated by polyacrylamide gel electrophoresis (figure 7). The specificity of the Y-12 antibody is shown by the absence of labelled material co-precipitating with an unrelated monoclonal antibody (Sca-1) raised against a murine haematopoietic cell surface antigen. From this analysis it is clear that only endogenous U1 snRNA transcripts, amongst some other snRNAs, are associated into stable particles which contain the Sm protein. No band is visible at the size expected for the ribozyme- or antisense-containing U1 RNA, even though the transcripts are easily detectable in these transfected cells (see figure 4).

Discussion

The aim of this project was to develop a nuclear RNA vector molecule which could direct antisense and ribozyme transcripts to the cellular target mRNAs with high efficiency, resulting in maximal levels of gene inhibition in transgenic mice. Such a system could be adapted to achieve controllable gene modulation in an inducible or tissue-specific manner. The U1 snRNA was modified to include antisense and ribozyme sequences targeting the mouse renin gene, and the ribozyme construct was found to express at high levels in cultured hepatoma cells and transgenic mice. Although the

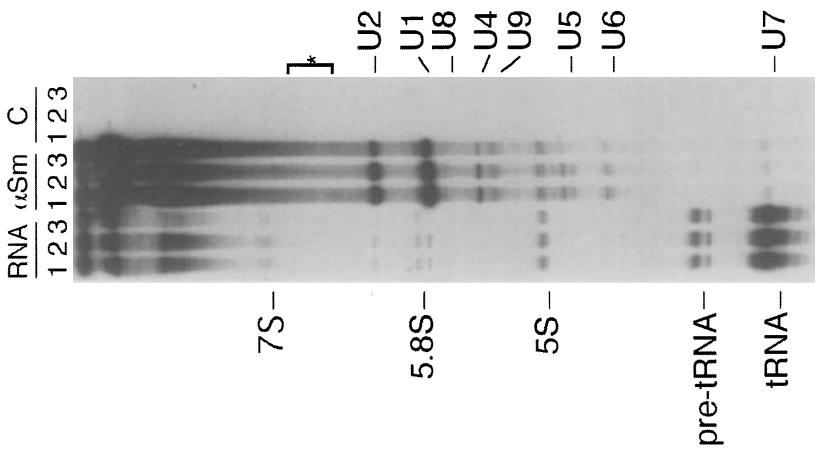

Figure 7. *Immunoprecipitation of ribozymes from hepatoma cells. Antibody specific for the Sm antigen common to many snRNPs was used to immunoprecipitate labelled RNAs from cultured HepRn20 cells expressing either human U1 alone (lanes 1), U1AS43 (lanes 2) or U1RZ43 (lanes 3). Labelled cellular RNA is shown for comparison (RNA). Immunoprecipitation was specific for the Sm antigen (Sm), as shown by the complete absence of labelled material immunoprecipitating with a control monoclonal antibody (C). Several of the more abundant Sm-containing snRNPs are indicated (Sm tracks), as are some cellular RNA species (RNA tracks). Modified U1 RNAs containing antisense or ribozyme sequences are not detectable, and should appear above the U2 snRNA (which is 187nt) in the region indicated (*).*

modified snRNA appeared to accumulate in the nucleus of hepatoma cells, proper association with a protein component of snRNPs (i.e. Sm antigen) does not occur. This fact may account for the moderate levels of gene inhibition achieved by these constructs, because improper snRNP formation will prevent co-localization of antisense and target RNAs within the splicing compartment of the nucleus. Thus, we have shown that molecular engineering of the 5' terminus of the U1 snRNA disrupts the association with the Sm protein, and probably blocks localization of the transcript to the splicing apparatus in the nucleus.

We chose to target two ribozyme cleavage sites that are close together in the substrate, such that one region of complementary sequence would bridge both sites, and allow a twin ribozyme moiety to cleave the target RNA. Construct pU1RZ43 was designed so that a long (41nt) region of the renin mRNA would hybridise to the complementary region of the U1RZ43 molecule (figures 1 and 2). This long duplex should be relatively stable, even in the denaturing environment of the cell nucleus [32,33]. Cleavage by both ribozymes at two points in the duplex breaks the regions of contiguous pairing into short, unstable segments, which will dissociate rapidly. The rapid dissociation of products from the ribozyme strand is essential for catalytic turnover. Cleavage of renin mRNA in vitro by RZ43 was observed (figure 3), and the reaction was reasonably rapid, with most of the full-length substrate converted in two hours, with a small (10-fold) excess of ribozyme RNA.

Antisense inhibition involves a stoichiometric interaction between the complementary RNA strands, and so it is necessary to have abundant expression of antisense RNA for efficient gene inhibition. Even then, the level of inhibition is not likely to reach 100%. The degree of depletion of the target mRNA required before a phenotypic change occurs will vary considerably, depending upon the particular system under study. However, it is known that mRNAs are not free to diffuse through the cell, they can be tethered to well-ordered and defined trafficking pathways as they travel from the site of transcription, through the processing machinery to the site of translation [34,35]. It would appear plausible that the siting of a catalytic molecule, such as a ribozyme, at a position on this pathway would greatly increase the inhibition needed for a physiological change to occur. The U1 snRNA molecule seems ideally suited for the purpose of localizing a ribozyme RNA near the potential substrate. Firstly, it is abundant, stable and found throughout the nucleus, where it binds to intron/exon splice sites in the newly transcribed pre-mRNA [36,37]. The U1 genes are highly active in mammalian cells, producing $\approx 5 \times 10^5$ RNA molecules per cell. By replacing only those U1 sequences which normally base-pair to splice donor sites [31,38] with a ribozyme domain specific for the mouse *Ren-2* mRNA, our aim was to use the functions of the U1 snRNP to co-localize the ribozyme and the substrate. This would not only greatly increase the efficiency with which the ribozyme RNA associates with the target, but also promotes cleavage of the target prior to nuclear export to the cytoplasm, the site of mRNA translation. However, the comparison of nuclear and cytoplasmic vector RNAs for ribozymes indicates that although nuclear ribozyme RNAs can be extremely stable, the cytoplasmic compartment allows much higher levels of gene inhibition [39]. The U1RZ43 gene used here is highly active in stably transfected cells (figure 4A) and in transgenic mice (figure 5) as detected by northern blotting, although it is less active

in transient expression assays (figure 4B). Interestingly, more sensitive assays of RNA expression such as ribonuclease protection and primer extension were consistently unable to detect this abundant expression of U1RZ43 RNA in transgenic mice (M. G. F. S., unpublished observations). The reason for this remains unclear, but the high degree of secondary structure in the U1RZ43 RNA may well interfere with solution hybridization or enzymatic polymerization steps during these procedures. Nuclear importation of U1 snRNPs is dependent upon modular signals, including the modified cap structure at the 5' end of the U1 RNA, and the Sm protein [40]. Although the ribozyme RNA studied here appears to be located in the nucleus (figure 4), there is no detectable association with the Sm antigen, in the transfected hepatoma cells at least (figure 7). For this type of modified snRNA to associate with nascent transcripts as part of the splicing pathway, different designs must be tried which do not inhibit association with snRNP protein components, or nuclear transport. Recently, it has been shown that the insertion of a single ribozyme domain into stem-loop III of U1 allows these RNAs to be localized to the nucleus of *Xenopus* oocytes, and also to associate with Sm antigen [41]. These constructs were shown to be efficient in the cleavage of the target pre-mRNA after injection into oocytes. Also, the replacement of the Sm-binding site between stem-loop regions of U1 with a hammerhead ribozyme allowed nuclear accumulation, and efficient cleavage of the target RNA (fibrillin 1) in cultured cells [42], thus indicating that association with the Sm antigen may not in fact be desirable. The importance of directing ribozymes to the same cellular compartment for high efficacy was clearly demonstrated by Sullenger and Cech [43]. These authors showed that efficient inactivation of reporter RNA (lacZ) by a retroviral ribozyme was dependent upon the packaging of both target and catalytic RNA into the same viral particle. Expression of both RNAs in the same cell (without viral packaging) resulted in no reduction in reporter gene expression [43].

We have shown that transgenic mice expressing the U1RZ43 ribozyme RNA had a reduction in the level of renal renin mRNA, and a significant reduction in the level of kidney active renin protein (figure 6). This reduction is remarkable, as the level of renin gene expression and renin protein accumulation is very high in renal juxtaglomerular cells [8]. Reduction in renin protein levels was not observed in another major site of renin synthesis, the SMG. The reasons for this are unclear at present, but it may be due to a number of factors, including tissue-specific differences in (i) nuclear processing pathways, (ii) transcript secondary structure or stability, (iii) U1 snRNA processing and location, or (iv) compensatory upregulation of renin expression. The levels of gene inhibition achieved by U1RZ43 are significant, but may be augmented by improving construct designs, such that proper co-localization with the target mRNA occurs in all cell types and under all conditions [18].

Ribozymes and antisense RNA offer a general approach to defining the function of a gene by controllable, tissue-specific reduction or ablation of gene function in transgenic animals. The U1 gene promoter used here is highly active in all mammalian cells [29], and it will be interesting to see if the same, or higher levels of gene inhibition can be produced by a tissue-specific promoter. Many promoter elements with restricted spatial and temporal patterns of expression are not as active as the U1 gene, and so successful application of ribozymes as general probes of gene function will be dependent upon

strategies such as the co-localization of the ribozyme with the target mRNA in the nucleus. The utility of an inducible ribozyme for developmentally-specific effects of gene inhibition has already been demonstrated in *Drosophila* [44]. Using the approach we have described it will soon be possible to achieve gene inhibition to defined levels, in a controllable way, by employing appropriate transcriptional control elements [45,46]. The detailed analysis of the threshold effects of gene inhibition at particular times or in particular tissues will soon be possible in transgenic mice, when the appropriate control elements are used. A robust system for intracellular navigation of ribozymes to their target RNAs with precision is desirable, and will be a powerful addition to the arsenal of weapons deployed against human disease.

Conclusion

In summary, we have attempted to develop efficient co-localization of ribozyme and substrate mRNA molecules within the target tissues of transgenic animals. The U1 snRNA is a candidate vector molecule for ribozyme and antisense appilcations, but the design constraints which permit proper location of modified U1 molecules within the cell remain to be defined clearly. Other candidate molecules might also be adapted for trafficking ribozymes to the substrate RNA, such as transfer RNA or ribosomal RNA species, and these strategies are being persued in other laboratories. What is clear is that exquisite control over when and where antisense molecules accumulate within a target cell is probably necessary before this exciting technology comes of age as a research tool.

Acknowledgements

We are grateful to Dr. I. C. Eperon for clone HSD2 and many helpful suggestions, and Drs. J. A. Steitz and N. Hole for Y-12 and Sca-1 antibodies. We are indebted to G. Brooker and R. Allan for generating transgenic mice, and H. A. K. Davidson-Smith for technical assistance. This work was supported by the European Union Concerted Action Transgeneur, the Biotechnology and Biological Sciences Research Council of the U.K., and the National Institutes of Health of the U.S.A. grant number 5-RO1-HL45468.

References

1. Sharp MGF, Fettes D, Brooker G, et al. Targeted inactivation of the Ren-2 gene in mice. Hypertension 1996;26:1126-31.
2. Clark AF, Sharp MGF, Morley SD, Fleming S, Peters J, Mullins JJ. Renin-1 is essential for normal renal juxtaglomerular cell granulation and macula densa morphology. J Biol Chem 1997;272:18185-90.
3. Mullins JJ, Peters J, Ganten D. Fulminant hypertension in transgenic rats harbouring the mouse Ren-2 gene. Nature 1990;344:541-44.
4. Véniant M, Ménard J, Bruneval P, Morley S, Gonzales MF, Mullins J. Vascular damage without hypertension in transgenic rats expressing prorenin exclusively in the liver. J Clin Invest 1996;98:1966-70.
5. Taugner R, Hackenthal E. The juxtaglomerular apparatus: Structure and function. Berlin: Springer Verlag, 1989.
6. Field LJ, Gross KW. *Ren-1* and *Ren-2* loci are expressed in mouse kidney. Proc Natl Acad Sci USA 1985;82:6196-200.
7. Dickinson DP, Gross KW, Piccini N, Wilson CM. Evolution and variation of renin genes in mice. Genetics 1984;108:651-67.
8. Sigmund CD, Gross KW. Structure, expression, and regulation of the murine renin genes. Hypertension 1991;18:446-57.
9. Wagner EGH, Simons RW. Antisense RNA control in bacteria, phages, and plasmids. Annu Rev Microbiol 1994;48:713-42.
10. Sokol DL, Murray JD. Antisense and ribozyme constructs in transgenic animals. Transgenic Res 1996;5:363-71.
11. Phillips MI, Wielbo D, Gyurko R. Antisense inhibition of hypertension: A new strategy for renin- angiotensin candidate genes. Kidney Int 1994;46:1554-56.
12. Wielbo D, Sernia C, Gyurko R, Phillips MI. Antisense inhibition of hypertension in the spontaneously hypertensive rat. Hypertension 1995;25:314-19.
13. Tomita N, Morishita R, Higaki J, Kaneda Y, Mikami H, Ogihara T. In-vivo transfer of antisense oligonucleotide against rat angiotensinogen with HVJ-liposome delivery resulted the reduction of blood pressure in SHR. Hypertension 1994;24:397-99.
14. Tomita N, Morishita R, Higaki J, et al. Transient decrease in high blood pressure by in vivo transfer of antisense oligodeoxynucleotides against rat angiotensinogen. Hypertension 1995;26:131-36.
15. Lu D, Raizada MK. Delivery of angiotensin II type 1 receptor antisense inhibits angiotensin action in neurons from hypertensive rat brain. Proc Natl Acad Sci USA 1995;92:2914-18.
16. Iyer SN, Lu D, Katovich MJ, Raizada MK. Chronic control of high blood pressure in the spontaneously hypertensive rat by delivery of angiotensin type I receptor antisense. Proc Natl Acad Sci USA 1996;93:9960-65.
17. Pedrazzini T, Cousin P, Aubert J-F, Brunner H-R. Transient inhibition of angiotensinogen production in transgenic mice bearing an antisense angiotensinogen gene. Kidney Int 1995;47:1638-46.
18. Rossi JJ. Controlled, targeted, intracellular expression of ribozymes: progress and problems. Trends Biotechnol 1995;13:301-06.
19. Sarver N, Cantin EM, Chang PS, et al. Ribozymes as potential anti-HIV-1 therapeutic agents. Science 1990;247:1222-25.
20. Manser T, Gesteland RF. Human U1 loci: Genes for human U1 RNA have dramatically similar genomic environments. Cell 1982;29:257-64.
21. Rougeon F, Chambraud B, Foote S, Panthier JJ, Nageotte R, Corvol P. Molecular cloning of a mouse submaxillary gland renin cDNA fragment. Proc Natl Acad Sci USA 1981;78:6367-71.
22. Chomczynski P, Sacchi N. Single-step method of RNA isolation by acid guanidinium

thiocyanate phenol chloroform extraction. Anal Biochem 1987;162:156-59.
23. Thomas PS. Hybridization of denatured RNA and small DNA fragments transferred to nitrocellulose. Proc Natl Acad Sci USA 1980;77:5201-05.
24. Church GM, Gilbert W. Genomic Sequencing. Proc Natl Acad Sci USA 1984;81:1991-95.
25. Peters J, Münter K, Bader M, Hackenthal E, Mullins JJ, Ganten D. Increased adrenal renin in transgenic hypertensive rats, TGR(mREN2)27, and its regulation by cAMP, angiotensin-II, and calcium. J Clin Invest 1993;91:742-47.
26. Hackenthal E, Hackenthal R, Hofbauer KG. No evidence for product inhibition of the renin-angiotensinogen reaction in the rat. Circulation Res 1977;41:49-57.
27. Kessler SW. Rapid isolation of antigens from cells with a staphylococcal protein A-antibody adsorbent: parameters of the interaction of antibody-antigen complexes with protein A. J Immunol 1975;115:1617-24.
28. Matter L, Schopfer K, Wilhelm JA, Nyffenegger T, Parisot RF, De Robertis EM. Molecular characterization of ribonucleoprotein antigens bound by antinuclear antibodies. A diagnostic evaluation. Arthritis Rheum 1982;25:1278-83.
29. Skuzeski JM, Lund E, Murphy JT, Steinberg TH, Burgess RR, Dahlberg JE. Synthesis of human U1 RNA. J Biol Chem 1984;259:8345-52.
30. Kastner B, Lührmann R. Electron microscopy of U1 small nuclear ribonucleoprotein particles: shape of the particle and position of the 5' RNA terminus. EMBO J 1989;8:277-86.
31. Zhuang Y, Weiner AM. A compensatory base change in U1 snRNA suppresses a 5' splice site mutation. Cell 1986;46:827-35.
32. Crisell P, Thompson S, James W. Inhibition of HIV-1 replication by ribozymes that show poor activity in vitro. Nucleic Acids Res 1993;21:5251-55.
33. Hormes R, Homann M, Oelze I, et al. The subcellular localization and length of hammerhead ribozymes determine efficacy in human cells. Nucleic Acids Res 1997;25:769-75.
34. Singer RH. The cytoskeleton and mRNA localization. Curr Opin Cell Biol 1992;4:15-19.
35. Zhang GH, Taneja KL, Singer RH, Green MR. Localization of pre-mRNA splicing in mammalian nuclei. Nature 1994;372:809-12.
36. Sharp PA. Split genes and RNA splicing. Cell 1994;77:805-15.
37. Eperon IC, Ireland DC, Smith RA, Mayeda A, Krainer AR. Pathways for selection of 5' splice sites by U1 snRNPs and SF2/ASF. EMBO J 1993;12:3607-17.
38. Yuo CY, Weiner AM. A U1 small nuclear ribonucleoprotein particle with altered specificity induces alternative splicing of an adenovirus E1A mRNA precursor. Mol Cell Biol 1989;9:3429-37.
39. Bertrand E, Castanotto D, Zhou C, et al. The expression cassette determines the functional activity of ribozymes in mammalian cells by controlling their intracellular localization. RNA 1997;3:75-88.
40. Hamm J, Darzynkiewicz E, Tahara SM, Mattaj IW. The trimethylguanosine cap structure of U1 snRNA is a component of a bipartite nuclear targeting signal. Cell 1990;62:569-77.
41. Michienzi A, Prislei S, Bozzoni I. U1 small nuclear RNA chimeric ribozymes with a substrate specificity for the Rev pre-mRNA of human immunodeficiency virus. Proc Natl Acad Sci USA 1996;93:7219-24.
42. Montgomery RA, Dietz HC. Inhibition of fibrillin 1 expression using U1 snRNA as a vehicle for the presentation of antisense targeting sequence. Hum Mol Genet 1997;6:519-25.
43. Sullenger BA, Cech TR. Tethering ribozymes to a retroviral packaging signal for destruction of viral RNA. Science 1993;262:1566-69.
44. Zhao JJ, Pick L. Generating loss-of-function phenotypes of the fushi tarazu gene with a targeted ribozyme in Drosophila. Nature 1993;365:448-51.
45. Gossen M, Bujard H. Tight control of gene expression in mammalian cells by tetracycline-responsive promoters. Proc Natl Acad Sci U S A 1992;89:5547-51.
46. Furth PA, St. Onge L, Böger H, et al. Temporal control of gene expression in transgenic mice by a tetracycline-responsive promoter. Proc Natl Acad Sci USA 1994;91:9302-06.

24. RECEPTOR-DEPENDENT CELL SPECIFIC DELIVERY OF ANTISENSE OLIGONUCLEOTIDES

Erik A.L. Biessen, and Theo J.C.van Berkel

Introduction

Oligodeoxynucleotides (ODNs) have been shown to inhibit gene expression at various levels both in vitro and in vivo [1-4]. In vivo, the efficacy of ODN-induced regulation of genes in specific cell types may be suboptimal due to poor accumulation of ODNs in these cells. In addition, untimely elimination of ODNs via renal clearance, degradation and scavenger receptor-mediated uptake [6] may further impair their therapeutic activity. These hurdles can be at least partly overcome by targeted delivery of the ODNs to the desired site of action. A number of approaches have been suggested to facilitate the entry of polyanionic ODNs into the aimed target cell [7-12]. Neutral and cationic liposomes are considered to be attractive ODN carriers since they markedly enhance cellular uptake under in vitro conditions. Like native ODNs, however, liposomally formulated ODNs are mainly captured by cells of the reticulo-endothelial system in lungs, spleen and liver [13-15], as a result of which the ODN concentration in the target cell will be suboptimal. After local delivery of ODNs encapsulated in virus capsid-coated liposomes, Morishita et al. [16] could enhance ODN uptake by vascular endothelial cells leading to cell-specific antisense effects. Nevertheless, this approach is not feasible for specific delivery of ODNs to most other cell types like the parenchymal liver cell (PC).

The PC is the aimed target for antisense mediated down-regulation of the expression of a number of clinically relevant target genes, including that of the atherogenic apolipoprotein(a) [17], cholesterol ester transfer protein [18], and viral proteins from hepatitis B/C virus [19-21]. A promising way to enhance the local bioavailability of ODNs in this cell type involves conjugation of the ODNs to a ligand for a receptor uniquely expressed by PCs, such as the asialoglycoprotein receptor [22]. In vitro, glycotargeted delivery to this receptor has been shown after non-covalent complexation of the ODNs to a conjugate of poly-L-lysine and asialoorosomucoid [23-26], while a study of Lu et al. [23] also indicated an altered biodistribution of glycotargeted ODNs in vivo. In comparison with the rather bulky ODN carriers based on poly-L-lysine/asialoorosomucoid conjugates, covalent attachment of ODNs to a low-molecular

P.A. Doevendans et al. (eds.), Cardiovascular specific gene expression, 285-99.

weight ligand for a cell-specific receptor confers the advantage that it is synthetically more accessible, less laborious and pharmaceutically applicable. Hangeland et al. [27] have reported enhanced uptake of a 7-mer heptathymidinylate (T_7) methylphosphonate by HepG2 cells after conjugation to a N-acetyl galactosamine-terminated glycopeptide. In vivo studies of Hangeland et al. [28] of this glycoconjugate in mice also showed an increased hepatic uptake of this conjugate. As short oligothymidinylates (and in particular if they are uncharged) are poor substrates for the liver scavenger receptors, which appear to be responsible for the rapid elimination of ODNs by cells of the reticulo-endothelial system, these results leave unanswered whether longer, charged and miscellaneous ODN sequences can also be redirected to the aimed target cell in vivo [29,6]. This emphasizes that it is crucial to analyse the tissue distribution and to identify the cellular uptake sites within the liver using full length antisense sequences. In this study in vivo evidence is provided that untimely elimination of a miscellaneous 20-mer ODN by the above scavenger pathways can be circumvented and, concomittantly, accumulation by parenchymal liver cells can be enhanced after derivatisation with a small-sized synthetic galactoside with high affinity for the asialoglycoprotein receptor.

Methods and Results

Concept for improved delivery of antisense

To improve the cellular uptake of antisense ODNs and to avoid untimely degradation we have conjugated the antisense directly to the homing device (see figure 1). The perspectives of glycotargeting for improving the local bioavailability of the antisense drug were illustrated for the asialoglycoprotein receptor on parenchymal liver cells.

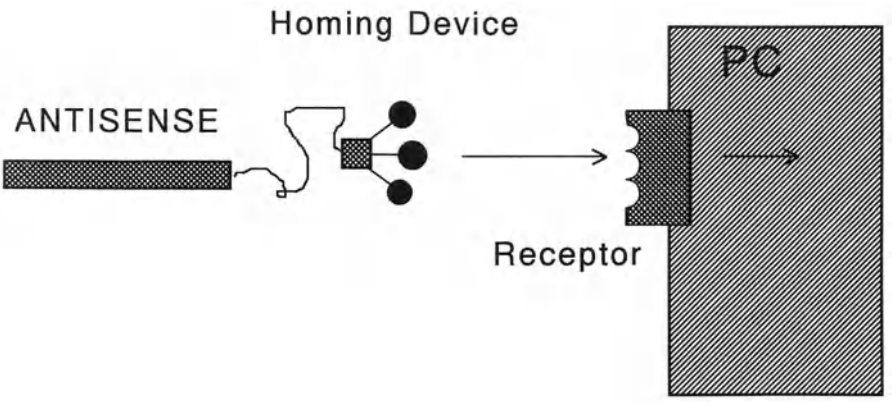

Figure 1. *Concept of glycotargeting of antisense ODNs to the asialoglycoprotein receptor on parenchymal liver cells.*

Synthesis of L_3G_4-ODN

The tetra-antennary cluster galactoside L_3G_4 (for a structure see scheme 1) was synthesized from trilysine and p-(•-D-galactopyranosyloxy)phenyl isothiocyanate in 67% yield. The structural identity of the product was established by NMR and mass spectrometry. The high affinity of L_3G_4 (see below) allows further application as targeting device to achieve specific delivery of antisense ODN to hepatocytes. Conjugation of L_3G_4 to the antisense ODN was accomplished via a two-step procedure. In the first step, L_3G_4 was linked to the 5'-end part of the antisense ODN for apolipoprotein(a) (nt 83-92; ODN-AS5').

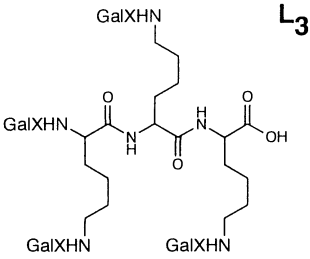

L_3G_4

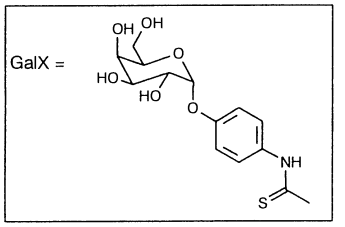

Scheme 1. *Chemical structures of L_3G_4 and L_3G_4-[^{32}P]-ODN.*

L_3G_4-[^{32}P]-ODN

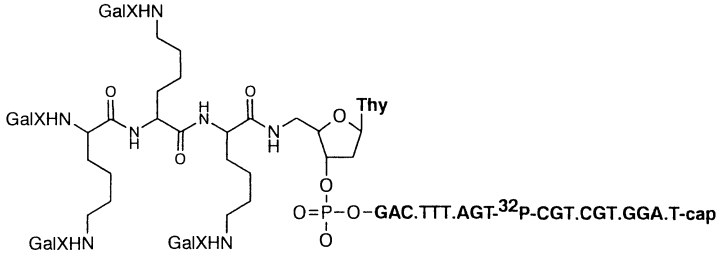

In the second step, this ODN was ligated to the phosphorylated and 3'-capped ODN-AS3' (nt 93-102 of the apo(a) gene). Coupling of L_3G_4 to the amino group of the terminal 5'-amino thymidinyl from ODN-AS5' was carried out in DMF/H_2O (1:1, v/v) using HBTU and HOBT as cross-linking reagents and DiPEA as catalyzing base. L_3G_4-conjugated ODN-AS5' was produced in 31% yield, and could be easily purified from

the non-conjugated ODN-AS5' and free L_3G_4 by gel electrophoresis on denaturing 19% polyacrylamide. It displayed an electrophoretic mobility comparable to that of a 20-mer ODN. The product was excised, eluted from the gel, and desalted over Sephadex G25. Mass spectrometry was in agreement with the presumed chemical structure. The coupling efficiency was moderate, despite the 100 molar-fold excess of L_3G_4, the coupling reagent and the catalyzing base. Attempts to increase the coupling yield by changes in solvent composition or coupling reagents were not successful. The pursued procedure led to markedly higher yields than DCC, DCC/HOBT, EDC, or EEDQ catalyzed reactions. Furthermore, DMF/H_2O appeared to be superior to DMA/H_2O, acetonitril/H_2O mixtures or pure H_2O. Efforts to couple L_3G_4 to the 5'-amino derivatized ODN using a Heinzer base according to the procedure of Oberhauser and Wagner [36] failed for phosphodiester ODNs longer than 10 bases, and gave only low yields for smaller ODN sequences. The phosphorylated ODN-AS3' was enzymatically ligated to the ligand-conjugated ODN-AS5' without prior purification. After incubation for 18h at 8°C in the presence of the complementary sense strand (ODN-SE), T4-DNA ligase and ATP, the ligation product could be isolated by gel electrophoresis. The ligation product (L_3G_4-[^{32}P]-ODN) ran at an electrophoretic mobility comparable to that of a 24-mer ODN, and considerably slower than [^{32}P]-ODN-AS3', L_3G_4-ODN-AS5' or non-conjugated [^{32}P]-ODN. An extended cooling protocol for annealing L_3G_4-ODN-AS5' and [^{32}P]-ODN-AS3' to the complementary ODN-SE strand appeared to be critical to obtain good ligation yields. The presence of the bulky L_3G_4 moiety did not significantly affect ligation yields.

In vitro binding and uptake studies

We further investigated whether the glycoconjugated ODN is also efficiently and specifically taken up by parenchymal liver cells in vitro. In vitro competition studies of ^{125}I-ASOR binding to isolated rat hepatocytes showed that free L_3G_4 is able to inhibit ^{125}I-ASOR binding to the asialoglycoprotein receptor in a competitive fashion. The affinity was 6.5 nM (pK_i=8.19±0.01) (data not shown). Subsequently, we tested whether L_3G_4 was also recognized by the asialoglycoprotein receptor upon conjugation to the decanucleotide ODN-AS5'. L_3G_4-ODN-AS5' inhibited ^{125}I-ASOR binding at an inhibition constant of 23 nM (pK_i= 7.63±0.11). Apparently, derivatisation of L_3G_4 with ODN-AS5' only slightly reduced its affinity for the asialoglycoprotein receptor. In contrast, underivatized ODN-AS5' was not able to displace ^{125}I-ASOR binding at concentrations of up to 200 nM.

To assess the relative contribution of the asialoglycoprotein receptor in the association of L_3G_4-[^{32}P]-ODN to hepatocytes, we studied the interaction of internally labelled L_3G_4-[^{32}P]-ODN with isolated hepatocytes. First, equilibrium conditions for L_3G_4-[^{32}P]-ODN binding at 4°C were assessed by analyzing the kinetics of its association to hepatocytes. Equilibrium binding at 1 nM of L_3G_4-[^{32}P]-ODN was achieved within 2h of incubation (data not shown). Saturation binding studies of L_3G_4-[^{32}P]-ODN indicated that binding was monophasic, saturable (B_{max}= 11±1 ng/mg) and of high affinity (Kd=68 ± 13 nM) (figure 2). Subsequently, we investigated the effect of various inhibitors of the asialoglycoprotein receptor on L_3G_4-[^{32}P]-ODN binding to hepatocytes (figure 3). ASOR, N-acetyl galactosamine or unlabelled L_3G_4-ODN were all able to

inhibit L_3G_4-[^{32}P]-ODN binding by 80-90%, whereas N-acetyl glucosamine was uneffective. From the competition curves, the inhibition constants (pK_i) could be calculated, amounting 6.59±0.20 (unlabelled L_3G_4-ODN), 7.94±0.10 (asialoorosomucoid), and 4.88±0.06 (GalNAc).

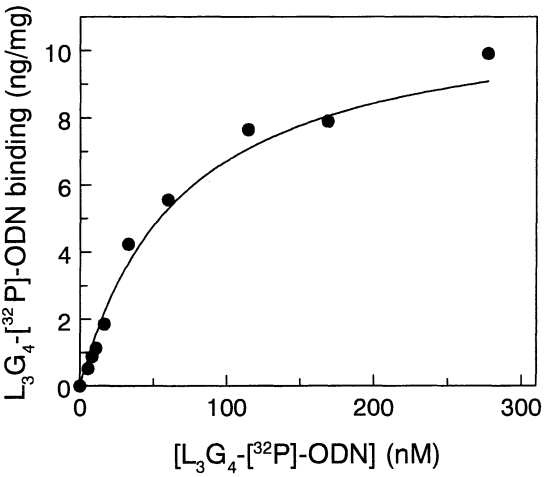

Figure 2. *Saturation binding of L_3G_4-[^{32}P]-ODN to isolated rat parenchymal liver cells. PCs (1.10^6 cells/500 µl) were incubated for 2h at 37°C in DMEM+ 2% (w/v) BSA with 0-300 nM L_3G_4-[^{32}P]-ODN in the absence or presence of 100 mM of GalNAc. Following incubation, cells were put on ice, washed thoroughly and membrane-bound radioactivity was determined and corrected for protein content. Specific binding, defined as the differential binding in the presence and absence of GalNAc (mean of a duplicate experiment), is plotted against the ligand concentration.*

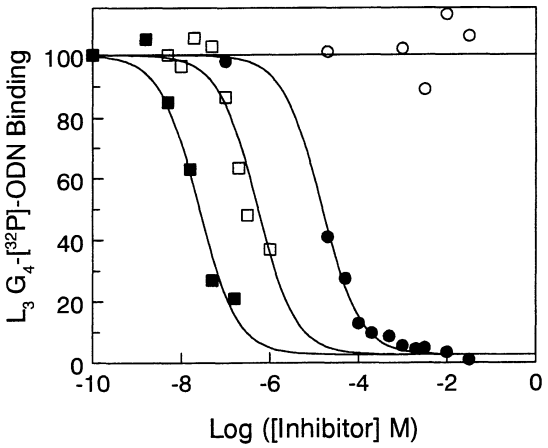

Figure 3. *In vitro competition of L3G4-[^{32}P]-ODN binding to rat PCs by various inhibitors. Rat PCs (1.10^6 cells/500 µl) were incubated for 2h at 4°C in DMEM+2% (w/v) BSA with ^{125}I-ASOR (10 nM) in the presence of asialoorosomucoid (?), GalNAc (?), unlabeled L_3G_4-ODN (?) or ODN (○). Following incubation, cells were washed thoroughly and cell-bound radioactivity was determined and corrected for protein content. Specific binding is expressed as percentage of control binding in the absence of inhibitor and is plotted against the log of the inhibitor concentration (in M).*

Subsequently, we have investigated whether these glycoconjugated ODNs are also efficiently and specifically taken up by parenchymal liver cells in vitro. Uptake of L_3G_4-[^{32}P]-ODN by PCs, i.e., total cell-associated radioactivity after removal of membrane-bound ligand by treatment with 5 mM EGTA, proceeded linearly in time for 10-15 min and tended to level off after 25 min of incubation (figure 4). Within the first 20 min, L_3G_4-[^{32}P]-ODN uptake was 35-fold more rapid than non-specific uptake in the presence of 100 mM GalNAc. To investigate whether L_3G_4-[^{32}P]-ODN uptake involves the classical pathway, we have measured the effect of various uptake inhibitors on the internalisation of L_3G_4-[^{32}P]-ODN by PCs in comparison with that of ^{125}I-ASOR (figure 5). Clearly, all of the tested agents reduced L_3G_4-[^{32}P]-ODN uptake. Sodium azide (10 mM), monensin (0.025 mM) and colchicine (0.1 mM) inhibited uptake by approximately 70%, while sucrose (200 mM) almost completely prevented uptake (circa 96% inhibition). In agreement, ^{125}I-ASOR uptake was similarly reduced after incubation with sodium azide, monensin, colchicine, and sucrose.

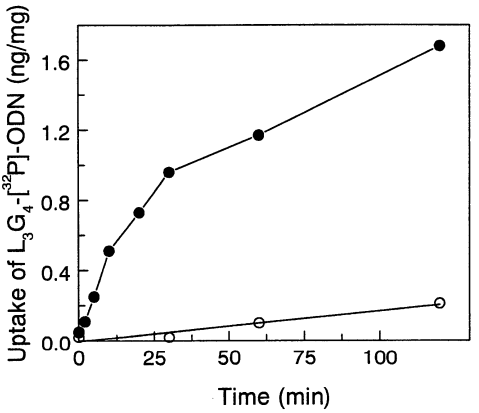

Figure 4. *Kinetics of uptake of L_3G_4-[^{32}P]-ODN by isolated rat parenchymal liver cells. PCs (1.10^6 cells/500 µl) were incubated for 0-2h at 37° C in DMEM+ 2% (w/v) BSA with 10 nM L_3G_4-[^{32}P]-ODN in the absence (•) or presence of 100 mM of GalNAc (◦). Following incubation, cells were put on ice, washed thoroughly and membrane-associated radioactivity was removed by a EGTA incubation step. After a subsequent cell wash, the cell-associated binding (uptake) were determined and corrected for protein content.*

Confocal laser scanning fluorescence of L_3G_4-ODN-Rho and ODN-Rho

From the above in vitro studies it is evident that PC uptake is greatly facilitated by derivatization of ODN with L_3G_4. To visualize the stimulatory effect of glycoconjugation on cell binding and uptake, we have analyzed the interaction of the rhodamine-labeled antisense ODNs (ODN-Rho and L_3G_4-ODN-Rho) with rat PCs in real time by confocal laser scan microscopy. L_3G_4-ODN-Rho or ODN-Rho were prepared as described above, in good yield, starting from 3'-rhodamine-modified ODN-AS3' (figure 1, lane F). Competition studies showed that the affinity of the rhodamine labeled glycoconjugates for the asialoglycoprotein receptor was very comparable to that of the underivatized compounds (K_i= 6.71±0.07 vs. 6.59±0.2 for underivatized L_3G_4-ODN, respectively (data not shown). Confocal laser scanning fluorescence analysis of

rat PCs was performed after 3 and 15 min of incubation at 37°C with ODN-Rho (100 nM) or L_3G_4-ODN-Rho (100 nM). No significant fluorescent staining was observed after incubation with ODN-Rho at both time-points. By contrast, PCs incubated with L_3G_4-ODN-Rho showed bright staining both at 3 min and at 15 min of incubation (figure 6). At 3 min, fluorescence was localized mainly in a bright cellular lining, indicative of membrane binding of the fluorescent label. After 15 min of incubation, the bulk of the fluorescence was observed intracellularly, both in punctate spots (indicative of the lyso- and endosomal compartment) and, in more diffuse form, in the cytosol. To establish that uptake of the fluorescently labeled ODNs was mediated by the asialoglycoprotein receptor, we have also analyzed cellular fluorescence after incubation of PCs with L_3G_4-ODN-Rho in the presence of the inhibitor ß-D-lactose (100 mM). Evidently, fluorescent staining of the cells is fully prevented by excess lactose.

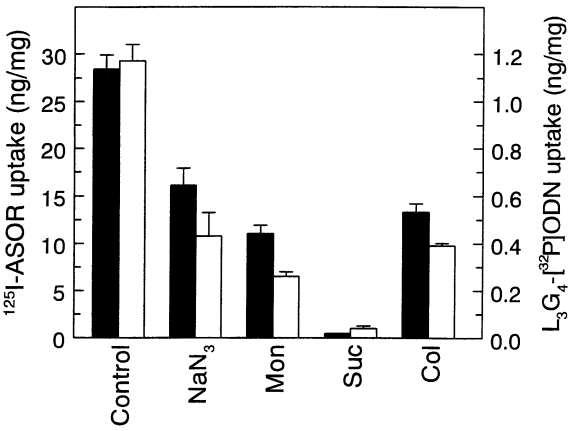

Figure 5. *Effect of various uptake inhibitors on L_3G_4-[^{32}P]-ODN (open bars) and ^{125}I-ASOR uptake (hatched bars) by rat PCs. Rat PCs (1.10^6 cells/500 µl) were incubated for 30 min at 37°C with DMEM/2% BSA (control) or DMEM/2% BSA supplemented with sodium azide (NaN_3, 10 mM), sucrose (suc, 250 mM), monensin (mon, 10 µM), or colchicine (col, 100 µM). Subsequently, L_3G_4-[^{32}P]-ODN or ^{125}I-ASOR was added to final concentrations of 100 and 10 nM, resp.. After incubation for 15 min at 37°C, the cells were put on ice, washed once with DMEM/2% (w/v) BSA and incubated for 10 min at 4°C with EGTA (5 mM in DMEM + 2% (w/v) BSA) to remove EGTA-releasable membrane-associated radioactivity. Finally, the cells were washed thoroughly, cell-associated radioactivity was determined, and corrected for protein content.*

In vivo studies

From the above in vitro studies it is clear that PC uptake is greatly facilitated by derivatization of ODN with L_3G_4. To validate that this glycoconjugation also improves specific accumulation of ODN into PCs in vivo, we monitored liver uptake and serum decay of intravenously injected L_3G_4-[^{32}P]-ODN and [^{32}P]-ODN in the rat. L_3G_4-conjugated and non-conjugated ODNs were equally rapidly cleared from the bloodstream (figure 7): within 2 min after injection only 11.5±1.5% and 14.3±1.7% of the injected dose, respectively, resided in the serum. Liver uptake of [^{32}P]-ODN amounted to 19.1±0.6%, whereas L_3G_4-[^{32}P]-ODN was almost quantitatively taken up by the liver (77±6% of the injected dose). Crucial for interpreting the above

pharmacokinetic data of L_3G_4-[^{32}P]-ODN is the stability of L_3G_4-[^{32}P]-ODN under in vivo conditions. Analysis of the stability of L_3G_4-[^{32}P]-ODN at 37°C in the presence of serum showed that the glycoconjugate is rather stable (figure 8). Only 40% of the ODN derivative is degraded within 3h of incubation. The half-life of the glycoconjugate in serum was calculated to be 200±20 min, which is about 10-fold higher than that of underivatized [^{32}P]-ODN (19±6 min).

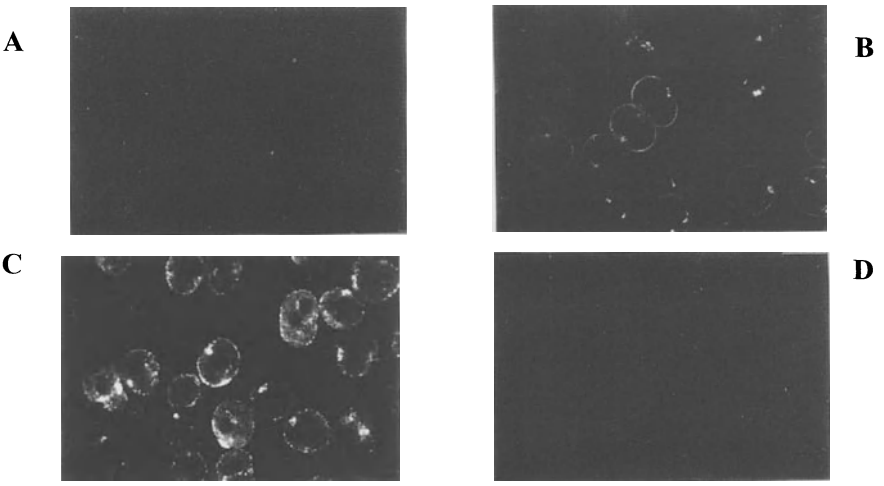

Figure 6. *Confocal laser scan microscopy study of L_3G_4-ODN-Rho and ODN-Rho uptake by rat PCs. Rat PCs (3.10^5 cells) were adhered to a glass layer matrix by a 15 min incubation at 37°C. Subsequently, the glass matrices were washed gently, ODN-Rho (A) or L_3G_4-ODN-Rho (B-D) was added to a final concentration of 100 nM (DMEM/2% BSA), and the cells were incubated for 0-15 min at 37°C in the absence (A-C) or presence of 100 mM β-D-lactose (D). At 3 (B) and 15 min (A,C,D), cells were confocally analyzed for fluorescence. Image analysis was performed using a Kalman filter (10 scans).*

The induced liver uptake could be almost completely prevented by preinjection of 400 mg/kg of N-acetyl galactosamine, which blocks galactose-receptor mediated uptake (figure 9). Preinjection of N-acetyl glucosamine, which does not interfere with galactose receptor-mediated substrate recognition, had no effect on liver uptake of L_3G_4-[^{32}P]-ODN. The underivatized ODN was primarily internalized by endothelial cells (54%) and Kupffer cells (41%), and not by PCs (5%). By contrast, liver uptake of L_3G_4-[^{32}P]-ODN could be mainly attributed to PCs (75±4% of the total liver uptake), whereas endothelial and Kupffer cells contributed only 16±7% and 13±3% to liver uptake, resp. (figure 10). Preinjection of N-acetyl galactosamine reduced PC uptake by 70% to 23±7%, but increased Kupffer and endothelial cell uptake, suggesting that only PC uptake is mediated by galactose-recognizing receptors. In order to verify the nature of the liver-associated ODN, we have investigated whether the liver-associated ODN could be released from the liver by displacing the extracellularly bound ODN through injection of 400 mg/kg of N-acetyl galactosamine at 5 and 10 min after administration of L_3G_4-[^{32}P]-ODN. It can be concluded from figure 9 that liver-associated radioactivity was not significantly affected fter N-acetyl galactosamine injection, suggesting that the liver-associated radioactivity reflects internalized, non-releasable rather than

extracellularly bound L_3G_4-[^{32}P]-ODN.

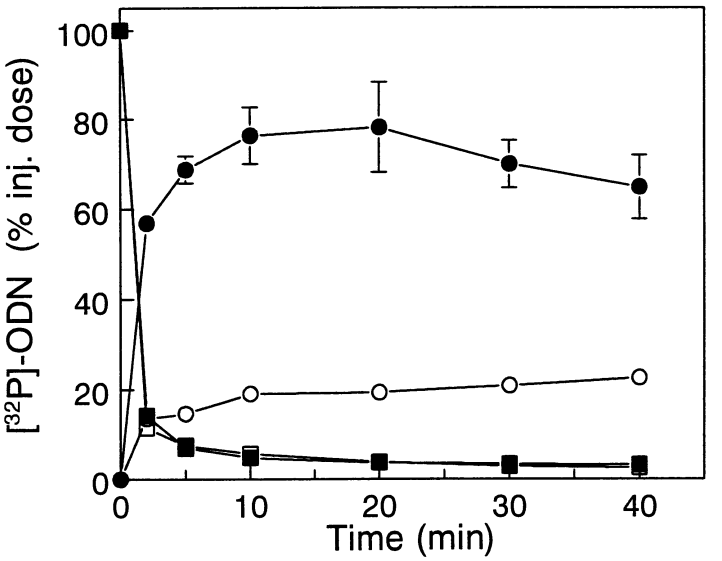

Figure 7. *Serum decay and liver uptake of L_3G_4-[^{32}P]-ODN in the rat. L_3G_4-[^{32}P]-ODN (•,■), or underivatized [^{32}P]-ODN (○,□) (4 μg in 500 μl PBS) was injected intravenously into rats. At the indicated times, radioactivities in serum (■,□) and the liver-associated radioactivities (•,○) were determined. Values are means ± S.E.M. of 3 experiments.*

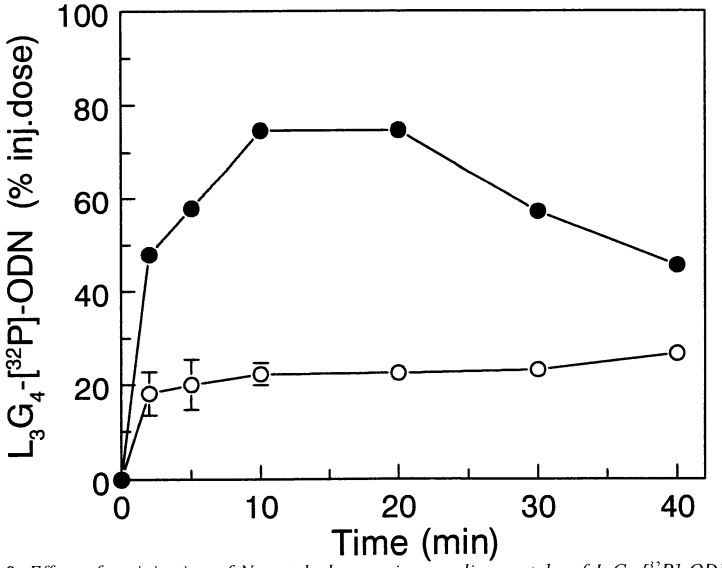

Figure 8. *Effect of preinjection of N-acetyl glycosamines on liver uptake of L_3G_4-[^{32}P]-ODN. N-acetyl galactosamine (○) or N-acetyl glucosamine (both 400 mg/kg in 250 μl PBS; •) were injected intravenously in rats. At 1 min after injection, L_3G_4-[^{32}P]-ODN (4 μg in 500 μl PBS) was administered by i.v. injection into the vena cava. At the indicated times, the liver-associated radioactivities were determined. Values are means of 2 experiments.*

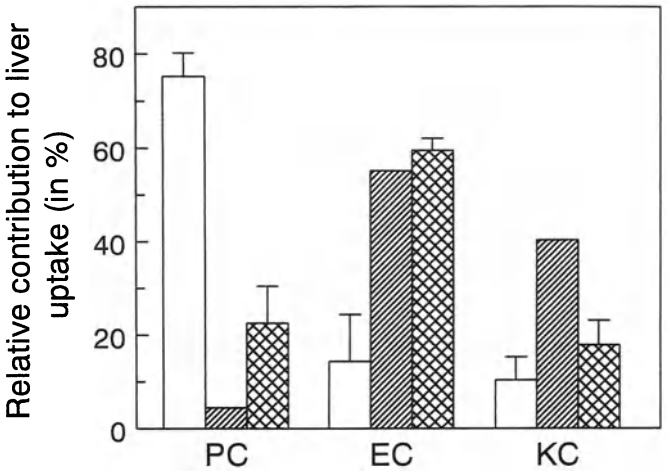

Figure 9. *Relative contribution of various cell types to the liver uptake of L_3G_4-[^{32}P]-ODN (open bar), L_3G_4-[^{32}P]-ODN after preinjection of GalNAC (hatched bars), or [^{32}P]-ODN (crossed bars). [^{32}P]-ODN (1 µg in 500 µl PBS) or L_3G_4-[^{32}P]-ODN (1 µg in 500 µl PBS) was injected into rats at 1 min after preinjection of PBS (250 µl) or GalNAc (150 mg in 250 µl PBS). Parenchymal, endothelial and Kupffer cells were isolated from the liver at 10 min after injection of the radiolabel and the cellular radioactivity was counted. Values (except that of GalNAc treated rats) are means of 3 experiments (± S.D.) and are expressed as percentage of the total liver uptake.*

Discussion

In vivo application of antisense ODNs for the modulation of the expression of target genes in the PC is seriously hampered because it does not markedly accumulate in this cell type. We show in the current study that this drawback can be overcome by glycoconjugating ODNs to a synthetic ligand for the asialoglycoprotein receptor. Previous studies already illustrated that the bioavailability of drugs and genes at the aimed site can be considerably improved through targeting [23-25,28,37-42]. Requisite for successful glycotargeting to the PC is the availibility of a high affinity ligand for a PC-specific receptor such as the asialoglycoprotein receptor [22]. Various research groups have recently designed glycopeptide mimics of multivalent N-linked oligosaccharides that display nanomolar affinities for the asialoglycoprotein receptor [40-43]. These ligands generally contain glycoside units that are attached to a small peptide scaffold. We have synthesized a tetra-antennary lysine based galactoside (L_3G_4) with an equally high affinity as the aforementioned glycopeptides (K_i=6.5 nM) using an accessible 2-step synthetic protocol. Although coupling yields may seem moderate, solution-phase acylation reactions between negatively charged ODNs and carboxylic groups are considered notoriously difficult [27]. Similar yields are reported for solution-phase coupling by Wagner and co-workers [36], while the two-step procedure used by Hangeland et al. [27] to conjugate a heptathymidine to a tri-antennary glycopeptide in solution using cystamine and a thiol/amine cross-linker only resulted in 14% overall yield.

Competition studies of ^{125}I-ASOR binding to hepatocytes established that the affinity

of L_3G_4 for the asialoglycoprotein receptor (ASGPr) was only slightly reduced after conjugation to ODN-AS5', suggesting that L_3G_4 may be an appropriate homing device for targeting of ODNs to the ASGPr. Hereto, the glycoconjugated ODN-AS5' was ligated to the ^{32}P-labelled 3'end f the antisense ODN (ODN-AS3'), to yield a glycosylated internaly labelled 20-mer. Ligation yields were comparable to that of underivatized ODN fragments. This indicates that the presence of the bulky L_3G_4 moiety did not interfere with hybridization to the complementary sense strand, which is a crucial criterium for antisense activity of ODNs. Next, it was evaluated whether recognition, internalization and processing of ODNs by hepatocytes was affected by its conjugation to L_3G_4. L_3G_4-[^{32}P]-ODN appeared to bind to hepatocytes in a saturable fashion. L_3G_4-[^{32}P]-ODN binding could be almost completely (>95%) displaced by unlabelled L_3G_4-ODN and by conventional ligands for the ASGPr (viz. N-acetyl galactosamine, ASOR), but not by N-acetyl glucosamine. The inhibition constants of N-acetyl galactosamine and ASOR for displacing L_3G_4-[^{32}P]-ODN were essentially similar to those reported in literature, suggesting that L_3G_4-[^{32}P]-ODN binding was almost fully mediated by the ASGPr. Moreover, after 2 h of incubation the specific L_3G_4-[^{32}P]-ODN uptake amounted 1.6 ng L_3G_4-[^{32}P]-ODN per mg cell protein, corresponding with an intracellular concentration of 40 nM. This is 4-fold higher than the L_3G_4-[^{32}P]-ODN concentration in the medium, confirming that L_3G_4-[^{32}P]-ODN uptake proceeds through an active transport- rather than a diffusion-mediated process. In vitro studies at 37EC demonstrated that the ASGPr not only binds glycoconjugated ODN but also mediates its uptake and processing. L_3G_4-[^{32}P]-ODN uptake was similarly reduced by established inhibitors of lysosomal uptake than that of ^{125}I-ASOR.

Confocal laser scan microscopy data were in close agreement with the in vitro binding experiments in that ODN uptake by PCs was also strongly stimulated after glycoconjugation. The kinetics of endocytosis of the glycoconjugate could be chased in real time, showing that, after binding, intracellular ODN is succesively concentrated in the endosomal compartiment (just below the membrane surface), in lysosomes (smaller and deeper in the cytosol) and, to a lesser extent diffusely in the cytosol.

In concert with the above in vitro data, in vivo liver uptake of ODNs appeared to be considerably enhanced to almost 80% of the injected dose by coupling to L_3G_4. Liver uptake is close to values reported for a bi-antennary cluster glycoside with high affinity for the asialoglycoprotein receptor [39] and to that of ASOR itself. As the serum degradation of the glycoconjugate proceeds at a much slower rate than hepatic uptake, as liver uptake can be inhibited by inhibitors of the asialoglycoprotein receptor, and as liver uptake of capped phosphodiester ODNs (or ODN degradation products) has been shown to be marginal [6], we can safely assume that liver association of the glycoconjugate reflects uptake of the intact glycoconjugate. Analysis of the liver cell types revealed that the PC was responsible for the induced liver uptake. Accumulation of L_3G_4-derivatized ODNs in this cell type was 60-fold higher upon derivatization with L_3G_4 as compared to underivatized ODNs. This implies that even at doses as low as 40 μg glycoconjugated ODN/kg body weight, intracellular ODN concentrations in the PC may be realized in the order of 100 nM, which is in the concentration range required for therapeutic antisense activity. Hangeland et al. [28] has recently reported enhanced hepatic uptake of a heptathymidinylate (methylphosphonate) conjugated to a tris-

galactosylated glycopeptide in the mouse. In agreement, we report in this study that elimination of a miscellaneous, charged and full length ODN sequences by a scavenger receptor mediated pathway can be prevented and liver uptake of the ODN be realized after derivatization of the ODN to a synthetic glycopeptide tag. Moreover, we demonstrate that uptake is mediated by the aimed target receptor, the asialoglycoprotein receptor, and that it reflects internalized ODN.

Conclusions

Glycotargeting of ODN sequences using homing devices is a very effective way to enhance the local concentration of ODN in the PC under in vivo conditions. Apparently, the natural tendency to be eliminated by the reticulo-endothelial system (i.e. macrophages, Kupffer and liver endothelial cells) and by cells that express scavenger receptor-type proteins [6,44,45] can be overcome through conjugation to a synthetic low-molecular weight ligand for the asialoglycoprotein receptor. Interestingly, the presence of the bulky L_3G_4 group did not markedly interfere with hybridization of the antisense sequence to the complementary target sequence, indicating that another crucial criterium for antisense activity in vivo is met.

Full names of compounds

HBTU - 2-(1H-benzotriazole-1-yl)-1,1,3,3-tetramethyluronium hexafluorophosphate
HOBT - N-hydroxybenzotriazole
DiPEA - N,N-diisopropylethylamine
DCC - N,N-dicyclohexylcarbodiimide
EDC - 1-(3-dimethylaminopropyl)-3-ethylcarbodiimide
EEDQ - 2-ethoxy-1-ethoxycarbonyl-1,2-dihydroquinoline
DMF - N,N-dimethylformamide
DMA - N,N-dimethylacetamide
ASOR - aialoorosomucoid

References

1. Stein CA, Cheng YC. Antisense oligonucleotides as therapeutic agents -is the bullet really magical. Science 1993;261:1004-11.
2. Wagner RW. Gene inhibition using antisense oligodeoxynucleotides Nature 1994;372:333-35.
3. Milligan JF, Matteucci MD, Martin JC. Current concepts in antisense drug design J Med Chem 1993;36:1923-37.
4. Szymkowski DE. Antisense Drug Discov Today 1996;1:415-28.
5. Wagner RW, Flanagan WM. Antisense technology and prospects for therapy of viral infections and cancer. Mol Med Today 1997;3:31-38.
6. Biessen EAL, Vietsch H, Kuiper J, Bijsterbosch MK, van Berkel ThJH. Liver uptake of phosphodiester oligonucleotides is mediated by scavenger receptors Mol Pharmacol 1998;53:1-8.
7. Felgner PL, Gadek TR, Holm M, Roman R, Chan HW, Wenz M, Northrop JP, Ringold GM, Danielsen M. Lipofectin, a highly specific lipid-mediated DNA-transfection procedure. Proc Natl Acad Sci USA 1993;84:7413-17.
8. Leventis R, Silvius JR. Interactions of mammalian cells with lipid dispersions containing novel metabolizable cationic amphiphiles. Bioch Biophys Acta 1990;1023:124-32.
9. Bennett CF, Chiang MY, Chan H, Shoemaker JE, Mirabelli CK. Cationic lipids enhance cellular uptake and activity of phosphorothioate antisense oligonucleotides. Mol Pharm 1992;41:1023-33.
10. Tari AM, Tucker SD, Deisseroth A, Lopez-Berestein G. Liposomal delivery of methylphosphonate antisense oligodeoxynucleotides in chronic myelogenous leukemia Blood 1994;80:601-607.
11. Lewis JG, Lin KY, Kothavale A, Flanagan WM, Matteucci MD, DePrince RB, Mook RA, Hendren RW, Wagner RW. A serum-resistant cytofectin for cellular delivery of antisense oligodeoxynucleotides and plasmid DNA. Proc Natl Acad Sci USA 1996;93:3176-81.
12. Crook ST. Delivery of oligonucleotides and polynucleotides J Drug Targeting 1995;3:185-90.
13. Sands H, Gorey-Feret LJ, Cocazza AJ, Hobbs FW, Chidester D, Trainer GL. Biodistribution and metabolism of internally ^{3}H-labeled oligonucleotides. Mol Pharmacol 1994;45:932-43.
14. Inagaki M, Togawa K, Carr BI, Ghosh K, Cohen JS. Antisense oligonucleotides: inhibition of liver cell proliferation and in vivo disposition. Transpl Proc 1994;24:2971-72.
15. Frese J, Wu CH, Wu GY. Targeting of genes to the liver with glycoprotein carriers. Adv Drug Deliver Rev 1994;14:137-52.
16. Morishita R, Gibbons GH, Kaneda Y, Ogihara T, Dzau VJ. Pharmacokinetics of antisense oligodeoxyribonucleotides (cyclin B1 and CDC 2 kinase) in the vessel wall in vivo: enhanced therapeutic utility for restenosis by HVJ-liposome delivery. Gene 1994;149:13-19.
17. Morishita R, Higaku J, Kida I, Aoki M, Moriguchi A, Lawn R, Kaneda Y, Ogihara T. Ribozyme oligonucleotides against apoliprotein(a) gene cleavages selectively apolipoprotein(a) but not plasminogen, gene: novel gene therapy strategy for atherosclerosis. Circulation 1996;94:I-39.
18. Sugano M, Makino N. Changes in plasma lipoprotein cholesterol levels by antisense oligonucleotides against CETP in cholesterol-fed rabbits. J Biol Chem 1996;271:19080-83.
19. Mizutani T, Kato N, Hirota M, Sugiyama K, Murakami A, Shimotohno K. Inhibition of hepatitis C virus replication by antisense oligonucleotide in culture cells. Biochem Biophys Res Comm 1995;212: 906-11.
20. Wakita T, Wands JR. Specific inhibition of hepatitis C virus expression by antisense oligodeoxynucleotides. J Biol Chem 1994;269:14205-10.
21. Nakazono K, Ito Y, Wu CH, Wu GY. Inhibition of hepatitis B virus replication by targeted pretreatment of complexed antisense DNA in vitro. Hepatology 1996;23:1297-303.

22. Wu GY, Wu CH. Specific inhibition of hepatitis B viral gene expression in vitro by targeted antisense oligonucleotides. J Biol Chem 1992;267:12436-39.
23. Lu XM, Fischman AJ, Jyawook SL, Hendricks K, Tompkins RG, Yarmusch ML. Antisense delivery in vivo: liver targeting by receptor-mediated uptake. J Nucl Med 1994;35:269-75.
24. Bunnell BA, Askari, FA, Wilson, JM. Targeted delivery of antisense oligonucleotides by molecular conjugates Somatic Cell Molecular Genetics 1992;18:559-59.
25. Reinis M, Damkova M, Korec E. Receptor-mediated transport of oligodeoxynucleotides into hepatic cells. J Virol Methods 1993;42:99-106.
26. Ashwell GG, Harford J. Carbohydrate-specific receptors of the liver Ann Rev Biochem 1982;51:531-54.
27. Hangeland JJ, Levis JT, Lee YC, Ts'o POP. Cell-type specific and ligand specific enhancement of cellular uptake of oligodeoxynucleoside methylphosphonates covalently linked with a neoglycopeptide, YEE(ah-GalNAc)3. Bioconjugate Chem 1995;6:695-701.
28. Hangeland JJ, Flesher JE, Deamond SF, Lee YC, Ts'o POP, Frost JJ. Tissue distribution and metabolism of [^{32}P]-labeled ODN methylphosphonate-neoglycopeptide conjugate, [YEE-(ah-GALNAc)$_3$]-SMC-AET-pUm-pT$_7$, in the mouse. Antisense Nucl Acid Drug Dev 1997;7:141-49.
29. Pearson AM, Rich A, Krieger M. Polynucleotide binding to macrophage scavenger receptors depends on the formation of base-quartet-stabilized four-stranded helices. J Biol Chem 1993;268:3546-54.
30. McLean JW, Tomlinson JE, Kuang WJ, Eaton DL, Chen EY, Fless GM, Scanu AM, Lawn RW. cDNA sequence of human apolipoprotein(a) is homologous to plasminogen. Nature 1987;330:132-37.
31. Biessen EAL, Bakkeren HF, Beuting DM, Kuiper J, van Berkel ThJC. Recognition of both fucose- and galactose-exposing particles by the hepatic fucose receptor depends on the particle size. Biochem J 1994;299:291-96.
32. Sambrook J, Frits EF, Maniatis T. Molecular Cloning: A Laboratory Manual, 2nd ed., Ed., Cold Spring Harbor Laboratory, Cold Spring Harbor, NY, 1989.
33. Biessen EAL, Beuting DM, Roelen HCPF, van de Marel GA, van Boom JH, van Berkel ThJC. Synthesis of cluster galactosides with high affinity for the hepatic asialoglycoprotein receptor. J Med Chem 1995;38:1446-52.
34. van Berkel ThJC, De Rijke YB, Kruijt JK. Differrent fate in vivo of oxidatively modified low-density lipoprotein in rats. J Biol Chem 1991;266:2282-89.
35. Biessen EAL, Norder JA, Horn AS, Robillard GT. Evidence for the existence of at least two different binding sites for 5HT-reuptake inhibitors within the 5HT-reuptake system from human blood platelets. BiochemPharm 1988;37:3959-66.
36. Oberhauser B, Wagner E. Effective incorporation of 2'-O-methyl-oligoribonucleotides into liposomes and enhanced cell association through modification with thiocholesterol. Nucleic Acids Res 1992;20:533-538.
37. Biessen EAL, Beuting DM, Vietsch H, Bijsterbosch MK, van Berkel ThJC. Specific targeting of the antiviral drug 5-iodo-2'deoxyuridine to the parenchymal liver cell using lactosylated poly-L-lysine. J Hepatology 1994;21:806-15.
38. Bonfils E, Dupiereux C, Midoux P, Thuong NT, Monsigny M, Roche AC. Drug targeting: synthesis and endocytosis of oligonucleotide-neoglycoprotein conjugates. Nucleic Acids Res 1992;20:4621-29.
39. Chiu M, Tamura T, Wadhwa MS, Rice KG. In vivo targeting function of N-linked oligosaccharides with terminating galactose and N-acetylgalactosamine residues. J Biol Chem 1994;269:16195-202.
40. Haensler J, Szoka FC. Synthesis and characterization of a trigalactosylated bisacridine compound to target DNA to hepatocytes. Bioconjugate Chem 1993;4:85-93.
41. Merwin JR, Noell GS, Thomas WC, Chion HC, De Rome ME, McKee TD, Findeis MA.

Targeted delivery of DNA using YEE(GalNAcAH)3, a synthetic glycopeptide ligand for the asialoglycoprotein receptor. Bioconjugate Chem 1994;5:612-20.

42. Plank C, Zatloukal K, Cotten M, Mechtler K, Wagner E. Gene transfer into hepatocytes using asialoglycoprotein receptor mediated endocytosis of DNA complexed with an artificial tetra-antennary galactose ligand. Bioconjugate Chem 1992;3:533-39.
43. Lee RT, Lee YC. Preparation of cluster glycosides and GalNAc that have sub-nanomolar binding affinity toward mammalian hepatic Gal/GalNAc-specific receptors. Glycoconjugate J 1987;4:317-28.
44. Bijsterbosch MK, Manoharan M, Rump ET, de Vrueh RLA, van Veghel R, Tivel KL, Biessen EAL, Bennett CF, Cook PD, van Berkel ThJC. In vivo fate of phosphorothioate antisense oligonucleotides: Predominant uptake by scavenger receptors on endothelial cells Nucl Acids Res 1997;25:3290-96.
45. Rifai A, Brysch W, Fadden K, Clark J, Slingensiepen KH. Clearance kinetics, biodistribution, and organ saturability of phosphorothioate oligodeoxynucleotides in mice. Am J Pathol 1996;149:717-25.

25. TISSUE-SPECIFIC GENE DELIVERY BY RECOMBINANT ADENOVIRUSES CONTAINING CARDIAC-SPECIFIC PROMOTERS

Wolfgang-Michael Franz, Thomas Rothmann, Matthias Müller, Norbert Frey, and Hugo Albert Katus

Introduction

Somatic gene therapy represents a promising approach for the treatment of inherited and acquired heart diseases including X-linked cardiomyopathies [1-3]. The risk-to-benefit ratio of gene therapy for patients with cardiomyopathy is higher than for patients suffering from cancer or AIDS in which treatment options are more limited. The safety of the vector system is therefore a major aspect of consideration for gene therapy of heart muscle diseases. An ideal vector system should be immunologically tolerated, gene delivery should be efficient and gene expression should be restricted to heart muscle cells only.

Recombinant adenoviruses have been shown to be the most efficient vector system to express recombinant genes in the myocardium of experimental animal model systems [4-6]. Adenoviruses, unlike retroviruses, can infect non dividing cardiomyocytes very efficiently and show 50-100 fold higher gene expression in rat myocardium after direct injection of viral particles compared with injection of plasmid DNA alone [4,7]. In addition, adenoviral vectors can accommodate large cDNA inserts, they are easy to produce and can be prepared in high titers (10^{10} - 10^{12} plaque forming units (pfu) / ml). They have been used safely for human vaccination and do not integrate into the genome [8]. In most models, however, gene expression is transient after adenoviral infection and inflammation is observed in tissues expressing the transgene [9]. Several groups have recently developed so called second and third generation adenoviral vectors to prolong gene expression and reduce the immune response, but their persistence in the heart has not yet been tested [10-17]. So far, only first generation adenoviral vectors have been tested by different routes of administration for the efficiency to transduce heart muscle cells *in vivo*. Infusion of adenoviruses into the tail vein of mice led to a poor transduction of the heart (approx. 0.2 % of cardiomyocytes transduced) with a distribution of the virus throughout the body [18]. More efficient ways to deliver genes

P.A. Doevendans et al. (eds.), Cardiovascular specific gene expression, 301-17.

to the heart *in vivo* include direct injection of viral particles into heart muscle or the cardiac cavity as well as percutaneous transluminal gene transfer (PTGT) [4-6,19,20]. In all methods examined, non-cardiomyocytes are also transduced. After direct injection into the heart many other tissues including thymus, lung and liver showed transgene expression [4,5,19,20]. Administration of adenovirus by PTGT is followed by transduction of the coronary vasculature and non-myocyte connective tissue cells throughout the region of the myocardium supplied by the injected coronary artery [6]. Of note, no inflammatory response was observed after PTGT administration of the virus. The important question of how to limit gene expression to heart muscle cells using adenoviral vectors has not yet been addressed.

The best characterized promoters for a tissue-specific expression in embryonic and adult ventricular myocardium derive from the myosin light chain-2 (MLC-2v) and the alpha-myosin heavy chain (α-MHC) genes [21]. In a transgenic animal model, we previously demonstrated the ventricular specific gene expression under the control of the 2.1 kb MLC-2v promoter [22,23]. In another transgenic animal model the α-MHC promoter was shown to be active in ventricular and atrial tissues [24,25]. In order to target genes and the corresponding proteins to defined regions within the heart such as atrium and/or ventricle, we compared the rat cardiac α-MHC promoter with the MLC-2v promoter with regard to their cardiac selectivity and their differences in atrial and ventricular gene expression [26,27].

Methods

Construction of recombinant plasmids

Plasmids pAd-Luc, pAd-RSVLuc, pAd-MHCLuc and pAd-MLCLuc are derivates of the plasmid pAd. RSV-βgal, in which the BamHI/KpnI RSV-βgal cassette is exchanged for luciferase cDNA containing the endogenous polyadenylation signal [18]. This was achieved by subcloning the HindIII/KpnI fragment of plasmid pSVOALΔ5', containing the luciferase gene, into HindIII/KpnI site of pBluescriptSK (Stratagene), thus generating the subclone pBluescript-Luc [27]. pBluescript-RSVLuc was engineered by subcloning the BamHI/HindIII 587 bp RSV-fragment of plasmid pAd.RSV-βgal into the BamHI/HindIII sites of subclone pBluescript-Luc. For the construction of plasmid pBluescript-MHCLuc the EcoRI/HindIII fragment of the α-MHC promoter (-612 bp to +420 bp) plus 32 bp of the 5' multiple cloning side of plasmid pGCATCalphaMHC were excised by BamHI and HindIII and subcloned into the BamHI/HindIII sites of pBluescript-Luc [28]. The BamHI/KpnI fragments of subclone pBluescript-Luc, pBluescript-RSVLuc and pBluescript-MHCLuc, were then cloned into the BamHI/KpnI sites of plasmid pAd.RSV-βgal to give rise to plasmid pAd-Luc, pAd-RSVLuc and pAd-MHCLuc. To generate plasmid pAd-MLCLuc, the BamHI/KpnI MLC-Luciferase fragment of plasmid pMLCLΔ5', containing approximately 800 bp of the MLC-2v promoter in front of the luciferase gene, was directly cloned into the BamHI/KpnI sites of plasmid pAd.RSV-βgal [30].

Construction of recombinant adenoviruses

Recombinant viruses were constructed by homologous recombination between plasmids pAd-Luc, pAd-RSVLuc and pAd-MLCLuc with adenovirus Ad del324 genomic DNA in HEK-293 cells [18,31]. Briefly, 2 x 10^6 HEK-293 cells were cotransfected with 5 μg AatII linearized plasmids and 5 μg of the large ClaI fragment of Ad del324 genomic DNA. Virus Ad-MHCLuc was generated after homologous recombination between plasmid pAd-MHCLuc and plasmid pBHG10 transfecting 1 x 10^6 911 cells [32,33]. After overlaying with agar and 8-10 days incubation at 37°C, plaques containing recombinant viruses were picked and screened for the correct integration of the transgene by restriction enzyme analysis (figure 1).

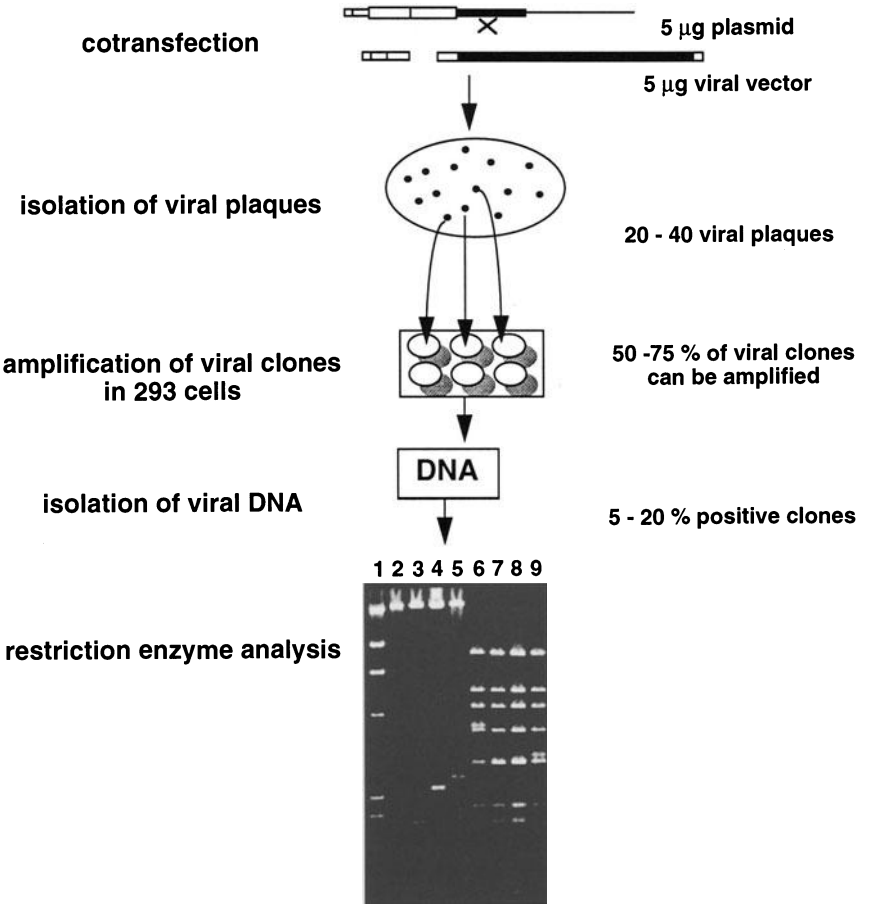

Figure 1. *Generation and characterization of recombinant adenoviruses. After cotransfection with 5 μg of ClaI digested Ad del324 and 5 μg of plasmids pAd-Luc, pAd-RSVLuc, pAd-MLCLuc, and pAdMHCLuc, into 293 cells up to 40 viral plaques were isolated and amplified. Restriction enzyme analysis of adenoviral DNA by ClaI (lanes 2 - 5) and HindIII (lanes 6-9) revealed up to 20% positive clones. λ-marker cut with HindIII (lane 1), Ad del324 (lanes 2 and 6), Ad-Luc (lanes 3 and 7), Ad-RSVLuc (lanes 4 and 8), Ad-MLC-Luc (lanes 5 and 9).*

Recombinant adenoviruses were again plaque purified before being propagated in HEK-293 cells and further purified by two rounds of cesium chloride density centrifugation [18]. Finally, the viruses were dialyzed against TD-buffer (137 mM NaCl, 5 mM KCl, 0.7 mM Na_2HPO_4, 0.5 mM $CaCl_2$, 1 mM $MgCl_2$, 10 % (v/v) glycerol, 25 mM Tris-HCl (pH 7.4) and stored at -70°C. The titer of the frozen viral stocks was determined by plaque assay using HEK-293 or 911 cells respectively [18]. All recombinant adenoviruses had a titer of approximately 10^{11} pfu per ml. DNA of the viral stocks was isolated and analyzed by restriction enzyme analysis (figure 1) and PCR for the correct integration of the insert. In addition, viral stocks were tested by PCR for wild type Ad-5, showing no contamination in 50 ng of recombinant viral DNA [34].

In vivo injections into the cardiac cavity and thigh muscle

For the injection experiments, two days old Sprague-Dawley rats were used. The investigation conforms with the Guide for the Care and Use of Laboratory Animals published by the US National Institute of Health (NIH Publication No. 8523, revised 1985). Prior to injections, rats were anaesthetized by a 3 - 5 minutes inhalation of methoxyfluran (Metofane, Janssen GmbH). 2 x 10^9 pfu of the recombinant adenoviruses Ad.RSV-βgal, Ad-Luc, Ad-RSVLuc, Ad-MHCLuc or Ad-MLCLuc were injected in a 20 μl volume using a 27½ gauge tuberculin syringe. Injections were carried out by transthoracal puncture of the cardiac cavity. The flashback of the pulsatile blood stream into the syringe indicated the intracavitary position of the needle tip. A slow rate of injection (20 μl/min.) was achieved using a self-constructed device. Injection into the quadriceps femoris was performed accordingly.

Reporter gene assays

For *in vivo* studies, animals were sacrificed five days post injection by decapitation. In a first set of experiments (data represented in figure 3, 4) several tissues were dissected (total heart, intercostal muscle, thymus, lung, diaphragm, abdominal wall muscle, liver, stomach, spleen, quadriceps femoris) and in a second set of experiments (data represented in figure 7) only ventricular and atrial tissues were excised using a stereo microscope. After dissection, tissues were immediately frozen in liquid nitrogen. Samples were weighed, homogenized in lysis buffer (1% (v/v) Triton X-100, 1 mM DTT, 100 mM potassium phosphate pH 7.8), centrifuged and the supernatant was used to perform luciferase assays as described [35]. Luciferase activity measured by a transilluminometer (Lumat LB 9501, Berthold) was given in relative light units (RLU) per mg wet tissue after correction for background luciferase activity measured in tissues of uninfected control animals.

Hearts of sacrificed animals were flash frozen in isopentane precooled in liquid nitrogen and embedded in OTC compound (Tissue Tek, Miles). 10 μm cryosections were taken, analyzed for β-galactosidase expression and counterstained with hematoxylin and eosin as described [36].

PCR analysis of adenoviral DNA

Simultaneously to luciferase assay measurements, genomic DNA was extracted from the same tissues using the QIAamp tissue kit (QIAGEN, Germany). Eight

representative animals, two for each of the four different adenoviruses, were analyzed for tissue distribution of the viruses using PCR as previously described, with minor modifications [34]. One hundred ng of genomic DNA was used as a template together with 40 ng of oligonucleotide primers E2B-1 and E2B-2 in a 25 μl reaction volume. Gel electrophoresis of the PCR product revealed a specific 860 bp band.
The sensitivity of the PCR reaction was determined by using 100 ng genomic DNA from uninfected rats, mixed with decreasing amounts of Ad del324 DNA, as a template. To increase sensitivity of detection the PCR products of the tested genomic DNAs were transferred to GeneScreenPlus membranes (NEN, Massachusetts) and analyzed by Southern blot hybridization [35]. Gel purified DNA, generated by positive control PCR, was labeled by random hexanucleotide primers and used as a hybridization probe [35]. Thus, sensitivity of detection was increased 10-100 fold.

Results

Construction of recombinant adenoviruses
To assess the specificity of gene expression driven by the α-MHC and MLC-2v promoter in the adenoviral vector system, four types of recombinant adenoviruses were constructed as shown in figure 2. Each of the replication defective adenoviruses (figure 2 A - D) contains the luciferase reporter gene under the control of a different upstream regulatory region, such as the 1.0 kb α-MHC, 0.8 kb MLC-2v and the 0.6 kb RSV promoter, substituting the E1 region 3' of the encapsidation signal Ψ [28-30,36,37]. The resulting recombinant adenoviruses Ad-MHCLuc, Ad-MLCLuc and Ad-RSVLuc were named according to their respective promoter. The adenoviral construct Ad-Luc (figure 2 D) containing only the luciferase reporter gene served as a negative control virus.

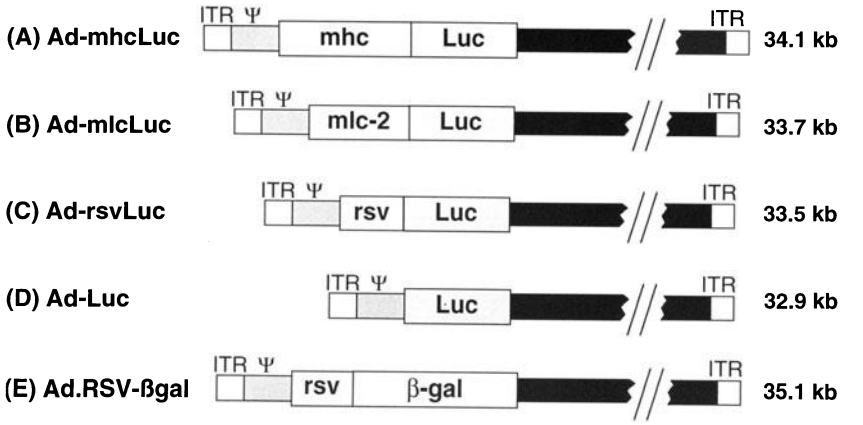

Figure 2. *Schematic drawing of the replication defective adenoviruses Ad-MHCLuc, Ad-MLCLuc, Ad-RSVLuc, Ad-Luc, and Ad.RSV-βgal. Viruses (A) - (D) were harboring the luciferase reporter gene (replacing the E1-region) driven by (A) the α-MHC promoter (B) the MLC-2v promoter, (C) the RSV promoter and (D) no promoter. (ITR = Inverted Terminal Repeat, Ψ = adenoviral packaging sequence, RSV = Rous Sarcoma Virus promoter, MLC-2v = myosin light chain-2 promoter, α-MHC = α-myosin heavy chain promoter, Luc = luciferase, ß-gal = ß-galactosidase).*

Transgene expression in neonatal rats after adenoviral injection into cardiac cavity and thigh muscle

In order to test whether the recombinant adenoviruses Ad-MHCLuc and Ad-MLCLuc are able to direct luciferase expression specifically into the heart muscle, a volume of 20 μl containing 2 x 10^9 pfu was injected into the cardiac cavity of newborn rats. The positive control virus Ad-RSVLuc and the negative control virus Ad-Luc were administered via the same route of injection. Luciferase activities determined five days after injection for nine different tissues are summarized in figure 3.

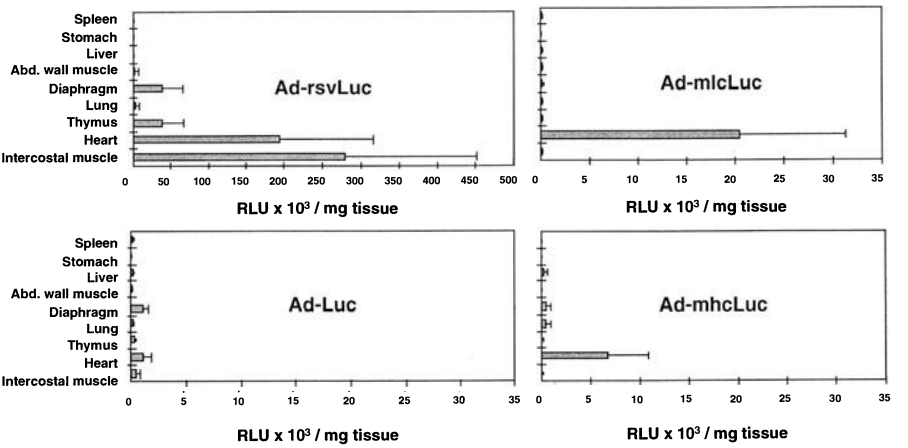

Figure 3. *Luciferase activity in 9 different tissues after intracavitary injection of recombinant adenoviruses Ad-RSVLuc, Ad-Luc, Ad-MLCLuc, or Ad-MHCLuc. 2 x 10^9 pfu in a total volume of 20 μl were injected into the left ventricle of neonatal rats. Tissues were analyzed five days post injection. Luciferase activity is expressed in Relative Light Units (RLU)/mg wet tissue. Bars show mean level of four experiments and lines represent the standard error of the mean.*

Injection of Ad-RSVLuc led to the highest luciferase activity in heart and intercostal muscle and showed a substantial level of reporter gene expression in thymus, diaphragm, lung and a lower abundance in the abdominal wall muscle, liver and spleen. The negative control virus Ad-Luc showed a low level luciferase activity in all tissues with a slightly higher value in diaphragm, heart, intercostal muscle and thymus due to the transthoracal gene transfer method. Adenovirus Ad-MHCLuc and Ad-MLCLuc harboring the heart muscle specific promoters revealed highest reporter gene expression in the heart. Compared to the promoterless control virus Ad-Luc, Ad-MHCLuc infected animals showed additional luciferase activity in lung and liver tissue (figure 4). By contrast, adenoviral Ad-MLCLuc transfer resulted in heart specific gene expression with background activities at or below the negative control virus Ad-Luc (figure 4). Light emission of Ad-MLCLuc in the heart was 20 fold higher in comparison to Ad-Luc and reached 11% of the activity obtained by Ad-RSVLuc. Ad-MHCLuc gave a 6.5 fold higher luciferase activity in the heart compared to Ad-Luc. This level corresponds to 3 % of the Ad-RSVLuc activity. These data demonstrate that in contrast to the 0.8 kb MLC-2v promoter gene expression driven by the 1.0 kb α-MHC promoter is not restricted to the heart.

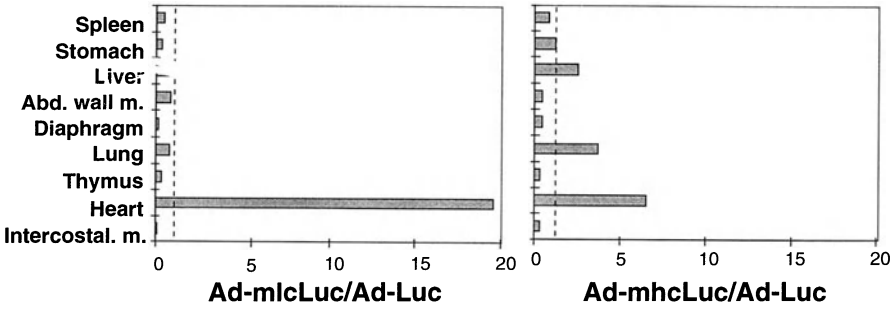

Figure 4. *Ratio of luciferase activity for recombinant adenovirus Ad-MLCLuc (A) and Ad-MHCLuc (B) related to the promoterless virus Ad-Luc in 9 different tissues expressed in two bar diagrams. All bars left of the dashed line representing a ratio of 1 express background luciferase activities.*

The distribution of transduced heart muscle cells after intracavitary injection of adenoviruses was assessed by injection of a recombinant adenovirus expressing the β-galactosidase (Ad.RSV-βgal) reporter-gene (figure 2 E) [18]. After sectioning and X-gal staining, visual inspection showed that approximately half of the myocardial β-galactosidase activity resulted from direct myocardial injection along the needle track into the heart (figure 5). In the needle track (figure 5 A), almost all of the cardiomyocytes revealed β-galactosidase activity, whereas in the remaining myocardium only a few cardiomyocytes stained blue (figure 5 B).

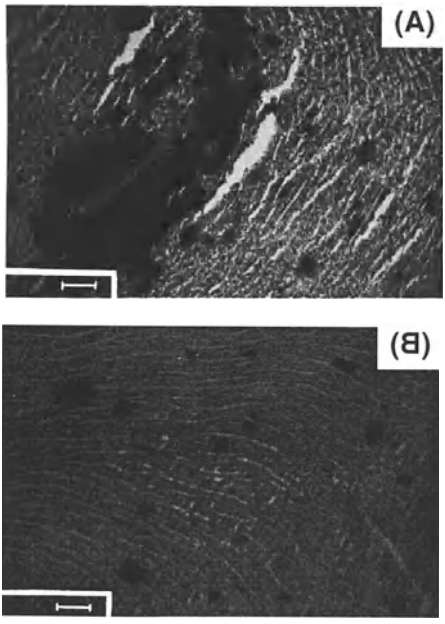

Figure 5. *Histological detection of β-galactosidase activity in the myocardium 5 days after intracavitary injection of Ad.RSV-βgal. (A) Photomicrograph of a histological section through the apical site of injection and (B) through the central part of the heart. In each panel blue staining shows β-galactosidase activity. Bar represents 100 μm [26].*

To test whether the adenoviral vector Ad-MHCLuc reveals reporter gene activity in skeletal muscle after a direct needle injection, a volume of 20 μl containing 2 x 10^9 pfu of recombinant adenovirus was injected into the right quadriceps femoris muscle. A luciferase activity of 3,4 ± 0,8 RLU per 10^{-3} mg tissue was measured five days after injection (n=4). This result was comparable to the negative control virus Ad-Luc and Ad-MLCLuc (figure 6). Adenoviruses containing the α-MHC or the MLC-2v promoter showed only background activities comparable to Ad-Luc. These data suggest, that in the adenoviral context the α-MHC promoter, like the MLC-2v promoter, has no skeletal muscle activity.

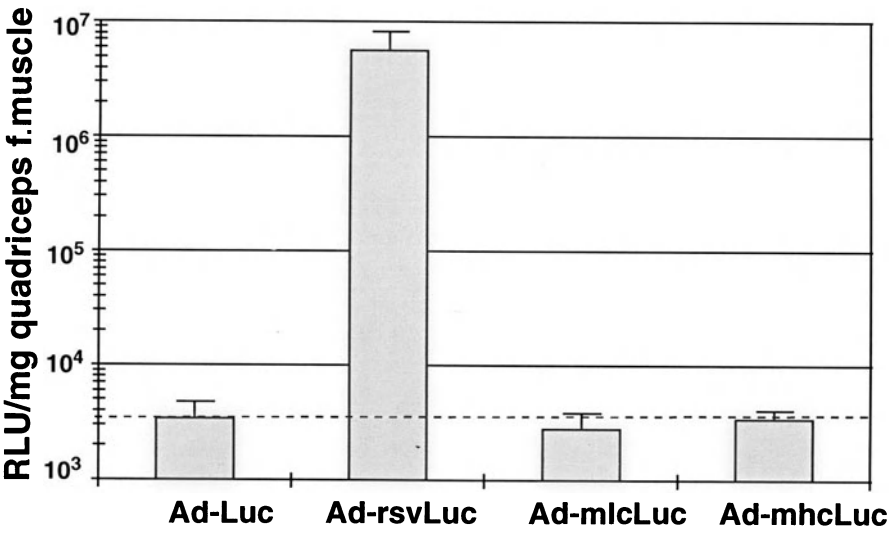

Figure 6. *Luciferase activity obtained after injection of the recombinant adenoviruses in thigh muscle. 2 x 10^9 pfu in a total volume of 20 μl were injected into the right quadriceps femoris muscle of neonatal rats. Tissues were analyzed five days post injection. Luciferase activities are expressed in Relative Light Units (RLU)/mg wet tissue. Bars show mean level of four experiments and lines represent the standard error of the mean.*

Ventricle versus atrium specific gene expression after adenoviral injection into cardiac cavity

To study the regional differences of reporter gene expression in atrial and ventricular myocardium the four recombinant adenoviruses containing the luciferase reporter gene were injected into the cardiac cavity accordingly. Five days after injection, light emission was determined in heart ventricle and atrium (figure 7). While Ad-MLCLuc showed high luciferase activity in the ventricle (figure 7 A), luciferase expression levels in the atrium were comparable to the negative control Ad-Luc (figure 7 B). The ratio of light emission for ventricular to atrial tissue is shown for the four recombinant adenoviruses (figure 7 C). While Ad-RSVLuc, Ad-MHCLuc and Ad-Luc injection led to an approximately 2-fold higher luciferase activity in the ventricle, Ad-MLCLuc

injection gave a 35-fold higher luciferase activity in the ventricular compared to the atrial tissue. These data demonstrate that Ad-MLCLuc is specifically active in the ventricle of neonatal rats.

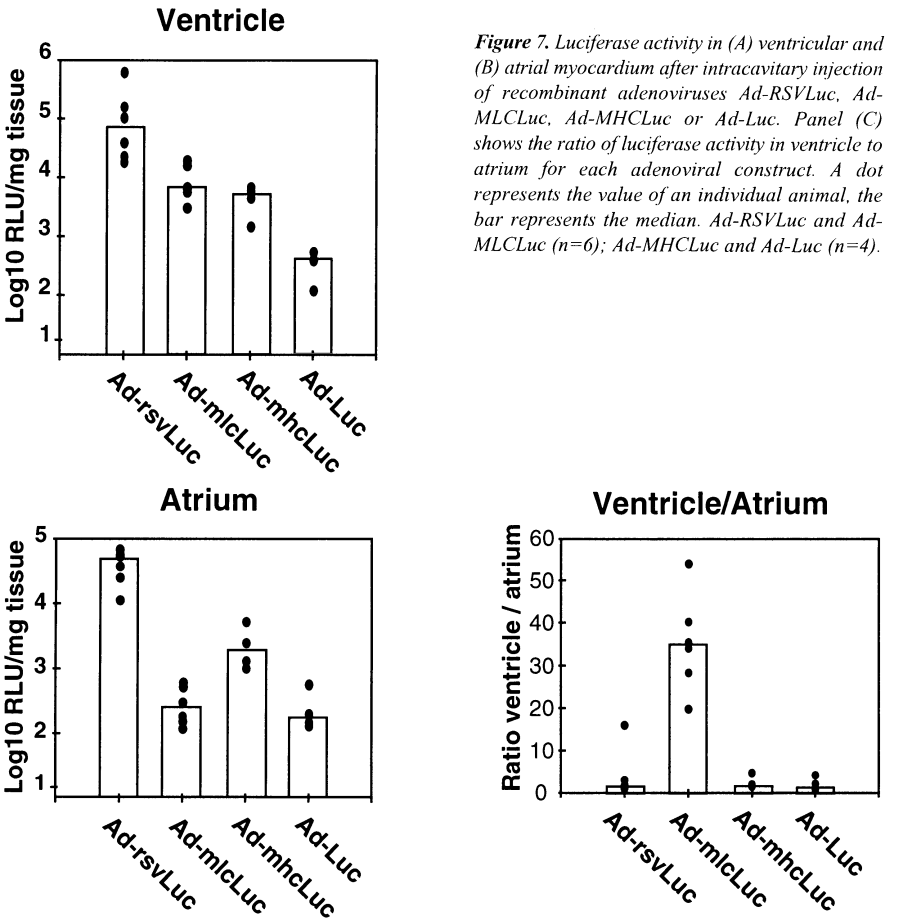

Figure 7. *Luciferase activity in (A) ventricular and (B) atrial myocardium after intracavitary injection of recombinant adenoviruses Ad-RSVLuc, Ad-MLCLuc, Ad-MHCLuc or Ad-Luc. Panel (C) shows the ratio of luciferase activity in ventricle to atrium for each adenoviral construct. A dot represents the value of an individual animal, the bar represents the median. Ad-RSVLuc and Ad-MLCLuc (n=6); Ad-MHCLuc and Ad-Luc (n=4).*

Extent of tissue infection in neonatal rats after injection of recombinant adenoviruses into cardiac cavity

To evaluate the extent of non-cardiac gene transfer and the adenoviral distribution within the heart following intracardiac injection of recombinant viruses, genomic DNA was isolated and assayed for the presence of adenoviral sequences by PCR. To assess the range of sensitivity, 100 ng of genomic DNA from an uninfected rat was mixed with decreasing amounts of adenoviral DNA Ad del324 (10 pg - 0.1 fg) and PCR was performed consecutively. These experiments demonstrated that approximately 10 fg of Ad del324 DNA can be detected in 100 ng of rat genomic DNA, corresponding to 1 copy of adenoviral genome per 600 cells (figure 8 A). In adenovirus infected animals, viral DNA could be detected in intercostal muscle, heart, thymus, lung, diaphragm and

liver, independent of the injected recombinant virus (figure 8 B). To increase sensitivity of adenoviral detection, PCR products were transferred to a nylon membrane and analyzed by Southern blot hybridization. This assay revealed the presence of adenoviral DNA in low amounts in all other tissues investigated, with minor variations between individual animals. Figure 8 C shows a representative Southern blot for one animal injected with the adenovirus Ad-MLCLuc.

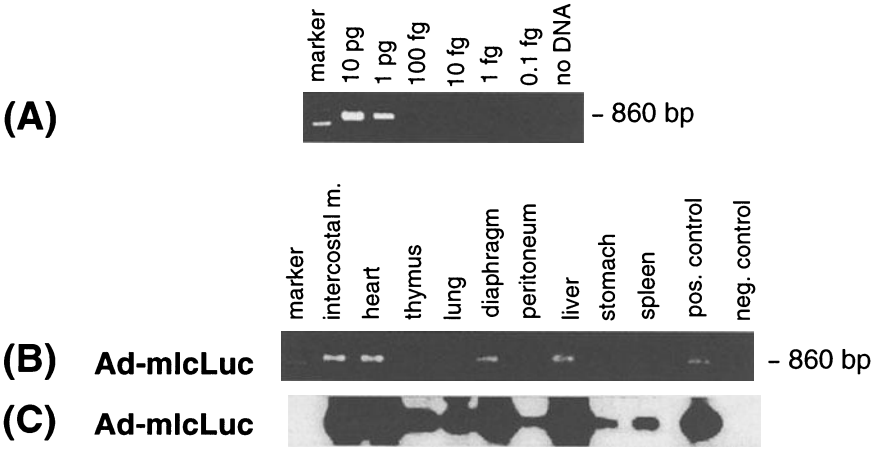

Figure 8. *Detection of adenoviral DNA in 9 tissues after intracavitary injection of the representative adenovirus Ad-MLCLuc. (A) Agarose gel (2.4 %) showing specific 860 bp PCR-product amplified from decreasing amounts of Ad del324 DNA. For templates, 100 ng of rat genomic DNA were mixed together with the following amounts of viral DNA: 10 pg (lane 1); 1 pg (lane 2); 100 fg (lane 3); 10 fg (lane 4); 1 fg (lane 5); 0.1 fg (lane 6); no viral DNA (lane 7). A 100 bp ladder served as the molecular weight standard (lane M). (B) Agarose gel (2.4 %) showing 860 bp PCR-product amplified from 100 ng genomic DNA isolated from the indicated organs after intracavitary injection of Ad-MLCLuc. PCR reactions containing 100 ng of rat genomic DNA mixed with 1 pg Ad del324 DNA or without addition of viral DNA served as positive and negative controls, respectively. (C) Southern blot analysis of the same Ad-MLCLuc infected animal using the specific, ^{32}P-radiolabeled 860 bp amplification product as a probe .*

To analyze the local distribution of viral DNA within the myocardium infected animals were analyzed 5 days after intracardiac injection. Adenoviral DNA was detected to similar amounts in both ventricular and atrial tissue (figure 9). This could be repeated independent of the injected recombinant adenovirus, indicating a similar intracardiac viral distribution after intracavitary application [27]. Thus, gene expression of Ad-MHCLuc and Ad-MLCLuc may result from the regulatory promoter sequence of α-MHC and MLC-2v and may not be due to a difference in tissue infection or tissue specific differences in local viral concentration.

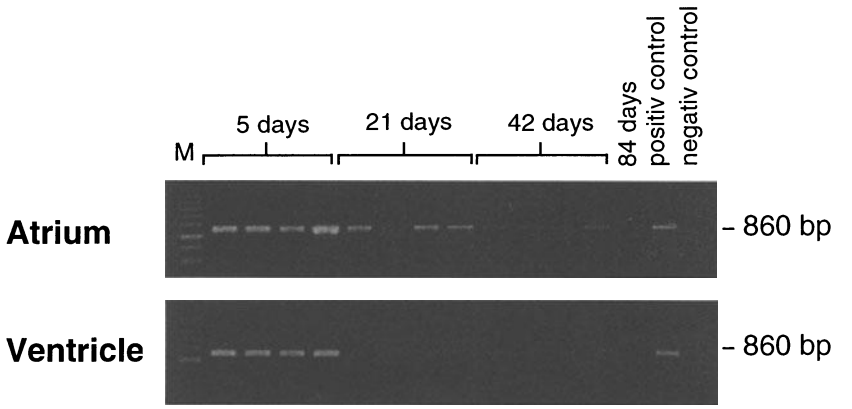

Figure 9. *Detection of adenoviral DNA in atrial and ventricular tissue for the representative adenovirus Ad-MLCLuc at different time points after infection. Genomic DNA from four animals was assayed for the presence of adenoviral sequences by PCR. Two Nusieve agarose gels (2.4 %) showing the 860 bp PCR-product amplified from 100 ng rat genomic DNA isolated from atrial and vertricular tissue after intracavitary injection. PCR reactions containing 100 ng of rat genomic DNA mixed with 1 pg Ad del324 DNA or without addition of viral DNA served as positive and negative controls, respectively. A 100 bp ladder served as the molecular weight standard (lane M).*

Long-term expression after adenoviral injection into cardiac cavity

Recombinant adenoviruses Ad-MLCLuc and Ad-RSVLuc were injected into the cardiac cavity of neonatal rats. Animals were sacrificed 5, 21, 42 and 84 days after infection followed by luciferase measurements in ventricular and atrial tissues (figure 10). Simultaneously genomic DNA was extracted and the amount of adenoviral DNA was measured by semiquantitative PCR analysis (figure 9).

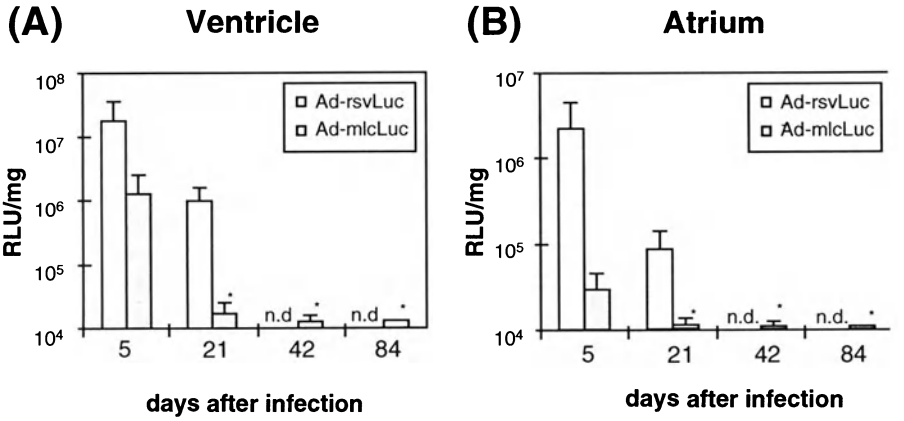

Figure 10. *Long term luciferase expression in (A) ventricular and (B) atrial myocardium after intracavitary injection of 20 µl containing 2 x 10^9 pfu of Ad-RSVLuc and Ad-MLCLuc (n = 4). Tissues were analyzed 5, 21, 42, and 84 days post injection. Luciferase activities are expressed in Relative Light Units (RLU)/mg wet tissue. Bars show mean level of four experiments and lines represent the standard error of the mean.*

Twenty-one days after Ad-RSVLuc application a 20-fold reduction of luciferase activity was detected in ventricular myocardium and a 40-fold decrease in the atria compared to light activities five days after infection. No luciferase activity was observed 42 and 84 days after cardiac infection, which correlated well with the loss of adenoviral DNA detected by PCR (figure 9). For Ad-MLCLuc no luciferase activity was detected in ventricles and atria 21 days post infection (figure 10).

Discussion

The experiments have demonstrated that the ventricular specific myosin-light-chain 2 promoter retains its *in vivo* specificity of gene expression in the myocardium [22,23] after incorporation into an adenoviral vector, Ad-MLCLuc [26]. Specific gene expression of Ad-MLCLuc was shown in the ventricular myocardium after injection into the cardiac cavity of newborn rats [27]. By contrast using the adenoviral shuttle vector Ad-MHCLuc, in which the α-myosin heavy chain promoter was used to drive luciferase, the reporter gene was active in ventricular and atrial myocardium, and revealed ectopic expression in lung as well as in liver tissue.

For gene therapy of cardiovascular diseases it is useful to target recombinant gene expression to the myocardium. Previous attempts of adenoviral gene transfer have not allowed a restricted gene expression in cardiac cells [4,19,20]. The finding that administration of recombinant adenovirus resulted in infection and expression of the transgene in many non-cardiac tissues raises important safety concerns. For example, a strong expression of the *Drosophila Shaker* potassium channel was reported in liver after intracardiac injection of the recombinant adenovirus AdShK [39]. As noted by the authors, this may have phenotypic consequences since the hepatocyte membrane potential determines the rate of bile acid uptake. Such undesired effects could be avoided by using the here described adenoviral vector Ad-MLCLuc, which allows a ventricular muscle-specific gene expression.

In concordance with tissue culture results in neonatal rat cardiomyocytes reported earlier by our group [26], a heart muscle-specific gene expression could be observed *in vivo* for the recombinant adenovirus Ad-MLCLuc, which contains a 800 bp fragment of the MLC-2v promoter. After intracavitary injection of the recombinant viruses into the cardiac cavity of neonatal rats, light emission after Ad-MLCLuc infection was 11% in relation to Ad-RSVLuc and 20 fold above the luciferase activity of the negative control virus Ad-Luc (figure 3). In the other 8 tissues tested, the MLC-2v promoter was inactive and light activity did not exceed the expression level of the promoterless construct Ad-Luc. Interestingly, Ad-MLCLuc showed only minor activity in atrial myocardium, but was restricted in its activity to the ventricular myocardium of neonatal rats (figure 4). The negative control virus Ad-Luc and the positive control virus Ad-RSVLuc revealed an approximately two times higher activity in ventricular as compared to atrial myocardium. However, Ad-MLCLuc was 35 times more active in the ventricular compartment. The detection of adenoviral DNA by a specific PCR in atrial and ventricular tissue did not depend on the injected type of adenovirus indicating a ventricular-specific regulation of Ad-MLCLuc by the MLC-2v promoter (figure 9).

Therefore, we conclude that in adenoviral vectors the MLC-2v promoter retains its ventricle specificity first demonstrated in the transgenic system [22,23].

In contrast to Ad-MLCLuc, Ad-RSVLuc induced luciferase activity was also observed in intercostal muscle, thymus, lung and diaphragm. Luciferase expression in these tissues has also been shown after intracavitary injection of an adenoviral construct in which the cytomegalovirus promoter was used to drive the luciferase gene [19]. When a PCR based method was used to test for adenoviral infection, viral DNA could be detected in heart, intercostal muscle, thymus, lung, diaphragm and liver, for each of the viruses injected. With the exception of liver, these are the same tissues that showed luciferase activity after infection of Ad-RSVLuc. Absence of hepatic reporter gene activity is in accordance with the lack of RSV driven gene expression in the liver observed in a transgenic mouse model [40]. Thus it appears that the presence of PCR-detectable adenoviral DNA correlates well with luciferase activity in the Ad-RSVLuc injected animals.

The two fold higher luciferase activity of the control constructs in the ventricular as compared to the atrial myocardium can be explained by the mode of intracavitary application. After injection of a recombinant adenovirus expressing the β-galactosidase (Ad.RSV-βgal) reporter gene, we reported recently that half of the β-galactosidase activity in the myocardium resulted from viral accumulation along the transventricular needle track [26], whereas in the remaining myocardium only 1-2% of the cardiomyocytes stained blue. For an efficient gene therapy approach, however, a catheter guided delivery system such as PTGT should be applied [6], which is not feasible in neonatal rats.

For some indications, it may be necessary to induce gene expression in both ventricular and atrial tissue. Based on transgenic experiments showing a ventricular and atrial activity of the α-MHC promoter [25], we constructed the adenoviral vector Ad-MHCLuc where the rat α-MHC promoter regulates expression of the luciferase reporter gene [29]. After intracavitary injection of the recombinant adenovirus Ad-MHCLuc the highest luciferase activity was found in the myocardium, which was 3-4 fold less compared to Ad-MLCLuc. In contrast to Ad-MLCLuc, luciferase activity under control of the α-MHC promoter was also detected at significant levels in atrium (figure 7), and to a lower extend in lung and liver (figure 3, 4). It has been shown before, that the α-MHC promoter drives gene expression in the lung of transgenic animals [24]. Expression in the liver, however, has not yet been reported. The non-specific activity of Ad-MHCLuc in the liver might be an unique sequel of the adenoviral vector system. In skeletal muscle tissue, however, Ad-MHCLuc was inactive and showed only background luciferase activity (0.05 % of Ad-RSVLuc) even when injected directly into the thigh muscle. We therefore conclude that only the MLC-2v promoter but not the α-MHC promoter may be potentially useful within adenoviral vectors to target gene expression to heart and ventricular muscle tissue respectively. To characterize the usefulness of this novel adenoviral gene shuttle system with potential ventricular specificity further investigations in adult rat myocardium and larger animals such as rabbit or pig are necessary. The low level of luciferase expression driven by the α-MHC promoter in comparison to the MLC-2v promoter may be due to the chosen neonatal rat model because of two promoter specific properties. First, it is known that neonatal rat

hearts express primarily the β-MHC rather than the α-MHC gene [41]. Second, MLC-2v promoter activity has been demonstrated to be higher in neonatal compared to adult mice [22]. Both effects may account for the 3 to 4 fold lower expression level of the Ad-MHCLuc viruses in the neonatal rat model.

Conclusions

In this study a first generation adenoviral vector was used [18]. Within the time frame of five days no cell necrosis, mononuclear cell infiltration or other signs of inflammation were observed as described previously [26]. The problem of a transient transgene expression may be overcome by second and third generation adenoviral vector systems [10-17,20]. When long lasting gene expression becomes an established reality, tissue specificity will be of critical importance to circumvent side effects caused by a long lasting gene expression. Combination of the tissue specificity of the MLC-2v promoter with improved adenoviral vectors may facilitate the use of recombinant adenoviruses to treat heart muscle diseases such as dilated or hypertrophic cardiomyopathies.

Acknowledgments

We thank Yvonne Müller for excellent technical assistance. We thank Professor Dr. Alex van der Eb (University of Leiden) for providing us the cell line 911, Professor Dr. Martin Paul (Free University of Berlin) for the gift of the 1.0 kb α-MHC promoter and Yvonne Müller for excellent technical assistance. The generous support of Professor Dr. Harald zur Hausen is highly appreciated. This work was supported by the Deutsche Forschungsgemeinschaft (SFB 320/B6 and Ka 493/3-1) and the Deutsche Forschungsanstalt für Luft- und Raumfahrt (01 KV 9560).

References

1. Perloff JK. Congenital heart disease in adults. In:Braunwald E, editor. Heart Disease. Saunders:Philadelphia, 1992, pp 1810-26.
2. Towbin JA, Hejtmancik JF, Brink P, Gelb B, Zhu XM, Chamberlain JS et al. X-linked dilated cardiomyopathy. Molecular genetic evidence of linkage to the Duchenne muscular dystrophy (dystrophin) gene at the Xp21 locus. Circulation 1993;87:1854-65.
3. Franz WM, Cremer M, Herrmann R, Grünig E, Fogel W, Scheffold T et al. X-linked dilated cardiomyopathy: Novel Mutation of the dystrophin gene. Ann N Y Acad Sci 1995;752:470-91.
4. Kass Eisler A, Falck Pedersen E, Alvira M, Rivera J, Buttrick PM, Wittenberg BA et al. Quantitative determination of adenovirus-mediated gene delivery to rat cardiac myocytes *in vitro* and *in vivo*. Proc Natl Acad Sci USA 1993;90:11498-502.
5. Guzman RJ, Lemarchand P, Crystal RG, Epstein SE, Finkel T. Efficient gene transfer into myocardium by direct injection of adenovirus vectors. Circ Res 1993;73:1202-07.
6. Barr E, Carroll J, Kalynych AM, Tripathy SK, Kozarsky K, Wilson JM et al. Efficient catheter-mediated gene transfer into the heart using replication defective adenovirus. Gene Ther 1994;1:51-58.
7. Kirshenbaum LA, MacLellan WR, Mazur W, French BA, Schneider MD. Highly efficient gene transfer into adult ventricular myocytes by recombinant adenovirus. J Clin Invest 1993;92:381-87.
8. Chanock RM, Ludwig W, Heubner RJ, Cate TR, Chu LW. Immunization by selective infection with type 4 adenovirus grown in human diploid tissue cultures. I. Safety and lack of oncogenicity and tests for potency in volunteers. J Am Med Assoc 1966;195:445-52.
9. Yang Y, Nunes FA, Berencsi K, Furth EE, Gonczol E, Wilson JM. Cellular immunity to viral antigens limits E1-deleted adenovirus for gene therapy. Proc Natl Acad Sci USA 1994;91:4407-11.
10. Krougliak V, Graham FL. Development of cell lines capable of complementing E1, E4 and protein IX defective adenovirus type 5 mutants. Hum Gene Ther 1995;6:1575-86.
11. Wang Q, Jia XC, Finer, MH. A packaging cell line for propagation of recombinant adenovirus containing two lethal gene-region deletions. Gene Ther 1995;2:775-83.
12. Yeh P, Dedieu JF, Orsini C, Vigne E, Denefle P, Perricaudet M. Efficient dual transcomplementation of adenovirus E1 and E4 regions from a 293-derived cell line expressing a minimal E4 functional unit. J Virol 1996;70:559-65
13. Engelhardt JF, Ye X, Doranz B, Wilson JM. Ablation of E2a in recombinant adenoviruses improves transgene persistence and decreases inflammatory response in mouse liver. Proc Natl Acad Sci USA 1994;91:6196-6200
14. Yang Y, Nunes FA, Berencsi K, Gonczol E, Engelhardt JF, Wilson JM. Inactivation of E2a in recombinant adenoviruses improves the prospect for gene therapy in cystic fibrosis. Nat Gen 1994;7:362-69.
15. Kochanek S, Clemens PR, Mitani K, Chen HH, Chan S, Caskey T. A new adenoviral vector: Replacement of all viral coding sequences with 28 kb of DNA independently expressing both full-length dystrophin and ß-galactosidase. Proc Natl Acad Sci USA 1996;93:5731-36.
16. Parks RJ, Chen L, Anton M, Sankar U, Rudnicki MA, Graham FL. A helper-dependent adenovirus vector system: removal of helper virus by Cre-mediated excision of the viral packaging signal. Proc Natl Acad Sci (USA) 1996;93:13565-70.
17. Hardy S, Kitamura M, Harris-Stansil T, Dai Y, Phipps ML. Construction of adenovirus vectors through Cre-lox recombination. J Virol 1997;71:1842-49
18. Stradtford-Perricaudet LD, Makeh I, Perricaudet M, Briand P. Widespread long-term gene transfer to mouse skeletal muscles and heart. J Clin Invest 1992;90:626-30.
19. Huard J, Lochmüller H, Acsadi G, Jani A, Massie B, Karpati G. The route of administration

is a major determinant of the transduction efficiency of rat tissues by adenoviral recombinants. Gene Ther 1995;2:107-15.
20. Kass Eisler A, Falck Pedersen E, Elfenbein DH, Alvira M, Buttrick PM, Leinwand LA. The impact of developmental stage, route of administration and the immune system on adenovirus mediated gene transfer. Gene Ther 1994;1:395-402.
21. Franz WM, Mueller OJ, Hartong R, Frey N, Katus HA. Transgenic animal models: new avenues in cardiovascular physiology. J Mol Med 1997;75:115-29.
22. Franz WM, Breves D, Klingel K, Brem G, Hofschneider PH, Kandolf R. Heart-specific targeting of firefly luciferase by the myosin light chain-2 promoter and developmental regulation in transgenic mice. Circ Res 1993;73:629-38.
23. Franz WM, Brem G, Katus HA, Klingel K, Hofschneider PH, Kandolf R. Characterization of a cardiac-selective and developmentally upregulated promoter in transgenic mice. Cardioscience 1994; 5:235-43.
24. Subramaniam A, Jones WK, Gulick J, Wert S, Neumann J, Robbins J. Tissue specific regulation of the alpha-myosin heavy chain gene promoter in transgenic mice. J Biol Chem 1991; 266:24613-20.
25. Subramaniam A, Gulick J, Neumann J, Knotts S, Robbins J. Transgenic analysis of the thryoid elements in the alpha-cardiac myosin heavy chain gene promoter. J Biol Chem 1993;268:4331-36.
26. Rothmann T, Katus HA, Hartong R, Perricaudet M, Franz WM. Heart muscle-specific gene expression using replication defective recombinant adenoviurs. Gene Ther 1996;3:919-26
27. Franz WM, Rothmann T, Frey N, Katus HA. Analysis of tissue-specific gene delivery by recombinant adenoviruses containing cardiac-specific promoters. Cardiovascular Research 1997;35:560-66.
28. de Wet JR, Wood KV, DeLuca M, Helinski DR, Subramani S. Firefly luciferase gene: Structure and expression in mammalian cells. Mol Cell Biol 1987;7:725-37.
29. Mahdavi V, Cahmber AP, Nadal-Ginard B. Cardiac alpha- and beta-myosin heavy chain genes are organized in tandem. Proc Natl Acad Sci USA 1984;81:2626-30.
30. Henderson SA, Spencer M, Sen A, Kumar C, Siddiqui MA, Chien KR. Structure, organization, and expression of the rat cardiac myosin light chain-2 gene. J Biol Chem 1989;264:1842-48.
31. Graham FL, Smiley J, Russel WC, Nairn R. Characteristics of a human cell line transformed by DNA from human adenovirus type 5. J Gen Virol 1977; 36:59-74.
32. Fallaux FJ, Kranenburg O, Cramer SJ, Houweling A, Van Ormondt H, Hoeben RC et al. Characterization of 911: a new helper cell line for the titration and propagation of early region 1-deleted adenoviral vectors. Hum Gene Ther 1996;7:215-22.
33. Bett AJ, Haddara W, Prevec L, Graham FL. An efficient and flexible system for construction of adenovirus vectors with insertions or deletions in early regions 1 and 3. Proc Natl Acad Sci USA 1994;91:8802-06.
34. Zhang WW, Koch PE, Roth JA. Detection of wild-type contamination in a recombinant adenoviral preparation by PCR. BioTechniques 1995;18:444-47.
35. Ausbel JM, Brent R, Kingston RR, Moore DD, Seidman JG, Smith JA, Struhl K. Current Protocols in Molecular Biology. New York: Greene and Wiley, 1989.
36. Hearing P, Shenk T. The adenovirus type 5 E1A transcriptional control region contains a duplicated enhancer element. Cell 1983;33:695-703.
37. Hearing P, Samulski RJ, Wishart WL, Shenk T. Identification of a repeated sequence element required for efficient encapsidation of the adenovirus type 5 chromosome. J Virol 1987;61:2555-58.
38. Acsadi G, Jani A, Massie B, Simoneau M, Holland P, Blaschuk K et al. A differential efficiency of adenovirus-mediated in vivo gene transfer into skeletal muscle cells of different maturity. Hum Mol Gen 1994;3:579-84.

39. Johns DC, Nuss HB, Chiamvimonvat N, Ramza BM, Marban E, Lawrence JH. Adenovirus-mediated expression of a voltage-gated potassium channel in vitro (rat cardiac myocytes) and in vivo (rat liver). J Clin Invest 1995;96:1152-58.
40. Overbeek PA, Lai SP, Van Quill KR, Westphal H. Tissue-specific expression in transgenic mice of a fused gene containing RSV terminal repeats. Science 1986;231:1574-77.
41. Lompre AM, Nadal-Ginard B, Mahdavi V. Expression of the cardiac ventricular α-and β-myosin heavy chain genes is developmentally and hormonally regulated. J Biol Chem 1984; 259:6437-46.

26. CATHETER-MEDIATED DELIVERY OF RECOMBINANT ADENOVIRUS TO THE VESSEL WALL TO INHIBIT RESTENOSIS

Olivier Varenne, Peter Sinnaeve, Désiré Collen, Stefan P. Janssens, and Robert D. Gerard

Introduction

Although percutaneous transluminal coronary angioplasty (PTCA) is widely used for the treatment of coronary artery disease, its therapeutic efficacy is still limited by the occurrence of restenosis in 20-50% of all patients [1]. Restenosis following PTCA is a complex process characterized by progressive arterial remodeling [2], extracellular matrix deposition [3, 4], smooth muscle cell (SMC) proliferation and hyperplasia [4]. Except for probucol [5,6], pharmacological agents have consistently failed to demonstrate a clear beneficial effect on restenosis in large randomized clinical trials [1,7].

Recently, a number of gene transfer strategies have been employed to address the problem of restenosis [8]. Cells within the vessel wall are attractive targets for gene therapy because of their direct participation in the local pathologic response to injury. Recombinant adenovirus vectors are useful for gene transfer because high titer purified viral stocks can be obtained which permit relatively efficient infection of the various proliferative and quiescent cell types within the vessel wall.

A variety of techniques has been used to accomplish adenoviral mediated gene transfer to the vessel wall *in vivo*. Techniques in which virus is simply infused into the lumen without disruption of the endothelial barrier or the internal elastic lamina (IEL) (local dwell, double balloon catheter) result in efficient and highly selective gene transfer into the endothelial layer and vasa vasorum [9]. This pattern reflects the permeability barriers posed by the intact endothelium and IEL to recombinant virus particles [10]. Nevertheless, since gene therapy for restenosis will primarily be directed to sites of angioplasty, the influence of vessel trauma on local gene transfer efficiency and pattern remains an important issue. When virus is delivered into the arterial wall under pressure or with prior disruption of the endothelial layer and IEL by PTCA, genetic modification of the medial SMCs is observed in regions of the arterial segment proximal to the

P.A. Doevendans et al. (eds), Cardiovascular specific gene expression, 319-24.

intimal disruption [9,11]. The cells accessible to adenoviral transduction are likely the same ones that contribute most to the migration and proliferation that characterize the process of restenosis. Indeed, adenoviral delivery of a therapeutic gene (herpesvirus thymidine kinase, tk) into injured porcine iliac arteries with the double-balloon catheter rendered infected SMCs sensitive to the nucleoside analog ganciclovir and reduced neointima formation [12]. Although the relatively long duration of infusion is a significant limitation to clinical application of local gene delivery into the coronary vasculature, the local dwell method remains a promising technique for vein graft transduction *ex vivo* before coronary bypass surgery or for *in situ* delivery to peripheral vessels.

The pattern of gene transfer into atherosclerotic vessels may differ significantly from that observed in normal arteries by virtue of the altered architecture and cell composition of the vessel wall associated with atherosclerotic plaques [13]. Instillation of a recombinant adenoviral vector encoding ß-galactosidase after balloon injury demonstrates efficient gene transfer into atherosclerotic rabbit iliac arteries [14]. Genetically modified cells are located in pockets within the layers of the neointima, media and adventitia immediately adjacent to dissection planes. Furthermore, transfer of tk followed by ganciclovir injection limits neointima formation in balloon-injured rabbit atherosclerotic arteries, thus demonstrating sufficient biological activity of the transgene to inhibit the proliferative response [15]. However, small animal models employing either normal or atherosclerotic peripheral elastic arteries only poorly imitate the clinical situation of post-PTCA restenosis in the relatively inelastic coronary arteries of humans. Whether restenosis or vascular remodeling plays the predominant role in luminal narrowing in patients is also an issue. Porcine coronary arteries have been suggested to more closely mimic the situation in man [16], but generally require prolonged exposure to achieve substantial transduction via passive diffusion. In the coronary vasculature of large mammals, such protracted balloon inflation generates unacceptable myocardial ischemia and has limited the use of catheter-based techniques.

Recombinant adenovirus delivery to the vascular wall

The Infiltrator™ catheter (InterVentional Technologies Inc., San Diego, CA) is a intramural delivery catheter with 21 microinjector ports penetrating the IEL upon balloon inflation (Figure 1). This catheter permits rapid local virus delivery without causing significant perforation, dissection or hemorrhage in the arterial segment [17].

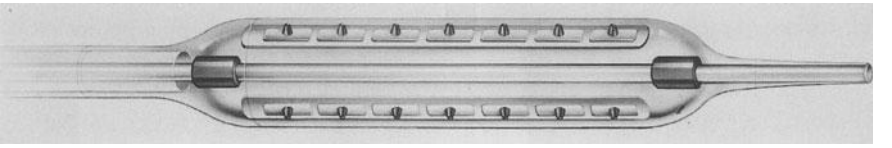

Figure 1. *Schematic diagram of the Infiltrator™ catheter, a device for combined PTCA and intramural drug delivery. A low pressure positioning balloon has three rows of seven conical microinjector ports mounted on its surface at 120° angles which radially penetrate the vessel wall upon balloon inflation. A specific delivery lumen allows injection of 0.3 ml viral solution through these ports over 10 to 20 sec.*

Qualitatively, gene transfer into vessels can be determined by histologic staining following ß-galactosidase virus (AdCMVßgal) transduction or immunohistochemical staining after infection with recombinant adenovirus carrying the constitutive endothelial nitric oxide synthase cDNA (AdCMVecNOS) [18]. Marked ß-galactosidase activity, as assessed by the blue staining of nuclei in infected cells, is detected in the media and the adventitia of AdCMVßgal-infected arteries. Virally-transduced cells are most frequently observed in the outer layers of the media and in the internal layers of the adventitia, often adjacent to dissection planes. Segments from coronary arteries infected with empty virus (AdRR5) show no blue staining within nuclei. Medial SMCs and adventitial cells of coronary arteries infected with AdCMVecNOS show diffuse ecNOS immunoreactivity in the deep layers of the media and adventitia resulting from gene transfer.

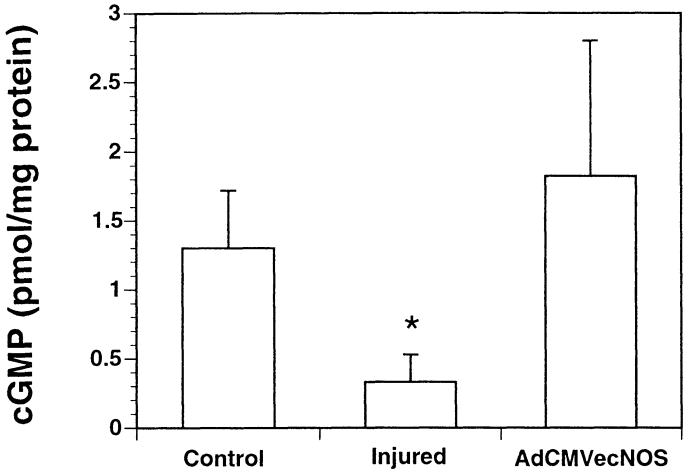

Figure 2. cGMP levels in frozen segments of porcine coronary arteries. cGMP levels were measured on day 5 after treatment in uninjured control coronary arteries (n=8), PTCA-injured arteries (n=8), and injured arteries infected with AdCMVecNOS (n=4). The asterisk indicates a value significantly reduced by comparison to both control and AdCMVecNOS groups.

In endothelial cells, ecNOS catalyzes the formation of nitric oxide (NO) from L-arginine [19]. NO is freely diffusible and plays a number of important roles in normal vascular homeostasis through pleiotropic effects on both smooth muscle cells in the vessel wall and platelets in the circulation, many of which are mediated by 3', 5'-cyclic guanosine monophosphate (cGMP). Injury to the endothelial protective barrier by PTCA results in the loss of a variety of vasoactive factors including NO which reduces guanylate cyclase activity. Vascular cGMP levels are significantly decreased following PTCA-induced injury to 0.33±0.20 pmol/mg protein compared with 1.30±0.42 pmol/mg protein in uninjured control arteries ($p<0.05$) (Figure 2), consistent with the loss of ecNOS from the injured vascular segment [18]. Adenovirus-mediated transfer of ecNOS to the SMC layer can restore vascular cGMP levels in injured arteries to 1.82±0.98 pmol/mg protein, which is not significantly different from uninjured controls.

In order to evaluate the ability of ecNOS gene transfer to limit restenosis using a strictly percutaneous catheter-based technique, porcine coronary arteries were treated with recombinant adenovirus after balloon-injury [18]. Juvenile domestic pigs underwent PTCA of the left anterior descending coronary artery (LAD) by three successive 30 sec inflations at 10 atmosphere. Adenoviral solution (AdCMVecNOS or AdRR5) was injected at the site of injury using the Infiltrator™ catheter. Control arteries in this study received AdRR5 to exclude the possibility that the adenovirus itself modulates the vascular response to angioplasty, perhaps by eliciting a host immune response to either the viral particle or virally-transduced cells. After four weeks, injured coronary arteries were harvested and prepared for morphometric analysis of neointima formation. The degree of injury in segments with maximal stenosis (estimated by both the injury score defined by Schwartz et al. [3] and the IEL fracture length normalized to the IEL perimeter) is similar in AdRR5- and AdCMVecNOS-infected pigs (2.30±0.48 vs. 2.20±0.47, p=NS, and 0.40±0.10 vs. 0.43±0.13, p=NS, respectively). The vessel size (measured as the area encompassed by the external elastic lamina (EEL)) is also similar in AdCMVecNOS- and AdRR5-infected arteries (2.55±0.79 mm^2 vs. 2.27±0.52 mm^2, respectively, p=NS).

Nevertheless, all parameters measuring neointima formation and luminal narrowing are significantly different between the two groups. The neointimal area normalized to IEL fracture length (Figure 3A) is significantly smaller in AdCMVecNOS-transduced arteries (0.59±0.14 mm) compared to AdRR5-infected vessels (0.80±0.19 mm, p=0.02). Maximal neointimal thickness (Figure 3B) is also significantly less in AdCMVecNOS-transduced arteries than those in AdRR5-infected animals (0.75±0.21 mm vs. 1.04±0.25 mm, p=0.019). Conversely, in AdCMVecNOS-infected pigs the minimal lumen area (Figure 3C) is larger than in the controls (0.70±0.35 vs. 0.32±0.18 mm^2, p=0.007), corresponding to a more severe stenosis rate (Figure 3D) in the AdRR5-infected control group than the AdCMVecNOS group (75±11% vs. 53±15%, p=0.006).

Discussion

These experiments demonstrate that the Infiltrator™ catheter permits efficient percutaneous adenoviral-mediated gene transfer into the medial and adventitial cells involved in the process of restenosis. Since efficient gene transfer is achieved with only a small volume of viral solution (0.3 ml) delivered within a very short time (about 15 sec), this catheter is also eminently compatible with standard interventional cardiology practices in the coronary vasculature. Further, intramural gene transfer results in the expression of sufficient levels of functional ecNOS capable of restoring vascular cGMP levels to normal values and reducing restenosis and luminal narrowing 28 days after PTCA. Increasing the local NO concentration within the injured vascular segment thus ameliorates the processes of cell proliferation and vascular remodeling that contribute to restenosis. Even though the anatomy of coronary arteries and the progression and morphology of neointima formation in the porcine model is similar to that observed in man, extrapolation of these data to patients requires both caution and further investigation into the efficacy and safety of gene therapy for restenosis. Nevertheless,

intramural gene transfer of ecNOS is a promising new therapeutic approach for restenosis after PTCA.

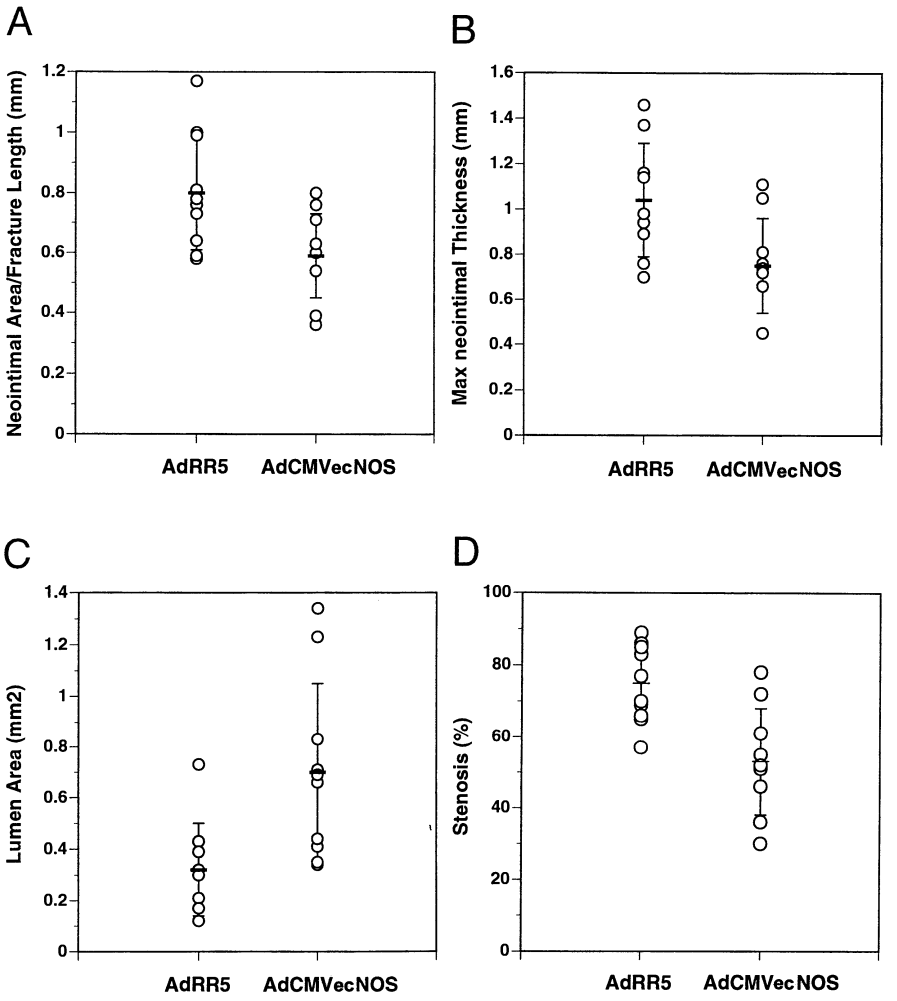

Figure 3. Response-to-injury in the porcine coronary artery following catheter-mediated gene therapy with AdCMVecNOS. Mean and standard deviation are indicated by the horizontal bar and error bars. **Panel A.** Neointimal area/ fracture length (mm) is significantly reduced in the AdCMVecNOS group (P=0.02) by comparison to the AdRR5 control. This parameter represents the vascular response to injury (neointimal area) normalized to the degree of injury defined by the IEL fracture length. **Panel B.** Maximal neointimal thickness (mm) is significantly reduced in the AdCMVecNOS group (P=0.019). **Panel C.** The minimal lumen area in each artery is significantly increased in the AdCMVecNOS group (P=0.007). **Panel D.** The resulting stenosis (%) is reduced in the AdCMVecNOS group (P=0.006). Percent stenosis is defined as (100 x (1-lumen area/IEL area).

References

1. Faxon DP, Currier JW. Prevention of post-PTCA restenosis. Ann N Y Acad Sci 1995; 748:419-27.
2. Post MJ, Borst C, Kuntz RE. The relative importance of arterial remodeling compared with intimal hyperplasia in lumen renarrowing after balloon angioplasty. A study in the normal rabbit and the hypercholesterolemic Yucatan micropig. Circulation 1994; 89:2816-21.
3. Schwartz RS, Edwards WD, Huber KC, et al. Coronary restenosis: prospects for solution and new perspectives from a porcine model. Mayo Clin Proc 1993; 68:54-62.
4. Carter AJ, Laird JR, Farb A, Kufs W, Wortham DC, Virmani R. Morphologic characteristics of lesion formation and time course of smooth muscle cell proliferation in a porcine proliferative restenosis model. J Am Coll Cardiol 1994; 24:1398-1405.
5. Tardif J-C, Cote G, Lesperance J, et al. Probucol and multivitamins in the prevention of restenosis after coronary angioplasty. N Engl J Med 1997; 337:365-72.
6. Yokoi H, Daida H, Kuwabara Y, et al. Effectiveness of an antioxidant in preventing restenosis after percutaneous transluminal coronary angioplasty: the Probucol Angioplasty Restenosis Trial. J Am Coll Cardiol 1997; 30:855-62.
7. Popma JJ, Califf RM, Topol EJ. Clinical trials of restenosis after coronary angioplasty. Circulation 1991; 84:1426-36.
8. Gerard RD, Collen D. Adenovirus gene therapy for hypercholesterolemia, thrombosis and restenosis. Cardiovasc Res 1997; 35:451-58.
9. Willard JE, Landau C, Glamann DB, et al. Genetic modification of the vessel wall. Comparison of surgical and catheter-based techniques for delivery of recombinant adenovirus. Circulation 1994; 89:2190-97.
10. Rome JJ, Shayani V, Flugelman MY, et al. Anatomic barriers influence the distribution of in vivo gene transfer into the arterial wall. Modeling with microscopic tracer particles and verification with a recombinant adenoviral vector. Arterioscler Thromb. 1994; 14:148-61.
11. French BA, Mazur W, Ali NM, et al. Percutaneous transluminal in vivo gene transfer by recombinant adenovirus in normal porcine coronary arteries, atherosclerotic arteries, and two models of coronary restenosis. Circulation 1994; 90:2402-13.
12. Ohno T, Gordon D, San H, et al. Gene therapy for vascular smooth muscle cell proliferation after arterial injury. Science 1994; 265:781-84.
13. Feldman LJ, Steg PG, Zheng LP, et al. Low-efficiency of percutaneous adenovirus-mediated arterial gene transfer in the atherosclerotic rabbit. J Clin Invest 1995; 95:2662-71.
14. Landau C, Pirwitz MJ, Willard MA, Gerard RD, Meidell RS, Willard SE. Adenoviral mediated gene transfer to atherosclerotic arteries after balloon angioplasty. Am Heart J 1995; 129:1051-57.
15. Simari RD, San H, Rekhter M, et al. Regulation of cellular proliferation and intimal formation following balloon injury in atherosclerotic rabbit arteries. J Clin Invest 1996; 98:225-35.
16. Muller DWM, Ellis SG, Topol EJ. Experimental models of coronary artery restenosis. J Am Coll Cardiol 1992; 19:418-32.
17. Barath P, Popov A, Dillehay GL, Matos G, McKiernan T. Infiltrator Angioplasty Balloon Catheter: a device for combined angioplasty and intramural site-specific treatment. Cathet Cardiovasc Diagn 1997; 41:333-41.
18. Varenne O, Pislaru S, Gillijns H, et al. Local adenoviral-mediated transfer of human endothelial nitric oxide synthase reduces luminal narrowing following coronary angioplasty in pigs. Circulation 1998;98:919-26.
19. Knowles RG, Moncada S. Nitric oxide synthases in mammals. Biochem J 1994; 298:249-58.

INDEX

actin-binding, 54
adenovirus, 209, 301, 319
angiogenesis, 135, 179, 194, 245
angiotensin II, 146, 163
antisense, 89, 105, 238, 269, 285
apoptosis, 3, 179, 238, 259
arterial remodeling, 204, 319
ATPase
  H^+-ATPase, 139
  Na^+/K^+-ATPase, 139
  plasmamembrane Ca^{2+}-ATPase, 139
  sarcoplasmatic reticulum Ca^{2+}-ATPase, 8, 139
atrial natriuretic factor, 8, 28, 70, 104, 122

brachytherapy, 3
brain natriuretic peptide, 99

Ca^{2+} transients, 142
cardiac hypertrophy, 28, 108, 144, 156, 166, 227, 258, 269
cardiogenesis, 12, 20, 70, 87, 100
cardiomyopathy
  dilated, 27, 93, 99
  hypertrophic, 1, 80, 99, 173, 227
cardioprotection, 247
catalytic RNA, 269
channelopathy
  long QT syndrome, 1, 125, 154, 171
  Brugada syndrome, 125, 171
cis elements
  AP2, 43
  AT-rich element, 76, 111
  CACC-box, 76
  CEF-2, 79
  E-boxes, 111, 122, 237
  enhancer, 39, 56, 76, 111, 196
  HRE, 111, 228
  initiator, 76
  TATA-box, 42, 56, 76, 122
compact myocardium, 11
congenital heart disease, 71
connexin, 29, 117, 161, 227
contractile proteins
  α-MHC, 11, 302
  myosin light chain - regulatory, 9, 99, 302
  myosin light chain - 3F, 8, 67
  tropomyosin, 75
  troponin C, 8, 75
  troponin I, 17, 75
  tropinin T, 17, 75
creatine kinase, 8, 78
cytoarchitecture, 31
cytoskeleton, 27, 62

dedifferentiation, 62, 109, 146
delayed rectification, 125

ectopic expression, 22, 312
electrogram, 172
endothelial nitric oxide synthase, 321
β-estradiol, 103, 228
excitation-contraction coupling, 144

fatty acids, 257

gender, 227
gene therapy, 38, 49, 112, 210, 301, 319
gene transfer, 202, 302, 319
Gln2, 8
growth factor
  angiopoietin, 37, 184, 194
  basic fibroblastic growth factor, 193
  cardiotrophin-1, 110
  CBF40, 79
  endothelin-1, 103
  insulin-like growth factor, 3, 199, 227, 245

platelet/ endothelial cell adhesion molecule, 202
placental growth factor, 37, 182, 197
platelet-derived growth factor, 37, 182, 194
transforming growth factor, 180, 194
vascular endothelial growth factor, 3, 37, 180, 194

heart failure, 2, 27, 87, 131, 144, 151, 171, 212
heart tube, 7, 35, 67, 100, 141
hemangioblast, 35, 193
heterotaxy, 71
hypertensive heart disease, 227
hypoxia-inducible factor, 43, 195

Infiltrator™ catheter, 320
inflammation, 193, 249, 301
inositol 1,4,5-triphosphate, 139
intussusception, 35, 179
ion channel
HERG, 154, 172
KvLQT1, 130, 154, 172
minK, 129, 154, 175
Na^+/Ca^{2+} exchanger, 139
ryanodine receptor, 139
SERCA-2, 8, 139
Na^+ channel, 129, 156

L_3G_4, 287
lavendustin A, 248
LIM-only protein, 27

malformation, 37, 71, 87
microembolization, 249
mitochondrial oxidation, 91, 261
morphogenesis, 87, 183
muscular artery, 56

necrosis, 58, 197, 247, 259, 313
neurohormones, 125
nuclear receptors, 87, 111, 231

palmitoylation, 258
percutaneous transluminal gene transfer, 302
peristaltoid contraction, 7
phenylephrine, 99, 142, 264
phospholamban, 142
plasminogen activator-inhibitor, 199
protein kinase
Ca^{2+}/calmodulin-dependent protein kinase, 142
cAMP-dependent protein kinase, 128, 142
cGMP-dependent protein kinase, 142
protein kinase A, 128, 142
protein kinase C, 131, 142, 185, 258
proteinases
gelatinase A, 199
gelatinase B, 199
metalloproteinases, 199
plasminogen activator, 182, 194
stromelysin-1, 199
stromelysin-2, 199
tissue-type plasminogen activator, 199
urokinase-type plasminogen activator, 199

Raf, 110, 180
Ras, 39, 99, 180, 258
receptors
α-adrenergic receptor, 110, 264
β-adrenergic receptor, 30, 127, 142
asialoglycoprotein, 285
estrogen, 110, 227
Flk-1, 36, 180, 195
Flt-1, 36, 180, 194
Flt-4, 36, 180, 197
vascular cell adhesion molecule, 194
TIE, 36, 186, 201
refractoriness, 172
regional specification, 23

restenosis, 3, 199, 237, 319
ribozyme cleavage assay, 271
rhodamine, 5, 290

sarcoplasmic reticulum, 139
septation, 7, 67
sequence tagged sites, 80
signal transduction, 61, 110, 155, 227, 245, 257
smoothelin, 49
snRNPs, 274
sprouting, 35, 179, 194, 250
stunning, 247
subtractive hybridization, 88
sulphonylureas, 155

targeting, 30, 72, 87, 132, 175, 198, 271, 286
thapsigargin, 146
tissue factor, 194
tissue factor pathway inhibitor, 204
tissue inhibitors of matrix metalloproteinase, 199
trabeculations, 11, 87, 100, 180
transcription factors
  AP2, 43, 172
  arylhydrocarbon-receptor nuclear translocator, 195
  CBF40, 79
  CEF-2, 79
  dermo-1, 239
  dHand, 12, 17, 70, 122, 238
  eHand, 17, 23, 70, 122, 238
  estrogen receptor, 111, 227
  GATA, 17, 42, 56, 76, 111
  M-CAT, 76
  MEF-2, 76
  MEF-3, 76
  MNF, 79
  MHox, 78
  NFκB, 43, 122
  Nkx 2.5, 17, 70, 112, 122, 240
  PPAR, 263
  Oct-1, 19, 78
  retinoid X receptor α, 87, 100, 263
  SP1, 17, 42, 77, 122
  TEF1, 17, 93, 112
  twist, 239

vasculogenesis, 35, 179, 194
vasomotor tone, 161
VEGF-related protein, 197
ventricular arrhythmias, 131, 156, 171
ventricular conduction system, 7, 117
visceral tissue, 54
voltage-dependent inactivation, 126
Von Hipple-Lindau, 195

Developments in Cardiovascular Medicine

170. S.N. Willich and J.E. Muller (eds.): *Triggering of Acute Coronary Syndromes.* Implications for Prevention. 1995 ISBN 0-7923-3605-4
171. E.E. van der Wall, T.H. Marwick and J.H.C. Reiber (eds.): *Advances in Imaging Techniques in Ischemic Heart Disease.* 1995 ISBN 0-7923-3620-8
172. B. Swynghedauw: *Molecular Cardiology for the Cardiologist.* 1995 ISBN 0-7923-3622-4
173. C.A. Nienaber and U. Sechtem (eds.): *Imaging and Intervention in Cardiology.* 1996 ISBN 0-7923-3649-6
174. G. Assmann (ed.): *HDL Deficiency and Atherosclerosis.* 1995 ISBN 0-7923-8888-7
175. N.M. van Hemel, F.H.M. Wittkampf and H. Ector (eds.): *The Pacemaker Clinic of the 90's.* Essentials in Brady-Pacing. 1995 ISBN 0-7923-3688-7
176. N. Wilke (ed.): *Advanced Cardiovascular MRI of the Heart and Great Vessels.* Forthcoming. ISBN 0-7923-3720-4
177. M. LeWinter, H. Suga and M.W. Watkins (eds.): *Cardiac Energetics: From Emax to Pressure-volume Area.* 1995 ISBN 0-7923-3721-2
178. R.J. Siegel (ed.): *Ultrasound Angioplasty.* 1995 ISBN 0-7923-3722-0
179. D.M. Yellon and G.J. Gross (eds.): *Myocardial Protection and the K_{ATP} Channel.* 1995 ISBN 0-7923-3791-3
180. A.V.G. Bruschke, J.H.C. Reiber, K.I. Lie and H.J.J. Wellens (eds.): *Lipid Lowering Therapy and Progression of Coronary Atherosclerosis.* 1996 ISBN 0-7923-3807-3
181. A.-S.A. Abd-Eyattah and A.S. Wechsler (eds.): *Purines and Myocardial Protection.* 1995 ISBN 0-7923-3831-6
182. M. Morad, S. Ebashi, W. Trautwein and Y. Kurachi (eds.): *Molecular Physiology and Pharmacology of Cardiac Ion Channels and Transporters.* 1996 ISBN 0-7923-3913-4
183. M.A. Oto (ed.): *Practice and Progress in Cardiac Pacing and Electrophysiology.* 1996 ISBN 0-7923-3950-9
184. W.H. Birkenhäger (ed.): *Practical Management of Hypertension.* Second Edition. 1996 ISBN 0-7923-3952-5
185. J.C. Chatham, J.R. Forder and J.H. McNeill (eds.): *The Heart in Diabetes.* 1996 ISBN 0-7923-4052-3
186. J.H.C. Reiber and E.E. van der Wall (eds.): *Cardiovascular Imaging.* 1996 ISBN 0-7923-4109-0
187. A-M. Salmasi and A. Strano (eds.): *Angiology in Practice.* 1996 ISBN 0-7923-4143-0
188. M.W. Kroll and M.H. Lehmann (eds.): *Implantable Cardioverter Defibrillator Therapy: The Engineering – Clinical Interface.* 1996 ISBN 0-7923-4300-X
189. K.L. March (ed.): *Gene Transfer in the Cardiovascular System.* Experimental Approaches and Therapeutic Implications. 1996 ISBN 0-7923-9859-9
190. L. Klein (ed.): *Coronary Stenosis Morphology: Analysis and Implication.* 1997 ISBN 0-7923-9867-X
191. J.E. Pérez and R.M. Lang (eds.): *Echocardiography and Cardiovascular Function: Tools for the Next Decade.* 1997 ISBN 0-7923-9884-X
192. A.A. Knowlton (ed.): *Heat Shock Proteins and the Cardiovascular System.* 1997 ISBN 0-7923-9910-2
193. R.C. Becker (ed.): *The Textbook of Coronary Thrombosis and Thrombolysis.* 1997 ISBN 0-7923-9923-4
194. R.M. Mentzer, Jr., M. Kitakaze, J.M. Downey and M. Hori (eds.): *Adenosine, Cardioprotection and Its Clinical Application.* 1997 ISBN 0-7923-9954-4
195. N.H.J. Pijls and B. De Bruyne: *Coronary Pressure.* 1997 ISBN 0-7923-4672-6
196. I. Graham, H. Refsum, I.H. Rosenberg and P.M. Ueland (eds.): *Homocysteine Metabolism: from Basic Science to Clinical Medicine.* 1997 ISBN 0-7923-9983-8
197. E.E. van der Wall, V. Manger Cats and J. Baan (eds.): *Vascular Medicine – From Endothelium to Myocardium.* 1997 ISBN 0-7923-4740-4
198. A. Lafont and E. Topol (eds.): *Arterial Remodeling.* A Critical Factor in Restenosis. 1997 ISBN 0-7923-8008-8
199. M. Mercury, D.D. McPherson, H. Bassiouny and S. Glagov (eds.): *Non-Invasive Imaging of Atherosclerosis* 1998 ISBN 0-7923-8036-3
200. W.C. De Mello and M.J. Janse (eds.): *Heart Cell Communication in Health and Disease.* 1997 ISBN 0-7923-8052-5

Developments in Cardiovascular Medicine

201. P.E. Vardas (ed.): *Cardiac Arrhythmias Pacing and Electrophysiology.* The Expert View. 1998 ISBN 0-7923-4908-3
202. E.E. van der Wall, P.K. Blanksma, M.G. Niemeyer, W. Vaalburg and H.J.G.M. Crijns (eds.): *Advanced Imaging in Coronary Artery Disease.* PET, SPECT, MRI, IVUS, EBCT. 1998 ISBN 0-7923-5083-9
203. R.L. Wilenski (ed.): *Unstable Coronary Artery Syndromes, Pathophysiology, Diagnosis and Treatment.* 1998 ISBN 0-7923-8201-3
204. J.H.C. Reiber and E.E. van der Wall (eds.): *What's New in Cardiovascular Imaging?* 1998 ISBN 0-7923-5121-5
205. J.C. Kaski and D.W. Holt (eds.): *Myocardial Damage.* Early Detection by Novel Biochemical Markers. 1998 ISBN 0-7923-5140-1
206. M. Malik (ed.): *Clinical Guide to Cardiac Autonomic Tests.* 1998 ISBN 0-7923-5178-9
207. G.F. Baxter and D.M. Yellon (eds.): *Delayed Preconditioning and Adaptive Cardioprotection.* 1998 ISBN 0-7923-5259-9
208. B. Swynghedauw: *Molecular Cardiology for the Cardiologist, Second Edition.* 1998 ISBN 0-7923-8323-0
209. G. Burnstock, J.G. Dobson, B.T. Liang and J. Linden (eds.): *Cardiovascular Biology of Purines.* 1998 ISBN 0-7923-8334-6
210. B.D. Hoit and R.A. Walsh (eds.): *Cardiovascular Physiology in the Genetically Engineerd Mouse.* 1998 ISBN 0-7923-8356-7
211. P. Whittaker and G.S. Abela (eds.): *Direct Myocardial Revascularization: History, Methodology, Technology.* 1998 ISBN 0-7923-8398-2
212. C.A. Nienaber and R. Fattori (eds.): *Diagnosis and Treatment of Aortic Diseases.* 1999 ISBN 0-7923-5517-2
213. J.C. Kaski (ed.): *Chest Pain with Normal Coronary Angiograms: Pathogenesis, Diagnosis and Management.* 1999 ISBN 0-7923-8421-0
214. P.A. Doevendans, R.S. Reneman and M. van Bilsen (eds.): *Cardiovascular Specific Gene Expression.* 1999 ISBN 0-7923-5633-0
215. G. Pons-Lladó, F. Carreras, X. Borrás, M. Subirana and L.J. Jiménez-Borreguero (eds.): *Atlas of Practical Cardiac Applications of MRI.* 1999 ISBN 0-7923-5636-5

Previous volumes are still available

KLUWER ACADEMIC PUBLISHERS – DORDRECHT / BOSTON / LONDON